

# FINAL PROGRAMME AND BOOK OF ABSTRACTS

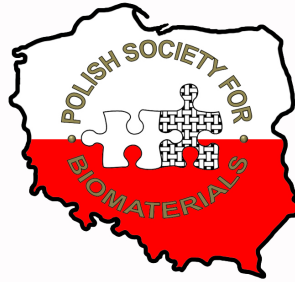
4th International Conference on  
Biomedical Polymers & Polymeric Biomaterials  
15–18 July 2018, Kraków, POLAND



[www.isbppb2018.org](http://www.isbppb2018.org)

# Organizers

Main Organizer



Supporting Scientific Organizers



# wimic

FACULTY OF MATERIALS SCIENCE AND CERAMICS  
AGH UNIVERSITY OF SCIENCE AND TECHNOLOGY



International Society for Biomedical  
Polymers and Polymeric Biomaterials

Endorsed by:



European  
Society for  
Biomaterials

Financially Supported by:



Ministry of Science  
and Higher Education

Republic of Poland



POLISH ACADEMY of SCIENCES



# Partners & Sponsors



CONGRESS BUREAU

JORDAN  
GROUP

# ARBURG



# polymers

an Open Access Journal by MDPI

ENGINEERING OF  
**BIOMATERIALS**  
INŻYNIERIA BIOMATERIAŁÓW  
JOURNAL OF POLISH SOCIETY FOR BIOMATERIALS AND FACULTY OF MATERIALS SCIENCE AND CHEMICALS AGH-UST  
Czasopismo Polskiego Stowarzyszenia Biomateriałów i Wydziału Inżynierii Materiałowej i Chemii AGH

Number 139  
Numer 139  
Volume XX  
Rok XX

JANUARY 2017  
STYCZEŃ 2017

ISSN 1429-7248

PUBLISHER:  
WYDAWCA:  
Polish Society  
for Biomaterials  
in Krakow  
Polskie  
Stowarzyszenie  
Biomateriałów  
w Krakowie

EDITORIAL  
COMMITTEE:  
KOMITET  
REDAKCYJNY:  
Editor-in-Chief  
Redaktor naczelny  
Jan Chłopek  
Editor  
Redaktor  
Elżbieta Pamała

Secretary of editorial  
Sekretarz redakcji  
Design  
Projekt  
Katarzyna Trala  
Augustyna Poremba

ADDRESS OF  
EDITORIAL OFFICE:  
ADRES REDAKCJI:  
AGH-UST  
30-043, Miskowicka Ave.  
30-059 Krakow, Poland  
Krakow  
Główna-Hutnicza 30/31  
30-059 Krakow

Issue: 292 copies  
Wydanie: 292 egz.

Scientific Publishing  
House ASLAPT  
Wydawnictwo Naukowe  
ASLAPT  
ul. Krakowska 100/101  
31-111 Krakow

ISSN: 0091-0037

International Journal of  
**Polymeric Materials and  
Polymeric Biomaterials**

Editor: Munmaya K. Mishra

Taylor & Francis  
Taylor & Francis Group

Included in this print edition:  
Volume 62, 2013  
Number 1, pages XX-XX  
Number 2, pages XX-XX  
Number 3, pages XX-XX  
Number 4, pages XX-XX

# Table of Contents



## FINAL PROGRAMME

• <b>Welcome Addresses</b>	<b>3</b>
ISBPPB 2018 Chair	3
PSB President	4
ISBPPB President	5
ISBPPB Founding Chairman	6
• <b>Committees</b>	<b>7</b>
Organizing Committee	7
International Scientific Committee	7
• <b>General Information</b>	<b>9</b>
• <b>Conference Venue Floor Plans</b>	<b>13</b>
• <b>Plenary Speakers</b>	<b>14</b>
• <b>Keynote Speakers</b>	<b>18</b>
• <b>Awards</b>	<b>24</b>
• <b>Social Events</b>	<b>25</b>
• <b>Detailed Scientific Programme</b>	<b>27</b>
• <b>Programme at a Glance</b>	<b>28</b>
• <b>Oral Presentations</b>	<b>30</b>
Monday, 16 <sup>th</sup> July	30
Tuesday, 17 <sup>th</sup> July	34
Wednesday, 18 <sup>th</sup> July	38
• <b>Rapid Fire and Poster Presentations</b>	<b>42</b>
• <b>Poster Presentations</b>	<b>44</b>
• <b>Authors Index</b>	<b>53</b>

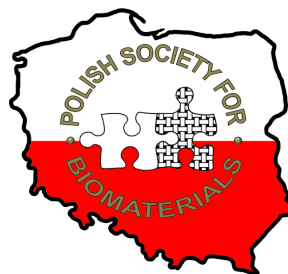
## BOOK OF ABSTRACTS

• <b>Plenary Lectures</b>	<b>L1 - L4</b>
• <b>Keynotes</b>	<b>K1 - K11</b>
• <b>Oral Presentations</b>	<b>1 - 86</b>
• <b>Rapid Fire and Poster Presentations</b>	<b>87 - 108</b>
• <b>Poster Presentations</b>	<b>109 - 217</b>

## Address of the Organizing Committee

Polish Society for Biomaterials  
AGH University of Science and Technology  
Faculty of Materials Science and Ceramics  
Department of Biomaterials and Composites

Al. Mickiewicza 30  
30-059 Kraków, Poland



© Copyright by the Polish Society for Biomaterials, Kraków 2018

Printed in Poland

**ISBN 978-83-65955-10-4**

## Publishing:



Scientific Publishing House „Akapit”, Kraków, Poland  
phone 48 608 024 572; [www.akapit.krakow.pl](http://www.akapit.krakow.pl)  
e-mail: [wn@akapit.krakow.pl](mailto:wn@akapit.krakow.pl)

# Welcome Address



On behalf of the Organizing Committee, I would like to welcome all of you to the 4<sup>th</sup> International Conference on Biomedical Polymers & Polymeric Biomaterials. It is also my great pleasure to welcome you to the Royal City of Kraków, its best technical university – AGH University of Science and Technology, and my home faculty – Faculty of Materials Science and Ceramics.

AGH is constantly growing and nowadays its educational offer includes not only traditional technical degrees but also more biology-related fields of study, like biomaterials science, biomedical engineering, medical physics, or biomechanics. The Faculty offers degree in materials science, with a major in biomaterials and composites, mostly focused on polymeric and composite biomaterials, as well as bioceramics.

The ISBPPB 2018 Conference is organized by two local biomaterial societies: the Polish Society for Biomaterials and the International Society for Biomedical Polymers and Polymeric Biomaterials based in the USA. This cooperation shows that it is possible to organize intercontinental meetings that support the exchange of people, ideas and facilitate formulating strategic goals in the field of biomaterials.

The most important in every endeavor are people and at this point I would like to express my sincere gratitude to the Presidents of both Societies - Dr. Gary Bowlin and Prof. Elżbieta Pamuła, as well as to Dr. Munmaya Mishra - the main initiator of the organization of this conference in Poland.

We are aware that this current initiative is a result of a well-organized European Conference on Biomaterials in 2015. The ESB 2015 conference was regarded as a success, hence during the organization of the ISBPPB 2018 we felt a lot of pressure not to disappoint our participants and maintain high standard of the meeting. The conference program created in cooperation with the International Scientific Committee covers such topics as: tissue engineering, cardiovascular applications, wound healing, surface modification, controlled delivery, smart materials, advanced manufacturing methods, cellular encapsulation and delivery, and many other aspects of biomedical polymers and polymeric biomaterials. I hope that you will enjoy both the scientific part, and the cultural events we have prepared for you.

Once again, thank you all for coming! Enjoy the ISBPPB 2018 Conference and your stay in our beautiful city!

## **Prof. Jan Chłopek**

*ISBPPB 2018 Chair*

*Head of the Department of Biomaterials and Composites,*

*AGH University of Science and Technology*

# Welcome Address



On behalf of the Polish Society for Biomaterials and the whole biomaterials community in Poland, I am delighted to welcome you to Kraków, to the 4<sup>th</sup> International Conference on Biomedical Polymers & Polymeric Biomaterials.

The Polish Society for Biomaterials was established 22 years ago and currently includes 213 members from all over Poland. The objective of the Society is to cooperate in creating interdisciplinary partner relations and initiatives serving the development of knowledge about materials for medicine, their promotion and application. The Society pursues its goals through scientific, research, educational and publishing activities. This year our Society is honored to co-organize the Conference of the International Society for Biomedical Polymers and Polymeric Biomaterials - ISBPPB 2018.

ISBPPB 2018 is a continuation of three previous conferences, which were organized by the International Society for Biomedical Polymers and Polymeric Biomaterials in the USA under the leadership of Dr. Gary Bowlin and Dr. Munmaya Mishra. This year, thanks to their initiative and collaboration between both our societies, the conference was moved to Europe, providing both our societies transcontinental dimension.

For ISBPPB 2018, we have had a strong record of 300 abstracts submissions and are expecting more than 250 participants from 36 countries. ISBPPB 2018 hosts an excellent set of 4 plenary and 11 keynote speakers from different countries and continents. Moreover, we will have the opportunity to listen to 86 podium presentations and discuss 130 poster contributions. Additionally, there will be 22 rapid-fire talks presented by young scientists.

This meeting could not have been organized without the contribution of all participants, speakers, reviewers, chairs of the sessions, members of the International Scientific Committee, members of the Local Organizing Committee, sponsors and partners. Let me thank all of you.

I hope that the value of the knowledge and inspiration generated during the next three days will result in many new collaborations and in the near future bring the benefits for the patients.

Welcome to the ISBPPB 2018, welcome to Kraków!

## **Prof. Elżbieta Pamuła**

*ISBPPB 2018 Vice-Chair*

*President of the Polish Society for Biomaterials*



# Powitanie! Welcome!



As the President of the International Society for Biomedical Polymers and Polymeric Biomaterials (ISBPPB), I would like to extend a very warm welcome, powitanie, to you to the historical city of Krakow, Poland as a valued attendee of the 4th International Conference on Biomedical Polymers and Polymeric Biomaterials.

I think all of you will enjoy the tremendous program developed by the local organizers and the International Scientific Committee. My deepest gratitude goes to Professor Jan CHŁOPEK as the chair of the organizing committee and the co-chair, Professor Elżbieta PAMUŁA both from the AGH University of Science and Technology for all their hard work and dedication. Without them, this meeting would not have been realized nor the success I am sure it will be. I would also like to acknowledge and thank the other honorary co-chair, Dr. Munmaya MISHRA, for all his vision and direction

during the development and growth of ISBPPB. We sure have come a long way in a short period of time as a new society. Finally, a big thank you to the sponsors, other organizers, supporting scientific organizers, and endorsing societies.

I make no secret that this has developed into one of my favorite conferences due to the diversity of the attendees, scientifically and culturally, and the fact that the environment maintained is one to promote comradery. ISBPPB prides itself on the international aspect of our society and conferences. I hope those that have attended our conferences in the past agree and that those attending for the first time will gain a similar experience. Please enjoy all that this meeting has to offer. Students and young investigators please be full participates in the meeting. You are the future and we are here to support and nurture you during your early-stage career.

In closing, thank you for attending. We hope that you will enjoy the scientific presentations and the wonderful social events that have been incorporated as a part of this conference. More importantly, we look forward to a very productive few days together continuing old friendships, developing new friendships, and creating new collaborations that are derived from our time together. I look forward to meeting everyone. Enjoy the meeting!

## **Dr. Gary Bowlin**

*ISBPPB 2018 Honorary Co-Chair*

*President of the International Society for Biomedical Polymers and Polymeric Biomaterials*

# Welcome Address



A VERY WARM WELCOME to all of you attending the 4th International Conference on Biomedical Polymers and Polymeric Biomaterials in Kraków, Poland. My special thanks go to Professor Jan CHŁOPEK who took our call and agreed to stage the conference in this historic town of Kraków. Please join me thanking the local Organizers and the International Scientific Committee for putting together such a wonderful program. Also, thanks to the sponsors, exhibitors, supporting scientific organizations, and endorsing societies. This is all possible by the tremendous leadership of Professor Jan CHŁOPEK (chair of the organizing committee) in association with Professor Elżbieta PAMUŁA (vice-chair). Without them, the meeting would not have been started in Kraków nor the success that we are sure to experience.

The International Society of Biomedical Polymers and Polymeric Biomaterials (ISBPPB) is still in its infancy but, we have come a long way since its debut in 2012. The idea of assembling the society was sparked during the publication of a multi-volume encyclopedia on the very title of this conference, published by CRC Press (T&F Group). Many thanks to Professor Gary BOWLIN as the president of the society who helped develop the infrastructure further. We would like to thank the publisher, Taylor & Francis Group for allowing us to designate the “International Journal of Polymeric Materials and Polymeric Biomaterials” as the official publication of ISBPPB. We hope the ISBPPB organization will serve as a platform for the scientists who are already in the field and for those who are entering this exciting arena.

It is worth noting ... for the first time the ISBPPB conference is being held outside of USA and we hope the trend continues. We look forward to enjoying the excellent scientific presentations and social events. Undoubtedly, it will be an exciting few days that we will be spending together. More importantly, our friendship will go a long way. Enjoy the meeting!

## **Dr. Munmaya K. Mishra**

*ISBPPB 2018 Honorary Co-Chair  
Founding Chairman, ISBPPB*

# Committees

## Organizing Committee

### Chair

**Prof. Jan CHŁOPEK**

Head of the Department of Biomaterials and Composites,  
Faculty of Materials Science and Ceramics,  
AGH University of Science and Technology, Kraków, Poland

### Vice-Chair

**Prof. Elżbieta PAMUŁA**

President of the Polish Society for Biomaterials,  
Faculty of Materials Science and Ceramics,  
AGH University of Science and Technology, Kraków, Poland

### Honorary Co-Chair

**Dr. Gary BOWLIN**

President of the International Society for Biomedical Polymers and Polymeric Biomaterials,  
The University of Memphis, USA

### Honorary Co-Chair

**Dr. Munmaya MISHRA**

Founding Chairman, International Society for Biomedical Polymers and Polymeric Biomaterials,  
Altria Research Center, Virginia, USA

### Members

**Katarzyna TRĄŁA**

**Patrycja DOMALIK-PYZIK**

**Barbara SZARANIEC**

**Karol GRYŃ**

Department of Biomaterials and Composites,  
Faculty of Materials Science and Ceramics  
AGH University of Science and Technology, Kraków, Poland

## International Scientific Committee

**Eben Alsberg**, Case Western Reserve University, Cleveland, United States

**Luigi Ambrosio**, National Research Council, Napoli, Italy

**Joelle Amedee**, Inserm, Bordeaux, France

**Iulian Antoniac**, University Politehnica of Bucharest, Bucharest, Romania

**Aldo Boccaccini**, University of Erlangen-Nuremberg, Erlangen, Germany

**Gary Bowlin**, University of Memphis, Memphis, United States

**Maria Chatzinikolaidou**, University of Crete, Heraklion, Greece

**Jan Chłopek**, AGH University of Science and Technology, Krakow, Poland  
**Wojciech Chrzanowski**, University of Sydney, Sydney, Australia  
**Gianluca Ciardelli**, Politecnico di Torino, Torino, Italy  
**Piotr Dobrzynski**, Centre of Polymer and Carbon Materials, Zabrze, Poland  
**Timothy Douglas**, Lancaster University, Lancaster, United Kingdom  
**Peter Dubruel**, Ghent University, Ghent, Belgium  
**Andrzej Dworak**, Polish Academy of Sciences, Zabrze, Poland  
**David Eglin**, AO Research Institute Davos, Davos Platz, Switzerland  
**Mirosława El Fray**, West Pomeranian University of Technology, Szczecin, Poland  
**Silvia Fare**, Politecnico di Milano, Milan, Italy  
**Michael Gelinsky**, TU Dresden, Dresden, Germany  
**Oguzhan Gunduz**, Marmara University, Istanbul, Turkey  
**Pamela Habibovic**, Maastricht University, Maastricht, Netherlands  
**Hitesh Handa**, University of Georgia, Athens, United States  
**Vasif Hasirci**, BIOMATEN Ctr of Excellence in Biomaterials and Tissue Engineering, Ankara, Turkey  
**Håvard J. Haugen**, University of Oslo, Oslo, Norway  
**Richard Hoogenboom**, Ghent University, Ghent, Belgium  
**Janusz Kasperczyk**, Medical University of Silesia, Sosnowiec, Poland  
**Charles James Kirkpatrick**, Goethe University of Frankfurt, Frankfurt/Main, Germany  
**Joachim Kohn**, New Jersey Center for Biomaterials, Rutgers, Piscataway, United States  
**Marek Kowalczyk**, University of Wolverhampton, Wolverhampton, United Kingdom  
**Veronique Larreta Garde**, Ermece Lab. University of Cergy Pontoise, Cergy Pontoise, France  
**Sébastien Lecommandoux**, Bordeaux INP, PESSAC, France  
**Didier Letourneur**, INSERM U 1148, Paris, France  
**Małgorzata Lewandowska-Szumieł**, Medical University of Warsaw, Warsaw, Poland  
**Suming Li**, National Center for Scientific Research, Montpellier, France  
**Munmaya Mishra**, Altria Research Center, Richmond, United States  
**Lorenzo Moroni**, Maastricht University, Maastricht, Netherlands  
**Maria Nowakowska**, Jagiellonian University, Krakow, Poland  
**Elżbieta Pamuła**, AGH University of Science and Technology, Kraków, Poland  
**Abhay Pandit**, CÚRAM Center for Research in Medical Devices, Galway, Ireland  
**Ki Dong Park**, Ajou University, Suwon, Korea  
**Ana Paula Pego**, INEB - Instituto de Engenharia Biomédica, Porto, Portugal  
**Rui L. Reis**, 3B's Research Group University of Minho, Guimaraes, Portugal  
**Janusz M. Rosiak**, Lodz University of Technology, Lodz, Poland  
**Frantisek Rypacek**, Institute of Macromolecular Chemistry, Prague, Czech Republic  
**Matteo Santin**, University of Brighton, Brighton, United Kingdom  
**Swadeshmukul Santra**, University of Central Florida, Orlando, United States  
**Dieter Scharnweber**, TU Dresden, Dresden, Germany  
**Alina Sionkowska**, Nicolaus Copernicus University in Torun, Torun, Poland  
**Wojciech Swieszkowski**, Warsaw University of Technology, Warsaw, Poland  
**Sandra Van Vlierberghe**, Ghent University, Ghent, Belgium  
**Hu Yang**, Virginia Commonwealth University, Richmond, United States  
**Dimitrios Zeugolis**, NUI Galway, Galway, Ireland  
**Meital Zilberman**, Tel-Aviv University, Tel-Aviv, Israel  
**Ewa Zuba-Surma**, Jagiellonian University, Krakow, Poland

# General Information

## CONFERENCE VENUE

The conference is being held in the newest building (B-8) of the Faculty of Materials Science and Ceramics located at the AGH University of Science and Technology campus, within walking distance to the historical center of Kraków. This modern research and educational center of the Faculty was designed to meet the highest, world-class requirements. Excellent location of the venue, its contemporary interiors and unique scientific atmosphere make it a perfect setting for the organization of international conferences. AGH University of Science and Technology, established in 1919, is a leading Polish technical university and one of the top-ranked higher education institutions in Poland. The AGH-UST is well recognized for its high quality research in different fields and disciplines of science.

Password-free **Wi-Fi** is available for the Conference Delegates. However, because of a large number of users, Wi-Fi should not be used for large file exchanges.

## TRANSPORT INFORMATION

The Conference venue is located close to the City Center - it is only a 15-mins walk. It is also possible to use different forms of public and private transportation to get to the venue, e.g. bus, tram or taxi.

Public transport connections can be found here:

<http://krakow.jakdojade.pl/?locale=en>

We recommend downloading the **Jakdojade** app (btw, 'jak dojade?' means 'how do I get to?')

To avoid overcharging and for safety reasons, Delegates are advised to use only licensed taxis (there are over a dozen licensed taxi companies in Kraków) - full list of those is available here:

<http://cracow.travel>

## REGISTRATION DESK

The Registration Desk is located on Level 0.

Opening times are as follows:

Sunday, 15 <sup>th</sup> July	16:00 - 20:00
Monday, 16 <sup>th</sup> July	07:30 - 18:00
Tuesday, 17 <sup>th</sup> July	08:00 - 18:00
Wednesday, 18 <sup>th</sup> July	08:00 - 14:00

Optional tours tickets can be bought at the Registration Desk. The Staff will be also happy to give extra tourist information and make travel or transport arrangements.

## ORGANIZING COMMITTEE INFORMATION DESK

Organizing Committee members can be found at the Information Desk on Level 0. Please do not hesitate to contact us with all the enquiries.



## BADGES

Name badges will be issued to all delegates upon registration. **These must be worn at all times.**

## CLOAKROOMS

Cloakrooms are located on Level 0 (you have to go pass the Registration Desk, and enter the adjacent B-6 building) and are free of charge. It is also possible to leave travel bags there.

Opening times are as follows:

Sunday, 15 <sup>th</sup> July	16:00 - 20:00
Monday, 16 <sup>th</sup> July	07:30 - 18:30
Tuesday, 17 <sup>th</sup> July	08:00 - 18:30
Wednesday, 18 <sup>th</sup> July	08:00 - 15:00

## CONFERENCE HALLS

Plenary Lectures will be held in the main lecture hall – Hall 1. This hall will be subsequently divided into two smaller halls – Hall 1A and Hall 1B for parallel sessions. On Wednesday morning, third parallel session, i.e. Rapid Fire Session, will be held in Hall 2 located on Level 0 to the right of the main staircase. Please refer to the Conference venue maps for the exact locations of the halls.

## COFFEE BREAKS AND LUNCH AREA

Coffee (together with other refreshments and sweet pastries) and lunches will be served in the Conference tent located at the back of the B-8 Building. To get there, please go to Level -1 using the main staircase (or lift located next to it) and take a left hallway. The passage will be clearly marked with signs. In case of any troubles with finding the right way, please ask Volunteers or Organizing Committee members for help.

## SPEAKER READY ROOM

Speaker Ready Room will be organized in Hall 2 (on Level 0, to the right of the main staircase; please refer to the Conference venue maps for its exact location). **All presentations (.ppt or .pptx) should be brought to the Speaker Ready Room at least half a day prior to a scheduled presentation time** (e.g. on Sunday for Monday morning sessions; no later than 8:30 a.m. for Monday afternoon sessions).

Speakers are advised to check with technicians available in the Room if the presentation or embedded videos run properly. The system is PC-based, thus Mac user should also ensure PowerPoint compatibility of their presentation.

Speaker Ready Room hours:

Sunday, 15 <sup>th</sup> July	16:00 - 18:00
Monday, 16 <sup>th</sup> July	07:30 - 16:00
Tuesday, 17 <sup>th</sup> July	08:00 - 16:00

PLEASE NOTE: Speaker Ready Room will not be operating on Wednesday. All presentations scheduled for Wednesday, 18<sup>th</sup> July have to be uploaded on Tuesday at the latest.

## ORAL PRESENTATIONS

To ensure that all sessions run smoothly, Oral Presenters are kindly requested to read following instructions.

- Speakers should check the Conference programme carefully for the scheduled session time and presentation order.
- Use of personal laptops to run the presentation will not be possible. Speakers must upload their presentations (.ppt or .pptx) in the Speaker Ready Room no later than 16:00 on the day prior to their allocated session.
- Speakers should arrive at their assigned session hall 10 minutes before the start of their session in order to introduce themselves to the Session Chairs and familiarize with the hall arrangement.
- Speakers will be provided with a microphone and a laser pointer for use in their presentations.
- Oral presentations should last no longer than 12 minutes, and then there should be 3 minutes for discussion. All Oral Presenters are kindly requested not to exceed their time. Session Chairs will monitor presentation timekeeping and will intervene if the time (maximum of 15 minutes) has been exceeded.
- Technical support and audiovisual operators are ready to attend any problem during presentations. In case of such an event, Speakers should continue their presentation; the problem will be fixed as quickly as possible.

## DISCUSSION

After each presentation, there should be enough time for longer or shorter discussion. Delegates wishing to ask a question or make a comment, should raise a hand or stand up to make a clear sign that they are willing to take part in the discussion. Our Volunteers will be ready to hand the microphone. Delegates are kindly asked not to speak without the microphone since it might be hard for the Presenter or the audience to hear.

## RAPID FIRE PRESENTATIONS

Rapid Fire Session will be held on Wednesday, from 09:00 to 11:30, in Hall 2 located on Level 0, to the right of the main staircase. Rapid Fire Presenters are kindly requested to read following instructions.

- Speakers should check in the Final Programme order of the presentation.
- Use of personal computers will not be possible.
- All Rapid Fire Presentations should be uploaded in the Speaker Ready Room no later than 16:00 on Tuesday, 17<sup>th</sup> July.
- Speakers should arrive at Hall 2 at least 10 minutes before the start of the session.
- Each rapid-fire presentation must last no longer than 4 minutes (it usually means a maximum of 5-6 slides). All presentations should be in PowerPoint format.
- Session Chair will monitor presentation timekeeping and will intervene if the time has been exceeded.
- Speakers will be provided with a slide changer/laser pointer for use in the presentation.

**POSTER SESSIONS**

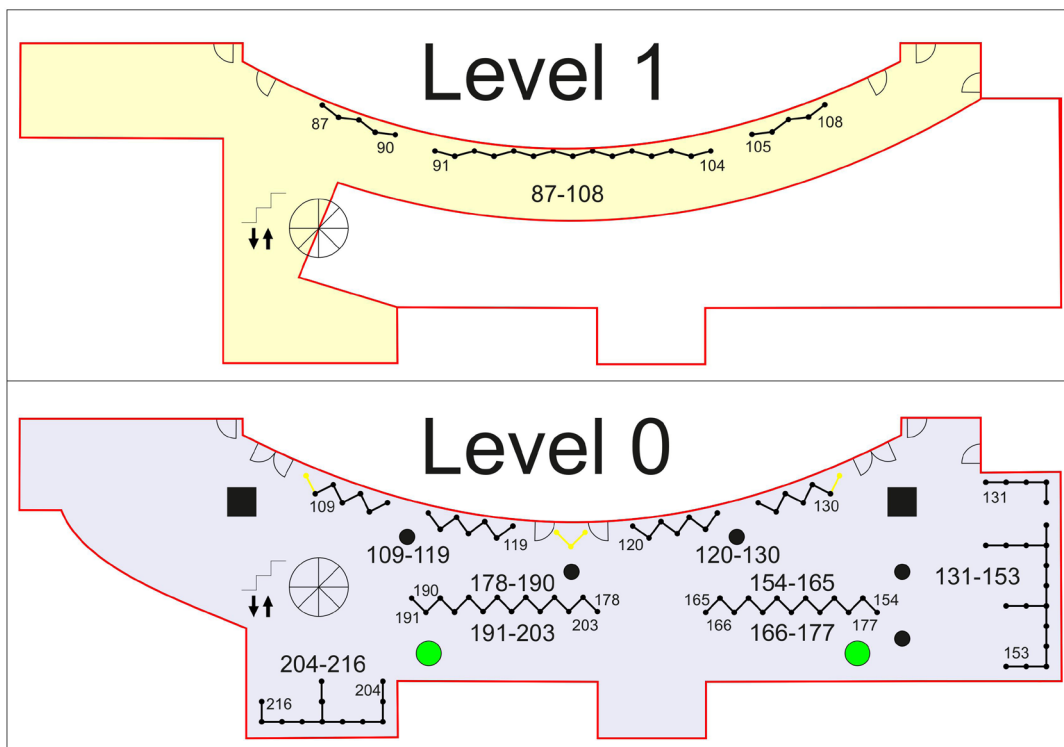
Poster Sessions will be held in the main foyer of the Conference venue on Level 0 and 1. All posters will be exposed during the whole Conference.

Poster Presenters are kindly requested to attach their poster (1189 mm (tall) x 841 mm (wide), Portrait style (A0 Size)) to their assigned poster panel on Sunday, 15<sup>th</sup> July (16:00 - 17:45) or on Monday morning, 16<sup>th</sup> July. Posters will be arranged numerically and organized by topics. Please check the Final Programme for the assigned poster number.

Poster presenters are strongly encouraged to be present at their posters during these times:

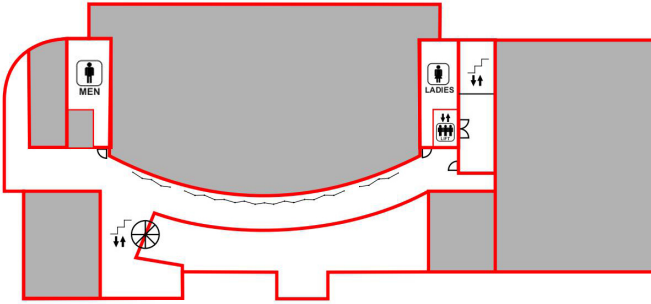
Monday, 16 <sup>th</sup> July	13:00 - 14:30
Tuesday, 17 <sup>th</sup> July	13:00 - 14:30

Posters must be removed until 12:00 on Wednesday, 18<sup>th</sup> July. After that time, all the remaining posters will be taken off and gathered at the Organizing Committee Information Desk, where it would be possible to collect them. Any posters not collected by 14:00 on Wednesday, 18<sup>th</sup> July will be discarded.

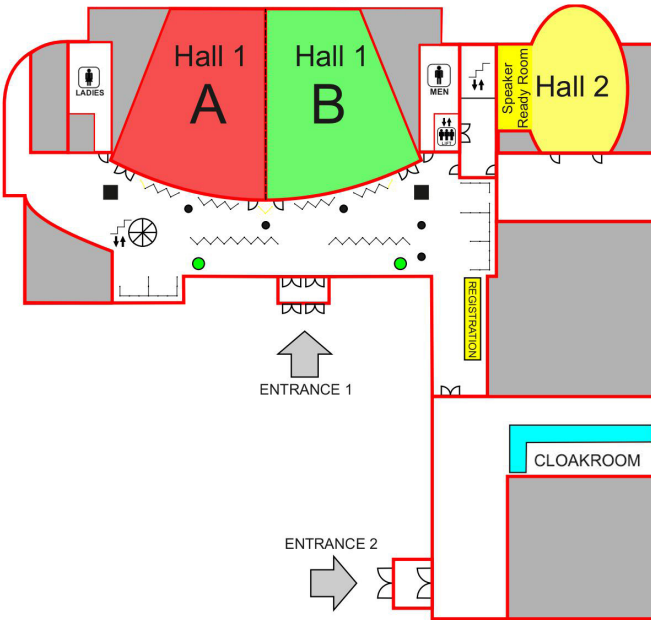


# Conference Venue Floor Plan

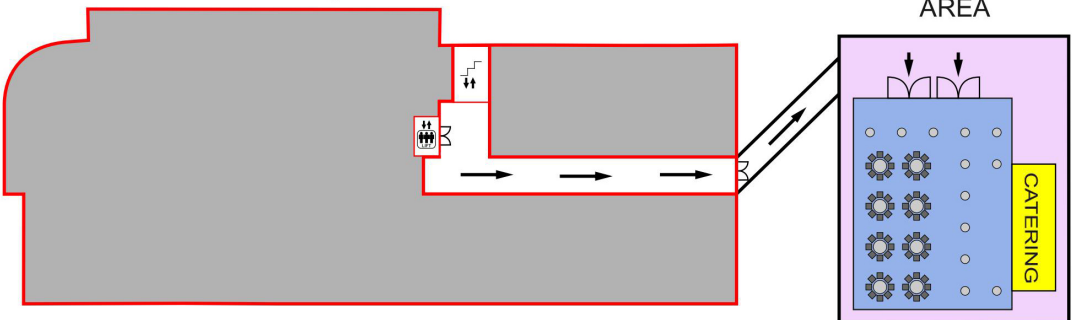
## Main Building - Level 1



## Main Building - Level 0



## Main Building - Level -1



# Plenary Speakers



## **Andreas LENDLEIN**

*The Helmholtz-Zentrum Geesthacht,  
GERMANY*

### **PL1**

***Title: “Implementing multifunctionality in polymeric biomaterials for medical applications”***

***Monday, 16<sup>th</sup> July***

***9:00 - 9:45, Hall 1***

Andreas Lendlein is Director of the Institute of Biomaterial Science at the Helmholtz-Zentrum Geesthacht in Teltow, Germany, and Professor for Materials in Life Sciences at University Potsdam. Prof. Lendlein received his doctoral degree in Materials Science from Swiss Federal Institute of Technology (ETH) in Zürich in 1996. He worked as a visiting scientist at the Massachusetts Institute of Technology in 1997-98 and completed his habilitation in Macromolecular Chemistry in 2002 at the RWTH Aachen University. In 2002 he joined the Helmholtz-Zentrum Geesthacht in Teltow and the University of Potsdam. Furthermore, he is honorary professor in Chemistry at the Freie Universität Berlin and member of the medical faculty of Charité University Medicine Berlin.

His research interests in material science & engineering are creation of material functions by design and implementation of multifunctionality in polymer-based materials with special emphasis given to stimuli-responsive polymers, especially shape-memory polymer actuators, biopolymer-based material systems and structured biomaterials. He also works on fabrication schemes for multifunctional materials including integrated processes and advanced manufacturing methods as well as on studies related to processes occurring at interfaces, e.g. biointerface or water/air interface. Biomaterial-based regenerative therapies, controlled drug delivery systems, health technologies and robotics recently are his interests in translational research.

Andreas Lendlein published more than 500 peer-reviewed papers (H-factor: 54), is an inventor on about 300 issued patents and published patent applications, and received more than 20 awards for his scientific work and his achievements as an entrepreneur including the BioFUTURE Award, Hermann-Schnell Award, and the World Technology Network Award in the category Health & Medicine. He is founding Editor-in-Chief of the journal Multifunctional Materials (IOP Publishing) and serves on the Executive Advisory Board of VCH-Wiley’s Macromolecular Journals.





## **Sandra VAN VLIERBERGHE**

*Ghent University,  
BELGIUM*

**PL2**

**Title: “Crosslinkable hydrogels tailored towards processing and biomedical needs”**

**Monday, 16<sup>th</sup> July  
14:30 - 15:15, Hall 1**

Sandra Van Vlierberghe is a full-time professor at the Centre of Macromolecular Chemistry (Ghent University) and holds a 20% professorship at the Faculty of Engineering of the Vrije Universiteit Brussel (VUB). She graduated as a Master in Chemistry with high distinction with majors in Polymer Chemistry in 2003 and received her PhD in Sciences in 2008, both at Ghent University. She has acquired expertise related to the synthesis, modification, characterization and processing of a variety of (bio)polymers including thermoplasts (e.g. polyesters) and hydrogels (e.g. proteins and polysaccharides) for a variety of applications in the fields of optics and regenerative medicine. She is experienced in the field of polymer processing using 3D printing, electrospinning and two-photon polymerization (2PP). Her research mainly focuses on the interplay between light and polymers and how this can further advance the biomedical field.

Sandra Van Vlierberghe authored 107 Web of Science Core Collection cited papers (h-index 23) of which 95 are high-impact journal papers and 11 full papers in international conference proceedings. In addition, she also authored more than 100 conference abstracts. She is supervisor of 17 PhDs, edited two books, authored 7 chapters in books of which 5 were invited. She was invited speaker at 10 international conferences, and keynote and plenary speaker at two international conferences.

Sandra Van Vlierberghe is YSF spokesperson and treasurer of the Belgian Polymer Group, editorial board member of the Biomaterials Network and associate editor of Journal of Materials Science: Materials in Medicine. She fulfils several refereeing activities for a number of journals including a.o. Advances in Polymer Technology, Biomaterials, European Polymer Journal, Biomacromolecules. Sandra Van Vlierberghe serves as evaluator for national, EU and international projects. She organized several national and international symposia and conferences including AMBA 2017, IMRC 2015, AMBA 2014, the Annual Meeting of the Belgian Polymer Group (2014) and Biofuture 2011. In 2017, she received the Jean Leray Award from the European Society for Biomaterials.



## **Eben ALSBERG**

Case Western Reserve University, Cleveland,  
UNITED STATES

### **PL3**

**Title: “Controlled spatiotemporal signal presentation within high-density cell culture systems for engineering complex tissues”**

**Tuesday, 17<sup>th</sup> July**  
**9:00 - 9:45, Hall 1**

Dr. Alsberg took a faculty position in 2005 at Case Western Reserve University, where he is currently Professor of Biomedical Engineering and Orthopaedic Surgery and serves as Director of the Stem Cell and Engineered Novel Therapeutics Laboratory. He received his B.S.E. in Mechanical Engineering and Material Science and Biomedical Engineering, cum laude, from Duke University in 1994. He then went to graduate school at the University of Michigan, Ann Arbor, where he received an M.S.E. in Mechanical Engineering (1998), an M.S.E. in Biomedical Engineering (1998), and a Ph.D. in Biomedical Engineering (2002). Following his graduate studies, he was a Postdoctoral Research Fellow in the Vascular Biology Program at Harvard Medical School.

His laboratory focuses on engineering functional biologic replacements to repair damaged or diseased tissues in the body. Complex signals implicated in tissue morphogenesis, repair, and homeostasis are used as inspiration for the development of innovative biomaterials for tissue regeneration. Through the precise temporal and spatial presentation of soluble bioactive factors, mechanical forces, and biomaterial physical and biochemical properties, his lab aspires to create microenvironments that regulate cell gene expression and new tissue formation.

He’s co-authored over 110 peer reviewed papers and book chapters, and his work has been recognized with the Ellison Medical Foundation New Scholar in Aging Award, the Biovalley Young Investigator Award from the Tissue Engineering Society International, the Crain’s Cleveland Business Forty Under 40 Award, a Visiting Professorship at Kyung Hee University (Korea), a Lady Davis Fellowship at the Technion (Israel), and election to the American Institute for Medical and Biological Engineering (AIMBE) College of Fellows. The NIH, DOD, NSF, the Ellison Medical Foundation, the Coulter Foundation, the Musculoskeletal Transplant Foundation, the State of Ohio and the AO Foundation have funded his lab’s research. He is active in many professional societies, and currently serves on the Americas Council of the Tissue Engineering and Regenerative Medicine International Society (TERMIS).



## **Joachim KOHN**

*The New Jersey Center for Biomaterials  
UNITED STATES*

**PL4**

**Title: “Understanding the effect of biomaterials on cell and stem-cell differentiation”**

**Tuesday, 17<sup>th</sup> July  
14:30 - 15:15, Hall 1**

Joachim Kohn, PhD, FBSE is a research entrepreneur, a multi-disciplinary translational scientist, and a national leader in the field of biomaterials science. In 1997, Kohn founded the New Jersey Center for Biomaterials (NJCBM), which has grown into a collaborative network spanning 25 institutions and 40 laboratories. Research at the NJCBM focuses on design, synthesis, characterization and fabrication of new biomaterials for regenerative medicine, tissue engineering and drug delivery. Kohn has pioneered the use of combinatorial and computational methods for the optimization of biomaterials for specific medical applications.

He is mostly known for his seminal work on „pseudo-poly(amino acid)s“- a new class of polymers that combine the non-toxicity of individual amino acids with the processability and strength of high-quality engineering plastics. Medical devices (a coronary stent and an antimicrobial device to prevent infections in pace maker patients) using these materials have been implanted in more than 250,000 patients and are currently approved for use in 46 countries. As a translational scientist, Kohn has 72 issued US Patents on novel biomaterials and seven companies have licensed his technologies. He is the scientific founder of three spin-off companies.

Professor Kohn’s selected Honors and Awards: Thomas Alva Edison Patent Award, best patent in New Jersey for invention of the first unique polymer used in the world’s first biodegradable and x-ray visible polymer stent (2017); Health Institute of New Jersey Life Sciences researcher of the year (2014); Inducted into the National Academy of Inventors (2013); Inducted into the New Jersey High-Tech Hall of Fame (2007); Thomas Alva Edison Patent Award, best patent in New Jersey for invention of the first combinatorially designed library of polyarylates (2006); Elected as a Fellow of Biomaterials Science & Engineering, serves as Chair (2004); Elected as a Fellow of AIMBE (2001); Thomas Alva Edison Patent Award, best patent in New Jersey for invention of tyrosine-derived polycarbonates (1999).

# Keynote Speakers



## **Maria CHATZINIKOLAÏDOU**

*Univeristy of Crete, GREECE*

### **K1**

***Title: “PLLA-based copolymeric biomaterials for bone tissue engineering”***

***Monday, 16<sup>th</sup> July***

***10:15 - 10:45, Hall 1A***

Dr. Maria Chatzinikolaïdou is an Assistant Professor in Biomaterials in Tissue Engineering at the Department of Materials Science and Technology, University of Crete (tenured in 2014) and affiliated researcher at the Foundation for Research and Technology – Hellas (FORTH). Her research interests focus on the development of biomaterials and scaffolds, in vitro and in vivo biocompatibility, tissue engineering (bone, dental, cardiovascular). Dr. Chatzinikolaïdou is actively involved in several competitive national and international projects, is author of more than 50 publications in international peer-reviewed journals, 3 book chapters, 120 peer-reviewed conference abstracts and inventor of 3 patents on osteoinductive implants. She is co-organizer of numerous national and international conferences. Since 2012, she is elected member of the Executive Board of the Hellenic Society for Biomaterials (and serves as vice president in the 2015-2018 term). She served as Chair of the 28th Conference of the European Society for Biomaterials (ESB 2017) hold in Athens, and is program chair of the TERMIS-EU 2019 conference to be held in Rhodes, Greece.



## **Ahmed FATIMI**

*Sultan Moulay Slimane University, MOROCCO*

### **K2**

***Title: “Chitosan-based embolizing hydrogel for endovascular therapies characterization of rheological and occlusive properties”***

***Monday, 16<sup>th</sup> July***

***10:15 - 10:45, Hall 1B***

Dr. Ahmed Fatimi is an Assistant Professor (Department of Chemistry) and affiliated researcher (Biological Engineering Laboratory) at Sultan Moulay Slimane University (Morocco). He has a Master degree (chemical engineering) from Polytech’Nantes School (France) and another Master degree (biopolymers engineering) from University of Nantes (France). In 2008, he obtained a PhD degree in biomaterials from University of Nantes in collaboration with French National Institute for Health and Medical Research (INSERM) on rheological behavior of biomaterials for osteoarticular and dental tissue engineering. From 2009 until 2012, he worked as post-doctoral research fellow at Canada Research Chair in Biomaterials and Endovascular Implants (development of an injectable radiopaque chitosan-based hydrogel for use in endovascular therapy). Dr. Ahmed Fatimi’s research is focused on developing and formulation of hydrogels for tissue engineering and biomedical use, and its physico-chemical, rheological and biological properties. He published 20 papers, 2 book chapters and 2 patents and presented around 40 conference communications.



## **Marta PEGUEROLES**

*Technical University of Catalonia UPC, SPAIN*

### **K3**

**Title: "Controlled drug delivery from 3D printed poly-L-lactic acid bioresorbable stent"**

**Monday, 16<sup>th</sup> July**

**15:45 - 16:15, Hall 1A**

Dr. Marta Pegueroles is head of the Cardiovascular Research line of the Biomaterials, Biomechanics and Tissue Engineering group of the Technical University of Catalonia (UPC). She obtained her PhD degree in Materials Science in 2009 from UPC focusing on the surface modification and the study of cell-material interactions for dental applications. She has performed research stays at the Université Paris XIII (Paris, France) and at the Instituto de Engenharia Biomédica (INEB) (Porto, Portugal). In 2016, she became Associate Professor at UPC and she has a sound experience in the development and modification of metal and polymer biomaterials and its physico-chemical and biological characterization. She has published around 20 papers and 2 book chapters. Her current research focuses on the development of (3D-printed) biofunctional polymeric scaffolds and stents with improved endothelialization properties and reduced risks of restenosis and thrombosis.



## **Andrzej KOTARBA**

*Jagiellonian University, POLAND*

### **K4**

**Title: "Tailoring of implant-tissue interface: PLGA-parylene C multifunctional coating"**

**Monday, 16<sup>th</sup> July**

**15:45 - 16:15, Hall 1B**

Andrzej Kotarba is a full professor at the Faculty of Chemistry, Jagiellonian University, Kraków, Poland. In his research carried out within Materials and Surface Chemistry Group, he is head of, he focuses on the processes taking place at the solid/liquid and solid/gas interfaces, with the aim to apply the acquired knowledge in designing surfaces with desired properties. Within this framework, the research includes catalysts and biomaterials, their preparation and characterization, the latter including their surface properties and reactivities. The research is typically interdisciplinary and is carried out at the interface of chemistry, biochemistry and materials science. Andrzej Kotarba co-authored more than 120 scientific papers and 30 national and international patents and patent applications.





## Achim AIGNER

Leipzig University, GERMANY

### K5

**Title: "Microparticulate poly vinyl alcohol hydrogel formulations for embedding and controlled release of polyethyleimine PEI -based nanoparticles"**

**Tuesday, 17<sup>th</sup> July**

**10:15 - 10:45, Hall 1A**

Achim Aigner is Full Professor for Clinical Pharmacology at the Rudolf-Boehm-Institute for Pharmacology and Toxicology, Faculty of Medicine, University of Leipzig (Germany). Diploma and PhD in Chemistry / Biochemistry, Technical University Darmstadt; Postdoc, Georgetown University, Lombardi Cancer Center, Washington DC, USA; Habilitation / Junior Research Group leader, Institute for Pharmacology and Toxicology, Philipps University Marburg; since 2011 in Leipzig. His research interests are in the (preclinical) development of novel therapeutic strategies based on small RNA molecules (siRNAs, miRNAs, anti-miRs) in oncology and other diseases. One major focus is on developing new polymer-based nanoparticles for in vivo use, including chemical modifications, combinations with lipids and embedding in sustained release systems. Nanoparticles are tested and utilized in various in vitro, ex vivo and in vivo models. To this end, different target genes (established and novel oncogenes) as well as tumor inhibitory miRNAs or the inhibition of oncogenic non-coding RNAs are explored.



## Gary BOWLIN

University of Memphis, UNITED STATES

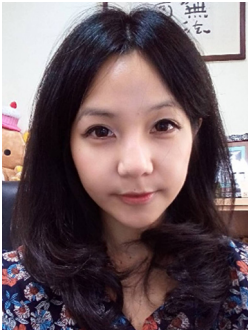
### K6

**Title: "Modular tissue engineering template constructs from fibrous branched clusters"**

**Tuesday, 17<sup>th</sup> July**

**10:15 - 10:45, Hall 1B**

Dr. Bowlin is a Professor and Herbert Herff Chair of Excellence at The University of Memphis in the Department of Biomedical Engineering. Dr. Bowlin's collaborative research focuses on the application of electrospun templates for tissue regenerative applications. Dr. Bowlin's laboratory has published extensively in these areas with over 130 peer-reviewed manuscripts. Google Scholar data shows his group's published works have been cited over 14,500 times (H-index of 51). Dr. Bowlin has been granted 13 U.S. Patents and over 30 foreign patents. These patents have helped to start five different companies and several commercially available and regulatory agency cleared products. One of the most recent technologies being developed by St. Teresa Medical, Inc. The latest company, Sweetbio, Inc., is Memphis based and commercializing novel guided tissue regeneration membranes for dental reconstruction procedures. He is a Fellow in the National Academy of Inventors and the Inaugural and current President of the International Society for Biomedical Polymers and Polymeric Biomaterials.



## Jiashing YU

National Taiwan University, TAIWAN

**K7**

**Title: "A 3D enzymatically crosslinked hydrogel promotes human adipose-derived stem cell spheroids proliferation and differentiation"**

**Tuesday, 17<sup>th</sup> July**

**15:45 - 16:15, Hall 1A**

Dr. Yu received her B.S. in Chemical Engineering in 2003 from National Taiwan University, Taiwan, R.O.C and Ph.D. in 2008 from UC Berkeley/UC San Francisco Joint Graduate Group in Bioengineering. Dr. Yu worked as a postdoctoral researcher at UCSF Medical School and Cardiovascular Research Institute from 2008-2010. She relocated back to her alma mater in 2010 and was an Assistant Professor from 2010-2015 and was promoted to Associate Professor from 2015 till now. Dr. Yu's group focuses on costumed-design of biomaterials including surface modification of biomaterials to enhance cell and extracellular matrix (ECM) interaction, antibody and peptides conjugated nanoparticles as biosensors and drug delivery vehicles for cancer therapy, cell encapsulation and 3D culture of hASCs (human adipose-derived stem cell) in alginate-based microspheres and various porous scaffold and hydrogel for stem cells differentiation.



## Ton LOONTJENS

University Groningen, NETHERLANDS

**K8**

**Title: "Contact-killing of gram positive and gram negative bacteria on silicone rubber sheets covered with a flexible immobilized hyperbranched coating"**

**Tuesday, 17<sup>th</sup> July**

**15:45 - 16:15, Hall 1B**

Ton Loontjens studied chemistry at the University of Nijmegen in the Netherlands. After his study (cum laude) he started working at DSM, an international chemical and biotechnology company, as research leader of the polypropylene polymerization group. After that he possessed a number of functions at DSM, such as researcher, principal scientist and head of several departments all in various areas of polymer chemistry. In 2005 he became in addition part-time professor in the area of biomedical polymers at the University of Groningen. His main interest is currently the development of antibacterial coatings for biomedical devices and implants in cooperation with several companies. Loontjens is co-author of 2 books, more than 80 publications and is (co)inventor of 70 patents.



## Silvia FARE

Politecnico di Milano, ITALY

**K9**

**Title: "Assessment of SIBS copolymer properties and suitability for biomedical applications"**

**Wednesday, 18<sup>th</sup> July**

**9:00 - 9:30, Hall 1A**

Silvia Farè (Ph.D) is Associate Professor in Industrial Bioengineering at Politecnico di Milano (IT), at the Department of Chemistry, Materials and Chemical Engineering "G. Natta". She obtained her PhD degree in Biomaterials at Politecnico di Milano on the in vitro study of oxidation mechanisms in polyurethanes. She performed a research stage at Laval University, Quebec, Canada. She is author of more than 80 publications in international peer-reviewed journals, 3 book chapters, more than 100 peer-reviewed conference abstracts and inventor of 3 patents on novel polymer formulation and silk fibroin structure for ligament replacement. She is involved in ESB council from 2017, editorial board member of the Journal of Applied Biomaterials and Functional Materials (Sage Journals). Her experience focuses on polymers and composites for biomedical applications, in particular for implantable devices, regenerative medicine and tissue engineering applications, 3D-printed bifunctional/smart polymeric in vitro models mimicking muscle-skeletal pathologies, advanced therapies.



## Sungho YANG

Korea National University of Education, REPUBLIC OF KOREA

**K10**

**Title: "Cytocompatible coating of individual living cells by atom transfer radical polymerization"**

**Wednesday, 18<sup>th</sup> July**

**9:00 - 9:30, Hall 1B**

Prof. Sung Ho Yang is an Associate Professor of Chemistry Education at Korea National University of Education (KNUE), Chungju, Republic of Korea. He obtained his Ph.D. from the Department of Chemistry in 2010 from Korea Advanced Institute of Science and Technology, Republic of Korea, under the supervision of Prof. Insung S. Choi. After postdoctoral work in Department of Bioengineering at University of California, Berkeley, he started his independent research career as a professor at KNUE since 2012. He started his research career with study on atom-transfer radical polymerization, biomimetic synthesis of inorganic materials, and Fabrication of Thin films. Since 2006, he applied biomimetic synthesis and of thin films fabrication to biological systems, leading to encapsulation of living cells with nanomaterials through chemical reactions on the interface of biological systems and aqueous medium. The concept of hard shell encapsulation promoted a new research field such as artificial spore and single cell biology. He is still working for encapsulation of mammalian cells and trying to expand the scope of cell-encapsulation.



## **Gianluca CIARDELLI**

*Politecnico di Torino, ITALY*

### **K11**

***Title: "Novel thermo-sensitive and photo-curable hydrogels as potential bioinks in regenerative medicine"***

***Wednesday, 18<sup>th</sup> July***

***12:00 - 12:30, Hall 1A***

Gianluca Ciardelli (Ph.D) has a Master Degree in Chemistry summa cum laude, from the University of Pisa (1994). In 1997 he received the PhD in Natural Sciences from the Swiss Federal Institute of Technology (ETH) of Zurich on synthetic degradable polyurethanes for biomedical applications. From 2002 and 2004 he was assistant professor at the University of Pisa at the Department of Chemical Engineering, Industrial Chemistry, Materials Science. In December 2004 he joined the Department of Mechanics at the Politecnico di Torino as associated professor. He became Full Professor in Biomedical Engineering in 2011. His research interests focus on polymeric and composite bio and nanomaterials design and technologies for implantable biomedical devices, tissue engineering, nanomedicine, advanced therapies. He has an h-index is 32 with around 4000 citations.

# Awards

## Best Oral/Poster/Rapid Fire Presentations

All candidates must be **students**, must have an accepted abstract as presenting author and should have indicated on the registration form their desire to be considered for these awards. The presentations will be assessed by the Conference Award Committee. Winners will be announced during the Closing Ceremony on **Wednesday, 18<sup>th</sup> July at 14:00**.

### Best Oral Presentations

First prize: **300€ + Certificate**  
Second prize: **250€ + Certificate**  
Third prize: **150€ + Certificate**

*Sponsored by:*



**ARBURG**

### Best Poster Presentations

First prize: **200€ + Certificate**  
Second prize: **150€ + Certificate**  
Third prize: **100€ + Certificate**

*Sponsored by:*



*polymers*  
an Open Access Journal by MDPI

### Best Rapid Fire Presentation

Prize: **100€ + Certificate**

*Sponsored by:*



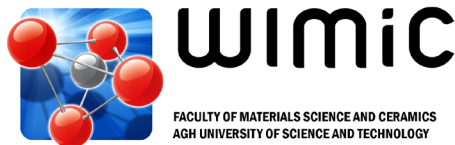
# Social Events

## Welcome Reception

Conference venue, AGH University of Science and Technology,  
Faculty of Materials Science and Ceramics (B-8 Building)  
al. Mickiewicza 30, 30-059 Krakow, Poland

Sunday, 15<sup>th</sup> July  
18:00 – 20:00

Kick off your ISBPPB 2018 journey at the appealing Welcome Reception! Say hello to your colleagues from all over the world and make new connections. Enjoy delicious food and drinks and get a first taste of famous Polish hospitality!



## Chairpersons Dinner *(by invitation only)*

'Szara Gęś' Restaurant,  
Main Market Square - Rynek Główny 17

Monday, 16<sup>th</sup> July  
19:00 - 21:00

To show our appreciation to all those who have helped us with the ISBPPB 2018 Conference organization. The Chairpersons Dinner will be hosted in the Szara Gęś Restaurant (The Grey Goose) situated in an iconic XIV century building in the Main Square. We hope that the splendid interiors of the Szara Gęś Restaurant and the historic character of the surrounding area and the building itself (Hetman House) combined with a modern Polish cuisine at its best will be a truly unique experience and a perfect way to say 'Thank you'.





# Gala Dinner

## The Zalesie Manor

Tuesday, 17<sup>th</sup> July

18:30 – as long as you wish

For the ISBPPB 2018 Conference Gala Dinner, we decided to invite all the participants to the astonishing Zalesie Manor.

This 200 years old complex is located 25 km away from Krakow’s Main Market Square on a hill with a beautiful, panoramic view of the Beskidy and Tatra Mountains. Its rural architecture buildings are surrounded by picturesque forests, fields, and meadows, creating perfect place for rustic-style celebration.

Come to experience Polish culture at its best. Be prepared for thrilling surprises.

We are certain that it will be an unforgettable evening!

PLEASE NOTE: Transport from the Conference Venue to the Zalesie Manor will be provided. The journey to the manor will take about 40 minutes. And most importantly, participation in the ISBPPB 2018 Conference Gala Dinner is already included in the conference fee.

**Please show your conference badge to board the bus.**





# DETAILED SCIENTIFIC PROGRAMME



# Programme at a Glance

	Sunday, 15th July	Monday, 16th July	
		Hall 1A	Hall 1B
7.00 - 8.00		07:30 Registration Opens	
8.00 - 9.00		8:30 Opening Ceremony	
9.00 - 10.00		PL1. Andreas Lendlein	
10.00 - 11.00		Coffee Break	
11.00 - 12.00		<b>K1. Chatzinikolaidou</b> 1. Thiré 2. Douglas 3. Liang 4. Gryń 5. Basu 6. Deszczynski 7. Uppstu	<b>K2. Fatimi</b> 8. Letourneur 9. Szczubialka 10. Azizova 11. Gonsior 12. Mzyk 13. Ahadpour 14. Pien
12.00 - 13.00		Lunch Poster session	
13.00 - 14.00			
14.00 - 15.00		PL2. Sandra van Vlierberghe	
15.00 - 16.00		Coffee Break	
16.00 - 17.00	Registration 16:00-20:00	<b>K3. Pegueroles</b> 15. Oktar 16. Gunduz 17. Włodarczyk-Biegun 18. Al-Taie 19. Kalkandelen 20. Moukbil 21. Sadaba	<b>K4. Kotarba</b> 22. Riool 23. Gajos 24. Civantos 25. Kavatzikidou 26. Kulikouskaya 27. Chattaway 28. Babaliari
17.00 - 18.00			
18.00 - 19.00	Welcome Reception <i>conference venue</i>		
19.00 - 20.00		Chairpersons Dinner <i>(by invitation only)</i>	
20.00 - 21.00			
21.00 - 22.00			



Tuesday, 17th July			Wednesday, 18th July							
Hall 1A	Hall 1B		Hall 1A	Hall 1B	Hall 2					
08:00 Registration Opens						7.00 - 8.00				
						8.00 - 9.00				
<b>PL3. Eben Alsberg</b>			<b>5A Biomedical polymers</b>	<b>K9. Fare</b>	<b>5B Cell encaps. and culture</b>	<b>K10. Yang S.</b>	<b>Rapid Fire Session</b>	9.00 - 10.00		
<b>Coffee Break</b>				57. Mauri		65. Yang Y.				
<b>3A Controlled deliv.</b>	<b>K5. Aigner</b>	<b>3B Wound healing</b>		<b>K6. Bowlin</b>		58. Mishra		66. Kroneková	67. Costa	10.00 - 11.00
	29. Paik			36. Younes		60. Lerf		68. Canal	69. Sotiropoulos	
	30. Darsey			37. Coentro		61. Puzska		70. Lu	71. Gering	
	31. Licea-Claverie			38. Contardi		62. Wach		72. Kim		
	32. Kronek		39. Mndlovu	63. Caba						
	33. Choi		40. Gupta	64. Akyol						
<b>Coffee Break</b>			<b>Coffee Break</b>			11.00 - 12.00				
<b>Lunch Poster session</b>			<b>6A Tissue eng.</b>	<b>K11. Ciardelli</b>	<b>6B Adv. manuf. 2</b>	79. Kandaswamy		12.00 - 13.00		
				73. Garcia-Fernández		80. Ochbaum		81. Domalik-Pyzik	13.00 - 14.00	
				74. Sobolewski		82. Lee		83. Oehmichen		
				75. Lyyra		84. Kim		85. Ozen		
				76. Dalgic		86. Hileuskaya				
				77. Metwally						
			78. Kraskouski							
			<b>14:00 Closing Ceremony</b>			14.00 - 15.00				
<b>PL4. Joachim Kohn</b>						15.00 - 16.00				
<b>Coffee Break</b>						16.00 - 17.00				
<b>4A Soft tissue eng.</b>	<b>K7. Yu</b>	<b>4B Smart materials</b>	<b>K8. Loontjens</b>	<b>Sessions:</b>  <b>1A</b> Bone tissue engineering <b>1B</b> Cardiovascular applications <b>2A</b> Advanced manufacturing 1 <b>2B</b> Surface modification <b>3A</b> Controlled delivery <b>3B</b> Wound healing <b>4A</b> Soft tissue engineering <b>4B</b> Smart materials <b>5A</b> Biomedical polymers <b>5B</b> Cell encapsulation and culture <b>6A</b> Tissue engineering <b>6B</b> Advanced manufacturing 2			17.00 - 18.00			
	43. El Fray		50. Scatto							
	44. Tavor Re em		51. Mielańczyk							
	45. Barros		52. Montanari							
	46. Wali		53. De Pieri							
	47. Pugliese		54. Son							
48. Becerril-Rodriguez	55. Zaborniak									
49. Ribeiro	56. Vukajlovic									
						18.00 - 19.00				
<b>Gala Dinner</b>						19.00 - 20.00				
<i>Zalesie Manor</i>						20.00 - 21.00				
						21.00 - 22.00				

# Oral presentations

Monday, 16<sup>th</sup> July

## PLENARY LECTURE 1

(Hall 1)

Session chairs: **Jan Chłopek, Gary Bowlin**

**09:00** **Andreas Lendlein** *The Helmholtz-Zentrum Geesthacht, Germany*  
*Implementing Multifunctionality in Polymeric Biomaterials for Medical Applications*

	<b>1A. BONE TISSUE ENGINEERING</b> (Hall 1A) Session chairs: <b>Gary Bowlin, Marek Kowalczyk</b>	<b>1B. CARDIOVASCULAR APPLICATIONS</b> (Hall 1B) Session chairs: <b>Marta Pegueroles, Jiashing Yu</b>
<b>10:15</b>	<b>K1. PLLA-based Copolymeric Biomaterials for Bone Tissue Engineering</b> Maria Kaliva, Anthie Georgopoulou, Costas Charitidis, <u>Maria Chatzinikolaidou</u> , Maria Vamvakaki	<b>K2. Chitosan-based Embolizing Hydrogel for Endovascular Therapies Characterization of Rheological and Occlusive Properties</b> <u>Ahmed Fatimi</u> , Fatemah Zehtabi, Sophie Lerouge
<b>10:45</b>	<b>1. In Vitro and In Vivo Evaluation of 3D-Printed PLA Scaffolds Coated with Biomimetic Apatite for Applications in Bone Tissue Engineering</b> Marianna Maia-Pinto, Leonardo Boldrini, Mônica Calasans-Maia, <u>Rossana Thiré</u>	<b>8. Polysaccharides for Target-Specific Imaging and Treatment of Atherothrombosis. From the Polymer Design to the Clinical Trial</b> <u>Didier Letourneur</u>
<b>11:00</b>	<b>2. Enzymatic Mineralization of Novel Whey-protein Isolate Hydrogels for Bone Regeneration</b> Anna Tryba, Magdalena Kocot, Julia Keppler, Elzbieta Pamula, <u>Timothy Douglas</u>	<b>9. Anticoagulative Activity of Aionic Block Polymers Structural and Mechanistic Considerations</b> Bartłomiej Kałaska, Kamil Kamiński, Joanna Mikłosz, Shin-Ichi Yusa, Emilia Sokołowska, Agnieszka Błażejczyk, Joanna Wietrzyk, Dariusz Pawlak, Maria Nowakowska, Andrzej Mogielnicki, <u>Krzysztof Szczubiałka</u>

11:15	<p><b>3. A Long-Lasting UV-cured Vinylbenzylated Atelocollagen Membrane for Guided Bone Regeneration</b></p> <p><u>He Liang</u>, Stephen Russell, David Wood, Giuseppe Tronci</p>	<p><b>10. Modification of PVC and PU with Cu and Se Species for NO Generation Purpose</b></p> <p><u>Liana Azizova</u>, Lyuba Mikhalovska, Sergey Mikhalovsky</p>
11:30	<p><b>4. PLA/TCP Nanocomposite Locking Bolt for Intramedullary Locking Nail System</b></p> <p><u>Karol Gryń</u>, Barbara Szaraniec, Jan Chłopek, Jarosław Michał Deszczyński, Jarosław Deszczyński</p>	<p><b>11. Biocompatible Polyurethane-Titanium Composite Utilisation in the Innovative Flexible Valve Designed for Pulsatile Ventricular Assist Devices</b></p> <p><u>Małgorzata Gonsior</u>, Artur Kapis, Przemysław Kurtyka, Roman Kustosz, Roman Major, Juergen Lackner, Mirosława El Fray, Andrzej Misztela</p>
11:45	<p><b>5. Inorganic Calcium Filled Bacterial Cellulose Based Hydrogel Scaffold: A Novel Three Dimensional Biomaterial for Bone Tissue Regeneration</b></p> <p><u>Probal Basu</u>, Nabanita Saha, Petr Saha</p>	<p><b>12. Cellular Response to Blow-Spun Scaffolds Modified by Polyelectrolyte Multilayer Films</b></p> <p><u>Aldona Mzyk</u>, Michal Wojasinski, Piotr Natkanski, Aleksandra Drewienkiewicz</p>
12:00	<p><b>6. Novel Intramedullary Nailing for Humerus Shaft Fractures</b></p> <p><u>Jaroslaw Michal Deszczynski</u>, Jaroslaw Deszczynski, Barbara Szaraniec, Karol Gryń, Jan Chłopek</p>	<p><b>13. Injectable Chitosan/Carrageenan/PNIPAM Hydrogel Designed with Au Nanoparticles Towards Conductive Scaffolds for Tissue Engineering Demands</b></p> <p>Mohadeseh Doroudian, <u>Amirkhashayar Ahadpour</u>, Ali Pourjavadi, Shahram Azari</p>
12:15	<p><b>7. Enhancing the Induced Membrane Technique for the Regeneration of Bone Defects</b></p> <p>Robert Björkenheim, Gustav Strömberg, Laura Aalto-Setälä, <u>Peter Uppstu</u>, Mari Ainola, Jukka Pajarinen, Leena Hupa, Nina Lindfors</p>	<p><b>14. Photo-crosslinkable Collagen-based Precursors for Vascular Tissue Engineering</b></p> <p><u>Nele Pien</u>, Daniele Pezzoli, Dimitria Camasao, Fabrice Bray, Christian Rolando, Madalina Albu, Diego Mantovani, Sandra Van Vlierberghe, Peter Dubruel</p>

## PLENARY LECTURE 2

(Hall 1)

Session chairs: **Elżbieta Pamuła, Munmaya Mishra**

**14:30** **Sandra van Vlierberghe** *Ghent University, Belgium*  
*Crosslinkable Hydrogels Tailored Towards Processing and Biomedical Needs*

	2A. ADVANCED MANUFACTURING 1 (Hall 1A) Session chairs: <b>Sandra van Vlierberghe, Elżbieta Pamuła</b>	2B. SURFACE MODIFICATION (Hall 1B) Session chairs: <b>Munmaya Mishra, Ton Loontjens</b>
<b>15:45</b>	<b>K3. <i>Controlled Drug Delivery from 3D Printed Poly-L-Lactic Acid Bioresorbable Stent</i></b> Mathilde Fiorletta, Cristina Canal, <u>Marta Pegueroles</u>	<b>K4. <i>Tailoring of Implant-Tissue Interface: PLGA-parylene C Multifunctional Coating</i></b> Monika Golda-Cepa, Aleksandra Chorylek, Paulina Chytrosz, Monika Brzychczy-Wloch, Minna Hakkarainen, Klas Engvall, <u>Andrzej Kotarba</u>
<b>16:15</b>	<b>15. <i>Polycaprolactone/Beta Tricalcium Phosphate/ Collagen as a 3D Printed Tissue Scaffold</i></b> Mehmet Aydogdu, Nazmi Ekren, <u>Faik Oktar</u> , Osman Kilic, Oguzhan Gunduz	<b>22. <i>Antimicrobial Supramolecular UPy-Based Biomaterials</i></b> Sabrina Zaccaria, Ronald van Gaal, <u>Martijn Riool</u> , Moniek Schmitz, Sebastian Zaat, Patricia Dankers
<b>16:30</b>	<b>16. <i>Electrohydrodynamic EHD Bioprinting of Bacterial Cellulose/Polycaprolactone Scaffolds</i></b> Esra Altun, Nazmi Ekren, Osman Kiliç, <u>Oguzhan Gunduz</u>	<b>23. <i>Silicon Biosensors Examined with Surface Techniques Molecular Arrangement and Composition Antibody Orientation and Binding Stoichiometry</i></b> <u>Katarzyna Gajos</u> , Andrzej Budkowski, Panagiota Petrou, Varvara Pagkali, Ioannis Raptis, Kamil Awsiuk, Jakub Rysz, Sotirios Kakabakos
<b>16:45</b>	<b>17. <i>3D Bioprinting of Medical Adhesives</i></b> <u>Malgorzata Wlodarczyk-Biegun</u> , Julieta Paez, Jun Feng, Maria Villiou, Aranzazu del Campo	<b>24. <i>High-fidelity Control of Nanostructured Poly(ether-ether ketone). Surfaces by Directed Irradiation Synthesis Towards a Tunable Osseointegration</i></b> <u>Ana Civantos</u> , Zak Koyn, Jean Paul Allain

17:00	<p><b>18.</b> <i>3D Printed Polyvinyl Alcohol Sampling Filters for the Entrapment of Exhaled Microorganisms</i></p> <p><u>Alaa Al-Taie</u>, Xiaoxiao Han, Caroline Williams, Mohamad Abdulwhhab, Andrew Abbott, Alex Goddard, Malgorzata Wegrzyn, Natalie Garton, Michael Barer, Jingzhe Pan</p>	<p><b>25.</b> <i>Effect of Topography and Chemical Cues of Biodegradable Polymeric Microstructured Replicas on Cellular Alignment and Proliferation</i></p> <p><u>Paraskevi Kavatzikidou</u>, Despina Angelaki, Lefki Chaniotaki, Eleftheria Babaliari, Anthi Ranella, Emmanuel Stratakis</p>
17:15	<p><b>19.</b> <i>Bioactive Scaffolds of 3D Bioprinted Gelatin/Alginate and Gelatine/Alginate/Tri-calcium Phosphate Composites as a Potential Biomaterial for Bone Tissue Engineering</i></p> <p>Burak Ozbek, Osman Kilic, Nazmi Ekren, Faik Nuzhet Oktar, <u>Cevriye Kalkandelen</u>, Mahir Mahirogullari, Oguzhan Gunduz</p>	<p><b>26.</b> <i>Formation and Physico-chemical Properties of Chitosan and Polyethyleneimine Containing LbL Films</i></p> <p><u>Viktoryia Kulikouskaya</u>, Kseniya Hileuskaya, Aliaksandr Kraskouski, Tsimafei Zhdanko, Vladimir Agabekov</p>
17:30	<p><b>20.</b> <i>3D Printing Bioactive Composite Scaffolds for Bone Tissue Engineering</i></p> <p><u>Yunis Moukbil</u>, Busra Isindag, Velican Gayir, Burak Ozbek, Ebru Toksoy Oner, Faik Oktar, Mehmet Eroglu, Oguzhan Gunduz</p>	<p><b>27.</b> <i>Nanostructured and Bifunctional Surfaces for Biomedical Applications</i></p> <p><u>Claire Chattaway</u>, Sabrina Belbekhouche, Filip E. Du Prez, Sophie Demoustier-Champagne, Karine Glinel</p>
17:45	<p><b>21.</b> <i>Bioresorbable, Radiopaque and 3D Printable Scaffolds for Bone Tissue</i></p> <p><u>Naroa Sadaba</u>, Jone Muñoz, Jose-Ramon Sarasua, Ester Zuza</p>	<p><b>28.</b> <i>Cellular Responses Under Static and Dynamic Conditions of Polymeric Micropatterned Substrates Fabricated via Ultrafast Laser Direct Writing</i></p> <p><u>Eleftheria Babaliari</u>, Paraskevi Kavatzikidou, Anna Mitraki, Anthi Ranella, Emmanuel Stratakis</p>



# Tuesday, 17<sup>th</sup> July

## PLENARY LECTURE 3

(Hall 1)

Session chairs: **Joachim Kohn, Jan Chłopek**

**09:00** **Eben Alsberg** *Case Western Reserve University, USA*  
*Controlled Spatiotemporal Signal Presentation within High-Density Cell Culture Systems for Engineering Complex Tissues*

### 3A. CONTROLLED DELIVERY

(Hall 1A)

Session chairs:

**Bożena Michniak, Didier Letourneur**

### 3B. WOUND HEALING

(Hall 1B)

Session chairs:

**Joelle Amedee, Mirosława El Fray**

**10:15** **K5. Microparticulate Poly Vinyl Alcohol Hydrogel Formulations for Embedding and Controlled Release of Polyethyleimine PEI-based Nanoparticles**  
 Jan Schulze, Stephan Hendrikx, Michaela Schulz-Siegmund, Achim Aigner

**K6. Modular Tissue Engineering Template Constructs from Fibrous Branched Clusters**  
 Benjamin Minden-Birkenmaier, Gary Bowlin

**10:45** **29. New Hollow Core-Shell Nanocapsules Facilitate Sustained Release of Immunomodulatory Drugs and Exhibit Adjuvant Properties**  
 Anil Yamala, Vinod Nadella, Yitzhak Mastai, Hridayesh Prakash, Pradip Paik

**36. Amoxicillin-loaded Poly( $\epsilon$ -caprolactone)/Poly (ethylene glycol) Biodegradable Electrospun Nanofibrous Mats for Wound Healing**  
Husam Younes, Sandi Ali-Adib, Shijimol Ma

**11:00** **30. DFT Modelling Studies of the LRRK2 Protein for Developing New Drug Treatments for Parkinson's Disease**  
Jerry Darsey, Hetvi Shah

**37. Multi-Compartment Collagen Devices as Modulators of Skin Fibrosis Through Controlled Synergistic Dual Delivery of Anti-fibrotics**  
João Coentro, Dimitrios I. Zeugolis

**11:15** **31. PEGylated Cationic/Anionic Nanogels with Gold Nanoparticles for Controlled Release of Anticancer Drugs**  
Angel Licea-Claverie, Ivan Zapata-Gonzalez, Lizbeth Manzanares-Guevara, Alejandra Gonzalez-Urias, Irasema Oroz-Parra, Alexei Licea-Navarro

**38. Polyvinylpyrrolidone/Ciprofloxacin-Based Transparent Films and Electrospun Nanofibers as Potential Wound Care Dressings**  
Marco Contardi, José A. Heredia-Guerrero, Giovanni Perotto, Paola Valentini, Pier Paolo Pompa, Raffaele Spanò, Luca Goldoni, Rosalia Bertorelli, Athanassia Athanassiou, Ilker S. Bayer

<p><b>11:30</b></p>	<p><b>32.</b> <i>Curcumin Loaded 2-Ethyl-2-Oxazoline-grad-2- 4-Dodecyloxyphenyl -2-Oxazoline Copolymer Nanoparticles with Excellent Chemical Stability and Bioavailability</i> Shubhashis Datta, Annamaria Jutková, Petra Šrámková, Lenka Lenkavská, Veronika Huntošová, Nadežda Petrenčíková, Dušan Chorvát, Pavol Miškovský, Daniel Jancura, <a href="#">Juraj Kronek</a></p>	<p><b>39.</b> <i>Partially-crosslinked Co-complexed Biomaterial Platforms for Potential Wound Healing Applications</i> <a href="#">Hillary Mndlovu</a>, Pradeep Kumar, Thashree Marimuthu, Lisa du Toit, Yahya Choonara, Viness Pillay</p>
<p><b>11:45</b></p>	<p><b>33.</b> <i>Dual Intracellular Targeting Nanosized Anticancer Drug Carriers with Intracellular Glutathione Responsiveness and Mitochondrial Targeting Activity</i> <a href="#">Yeon Su Choi</a>, Han Chang Kang</p>	<p><b>40.</b> <i>Biosynthetic Cellulose based Hydrogels of Curcumin Encapsulated in Cyclodextrins as Wound Dressings</i> <a href="#">Abhishek Gupta</a>, Marek Kowalczuk, Claire Martin, Iza Radecka</p>
<p><b>12:00</b></p>	<p><b>34.</b> <i>Controlled release of Metformin Hydrochloride from Core-Shell Nanofibers with Fish Sarcoplasmic Protein</i> Sena Su, <a href="#">Nalan Sumeyra Korkmaz</a>, <a href="#">Ulku Gul Guven</a>, Mehmet Sayip Eroglu, Nazmi Ekren, Osman Kilic, Faik Nuzhet Oktar, Oguzhan Gunduz</p>	<p><b>41.</b> <i>Modification of Alginate Based-Hydrogel for Therapeutical Applications Using Cold Atmospheric Plasma</i> <a href="#">Inès Hamouda</a>, Cédric Labay, Maria Pau Ginebra, Cristina Canal</p>
<p><b>12:15</b></p>	<p><b>35.</b> <i>Emulsion Technology for the Development of Bio-based Materials for Controlled Drug Delivery Applications</i> <a href="#">Chiara Setti</a>, Giulia Suarato, Athanassia Athanassiou, Ilker S. Bayer</p>	<p><b>42.</b> <i>Monitoring of Matrix Remodeling during Living Cell Culture by Microrheological Measurements</i> <a href="#">Johanna Roether</a>, Claude Oelschlaeger, Norbert Willenbacher</p>



## PLENARY LECTURE 4

(Hall 1)

Session chairs: **Eben Alsberg, Andrzej Kotarba**

**14:30** **Joachim Kohn** *The New Jersey Center for Biomaterials, USA*  
*Understanding the Effect of Biomaterials on Cell and Stem-Cell Differentiation*

### 4A. SOFT TISSUE ENGINEERING

(Hall 1A)

Session chairs:

**Veronique Larreta-Garde, Jerry Darsey**

### 4B. SMART MATERIALS

(Hall 1B)

Session chairs:

**Achim Aigner, Krzysztof Szczubiałka**

**15:45** **K7. A 3D Enzymatically Crosslinked Hydrogel Promotes Human Adipose-Derived Stem Cell Spheroids Proliferation and Differentiation**

Ching-Cheng Tsai, Nai-Chen Cheng,  
Jiashing Yu

**K8: Contact-killing of Gram Positive and Gram Negative Bacteria on Silicone Rubber Sheets Covered with a Flexible Immobilized Hyperbranched Coating**

Ton Loontjens, Jia Jia Dong, Agnieszka Muszanska, Betsy van der Belt-Gritter, Henk Busscher, Henny van der Mei

**16:15** **43. Photocurable Polymer Materials for Innovative Hernia Repair**  
Mirosława El Fray

**50. Melt Compounded Polymer Nanocomposite for the Production of 3D Printing Scaffold in Regenerative Medicine**  
Marco Scatto, Maria Bastianini, Michele Sisani, Paolo Scopece, Maria Camara Torres, Ravi Sinha, Ainhoa Egizabal Luzuriaga, Carlos Mota, Alessandro Patelli, Lorenzo Moroni

**16:30** **44. Construction of a Three Dimensional in Vitro Embryo Implantation Model Using Alginate Macroporous Scaffold**  
Dganit Stern, Reuven Reich,  
Tali Tavor Re em

**51. Stimuli Responsive Homoarm and Miktoarm Stars - The Influence of Composition on Phase Transition and Morphology**  
Anna Mielańczyk, Maria Kupczak, Małgorzata Burek, Łukasz Mielańczyk, Olesya Klymenko, Ilona Wandzik, Dorota Neugebauer

**16:45** **45. Engineered Substrates with Site-Specific Immobilized Laminin for Neural Stem Cells**  
Daniela Barros, Paula Parreira, Joana Furtado, Frederico Ferreira-da-Silva, Andrés J. García, M. Cristina L. Martins, Isabel Freitas Amaral, Ana Paula Pêgo

**52. Hyaluronan-Based Nanogels as Trojan Horse: Chasing Intracellular Pathogens**  
Elita Montanari, Chiara Di Meo, Tommasina Coviello, Patrizia Mancini, Luciana Mosca, Pietro Matricardi

Tuesday, 17<sup>th</sup> July

17:00	<p><b>46.</b> <i>Electrospinning of Non-Ionic Cellulose Ether Nanofibers with Silver Nanoparticles Having Antibacterial Activity</i></p> <p><u>Ashwini Wali</u>, Manohar Inamdar, Satish Badiger</p>	<p><b>53.</b> <i>Anisotropic Thermoresponsive Nanofibers for Engineering Extracellular Matrix-Rich Living Substitutes</i></p> <p><u>Andrea De Pieri</u>, Alexander Gorelv, Yuri Rochev, Dimitrios Zeugolis</p>
17:15	<p><b>47.</b> <i>Collagen-Based Devices as Multi Cargo Delivery Vehicles for Tendon Treatments</i></p> <p><u>Eugenia Pugliese</u>, Yves Bayon, Dimitrios Zeugolis</p>	<p><b>54.</b> <i>UV Vis- Reactive Natural Polymer Derivatives and Stabilization of Protein Drugs</i></p> <p><u>Tae Il Son</u>, Shin-Woong Kim, Jae-Won Kim, Seung-Hyun Noh, Yoshihiro Ito</p>
17:30	<p><b>48.</b> <i>Design of a Novel Microfeatured Poly Glycerol Sebacate Methacrylate PGSM Scaffolds for Corneal Regeneration</i></p> <p><u>Iris Becerril-Rodriguez</u>, Sheila MacNeil, Frederik Claeysens</p>	<p><b>55.</b> <i>Synthesis of Naturally-Derived Star-Shaped Polymers Through ATRP Methods with Diminished Catalyst Concentration</i></p> <p><u>Izabela Zaborniak</u>, Paweł Chmielarz</p>
17:45	<p><b>49.</b> <i>Design and Characterization of Synthetic Biodegradable Films for Tendon Tissue Engineering</i></p> <p><u>Sofia Ribeiro</u>, Vit Novacek, Emanuel M. Fernandes, Manuela E. Gomes, Rui L. Reis, Yves Bayon, Dimitrios I. Zeugolis</p>	<p><b>56.</b> <i>Fluorescence Mechanical and Swelling Properties of Chitosan-Genipin and Chitosan-Genipin-PVP Hydrogels</i></p> <p><u>Durda Vukajlovic</u>, Oana Bretcanu, Julie Parker, Katarina Novakovic</p>

## Wednesday, 18<sup>th</sup> July

	5A. BIOMEDICAL POLYMERS (Hall 1A) Session chairs: <b>Maria Chatzinikolaïdou, Oguzhan Gunduz</b>	5B. CELL ENCAPSULATION AND CULTURE (Hall 1B) Session chairs: <b>Ewa Zuba-Surma, Gianluca Ciardelli</b>	RAPID FIRE SESSION (Hall 2)
<b>09:00</b>	<p><b>K9. <i>Assessment of SIBS Copolymer Properties and Suitability for Biomedical Applications</i></b></p> <p>Serena Bertoldi, Nicola Contessi Negrini, Manuele Lofaro, Maria Cristina Tanzi, <u>Silvia Fare</u></p>	<p><b>K10. <i>Cytocompatible Coating of Individual Living Cells by Atom Transfer Radical Polymerization</i></b></p> <p><u>Sung Ho Yang</u></p>	<b>RAPID FIRE PRESENTATIONS</b> (see page 42 for details)
<b>09:30</b>	<p><b>57. <i>RGD-Functionalized Hydrogels to Deliver Factors Secreted by Human Mesenchymal Stem Cells in Spinal Cord Injury</i></b></p> <p><u>Emanuele Mauri</u>, Pietro Veglianesi, Monica Sani, Alessandro Sacchetti, Filippo Rossi</p>	<p><b>65. <i>Enhancing Pseudoislet Biofunctionality using Microparticle Technology</i></b></p> <p>Ajile Elttayef, Catriona Kelly, <u>Ying Yang</u></p>	
<b>09:45</b>	<p><b>58. <i>Polymer Assisted Housing of Actives for Designed Release</i></b></p> <p><u>Munmaya Mishra</u></p>	<p><b>66. <i>Unraveling the Structural Changes of Alginate-Based Microspheres In Vitro and In Vivo Using Confocal Raman Microscopy</i></b></p> <p><u>Zuzana Kronekova</u>, Michal Pelach, Petra Mazancová, Lucia Uhelská, Lucia Kleščíková, Dušana Treľová, Filip Rázga, Veronika Némethová, Eva Majková, Peter Šiffalovič, Vladimír Raus, Dušan Chorvát, James J. McGarrigle, Mustafa Omami, Douglas Isa, Sofia Ghani, José Oberholzer, Igor Lacík</p>	
<b>10:00</b>	<p><b>59. <i>Unravelling Mechanical Properties of Biopolymer Films by Means of Force Spectroscopy</i></b></p> <p><u>Jagoba Iturri</u>, Maria Sumarokova, Andreas Weber, José Luis Toca-Herrera</p>	<p><b>67. <i>Targeting Cellular Organelles with Therapeutic Fluorescent Nanoparticles</i></b></p> <p><u>Diana Costa</u>, João Queiroz, Carla Cruz</p>	

10:15	<p><b>60.</b> <i>How a Minute Addition of a Vitamin Can Enhance Polyethylene for Young and Active Patients</i> Daniel Delfosse, <a href="#">Reto Lerf</a>, Peter Muenger</p>	<p><b>68.</b> <i>Cold Atmospheric Plasma Generation and Quantification of Reactive Oxygen and Nitrogen Species in Biocompatible Hydrogels</i> Cédric Labay, Ines Hamouda, Maria-Pau Ginebra, <a href="#">Cristina Canal</a></p>
10:30	<p><b>61.</b> <i>New Thermoplastic Polyurethane Elastomers for Biomedical Applications Synthesis and Characterization</i> <a href="#">Andrzej Puszka</a>, Magdalena Rogulska, Pavel Yakushev, Vladimir Bershtein</p>	<p><b>69.</b> <i>Identification of Hematopoietic Stem Cells Microparticles from Cord Blood transplants</i> <a href="#">Damianos Sotiropoulos</a>, Angeliki Xagorari, Marina Geroussi, Antonia Sioga, Dimitris Bougiouklis, Anagnostis Argiriou, Achilles Anagnostopoulos</p>
10:45	<p><b>62.</b> <i>Selection of the Sterilization Method for an Implantable Device for Therapeutics Delivery</i> <a href="#">Radoslaw Wach</a>, Alicja Olejnik, Agnieszka Adamus-Wlodarczyk</p>	<p><b>70.</b> <i>Synthesis and Self-Assembly of Amphiphilic Block Copolymers from Bio-based Hydroxypropyl Methyl Cellulose and Poly L-lactide</i> <a href="#">Aijing Lu</a>, Suming Li</p>
11:00	<p><b>63.</b> <i>A Green and Simple Process to Develop Conductive Polyurethane Foams for Biomedical Applications</i> <a href="#">Valentina Caba</a>, Laura Borgese, Silvia Agnelli, Laura E. Depero</p>	<p><b>71.</b> <i>Avidin-functionalized Gellan Gum as Modular Hydrogel for 3D Cell Culture</i> <a href="#">Christine Gering</a>, Janne Koivisto, Jenny Parraga, Jenni Leppiniemi, Vesa Hytönen, Minna Kellomäki</p>
11:15	<p><b>64.</b> <i>In vitro and In vivo Biodegradability of Soybean Oil and Polylactic Acid PLA Blended Films</i> <a href="#">Elvan Akyol</a>, R. Seda Tigli Aydın, Baki Hazer</p>	<p><b>72.</b> <i>3D Cell-Laden Collagen Villi Model for Mimicking Intestinal Villus Epithelium and Capillary</i> <a href="#">WonJin Kim</a>, Minseong Kim, Gi Hoon Yang, JaeYoon Lee, Miji Yeo, YoungWon Koo, JiUn Lee, HaeRi Kim, GeunHyung Kim</p>

**RAPID FIRE PRESENTATIONS**  
(see page 42 for details)

Wednesday, 18<sup>th</sup> July

	<p style="text-align: center;"><b>6A. TISSUE ENGINEERING</b> (Hall 1A) Session chairs: <b>Sungho Yang, Timothy Douglas</b></p>	<p style="text-align: center;"><b>6B. ADVANCED MANUFACTURING 2</b> (Hall 1B) Session chairs: <b>Silvia Fare, Ahmed Fatimi</b></p>
12:00	<p><b>K11. Novel Thermo-sensitive and Photocurable Hydrogels as Potential Bioinks in Regenerative Medicine</b></p> <p>Stefano Calzone, Monica Boffito, Deepak Choudhury, Arianna Grivet-Brancot, Prabhu Pannirselvam, May Win Naing, <u>Gianluca Ciardelli</u></p>	<p><b>79. Melt Processing and Characterization of Tricalcium Phosphate Filled Poly(butylene adipate-co-terephthalate)/Poly(methyl methacrylate) Composites for Biomedical Applications</b></p> <p><u>Ravichandran Kandaswamy</u>, Girija Bheemaneni</p>
12:15		<p><b>80. Tuning the Mechanical Properties of Alginate-Peptide Hydrogels</b></p> <p><u>Guy Ochbaum</u>, Ronit Bitton</p>
12:30	<p><b>73. Development of Novel Injectable Hydrogels for Osteochondral Regeneration</b></p> <p><u>Luis García-Fernández</u>, Marta Olmeda-Lozano, Blanca Vázquez-Lasa, Julio San Román</p>	<p><b>81. Double-Layered Polymer Scaffolds Fabricated by Combination of Electrospinning and Thermally Induced Phase Separation</b></p> <p><u>Patrycja Domalik-Pyzik</u>, Anna Morawska-Chochół, Jan Chlopek</p>
12:45	<p><b>74. Wet Electrospinning and In Situ Biofunctionalization of Degradable Multiblock Copolyester</b></p> <p><u>Peter Sobolewski</u>, Julia Buwała, Karolina Stępień, Rahul Sahay, Mirosława El Fray</p>	<p><b>82. Development of Cryopreserved Cell-laden Scaffold Using a Cell Printing System Supplemented with Low-temperature Processing Method</b></p> <p><u>JaeYoon Lee</u>, Minseong Kim, Gi Hoon Yang, Miji Yeo, WonJin Kim, JiUn Lee, YoungWon Koo, Hae Ri Kim, YoungEun Choe, GeunHyung Kim</p>
13:00	<p><b>75. Mechanical and In Vitro Properties of PLA/Bioactive Glass Composites</b></p> <p><u>Inari Lyyra</u>, Katri Leino, Terttu Hukka, Minna Kellomäki, Jonathan Massera</p>	<p><b>83. Plasma Modification of PCL Fiber Mats and the Possibility of a Graded Functionalization</b></p> <p><u>Sarah Oehmichen</u>, Anna Lena Hoheisel, Steffen Sydow, Nadeschda Schmidt, Birgit Glasmacher, Peter Behrens, Henning Menzel</p>





13:15	<p><b>76. PHBV Based Bone Tissue Engineering Scaffolds Doped with Diatom Shells</b>  <u>Ali Deniz Dalgic</u>, Deniz Atila, Ayten Karatas, Aysen Tezcaner, Dilek Keskin</p>	<p><b>84. Fabrication of Fibrous 3D Collagen Scaffold Mimicking Extracellular Matrix</b>  <u>Minseong Kim</u>, Gi Hoon Yang, JaeYoon Lee, Miji Yeo, WonJin Kim, YoungWon Koo, JiUn Lee, HaeRi Kim, YoungEun Choe, GeunHyung Kim</p>
13:30	<p><b>77. PCL Fibers Porosity Impact on Cells Attachment and Proliferation for Tissue Engineering</b>  <u>Sara Metwally</u>, Joanna Karbowniczek, Adam Gruszczynski, Piotr K. Szewczyk, Urszula Stachewicz</p>	<p><b>85. Production of the GO-doped PLA-Based Nanofibers and Investigation of Their Electrical Properties</b>  <u>Sertan Ozen</u>, Mehmet Aydogdu, Zeynep Ege, Sumeyye Cesur, Umit Terzi, Hayriye Korkmaz, Nazmi Ekren, Faik Oktar, Osman Kilic, Beyhan Kilic, Oguzhan Gunduz</p>
13:45	<p><b>78. Formation of 3D Porous Scaffolds Based on Pectins for Tissue Engineering</b>  <u>Aliaksandr Kraskouski</u>, Alexandr Zhura, Kseniya Hileuskaya, Viktoryia Kulikouskaya, Stanislau Tratyak, Vladimir Agabekov</p>	<p><b>86. Fabrication and Antibacterial Activity of Films Based on Pectin-Ag Nanocomposites</b>  <u>Kseniya Hileuskaya</u>, Aliaksandr Kraskouski, Alena Ladutska, Galina Novik, Vladimir Agabekov</p>

# Rapid Fire and Poster Presentations

Wednesday, 18<sup>th</sup> July, 9:00-11.30

(Rapid Fire Session - Hall 2)

Session chairs: **Patrycja Domalik-Pyzik, Timothy Douglas, Karol Gryń**

87.	<i>Alginate of Azotobacter Origin</i> <u>Elizaveta Akoulina</u> , Andrej Dudun, Anton Bonartsev, Vera Voinova, Garina Bonartseva
88.	<i>Fabrication and Characterization of PLA/SA/HA Composite Nanofiber by Electrospinning for Bone Tissue Engineering Applications</i> <u>Sumeyye Cesur</u> , Nazmi Ekren, Osman Kilic, Faik Oktar, Dilek Bilgic Akkaya, Serap Ayaz Seyhan, Zeynep Ruya Ege, Oguzhan Gunduz
89.	<i>Sonochemical synthesis of nanoparticles of bioactive molecules for their direct embedding into polymeric surfaces</i> <u>Paulina Chytrosz</u> , Monika Golda-Cepa, Andrzej Kotarba
90.	<i>The New Inorganic/Organic Bone Cement Based on Si Doped Alpha TCP</i> <u>Ewelina Cichoń</u> , Aneta Zima, Joanna Czechowska, Anna Ślósarczyk
91.	<i>Electrospun Multilayer Nanofiber Based Intelligent Drug Delivery and Release System</i> <u>Zeynep Ruya Ege</u> , Faik Nuzhet Oktar, Aydin Akan, Durdane Serap Kuruca, Betul Karademir, Gokce Erdemir, Sumeyye Cesur, Oguzhan Gunduz
92.	<i>Melt Compounded Biocompatible Thermoplastic Polyurethane TPU for the Engineering of 3D Printed Aortic Heart Valve Ring Design Fabrication Testing and Simulation</i> <u>Emanuele Gasparotti</u> , Emanuele Vignali, Giorgio Soldani, Paola Losi, Marco Scatto, Simona Celi
93.	<i>Comparison of PCL, PLC70:30, PLC85:15, PLG82:18 as a Matrix for Biodegradable X-rays Visible Composites</i> <u>Żaneta Górecka</u> , Emilia Choinska, Wojciech Świąszkowski
94.	<i>Multiphase Hydrogel System Modified with Graphene Oxide and Hydroxyapatite for Cartilage Tissue Engineering - Preliminary Study</i> <u>Martyna Hunger</u> , Patrycja Domalik-Pyzik, Jan Chłopek
95.	<i>Biopolymers for Advanced Medical Applications Based on Polyhydroxyalkanoates PHAs Derived from Polyolefin Waste Materials</i> <u>Brian Johnston</u> , David Hill, Marek Kowalczyk, Iwona Kwiecień, Jennifer Gonzalez Ausejo, Iza Radecka
96.	<i>Nitric Oxide-Generating Bioreducible Polymeric Nanoparticles for Site-Specific Vasodilation in Tumour Tissue</i> <u>Hyewon Ko</u> , Jae Hyung Park



97.	<i>Chitosan-Matrix Hydrogels Modified with Graphene Additives - Variations in Physicochemical Properties</i> <u>Karolina Kosowska</u> , Patrycja Domalik-Pyzik, Jan Chłopek
98.	<i>A Study on the Degradation Properties of Pectin/Chitosan Scaffold</i> <u>Maryna Lazouskaya</u> , Viktoriya Kulikouskaya, Vladimir Agabekov
99.	<i>Moldable Hyaluronic Acid Hydrogel Based on Dynamic Chemistry as Skin Regenerative Material</i> <u>Liyang Shi</u> , Yannan Zhao, Jöns Hilborn, Jianwu Dai, Dmitri Ossipov
100.	<i>Preparation and Characterization of Polyurethane-based Multifunctional Bone Cements</i> <u>Klaudia Ordon</u> , Kinga Pielichowska
101.	<i>Design of Poly <math>\epsilon</math>-Caprolactone /Zein Blends for Delivery of Essential Oils as Antimicrobial Biomaterials</i> <u>Binh Thi Thanh Phan</u> , Christopher Lovell, Wolfgang H. Goldmann, Aldo R. Boccaccini
102.	<i>The Influence of the Solvent Type on the Structure of Thermosensitive Chitosan Hydrogels Containing Graphene Oxide</i> <u>Katarzyna Pieklarz</u> , Michał Tylman, Zofia Modrzejewska
103.	<i>Tumour Microenvironment-Recognizable Polymeric Conjugate for Cancer Immunotherapy</i> <u>Jung Min Shin</u> , Seok Ho Song, Jae Hyung Park
104.	<i>Synthesis and Characterization of Drug Loaded PVA/<math>\beta</math>- Tri Calcium Phosphate Powders for Bone Engineering Applications</i> <u>Aysenur Topsakal</u> , Nazmi Ekren, Osman Kilic, Faik Oktar, Mahir Mahirogullari, Oguzhan Gunduz
105.	<i>Photo-crosslinkable Nature-inspired Synthetic Polymers for Adipose Tissue Regeneration</i> <u>Liesbeth Tytgat</u> , Marica Markovic, Taimoor Qazi, Heidi Ottevaere, Hugo Thienpont, Aleksandr Ovsianikov, Peter Dubruel, Sandra Van Vlierberghe
106.	<i>Evaluation of the Degradation Process of Scaffolds Fabricated by Compression Molding with Particulate Leaching</i> <u>Anna Wiśniewska</u> , Aneta Liber-Kneć
107.	<i>Antibacterial Nanofibrous Wound Dressing Material by Electrospinning Method</i> <u>Eda Yeniay</u> , Leyla Öcal, Esra Altun, Faik Oktar, Nazmi Ekren, Osman Kilic, Oguzhan Gündüz
108.	<i>Study the Schiff-base Reaction in the Alginate-Gelatin Hydrogels</i> <u>Zahra Emami</u> , Morteza Ehsani, Mojgan Zandi, Reza Foudazi

# Poster Presentations

Monday and Tuesday, 12:30-14:30

109.	<i>The Comparison of Crosslinking Methods of Bicomponent PCL/Gelatin Electrospun Nanofibres</i> <u>Judyta Dulnik</u> , Paweł Sajkiewicz
110.	<i>Polymers for 3D Printing for Head and Neck Applications</i> <u>Sibylle Voigt</u> , Gabriele Grimm, Katja Otto, Astrid Enkelmann, Uwe Brick, Matthias Schnabelrauch, Gerlind Schneider
111.	<i>Assessment of Antibacterial Behavior of Some Polymer Composites Used for 3D Printing</i> <u>Dan Batalu</u> , Anamaria Bunescu, Marcela Bucur, Luminita Marutescu, Mariana Carmen Chifiriuc, Petre Badica
112.	<i>Acetylcholinesterase from Eisenia Foetida as Biosensor for Pesticides</i> <u>Erika Flores-Loyola</u> , Magdalena Galindo-Guzman, Selene Sepulveda-Guzman
113.	<i>In Vitro Bioactivity and Long-term Hydrolytic Degradation of Poly <math>\epsilon</math>-Caprolactone/Bioactive Glass Composites</i> <u>Michał Dziadek</u> , Barbara Zagrajczuk, Katarzyna Cholewa-Kowalska
114.	<i>Surface Charge Controlled Cell Proliferation on Electrospun Polyvinylidene Fluoride Fibers</i> <u>Piotr K. Szewczyk</u> , Sara Metwally, Joanna Karbowniczek, Adam Gruszczyński, Mateusz Marzec, Andrzej Bernasik, Urszula Stachewicz
115.	<i>Solution Blow Spun Poly-L-Lactic Acid/Ceramic Fibrous Composites</i> <u>Michał Wojasiński</u> , Joanna Latocha, Paweł Sobieszuk, Tomasz Ciach
116.	<i>Cefuroxime Axetil Loaded PHBV/PCL Electrospun Scaffolds for Bone Tissue Engineering</i> Ali Deniz Dalgiç, <u>Deniz Atıla</u> , Ayten Karataş, Ayşen Tezcaner, Dilek Keskin
117.	<i>Controlled Delivery of bFGF and TGF-<math>\beta</math>1 via Polymeric Nanoparticles within Hybrid Hydrogels for Articular Cartilage Tissue Engineering</i> <u>Milad Fathi Achachelouei</u> , Nihal Engin Vrana, Erhan Bat, Dilek Keskin, Aysen Tezcaner
118.	<i>Various Approaches to the In Vitro Bioactivity Evaluation of the Polymer-Ceramics Composites for Bone Tissue Engineering</i> <u>Barbara Zagrajczuk</u> , Michał Dziadek, Agata Flis, Katarzyna Cholewa-Kowalska, Maria Laczka
119.	<i>Alginate-based Hydrogels Modified with Graphene Oxide for Cartilage Regeneration</i> <u>Klaudia Ordon</u> , Aleksandra Lach, Monika Skoczeń, Kinga Pielichowska
120.	<i>Electron-crosslinked Gelatin Hydrogels Mineralized Enzymatically for Bone Regeneration</i> Stefanie Riedel, Karolina Mazur, Danny Ward, Lorna Ashton, Stefan Mayr, <u>Timothy Douglas</u>



121.	<i><math>\beta</math>-TCP/PHO Biocomposites for Bone Tissue Engineering</i> <u>Ewelina Cichoń</u> , Katarzyna Harażna, Maciej Guzik, Aneta Zima, Anna Ślósarczyk
122.	<i>Polymeric Orthopaedic Textiles Ultrasonically Coated with Bioactive Nanoparticles and Their Stability in Human Body Simulated Environment</i> <u>Julia Rogowska-Tylman</u> , Bartosz Woźniak, Agnieszka Chodara, Sylwia Dąbrowska, Robert Mrugas, Witold Łojkowski
123.	<i>Enzymatically Mineralized Gellan Gum/Alginate Porous Scaffolds for Bone and Cartilage Regeneration</i> <u>Krzysztof Pietryga</u> , Violeta Rodriguez, Véronique Larreta-Garde, Elżbieta Pamuła
124.	<i>Assessment of Cytocompatibility of PLLA/PLLATMC Scaffolds Prepared by Low-cost 3D Printing</i> <u>Jakub Marchewka</u> , Bartosz Mielan, Elżbieta Pamuła, Jadwiga Laska
125.	<i>Preparation of Microspheres with Different Topologies for Cell Culture in Tissue Engineering</i> <u>Bartosz Mielan</u> , Małgorzata Krok-Borkowicz, Elżbieta Pamuła
126.	<i>Poly lactide Based Nanocomposites Reinforced with Graphene Oxide for Bone Surgery Implants</i> Nerea Uriarte Losada, Bartosz Mielan, <u>Barbara Szaraniec</u> , Elżbieta Pamuła, Jan Chłopek
127.	<i>Structuring of Surfaces Dedicated for the Integration with the Cardiovascular Tissue</i> <u>Klaudia Trembecka-Wójciga</u> , Roman Major, Jurgen Lackner, Bogusław Major
128.	<i>Chemoselective Functionalization of Hydrogels for Tunable pH-sensitive Drug Delivery</i> <u>Emanuele Mauri</u> , Alessandro Sacchetti, Filippo Rossi
129.	<i>The Content of Collagen in Collagen-Polyester Material and Hemostatic Research</i> Chun-Hui Huang, Yi-Ting Wang, Pei-Ni Huang, <u>Hsiao-Cheng Yen</u>
130.	<i>Nanocapsules Based on Amphiphilic Polysaccharides as Nanocarriers for Biomedical Applications</i> <u>Małgorzata Janik</u> , Joanna Szafranec, Mikel Felipe, Szczepan Zapotoczny
131.	<i>Study on the Influence of pH upon the Doxorubicine Loading in Core/Multilayer Shell Microcapsules of BSA Gel/Polyelectrolite Complexes Pectin/Chitosan/Hyaluronic Acid</i> <u>Violeta Paşcalău</u> , Codruta Pavel, Alina Pinte, Cecilia Cristea, Eموke Pall, Nicodim Fit, Horea Chicinas, Traian Marinca, Catalin Popa
132.	<i>Nanocapsules Based on Chitosan Carboxylate and Poly N-Vinylpyrrolidone-alt-Itaconic Anhydride - A Promising Alternative for the Basal Cell Carcinoma Treatment</i> <u>Delia Mihaela Raţă</u> , Anca Niculina Cadinoiu, Leonard Ionut Atanase, Luiza Madalina Gradinaru, Marcel Popa

133.	<i>Aptamer-Functionalized Liposomes - A New Attempt to Treat Basal Cell Carcinoma</i> <u>Anca-Niculina Cadinoiu</u> , Delia-Mihaela Rață, Leonard-Ionuț Atanase, Marcel Popa
134.	<i>Chitosan-g-Poly Glycidyl Methacrylate Microparticles as Sustained Drug Delivery System for Oral Administration</i> Silvia Vasiliu, Stefania Racovita, Ionela Gugoasa, Marcel Popa, <u>Anca - Niculina Cadinoiu</u>
135.	<i>Poly(ethylene glycol) methyl ether acrylate Grafted Chitosan Micro and Nanoparticles with Potential Applications in Ophthalmology</i> Corina-Lenuta Savin, <u>Delia Mihaela Rata</u> , Marcel Popa, Christelle Delaite, Gerard Riess, Catalina Anisoara Peptu
136.	<i>Microcapsules Consisting of a BSA Gel Core and a Multilayer Shell of Polysaccharides Polyelectrolite Complexes with the Outer Layer Containing Hyaluronic Acid</i> <u>Codruta Pavel</u> , Violeta Pascalau, Alina Pinte, Horea Chicinas, Florin Popa, Catalin Popa
137.	<i>Control of Paclitaxel Release from 3D Matrices Produced by Electrospinning</i> Konstantin Kuznetsov, Alena Stepanova, Olga Novikova, Ren Kvon, Irina Romanova, Andrey Karpenko, Evgeny Pokushalov, Alexander Karaskov, <u>Pavel Laktionov</u>
138.	<i>Preparation and Characterization of Liposomal Curcumin</i> <u>Katsiaryna Dubatouka</u> , Vladimir Agabekov
139.	<i>Polysachcarides-based Capsules Loaded with Magnetic Nanoparticles</i> <u>Elżbieta Gumieniczek-Chłopek</u> , Joanna Odrobińska, Czesław Kapusta, Szczepan Zapotoczny
140.	<i>Click-Nanohydrogels Based on Riboflavin-modified Hyaluronan</i> Nicole Zoratto, Giuliana Manzi, <u>Elita Montanari</u> , Tommasina Coviello, Pietro Matricardi, Chiara Di Meo
141.	<i>Dexamethasone-loaded Bioreducible Branched Polyethyleneimine for Enhanced Nonviral Transfection</i> <u>Sang Jun Park</u> , Han Chang Kang
142.	<i>Effective Cytotoxic Efficacy of Doxorubicin-loaded Reducible Polycation to Cancer Cells</i> <u>Dong U Ju</u> , Kitae Ryu, Han Chang Kang
143.	<i>Evaluation of the In Vitro Response of Keratinocytes and Fibroblasts to Collagen-Hydroxyethyl Cellulose Matrices with Incorporated Collagen-Gelatin Microspheres</i> <u>Justyna Kozłowska</u> , Natalia Stachowiak, Anna Bajek, Alina Sionkowska, Lukasz Kazmierski
144.	<i>Effect of Assembly pH and Ionic Strength of Chitosan/Casein Multilayers on Benzylamine Hydrochloride Release</i> <u>Maria Marudova</u> , Antoaneta Marinova, Asya Viraneva, Sotir Sotirov, Bissera Pilicheva, Ivan Bodurov, Ivanka Vlaeva, Ginka Exner, Yordanka Uzunova, Temenuzhka Yovcheva
145.	<i>Chitosan/Poly(lactic Acid) Blends as Drug Delivery Systems</i> <u>Maria Marudova</u> , Tsvetan Yorov, Sotir Sotirov

146.	<i>Poly lactide as Drug Carrier in Composite Implant</i> <u>Agnieszka Skórska-Stania</u> , Agnieszka Jelonek, Monika Brzychczy-Włoch
147.	<i>Development and Characterization Minocycline Loaded Chitosan Nanoparticles for Local-Drug-Delivery</i> Victor Martin, <u>Catarina Santos</u> , Marta Alves, Lídia Gonçalves, Isabel C. Ribeiro, Ana Bettencourt
148.	<i>Polymer-clay Nanocomposites with Antibacterial Activity</i> <u>Alicja Rapacz-Kmita</u> , Maciej Mikołajczyk, Barbara Szaraniec, Marta Ludwicka, Ewa Stodolak-Zych
149.	<i>Multifunctional Porous Membranes with Antibacterial Properties</i> Ewa Dzierzkowska, Ewa Stodolak-Zych, Maciej Mikołajczyk, Marcin Gajek, <u>Alicja Rapacz-Kmita</u>
150.	<i>Novel Temperature Responsive Nanocapsules for Anti-aging Skin Care Applications</i> <u>Sergiy Grishchuk</u> , Liudmyla Gryshchuk
151.	<i>Electrosprayed Chitosan Micro/Nanoparticles for Drug Delivery Applications</i> Badriya Baig, <u>Yaser Greish</u> , Amr Amin
152.	<i>Controlled Growth Factor Release by Nanoparticulate Multilayer Systems for Graded Implants</i> <u>Steffen Sydow</u> , Dominik de Cassan, Yvonne Roger, Julius Sundermann, Heike Bunjes, Andrea Hoffmann, Henning Menzel
153.	<i>Gentamicin Loaded Poly D,L - Lactide-co-Glycolide Nanoparticles as Drug Delivery Carriers</i> <u>Katarzyna Reczyńska</u> , Anna-Maria Tryba, Krzysztof Pietryga, Juergen M. Leckner, Elżbieta Pamuła
154.	<i>Characterization of Compound Loading into Polymer Nanospheres for Dermal Application</i> Rose Soskind, <u>Bozena Michniak-Kohn</u>
155.	<i>Edible Biopolymers Films and Coatings Prepare from Cactus Mucilage and Whey Protein</i> <u>Jolanta E. Marszałek</u> , Erika Flores Loyola, Jorge A. De La Rosa Martínez
156.	<i>Synthesis of Poly Lactic co-Glycolic Acid Based Biomaterials and Study of Wettability of Their Films</i> <u>Muhammad Ayyoob</u> , Xin Yang, Young Jun Kim
157.	<i>Controlled Degradation Time of Polylactide and Polypropylene</i> <u>Ewelina Niedzielska</u> , Anna Masek
158.	<i>The Influence of Soft Segments on Properties of New Segmented Polyurethanes Based on Cycloaliphatic Diisocyanate</i> <u>Andrzej Puszka</u>



159.	<i>Physicochemical and Biological Properties of Biomimetic Hydrogel Materials for Tissue Engineering Application</i> <u>Adriana Gilarska</u> , Joanna Lewandowska-Łańcucka, Maria Nowakowska
160.	<i>Barrier Properties of Bilayer Films of FucoPol and Chitosan</i> Ana Rita Ferreira, Vitor Alves, <u>Isabel Coelho</u>
161.	<i>Influence of Friction on Hydrolytic Degradation Polymeric Biomaterials</i> <u>Wojciech Karalus</u> , Jan Dabrowski
162.	<i>Production of Hydroxyapatite Poly vinyl alcohol Based Scaffold for Drug Delivery from Orange Spiny Oyster Seashell Spondylus Barbatulus</i> <u>Serap Ayaz Seyhan</u> , Dilek Bilgiç Alkaya, Sumeyye Cesur, Faik Nuzhet Oktar, Oguzhan Gunduz
163.	<i>Investigation of Chitosan / Tricalcium Phosphate TCP Composite Powders from Scotch Bonnets Semicassis granulata as a Drug Controlled Release Matrices</i> <u>Dilek Bilgiç Alkaya</u> , Serap Ayaz Seyhan, Sumeyye Cesur, Oguzhan Gunduz, Faik Nuzhet Oktar
164.	<i>Luminescence Phenomena of Carbon Dots Molecular Insight</i> <u>Wiktor Kasprzyk</u> , Tomasz Świergosz, Szczepan Bednarz, Karolina Walas, Dariusz Bogdał
165.	<i>The Influence of CNT Modification on Osteo-differentiation</i> <u>Eliška Mázl Chánová</u> , Kristýna Venclíková, Petr Knotek, Dana Kubies, Olga Janoušková, Jana Kredatusová, Ying Yang
166.	<i>Fluorescent Molecular Sensors for Rapidly and Nondestructive Measurement of Polymer Materials</i> <u>Wiktor Kasprzyk</u> , Joanna Ortyl, Anna Chachaj-Brekiesz, Monika Topa, Maciej Pilch, Emilia Hola, Paweł Fiedor
167.	<i>Biocompatibility of the Polymer Middle Ear Prosthesis</i> <u>Magdalena Ziabka</u>
168.	<i>Adjunctive Hemostatic Application of Highly Adhesive Drug Loadable Powder for Partial Hepatectomy Bleeding in a Swine Model</i> <u>Eunhye Lee</u> , Sukyung Ahn, Yonghai Nam, Keunsu Kim, Don Haeng Lee
169.	<i>New Crosslinking Diluents for Dental Materials</i> <u>Norbert Moszner</u> , Jörg Angermann, Urs Fischer
170.	<i>Polymers with Non-Carcinogenic Precursors for Green Electronic Devices</i> <u>Cristian Ravariu</u> , Dan Eduard Mihaiescu, Bogdan Purcareanu
171.	<i>Smart Chitosan-based Hydrogels for Targeted Drug Delivery Application</i> <u>Nga Vo</u> , Lei Huang, Henrique De Paula Lemos, Andrew Mellor, Katarina Novakovic

172.	<i>In Vitro Testing of a Polylactic Polymer Synthesized from Whey</i> <u>Alexandra Dreanca</u> , Radu Popescu, Marioara Moldovan, Laura Silaghi Dumitrescu, Anca Jurj, Ioana Berindan-Neagoe, Ioan Marcus
173.	<i>Microneedle Arrays Coated with pH-sensitive Charge Reversal Copolymers Improve Dendritic Cell-homing DNA Vaccine Delivery and Immune Responses</i> <u>Thambi Thavasyappan</u> , Duong Huu Thuy Trang , Lee Doo Sung
174.	<i>The Effect of Chemical Composition on Crosslinking Kinetics of Methylcellulose/Agarose Hydrogel</i> <u>Beata Niemczyk</u> , Paweł Sajkiewicz, Arkadiusz Gradys
175.	<i>Synthesis of Biopolymers by Bacterial Strain Azotobacter Agile 12</i> <u>Andrei Dudun</u> , Elizaveta Akoulina, Anton Bonartsev, Vera Voinova, Tatiana Makhina, Garina Bonartseva
176.	<i>Hydrogels Cross-linked by Trehalose Diacetals with Tunable Degradation Rate in Acidic Solutions as Carriers for pH-Triggered Protein Release</i> <u>Małgorzata Burek</u> , Sylwia Waśkiewicz, Klaudia Kubic, Izabela Nabałczyk, Ilona Wandzik
177.	<i>Effect of Bacterial Alginate on Growth of Mesenchymal Stem Cells</i> <u>Elizaveta Akoulina</u> , Anton Bonartsev, Garina Bonartseva, Vera Voinova
178.	<i>Biodegradable Non-thermosensitive Pseudo Double Networks as Potential Hydrogels to Release Viable Cell Sheets for tissue Regeneration</i> <u>Ana Fatima Civantos</u> , Isabel Casado Losada, David Acitores, María Eugenia Perez-Ojeda, Enrique Martinez Campos, Viviana Ramos, Alberto Gallardo
179.	<i>Surface Functionalization of Ti6Al7Nb Alloy with Biopolymers and DLC-based Coatings Using Plasmochemical Activation</i> <u>Karol Kyzioł</u> , Julia Oczkowska, Karol Wolski, Agnieszka Kyzioł, Łukasz Kaczmarek
180.	<i>One-step Sonochemical Fabrication and Embedding of Gentamicin Nanoparticles into Parylene C Implant Coating</i> Monika Golda-Cepa, Paulina Chytrosz, Aleksandra Chorylek, <u>Andrzej Kotarba</u>
181.	<i>Assessment of Haemo- and Biocompatibility of Different Polyurethane-based Electrospun Vascular Grafts</i> <u>Vera Chernonosova</u> , Alexander Gostev, Andrey Karpenko, Alexander Karaskov, Evgeny Pokushalov, Pavel Laktionov
182.	<i>PLA/Mg Composites Treated with LSP against the Adhesion of Microorganisms</i> <u>Miguel A. Pacha-Olivenza</u> , Amparo M. Gallardo-Moreno, José L. González-Carrasco, José L. Ocaña-Moreno, M. Luisa González-Martín

183.	<i>Physical Surface Changes on a PLA/Mg Composite after Degradation under Physiological Conditions</i> Daniel Romero-Guzmán, Laura Vazquez-Serrano, <u>Miguel A. Pacha-Olivenza</u> , Amparo M. Gallardo-Moreno, M. Luisa González-Martín
184.	<i>Characterisation of Partially Polymer Covered Self-expandable Metallic Stents in Esophageal Cancer Treatment Impact of Long-term Usage in the Body</i> Monika Golda-Cepa, Janusz Włodarczyk, Jarosław Kuzdzal, <u>Paulina Chytrosz</u> , Andrzej Kotarba
185.	<i>Surface Functionalisation Nanoroughness and Drug Delivery by Atmospheric Plasma Jet on Scaffolds</i> Alessandro Patelli, Federico Mussano, Paola Brun, Tullio Genova, Emmanuele Verga, Emmanuele Ambrosi, T Michieli, Giovanni Mattei, Paolo Scopece, <u>Marco Scatto</u>
186.	<i>Improvement of Short Ca-P Whiskers/Polylactide Composites by Surface Modification with Lauric Acid</i> <u>Monika Biernat</u> , Zbigniew Jaegermann, Paulina Tymowicz-Grzyb, Zdzisław Wiśniewski
187.	<i>PEO-based Films Prepared by Plasma Polymerization from Bulk Precursors</i> <u>Jana Sedlarikova</u> , Zuzana Kolarova-Raskova, Jaroslav Kousal, Anna Hurajová, Marian Lehocky
188.	<i>Chitosan and Its Derivatives as Biocompatible Coatings and Scaffold Materials</i> <u>Adriana Gilarska</u> , Sylwia Fiejdasz, Czesław Kapusta, Maria Nowakowska, Szczepan Zapotoczny
189.	<i>Excimer Laser Micromachining-Forming without Influencing the Mechanical Behaviour of Biodegradable Polymers</i> <u>Magdalena Tomanik</u> , Magdalena Kobielarz, Bogusz Stępak, Arkadiusz Antończak, Celina Pezowicz, Jarosław Filipiak
190.	<i>Topographic Evaluation of the Micropatterned Poly L-Lactide Thin Sheets</i> <u>Magdalena Tomanik</u> , Katarzyna Łęcka, Arkadiusz Antończak, Celina Pezowicz, Jarosław Filipiak
191.	<i>Extracellular Matrix Substitute with Natural Polysaccharides and Small Peptide</i> <u>Ewa Stodolak-Zych</u> , Agnieszka Solecka, Julia Golańska, Wiktor Niemiec, Maciej Bogun, Zbigniew Darczynski, Beata Kolesinska
192.	<i>Effective Immobilization of BMPs on Diazo-resin Substrates Composed from Pectin or Chondroitin Sulfate</i> <u>Magdalena Wytrwal-Sarna</u> , Agata Pomorska, Michał Sarna, Zbigniew Adamczyk, Krzysztof Szczubiałka, Andrzej Bernasik

193.	<i>Raman Microspectroscopic Investigations of Polymer Nanocomposites - Evaluation of Physical and Biophysical Properties</i> <u>Aleksandra Weselucha-Birczynska</u> , Anna Kołodziej, Małgorzata Świętek, Łukasz Skalniak, Marta Błażewicz
194.	<i>2D-Correlation Raman Studies on the Effect of Modifications of Carbon Nanofibers on their Properties and Molecular Structure</i> <u>Aleksandra Weselucha-Birczynska</u> , Elżbieta Długoń, Krzysztof Morajka, Marek Michalec, Marta Błażewicz
195.	<i>Chitosan-based ZnO-doped Bioglass Composite as Carriers of Bioactive Peptides</i> <u>Lidia Ciołek</u> , Monika Biernat, Zbigniew Jaegermann, Artur Oziębło, Justyna Sawicka, Maria Dzierżyńska, Sylwia Rodziewicz-Motowidło, Milena Deptuła, Michał Pikuła
196.	<i>The Development of the Bioactive Particles Combined with Collagen Hydrogels for Tissue Engineering</i> <u>Justyna Pawlik</u> , Karolina Zazakowny, Katarzyna Cholewa-Kowalska
197.	<i>Synthesis and Characterization of Chitosan-coated Magnetite Using a Modified Wet Method for Drug Delivery Applications</i> <u>Yaser Greish</u>
198.	<i>Stability and Mechanical Properties of Hybrid Hydrogel Materials with Variation of TiO<sub>2</sub> Nanoparticle Concentration with Potential Use as Bones Scaffolds</i> <u>Karolina Zazakowny</u> , Justyna Pawlik, Joanna Lewandowska-Łańcucka, Joanna Mastalska-Popławska, Kamil Kamiński, Maria Nowakowska, Marta Radecka
199.	<i>Plasma-modified Polystyrene Solution Blow Spun Fibrous Scaffolds for 3D Cell Culture</i> <u>Michał Wojasiński</u> , Marta Błaszczak, Tomasz Ciach
200.	<i>Surface Functionalization of Poly L-Lactide-co-Glycolide with Poly 2-Oxazolines</i> <u>Anna-Maria Tryba</u> , Katarzyna Reczyńska, Krzysztof Pietryga, Elżbieta Pamuła
201.	<i>Self-Assembling Peptides with RGD Motifs as Scaffolds for Tissue Engineering</i> <u>Graziano Deidda</u> , Sai Vamshi Jonnalagadda, Anthi Ranella, Estelle Mossou, Trevor Forsyth, Phanourios Tamamis, Maria Farsari, Anna Mitraki
202.	<i>HypACT Inject Auto device an Easy Fast and Sterile Method to Produce the Best Quality Platelet Rich Fibrin Membrane</i> <u>Dorottya Kardos</u> , István Hornyák, Melinda Simon, Adél Hinsenkamp, Bence Marshall, Róbert Várdai, Balázs Pinke, László Mészáros, Alfréd Kállay-Menyhárd, Zsombor Lacza
203.	<i>Wetting Properties and Morphology of Electrospun Fibers from Hydrophobic and Hydrophilic Polymers</i> <u>Joanna Knapczyk</u> , Marcin Gajek, Urszula Stachewicz
204.	<i>Charge Assisted Tailoring of Electrospun PMMA Fibers Surface Chemistry and Wetting Properties</i> <u>Daniel Ura</u> , Mateusz Marzec, Andrzej Bernasik, Urszula Stachewicz

205.	<i>Composite Scaffolds from Poly 3-Hydroxybutyrate and Sodium Alginate for Tissue Engineering</i> <u>Andrei Dudun</u> , Anton Bonartsev, Irina Zharkova, Elizaveta Akoulina, Vsevolod Zhuikov, Dariana Chesnokova, Tatiana Makhina, Sergey Yakovlev, Garina Bonartseva, Vera Voinova
206.	<i>Biophysical Studies on Biocompatible Polymers for Medical Applications - Polyhydroxyoctanoate PHO</i> <u>Katarzyna Haraźna</u> , Tomasz Witko, Daria Solarz, Małgorzata Witko, Marcel Krzan, Andrzej Bojarski, Maciej Guzik
207.	<i>Fabrication and Evaluation of Nanofibrous Scaffolds with Polylactide and Hyaluronic Fibers for Skin Substitute</i> <u>Ewa Stodolak-Zych</u> , Katarzyna Rozmus, Joanna Kubacka, Łukasz Zych, Magdalena Gargas, Elżbieta Kolaczkowska, Magdalena Cieniawska, Katarzyna Książek, Anna Ścisłowska-Czarnecka
208.	<i>Bacterial Response to PVA/Silver Nanoparticles Wound Dressing</i> Noemi Monteiro, Jean Silva, Renata Oliveira, <u>Rossana Thiré</u> , Olney Motta, João Almeida
209.	<i>Tuning the Mechanical Properties of Alginate-Peptide Hydrogels</i> <u>Guy Ochbaum</u> , Ronit Bitton
210.	<i>Highly Porous 3D Fibrous Scaffolds for Tissue Regeneration</i> <u>ChaeHwa Kim</u> , Taehee Kim
211.	<i>Preparation and Characterization of Absorbent Nonwoven Fabrics for Wound Care</i> <u>YoonJin Kim</u> , Chae-Hwa Kim, Jung Nam Im, Tae-Hee Kim
212.	<i>L-arginine and Manuka Honey Loaded Nanofibers for Wound Healing Applications</i> <u>Oana Maria Ionescu</u> , Lenuta Profire, Arn Mignon, Sandra Sandra Van Vlierberghe
213.	<i>Collagen Hydrogels Modified by Cyclodextrines Addition</i> Joanna Skopinska-Wisniewska, <u>Justyna Kozłowska</u> , Alina Sionkowska
214.	<i>Interactions between Dermal Papilla Spheroid Array and Acellular Skin Dermis During Hair Follicle Regeneration</i> <u>Yi-You Huang</u>
215.	<i>Correlation between Viscoelastic Properties and Curcumin Release Rate from PVA-Borax/Cellulose Nanofiber Hydrogels</i> Gelareh Rezvan, <u>Gholamreza Pircheraghi</u> , Reza Bagheri
216.	<i>Innovative PCL/graphene filament for 3D printing of cartilage scaffolds using fused deposition modeling</i> Anna Kurowska, Arkadiusz Matuszek, Dawid Holisz, Adam Jabłoński, Magdalena Ziąbka, Ryszard Kwiatkowski, Izabella Rajzer
217.	<i>Novel Perspectives of Polymer-based Scaffolds for Biomedical Applications</i> <u>Małgorzata Sekuła</u> , Patrycja Domalik-Pyzik, Sylwia Noga, Elżbieta Karnas, Karolina Kosowska, Martyna Hunger, Natalia Złocista-Szewczyk, Joanna Jagiełło, Ludwika Lipińska, Kinga Pielichowska, Jan Chłopek, Ewa Zuba-Surma

# Authors Index

## A

Aalto-Setälä Laura 7  
Abbott Andrew 18  
Abdulwhhab Mohamad 18  
Achachelouei Milad Fathi 117  
Acitores David 178  
Adamczyk Zbigniew 192  
Adamus-Wlodarczyk Agnieszka 62  
Agabekov Vladimir 26, 78, 86, 98, 138  
Agnelli Silvia 63  
Ahadpour Amirkhashayar 13  
Ahn Sukyung 168  
Aigner Achim K5  
Ainola Mari 7  
Akan Aydin 91  
Akkaya Dilek Bilgic 88  
Akoulina Elizaveta 87, 175, 177, 205  
Akyol Elvan 64  
Albu Madalina 14  
Ali-Adib Sandi 36  
Alkaya Dilek Bilgic 162, 163  
Allain Jean Paul 24  
Almeida Joao 208  
Alsberg Eben PL3  
Al-Taie Alaa 18  
Altun Esra 16, 107  
Alves Marta 147  
Alves Vitor 160  
Ambrosi Emmanuele 185  
Amin Amr 151  
Anagnostopoulos Achilles 69  
Angelaki Despina 25  
Angermann Jörg 169  
Antończak Arkadiusz 189, 190  
Argiriou Anagnostis 69  
Arslan Aysu PL2  
Ashton Lorna 120  
Atanase Leonard Ionut 132, 133  
Athanassiou Athanassia 35, 38  
Atila Deniz 76 116  
Ausejo Jennifer Gonzalez 95  
Awsuik Kamil 23  
Aydin R. Seda Tigli 64  
Aydogdu Mehmet 15, 85  
Ayyoob Muhammad 156  
Azari Shahram 13  
Azizova Liana 10

## B

Babaliari Eleftheria 25, 28  
Badica Petre 111  
Badiger Manohar 46  
Bagheri Reza 215  
Baig Badriya 151  
Bajek Anna 143  
Barer Michael 18

Barros Daniela 45  
Bastianini Maria 50  
Basu Probal 5  
Bat Erhan 117  
Batalu Dan 111  
Bayer Ilker S. 35, 38  
Bayon Yves 47, 49  
Becerril-Rodriguez Iris 48  
Bednarz Szczepan 164  
Behrens Peter 83  
Belbekhouche Sabrina 27  
Berindan-Neagoe Ioana 172  
Bernasik Andrzej 114, 192, 204  
Bershtein Vladimir 61  
Bertoldi Serena K9  
Bertorelli Rosalia 38  
Bettencourt Ana 147  
Bheemaneni Girija 79  
Biernat Monika 79, 186  
Bitton Ronit 80, 209  
Björkenheim Robert 7  
Błaszczak Marta 199  
Błażejczyk Agnieszka 9  
Błażewicz Marta 193, 194  
Boccaccini Aldo R. 101  
Bodurov Ivan 144  
Boffito Monica K11.  
Bogdał Dariusz 164  
Bogun Maciej 191  
Bojarski Andrzej 206  
Boldrini Leonardo 1  
Bonartsev Anton 87, 175, 177, 205  
Bonartseva Garina 87, 175, 177, 206  
Borgese Laura 63  
Bougiouklis Dimitris 69  
Bowlin Gary K6  
Bray Fabrice 14  
Bretcanu Oana 56  
Brick Uwe 110  
Brun Paola 185  
Brzychczy-Wloch Monika K4, 146  
Bucur Marcela 111  
Budkowski Andrzej 23  
Bukata Julia 74  
Bunescu Anamaria 111  
Bunjjes Heike 152  
Burek Małgorzata 51, 176  
Busscher Henk K8

## C

Caba Valentina 63  
Cadinoiu Anca Niculina 132, 133  
Calasans-Maia Mônica 1  
Calzone Stefano K11  
Camasao Dimitria 14  
Campos Enrique Martinez 178  
Canal Cristina K3, 41, 68  
Casado Losada Isabel 178  
Celi Simona 92

Cesur Sumeyye 85, 88, 91, 162, 163  
 Chachaj-Brekiesz Anna 166  
 Chaniotaki Lefki 25  
 Charitidis Costas K1  
 Chattaway Claire 27  
 Chatzinikolaidou Maria K1  
 Cheng Nai-Chen K7  
 Chernonosova Vera 181  
 Chesnokova Dariana 205  
 Chicinas Horea 131, 136  
 Chifiriuc Mariana Carmen 111  
 Chłopek Jan 4, 6, 81, 94, 97, 126, 217  
 Chmielarz Paweł 55  
 Chodara Agnieszka 122  
 Choe Young Eun 82, 84  
 Choi YeonSu 33  
 Choinska Emilia 93  
 Cholewa-Kowalska Katarzyna 113, 118, 196  
 Choonara Yahya 39  
 Chorvát Dušan 32, 66  
 Chorylek Aleksandra K4, 180  
 Choudhury Deepak K11  
 Chytrosz Paulina K4, 89, 180, 184  
 Ciach Tomasz 115, 199  
 Ciardelli Gianluca K11  
 Cichoń Ewelina 90, 121  
 Cieniawska Magdalena 207  
 Ciołek Lidia 195  
 Civantos Ana 24  
 Claeysens Frederik 48  
 Coelho Isabel 160  
 Coentro Joao 37  
 Contardi Marco 38  
 Contessi Negrini Nicola K9  
 Costa Diana 67  
 Coviello Tommasina 52, 140  
 Cristea Cecilia 131  
 Cruz Carla 67  
 Czechowska Joanna 90

## D

Dąbrowska Sylwia 122  
 Dabrowski Jan 161  
 Dai Jianwu 99  
 Dalgic Ali Deniz 76, 116  
 Dankers Patricia 22  
 Darczynski Zbigniew 191  
 Darsey Jerry 30  
 Datta Shubhashis 32  
 De Cassan Dominik 152  
 De La Rosa Martínez Jorge A. 155  
 De Paula Lemos Henrique 171  
 De Pieri Andrea 53  
 Deidda Graziano 201  
 Del Campo Aranzazu 17  
 Delaite Christelle 135  
 Delfosse Daniel 60  
 Demoustier-Champagne Sophie 27

Depero Laura E. 63  
 Deptuła Milena 195  
 Deszczyński Jarosław 4, 6  
 Deszczyński Jarosław Michał 4, 6  
 Di Meo Chiara 52, 140  
 Długoń Elżbieta 194  
 Domalik-Pyzik Patrycja 81, 94, 97, 217  
 Dong Jia Jia K8  
 Doroudian Mohadeseh 13  
 Douglas Timothy 2, 120  
 Dreaanca Alexandra 172  
 Drewienkiewicz Aleksandra 12  
 Du Prez Fili E. 27  
 Du Toit Lisa 39  
 Dubatouka Katsiaryna 138  
 Dubruel Peter PL2, 14, 105  
 Dudun Andrei 87, 175, 205  
 Dulnik Judyta 109  
 Dumitrescu Laura Silaghi 172  
 Dziadek Michał 113, 118  
 Dzierzkowska Ewa 149  
 Dzierżyńska Maria 195

## E

Ege Zeynep 85  
 Ege Zeynep Ruya 88, 91  
 Ehsani Morteza 108  
 Ekren Nazmi 15, 16, 19, 34, 85, 88, 104, 107  
 El Fray Mirosława 11, 43, 74  
 Elttayef Ajile 65  
 Emami Zahra 108  
 Engvall Klas K4  
 Enkelmann Astrid 110  
 Erdemir Gokce 91  
 Eroglu Mehmet 20  
 Eroglu Mehmet Sayip 34  
 Exner Ginka 144

## F

Fare Silvia K9  
 Farsari Maria 201  
 Fatima Civantos Ana 178  
 Fatimi Ahmed K2  
 Felipe Mikel 130  
 Feng Jun 17  
 Fernandes Emanuel 49  
 Ferreira-da-Silva Frederico 45  
 Fiedor Paweł 166  
 Fiejdasz Sylwia 188  
 Filipiak Jarosław 189, 190  
 Fiorletta Mathilde K3  
 Fischer Urs 169  
 Fit Nicodim 131  
 Flis Agata 118  
 Flores-Loyola Erika 112, 155  
 Forsyth Trevor 201  
 Foudazi Reza 108  
 Freitas Amaral Isabel 45  
 Furtado Joana 45



## G

Gajek Marcin 149, 203  
Gajos Katarzyna 23  
Galindo-Guzman Magdalena 112  
Gallardo Alberto 178  
Gallardo-Moreno Amparo M. 182, 183  
García Andrés J. 45  
García-Fernández Luis 73  
Gargas Magdalena 207  
Garton Natalie 18  
Gasparotti Emanuele 92  
Gayir Velican 20  
Genova Tullio 185  
Georgopoulou Anthie K1  
Gering Christine 71  
Geroussi Marina 69  
Ghani Sofia 66  
Gilariska Adriana 159, 188  
Ginebra Maria-Pau 68  
Glasmacher Birgit 83  
Glinel Karine 27  
Goddard Alex 18  
Golańska Julia 191  
Golda-Cepa Monika K4, 89, 101, 180, 184  
Goldmann Wolfgang H. 101  
Goldoni Luca 38  
Gomes Manuela 49  
Gonçalves Lídia 147  
Gonsior Małgorzata 11  
González-Carrasco José L. 182  
González-Martín M. Luisa 182, 183  
Gonzalez-Urias Alejandra 31  
Górecka Żaneta 93  
Gorelv Alexander 53  
Gostev Alexander 181  
Gradinaru Luiza Madalina 132  
Gradys Arkadiusz 174  
Greish Yaser 151, 197  
Grimm Gabriele 110  
Grishchuk Sergiy 150  
Grivet-Brancot Arianna K11  
Gruber Peter PL2  
Gruszczyński Adam 77, 114  
Gryń Karol 4, 6  
Gryshchuk Liudmyla 150  
Gugoasa Ionela 134  
Gumieniczek-Chłopek Elżbieta 139  
Gunduz Oguzhan 15, 16, 19, 20, 34, 85, 88, 91, 104, 107, 162, 163  
Gupta Abhishek 40  
Guven Ulkugul 34  
Guzik Maciej 121, 206

## H

Haeng Lee Don 168  
Hakkarainen Minna K4  
Hamouda Ines 41, 68  
Han Xiaoxiao 18  
Harażna Katarzyna 121, 206  
Hazer Baki 64  
Hendriks Stephan K5  
Heredia-Guerrero José A. 38  
Hilborn Jöns 99  
Hileuskaya Kseniya 26, 86, 78  
Hill David 95  
Hinsenkamp Adél 202  
Hoffmann Andrea 152  
Hoheisel Anna Lena 83  
Hola Emilia 166  
Holisz Dawid 216  
Hornýák István 202  
Huang Chun-Hui 129  
Huang Lei 171  
Huang Pei-Ni 129  
Huang Yi-You 214  
Hukka Terttu 75  
Hunger Martyna 94, 217  
Huntošová Veronika 32  
Hupa Leena 7  
Hurajová Anna 187  
Hytönen Vesa 71

## I

Il Son Tae 54  
Im Jung Nam 211  
Inamdar Satish 46  
Ionescu Oana Maria 212  
Isa Douglas 66  
Isindag Busra 20  
Ito Yoshihiro 54  
Iturri Jagoba 59

## J

Jabłoński Adam 216  
Jaegermann Zbigniew 186, 195  
Jagiełło Joanna 217  
Jancura Daniel 32  
Janik Małgorzata 130  
Janoušková Olga 165  
Jelonek Agnieszka 146  
Johnston Brian 95  
Jonnalagadda Sai Vamshi 201  
Ju Dong U 142  
Jun Park Sang 141  
Jurj Anca 172  
Jutková Annamaria 32

## K

Kaczmarek Łukasz 179  
 Kakabakos Sotirios 23  
 Kałaska Bartłomiej 9  
 Kaliva Maria K1.  
 Kalkandelen Cevriye 19  
 Kállay-Menyhárd Alfréd 202  
 Kamiński Kamil 9, 198  
 Kandaswamy Ravichandran 79  
 Kang Han Chang 33, 141, 142  
 Kapis Artur 11  
 Kapusta Czesław 139, 188  
 Karademir Betül 91  
 Karalus Wojciech 161  
 Karaskov Alexander 137, 181  
 Karatas Ayten 76, 116  
 Karbowniczek Joanna 77, 214  
 Kardos Dorottya 202  
 Karnas Elżbieta 217  
 Karpenko Andrey 137, 181  
 Kasprzyk Wiktor 164, 166  
 Kavatzikidou Paraskevi 25, 28  
 Kazmierski Łukasz 143  
 Kellomäki Minna 71, 75  
 Kelly Catriona 65  
 Keppler Julia 2  
 Keskin Dilek 76, 116, 117  
 Kilic Beyhan 85  
 Kilic Osman 15, 16, 19, 34, 85, 88, 104, 107  
 Kim Chae-Hwa 210, 211  
 Kim Geun Hyung 72, 82, 84  
 Kim Hae Ri 72, 82, 84  
 Kim Jae-Won 54  
 Kim Keunsu 168  
 Kim Minseong 72, 82, 84  
 Kim Shin-Woong 54  
 Kim Taehee 210  
 Kim Tae-Hee 211  
 Kim Won Jin 72, 82, 84  
 Kim Yoon Jin 211  
 Kim Young Jun 156  
 Kleščiková Lucia 66  
 Klymenko Olesya 51  
 Knapczyk Joanna 203  
 Knotek Petr 165  
 Ko Hyewon 96  
 Kobielarz Magdalena 189  
 Kocot Magdalena 2  
 Kohn Joachim PL4  
 Koivisto Janne 71  
 Kolaczowska Elżbieta 207  
 Kolarova-Raskova Zuzana 187  
 Kolesinska Beata 191  
 Kołodziej Anna 193  
 Koo YoungWon 72, 82, 84  
 Korkmaz Hayriye 85  
 Korkmaz Nalan Sumeyra 34  
 Kosowska Karolina 97, 217

Kotarba Andrzej K4, 89, 180, 184  
 Kousal Jaroslav 187  
 Kowalczuk Marek 40, 95  
 Koyn Zak 24  
 Kozłowska Justyna 143, 213  
 Kraskouski Aliaksandr 26, 78, 86  
 Kredatusová Jana 165  
 Krok-Borkowicz Małgorzata 125  
 Kronek Juraj 32  
 Kronekova Zuzana 66  
 Krzan Marcel 206  
 Książek Katarzyna 207  
 Kubacka Joanna 207  
 Kubic Klaudia 176  
 Kubies Dana 165  
 Kulikouskaya Viktoriya 26, 78, 98  
 Kumar Pradeep 39  
 Kupczak Maria 51  
 Kurowska Anna 216  
 Kurtyka Przemysław 11  
 Kuruca DurdaneSerap 91  
 Kustos Roman 11  
 Kuzdzal Jarosław 184  
 Kuznetsov Konstantin 137  
 Kvon Ren 137  
 Kwiatkowski Ryszard 216  
 Kwiecień Iwona 95  
 Kyzioł Agnieszka 179  
 Kyzioł Karol 179

## L

Labay Cédric 41, 68  
 Lach Aleksandra 119  
 Lacić Igor 66  
 Lackner Juergen 11, 127  
 Lacza Zsombor 202  
 Laczka Maria 118  
 Ladutska Alena 86  
 Laktionov Pavel 137, 181  
 Larreta-Garde Véronique 123  
 Laska Jadwiga 124  
 Latocha Joanna 115  
 Lazouskaya Maryna 98  
 Łęcka Katarzyna 190  
 Leckner Juergen M. 153  
 Lee Eunhye 168  
 Lee Jae Yoon 72, 82, 84  
 Lee Ji Un 72, 82, 84  
 Lehocky Marian 187  
 Leino Katri 75  
 Lendlein Andreas PL1  
 Lenkavská Lenka 32  
 Leppiniemi Jenni 71  
 Lerf Reto 60  
 Lerouge Sophie K2  
 Letourneur Didier 8  
 Lewandowska-Łańcucka Joanna 159, 198  
 Li Suming 70

Liang He 3  
Liber-Kneć Aneta 106  
Licea-Claverie Angel 31  
Licea-Navarro Alexei 31  
Lindfors Nina 7  
Lipińska Ludwika 217  
Lofaro Manuele K9  
Łojkowski Witold 122  
Loontjens Ton K8  
Losi Paola 92  
Lovell Christopher 101  
Lu Aijing 70  
Ludwicka Marta 148  
Luzuriaga Ainhoa Egizabal 50  
Lyyra Inari 75

## M

Ma Shijimol 36  
MacNeil Sheila 48  
Mahirogullari Mahir 19, 104  
Maia-Pinto Marianna 1  
Majková Eva 66  
Major Bogusław 127  
Major Roman 11, 127  
Makhina Tatiana 175, 205  
Mancini Patrizia 52  
Mantovani Diego 14  
Manzanares-Guevara Lizbeth 31  
Manzi Giuliana 140  
Mao Yong PL4  
Marchewka Jakub 124  
Marcus Ioan 172  
Marimuthu Thashree 39  
Marinca Traian 131  
Marinova Antoaneta 144  
Markovic Marica PL2, 105  
Marshall Bence 202  
Marszałek Jolanta E. 155  
Martin Claire 40  
Martin Victor 147  
Martins M. Cristina L. 45  
Marudova Maria 144, 145  
Marutescu Luminita 111  
Marzec Mateusz 114, 204  
Masek Anna 157  
Massera Jonathan 75  
Mastai Yitzhak 29  
Mastalska-Popławska Joanna 198  
Matricardi Pietro 52, 104  
Mattei Giovanni 185  
Matuszek Arkadiusz 216  
Mauri Emanuele 57, 128  
Mayr Stefan 120  
Mazancová Petra 66  
Mázl Chánová Eliška 165  
Mazur Karolina 120  
McGarrigle James J. 66  
Mellor Andrew 171  
Menzel Henning 83, 152  
Mészáros László 202

Metwally Sara 77, 114  
Michalec Marek 194  
Michieli T 185  
Michniak-Kohn Bożena 154  
Mielan Bartosz 124, 125, 126  
Mielarńczyk Anna 51  
Mielarńczyk Łukasz 51  
Mignon Arn 212  
Mihaiescu Dan Eduard 170  
Mikhalovska Lyuba 10  
Mikhalovsky Sergey 10  
Mikłosz Joanna 9  
Mikołajczyk Maciej 148, 149  
Minden-Birkenmaier Benjamin K6  
Mishra Munmaya 58  
Miškovský Pavol 32  
Misztela Andrzej 11  
Mitraki Anna 28, 201  
Mndlovu Hillary 39  
Modrzejewska Zofia 102  
Moghe Prabhas PL4  
Mogielnicki Andrzej 9  
Moldovan Marioara 172  
Montanari Elita 52, 140  
Monteiro Noemi 208  
Morajka Krzysztof 194  
Morawska-Chochół Anna 81  
Moroni Lorenzo 50  
Mosca Luciana 52  
Mossou Estelle 201  
Moszner Norbert 169  
Mota Carlos 50  
Motta Olney 208  
Moukbil Yunis 20  
Mrugas Robert 122  
Muenger Peter 60  
Munoz Jone 21  
Mussano Federico 185  
Muszanska Agnieszka K8  
Mzyk Aldona 12

## N

Nabiałczyk Izabela 176  
Nadella Vinod 29  
Naing May Win K11  
Nam Yonghai 168  
Natkanski Piotr 12  
Némethová Veronika 66  
Neugebauer Dorota 51  
Niculina Cadinoiu Anca 134  
Niedzielska Ewelina 157  
Niemczyk Beata 174  
Niemiec Wiktor 191  
Noga Sylwia 217  
Noh Seung-Hyun 54  
Novacek Vit 49  
Novakovic Katarina 56, 171  
Novik Galina 86  
Novikova Olga 137  
Nowakowska Maria 9, 159, 188, 198

## O

Oberholzer José 66  
 Öcal Leyla 107  
 Ocana-Moreno José L. 182  
 Ochbaum Guy 80, 209  
 Oczkowska Julia 179  
 Odrobińska Joanna 139  
 Oehmichen Sarah 83  
 Oelschlaeger Claude 42  
 Oktar Faik 15, 20, 85, 88, 104, 107  
 Oktar Faik Nuzhet 19, 34, 91, 162, 163  
 Olejnik Alicja 62  
 Oliveira Renata 208  
 Olmeda-Lozano Marta 73  
 Omami Mustafa 66  
 Oner EbruToksoy 20  
 Ordon Klaudia 100, 119  
 Oroz-Parra Irasema 31  
 Ortyl Joanna 166  
 Ossipov Dmitri 99  
 Ottevaere Heidi 105  
 Otto Katja 110  
 Ovsianikov Aleksandr PL2, 105  
 Ozbek Burak 19, 20  
 Ozen Sertan 85  
 Oziębło Artur 195

## P

Pacha-Olivenza Miguel A. 182, 183  
 Paez Julieta 17  
 Pagkali Varvara 23  
 Paik Pradip 29  
 Pajarinen Jukka 7  
 Pall Emoke 131  
 Pamula Elżbieta 2, 123, 124, 125, 126, 153, 200  
 Pan Jingzhe 18  
 Pannirselvam Prabhu K11  
 Park Jae Hyung 96, 103  
 Parker Julie 56  
 Parraga Jenny 71  
 Parreira Paula 45  
 Pascalau Violeta 131, 136  
 Pastino Alexandra PL4  
 Patelli Alessandro 50, 185  
 Pau Ginebra Maria 41  
 Paula Pego Ana 45  
 Pavel Codruta 131, 136  
 Pawlak Dariusz 9  
 Pawlik Justyna 196, 198  
 Pegueroles Marta K3  
 Pelach Michal 66  
 Peptu Catalina Anisoara 135  
 Perez-Ojeda María Eugenia 178  
 Perotto Giovanni 38  
 Petrenčíková Nadežda 32  
 Petrou Panagiota 23  
 Pezowicz Celina 189, 190

Pezzoli Daniele 14  
 Pieklarz Katarzyna 102  
 Pielichowska Kinga 100, 119, 217  
 Pien Nele 14  
 Pietryga Krzysztof 123, 153, 200  
 Pikuta Michał 195  
 Pilch Maciej 166  
 Pilicheva Bissera 144  
 Pillay Viness 39  
 Pinke Balázs 202  
 Pintea Alina 131, 136  
 Pircheraghi Gholamreza 215  
 Pokushalov Evgeny 137, 181  
 Pomorska Agata 192  
 Pompa Pier Paolo 38  
 Popa Catalin 131, 136  
 Popa Florin 136  
 Popa Marcel 132, 133, 134, 135  
 Popescu Radu 172  
 Pourjavadi Ali 13  
 Prakash Hridayesh 29  
 Profire Lenuta 212  
 Pugliese Eugenia 47  
 Purcureanu Bogdan 170  
 Puszka Andrzej 61, 158

## Q

Qazi Taimoor 105  
 Queiroz Joao 67

## R

Racovita Stefania 134  
 Radecka Iza 40, 95  
 Radecka Marta 198  
 Rajzer Izabella 216  
 Ramos Viviana 178  
 Ranella Anthi 25, 28, 201  
 Rapacz-Kmita Alicja 148, 149  
 Raptis Ioannis 23  
 Rata DeliaMihaela 132, 133, 135  
 Raus Vladimír 66  
 Ravariu Cristian 170  
 Rázga Filip 66  
 Re em Tali Tavor 44  
 Reczyńska Katarzyna 153, 200  
 Reich Reuven 44  
 Reis Rui 49  
 Rezvan Gelareh 215  
 Ribeiro Isabel C. 147  
 Ribeiro Sofia 49  
 Riedel Stefanie 120  
 Riess Gerard 135  
 Riool Martijn 22  
 Rita Ferreira Ana 160  
 Rochev Yuri 53  
 Rodriguez Violeta 123  
 Rodziewicz-Motowidło Sylwia 195

Roether Johanna 42  
Roger Yvonne 152  
Rogowska-Tylman Julia 122  
Rogulska Magdalena 61  
Rolando Christian 14  
Romanova Irina 137  
Romero-Guzmán Daniel 183  
Rossi Filippo 57, 128  
Rozmus Katarzyna 207  
Russell Stephen 3  
Rysz Jakub 23  
Ryu Kitae 142

## S

Sacchetti Alessandro 57, 128  
Sadaba Naroa 21  
Saha Nabanita 5  
Saha Petr 5  
Sahay Rahul 74  
Sajkiewicz Paweł 109, 174  
San Román Julio 73  
Sani Monica 57  
Santos Catarina 147  
Sarasua Jose-Ramon 21  
Sarna Michal 192  
Savin Corina-Lenuta 135  
Sawicka Justyna 195  
Scatto Marco 50, 92, 185  
Schmidt Nadeschda 83  
Schmitz Moniek 22  
Schnabelrauch Matthias 110  
Schneider Gerlind 110  
Schulze Jan K5  
Schulz-Siegmund Michaela K5  
Ścisłowska-Czarnecka Anna 207  
Scopece Paolo 50, 185  
Sedlarikova Jana 187  
Sekuła Małgorzata 217  
Sepulveda-Guzman Selene 112  
Setti Chiara 35  
Seyhan Serap Ayaz 88, 162, 163  
Shah Hetvi 30  
Shi Liyang 99  
Shin Jung Min 103  
Šiffalovič Peter 66  
Silva Jean 208  
Simon Melinda 202  
Sinha Ravi 50  
Sioga Antonia 69  
Sionkowska Alina 143, 213  
Sisani Michele 50  
Skalniak Łukasz 193  
Skoczeń Monika 119  
Skopinska-Wisniewska Joanna 213  
Skórska-Stania Agnieszka 146  
Ślósarczyk Anna 90, 121  
Sobieszuk Paweł 115  
Sobolewski Peter 74  
Sokołowska Emilia 9

Solarz Daria 206  
Soldani Giorgio 92  
Solecka Agnieszka 191  
Song Seok Ho 103  
Soskind Rose 154  
Sotiropoulos Damianos 69  
Sotirov Sotir 144, 145  
Spano Raffaele 38  
Šrámková Petra 32  
Stachewicz Urszula 77, 114, 203, 204  
Stachowiak Natalia 143  
Steele Joseph PL4  
Stępak Bogusz 189  
Stepanova Alena 137  
Stępień Karolina 74  
Stern Dganit 44  
Stodolak-Zych Ewa 148, 149, 191, 207  
Stratakis Emmanuel 25, 28  
Strömberg Gustav 7  
Su Sena 34  
Suarato Giulia 35  
Sumarokova Maria 59  
Sundermann Julius 152  
Sung Lee Doo 173  
Świergosz Tomasz 164  
Świąszkowski Wojciech 93  
Świętek Małgorzata 193  
Sydow Steffen 83, 152  
Szafraniec Joanna 130  
Szaraniec Barbara 4, 6, 126, 148  
Szczubiałka Krzysztof 9, 192  
Szewczyk Piotr K. 77, 114

## T

Tamamis Phanourios 201  
Tanzi Maria Cristina K9  
Terzi Umit 85  
Tezcaner Aysen 76, 116, 117  
Thanh Phan Binh Thi 101  
Thavasyappan Thambi 173  
Thienpont Hugo 105  
Thiré Rossana 1, 208  
Thuy Trang Duong Huu 173  
Toca-Herrera José Luis 59  
Tomanik Magdalena 189, 190  
Topa Monika 166  
Topsakal Aysenur 104  
Torres Maria Camara 50  
Tratyak Stanislaw 78  
Trelová Dušana 66  
Trembecka-Wójciga Klaudia 127  
Tronci Giuseppe 3  
Tryba Anna 2  
Tryba Anna-Maria 153, 200  
Tsai Ching-Cheng K7  
Tylman Michał 102  
Tymowicz-Grzyb Paulina 186  
Tytgat Liesbeth PL2, 105

## U

Uhelská Lucia 66  
 Uppstu Peter 7  
 Ura Daniel 204  
 Uriarte Losada Nerea 126  
 Uzunova Yordanka 144

## V

Valentini Paola 38  
 Vamvakaki Maria K1  
 Van der Belt-Gritter Betsy K8  
 Van der Mei Henny K8  
 Van Gaal Ronald 22  
 Van Hoorick Jasper PL2  
 Van Vlierberghe Sandra PL2, 14, 105, 212  
 Várdai Róbert 202  
 Vasiliu Silvia 134  
 Vázquez-Lasa Blanca 73  
 Vazquez-Serrano Laura 183  
 Veglianesi Pietro 57  
 Venclíková Kristýna 165  
 Verga Emmanuele 185  
 Vignali Emanuele 92  
 Villiou Maria 17  
 Viraneva Asya 144  
 Vlaeva Ivanka 144  
 Vo Nga 171  
 Voigt Sibylle 110  
 Voinova Vera 87, 175, 177, 205  
 Vrana Nihal Engin 117  
 Vukajlovic Durda 56

## W

Wach Radoslaw 62  
 Walas Karolina 164  
 Wali Ashwini 46  
 Wandzik Ilona 51, 176  
 Wang Yi-Ting 129  
 Ward Danny 120  
 Waśkiewicz Sylwia 176  
 Weber Andreas 59  
 Wegrzyn Małgorzata 18  
 Weselucha-Birczynska Aleksandra 193, 194  
 Wietrzyk Joanna 9  
 Willenbacher Norbert 42  
 Williams Caroline 18  
 Wiśniewska Anna 106  
 Wiśniewski Zdzisław 186  
 Witko Małgorzata 206  
 Witko Tomasz 206  
 Włodarczyk Janusz 184  
 Włodarczyk-Biegun Małgorzata 17  
 Wojasinski Michal 12, 115, 199

Wolski Karol 179  
 Wood David 3  
 Woźniak Bartosz 122  
 Wytrwal-Sarna Magdalena 192

## X

Xagorari Angeliki 69

## Y

Yakovlev Sergey 205  
 Yakushev Pavel 61  
 Yamala Anil 29  
 Yang Gi Hoon 72, 82, 84  
 Yang Sung Ho K10  
 Yang Xin 156  
 Yang Ying 65, 165  
 Yen Hsiao-Cheng 129  
 Yeniay Eda 107  
 Yeo Miji 72, 82, 84  
 Yorov Tsvetan 145  
 Younes Husam 36  
 Yovcheva Temenuzhka 144  
 Yu Jiasheng K7  
 Yusa Shin-Ichi 9

## Z

Zaat Sebastian 22  
 Zaborniak Izabela 55  
 Zaccaria Sabrina 22  
 Zagrajczuk Barbara 113, 118  
 Zandi Mojgan 108  
 Zapata-Gonzalez Ivan 31  
 Zapotoczny Szczepan 130, 139, 188  
 Zazakowny Karolina 196, 198  
 Zehtabi Fatemah K2  
 Zeugolis Dimitrios 37, 47, 49, 53  
 Zhao Yunnan 99  
 Zharkova Irina 205  
 Zhdanko Tsimafei 26  
 Zhuikov Vsevolod 205  
 Zhura Alexandr 78  
 Ziąbka Magdalena 167, 216  
 Zima Aneta 90, 121  
 Złocista-Szewczyk Natalia 217  
 Zoratto Nicole 140  
 Zuba-Surma Ewa 217  
 Zuza Ester 21  
 Zych Łukasz 207



# MAASTRICHT ESB2018

**29<sup>TH</sup> EUROPEAN CONFERENCE ON BIOMATERIALS**  
the annual conference of the European Society for Biomaterials  
9-13 September 2018 MECC | Maastricht, The Netherlands



[WWW.ESB2018MAASTRICHT.ORG](http://WWW.ESB2018MAASTRICHT.ORG)

SAVE  
THE  
DATE



# 27th Biomaterials in Medicine and Veterinary Medicine Annual Conference

11 – 14 October 2018 Rytyro, Poland



SAVE THE DATE

11-14

OCTOBER  
2018

[www.biomat.agh.edu.pl](http://www.biomat.agh.edu.pl)



REGISTER  
AND  
SUBMIT  
AN ABSTRACT





# BOOK OF ABSTRACTS

## Implementing Multifunctionality in Polymeric Biomaterials for Medical Applications

Andreas Lendlein<sup>1,2</sup>

<sup>1</sup>Institute of Biomaterial Science and Berlin-Brandenburg Centre for Regenerative Therapies (BCRT),  
Helmholtz-Zentrum Geesthacht, Kantstraße 55, 14513 Teltow, Germany

<sup>2</sup>University of Potsdam, Karl-Liebknecht-Straße 24-25, 14476 Potsdam, Germany  
[andreas.lendlein@hzg.de](mailto:andreas.lendlein@hzg.de)

The combination of multiple functions in biomaterials is needed to fulfil the complex demands in modern medicine. There is no uniform concept to achieve multifunctionality. Different concepts can be followed to integrate different functions in one material system. Such systems can be complex molecular polymer network architectures, which are potentially equipped with side chains or specific functional groups. Multi-material systems can be designed in a way that novel functions are created by the clever combination of different materials (e.g. rigid structures in combination with thermosensitive gels resulting in directed stimuli-controlled shape changes). Function can also be assigned to different length scales in hierarchically structured materials.

Temporal and spatial separation of functions are also versatile options for achieving multifunctionality. In this presentation examples for multifunctional polymeric biomaterials will be given. Structured bio-based polymers are formed as 3D-structural hydrogels, which are able to modulate tissue regeneration *in vivo*.<sup>1,2</sup> In ocular microstents from hydrophobic copolymers, the structural support to keep drainage pathways open was combined with a spatially directed drug release functionality.<sup>3</sup>

Polycationic blocks conjugated with a hydrophobic macromolecular linker have attracted attention to combine high transfection efficiencies with low toxicity in gene delivery, where nucleic acid binding, transportation, and intracellular targeting functions have to be implemented. The design of hydrophobic blocks that are degradable, a function of particular interest for sensitive primary cells, was explored by introducing weak links into degradable copolyester blocks. These carriers enabled a remarkably efficient siRNA delivery *in vitro*.<sup>4</sup>

### REFERENCES

1. Neffe A. T., *et al.*, *Adv. Mater.* 27, 1738-1744, 2015
2. Lohmann P. *et al.*, *Biomaterials* 113, 158-169, 2017
3. Wischke C. *et al.*, *J. Controlled Release* 172, 1002-1010, 2013
4. Wang W., *et al.*, *J. Controlled Release* 242, 71-79, 2016

## Crosslinkable Hydrogels Tailored towards Processing and Biomedical Needs

Jasper Van Hoorick<sup>1,2</sup>, Liesbeth Tytgat<sup>1,2</sup>, Aysu Arslan<sup>1</sup>, Peter Gruber<sup>3,4</sup>, Marica Markovic<sup>3,4</sup>, Aleksandr Ovsianikov<sup>3,4</sup>, Peter Dubrue<sup>1</sup>, Sandra Van Vlierberghe<sup>1,2</sup>

<sup>1</sup>Polymer Chemistry & Biomaterials Group, Centre of Macromolecular Chemistry, Ghent University, Belgium

<sup>2</sup>Brussels Photonics, Vrije Universiteit Brussel, Belgium

<sup>3</sup>Institute of Materials Science and Technology, Vienna University of Technology (TU Wien), Austria

<sup>4</sup>Austrian Cluster for Tissue Regeneration (www.tissue-regeneration.at)

[Sandra.VanVlierberghe@UGent.be](mailto:Sandra.VanVlierberghe@UGent.be)

### INTRODUCTION

Biofabrication is a specific area within the field of tissue engineering which takes advantage of rapid manufacturing (RM) techniques to generate 3D structures which mimic the natural extracellular matrix (ECM). A popular material in this respect is gelatin, as it is a cost-effective collagen derivative, which is the major constituent of the natural ECM. The material is characterized by an upper critical solution temperature making the material soluble at physiological conditions. To tackle this problem, the present work focusses on different gelatin functionalization strategies which enable covalent stabilization of 3D gelatin structures.

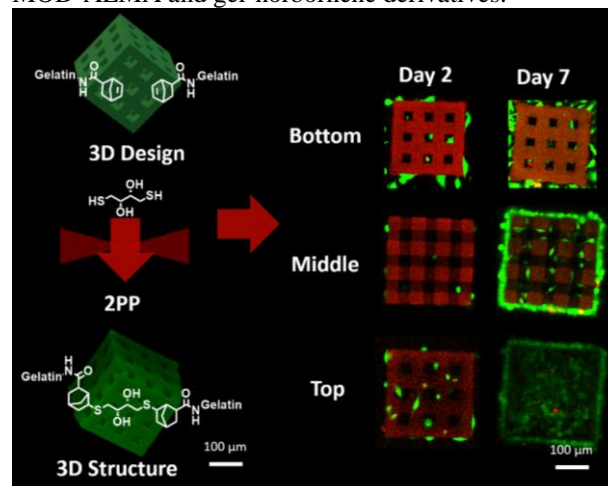
In a second part, synthetic acrylate-encapped, urethane-based precursors will be discussed with exceptional solid state crosslinking behaviour compared to conventional hydrogels.<sup>1,2</sup>

### RESULTS AND DISCUSSION

The first modification consists of methacrylation of the primary amines present in gelatin type B using methacrylic anhydride to obtain gel-MOD. As a consequence, the material becomes (photo-) crosslinkable using a chain growth polymerization mechanism. As a result, both extrusion- (e.g. Bioplotting) as well as irradiation-based rapid manufacturing (RM) techniques (e.g. two-photon-polymerization or 2PP) can be applied for biofabrication. Despite the proven material track record in biofabrication, it exhibits limitations in terms of post-production swelling and mechanical properties. To overcome these limitations, additional crosslinkable methacrylates can be introduced by additional carboxylic acid modification of the glutamic and aspartic acid side chains in gel-MOD with aminoethyl methacrylate via conventional carbodiimide coupling chemistry (EDC/NHS) to generate gel-MOD-AEMA.<sup>3</sup> As a result, more densely crosslinked hydrogels can be obtained with a low to fully absent swelling degree, making the material more suitable towards high resolution RM techniques including 2PP.

To further increase the gelatin versatility, a third modification strategy was pursued during which norbornene functionalities were introduced to the primary amines.<sup>4</sup> These functionalities have a very interesting reactivity towards thiols, as they can be applied for very fast, "spring-loaded" orthogonal thiol-ene "photo-click" reactions. When using multivalent thiol crosslinkers, crosslinked hydrogels can be obtained using significantly shorter irradiation times and/or doses. All developed derivatives were characterized in depth for their material properties

(NMR, rheology, swelling,...) as well as biocompatibility by monitoring the metabolic activity of L929 fibroblasts and MC3T3 osteoblasts seeded onto thin crosslinked films. The metabolic assay indicated no significant difference between the gelatin derivatives in terms of biocompatibility. Furthermore, proof of concept biofabrication experiments were performed. Micro-scaffolds were generated using 2PP which indicated superior processing capabilities for the gel-MOD-AEMA and gel-norbornene derivatives.



### CONCLUSION

Chemistry is a valuable tool to tailor the properties of hydrogels towards processing while preserving the material biocompatibility.

### REFERENCES

1. Houben. *et al.*, Materials Today Chemistry. 4:84-89, 2017
2. Houben. *et al.*, WO 2017/005613
3. Van Hoorick. *et al.*, Biomacromolecules. 18:3260-3272, 2017
4. Van Hoorick. *et al.*, Macromolecular Rapid Communications, accepted, 2018

### ACKNOWLEDGMENTS

The Research Foundation Flanders (FWO, Belgium) is acknowledged for financial support under the form of PhD grants (J.V.H. and L.T.) and research grants (FWOKN273, G005616N, G0F0516N). The FWO-FWF grant (Austrian Science fund project, FWF) is acknowledged for financial support (FWOAL843, #I2444N28). A.O. would like to acknowledge the European Research Council for financial support (Starting Grant No. 307701).

## Controlled Spatiotemporal Signal Presentation within High-Density Cell Culture Systems for Engineering Complex Tissues

Eben Alsberg

Department of Biomedical Engineering, Department of Orthopaedic Surgery,  
National Center for Regenerative Medicine, Division of General Medical Sciences,  
Case Western Reserve University, USA  
[exa46@case.edu](mailto:exa46@case.edu)

Tissue engineering holds the promise of producing functional biological replacements to treat lost or damaged tissues. Biomaterials can be designed to partially recapitulate the intricate signals that are implicated in tissue development and healing to regulate cell gene expression and new tissue formation. This talk will introduce high-density cultures of cells that can mimic immature condensates present during many developmental and healing processes. Delivering specific soluble signals exogenously in tissue culture media can regulate cell behavior in these cultures and promote new tissue formation. However, shortcomings of this approach include transport issues, limited spatial control over signal presentation, and required repeated dosing in the media. Incorporating biopolymer microparticles containing bioactive signals within the high-density cell cultures can overcome these challenges and permit localized spatial and temporal control over the presentation of regulatory cues to the cells. I will present our research using this strategy to engineer a variety of tissues, including bone, cartilage and trachea. The capacity to deliver diverse signals, including growth factors and plasmid DNA, for driving new tissue formation will be demonstrated. In addition, the value of this technology for engineering a wide range of tissue shapes, including spheres, sheets, rings and tubes will be examined. Finally, the utility of providing cell-instructive bioactive factors from biomaterials in a controlled manner for the assembly of modular tissue units to engineer complex constructs comprised of multiple tissue types will be explored.



## Understanding the Effect of Biomaterials on Cell and Stem-cell Differentiation

Alexandra Pastino<sup>1</sup>, Joseph Steele<sup>1</sup>, Yong Mao<sup>1</sup>, Prabhas Moghe<sup>2</sup>, Joachim Kohn<sup>1</sup>

<sup>1</sup>New Jersey Center for Biomaterials at Rutgers University, USA

<sup>2</sup>Department of Biomedical Engineering, Rutgers University, USA

[joachimkohn@gmail.com](mailto:joachimkohn@gmail.com)

### INTRODUCTION

Starting about 60 years ago, biomaterials scientists recognized the importance of the integrin-mediated signalling that influences key cellular responses such as attachment, migration, and proliferation. Since then, thousands of research publications have provided an increasingly detailed understanding of the effects of specific substrate properties on cell behaviour. Particularly fascinating were early studies showing how chemical composition, topography and surface architecture of 2D substrates and 3D scaffolds can affect the cellular response. These insights resulted in a significant shift from the early biomaterials (stable, inert materials such as polypropylene, polytetrafluoroethylene (PTFE), stainless steel) to biodegradable materials (such as the family of polyesters made of lactic and glycolic acid), to bioactive materials that are specifically designed to elicit unique cellular responses. An additional research direction was opened up when it was realized that stem cell differentiation is also profoundly affected by the properties of the substratum on which the cells are cultured. While cell biologists often limit their studies of stem cell differentiation on the effect of soluble factors (such as cytokines or growth factors that are added to the culture medium), an increasing body of knowledge indicates that the substratum has an equally important effect on stem cell differentiation. Recently, we discovered that high content imaging methods can be used to predict the differentiation pathway of cultured stem cells.

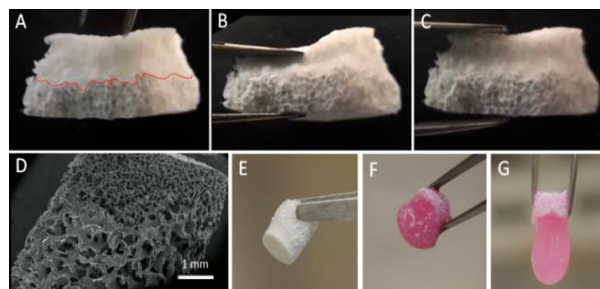
### RESULTS AND DISCUSSION

Fig. 1 illustrates current work aiming to design bioactive scaffolds for specific cell types. In this case, an attempt was made to build a scaffold for the regeneration of the osteochondral interface, the area in all articulating joints where bone transitions into cartilage. Osteoblasts and chondrocytes require different substrata for optimum proliferation and to retain their respective phenotypes. This requirement is met by a biphasic scaffold consisting of a layer optimized for bone growth and a layer optimized for cartilage.

Fig. 2 illustrates that stem cell fates on biomaterials are influenced by the complex confluence of micro-environmental cues.<sup>1</sup> Cell–microenvironment interactions influence the cell fate by initiating a series of outside-in signaling events that traverse from the focal adhesions to the nucleus and modulate the sub-nuclear protein organization and gene expression. The splicing factor SC-35 in the nucleoplasm is a potent marker to distinguish between minute differences of stem cell lineage pathways in response to changes in substrate properties. Using High Resolution Image Acquisition (HR IA) of SC-35 domains, followed by feature extraction and machine learning, it was possible to correlate the differentiation pathway of hMSCs with selected substrate properties.

### CONCLUSION

The field of biomaterials science is developing new insights of the biological mechanisms by which substrate chemistry and topography can affect cell behavior, including stem cell differentiation. This research effort will provide the foundation for significant advances in the future.



*Fig. 1: Design of bioactive scaffolds: (A) Red line indicates phase interface. (B) compressed and (C) after release, showing the different mechanical properties of the two components of the scaffold. (D) SEM of pore structure and interface. (E-G) Scaffolds held at bone phase: (E) after sterilization; (F) after 2 day and (G) after 9 days in medium.*

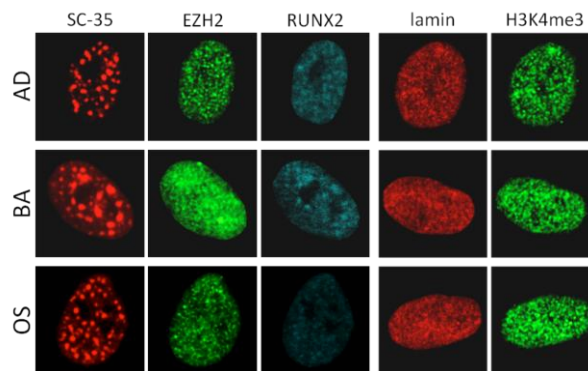


*Fig. 2: hMSCs were grown in adipogenic (AD), basal (BA), and osteogenic media (OS). The texture of five reporter proteins in the nucleus (SC-25, EZH2, RUNX2, lamin, H3K4me3) was captured by High Resolution Image Acquisition (HR IA).*

### REFERENCES

1. Vega, S.L. et al., Integrative Biology, *Integr. Biol.*, 2015,7, 435-446

### ACKNOWLEDGMENTS

This work was supported by NIH Grant P41 EB001046 through RESBIO, a national resource for polymeric biomaterials and the New Jersey Center for Biomaterials at Rutgers University

## PLLA-based Copolymeric Biomaterials for Bone Tissue Engineering

Maria Kaliva<sup>1,2</sup>, Anthie Georgopoulou<sup>1</sup>, Costas Charitidis<sup>3</sup>, Maria Chatzinikolaidou<sup>1,2</sup>, Maria Vamvakaki<sup>1,2</sup>

<sup>1</sup>Department of Materials Science and Technology, University of Crete, Greece

<sup>2</sup>Institute of Electronic Structure and Laser, Foundation for Research and Technology Hellas, Greece

<sup>3</sup>School of Chemical Engineering, National Technical University of Athens, Greece

[mchatzin@materials.uoc.gr](mailto:mchatzin@materials.uoc.gr)

### INTRODUCTION

This study focuses on the development of graft copolymeric biomaterials based on poly(L-lactide) (PLLA) and chitosan (CS) with tunable chemical and mechanical properties, and the evaluation of the biological response of pre-osteoblastic cells cultured on them.

CS, a natural polysaccharide, is a biocompatible polymer, slightly soluble in the aqueous culture medium with poor mechanical properties<sup>1</sup>. PLLA, is a biocompatible synthetic polymer with excellent mechanical properties<sup>2</sup>. Grafting the synthetic polymer along the CS backbone is an attractive way to regulate the physical and mechanical properties of the latter. In this work, we present the preparation of two CS-g-PLLA graft copolymers, CS-g-PLLA(20) and CS-g-PLLA(50), with 20 wt% and 50 wt% PLLA content, respectively, their mechanical properties and biological evaluation in pre-osteoblastic cells.

### EXPERIMENTAL METHODS

The CS-g-PLLA copolymers were synthesized by grafting PLLA chains, carrying a terminal carboxylic acid group, along the CS backbone<sup>3</sup> and were characterized in terms of their physicochemical and nanomechanical properties. Discs and thin films of the CS-g-PLLA(20) and CS-g-PLLA(50) copolymers were prepared to study the degradation profile and the nanomechanical properties of the copolymers, respectively, and also investigate the morphology, viability, proliferation and osteogenic response of MC3T3-E1 pre-osteoblastic cells on them.

### RESULTS AND DISCUSSION

We prepared CS-g-PLLA graft copolymers with PLLA content of 20 wt% and 50 wt%. Analysis of the <sup>1</sup>H NMR data allowed to calculate the copolymer grafting density, which was found to be one PLLA chain every 180 CS monomer repeat units for CS-g-PLLA(20) and one PLLA chain every 25 CS monomer repeat units for CS-g-PLLA(50). Degradation studies showed a total weight loss of 9% after 21 days in cell culture medium for both copolymers. Nanomechanical characterization indicated significantly higher Young modulus and hardness values for CS-g-PLLA(20) compared to CS-g-PLLA(50), which may be attributed to the higher viscoelasticity of the sample with the higher CS content. Biological experiments showed that both CS-g-PLLA copolymers promote pre-osteoblastic cell adhesion, viability and proliferation, and increase the levels of osteogenic markers, with the CS-g-PLLA(50) material exhibiting a significant increase in cell proliferation.

### CONCLUSION

We have synthesized CS-g-PLLA copolymers by grafting end-functionalized PLLA chains along the CS backbone, varying the PLLA content at 20 wt% and 50 wt% and controlling their nanomechanical properties. The biological assessment of the copolymers shows strong cell adhesion, increased proliferation for a time period up 7 days in culture, and increased osteogenic response of pre-osteoblastic cells on both CS-g-PLLA materials.

### REFERENCES

1. Madhally S.V. *et al.*, *Biomaterials* 20:1133-42, 2009.
2. Nampoothiri K.M. *et al.*, *Bioresource Technology* 101:8493–8501, 2010
3. Chatzinikolaidou M. *et al.*, *Curr. Pharm. Des.* 20:2030-2039, 2014

### ACKNOWLEDGMENTS

The authors acknowledge financial support from the General Secretariat for Research and Technology Aristeia II Grant ‘Osteobiomimesis 3438’ MIS 525089.



## Chitosan-based Embolizing Hydrogel for Endovascular Therapies: Characterization of Rheological and Occlusive Properties

Ahmed Fatimi<sup>1,2,3,4</sup>, Fatemeh Zehtabi<sup>3,4</sup>, Sophie Lerouge<sup>3,4</sup>

<sup>1</sup>LGB, FST, Sultan Moulay Slimane University, Mghila BP.523, Béni-Mellal 23000, Morocco

<sup>2</sup>Department of Chemistry, FP, Sultan Moulay Slimane University, Mghila BP.592, Béni-Mellal 23000, Morocco

<sup>3</sup>Department of Mechanical Engineering, ETS, 1100 Notre-Dame Street West, Montréal H3C1K3, Canada

<sup>4</sup>LBeV, Research Centre of CHUM, 900 St Denis, Tour Viger, Montréal H2X0A9, Canada

[a.fatimi@usms.ma](mailto:a.fatimi@usms.ma)

### INTRODUCTION

In the last years biopolymers have been investigated for potential applications in the biomedical field, mainly as hydrogels for minimally invasive procedures and tissue engineering strategies. Among the natural polymers, chitosan, obtained by alkaline deacetylation of chitin, has been one of the most widely studied, notably because of its ability to form in situ gelling hydrogels at room temperature and physiological pH when combined with a weak base such as  $\beta$ -glycerophosphate ( $\beta$ GP).<sup>1</sup>

Recently, chitosan hydrogel was shown to be a potential candidate for the embolization of blood vessels especially to treat or prevent endoleaks following endovascular aneurysm repair (EVAR).<sup>2</sup>

For these applications, chitosan gels must be made radio-opaque since successful embolization is largely dependent on controlled injection and real-time monitoring during injection using X-ray fluoroscopy.

The aim of this study was to develop and characterize an injectable radio-opaque hydrogel. We studied the effect of the contrast agent and  $\beta$ GP concentration on the chitosan hydrogel behavior, with respect to their gelation kinetics, rheological and occlusive properties, morphology, radiopacity and swelling.

### EXPERIMENTAL METHODS

Chitosan hydrogels with different concentrations of visipaque (contrast agent containing iodixanol) and  $\beta$ GP were prepared. The gelation kinetic and rheological properties were studied by rheology on a Physica MCR301 (Anton Paar), by following the evolution of both storage ( $G'$ ) and loss ( $G''$ ) moduli as a function of time at 37°C. Gel occlusive properties were assessed on a custom-made embolization bench system designed to evaluate the ability of the gel to occlude blood flow by measuring the maximal pressure of liquid sustained by the gel-embolized tubular structure. The system consists in a syringe filled with water mixed with glycerol 40% to mimic blood viscosity.

The morphology of chitosan hydrogels was carried out on an SU-70 electron microscope (Hitachi Ltd.).

The chitosan hydrogel samples were observed by fluoroscopy using an angiography X-ray system (Hicor/ACOMTop, Siemens Medical). The radiopacity of different hydrogels was then evaluated by calculating the mean X-ray attenuation in Hounsfield units.

The swelling property of chitosan hydrogels was assessed gravimetrically.

### RESULTS AND DISCUSSION

The initial  $G'$  was already higher than  $G''$ , indicating that chitosan samples gelled immediately. The  $G'$

modulus increases with time, while  $G''$  reaches a pseudo-plateau. This dramatic increase in  $G'$  is attributed to the fast initial rate of the network formation.  $\beta$ GP concentration has a strong effect on the gelation time and the gelation rate. The gelation of chitosan containing 20% visipaque was immediate for  $\beta$ GP concentrations of 12% or above.

After 1 day, all hydrogels were able to occlude blood flow up to the maximal pressure applied in this bench test (220mmHg). However, for shorter gelation times, the maximal pressure sustained by the gels varied strongly as a function of their composition. The maximal pressure sustained by chitosan and 20% visipaque hydrogels prepared with 12% and 20%  $\beta$ GP. When hydrogels were prepared with 20%  $\beta$ GP, they were able to immediately occlude the tubular structure, up to the maximal pressure.

The structure of the cross-sectional area of each hydrogel showed clear differences in the matrix structure as a function of the amount of contrast agent. Chitosan hydrogels exhibited an open and a porous structure, and the porosity decreased as the visipaque concentration increased. The cross-sectional areas of the same hydrogels, but which were rinsed in saline beforehand, were also examined. Rinsing had an effect on the morphology of CH/VIS, which tend back to the typical open porous structure of pure chitosan.

Radiopacity expressed in Hounsfield units increased with the percentage of visipaque in a relatively linear fashion. As expected, the radiopacity strongly decreased after immersion for 24 hours in saline, which is consistent with a rapid release of the contrast agent, as already observed.<sup>3</sup> The release was not completed after 24 hours since the gels were still significantly more radiopaque than chitosan controls.

Swelling results showed that swelling was strongly reduced when increasing the visipaque concentration in the hydrogel, confirming that chitosan becomes much less hydrophilic when visipaque is added.

### CONCLUSION

Chitosan was combined with  $\beta$ GP and visipaque contrast agent (iodixanol), and the thermogels were characterized by complementary techniques (rheology, embolization, SEM, X-ray and swelling) to optimize and evaluate their potential as injectable occlusive agents for endovascular therapies.

### REFERENCES

1. Chenite A. *et al.*, Biomaterials. 21:2155-2161, 2000
2. Fatimi A. *et al.*. Acta Biomater. 8:2712-2721, 2012
3. Fatimi A. *et al.*, Adv Mat Res. 409:129-135, 2012

## Controlled drug delivery from 3D printed poly-l-lactic acid bioresorbable stent

Mathilde Fiorletta<sup>1</sup>, Cristina Canal<sup>1,2</sup>, Marta Pegueroles<sup>1,2</sup>

<sup>1</sup>Dept. Materials Science and Metallurgical Engineering, EEBE, Technical University of Catalonia (UPC), Spain

<sup>2</sup>Barcelona Research Center in Multiscale Science and Engineering, UPC, Spain

[marta.pegueroles@upc.edu](mailto:marta.pegueroles@upc.edu)

### INTRODUCTION

Bioresorbable stents (BRS) are designed to overcome perceived limitations of drug-eluting stents (DES) by providing temporary support to the vessel wall, whilst simultaneously allowing the release of an anti-proliferative drug to limit the uncontrolled neointimal hyperplasia and tissue proliferation in response to vessel injury that occurs during balloon deployment of the stent<sup>1-2</sup>.

However, BRS in clinical use have three major limitations: (a) the low expandable capacity of stents related to low mechanical properties; (b) the high thickness of the struts and; (c) the risk of late thrombosis associated with the surface qualities of the implant. The main objective of this project is the development of a 3D printed BRS with enhanced mechanical properties and antithrombotic drug delivery fabricated by solvent-cast direct-write technique.

### EXPERIMENTAL METHODS

3D printed stents were obtained with a fused deposition modelling (FDM) 3D printer (BCN 3D+, BCN 3D technologies) modified by introducing a rotating mandrel to print cylindrical monolayer structures. The ink was a solution of poly-l-lactic acid (PLLA, PL65, Purasorb) w/w acetylsalicylic acid (ASA) in chloroform dissolved in a speed mixer (SpeedMixer™, FlackTek). 3 mm diameter stents were printed by solvent-cast direct-write (SC-DW) with different number of peaks at the end of the stent: 10 and 15 (P10 and P15) and a final ASA loading of 2.2 or 3.3 mg for each stent. They were subsequently treated thermally for 12 h at 80°C.

The obtained stents were characterised by SEM and DSC. Compression test between parallel plates were carried at a crosshead speed of 0.2 mm/s with a materials tester (SMS Materials test, Texture analyser model MT-LQ). Drug delivery assays were performed in PBS during 12 days at 37°C with stirring. The detection of the drug was performed by adding 0.8% of 1 M NaOH and the solution was diluted with a 0.02 M iron (III) solution and absorbance measured  $\lambda_{\max} = 530$  nm. Cytotoxicity with HUVEC was performed by means of lactate dehydrogenase test (LDH, Roche). Statistical analysis was realised by non-parametric Mann-Whitney U-test using Minitab software.

### RESULTS AND DISCUSSION

Drug loaded PLLA biodegradable stents of 3 mm diameter and 15-20 mm length were obtained by means of a modified FDM 3D printer with 130  $\mu$ m strut diameter (Fig. 1).

SEM images showed porosity at the external surface of the struts due to chloroform evaporation in non-loaded ASA stents. The addition of ASA affected the solvent evaporation rate reducing the porosity (Fig. 1).

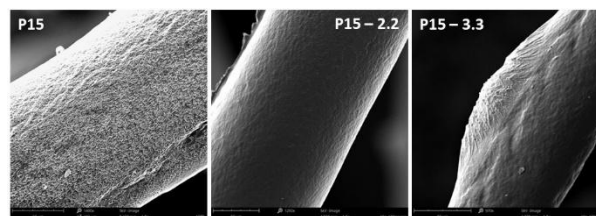


Fig. 1. SEM images of stents without (P15) or with ASA (P15-2.2 and P15-3.3).

Drug release depends on the initial concentration and the exposed surface to the PBS. Stents with higher loadings (P10-3.3) showed a certain burst released followed by sustained release. In contrast, in stents with lower loading the release was linear for 2 weeks and with potential for longer release. After 12 days, all stents presented a final release of 60-70%.

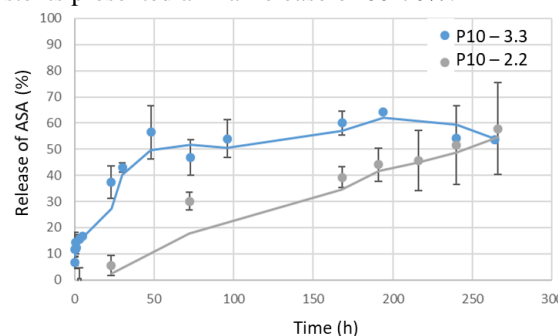


Fig. 2. Release percentage of ASA on P10 stents.

Compression tests indicated a higher radial strength as increases the number of peaks of the stent also correlated with the increasing crystallinity. The addition of ASA up to 2.2 mg did not change the mechanical properties while series with 3.3 mg decreased significantly. After stents degradation into PBS, radial strength decreased more than 50% for the non-loaded ASA stents while only a 2-4% for drug loaded stents. Finally, biological tests confirmed that the 3D printed stents were not cytotoxic.

### CONCLUSION

The fabrication of a drug eluting stent by 3D printing was successfully achieved by SC-DW with a self-modified FDM. Its sustained release properties depended on the drug concentration and construction characteristics of the stent. Biological assays confirmed that 3D printed stents were not cytotoxic.

### REFERENCES

1. Busch R. *et al.*, Acta Biomater. 10(2): 688-700, 2014
2. Tenekecioglu E. *et al.*, BMC Cardiovasc Disord. 16(1):38, 2016

### ACKNOWLEDGMENTS

Spanish Government, MINECO/FEDER, (Grant no: MAT2015-67183-R and Grant no: DTS16/00133).

## Tailoring of Implant-tissue Interface: PLGA-Parylene C Multifunctional Coating

Monika Golda-Cepa<sup>1</sup>, Aleksandra Chorylek<sup>1</sup>, Paulina Chytrosz<sup>1</sup>, Monika Brzychczy-Wloch<sup>2</sup>, Minna Hakkarainen<sup>3</sup>, Klas Engvall<sup>4</sup>, Andrzej Kotarba<sup>1</sup>

<sup>1</sup>Faculty of Chemistry, Jagiellonian University, Poland

<sup>2</sup>Department of Bacteriology, Microbial Ecology and Parasitology, Jagiellonian University Medical College, Poland

<sup>3</sup>Department of Fiber and Polymer Technology, KTH Royal Institute of Technology, Sweden

<sup>4</sup>Department of Chemical Engineering and Technology, KTH Royal Institute of Technology, Sweden  
[kotarba@chemia.uj.edu.pl](mailto:kotarba@chemia.uj.edu.pl)

### INTRODUCTION

The challenges of metal implant surface engineering are to introduce specific properties which result in optimization of the metal-implant tissue interface. One of the most explored approaches is coating metal implants with a polymer which can be additionally furnish with functions essential for a long-term implantation success, namely: anti-corrosive, biocompatibility, anti-infection and therapeutic. Extensive research worldwide is carried out on improving biocompatibility of implant surfaces in terms of osteoblasts adhesion and anti-bacterial function. Furthermore, the most common post-operation complications include prolonged inflammation and biomaterial-centered infection. For these reasons, main strategies rely on surface functionalization and/or controlled local drug release from the inserted implant, bringing a number of benefits to patients. The aim of the study was to develop a multifunctional polymer coating based on drug+PLGA/parylene C with four essential functions. The general concept of the integrated research is highlighted.

### EXPERIMENTAL METHODS

Parylene C micrometric films were prepared by CVD technique. To generate oxygen-containing surface functional groups and nanotopography, polymeric samples were modified using oxygen plasma. For the therapeutic layer preparation, the biodegradable copolymer PLGA (85/15) was used.<sup>1</sup> PLGA was dissolved with ibuprofen or gentamicin and deposited on the modified parylene C. The obtained multifunctional coating was then thoroughly characterized using physicochemical (SEM,  $\mu$ FTIR, LDI-MS) and biological (*in vitro* cells and microbiological) methods. In order to identify drugs elution kinetics, *in vitro* drug release studies were carried out. The release data were fitted into kinetic models.<sup>2</sup>

### RESULTS AND DISCUSSION

The key functions of the designed coating are the anti-corrosive properties, biocompatibility, anti-infection and therapeutic (Fig. 1). It was found that Parylene C micrometric coatings provides superior increase in corrosion resistance ( $1 \times 10^9 \Omega \text{ cm}^2$ ) comparing with uncoated SS 316L ( $1 \times 10^4 \Omega \text{ cm}^2$ ).<sup>3</sup> Plasma induced modifications of parylene C consist in changes in its surface chemical composition by generation of functional groups ( $-\text{COOH}$ ,  $-\text{OH}$ ) as well as nanotopography. The staining of focal contacts of MG-

63 cells together with SEM observations revealed improved biocompatibility of oxygen plasma modified parylene C. Moreover, the generated nanotopography, effectively limited the surface area available for bacteria. SEM observations revealed, that early-stage biofilm formation on unmodified parylene C takes place after 4 h of incubation, after the same time interval, on the surface of oxygen plasma treated samples not agglomerated; single bacteria cells dominated the picture. The studies of drug+PLGA/parylene C systems revealed that the drugs molecules remain unchanged upon interaction with the PLGA matrix and the drugs distribution were homogenous. The obtained release profiles revealed that both of the investigated systems (ibuprofen- and gentamicin-loaded) are suitable for prolonged elution up to 21 days. However, they follow different kinetic models.<sup>3</sup>

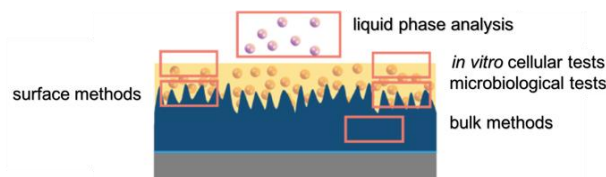


Fig. 1. The graphical representation of the integral approach for the design and development of PLGA+drug/parylene C systems

### CONCLUSION

Oxygen insertion into the parylene C surface provides a suitable substrate for MG-63 cells attachment and spread while nanoroughness effectively limits risk of infection. Modified parylene C allows also further tuning of the coating functionality by covering it with a biodegradable drug-loaded PLGA layer, which results in prolonged in-site drug release.

### REFERENCES

1. Dobrzyński P. *et al.*, *Macromolecules* 34: 5090-5098 2001
2. Costa P. *et al.*, *Eur. J. Pharm. Sci.* 13:123-133 2001
3. Golda-Cepa M. *et al.*, *ACS Appl. Mater. Interfaces* 8.34: 22093-22105 2016

## Microparticulate Poly(vinyl alcohol) Hydrogel Formulations for Embedding and Controlled Release of Polyethylenimine (PEI)-based Nanoparticles

Jan Schulze<sup>1</sup>, Stephan Hendrikx<sup>2</sup>, Michaela Schulz-Siegmund<sup>2</sup>, [Achim Aigner](mailto:achim.aigner@medizin.uni-leipzig.de)<sup>1</sup>

<sup>1</sup>Rudolf Boehm-Institute for Pharmacology and Toxicology, Clinical Pharmacology, Leipzig University, Germany

<sup>2</sup>Pharmaceutical Technology, Institute of Pharmacy, Leipzig University, Germany  
[achim.aigner@medizin.uni-leipzig.de](mailto:achim.aigner@medizin.uni-leipzig.de)

### INTRODUCTION

Nucleic acid-based therapeutics offer enormous potential in the treatment of various pathologies. For DNA or RNA delivery, nanoparticle systems based on lipids or polymers have been developed. Among those, polyethylenimine (PEI) is a promising candidate due to its high biological activity. The combination of PEI-based polyplexes (PP) with liposomes, leading to lipopolyplexes (LPP), further improves nanoparticle properties by combining the beneficial features of both systems. However, colloidal instability in solution, poor storage properties especially as dry powder and little stability against an aggressive environment, e.g. after oral application, are major issues. Furthermore, there is an urgent need for sustained release systems that allow for fine-tuned, long-term temporal and spatial nanoparticle release.

Here, we describe the embedding of PEI-based polyplexes and their corresponding liposome-modified analogues (lipopolyplexes), into microparticulate poly(vinyl alcohol) (PVA) hydrogels, leading to Nanoparticles-in-Microparticle Delivery Systems (NiMDS).

### EXPERIMENTAL METHODS

**Materials:** 10 kDa PEI was purchased from Polyscience (Eppelheim, Germany). DPPC was obtained from Avanti Polar Lipids (Alabaster, USA). PVA 30-70 kDa was purchased from Sigma Aldrich (St. Louis, USA) while 190 kDa PVA (Mowiol® 55-96) was kindly provided from Kuraray (Chiyoda, JPN).

**Preparation of PEI complexes and lipopolyplexes** PEI polyplexes were prepared at PEI/nucleic acid ratio 5 as described<sup>1</sup>. For lipopolyplex preparation, an appropriate amount of preformed liposomes was mixed with PEI complexes and incubated for 60 min.

**Preparation of PVA hydrogels.** Preformed (lipo-) polyplexes were suspended in a PVA solution and stirred until homogeneously suspended. Then, Span® 80 and Miglyol® 812 were added. The resulting emulsion was homogenized and added dropwise to a larger volume of acetone in order to precipitate the microparticles. For modifying their release kinetics from the NiMDS, the nanoparticles were suspended in 190 kDa PVA and the emulsion was frozen and thawed to crosslink the PVA, prior to precipitation in acetone. For spray drying of PVA microparticles, a Büchi Mini Spray Dryer B-191 (Essen, Germany) was used.

**Various parameters were modified:** PVA was explored with two different molecular weights and at different concentrations, different emulsifiers and acetone for extraction were employed, and the protocol was performed with or without repetitive freeze/thaw cycles for physical PVA crosslinking.

### RESULTS AND DISCUSSION

We show that polyplexes or lipopolyplexes released from PVA-MPs do not change in size compared to their freshly prepared counterparts<sup>2</sup>. Quite in contrast, a marked alteration of the zeta potential is observed after PVA encapsulation. The released nanoparticles show profound cellular uptake and transfection efficacy, resulting in high luciferase or EGFP expression. All tested formulations were nontoxic. Sizes of released nanoparticles remained unchanged during their storage as suspension in pure water, revealing a stabilizing 'PVA corona effect'. This was paralleled by biological activities of the nanoparticles remaining at the high levels, even after storage for at least 12 weeks at r.t.

Aiming at the modification of nanoparticle release kinetics from the PVA microparticles, we employed a freeze/thaw method for physical crosslinking. This led to a sustained release of encapsulated, bioactive nanoparticles over several days, as determined in release studies and in tissue culture experiments.

After spray drying, we obtained this nanoparticle-in-microparticle delivery system as ready-to-use dry powder for the encapsulation of the polyplexes or lipopolyplexes, without requiring additional stabilizing agents<sup>3</sup>. It proved to be an efficient device for the inhalative delivery of lipopolyplexes *in vivo*, as demonstrated by transgene expression in mice lung after only one administration.

### CONCLUSION

Our study shows that embedding PEI-based nanoparticles in a PVA matrix is a suitable system for their controlled release. The PVA matrix provides an easy platform for handling of the (lipo-)polyplexes, preserving their size and integrity, also in the presence of serum. Another favorable property is the preservation of transfection efficacy even upon very prolonged storage at room temperature. The unique character of PVA to crosslink during freeze/thaw cycles offers an attractive approach for fine-tuned, long-term nanoparticle release in possible therapeutic applications. Spray-drying leads to a dry powder allowing prolonged storage as easy-to-handle formulation without loss of nanoparticle activity, also suitable for inhalation.

### REFERENCES

1. Ewe A. *et al.*, *Meth. Mol. Biol.* 1445:198-200, 2016
2. Schulze J. *et al.*, *Acta Biomaterialia* 45:210-22, 2016
3. Schulze J. *et al.*, *Small*, in press.

### ACKNOWLEDGMENTS

This work was supported by grants from the Saxonian Ministry for Science and Art (SMWK), the Deutsche Krebshilfe and the Sächsische Aufbaubank (SAB).



## Modular Tissue Engineering Template Constructs from Fibrous Branched Clusters

Benjamin Minden-Birkenmaier, Gary Bowlin

Biomedical Engineering, University of Memphis, United States of America  
[gbowlin@memphis.edu](mailto:gbowlin@memphis.edu)

### INTRODUCTION

Over the past 20 years, electrospinning has become a commonly accepted method of template fabrication in the field of tissue engineering<sup>1,2</sup>. This method, which involves randomized fiber deposition in two dimensions, has severe limitations with regards to pore size and connectivity which impede cellular infiltration of the template<sup>3</sup>. To address this limitation, in this study electrospun templates were minced into fibrous branched-clusters. These clusters were separated by size and combined with cells in culture. This study tested the hypothesis that cells would bind these branched-clusters into three-dimensional, fully cellularized, modular, three-dimensional tissue engineering constructs.

### EXPERIMENTAL METHODS

#### Branched-cluster Creation

Templates were electrospun from a blend of polydioxanone (PDO) and collagen type II. Templates (fiber diameter:  $1.1 \pm 0.4 \mu\text{m}$ ) were cooled in ethanol to  $-80^\circ\text{C}$  and then minced using a Dremel<sup>®</sup>-driven razor-blade template mincer based on work by Thieme *et al.* at 15,000 rpm for 1 hour<sup>4</sup>. The resulting pulp was separated by centrifugation and filtration into groups of “small”, “medium”, and “large” branched-clusters.

#### Cell Culture

Adult human dermal fibroblasts (HDFs) or porcine chondrocytes (PCs) were combined in 5 mL culture medium (DME/F) in 15 mL conical centrifuge tubes along with various amounts of the different fibrous branched-cluster size groups. These tubes were mixed by inversion every half hour during the first 2 hours of  $37^\circ\text{C}$  incubation, then half of their volume was removed, placed in another 15 mL tube, and centrifuged down to pellet, while the original volume was allowed to settle by gravity. Caps were loosened, and samples were cultured for 21 days, changing medium every 3-4 days. PC constructs were cultured with or without the presence of TGF- $\beta$  and dexamethasone. After 21 days, all samples were formalin fixed.

#### Construct Analysis

Samples, varying in diameter from 1.3 mm to 3.2 mm, were cryosectioned, DAPI-stained, imaged, and analysed with ImageJ to determine cell density and distribution throughout the construct. Other sections were immunostained for Ki-67 to determine cellular proliferation throughout the constructs. Select whole constructs were also analysed via pycnometry to determine their density.

#### Statistical Analysis

A one-way ANOVA with a Holmes-Sidak post hoc test ( $\alpha=0.05$ ) was used to establish statistical significance.

### RESULTS AND DISCUSSION

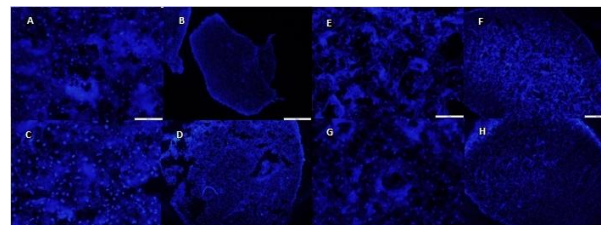


*Fig. 1. Fluorescent images of DAPI-stained HDF samples. These constructs had 500,000 HDFs with (A) and (B): 0.5 mg small, 0.5 mg medium branched-clusters, settled by gravity. (C) and (D): 0.5 mg small, 0.5 mg medium branched-clusters, centrifuged down (E) and (F): 1 mg large branched-clusters, settled by gravity. (G) and (H): 1 mg large branched-clusters, centrifuged down. (A, C, E, G): Scale bar = 100  $\mu\text{m}$ . (B, D, F, H): Scale bar = 500  $\mu\text{m}$ .*

In general, HDFs formed three-dimensional constructs that were cellularized throughout and maintained their form during handling. However, the only chondrocyte constructs to maintain their form were the ones made with small or medium branched-clusters and cultured with TGF- $\beta$  and dexamethasone, or cultured without any branched-clusters at all. Ki-67 staining of the HDF constructs showed low expression (0-2.5% of cells) throughout all sample types, indicating little-to-no proliferation after 3 weeks of culture. Pycnometry of these HDF constructs showed densities ranging from 1.2-1.6 g/mL, above that of skin (1.103 g/mL)<sup>5</sup>.

### CONCLUSION

These results indicate that both HDFs and PCs are able to bind together these branched-clusters into solid, three dimensional tissue-mimicking constructs which are well-cellularized throughout, with no necrosis or necrotic core. This cell distribution was superior to that seen in whole electrospun templates in literature, even when increasing template porosity via sacrificial fibers or air-impedance electrospinning<sup>3,6</sup>.

### REFERENCES

1. Pham Q. *et al.*, Tissue Eng. 12:1197-1211, 2006.
2. Yoo S. *et al.*, Adv Drug Deliver Rev. 61:1033-1042, 2009.
3. McClure M. *et al.*, Biomaterials 33:771-779, 2012.
4. Thieme M *et al.*, Polym Advan Technol 22: 1335-1344, 2011.
5. Allen T. *et al.*, J Appl Physiol. 14: 1005-1008, 1959.
6. Selders G. *et al.*, Electrospinning 1:20-30, 2016.

### ACKNOWLEDGMENTS

The authors thank the Memphis Research Consortium, and the Van Vleet Memorial Doctoral Award for their financial support of this study.

## A 3D Enzymatically Crosslinked Hydrogel Promotes Human Adipose-Derived Stem Cell Spheroids Proliferation and Differentiation

Ching-Cheng Tsai<sup>1</sup>, Nai-Chen Cheng<sup>2</sup>, Jiashing Yu<sup>1</sup>

<sup>1</sup>Department of Chemical Engineering, National Taiwan University, Taipei, Taiwan

<sup>2</sup>Department of Surgery, National Taiwan University Hospital, Taipei, Taiwan

[jiayu@ntu.edu.tw](mailto:jiayu@ntu.edu.tw)

### INTRODUCTION

hASCs have the ability to differentiate into different lineage. However, maintaining the stemness of hASCs during in vitro culture is still a challenging issue. Many studies have reported that hASC spheroids could induced significant upregulation of pluripotency marker genes which have a great influence on the cell renewal and differentiation capabilities.

Gelatin, a well-known biological material because of its good biocompatibility, has been widely used in the tissue engineering. Compared to the physical and chemical crosslinking methods which may lead to cell death, enzymatic crosslinking provide the milder reaction to encapsulate cells. mTG, a kind of enzyme, performs high specific activity over a wide range of temperature and pH. At present, few studies have reported on gelatin hydrogel crosslinked by mTG as a cell scaffold material.

In this research, we would assess the performance of hASC spheroids in the 3D gelatin/mTG hydrogel.

### EXPERIMENTAL METHODS

In this study, gelatin hydrogel crosslinked with microbial transglutaminase (mTG) which is a kind of enzyme that performs high specific activity over a wide range of temperature and pH. In addition, enzymatic crosslinking reaction is milder than physical and chemical methods which may lead to cell death. hASC spheroids formed by seeding cells in the agarose microwells plate, followed by the examination of the pluripotency genes markers expression in spheroids. The properties of gelatin/mTG hydrogel was evaluated including the gelatin time, crosslinking extent, mechanical strength and enzymatic degradation test. To investigate the performance of spheroids in the 3D hydrogel, after the spheroids were encapsulated and cultured in the hydrogel, cell cytotoxicity, proliferation and differentiation potential were assessed.

### RESULTS AND DISCUSSION

#### *hASC spheroids formation and stemness property*

hASCs were seeded into the microwells plate and the cells aggregate spontaneously after 1 day culture. In order to obtain intact cell spheroids, spheroids were collected after 3 days culture. To evaluate the stemness properties of spheroids, the gene expression of Sox-2, Oct-4, Nanog was analyzed by quantitative polymerase chain reaction (qPCR). The qPCR results demonstrated that Sox-2, Oct-4, Nanog were upregulated significantly increase in cell spheroids compared to the cell suspension group.

#### *Cell viability and proliferation in 3D hydrogel*

Live/Dead staining was used to assess cell viability in the hydrogel. It could show the viability of cells in the hydrogel and the distribution of cells survival of the spheroid. We found that the encapsulated cells and cell spheroids presented good viability and the less dead cells signal were detected after 7 days culture. The cell proliferation in the hydrogel was examined by the Alamar Blue assay. Both cells and spheroids performed great cell viability after 14 days culture and the cell suspension group significantly higher growth in comparison to the cell spheroid group.

#### *Cell differentiation capability in 3D hydrogel*

To evaluate the cell differentiation capability in the hydrogel, cells and spheroids were cultured in the appropriate induction medium. After 14 days culture both cells and spheroids maintained the capabilities of adipogenic, chondrogenic and osteogenic differentiation demonstrated by the histology staining specific for oil, glycosaminoglycan (GAG), and calcium, respectively. For the adipogenic differentiation, both PPAR- $\gamma$  and C/EBP- $\alpha$  genes showed the significantly upregulated in spheroids compared to cell suspension group. For the chondrogenic differentiation, COL II and Sox-9 genes revealed the significantly upregulated after cells formed cell spheroids either growth or induction medium group. For the osteogenic differentiation, compared with the suspension group in growth medium, the suspension and spheroid groups in induction medium demonstrated the significantly different for COL I gene. And there is no significant difference for Runx2 gene.

### CONCLUSION

In this study, qPCR analysis of stemness property of spheroids revealed the significantly upregulated. After spheroids were encapsulated in the hydrogel, they showed the great performance in cell adhesion, proliferation, and differentiation. And the results of qPCR analysis showed that cell spheroids have the better differentiation potential than cells.

### REFERENCES

[1]“Enzymatically crosslinked gelatin hydrogel promotes the proliferation of adipose tissue-derived stromal cells” Gang Yang et al., 2016, PeerJ.

### ACKNOWLEDGEMENTS

We acknowledged the funding from Ministry of Science of Technology, Taiwan, R.O.C.

## Contact-killing of Gram Positive and Gram Negative Bacteria on Silicone Rubber Sheets Covered with a Flexible Immobilized Hyperbranched Coating

Ton Loontjens<sup>1</sup>, Jia Jia Dong<sup>1</sup>, Agnieszka Muszanska<sup>2</sup>, Betsy van de Belt-Gritter<sup>2</sup>, Henk Busscher<sup>2</sup>, Henny van der Mei<sup>2</sup>

<sup>1</sup>Polymer Chemistry Department, University of Groningen, the Netherlands

<sup>2</sup>Biomedical engineering, University Medical centre Groningen, the Netherlands

[J.A.Loontjens@rug.nl](mailto:J.A.Loontjens@rug.nl)

### INTRODUCTION

Biomaterial based implants and devices are widely applied to restore human function and shape once beyond natural repair, such as after trauma, invasive oncological surgery or wear. Their use is increasing due to an increased life expectancy worldwide and the growing demands of patients for “healthy aging”. However, biomedical material related infections are still a major drawback of implants.

### EXPERIMENTAL METHODS

We developed a versatile technology<sup>1</sup> to prepare in one step and in quantitative yields AB<sub>2</sub> monomers of which the A-group is a secondary amine and the B-groups are BIs by reacting bishexamethylene triamine with carbonyl biscaprolactam (CBC).<sup>2</sup> Polymerization yields hyperbranched polymers with in the focal point the secondary amine as anchor point and polymer branches provided with BI at each branch, allowing functionalization.

### RESULTS AND DISCUSSION

Soluble quaternary ammonium compounds (QUATs) are very potent biocides, but not harmless for the humans. Therefore in the last decade much attention has been paid to immobilize QUATs on biomedical devices. Antibacterial coatings may offer a technology to prevent infections on all devices. Immobilization of coatings must be mediated by a coupling agent able to react with a substrate and with a coating.  $\gamma$ -aminopropyl triethoxysilane is converted in one step by CBC into a coupling agent having a trisiloxy moiety to bind covalently to substrates and a BI-group to immobilize amino functional polymers (Fig. 1). After an air-plasma treatment PDMS surface was covered with silanol groups. Importantly, the BIs do not react with the silanol groups under those conditions, remaining available to covalently couple the hyperbranched coatings via the secondary amino group (A-group). Subsequently, polyethyleneimine (PEI) was tethered via the BIs yielding amino functional surfaces.

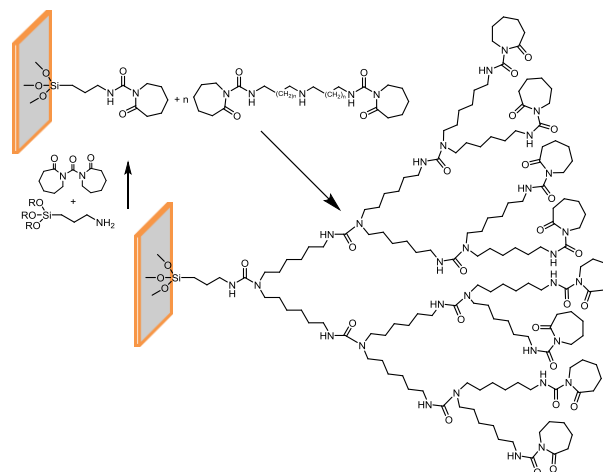


Fig. 1. Preparation of coupling agent and application of hyperbranched coating on substrate.

PEI offers control on the crosslink density of the coating by varying the reaction time. The amines were quaternized with hexylbromide. The antibacterial properties of 10 bacterial strains, 5 Gram positive and 5 Gram negative, were evaluated. The Gram positive bacteria were killed for >99%, whereas the Gram negative bacteria killed for >90%. In the presence of a permeabilisator the killing of Gram negative bacteria raised to >99% as well.

### Conclusions

Immobilized antibacterial hyperbranched coatings mediated by a novel coupling agent were successfully applied on PDMS. The coating killed Gram positive bacteria of 5 different strains and nearly all bacteria of 5 Gram negative strains.

### References

1. J.A.Loontjens, Journal of Polymer Science: Part A: Polymer Chemistry, Vol. 41, 3198–3205 (2003).
2. F. Xiang, J.A.Loontjens, Macromol. Chem. Phys. 2012, 213, 1841–1850.
3. L.Asri, M.Crismaru, S.Roest, Y.Chen, O.Ivashenko, P.Rudolf, J.Tiller, H.van der Mei, J.Loontjens, H.Busscher, Adv. Funct. Mater. 2014, 24, 346–355

### Acknowledgement

The Authors want to thank STW and Zorginnovatie for their financial support.



## Assessment of SIBS Copolymer Properties and Suitability for Biomedical Applications

Serena Bertoldi<sup>1,2</sup>, Nicola Contessi Negrini<sup>1,2</sup>, Rocco Manuele Lofaro<sup>1</sup>, Maria Cristina Tanzi<sup>2</sup>, Silvia Fare<sup>1,2</sup>

<sup>1</sup>Department of Chemistry, Materials and Chemical Engineering "G. Natta", Politecnico di Milano, Milan, Italy

<sup>2</sup>National Interuniversity Consortium of Materials Science and Technology (INSTM), Local Unit Politecnico di Milano, Florence, Italy

[silvia.fare@polimi.it](mailto:silvia.fare@polimi.it)

### INTRODUCTION

Biostable elastomers can find advantageous applications in the biomedical field, in particular for devices subjected to oxidation, hydrolysis, mechanical stresses and enzymatic or bacterial attack that might lead to device failure. For this particular purpose, Styrene-block-IsoButylene-block-Styrene (SIBS) potentially offer outstanding features to be exploited as biostable copolymers<sup>1</sup>. In fact, SIBS possesses properties overlapping both silicone rubbers and polyurethanes advantages. Up to now, only one SIBS formulation was certified as biomedical-grade material produced by Innovia LCC, while SIBS produced by other companies (e.g., SIBSTAR<sup>®</sup>, Kaneka) are presently used for industrial applications (e.g., pipes, caps and components for dumpers of noise and vibration), thus limiting SIBS potential different and versatile applications. The aim of this work is to evaluate the suitability of SIBS elastomers for biomedical uses, by comparing different not biomedical-grade SIBS copolymers, provided by Kaneka, with a biomedical-grade one (i.e., Innovia).

### EXPERIMENTAL METHODS

Six different SIBS compositions (five from Kaneka, 062M, 062T, 072T, 073T, 102T with different molecular weight and styrene content, and one from Innovia, INN) were considered. Solvent cast films (thickness 500  $\mu\text{m}$ ) were prepared by dissolving SIBS in two different selected solvents, namely chloroform, c (15% w/v SIBS) and hexane, e (7.5% w/v SIBS). Films were characterized for morphology (SEM), laser profilometry, ATR-FTIR to quantitatively evaluate the styrene content of the films by considering the parameter  $R=H_{757}/H_{950}$ , ( $H_{757}$ : peak height at 757  $\text{cm}^{-1}$ , characteristic of PS, and  $H_{950}$ : peak height at 950  $\text{cm}^{-1}$ , characteristic of isobutylene), mechanical properties, i.e. tensile and creep/recovery tests by the use of a Dynamic Mechanical Analyzer (DMA). Cytotoxicity and cytocompatibility were then investigated *in vitro* with L929 murine fibroblasts cell line L929, by assessing cell viability with Alamar Blue assay and cell morphology by SEM at different time points ( $t = 1, 4$  and 7 days).

### RESULTS AND DISCUSSION

All the films showed smooth surfaces with limited roughness, independently from the solvent used for the solvent casting procedure. The  $R$  parameter values obtained by ATR-FT IR analysis for the Kaneka SIBS were in agreement with the styrene content declared by the producer. The  $R$  value of INN SIBS was similar to the one of 073T. Therefore, it was assumed that 073T and INN have approximately the same styrene content (i.e., 30%). Comparing the IR spectra of the films of the

same SIBS prepared with a different solvent, no considerable differences were detected. Tensile mechanical tests (Fig. 1a) confirmed an elastomeric behaviour, evidencing variable stiffness values correlated to a different soft/hard segment organization in the copolymers, styrene content and molecular weight. In addition, creep/ recovery behaviour (Fig. 1b) highlighted a different viscous contribution by varying the aforementioned characteristics.

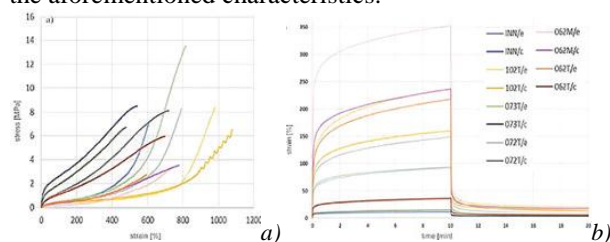


Fig. 1. (a) Representative tensile stress-strain and (b) creep/recovery curves of SIBS.

Considering the comparison of the two solvents used for film preparation, the films prepared with hexane were significantly ( $p < 0.05$ ) less stiff, thus more deformable, than the ones obtained with chloroform, probably related to a different soft/hard organization related to the possible chains mobility in the solution during the film preparation.

The *in vitro* cytotoxicity test proved no release of cytotoxic low molecular weight products. In cytocompatibility tests, cells exhibited good cells proliferation and viability (Fig. 2), with confluent elongated cells covering the films surface after 7 days of *in vitro* culture.

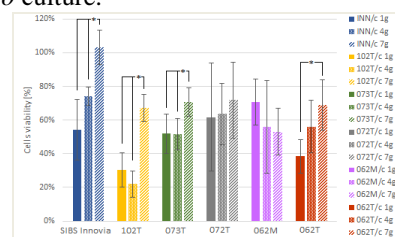


Fig. 2. Cell viability at 1, 4 and 7 days obtained by *in vitro* cytocompatibility tests performed on the considered SIBS. (\*):  $p < 0.05$ .

### CONCLUSION

The obtained results allowed to assess the main properties of SIBS, in particular depending on their composition and features, and confirmed the suitability of the INN SIBS for applications in contact with cells, but also demonstrated that SIBSTAR<sup>®</sup> SIBS could be used in biomedical applications.

### REFERENCES

- Pinchuk L. *et al.*, Biomaterials. 29:448-460, 2008
- Bertoldi S. *et al.*, J Dent Appl. 1:119-123, 2014

## Cytocompatible Coating of Individual Living Cells by Atom Transfer Radical Polymerization

Sung Ho Yang

Department of Chemistry and Chemistry Education, Korea National University of Education, Republic of Korea  
[sunghoyang@knue.ac.kr](mailto:sunghoyang@knue.ac.kr)

### INTRODUCTION

Simple but highly versatile in the formation of polymer brushes on solid substrates is surface-initiated, atom transfer radical polymerization (SI-ATRP), where polymers are grown, by controlled radical reactions, from the ATRP initiators that are introduced onto a substrate. During the last few decades, the target materials of SI-ATRP have recently been expanded to functional biomaterials, such as self-assembled peptides, polysaccharide crystals, proteins, and viruses, for enhancing their physical stability, chemical activity, or therapeutic utility. Although hybrid structures of living cells and synthetic polymers have a great deal of potential in cell-based applications, such as cell-based sensors, biomotors, biocatalysis, theranostics and cell therapy, and cells-on-a-chip, it is extremely challenging to perform SI-ATRP (and of course other polymerization protocols) from the surfaces of individual living cells, because its reaction conditions are lethal to chemically labile cells.<sup>1</sup> In this work, synthetic polymers are grafted from the surface of individual yeast cells without significant loss of cell viability, and the uniform and dense grafting is confirmed by various characterization methods including agglutination assay and cell-division studies.

### EXPERIMENTAL METHODS

The dopamine-based ATRP initiator was synthesized by following the previous report<sup>2</sup> and dissolved in a TRIS-buffered solution (pH 8.5). Yeast was incubated for 3 h in the initiator solution for PDi priming, and transferred to the aqueous ATRP solution that contained sodium methacrylate (SMA, 1 M), CuBr<sub>2</sub> (1 mM), 2,2'-bipyridyl (2 mM), and ascorbic acid (10 mM). After 1 h of polymer grafting, the resulting yeast@SMA was concentrated by centrifugation and washed with DI water. For generation of cell-polymer hybrids, yeast cells were individually primed with PDi for 3 h (formation of yeast@PDi), and SI-ARGET ATRP was performed from yeast@PDi with SMA as a monomer for predetermined time (30, 60, or 120 min) (generation of yeast@SMA).

### RESULTS AND DISCUSSION

The viability of yeast@PDi was calculated to be 82.2%, which was higher than or similar to our previous results from the PD coating of yeast cells (70%).<sup>3</sup> After 30 min of ARGET ATRP, the survival rate was 66.96%. The value was similar after 1 h of polymerization. These results implied that the PDi layer effectively protected the cell surfaces from peroxidation due to its radical scavenging capability. The development of fast-polymerizing reactions, therefore, would further contribute to cytocompatible polymer grafting.

The scanning electron microscopy images showed dramatic morphological changes after SI-ARGET ATRP. Compared with native yeast and yeast@PDi, the surface of yeast@SMA was rougher, composed of nanometer-scaled polymer particles, indicating the presence of poly(SMA) on the cell surface. We thought that this difference was caused by strong interactions between polymers and the yeast surface, which maintained the original shape without structural changes. 3-Azido-2-hydroxypropyl methacrylate (AzHPMA) was used as a co-monomer with SMA (SMA: AzHPMA = 100:1), and the polymer layer was visualized, after azide-alkyne cycloaddition of alkyne-linked Alexa Fluor® 594, by CLSM. Red rings were observed only for azide-functionalized yeast@SMA, and native yeast and yeast@SMA did not show any red-fluorescence signals.

The uniform poly(SMA) grafting was further confirmed by agglutination assay. Yeast cells make aggregates, when they are mixed with *Escherichia coli*. When mixed with *E. coli*, rapidly aggregated into a cell cluster within 3 min. However, the dense polymer layer of yeast@SMA physically blocked the binding of *E. coli* and prevented the agglutination. The formation of dense (and durable) polymer layers was also supported by the retarded cell division.<sup>4</sup>

### CONCLUSION

Polymer synthesis has so far never come along with living cells, while several cytocompatible bioorthogonal reactions have been developed for chemical manipulation of cells with small molecules. In this work, we developed a cytocompatible SI-ARGET ATRP method for grafting polymers from living cells with use of polydopamine priming. Modulation of cell-surface properties and cellular activities was demonstrated, along with post-functionality of polymer coats. Considering a plethora of functional and structural variations in synthetic polymers, we believe that grafting polymers from (or to) cell surfaces would generate multifunctional cellular hybrids for many biotechnological and biomedical applications, not to mention providing an advanced tool for chemically manipulating the cells.

### REFERENCES

1. Kim J. *et al.*, *Angew. Chem. Int. Ed.* 55:15306-15309, 2016
2. Kang S. M. *et al.*, *J. Nanosci. Nanotechnol.* 8:5347-5350, 2008
3. Yang, S. H. *et al.*, *J. Am. Chem. Soc.* 133:2795-2797, 2011
4. Yang, S. *et al.*, *Small* 9:178-186, 2013

### ACKNOWLEDGMENTS

This work was supported by National Research Foundation of Korea (2016R1C1B2013788).

## Novel Thermo-sensitive and Photo-curable Hydrogels as Potential Bioinks in Regenerative Medicine

Stefano Calzone<sup>1,2</sup>, Monica Boffito<sup>1</sup>, Deepak Choudhury<sup>2</sup>, Arianna Grivet-Brancot<sup>1</sup>,  
Prabhu Pannirselvam<sup>2</sup>, May Win Naing<sup>2</sup>, [Gianluca Ciardelli](mailto:gianluca.ciardelli@polito.it)<sup>1</sup>

<sup>1</sup>Department of Mechanical and Aerospace Engineering, Politecnico di Torino, Italy

<sup>2</sup>Bio-Manufacturing Programme, Singapore Institute of Manufacturing Technology, Singapore  
[gianluca.ciardelli@polito.it](mailto:gianluca.ciardelli@polito.it)

### INTRODUCTION

Tissue engineering/regenerative medicine (TERM) aims at the development of bioengineered scaffolds, which are able to provide a physical support to a damaged tissue/organ and prevent adverse remodeling and dysfunction. Biofabrication technologies based on additive manufacturing (AM) principles are emerging as promising tools for the fabrication of three-dimensional (3D) scaffolds for the repair of a broad range of tissues as well as complete organs, showing well-defined and controlled geometry, thus overcoming the typical drawbacks of conventional scaffold fabrication techniques<sup>1</sup>. The high technological versatility of AM methods allows a fine modulation of scaffold architecture, while the wide platform of available technologies offers the possibility to microfabricate almost all commercially available and custom-made polymers. Among the latter, polyurethanes (PUs) are a valuable and promising alternative due to their characteristic chemical versatility that can be exploited to design a wide variety of degradable biomaterials (thermoplastic and amphiphilic PUs) showing different physico-chemical properties, depending on the selected building blocks. The smart and fine combination of the previously mentioned high chemical and technological versatility of PUs and AM techniques, respectively, could be exploited to design biomimetic biomaterials and scaffolds to adequately stimulate cells they interface with. In this contribution, novel thermo- and photo-sensitive PU-based hydrogels were designed and characterized in order to obtain injectable and printable bioinks for the bioprinting of cellularized constructs.

### EXPERIMENTAL METHODS

Thermo- and photo-sensitive hydrogels were designed starting from aqueous solutions of (i) custom-made PUs containing Poloxamer 407 (P407) and pendant acrylate moieties in their backbone (solution concentration in the range 10-15 %w/v), or (ii) a blend of a P407-based PU and diacrylated poly(ethylene glycol) (PEGDA) (tested range: 10-17.5 %w/v for the thermo-sensitive PU and 5-10 %w/v for PEGDA). PUs were synthesized according to a previously published protocol<sup>2</sup>. The thermo-sensitive properties of the designed sol-gel systems were assessed by tube inverting tests, gelation time tests at 37 °C and rheological characterization, while injectability was evaluated through different needles (G14, G18, G22) at different temperatures (5, 25 and 37°C). Photo-sensitivity was then analysed on circular-shaped samples (approx. 10 mm diameter and 2 mm thickness) photo-crosslinked in conditions suitable for cell survival in terms of photo-initiator concentration (0.05% w/v Irgacure 2959), intensity and wavelength of UV light (10 mW/cm<sup>2</sup>, 365 nm) and time

of exposure (7 min). The kinetics of hydrogel photo-polymerization was studied by photorheology. Stability in aqueous environment of the designed gels was also assessed up to 2 months of incubation. Cellularized PU-based hydrogels encapsulating human bone marrow-derived mesenchymal stem cells (hMSCs) were then printed and photo-crosslinked at 365 nm layer-by-layer. The printing protocol (e.g. applied pressure - 30-200 kPa -, needle diameter - 200-450 µm -) was optimized to minimize cell death.

### RESULTS AND DISCUSSION

PUs were successfully synthesized as assessed by Size Exclusion Chromatography and Fourier-Transformed Infrared Spectroscopy. Sol-gel systems with different compositions were designed and characterized for their thermosensitivity, showing gelation in physiological conditions within 3-5 min and a sol-to-gel transition temperature in the range 25-37°C. Injectability tests confirmed the possibility to easily extrude the developed hydrogels through different needles (G14, G18, G22) at different temperatures (5, 25 and 37°C). All the designed sol-gel systems successfully underwent photo-polymerization, with different kinetics depending on their composition and degree of acrylation. Nevertheless, all the tested hydrogels were completely photo-polymerized within 3 min of exposure to UV-light at 365 nm and 10 mW/cm<sup>2</sup>. Stability in aqueous environment of circular-shaped photo-crosslinked gels was confirmed till 56 days of incubation. hMSCs were successfully encapsulated in the developed PU-based hydrogels and printed in multi-layered (up to 8 layers) 3D structures with high resolution (approx. 30 µm) and homogeneous cell distribution. Viability tests performed immediately after printing and photo-polymerization suggested that the scaffold fabrication process itself did not induce cell death, and no significant drop in cell viability was observed up to 10 days of cell culture.

### CONCLUSION

Thermo- and photo-sensitive injectable PU-based hydrogels were successfully designed, showing fast gelation, sol-to-gel transition temperature within the physiological range and long-term residence time in aqueous environment. The designed sol-gel systems showed high potential in bioprinting technology as cellularized bioinks with highly tuneable degradation /dissolution kinetics and mechanical strength, thus opening the way to a wide range of potential applications in the biomedical field.

### REFERENCES

1. Boffito M. *et al.*, Polym. Int. 63:2-11, 2014
2. Boffito M. *et al.*, Polym. Int. 65:756-769, 2016



## *In Vitro* and *In Vivo* Evaluation of 3D-Printed PLA Scaffolds Coated With Biomimetic Apatite for Applications in Bone Tissue Engineering

Marianna O. C. Maia-Pinto<sup>1</sup>, Leonardo C. Boldrini<sup>2</sup>, Mônica D. Calasans-Maia<sup>3</sup>, Rossana M. S. M. Thiré<sup>1</sup>

<sup>1</sup>Federal University of Rio de Janeiro – UFRJ, COPPE/Program of Metallurgical and Materials Engineering, Rio de Janeiro - RJ, Brazil

<sup>2</sup>National Institute of Metrology, Quality and Technology – INMETRO/Division of Applied Metrology the Life Sciences – DIMAV, Duque de Caxias - RJ, Brazil.

<sup>3</sup>Dental Clinical Research Center/Dentistry School, Fluminense Federal University – UFF, Niterói - RJ, Brazil  
[rossana@metalmat.ufrj.br](mailto:rossana@metalmat.ufrj.br)

### INTRODUCTION

Three-dimensional (3D) printing technologies, such as Fused Deposition Modeling (FDM), have been used to produce porous, customized scaffolds for tissue engineering<sup>1</sup>. Polylactic acid (PLA) is a biodegradable, synthetic polymer that has been widely investigated as scaffolding material mainly due to its biocompatibility and good thermal and physical properties. However, PLA is a hydrophobic polymer with low bioactivity<sup>2</sup>. It is known that calcium phosphate (CaP) coatings can be used to increase the bioactivity of synthetic scaffolds. In this study, we focus on the biological, chemical and physical characterization of 3D-printed PLA scaffolds coated with biomimetic apatite aiming their application in bone tissue engineering.

### EXPERIMENTAL METHODS

Cubic digital model with layer orientation of 0-90°, distance between struts of 0.68 mm and diameter of each strut of 0.30 mm was created in SolidWorks® 2014 software. Scaffolds were printed with commercial PLA white filament (eSun, China) in a 3D Cloner FDM printer (Microbrás, Brazil). PLA scaffolds were treated with 0.1 M NaOH at 65°C for 45 min and then, were immersed in simulated body fluid (SBF) for 14 days. Scanning electron microscopy (SEM), X-ray diffraction (DRX), Fourier-transform Infrared spectroscopy (FTIR) and thermogravimetric analysis (TGA) were used for physical, chemical and morphological characterization. *In vitro* cell viability was assessed with the methyl tetrazolium (MTT) assay, lactate dehydrogenase leakage assay (LDH) and interleucine-6 (IL-6) tests. MC3T3-E1 cells were directly cultivated on uncoated and coated PLA scaffolds for 24 h. *In vivo* study was approved by the Ethical Commission on Teaching and Research in Animals (CEUA/UFF n° 780/16). Under general anesthesia, a critical size defect measuring 8 mm in diameter was produced in Wister rat calvaria and filled with the biomaterials. The animals were euthanized after 180 days for bone block contain biomaterials removal. Tissue response was assessed by histology/histomorphometry.

### RESULTS AND DISCUSSION

SEM images show that SBF immersion provided the formation of a continuous CaP layer deposited over PLA scaffolds struts (Fig. 1).

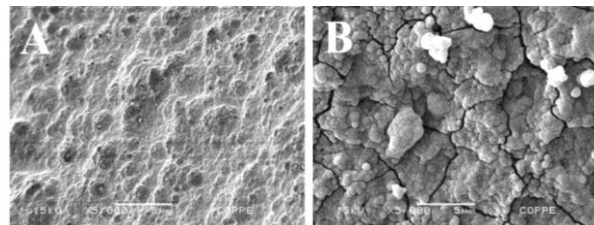


Fig. 1. SEM images of uncoated (A) and CaP-coated (B) PLA scaffolds.

FTIR spectra show the presence of phosphate groups (1020 cm<sup>-1</sup>) and carbonate group (867 cm<sup>-1</sup>) after exposure to SBF solution. The deposition of the bioceramic phase was also confirmed by XRD diffractograms. Considering the amount of the residues obtained in TGA analysis of uncoated and coated scaffolds, it was possible to infer that approximately 2% w/w of apatite was deposited onto the scaffolds.

No cytotoxicity was observed for any scaffold when the MTT (Fig. 2A), LDH leakage (Fig. 2B) and the protein assay were employed (data not shown). *In vivo* test results suggest that both scaffolds integrated with the host bone and were biocompatible.

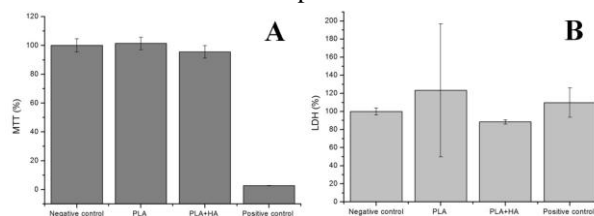


Fig. 2. Results of MTT (A) and LDH (B) assays for PLA scaffolds.

### CONCLUSION

Bioactive 3D-printed PLA scaffolds coated with continuous apatite layer were successfully obtained by immersion in SBF solution. These scaffolds showed no *in vitro* and *in vivo* toxicity. Accordingly, these materials can be considered potential candidates for bone regeneration applications.

### REFERENCES

- Turnbull G. *et al.*, *Bioactive Materials*, <https://doi.org/10.1016/j.bioactmat.2017.10.001>, 2017.
- Serra T. *et al.*, *Organogenesis*, 9:239–244, 2013.

### ACKNOWLEDGMENTS

CNPq and FAPERJ for financial support.

## Enzymatic Mineralization of Novel Whey-protein Isolate Hydrogels for Bone Regeneration

Anna Maria Tryba<sup>1</sup>, Magdalena Kocot<sup>1</sup>, Julia K. Keppler<sup>2</sup>, Elżbieta Pamuła<sup>1</sup>, Timothy E.L. Douglas<sup>3,4</sup>

<sup>1</sup>Dept. Biomaterials & Composites, Faculty of Materials Science and Ceramics, AGH University of Science and Technology, Krakow, Poland

<sup>2</sup>Dept. Food Technology, Christian-Albrechts-Universität zu Kiel, Germany

<sup>3</sup>Engineering Dept., Lancaster University, United Kingdom

<sup>4</sup>Materials Science Institute (MSI), Lancaster University, United Kingdom

[t.douglas@lancaster.ac.uk](mailto:t.douglas@lancaster.ac.uk)

### INTRODUCTION

Proteins derived from dairy sources, especially waste streams, are of interest for biomedical applications for environmental and financial reasons (recycling, low cost). One by-product from the production of cheese and Greek yoghurt is whey protein isolate (WPI), which consists mainly of  $\beta$ -lactoglobulin and is used by bodybuilders as a dietary supplement.

Heating of WPI solution induces formation of WPI hydrogels, i.e. highly hydrated three-dimensional polymer networks. Hydrogels are used increasingly as biomaterials for tissue regeneration due to the ease of incorporation of biologically active substances such as enzymes, including alkaline phosphatase (ALP), the enzyme responsible for the mineralization of bone tissue with calcium phosphate (CaP) *in vivo* by cleaving phosphate from organophosphates such as glycerophosphate (CaGP). Previous work has shown that WPI in solution can improve proliferation and osteogenic differentiation of bone-forming cells<sup>1</sup>. Hence, we consider WPI to be a good starting substance to fabricate biomaterials for bone regeneration.

Mineralization of hydrogels with CaP leads to mechanical reinforcement and promotion of attachment, proliferation and osteogenic differentiation of bone-forming cells. WPI hydrogels were formed by heating WPI solution. WPI hydrogels were mineralized with CaP by incorporation of ALP during hydrogel formation and incubation in a solution of CaGP, which served as a source of calcium ions and ALP substrate.

### EXPERIMENTAL METHODS

WPI was obtained from Davisco, USA. ALP and CaGP were obtained from Sigma-Aldrich, UK. WPI was dissolved in ddH<sub>2</sub>O at a concentration of 50% (w/v). If necessary, ALP was added to WPI solution in powder form to obtain a final ALP concentration of 3.125 mg/ml. Gelation was induced by heating at 60°C for 1 h. Both ALP-loaded and ALP-free hydrogels were prepared. Hydrogels were incubated in either mineralization solution (0.1 M CaGP) or ddH<sub>2</sub>O for 7 days, weighed, dried and re-weighed. The dry mass percentage, i.e. the percentage mass attributable to polymer and mineral and not water, was calculated as (mass after drying/mass before drying)\*100% and served as a measure of mineralization extent. FTIR and SEM were performed using a Cary 630 (Agilent) and a JSM-7800F (Jeol (UK) Ltd.), respectively, after drying.

### RESULTS AND DISCUSSION

After 7 days of incubation in mineralization solution, ALP-loaded hydrogels showed higher values of dry mass percentage than ALP-free hydrogels (not shown). This indirectly suggests formation of CaP in hydrogels. FTIR analysis revealed bands characteristic for CaP in ALP-loaded hydrogels, demonstrating CaP formation (Fig. 1). CaP deposits were detected by SEM (Fig. 2).

### CONCLUSION

ALP added to the WPI solution retained bioactivity upon hydrogel formation and induced formation of CaP.

### REFERENCES

1. Douglas TEL, *et al.* J Dairy Sci. 101:28-36, 2018

### ACKNOWLEDGMENTS

Financial support from: (1) United Kingdom Society for Biomaterials (UKSB) Lab-2-Lab award, (2) Lancaster University, Faculty of Science and Technology grant and (3) N8 Agrifood Pump Priming Grant (all T.E.L.D.)

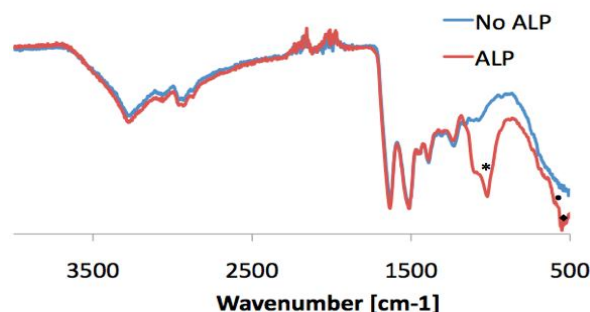


Fig. 1. FTIR of WPI hydrogels containing ALP or without ALP after mineralization. Asterisks and dots indicated bands specific for the presence of CaP.

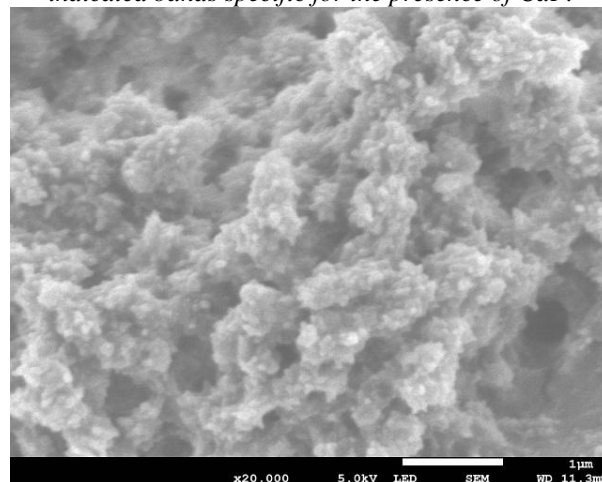


Fig. 2. SEM image of WPI hydrogel containing ALP after mineralization. Scale bar = 1  $\mu$ m.

## A Long-lasting UV-cured Vinylbenzylated Atelocollagen Membrane for Guided Bone Regeneration

He Liang<sup>1,2</sup>, Stephen J. Russell<sup>1</sup>, David J. Wood<sup>2</sup>, Giuseppe Tronci<sup>1,2</sup>

<sup>1</sup>Textile Technology Research Group, School of Design, University of Leeds, United Kingdom

<sup>2</sup>School of Dentistry, St James's University Hospital, University of Leeds, United Kingdom

[h.liang@leeds.ac.uk](mailto:h.liang@leeds.ac.uk)

### INTRODUCTION

Collagen membranes are a key component of guided bone regeneration (GBR) dental therapy for the treatment of localised bone defects in the jaws [1]. Here, the collagen membrane is implanted *in vivo* and is expected to display controlled biodegradability and barrier functionality to prevent soft tissue invasion and to guide the bone regeneration. However, currently-available collagen membranes still display fast mass loss *in vivo*, mainly due to the lack of effective crosslinking strategies resulting in restricted structure-property relationships [2]. This inherently leads to clinically-underperforming materials and poor quality of bone formed. New synthetic and manufacturing approaches should therefore be developed to enable the design of next generation long-lasting GBR devices.

### EXPERIMENTAL METHODS

To address previously-mentioned challenges, type I atelocollagen (AC) triple helices were selected as membrane building block [3], and covalently functionalised with photoactive moieties, e.g. 4-vinylbenzyl chloride (4VBC), aiming to achieve a water-insoluble, UV-cured covalent network [4]. At the same time, selective conjugation of metal-chelating factors to the collagen molecule was also explored in order to achieve local regulation of proteolytic activity and long lasting barrier function *in vivo* [5]. 2,4,6-trinitrobenzenesulfonic acid (TNBS) and ninhydrin assays as well as <sup>1</sup>H-NMR were employed to assess the degree of covalent functionalisation in reacted products, together with circular dichroism (CD) and SDS-PAGE aiming to elucidate the protein organisation and the occurrence of any reaction-induced collagen degradation. UV irradiation was employed to trigger gelation of the aqueous solution containing AC product and 2-hydroxy-1-[4-(2-hydroxyethoxy) phenyl]-2-methyl-1-propanone (I2959) [6]. UV-cured AC networks were characterised *in vitro* with regards to their water content, gel content, hydrated compression properties, UV curing rheometry, cell tolerability and enzymatic degradability (1–2.5 CDU·ml<sup>-1</sup> collagenase, 37°C).

### RESULTS AND DISCUSSION

Reacted AC product could be successfully obtained with varied chemical configurations and customised degree of covalent functionalisation (*F*: 20-90 Lys%). CD revealed a preserved triple helix organisation, whilst comparable electrophoretic patterns were detected in both native and reacted AC products. Full UV-cured networks were readily formed (Gel content > 90 wt.-%) with an averaged compression modulus and swelling ratio of at least 80 kPa and 800 wt.-%, respectively. The membrane displayed less than 50 wt.-% mass loss

following 2-week incubation in a collagenase-containing medium *in vitro*. After 4-day incubation, the enzymatic activity of the membrane-treated supernatant proved to be substantially downregulated (13-50 RFU%) compared to the activity of sample-free supernatant, supporting previously-obtained gravimetric data. Noteworthy, a commercial collagen-based GBR membrane was completely dissolved in the same experimental conditions *in vitro*. The superior proteolytic stability of obtained AC membrane was also confirmed via a 1-month subcutaneous implantation pilot study in rats. Further to that, a preclinical *in vivo* study is ongoing using a GBR model in rats.

### CONCLUSION

A superior GBR membrane could be successfully obtained by selectively manipulating the chemical configuration of the AC triple helix. The presented synthetic route enabled the formation of UV-cured networks at the molecular scale with customisable macroscopic properties and long-lasting proteolytic stability. The flexibility of this AC system could be exploited to design GBR membranes with complex micro- and macrostructure, e.g. fibres, fabrics and long-lasting coatings.

### REFERENCES

- [1] Elgali I. *et al.*, Eur. J. Oral. Sci. 125: 315-337, 2017
- [2] Wessing B. *et al.*, Clin. Oral. Impl. Res. 28: e218-e226, 2017
- [3] Holmes R. *et al.*, Mater. Sci. Eng. C 77: 823-827, 2017
- [4] Tronci G. *et al.*, J. R. Soc. Interface 12: 20141079, 2015
- [5] Tronci G. *et al.*, J. Mater. Chem. B 4: 7249-7258, 2016
- [6] Holmes R. *et al.*, Polymers 9: 226, 2017

### ACKNOWLEDGMENTS

The authors gratefully acknowledge financial support from the Clothworkers' Centre for Textile Materials Innovation for Healthcare (CCTMIH). The EPSRC Centre for Innovative Manufacturing in Medical Devices (MeDe Innovation), University of Leeds-MRC Confidence in Concept scheme, and the University of Leeds-EPSRC Impact Acceleration Account (IAA) are also gratefully acknowledged.



## PLA/TCP Nanocomposite Locking Bolt for Intramedullary Locking Nail System

Karol Gryń<sup>1</sup>, Barbara Szaraniec<sup>1</sup>, Jan Chłopek<sup>1</sup>, Jarosław M. Deszczyński<sup>2</sup>, Jarosław Deszczyński<sup>3</sup>

<sup>1</sup>Faculty of Materials Science and Ceramics, AGH University of Science and Technology, Krakow, Poland

<sup>2</sup>Clinical Rehabilitation Clinic IInd Medical Faculty, Warsaw Medical University, Warsaw, Poland

<sup>3</sup>Orthopaedic and Rehabilitation Department IInd Medical Faculty, Warsaw Medical University, Warsaw, Poland  
[kgryn@agh.edu.pl](mailto:kgryn@agh.edu.pl)

### INTRODUCTION

Intramedullary nailing has received increased attention for the treatment of distal femoral fractures. There are many types of nailing systems commonly used. Among them there is locked intramedullary nailing, which combines closed nailing with a special locking piece, which expands distal part of a nail and anchors it when a central screw is tightened. Compared to other interlocking nail systems it is very effective and not very invasive way of treatment of long bones fractures. However, it is not perfect and has one major disadvantage. Related to a material it is usually made of (metal) there is necessity of removing all parts of the system after the bone is recovered thus a better multifunctional material for the locking piece which is biodegradable, have bioactive function and is strong enough to maintain its mechanical requirements at the same time needs to be elaborated.

Poly-L-lactide (PLA) is nowadays one of the mostly used bioabsorbable materials in medicine. Unfortunately, this polymer may not meet some application requirements due to inadequate mechanical properties and its degradation characteristics. One of the easiest ways to overcome these obstacles is to introduce an inorganic phase into the polymer matrix to create a composite. That is the way to strengthen polymer matrix, to control the degradation rate and to give the composite an additional functions eg. improving bone tissue regeneration.

### EXPERIMENTAL METHODS

In this article biodegradable nanocomposite (PLA/nano  $\beta$ TCP, 90/10wt%) was prepared [PLA Ingeo 3251D, NatureWorks LLC;  $\beta$ TCP Sigma Aldrich]. To form a composite locking piece of an interlocking intramedullary nail called "OLIVE" injection molding was applied ( $T=170^{\circ}\text{C}$ ,  $p=70\text{ kg/cm}^2$ ). To simulate body environment, samples were incubated in PBS in  $36^{\circ}\text{C}$ . After 1, 2, 4, 7, 14 days pH and electrical conductivity of solution was measured.

Along with degradation monitoring mechanical tests were conducted at the same time intervals, to investigate and describe the inner thread shear strength of an "OLIVE". For this purpose a special device imitating real working conditions was fabricated. For structural analyses SEM observations were made.

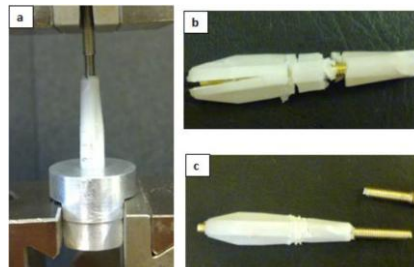


Fig. 1. a) The inner thread shear strength test; b) Olive after the test – despite fragmentation mechanical function was retained; c) Damaged locking screw – olive untouched.

### RESULTS

Preliminary results indicate that injection molding is a proper fabrication method for PLA/nanoTCP composite. It gives very good quality of an implant and allows for mass production, keeping production costs at low level.

Mechanical testing showed high strength of an implant. No inner thread destruction was discovered after uniaxial tensile strength, even after 14 days of incubation, contrary to a metallic screws used in simulating conditions, which in all cases broke. That indicates, that composite "olive" fulfill mechanical requirements for such a device (Fig. 1).

SEM analyses revealed good homogenization of nanoTCP in the composite. No agglomeration of nanopowder was revealed.

### CONCLUSION

This study shown that nanocomposite locking bolt for intramedullary locking nail system called "olive", made of proposed material in injection molding process, even though undergoing degradation process, maintains very good mechanical properties. Also, bioceramic ions released from the polymer matrix during degradation, should support the bone tissue regeneration process. It has to be underline that there is no necessity of removing such implant after bone is completely healed.

### REFERENCES

1. Minos Tyllianakis, Pantelis Tsoumpos, Kostas Anagnostou, Anna Konstantopoulou, Andreas Panagopoulos: "Intramedullary nailing of humeral diaphyseal fractures. Is distal locking really necessary?" – *Int. Jou. Of Shoulder Surgery*, 2013, Vol. 7, Issue : 2, 65-69

### ACKNOWLEDGMENTS

This research was financed by the statutory research No 11.11.160.182 of Faculty of Materials Science and Ceramics, AGH University of Science and Technology, Krakow, Poland.



## Inorganic Calcium Filled Bacterial Cellulose Based Hydrogel Scaffold: A Novel Three Dimensional Biomaterial for Bone Tissue Regeneration

Probal Basu, Nabanita Saha, Petr Saha

Centre of Polymer Systems, University Institute,  
Tomas Bata University in Zlin, Trida Tomase Bati 5678, 760 01 Zlín, Czech Republic  
[nabanita@ft.utb.cz](mailto:nabanita@ft.utb.cz)

### INTRODUCTION

Bone is the structural framework of our body. Studies showed that osteoporosis causes more than 8.9 million fractures worldwide annually<sup>1</sup>. The treatment methods related to the fracture resulted are expensive for application<sup>2</sup>. Thus, in this context, the application of bioactive hydrogel scaffold can become a significant approach in bone tissue engineering. Interestingly, bacterial cellulose (BC) based hydrogel scaffolds has the attributes to become a potential biomaterial. This work focuses the development of novel inorganic calcium filled BC based hydrogel scaffolds. The analysis of structure, function and biological efficiency study with the novel inorganic calcium filled BC based hydrogel scaffolds were the principal goal of investigation in regard to its potential utilization in bone tissue engineering application.

### EXPERIMENTAL METHODS

BC based hydrogel scaffolds were developed by applying the homogeneous suspension of BC (holding 99% water) with carboxymethyl cellulose (CMC), polyvinyl pyrrolidone (PVP), and polyethylene glycol (PEG), agar and glycerine. Additionally, bioactive compounds,  $\beta$ -tricalcium phosphate ( $\beta$ -TCP) and hydroxyapatite (HA) were incorporated to achieve the  $\text{CaPO}_4$  filled BC based hydrogel scaffolds (termed as “BC-PVP- $\beta$ -TCP/HA” and “BC-CMC- $\beta$ -TCP/HA”). Further, these  $\text{CaPO}_4$  filled BC based hydrogel scaffolds were placed for *in vitro* bio-mineralization to incorporate  $\text{CaCO}_3$ . Two different ionic solutions i.e.,  $\text{Na}_2\text{CO}_3$  (5.25/100 mL) and  $\text{CaCl}_2$  (7.35/100 mL) were used to achieve inorganic  $\text{CaPO}_4$  and  $\text{CaCO}_3$  filled bio-mineralized BC based hydrogel scaffolds (termed as “BC-PVP- $\beta$ -TCP/HA- $\text{CaCO}_3$ ” and “BC-CMC- $\beta$ -TCP/HA- $\text{CaCO}_3$ ”). BC-PVP and BC-CMC hydrogel scaffolds were used as control set. The characterization of the hydrogel scaffolds was performed on the basis of morphological, chemical, thermal analysis. Mechanical property was analysed through compression study. The absorptivity of the hydrogel scaffolds was investigated by swelling study. The cell biological efficiency with the extracts of the calcium filled hydrogel scaffolds were analysed (with Lep-3 cells) and recorded until 72, 120 and 168 hours. All data are analysed as mean $\pm$ standard error of the mean. Statistical differences were assessed using one-way analysis of variance (ANOVA) followed by suitable post-hoc test.

### RESULTS AND DISCUSSION

FTIR (Fourier Transform Infrared Spectroscopy) and TGA (Thermogravimetric analysis) indicate the presence of BC and inorganic calcium within BC matrix. SEM (Scanning electron microscopy) study

indicates the surface of the calcium filled hydrogel scaffolds (BC-PVP- $\beta$ -TCP/HA”, “BC-CMC- $\beta$ -TCP/HA, BC-PVP- $\beta$ -TCP/HA- $\text{CaCO}_3$ ” and “BC-CMC- $\beta$ -TCP/HA- $\text{CaCO}_3$ ) are rough compared to the control samples. Significant porous structures (50-200  $\mu\text{m}$ ,  $P < 0.05$ ) were observed in all the hydrogel scaffolds. Swelling study indicates the significant swelling ability of the calcium filled hydrogel scaffolds and also confirm about the development of three dimensional structures within the hydrogel. BC-CMC based samples were found to have higher absorptivity than BC-PVP based samples. Moreover, the *in vitro* bio-mineralized scaffolds (BC-PVP- $\beta$ -TCP/HA- $\text{CaCO}_3$ ” and “BC-CMC- $\beta$ -TCP/HA- $\text{CaCO}_3$ ) reach to nearly equilibrium level of absorptivity after 5 minutes, whereas  $\text{CaPO}_4$  filled hydrogel scaffolds were showing significant increase ( $P < 0.0001$ ) of absorptivity at the same time of duration. On the other hand, the compressive strength (0.24-0.60 MPa) of inorganic calcium filled BC based hydrogel scaffolds are similar like trabecular bone. Furthermore, significant cell viability (with Lep-3 cell) was noticed in presence of the extract of inorganic calcium filled BC based scaffolds ( $\text{CaPO}_4$  filled scaffolds,  $\text{CaPO}_4$  and  $\text{CaCO}_3$  filled BC based scaffolds), recorded until 72, 120 and 168 hours. This indicates the inorganic calcium filled BC based hydrogel scaffolds has the required biocompatibility.

### CONCLUSION

The present work focuses the preparation of novel inorganic calcium filled BC based hydrogel scaffolds which contains  $\text{CaPO}_4$  (in the form of  $\beta$ -TCP and HA) and  $\text{CaCO}_3$ . The SEM study revealed porous structures within all six BC based hydrogel samples. Furthermore, the inorganic calcium filled BC based hydrogel scaffolds have the similar compressive strength (0.24-0.60 MPa) like the trabecular bones. Finally, cell viability study demonstrates the cell biological efficiency of the scaffolds. Thus, the calcium filled BC based hydrogel scaffolds has the necessary attributes for the soft bone tissue engineering.

### REFERENCES

1. IOF, 2017, <https://www.iofbonehealth.org/facts-statistics>, accessed on 30.08.2017
2. Castilho et al., 2014. *Biofabrication*, 6 (025005), 1-13.

### ACKNOWLEDGMENTS

This work is supported by the Internal Grant Agency (Project No. IGA/CPS/2018/008), Tomas Bata University in Zlin, Czech Republic and Ministry of Education, Youth and Sports of the Czech Republic – NPU Program I (LO1504).

## Novel Intramedullary Nailing for Humerus Shaft Fractures

Jarosław Michał Deszczyński<sup>1</sup>, Jarosław Deszczyński<sup>2</sup>, Barbara Szaraniec<sup>3</sup>, Karol Gryń<sup>3</sup>, Jan Chłopek<sup>3</sup>

<sup>1</sup>Clinical Rehabilitation Clinic IInd Medical Faculty, Warsaw Medical University, Poland

<sup>2</sup>Orthopaedic and Rehabilitation Department IInd Medical Faculty, Warsaw Medical University, Poland

<sup>3</sup>Faculty of Material Sciences and Ceramics, AGH – University of Science and Technology, Krakow, Poland

[jm.deszczynski@me.com](mailto:jm.deszczynski@me.com)

### INTRODUCTION

Intramedullary fixation of long bones fractures is increases as an osteosynthesis method performed in the daily work of physicians at trauma and orthopedic departments. Therefore, it is still required to search for newer solutions of this method together with the use of modern biomaterial solutions, as well as to develop their clinical and biomechanical design solutions and implantation techniques. We introduce a new concept of the intramedullary nail with a new innovative construction, especially in the aspect of locking mechanism. An important element of the nail is the so-called "Olive" - element in the shape of a double-cone made of absorbable material. The conical part is the first to be inserted into the medullar cavity, it makes it easier to cross the fracture, while the other part of the cone allows the opening and directing of the extending parts of the nail. Humeral shaft fractures account for 1–3% of all fractures and 20% of the fractures involving the humerus. Internal fixation continues to be the surgical treatment of choice for humerus shaft fractures. A new concept of intramedullary nail without distal locking has been developed with the aim to reduce the damage to the radial nerve and shortening the time of surgery.

### EXPERIMENTAL METHODS

The purpose of this study was to evaluate the functional outcome, union and complication rates after surgical treatment of unstable or displaced humeral shaft fractures using a novel concept of intramedullary nail.

19 patients went under surgery of humeral shaft fracture using the novel intramedullary nail. Fractures were classified according to AO classification. Parameters such as patient demographics, mechanism of the injury, operative time, time of union and any complications were recorded. Functional outcome was evaluated using the Constant Shoulder Score. A comparison of the functional outcomes was done for two groups of patients. Patients >60 years in one group and patients < 60 in the second group.

### RESULTS AND DISCUSSION

One patient was lost to follow-up and was excluded from the analysis. For the fourteen patients (mean age: 51 years), the mean follow-up was 35 months. The union rate was 94% (mean time to union: 4,3 months). The mean Constant score was 73.8 (range: 39–91). No differences were observed in Patients under the age of 60 compared to patients > 60 years of age ( $p < 0.05$ ). Once incidence of non-union was observed. No complications regarding fixation failure, infection and impingement were noted.

### CONCLUSION

The new concept of intramedullary nail was found to be an effective implant for stabilization of humeral shaft fractures. Functional outcome for the greater majority of the cases was excellent or good. Operating technique of this implant doesn't require the distal locking of the nail what eliminates the risk of radial nerve damage and additionally may shorten the surgery duration. Those promising results are encouraging enough to perform the randomized trial studies on wider patient population.

### REFERENCES

1. Ekholm R, Adami J, Tidermark J, Hansson K, Tornkvist H, Ponzer S: "Fractures of the shaft of the humerus. An epidemiological study of 401 fractures" - *J Bone Joint Surg (Br)* 2006, 88(11):1469–1473.
2. Zhao J-G, Wang J, Meng X-H, Zeng X-T, Kan S-L (2017): "Surgical interventions to treat humerus shaft fractures: A network meta-analysis of randomized controlled trials" - *PLoS ONE* 12(3): e0173634 <https://doi.org/10.1371/journal.pone.0173634>

## Enhancing the Induced Membrane Technique for the Regeneration of Bone Defects

Robert Björkenheim<sup>1</sup>, Gustav Strömberg<sup>1</sup>, Laura Aalto-Setälä<sup>2</sup>, Peter Uppstu<sup>3</sup>, Mari Ainola<sup>4</sup>, Jukka Pajarinen<sup>4</sup>, Leena Hupa<sup>2</sup>, Nina Lindfors<sup>1</sup>

<sup>1</sup>Department of Musculoskeletal and Plastic Surgery, University of Helsinki and Helsinki University Central Hospital, Helsinki, Finland

<sup>2</sup>Johan Gadolin Process Chemistry Centre, Åbo Akademi University, Turku, Finland

<sup>3</sup>Laboratory of Polymer Technology, Åbo Akademi University, Turku, Finland

<sup>4</sup>Department of Medicine, Clinicum, University of Helsinki, Helsinki, Finland  
[peter.uppstu@abo.fi](mailto:peter.uppstu@abo.fi)

### INTRODUCTION

The induced membrane technique or the Masquelet technique is a clinically used two-stage procedure for regeneration of critical-sized segmental defects in long bones.<sup>1</sup> In the first operation, the bone segment containing the defect is removed and replaced with a poly(methyl methacrylate) (PMMA) spacer, around which a synovial-like membrane secreting growth factors which enhance bone regeneration will be induced over time. In the second operation 6–8 weeks after the first operation, a cut is made in the induced membrane, the spacer is removed and the gap is filled with non-vascularized bone graft or synthetic bone substitute. The clinical outcome is generally good, but complications in the form of persistence of infection or non-union have been reported in 18% of the cases.<sup>2</sup> Our aim is to enable a one-step procedure by using a biodegradable spacer of porous bioactive glass S53P4 (BonAlive®) coupled with a membrane-inducing quickly degradable coating of poly(D,L-lactide-co-glycolide) (PLGA), thus eliminating the need for a second operation. In the first in vivo trial we studied the regeneration of bone and the induction of a membrane in a metaphyseal bone defect in rabbits.

### EXPERIMENTAL METHODS

A bone defect was created in skeletally mature NZW rabbits by drilling a 6mm wide horizontal hole in the distal metaphyseal region of the femur. Rods of either sintered bioactive glass S53P4, PLGA-coated S53P4 or PMMA were implanted for follow-up of 2, 4 or 8 weeks with 3 parallels for each implant type and time point. For control, 3 holes were left empty for each time point. The induced membrane on the bone surface was recovered and VEGF and TNF expression was analysed with RT-qPCR. Capillary vessel count was determined from histological sections. Bioactive glass reactions and bone growth were studied by SEM analysis of cross-sections of the implant area. In statistical analysis, p-values <0.05 were considered significant.

### RESULTS AND DISCUSSION

Analysis of the induced membranes showed that the expression of VEGF (fig. 1) for the PLGA-coated S53P4 was rising over time and was significantly higher than for PMMA at 8 weeks.<sup>3</sup> Similarly the capillary count was significantly higher for PLGA-coated S53P4 than for both empty control and PMMA at 8 weeks. The expression of VEGF and TNF and capillary count for the uncoated S53P4 rods were largely similar to PMMA at all time points.

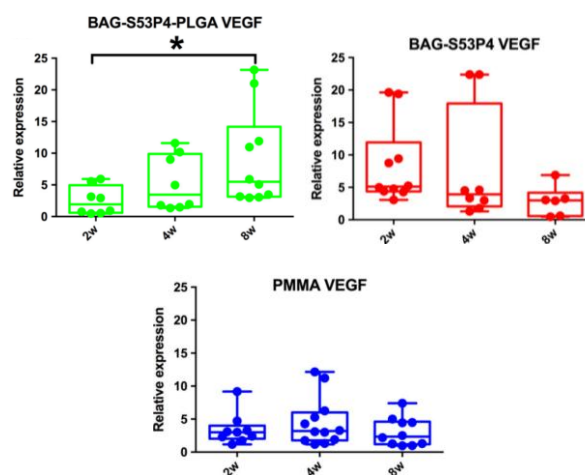


Fig. 1. VEGF expression for PLGA-coated S53P4 scaffolds, uncoated S53P4 scaffolds and PMMA spacers at 2, 4 and 8 weeks after surgery.

Analysis of cross-sectional SEM images showed that there was significant bone ingrowth into the porous bioactive glass rods. At 8 weeks, most of the bioactive glass had reacted, and only a small portion of unreacted glass remained.

### CONCLUSION

Our first results regarding VEGF and TNF expression and number of capillary beds show that both uncoated and PLGA-coated bioactive glass S53P4 scaffolds induced a membrane as good as or exceeding that of PMMA spacers, the “gold standard” material used in the induced membrane technique. In contrast to PMMA spacers, pro-angiogenic activity was shown to be increasing over time for PLGA-coated scaffolds. Bone growth was prominent inside of the porous bioactive glass rods. In our current research we are testing an improved scaffold design in a more demanding scenario in a critical sized segmental femoral defect.

### REFERENCES

- Masquelet A. *et al.*, *Orthop. Clin. North. Am.* 41:27-37, 2010
- Morelli I. *et al.*, *Injury* 47:S68-S76, 2016
- Björkenheim R. *et al.*, *J. Mater. Sci.* 52:9055-9065, 2017

## Polysaccharides for Target-Specific Imaging and Treatment of Atherothrombosis: From the Polymer Design to the Clinical Trial

Didier Letourneur

Cardiovascular Bio-engineering - INSERM U1148 – LVTS; X. Bichat Hospital; University Paris 13, 93430 Villetaneuse,  
University Paris Diderot, 75018 Paris; France  
[didier.letourneur@inserm.fr](mailto:didier.letourneur@inserm.fr)

### INTRODUCTION

Atherothrombotic diseases remain the main cause of morbidity and mortality with clinical manifestations of angina, heart attack and stroke. There is a need for new approaches for early diagnosis and improved therapies for cardiovascular diseases.

We have previously identified and patented a low molecular weight polysaccharide, fucoidan, as a powerful ligand of intravascular thrombi in vivo. Fucoidan refers to a type of polysaccharide mainly extracted from brown seaweed, which contains L-fucose and sulphate ester groups, able to mimic Sialyl Lewis X, the endogenous saccharidic motif recognized by platelet P-selectin expressed in thrombi. Our aims were to 1) visualize thrombus with Fucoidan by SPECT imaging 2) evidence in preclinical models the ability of Fucoidan on several nano/microsystems to target the thrombus 3) prepare a clinical grade Fucoidan 4) prepare the demonstration in a clinical setting.

### EXPERIMENTAL METHODS

Fucoidans from brown algae, containing low molecular weight polysaccharide species were prepared. The molecular weight, structure and composition of the purified fucoidan were determined by High Performance Size Exclusion Chromatography (HPSEC), Multi-Angle Laser Light Scattering (MALLS), viscosimetry, differential Refractive Index (dRI), colorimetric assays, Fourier Transform InfraRed spectroscopy (FT-IR) and Nuclear Magnetic Resonance (NMR). Fucoidan was directly complexed with  $^{99m}\text{Tc}$  for SPECT imaging<sup>1</sup>.

Several nano/microsystems containing Fucoidan were investigated: i) We have designed ultrasmall superparamagnetic iron-oxide (USPIO) nanoparticles associated with fucoidan to visualize by MRI arterial thrombi<sup>2</sup>. ii) Microparticles of 2.5  $\mu\text{m}$  were prepared by a water-in-oil emulsification combined with a cross-linking process of polysaccharides dextran, pullulan and fucoidan<sup>3</sup>. iii) Stable microcapsules (2-6  $\mu\text{m}$ ) made polysaccharide and functionalized with fucoidan were designed<sup>4</sup>. iv) Solid spherical nanoparticles (136 $\pm$ 4 nm) containing fucoidan were synthesized and then also loaded with a clinical thrombolytic drug<sup>5</sup>.

We have analysed in vitro the binding efficiency to recombinant P-selectin and to activated platelet aggregates under venous and arterial flows, and the efficiency in a mouse model of thrombosis by monitoring the platelet density with intravital microscopy, and in the intraluminal thrombus associated with progression of abdominal aortic aneurysms in rats.

### RESULTS AND DISCUSSION

- 1) Fucoidan with  $^{99m}\text{Tc}$  (Radio-purity >95%) efficiently bind to P-selectin in several animal models of thrombus.
- 2) In vitro experiments on human activated platelets, ex vivo flow chamber assays under arterial and venous shear stress conditions, and in vivo experiments on rat and mouse models evidenced targeting of fucoidan on P-selectin in thrombi. This effect has been observed for the fucoidan alone or on the surface of several nano/microsystems. Polysaccharide based-nanoparticles targeted with fucoidan improved the thrombolysis efficiency of a loaded clinical drug in thrombosis acute phase.
- 3) The purification techniques have been optimized for industrial development of a pharmaceutical grade fucoidan. We obtained in 2015 from the French regulatory agency ANSM the label "raw material for pharmaceutical use".
- 4) The Investigational Medicinal Product Dossier containing all regulatory safety data and product descriptions, the Investigator's Brochure and the clinical protocol were then prepared. We obtained in January 2018 and March 2018 the agreements from French and Dutch medical agencies, respectively, to start the phase I clinical trials of the polysaccharide as a contrast agent for SPECT imaging of atherothrombosis. These clinical trials are expected to start in summer 2018 in Paris and Amsterdam.

### CONCLUSION

Fucoidan efficiently bind to P-selectin in several animal models of thrombus. Clinical grade fucoidan was prepared and clinical trials are expected in summer 2018 for molecular imaging of thrombus. Fucoidan-functionalized polymeric nano/microparticles were also developed with fucoidan acting as a targeting agent in several delivery systems. The discovery of polymers as molecular targets, as well as the demonstration of their efficacy in preclinical and clinical trials for imaging and therapy, could improve the prevention, diagnosis and treatment of atherosclerosis.

### REFERENCES

1. Rouzet F *et al.*, J Nucl Med 2011;2:1433-40
2. Bonnard T *et al.*, Theranostics 2014;4:592-603
3. Suzuki M *et al.*, Nanomedicine 2015;10:73-87
4. Li B, *et al.*, Adv Healthc Mater 2017;6:4
5. Juenet M, *et al.*, Biomaterials 2018;156:204-216

### ACKNOWLEDGMENTS

This work received the financial supports of the ANR-13-LAB1-0005-01 "Fuco-Chem", ANR-13-RPIB-0006 "Fucothrombo" and the EU project FP7-NMP-2012-LARGE-6-309820 "NanoAthero".



## Anticoagulative Activity of Anionic Block Polymers – Structural and Mechanistic Considerations

Bartłomiej Kałaska<sup>1</sup>, Kamil Kamiński<sup>2</sup>, Joanna Mikłosz<sup>1</sup>, Shin-Ichi Yusa<sup>3</sup>, Emilia Sokołowska<sup>1</sup>, Agnieszka Błazejczyk<sup>4</sup>, Joanna Wietrzyk<sup>4</sup>, Dariusz Pawlak<sup>1</sup>, Maria Nowakowska<sup>2</sup>, Andrzej Mogielnicki<sup>1</sup>, Krzysztof Szczubiałka<sup>2</sup>

<sup>1</sup>Department of Pharmacodynamics, Medical University in Białystok, Poland

<sup>2</sup>Faculty of Chemistry, Jagiellonian University, Poland

<sup>3</sup>Department of Applied Chemistry, University of Hyogo, Japan

<sup>4</sup>Institute of Immunology and Experimental Therapy, Polish Academy of Sciences, Poland

[szczubia@chemia.uj.edu.pl](mailto:szczubia@chemia.uj.edu.pl)

### INTRODUCTION

Maintaining blood coagulation processes at equilibrium with fibrinolysis, i.e., hemostasis, is a very complicated process. A pathological deviation to any direction from this state, either towards insufficient or excessive tendency of blood to coagulate, is a potentially life-threatening state. On one hand, inability of blood to coagulate fast enough brings the risk of hemorrhage, while on the other, too quick blood coagulation may cause brain stroke or myocardial infarct.

Blood coagulation can be brought to normal using drugs such as Vitamin K, which restores blood coagulation, or heparin, which prevents blood coagulation and is one of the most widely applied anticoagulants. Use of anticoagulants is inherently connected with the risk of hemorrhage, e.g. due to overdose or trauma. The need to quickly stop anticoagulant action may thus occur by the administration of a proper antidote. However, many of the currently used anticoagulants do not have a safe and quickly acting antidote. Protamine, the only antidote to heparin, is an example of a drug with many severe side effects. Therefore, the search is continued for new anticoagulants and, in parallel, their antidotes.

We have synthesized antidotes for heparin based on cationically-modified polysaccharides<sup>1,2</sup> and synthetic polycations<sup>3</sup>. The optimal efficiency/safety profiles was shown cationically-modified dextran<sup>4</sup> and synthetic block polycations<sup>5</sup>. More recently, we have synthesized block polyanions which show anticoagulative properties, on one hand, and can be reversed with block polycations by the formation of polyelectrolyte complexes (PECs).

### EXPERIMENTAL METHODS

The block copolymers of PEG and PAMPS (polyanions), PEG and PMPC (zwitterionic polymers) and PEG and PMAPTAC (polycations) were synthesized using the RAFT technique. Cationically-modified dextran was synthesized by substitution of 40 kDa dextran with GTMAC.

### RESULTS AND DISCUSSION

Block copolymers were synthesized containing anionic poly(sodium 2-acrylamido-2-methylpropanesulfonate) (PAMPS) block as an anticoagulative component. To lower the toxicity of PAMPS it was copolymerized either with poly(ethylene glycol) (PEG) or poly(2-(methacryloyloxy)ethyl phosphorylcholine) (PMPC). The polymers showed anticoagulative properties both *in vitro* and *in vivo*. The influence of the polymer architecture and composition on the efficacy of anticoagulation and safety parameters was evaluated.

PEG-b-PAMPS copolymers could be reversed with a copolymer of PEG and poly(3-(methacryloylamino)propyl trimethylammonium chloride) (PMAPTAC) (PEG41-b-PMAPTAC53, HBC), which also effectively neutralized heparin. Neutralization of PEG-b-PAMPS could be attributed to the formation of polyelectrolyte complexes (PICs) with neutral PEG shells and cores composed of a mixture of cationic and anionic blocks of both copolymers. The PICs show no anticoagulative properties. PEG-b-PAMPS copolymers increased activated partial thromboplastin time (aPTT), prothrombin time and showed significant anti-FXa activity. The polymers inhibited platelet aggregation *in vitro* but not *in vivo*. All the studied polymers showed anti-inflammatory properties.

### CONCLUSION

The PEG-PAMPS and PEG-PMAPTAC block copolymers constitute a well-matching anticoagulant-antidote pair which can be further optimized by adjusting the relative block lengths and molecular weights.

### REFERENCES

1. K. Kamiński, K. Szczubiałka, K. Zazakowny, R. Lach, M. Nowakowska. *J.Med.Chem.* 2010, 53, 4141–4147.
2. Kałaska, B.; Sokołowska, E.; Kamiński, K.; Szczubiałka, K.; Kramkowski, K.; Mogielnicki, A.; Nowakowska, M.; Buczek, W. *Eur. J. Pharmacol.* 2012, 686 (1–3), 81–89.
3. K. Kamiński, B. Kałaska, P. Koczurkiewicz, M. Michalik, K. Szczubiałka, A. Mogielnicki, W. Buczek, M. Nowakowska *MedChemComm* 2014, 5, 489–495.
4. E. Sokołowska, B. Kałaska, K. Kamiński, A. Lewandowska, A. Błazejczyk, J. Wietrzyk, I. Kasacka, K. Szczubiałka, D. Pawlak, M. Nowakowska, A. Mogielnicki *Front. Pharmacol.* 2016, 7, 60.
5. B. Kałaska, K. Kamiński, J. Mikłosz, S.-I. Yusa, E. Sokołowska, A. Błazejczyk, J. Wietrzyk, I. Kasacka, K. Szczubiałka, D. Pawlak, M. Nowakowska, A. Mogielnicki, A. *Transl. Res.* 2016, 177, 98–112.

### ACKNOWLEDGMENTS

Grants 2011/03/B/NZ7/00755 and 2016/21/B/ST5/00837 from Polish National Science Centre (NCN) are gratefully acknowledged.

## Modification of PVC and PU with Cu and Se species for NO generation purpose

Liana Azizova, Lyuba Mikhailovska, Sergey Mikhailovsky

School of Pharmacy and Biomolecular Sciences/University of Brighton, UK

[liana.azizova@yahoo.com](mailto:liana.azizova@yahoo.com)

### INTRODUCTION

Biocompatible blood-contacting polymer should have both antithrombotic and antibacterial properties. Nitric oxide is a molecule which reduces clotting by its capacity to inhibit platelet adhesion and aggregation. Nitric oxide shows also an antibacterial activity by preventing bacterial film formation on the polymer surface. The endogenous S-nitrosothiols (RSNO) which are able to be decomposed by some transition metals may serve as NO-donors in human blood plasma. In this project we aimed to modify PVC and PU, two commonly used in blood-contacting devices polymers with Se and Cu species and show their capacity for NO generation in physiological conditions.

### EXPERIMENTAL METHODS

Film of polyvinylchloride (PVC) was purchased from Goodfellow (UK) and polyurethane (PU) was gifted by DelStar (UK). Polydopamine (PDA) and poly(norepinephrine) (PNE) form stable thin films firmly attached to the polymer surface. These two reagents were used as the intermediate modifying reagents with an aim to introduce reactive groups, including  $\text{NH}_2$ , to the polymers surface. The density of surface amine groups on PDA and PNE coatings was controlled by orange II assay<sup>1</sup> in order to optimise the amount of  $\text{NH}_2$  groups on the polymer surface for further immobilisation of Se species. Selenium species were attached using a 3,3'-diselenodipropionic acid (dSdPA) via EDC/NHS method. dSdPA was synthesized as described<sup>2</sup>. Copper nanoparticles were immobilized on polymers coated with PDA/PNE using their redox activity and ability of phenolic hydroxyl groups to chelate metal ions. In short, PDA/PNE-coated films were incubated in copper salt solutions in the range of concentration 1- 10 mg/mL at room temperature<sup>3</sup>. The chemical structure of the molecules attached to the surface was investigated by PerkinElmer Spectrum 65 FT-IR Spectrometer. The amount of surface immobilised Selenium and Copper were measured using Perkin-Elmer Optima 2100 DV inductively coupled plasma – optical emission spectrometer.

### RESULTS AND DISCUSSION

Films of PVC and PU modified by polydopamine (PDA) and poly(norepinephrine) (PNE) were obtained. It was found that amount of  $\text{NH}_2$  surface groups can vary from 0.9 nmole/cm<sup>2</sup> to 3.7 nmole/cm<sup>2</sup>. The functionalization of PVC and PU by PDA/PNE has also been confirmed by FTIR spectroscopy: ~3340 cm<sup>-1</sup>, is assigned to  $\nu(\text{N-H})$  and  $\nu(\text{O-H})$  stretching modes, ~1605 cm<sup>-1</sup>, representative of aromatic C=C stretching mode and N-H bending vibration (Fig. 1). Selenium was attached to the PVC and PU surface via COOH groups of dSdPA and  $\text{NH}_2$  groups of PDA/PNE coatings using

EDC/NHS coupling. The selenium content on the PU and PVC modified surfaces lies within a range of 0.0463 to 0.679  $\mu\text{mole}/\text{cm}^2$ .

Copper nanoparticles (CuNPs) were also immobilized on both, PVC and PU surfaces. Copper content of the PVC and PU surfaces was measured in the range from 94 to 385 nmole/cm<sup>2</sup>.

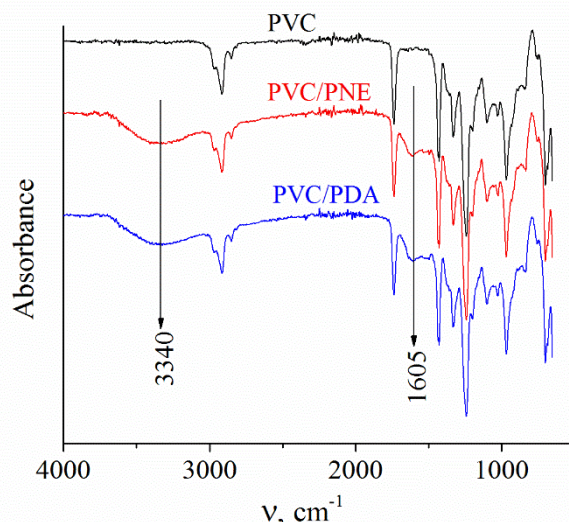


Fig. 1. FTIR spectra of PVC, PVC modified by PNE, and PVC modified by PDA.

### CONCLUSION

Two polymers, PVC and PU were modified with PDA/PNE in order to attach optimum amount Se and Cu species. FTIR spectra confirm modification of PVC and PU films by PDA/PNE. The measured amount of Se and Cu species on the surface of modified polymers is in the range of concentration which can produce the amount of NO similar to that generated in vivo<sup>4</sup>.

Preliminary assessment of NO release at physiologic conditions showed that both surfaces are capable of NO generation. Measurements of antimicrobial activity of materials are under development.

### REFERENCES

1. Noel S. *et al.*, *Bioconjugate Chem.* 22:1690–1699, 2011
2. Koch T. *et al.*, *Bioconjugate Chem.* 1:296–304, 1990
3. Wang Z. *et al.*, *Chem. Mater.* 29:8195–8201, 2017
- 4.a) Yang J. *et al.*, *Langmuir.* 16:10265–10272, 2008;  
b) Hwang S. *et al.*, *Biomaterials.* 29:2443–2452, 2008

### ACKNOWLEDGMENTS

This work is supported by the Marie Skłodowska-Curie Action of the European Union (H2020- MSCA-IF-2016, grant agreement no. 749207) and IRSES Nanobiomat; PIRSES-GA-2013-612484.

## Biocompatible Polyurethane-Titanium Composite Utilisation in the Innovative Flexible Valve Designed for Pulsatile Ventricular Assist Devices

Małgorzata Gonsior<sup>1</sup>, Artur Kapis<sup>1</sup>, Przemysław Kurtyka<sup>1</sup>, Roman Kustos<sup>1</sup>, Roman Major<sup>2</sup>, Juergen M. Lackner<sup>3</sup>, Mirosława El Fray<sup>4</sup>, Andrzej Misztela<sup>5</sup>

<sup>1</sup>Artificial Heart Laboratory, Prof Zbigniew Religa Foundation for Cardiac Surgery Development, Poland

<sup>2</sup>Institute of Metallurgy and Materials Science Polish Academy of Sciences Cracow, Poland

<sup>3</sup>Joanneum Research Forschungs-GmbH, Materials – Functional Surfaces, Leoben, Austria

<sup>4</sup>Division of Biomaterials and Microbiological Technologies, Nanotechnology Centre, West Pomeranian University of Technology, Szczecin, Poland

<sup>5</sup>Medical Tools Factory CHIRMED Rudniki near Czestochowa, Poland

[m.gonsior@frk.pl](mailto:m.gonsior@frk.pl)

### INTRODUCTION

Extracorporeal pulsatile ventricle assist devices (PVAD) are a well-known method for prolonged heart support in end-stage heart insufficiency, especially for children as the only common applicable method. However, major problem of PVADs is thrombus formation due to inadequate blood flow dynamics of mechanical valves. The new polyurethane valves (PUV) were designed for Polish ReligaHeart PVADs: single-leaflet inflow valve and two-leaflet outflow valve, consisting of flexible leaflets and valve house, equipped with titanium cores (Fig.1). The flexible valve design has to guarantee athrombogenic construction, by reduction of turbulence and sufficient valve wall washing [1].

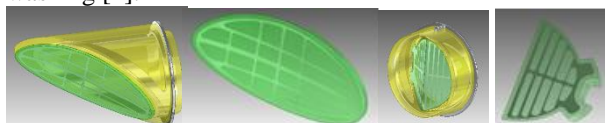


Fig. 1. New inflow and outflow flexible valves design

### EXPERIMENTAL METHODS

The single-leaflet inflow and double-leaflet outflow valve were designed using ANSYS stress numerical analysis. The titanium valve leaflets meshes were manufactured using precise laser cutting and investigated with SEM, TEM and CLSM utilisation, following with athrombogenic DLC and a-C:H carbon surface layer modification. The polyurethane Bionate 90A thin wall flexible valve leaflets with immersed titanium mesh were manufactured, utilizing temperature controlled pressing. The polyurethane wear resistance, mechanical thermal analysis (T=-100°C;+150°C), elasticity properties according to PN-ISO 37 as well as rheological tests (MFI) were carried out, in order to develop the proper temperature controlled pressing technology for leaflets prototypes manufacturing. Analysis of platelets wear after contact with the investigated material in hydrodynamic test was performed, investigating platelets activation and aggregation by flow cytometry and confocal microscopy.

### RESULTS AND DISCUSSION

The titanium Grade2 meshes size 0,06mm were manufactured as well as the PU valves leaflets (Fig. 2).

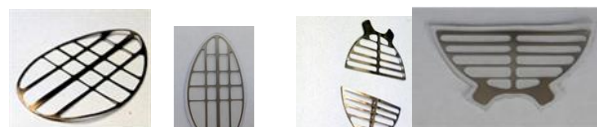


Fig. 2. Titanium meshes and PU valve leaflets

The microscopic evaluation confirmed the good properties of manufactured titanium mesh surface (Fig. 3).

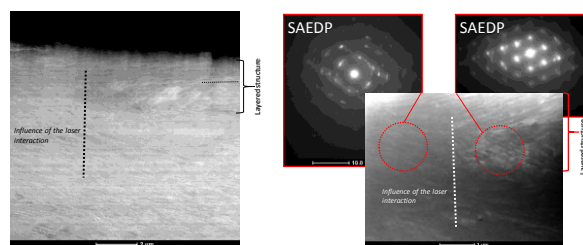


Fig. 3. TEM analysis of titanium mesh

Elasticity tests shown significant polyurethane mechanical properties change in increasing temperature: in T = 50°C the 30% Young's modulus and 60 % wear resistance decreasing was observed. Rheological polyurethane test results: MFI (T=200°C, 2,16kg)= 4,73±0,35 [g/10min]; and MFI (T=210°C, 2,16kg)= 6,22±0,41 [g/10min].

All samples in biological study similarly affected the activation of the PAC-1 and P-selectin antigens. The amount of active platelets were comparable for all samples except a-C:H 106 nm and 60 nm layers, which exhibited a slightly higher content of platelets. The total number of platelet aggregates was maintained at a constant level for all materials. Slight differences were observed within the small and large aggregates.

### CONCLUSION

The flexible polyurethane - titanium composite leaflet valves were constructed and manufactured as the inlet and outlet valves for pulsatile heart assist device, presenting good mechanical and biological properties. Further biological investigation of ReligaHeart PVAD equipped with polyurethane valves is continued.

### REFERENCES

1. Kapis A. *et al.*, Int J Artif Organs 40(8): 430-469, P74, 2017

### ACKNOWLEDGMENTS

The authors would like to thank NCBIR (Grant bioVALVE in M-Era.Net programme) for providing financial support to this project.



## Cellular response to blow-spun scaffolds modified by Polyelectrolyte Multilayer Films

Aldona Mzyk<sup>1</sup>, Michal Wojasinski<sup>2</sup>, Piotr Natkanski<sup>3</sup>, Aleksandra Drewienkiewicz<sup>1</sup>

<sup>1</sup>Institute of Metallurgy and Materials Science, Polish Academy of Sciences, Cracow, Poland

<sup>2</sup>Department of Biotechnology and Bioprocess Engineering, Warsaw University of Technology, Warsaw, Poland

<sup>3</sup>Faculty of Chemistry, Jagiellonian University, Cracow, Poland

[aldonamzyk@gmail.com](mailto:aldonamzyk@gmail.com)

### INTRODUCTION

Biomaterials engineering gives a great promise for the damaged myocardium reconstruction. For this purpose, it is necessary to design materials with properties regulating niche-specific cellular response. This is not possible without knowledge about fundamental relationship between scaffold parameters and cell response. There are several attempts dealing with explanation of cellular response to the applied scaffolds according to an effect of material mechanical properties [1-3]. However, mechano-activation of cardiac progenitor cells has not been studied so far. Therefore, we aim to develop and functionalized a new blow spun patch as smart carrier of cardiac progenitor cells for myocardium regeneration.

### EXPERIMENTAL METHODS

#### Porous patches fabrication

The porous polyurethane/albumin mats were fabricated by solution blow spinning method. The manufacturing process of materials was optimized toward macroscopic mechanical properties similar to the physiological values characteristic for pericardium. The SBS system consisted of: 1) the concentric nozzles system (inner and outer nozzles), 2) supply of compressed air, 3) supply of a polymer solution and 4) rotating drum as a collector.

#### Surface functionalization of blow spun patches

The blow spun scaffolds were functionalized by chitosan/chondroitin sulfate Polyelectrolyte Multilayer Films (PEMs). Stiffness of PEMs was regulated by chemical cross-linking based on NHS/EDC chemistry and nanoparticles incorporation (silver and graphene oxide flakes).

### RESULTS AND DISCUSSION

The novel type of polymer blow-spun patches was fabricated and functionalized by PEMs (Fig.1) that facilitated control over surface properties such as stiffness, roughness, surface wettability (Table 1) and thus proteins adsorption as well as cellular response (Fig.2). Properties of PEMs were controlled by structural changes through the chemical cross-linking process and nanoparticles incorporation. The obtained results of cardiac progenitor cells – scaffold interaction indicated that PEMs modification has improved cell adhesion and proliferation rate. Scaffolds modification by PEMs was essential for the cell paracrine activity. The crucial parameter that influenced cellular response was an architecture of scaffold and the PEMs stiffness.

Table 1. Scaffold properties before and after functionalization.

Material	Mean Fiber diameter $\pm$ SE [nm]	Porosity $\pm$ SD [%]	Pore size $\pm$ SD [ $\mu$ m]	Contact angle $\pm$ SD [°]	Young modulus $\pm$ SD [MPa]
CF/BSA 4:1	449 $\pm$ 17	93.6 $\pm$ 1.0	13.5 $\pm$ 1.4	107.4 $\pm$ 11.8	14.0 $\pm$ 2.0
CF/BSA PEMs	1062 $\pm$ 10	73.4 $\pm$ 1.0	8.5 $\pm$ 0.8	58.3 $\pm$ 4.4	12.5 $\pm$ 2.0

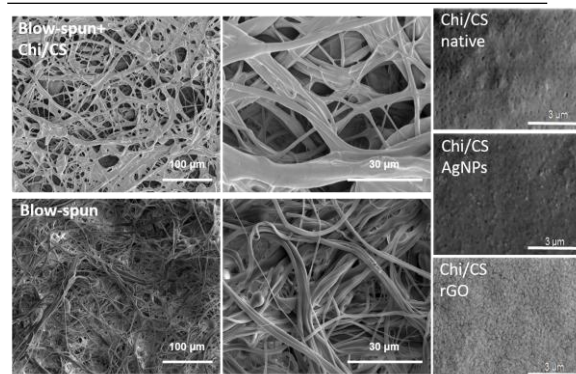


Fig.1. SEM images of scaffolds before and after functionalization.

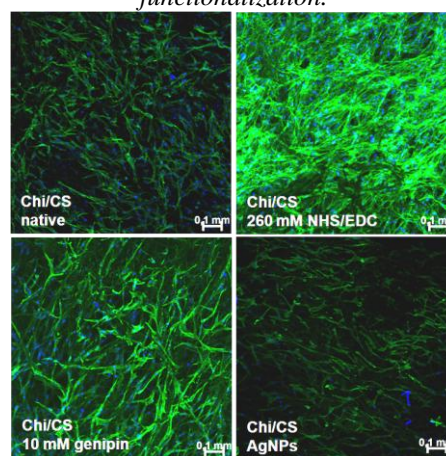


Fig. 2. Cell response depends on the scaffold modification.

### CONCLUSION

The presented experimental approach allowed to develop and functionalized a new blow spun patch as smart carrier of cardiac progenitor cells for myocardium regeneration.

### REFERENCES

1. Picart C. *et al.* *Curr Med Chem.* 7:685-97, 2008
2. Gribova V. *et al.* *Acta Biomaterialia.* 9:6468–6480, 2013
3. McMurray R.J. *et al.* *Tissue Eng Regen Med.* 5, 2014

### ACKNOWLEDGMENTS

The research was financially supported by the grant No. 2014/15/N/ST8/02601 of the Polish National Center of Science.

## Injectable Chitosan/Carrageenan/PNIPAM Hydrogel Designed with Au Nanoparticles: Towards Conductive Scaffolds for Tissue Engineering Demands

Mohadeseh Doroodian<sup>1</sup>, Amirhashayar Ahadpour<sup>1</sup>, Ali Pourjavadi<sup>1</sup>, Shahram Azari<sup>2</sup>

<sup>1</sup>Department of Chemistry, Sharif University of Technology, Iran

<sup>2</sup>National Cell Bank of Iran, Pasteur Institute of Iran, Tehran, Iran

[m.doroodian@gmail.com](mailto:m.doroodian@gmail.com)

[amirhashayarahadpour@yahoo.com](mailto:amirhashayarahadpour@yahoo.com)

### INTRODUCTION

Scaffolds for tissue engineering of specific sites such as cardiac tissues need a comprehensive design of 3 dimensional materials that covers all aspects of chemical composition and physical structures required for regeneration of desired cells.<sup>1</sup> Hydrogels possessing highly hydrated and interconnected structures are promising materials for tissue engineering applications.<sup>2</sup> Improvement of an injectable hydrogel from biocompatible polysaccharides and poly-N-isopropyl acryl amide enriched with Au nanoparticles are the main goal of this study. Two main enhancements are included mixture design of the components and addition of Au nanoparticles to access a homogeneous mixture that have potential application in tissue engineering.

### EXPERIMENTAL METHODS

- a) Preparation of chitosan loaded with Au nanoparticles

Chitosan solution was prepared by dissolving 0.100 g of chitosan in 10.0 mL of acetic acid solution (2% in deionized water). Then, 200  $\mu$ L of HAuCl<sub>4</sub> solution (0.1% weight/volume) was added to the chitosan solution and the mixture was stirred in 70°C for two hours.

- b) Preparation of thermo-sensitive hydrogel

Thermo-sensitive hydrogel was synthesized in two steps. At first, radical polymerization of NIPAM in the presence of APS was done through dissolving 2.000 g of NIPAM in 15.0 mL of deionized water, degassing of the solution for 15 minutes with N<sub>2</sub>, addition of 0.150 g of APS, and next refluxing the mixture in 80°C for 12 hours. Afterwards, the white resinous solid (PNIPAM) was separated and washed with hot water several times to remove the unreacted monomers, and then dried in 70°C for three days. 5% (W/V) solution of PNIPAM in deionized water was prepared and used for subsequent experiments.

At second step, a mixture from chitosan loaded with Au NPs and  $\kappa$ -carrageenan was prepared via formation of electrostatic interactions between NH<sup>3+</sup> of chitosan and SO<sup>3-</sup> of  $\kappa$ -carrageenan. To form a homogeneous mixture between two components a new method was applied to mix the polysaccharides. At first, 5 mL of concentrate chitosan/Au NPs and  $\kappa$ -carrageenan solutions (1% W/V) were diluted to 100.0 mL separately. These two solutions were added to a 250 mL beaker gradually (5 mL/min) under vigorous stirring and then concentrate to 10 mL at 40°C to reach the initial concentration.

Finally, the PNIPAM solution and polyelectrolyte mixture of chitosan/Au and  $\kappa$ -carrageenan were mixed with determined ratio and the mixtures were stirred for one day.

### RESULTS AND DISCUSSION

FESEM, TEM, XRD analyses and rheological behaviour studies have been applied to investigate physical structure of the composite. Addition of Au nanoparticles as a conductive component to enhance cell attachment and growth is a critical spot that is investigated through MTT assay.

### CONCLUSION

Injectable hydrogel was synthesized through electrostatic interactions. Au nanoparticles enhance cell growth as shown by MTT assay.

### REFERENCES

1. Baei, Payam, et al. "Electrically conductive gold nanoparticle-chitosan thermosensitive hydrogels for cardiac tissue engineering." *Materials Science and Engineering: C* 63 (2016): 131-141.
2. Radhakrishnan, Janani, et al. "Injectable and 3D bioprinted polysaccharide hydrogels: from cartilage to osteochondral tissue engineering." *Biomacromolecules* 18.1 (2016): 1-26.

## Photo-crosslinkable Collagen-based Precursors for Vascular Tissue Engineering

Nele Pien<sup>1,2</sup>, Daniele Pezzoli<sup>2</sup>, Dimitria Camasao<sup>2</sup>, Fabrice Bray<sup>3</sup>, Christian Rolando<sup>3</sup>, Madalina Albu<sup>4</sup>,  
Diego Mantovani<sup>2</sup>, Sandra Van Vlierberghe<sup>1,5</sup>, Peter Dubruel<sup>1</sup>

<sup>1</sup>Polymer Chemistry & Biomaterials Research Group, Centre of Macromolecular Chemistry, Ghent University, Belgium

<sup>2</sup>Laboratory for Biomaterials and Bioengineering, CRC-I, Laval University, Canada

<sup>3</sup>Miniaturisation pour la Synthèse, l'Analyse & la Protéomique (MSAP), Université Lille 1, France

<sup>4</sup>Department of Collagen Research, National Research & Development Institute for Textiles and Leather, Romania

<sup>5</sup>Brussels Photonics, Vrije Universiteit Brussel, Belgium

[nele.pien@ugent.be](mailto:nele.pien@ugent.be)

### INTRODUCTION

The aim of vascular tissue engineering (VTE) is the design of responsive, living conduits, with properties similar to those of native tissue.<sup>1</sup> Collagen type I, being the main component of native vessels, is a promising scaffold material for vascular TE owing to its favourable biological properties and to the ability of cells to remodel its matrix.<sup>2</sup> The present work targets the development of collagen precursors functionalized with photo-crosslinkable moieties while preserving the biocompatibility, to develop stable collagen-based hydrogel films.

### EXPERIMENTAL METHODS

Bovine skin collagen was provided by the Department of Collagen Research. In brief, methacrylated collagen was prepared by reaction of the primary amines of collagen with methacrylic anhydride (MeAnH). First, collagen (10 w/v%) was dissolved in phosphate buffer (pH = 7.8) at 40°C. Next, 0.5, 1 or 2 equivalents of MeAnH with respect to the primary amines were added followed by stirring for 1 hour. Next, the reaction mixture was dialyzed (MWCO 12-14 kDa) against distilled water (40°C, 24 h), followed by freeze-drying. <sup>1</sup>H-NMR spectroscopy (500 MHz) at 40°C was applied as a qualitative tool to evaluate the functionalization of collagen. The molecular weight of the collagen precursors was determined using gel permeation chromatography (GPC). The effect of functionalization on its physical gelation behaviour was studied using differential scanning calorimetry (DSC). Identification of the biopolymer peptide sequence was performed via mass spectrometry analysis (Orbitrap) along with bioinformatic analysis on unmodified and functionalized collagen precursors. Furthermore, crosslinked collagen films were characterized in depth in terms of gel fraction, swelling ratio and mechanical properties using rheology. Potential cytotoxicity of the functionalized collagen was evaluated using human umbilical vein endothelial cells (HUVECs). Cell viability, proliferation and morphology were examined via indirect (i.e. using material extracts) and direct (i.e. cell seeding) *in vitro* assays.

### RESULTS AND DISCUSSION

GPC measurements indicated moderate hydrolysis (~10%) comparable to observed hydrolysis for gelatin modifications.<sup>4</sup> DSC measurements indicated similar denaturation temperatures (~30°C) for all developed derivatives irrespective of the degree of substitution (DS). Since the denaturation temperature is related to

the transition of the triple helix to a statistic coil conformation<sup>3</sup>, these results imply similar triple helix formation is still observed, although the denaturation enthalpy indicates that the length of the formed triple helices is somewhat hampered by the introduction of the functionalities. Proteomics results showed that the targeted lysine groups were successfully modified. More specifically, 33, 38 and 57% of the lysines present were functionalized upon applying 0.5, 1 or 2 eq MeAnH. In addition to the amino acid quantification and localization, the position of the introduced double bonds was also determined via proteomics, which indicated a homogeneous methacrylamide distribution throughout the collagen backbone. Rheological measurements confirmed that an increasing number of crosslinkable moieties yields a higher storage modulus, due to a higher network density. Since the final goal is to develop materials that will be used in the presence of vascular cells, evaluation of cytocompatibility of the functionalized collagen precursors was also pursued. Indirect *in vitro* assays using HUVECs indicated excellent cell viability (i.e. 97, 94 and 96% upon addition of 0.5, 1 and 2 eq MeAnH). The direct assay of HUVEC seeding on the functionalized collagen films is still ongoing, so no conclusions can be discussed yet.

### CONCLUSION

Collagen type I has been successfully functionalized with photo-crosslinkable moieties. Different equivalents of MeAnH have resulted in varying degrees of functionalization. The modified collagen precursors have proven to be photo-crosslinkable and biocompatible materials with tunable mechanical properties.

### REFERENCES

1. Seifu, D. *et al.*, Nat. Rev. Cardiol. 10(7), 2013
2. Loy, C. *et al.*, Biomater. Sci. 5, 153, 2017
3. Ryglova, S. *et al.*, Macromol. Mater. Eng. 302, 2017
4. Van Hoorick, J. *et al.*, Biomacromolecules, 18, 2017

### ACKNOWLEDGMENTS

This work has been supported by the Research Foundation Flanders (FWO, G0F0516N).



## Polycaprolactone/ Beta Tricalcium Phosphate / Collagen as a 3D Printed Tissue Scaffold

Mehmet Onur Aydogdu<sup>1,2</sup>, Nazmi Ekren<sup>1,3</sup>, Faik Nuzhet Oktar<sup>\*4,1</sup>, Osman Kilic<sup>5</sup>, Oguzhan Gunduz<sup>1,6</sup>

<sup>1</sup>Advanced Nanomaterials Research Laboratory/ Department of Metallurgical and Materials Engineering, Marmara University, Turkey

<sup>2</sup>Department of Metallurgical and Materials Engineering, Master of Science, Institute of Pure and Applied Sciences, Marmara University, Turkey

<sup>3</sup>Department of Electrical - Electronics Engineering, Faculty of Technology, Marmara University, Turkey

<sup>4</sup>Department of Bioengineering, Faculty of Engineering, Marmara University, Turkey

<sup>5</sup>Department of Electrical and Electronics Engineering, Faculty of Technology, Marmara University, Turkey

<sup>6</sup>Department of Metallurgical and Materials Engineering, Faculty of Technology, Marmara University, Turkey

[foktar@marmara.edu.tr](mailto:foktar@marmara.edu.tr)

### INTRODUCTION

Additive Manufacturing techniques (AMT) for tissue engineering researches can be considered as a big breakthrough since the AMT allows higher degree of control to be available over architecture of scaffold compared to the traditional methods [1,2]. Therefore, production of the tissue scaffolds using AMT can be very promising. However, requirements are not only limited with the production method, selection of the materials is also crucial because of the inevitable requirements of a proper scaffold such as biodegradability and biocompatibility. Hence, Polycaprolactone (PCL) as a synthetic polymer and collagen as a natural polymer with the presence of beta Tricalcium phosphate ( $\beta$ -TCP) may provide a unique synergy to create proper tissue scaffolds because of the individual advantages of each material [3,4].

### EXPERIMENTAL METHODS

Three identical 10 wt. % of PCL solutions were prepared using dichloromethane as a dissolving agent., 2, 5, and 10 wt.% of  $\beta$ -TCP was added to the different PCL solutions. Afterwards collagen with 0.1 wt. % were added to each solution. 3D bioprinting of the scaffolds was performed using a bioprinter. Bioprinting were carried out under 50 mm/s printing speed, 1ml/hr flow rate. After the production phase, physical properties such as viscosity, surface tension and density for each solution was measured using calibrated equipment. Additionally, morphological structure of the scaffolds was revealed using scanning electron microscope and chemical structure of scaffolds was determined by Fourier-Transform Infrared Spectroscopy (FTIR). Finally, biocompatibility of the scaffolds were examined using Saos-2 human osteosarcoma cells.

### RESULTS AND DISCUSSION

Results indicated that the layer by layer production was successfully achieved. One of the major challenges in AMT is to keep uniform morphology and structural integrity during the bioprinting process. Therefore, solution properties are important and can create limitations since they have direct influence over the quality of the final product. Therefore, optimized viscosity for different solutions were measured between the range of 1540 cP to 6200 cP. Morphology of the scaffold was also revealed and results indicated that the increasing concentration of the  $\beta$ -TCP was corrected imperfections of the scaffold macrostructure.

Furthermore, pore diameter frequency of the scaffolds was also measured. Uniform pore size distribution was observed between 1,15 – 1,35 mm diameters for samples with 10 wt. %  $\beta$ -TCP ratio. Chemical composition of the polymer was revealed by FTIR. Characteristic FTIR peaks of  $\beta$ -TCP at 1026  $\text{cm}^{-1}$ , 602  $\text{cm}^{-1}$  and 562  $\text{cm}^{-1}$ , collagen at 1,633  $\text{cm}^{-1}$ , 1550  $\text{cm}^{-1}$  were observed. Additionally, all peaks of PCL were also clearly observed [5,6,7].

### CONCLUSION

Production of a composite tissue scaffold was demonstrated in this study with optimised parameter of the process as well as the comparative analysis of morphology directly affected by the increased concentration of  $\beta$ -TCP.

### REFERENCES

1. Groll J. *et al.*, Biofabrication 8, 2016
2. Peltola S. M. *et al.*, Ann. Med. 40:268-280, 2008
3. Gautam S. *et al.*, Mater. Sci. Eng. C 33:1228-1235, 2013
4. Holmes R. E. *et al.*, J. Bone Joint Surg. Am. 68:904-911, 1968
5. Elzein T. *et al.*, J. Colloid Interface Sci. 273:381-387, 2004
6. Tavares D. S. *et al.*, Appl. Oral Sci. 21:37-42, 2013
7. Kim B. S. *et al.*, Biotechnol Prog, 28:973-980, 2012

### ACKNOWLEDGEMENTS

This study has been funded by Ministry of Development, Turkey; project no: 2016K121280

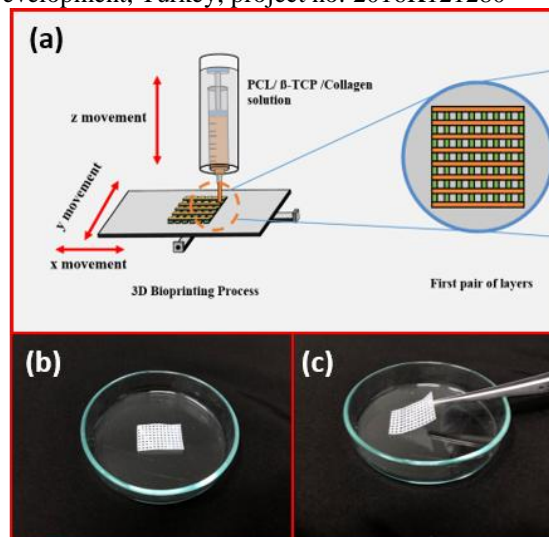


Fig. 1. Schematic representation of the 3D bioprinting (a) and camera images of the product (b,c).

## Electrohydrodynamic (EHD) Bioprinting of Bacterial Cellulose / Polycaprolactone Scaffolds

Esra Altun<sup>1,2</sup>, Nazmi Ekren<sup>1,3</sup>, Osman Kilic<sup>1,4</sup>, Oguzhan Gunduz<sup>1,5</sup>

<sup>1</sup>Advanced Nanomaterials Research Laboratory, Marmara University, Turkey

<sup>2</sup>Department of Metallurgical and Materials Engineering, Master of Science, Institute of Pure and Applied Sciences, Marmara University, Turkey

<sup>3</sup>Department of Electrical-Electronics Engineering, Faculty of Technology, Marmara University, Turkey

<sup>4</sup>Department of Electrical and Electronics Engineering, Faculty of Engineering, Marmara University, Turkey

<sup>5</sup>Department of Metallurgical and Materials Engineering, Faculty of Technology, Marmara University, Turkey  
[oguzhan@marmara.edu.tr](mailto:oguzhan@marmara.edu.tr)

### INTRODUCTION

Poly( $\epsilon$ -caprolactone) (PCL) is a biodegradable aliphatic polyester, which has biocompatibility and bioresorbability<sup>1</sup>. Also it can be combined with other biomaterials as Bacterial Cellulose (BC) biomaterial. Bacterial Cellulose is a highly hydrophilic natural polymer with high water absorption capacity and biocompatibility<sup>2</sup>. 3D patterned porous scaffold plays an important role in tissue engineering for better cell proliferation and tissue formation<sup>3</sup>. In this study, the basics of 3D printing and Electrohydrodynamic (EHD) method are combined and used to produce 3D patterned porous scaffold from two different BC:PCL polymer blend solutions.

### EXPERIMENTAL METHODS

#### 1. Solution Preparation

Polycaprolactone (PCL) solution was prepared by dissolving as 10 wt% in Dichloromethane (DCM) with continuous magnetic stirring for 2 hours. 5 wt% Bacterial Cellulose (BC) was sonicated in Dimethylformamide (DMF) using a sonifier for 1 h. The solution was centrifuged for 20 minutes and the DMF on the surface of fragmented BC was removed. After the centrifugation method, fragmented BC was added to 10 wt% PCL solution as 5 and 7 wt%. To be used final blends were magnetically stirred at the ambient temperature (23°C) for 1 h.

#### 2. EHD Bioprinting



Fig. 1. Digital image of EHD bioprinting

Pre-designated (with SolidWorks software) pattern model was used for EHD bioprinting. 3D scaffold patterns were printed on a microscope slide. Each prepared solution was loaded in a 10 mL standard syringe and electric potential was set to nozzle, which is mounted to system. According to the values of the previous studies, 1 to 2 kV were applied on the solutions. After the EHD bioprinting, all the samples were kept in laboratory oven at 25°C for 24 hours to evaporate residue DCM.

### RESULTS AND DISCUSSION

Fig. 2 shows comparative optical microscope and SEM images for 5 wt% BC:PCL, 7wt% BC:PCL and 10 wt% PCL samples for 1 to 2 kV. As can be seen on the images, while BC concentration increasing 5 to 7 wt%, structures of the patterned scaffolds were started to change their pore structures. 5 wt% BC:PCL sample was found to be significantly better pore structure comparing with 7 wt% BC:PCL sample.

Sample Name	kV Value	Optical Microscope Images	Scanning Electron Microscope Images
10 wt% PCL	2 kV		
5 wt% BC in PCL	2 kV		
10 wt% PCL	1 kV		
7 wt% BC in PCL	1 kV		

Fig. 2. Optical and SEM images of the EHD bioprinted scaffold samples.

### CONCLUSION

This work is demonstrated the potential of using EHD bioprinting for layer by layer printed BC:PCL scaffolds. 5 wt% BC:PCL scaffolds successfully fabricated with sub-200 $\mu$ m pore structure and the sample can be used variety applications of biomedical engineering.

### REFERENCES

- Woodruff M.A. and Hutmacher D.W., Progress in Polymer Science 35-1217, 2010.
- Qiu Y., *et al.*, Materials Science and Engineering C 59-303, 2016.
- Zhong S., *et al.*, Tissue Eng. Part B Rev. 18-77, 2011.

### ACKNOWLEDGMENTS

This study has been supported by BAPKO, Marmara University; project no: FEN-C-YLP-110117-0021 and Ministry of Development, Turkey; project no: 2016K121280.

## 3D Bioprinting of Medical Adhesives

Malgorzata K. Wlodarczyk-Biegun, Julieta Paez, Jun Feng, Maria Villiou, Aránzazu del Campo

Dynamic Biomaterials, Leibniz Institute for New Materials (INM), Germany  
[Malgorzata.Wlodarczyk@leibniz-inm.de](mailto:Malgorzata.Wlodarczyk@leibniz-inm.de); [aranzazu.delcampo@leibniz-inm.de](mailto:aranzazu.delcampo@leibniz-inm.de)

## INTRODUCTION

3D bioprinting is a booming technique allowing to build up 3 dimensional, well define structures. The process is based on precise deposition of biologically relevant material, usually hydrogel-based<sup>1,2</sup>. Development of biomedical inks is challenging since they need to combine printability with biocompatibility<sup>2</sup>, printable medical glues additional need to meet requirement of adhesiveness in wet and dry environment<sup>3</sup>. Therefore, such formulations are currently not available. In our lab we have developed printable tissue glues, envisioning their great potential in minimal surgery applications, where high precision in material deposition is required.

## EXPERIMENTAL METHODS

Bioinks based on catechol functionalized polymers, with various compositions, were prepared and printed with extrusion and inkjet technique. Different bioinspired chemistries leading to crosslinked networks at close-to-physiological conditions were tested. Resolution of printing and shape fidelity of prints were assessed based on brightfield microscopy and scanning electron microscopy images. Rheology measurement of viscosity, stiffness and relaxation time of proposed systems were used to compare the formulations. Influence of ink composition, crosslinking chemistry and pH on the rheological properties were studied. Additionally, cell viability on the printed scaffolds was tested. Tensile tests were used to analyse adhesiveness of developed material in wet and dry conditions.

## RESULTS AND DISCUSSION

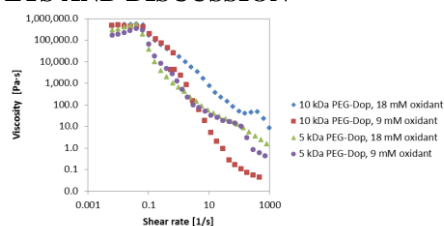


Fig. 1. Viscosity of proposed medical glues.

Developed hydrogel-based materials showed appropriate rheological properties, including shear thinning effect (Fig. 1), for facilitated printability and good resolution and shape fidelity of printed features. Depending on their chemical design, the formulations were successfully used for inkjet or extrusion printing (Fig. 2), with optional secondary cross-linking.

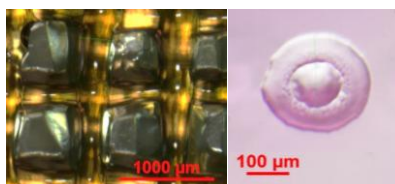


Fig. 2. Adhesives printed with extrusion (left) and inkjet (right) technique.

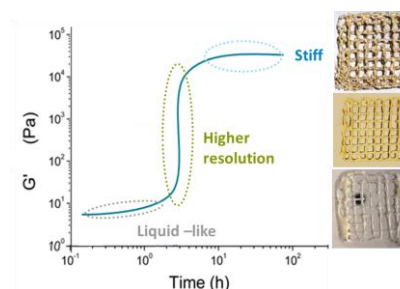


Fig. 3. Time dependent printability of one of the proposed formulations.

Final mechanical properties of the glues were controlled by the applied cross-linking chemistry, molecular weight, concentration of components (polymer, oxidant, metal ions), pH and waiting time in relation to gelation kinetics (Fig. 3).

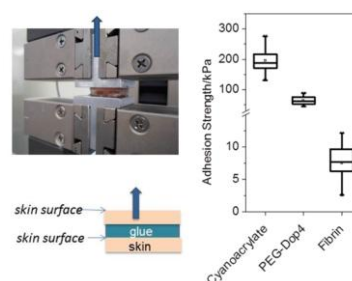


Fig. 4. Adhesive properties of the developed glue in comparison with two other commonly used tissue glues<sup>4</sup>.

Developed inks showed great adhesive properties (Fig. 4) in dry and wet environments. Additionally, cells seeded on the printed scaffolds revealed high viability (<96%).

Proposed system offers flexible formulation and possibility to adjust compositional and printing parameters, enabling to meet application-specific working conditions, adhesive and mechanical properties. Moreover, constructed hydrogel-based, stable scaffolds with high shape fidelity, are compatible with cells. In addition, cell-gel bioinks for building self-adhesive 3D structures allow straightforward affixing of the scaffolds. As a lack of new, functional bioinks is a main obstacle in the progress in 3D bioprinting<sup>2</sup>, and printable medical glues are not available, we believe that our study is of high significance.

## CONCLUSION

We have developed printable medical glues, based on variability of catechol chemistry. We believe that these materials have great application potential in regenerative medicine approaches and can be translated into clinical products for surgery.

## REFERENCES

1. Wlodarczyk-Biegun *et al.*, *Biomaterials* 134:180-201, 2017
2. Malda *et al.*, *Adv.Mater.* 25: 5011–5028, 2013
3. Mehdizadeh and Yang, *Macromol Biosci.*13: 271–288, 2013.
4. Feng *et al.*, *Biomimetics* 2(4), 23, 2017



### 3D Printed Polyvinyl Alcohol Sampling Filters for the Entrapment of Exhaled Microorganisms

Alaa Al Taie<sup>1</sup>, Xiaoxiao Han<sup>2</sup>, Caroline Williams<sup>3</sup>, Mohamad Abdulwhhab<sup>3</sup>, Andrew P Abbott<sup>4</sup>, Alex Goddard<sup>4</sup>, Malgorzata Wegrzyn<sup>3</sup>, Natalie J. Garton<sup>3</sup>, Michael R. Barer<sup>3</sup>, Jingzhe Pan<sup>1</sup>

<sup>1</sup>Department of Engineering, University of Leicester, Leicester, LE1 7RH, UK

<sup>2</sup>Wolfson School of Mechanical, Electrical and Manufacturing Engineering, Loughborough University, LE11 3TU, UK

<sup>3</sup>Department of Infection, Immunity and Inflammation, University of Leicester, Leicester, UK

<sup>4</sup>Department of Chemistry, University of Leicester, Leicester LE1 7RH, UK

[aaajat2@le.ac.uk](mailto:aaajat2@le.ac.uk)

#### INTRODUCTION

3D printing using Fused Deposition Modelling (FDM) has been used to produce scaffolds and complex designs<sup>1</sup>. FDM can be used to develop membranes, which can be used for biological sampling and diagnosis. Many infectious diseases including TB and flu are transmitted via air through the inhalation of droplet nuclei. The collection efficiency of cotton, cellulose, PTFE, polycarbonate and Sartorius gelatin filters have been studied when sampling airborne microbes. These filters differ from each other in composition, thickness and pore size. Gelatin filters show good collection efficiency for hydrophilic viruses<sup>2</sup>, however, they may be unsuitable for delicate organisms<sup>3</sup>. Williams *et al.* used gelatin filters in face masks for *Mycobacterium tuberculosis* detection<sup>4</sup>. Fragility of gelatin filters can limit their utility and they may degrade in the high humidity when sampling in masks. Furthermore, gelatin is not DNA-free material. In the work presented here, we show that biodegradable polymers can be printed as multilayers to create a porous matrix for microbial capture. PVA is considered promising material to be used for cell entrapment as its cryogel has been used as matrices for cell immobilization<sup>5</sup>. Also, the maintenance of *E. coli* within a PVA scaffold microstructure has been studied recently<sup>6</sup>. The goal of this study is to i) design and print a full face mask, nasal sampler and sampling filters from PVA and examine the matrix for *Mycobacterium* detection. ii) Study surface and mechanical features of the matrix.

#### EXPERIMENTAL METHODS

The PVA filament was used to print the designed models of filters and face mask. PVA filters were either inoculated with bacteria or exposed to aerosols generated by an Omron A3 nebuliser. *Mycobacterium bovis* BCG and *M. abscessus* (rough and smooth morphotypes) were used. Quantitative polymerase chain reactions (qPCR) were used to determine bacterial recovery rate from both PVA and gelatin filters. These were dissolved in water, bacteria pelleted followed by DNA extraction and qPCR. Tensiometer, X-ray CT Scans, SEM, Optical Profilometry, Theta Lite Optical Tensiometer, and Fluorescence Microscopy were used to study the mechanical and other characteristic features of PVA printed filters including tensile strength, porosity, surface topography, roughness and wettability.

#### RESULTS AND DISCUSSION

The 3D printed PVA samples shown in Fig. 1 yielded results comparable to gelatin filters for *Mycobacterial*

analyses but offer several advantages over the latter material. PVA can be handled and fabricated into fully printed face mask due to its toughness, as the absorbed energy at break is 714.27 mJ for PVA compared with 0.04 mJ for gelatin for the same samples dimensions. The hydrophilicity of the PVA matrix surface and its roughness of (Ra >1) may enhance the capture of bacteria. The formed pores between PVA layers of the model could reinforce the entrapment of organisms into the matrix.

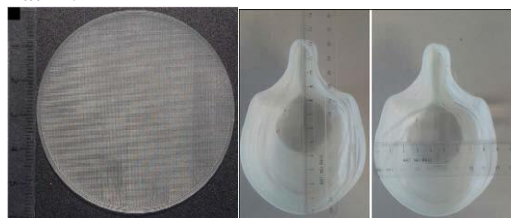


Fig. 1. Sampling filter (left), full face mask (right).

#### CONCLUSION

3D printed PVA filters were quantitatively examined for bacterial diagnostic objectives. FDM offers printing novel products for microbiology applications, saving time and cost. PVA is economic, can be dissolved in water and contains no background DNA. 3D designs may be the future innovative technology for microbiology applications.

#### REFERENCES

1. Zein, I., et al., Fused deposition modeling of novel scaffold architectures for tissue engineering applications. *Biomaterials*, 2002. 23(4): p. 1169-1185.
2. Tseng, C.-C. and C.-S. Li, Collection efficiencies of aerosol samplers for virus-containing aerosols. *Journal of Aerosol Science*, 2005. 36(5): p. 593-607.
3. Li, C.-S., Evaluation of microbial samplers for bacterial microorganisms. *Aerosol Science and Technology*, 1999. 30(2): p. 100-108.
4. Williams, C.M., et al., Face mask sampling for the detection of *Mycobacterium tuberculosis* in expelled aerosols. 2014. 9(8).
5. Lozinsky, V. and F. Plieva, Poly (vinyl alcohol) cryogels employed as matrices for cell immobilization. 3. Overview of recent research and developments. *Enzyme and microbial technology*, 1998. 23(3): p. 227-242.
6. Gutiérrez, M.C., et al., Hydrogel scaffolds with immobilized bacteria for 3D cultures. *Chemistry of materials*, 2007. 19(8): p. 1968-1973.

#### ACKNOWLEDGMENTS

Alaa Al-Taie gratefully acknowledges the Iraqi Ministry of Higher Education and scientific research (MOHESR) and the University of Leicester which supported this work.



## Bioactive Scaffolds of 3D Bioprinted Gelatin/Alginate and Gelatine/Alginate/Tri-calcium Phosphate Composites as a Potential Biomaterial for Bone Tissue Engineering

Burak Ozbek<sup>1,2</sup>, Osman Kılıç<sup>3,2</sup>, Nazmi Ekren<sup>4,2</sup>, Faik Nuzhet Oktar<sup>5,2</sup>, Cevriye Kalkandelen<sup>6,2</sup>, Mahir Mahirogullari<sup>7</sup>, Oguzhan Gunduz<sup>8,2</sup>

<sup>1</sup>Metallurgical and Materials Engineering/Institute of Pure and Applied Sciences, Marmara University, Turkey

<sup>2</sup>Metallurgical and Materials Engineering/Advance Nanomaterials Research Laboratory, Marmara University, Turkey

<sup>3</sup>Electrical and Electronics Engineering/Faculty of Engineering, Marmara University, Turkey

<sup>4</sup>Electrical-Electronics Engineering/Faculty of Technology, Marmara University, Turkey

<sup>5</sup>Biomedical Engineering/Faculty of Engineering, Marmara University, Turkey

<sup>6</sup>Biomedical Devices Technology/Vocational School of Technical Sciences, Turkey

<sup>7</sup>Department of Orthopaedics and Traumatology, Memorial Hospital, Turkey

<sup>8</sup>Metallurgical and Materials Engineering/Faculty of Technology, Marmara University, Turkey

[kalkan@istanbul.edu.tr](mailto:kalkan@istanbul.edu.tr)

### INTRODUCTION

Biomaterials which are used for regenerative medicine aims and objectives to heal damaged organs and tissues by merging cells and scaffold materials<sup>1</sup>. In the last decade, direct writing of the materials with 3D printing has become more important than other methods, because it has ability to manage the scaffold layer-by-layer. In addition to that, design of the scaffold can be adjusting by computer design software<sup>2</sup>. In this study, combination of biomaterials like gelatin, alginate and tri-calcium phosphate (TCP) were used as hydrogels to produce 3D printed scaffolds which were biologically active and biodegradable to heal injured tissues in bone and cartilage.

### EXPERIMENTAL METHODS

#### Preparation of hydrogels

Gelatin/alginate and gelatin/alginate/TCP hydrogels prepared by dissolving and mixing materials in deionized water heated to 90°C. 20 wt% gelatin (Halavet A.Ş., Istanbul, Turkey) solution was mixed with 10, 13, 15 wt% TCP. Following TCP addition, 2 wt% alginate powder mixed with solution to obtain hydrogel under magnetic stirring at 500 rpm and 90°C. Same weight percentages used for gelatin/alginate solution.

#### Fabrication of scaffolds

Scaffolds with 21x41x3 mm<sup>3</sup> (with 60% porosity) were produced by using 3D plotting machine, which were manufactured and modified by Tribot (Istanbul, Turkey) Solutions loaded to 10 ml syringes and syringe were placed into syringe holder with heating pad. Process achieved under sufficient pressure, 30°C temperature and with 19G luer lock needle.

#### Characterization of scaffolds

Fourier transform infrared spectrometer (FTIR) study were completed in transmission mode (Jasco, Easton, USA). Scanning electron microscopy (SEM) and cell culture study of the scaffolds were analysed.

### RESULTS AND DISCUSSION

Scaffolds were successfully produced (Figure 1) at 30°C temperature. Gelatin gel behave like solid at low temperatures while it liquefies at high temperatures. Therefore, optimized temperature selected for the process<sup>3,4</sup>. FTIR spectra of the structures were given in Fig. 2. For gelatin, absorption bands at 1629 cm<sup>-1</sup>, 1550 cm<sup>-1</sup> and 1240 cm<sup>-1</sup> were represent C=O, C-N stretching and N-H bending vibration, respectively. For alginate,

1452 cm<sup>-1</sup> were stood for symmetric stretching vibration of COO- group<sup>5</sup>.

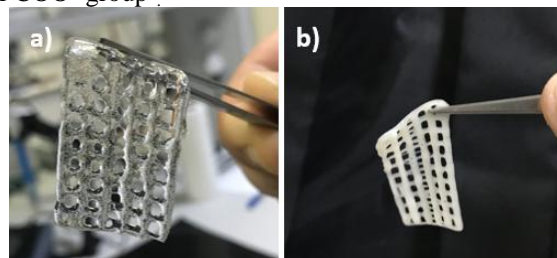


Fig. 1. Produced scaffolds, a) gelatin/alginate scaffold, b) gelatin/alginate/TCP scaffold.

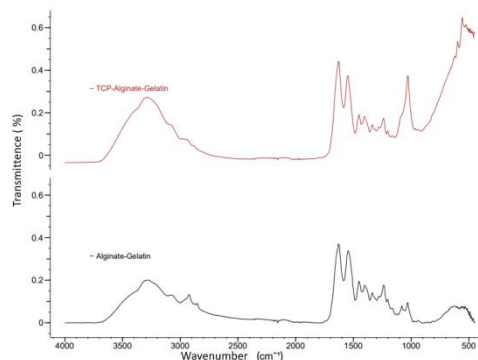


Fig. 2. FTIR spectra of the scaffolds.

### CONCLUSION

Gelatin/alginate and gelatin/alginate/TCP scaffolds were successfully produced with 3D bioprinting. Due to biocompatible profiles of the materials, manufactured structures can be perfect candidate for bone tissue engineering, which will be supported with future studies.

### REFERENCES

- Schuurman W. *et al.* Macromol. Biosci. 13:551-561, 2013
- A. Ito *et al.* Biosci. Bioeng. 95:196-199, 2003
- Luo Y. *et al.* RSC Advan. 5:43480-43488, 2015
- C. Kalkandelen. *et al.* IOP Conf. Ser. Mater. Sci. Eng. 293:012001, 2017
- Dong Z. *et al.* J. Membr. Sci. 280:37-44, 2006

### ACKNOWLEDGMENTS

This study is granted by Marmara University, BAPKO foundation (Project No: FEN-C-YLP-120417-0177) and Republic of Turkey Ministry of Development (Project No: 2016K121280). We also Thank Halavet A.Ş. company for giving us gelatin powder and thank Tribot Company for custom made 3d bioprinting.

### 3D Printing Bioactive Composite Scaffolds for Bone Tissue Engineering

Yunis Moukbil<sup>1</sup>, Busra Isindag<sup>1</sup>, Velican E. Gayir<sup>1</sup>, Burak Ozbek<sup>2,3</sup>, Ebru Toksoy Oner<sup>4</sup>, Faik N. Oktar<sup>1,2</sup>, Mehmet S. Eroglu<sup>5</sup>, Oguzhan Gunduz<sup>6,2</sup>

<sup>1</sup>Bioengineer. Dept., Faculty of Engineer., Marmara Univ., Istanbul, Turkey.

<sup>2</sup>Advanced Nanomaterial. Research Lab., Faculty of Technology, Marmara Univ., Istanbul, Turkey.

<sup>3</sup>Dept. of Metallurgical and Materials Engineer., Inst. of Pure and Applied Sciences, Marmara Univ., Istanbul, Turkey.

<sup>4</sup>IBSB, Department of Bioengineer., Marmara Univ., Istanbul, Turkey

<sup>5</sup>Dept. of Chemistry, Faculty of Engineering, Marmara Univ., Istanbul, Turkey.

<sup>6</sup>Department of Metallurgy and Material. Engineer., Faculty of Technology, Marmara Univ., Istanbul, Turkey.

[Yunismsm@gmail.com](mailto:Yunismsm@gmail.com)

#### INTRODUCTION

High intensity life style that cause, more and more injures and fractures, which are inevitable<sup>1</sup>. More often than not they are bone related and can affect the life style of the individual. To overcome such a problem invasive methods such as surgery or the application of autogenous grafts are used. Even though autogenous grafts are useful, they are quite limited in application<sup>2</sup>. Therefore, engineering is integrated with life sciences to create a more viable solution, such as bioscaffolds<sup>1</sup>. Biodegradable scaffolds are used to remedy the aforementioned defects and create a solution and a quick regeneration of different tissues<sup>3</sup>. There has been a lot of research of different biodegradable substances that can be used in the fabrication of the scaffolds. In this study, we research the effects of 3D printed PLA/TCP/HA scaffolds on cell growth both from the mechanical aspect and from the cell growth and proliferation.

#### EXPERIMENTAL METHODS

In this experiment to create the 3D bioscaffolds THF (Tetrahydrofuran) solution was used to dissolve PCL (Polycaprolacton), TCP (tricalcium phosphate) and BHA (Bovine hydroxyapatite). These substances were added in a consecutive order respectively upon the complete dissolution of the previous substance. The mixing took place at 50°C. Then they were loaded into a syringe and placed in a mechanical pump. The scaffolds had been printed with a 3D Ulitimaker 2<sup>+</sup>. Biocompatibility of the samples will be investigated in-vitro with human osteoblast (HOB) cell line and analysed with the use of a SEM (Scanning Electron Microscope). Scaffold composition was investigated with the use of Jasco FT/IR 4700 (Fourier Transform Infrared Spectrometer) device in terms of percent transmittance to wave number.

#### RESULTS AND DISCUSSION

In this study the scaffolds were printed with a 3D printer using the concept that can be seen in Fig. 1.

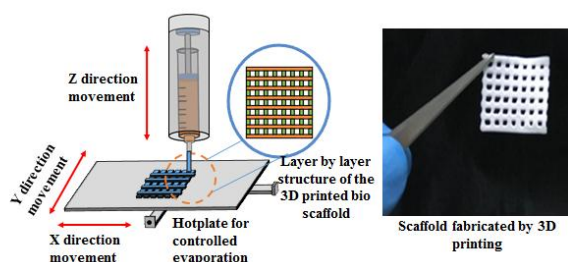


Fig. 1. Operating concept of the 3D printer.

A detailed investigation of the scaffold composition was conducted and the samples have showed to have all the desired components and all the initial components, (PCL, TCP and BHA) as can be seen from Fig. 2.

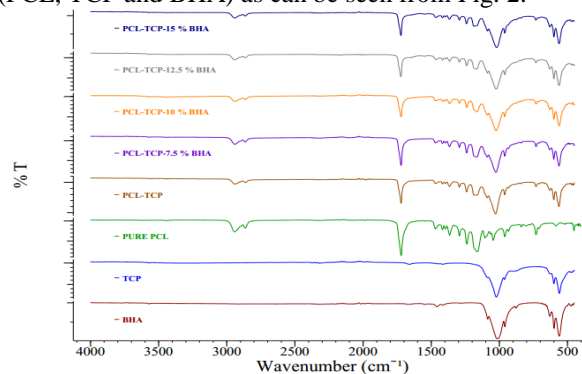


Fig. 2. FT/IR analysis of the scaffold composition.

#### CONCLUSION

Scaffolds were successfully created by using 3D printing with different concentrations of BHA. The most optimal concentration of BHA fabricated was chosen for growth and proliferation of HOB cells and further studies are to be conducted in vitro. The cell studies are to be made including cell proliferation and osteoblastic differentiation.

The cells have shown positive growth and integration with the scaffold. Further studies will be conducted for a deeper understanding of the cell behaviour with the scaffolds.

#### REFERENCES

1. Y. Liu, *et al.*, Review: development of clinically relevant scaffolds for vascularized bone tissue engineering, *Biotechnol. Adv.* 31 (2013) 688–705.
2. J.D. Boerckel, *et al.*, Effects of in vivo mechanical loading on large bone defect regeneration, *J.Orthop.Res.*30(2012)1067–1075.
3. K. Rezwan, *et al.*, Biodegradable and bioactive porous polymer/inorganic composite scaffolds for bone tissue engineering, *Biomaterials* 27(2006)3413–3431.

#### ACKNOWLEDGMENTS

This study was supported by Marmara University, BAPKO foundation (Project No: FEN-C-YLP-120417-0177). As well as the Ministry of Development of the Republic of Turkey (project No: 2016K121280)

## Bioresorbable, Radiopaque and 3D Printable Scaffolds for Bone Tissue

Naroa Sadaba, Jone Muñoz, Jose-Ramon Sarasua, Ester Zuza

Department of Mining-Metallurgy Engineering and Materials Science Institute of Polymer Materials (POYMAT)  
University of the Basque country (UPV/EHU) faculty of Engineering Alameda de Urquijo s/n 48013 Bilbao (Spain)

[Naroa.sadaba@polymat.eu](mailto:Naroa.sadaba@polymat.eu)

### INTRODUCTION

The so called “Additive manufacturing” is a new manufacturing process which consists in translating virtual solid model data into physical models in a quick and easy process. The most known example is 3D printing. In the present work, this novel technology will be used to print scaffolds with biomaterials.

Tissue engineering emerged from the need to repair a tissue or organ failure due to damage or injury. This area of knowledge comprehends different fields, such as the Materials Engineering, the Biology and the Medicine. During the last decade the number of studies related to tissue engineering has significantly increased. Due to all these efforts, currently, many different tissues and organs such as vascular graft<sup>1</sup>, skin graft<sup>2</sup> and bone<sup>3</sup> amongst others can be replaced, resulting in the improvement of the quality of life of the human being. Focusing on biomaterials, during the last decade the tissue engineering applications have moved forward to the use of biodegradable and bioactive materials. One application for these materials can be the graft or bone implants. Unlike traditional metal implants, polymer implants have the advantage of enabling the regeneration of the tissue or the bone, and disappearing some time after the procedure through the absorption by the body. Therefore, in the last years the polymers and especially the biocompatible polymers have experienced a great increase in both research and practical applications. One of the most used polymers nowadays are the polyesters because of their great diversity. Amongst the most used polyesters for medical applications, it can be cited the polylactide (PLA) and their derivatives<sup>4</sup>.

Despite all the advantages that these materials offer in comparison to others, their use has been limited so far, due to the fact that it is not possible to monitor the implant properly. In order to overcome this problem, it was decided to mix these polymers with radiopaque markers. As a consequence, the polymer becomes visible to the X-rays. It should be noted that X-ray visible substances are those with high atomic weight, such as barium sulphate ( $\text{BaSO}_4$ ), bismuth salts, tantalum or tungsten<sup>5</sup>.

The aim of the present study is to make scaffolds with radiopaque composite materials. In order to achieve this goal, a 3D-biploter printer is used. As this printer is based on the FDM technology, the thermal and rheological behaviour of the materials has been studied. Once the scaffold is printed, the mechanical properties of the scaffold are studied. By adding radiopaque particles, the mechanical properties of these scaffolds are improved in comparison to the scaffolds of unfilled PLLA.

### EXPERIMENTAL METHODS

For appropriate use of the 3D printing it is necessary to study the rheological and thermal behavior of polymers. For the radiopaque material, it is necessary to analyse the dispersion of the material, mechanical properties, radiopacity and cytotoxic test.

### RESULTS AND DISCUSSION

This printable system based on polylactide with barium sulphate has mechanical properties that fits with the natural bone and reduce the fragility of the actually implantable and resorbable devices.

AlamarBlue® and PicoGreen® assays were performed to quantify proliferation and metabolic activity of human dermal fibroblast (HDFs) seeded on these samples. Taken together, metabolic activity and proliferation results demonstrate that the materials employed in this work are not cytotoxic and provide a valid substrate for cells to attach and proliferate.

As shown in Figure 1, these materials are suitable for 3D impression, it begins with the construction of scaffolds.



Fig.1. Scaffold of PLLA/ $\text{BaSO}_4$  manufactured by 3D printing

### CONCLUSION

Poly(lactide)/barium sulphate composite system, that has good properties obtained in solid state (i. e. injected pieces or sheets obtained by compression molding) could be 3D printed.

Due to the radiopacity and the great toughness of this material, a broad range of possibilities of applying this composite as fixation devices or bone reconstruction in the biomedical field should be considered for future studies.

### REFERENCES

1. Bhowmick, S *et al.* Materials Science and Engineering: C 79: 15–22. 2017.
2. Cheng, L, *et al.* Biomaterials 83:169–81.2016.
3. Esmailzadeh, J, *et al.* Materials Science and Engineering: C 77: 978–89. 2017
4. Komae, H. *et al.* Tissue Eng. Regen. Med. 11, 926–935. 2017
5. Matthew J. *et al.* J. of Nanoparticle Research 15, 2146/1-2146/10. 2013.

### ACKNOWLEDGMENTS

Authors are thankful for funds of Basque Government (GV/EJ) Department of Education (IT-927-16) and from MINECO (MAT 2016-78527-P). N. Sadaba is thankful for the predoctoral fellowship to POLYMAT Fundazioa-Basque Center for Macromolecular Design and Engineering.



## Antimicrobial Supramolecular UPy-Based Biomaterials

Sabrina Zaccaria<sup>1,2</sup>, Ronald C. van Gaal<sup>2,3</sup>, Martijn Riool<sup>4</sup>, Moniek Schmitz<sup>1,2</sup>, Sebastian A.J. Zaat<sup>4</sup>,  
Patricia Y.W. Dankers<sup>1,2,3</sup>.

<sup>1</sup>Lab. of Chemical Biology, <sup>2</sup>Institute for Complex Molecular Systems and <sup>3</sup>Lab. for Cell and Tissue Engineering, Eindhoven University of Technology, Eindhoven, The Netherlands.

<sup>4</sup>Dept. of Medical Microbiology, Amsterdam Infection and Immunity Institute, Academic Medical Center (AMC), Amsterdam, The Netherlands.

[m.riool@amc.uva.nl](mailto:m.riool@amc.uva.nl)

### INTRODUCTION

The use of biomaterials inside the body always entails the risk of infection. The risk of infection might even be higher in so-called *in situ* tissue engineering applications, where population/infiltration of the scaffold material by endogenous cells and thereby the formation of new/healed tissue occurs as a spatiotemporal process. Since the porous scaffold materials can form a niche for invading bacteria, the intended *in situ* production of novel tissue may be severely compromised by infection. Therefore, we aim to develop a new polymeric supramolecular scaffold material, exerting two important functions: preventing microbial adhesion and thereby preventing biofilm formation, and inducing endogenous (eukaryotic) cells to repair the body.

### EXPERIMENTAL METHODS

#### *Synthesis of UPy-modified antimicrobial peptides*

The antimicrobial polymers were prepared by simply mixing-and-matching of Ureido-Pyrimidinone (UPy) based supramolecular polymers<sup>1</sup> with the antimicrobial peptides (AMPs) SYM11KK (KKFPWWPFKK), L<sub>9</sub>K<sub>6</sub> (LKLLKLLKLLKLL) and LASIO III (VNWKKILGKIIVVK) modified with a supramolecular UPy moiety. The AMPs were synthesized by manual 9-fluorenylmethoxycarbonyl (Fmoc)-based solid phase peptide synthesis, and coupled to the UPy-synthon in solution. Successful coupling was confirmed by LC/MS. The secondary structure of the UPy-AMPs in the presence and absence of sodium dodecyl sulphate (SDS, 30 mM) was investigated by circular dichroism (CD) spectroscopy using a Jasco J-815 spectropolarimeter.

#### *Drop cast preparation*

Solid samples were prepared by drop-casting 50 µL of a 5 w/v% of polycaprolactone (PCL<sub>2k</sub>)-diUPy solution in hexafluoroisopropanol (HFIP) with 0, 0.5, 1, 2 and 4 mol % AMPs or UPy-AMPs on glass coverslips.

#### *Antimicrobial activity*

The antimicrobial activity in solution of the UPy-AMPs against *Escherichia coli* ATCC8937, *Staphylococcus aureus* RN4220 and methicillin-resistant *S. aureus* (MRSA) AMC201 was evaluated. The minimal inhibitory concentration (MIC) was determined after 24 h of incubation as the lowest concentration (in µM) at which there was no visible bacterial growth. The lowest concentration of AMP (in µM) that killed at least 99.9% of the inoculum (LC<sub>99.9</sub>) after 24 h was determined by colony counting.

The Japanese Industrial Standard test (JIS Z 2801) was performed to evaluate the antimicrobial activity of the drop-cast samples against the above mentioned bacterial strains.

### RESULTS AND DISCUSSION

The AMPs were coupled in solution to a UPy-COOH synthon through formation of a new amidic bond with the peptide N-terminus. The UPy-functionalization of the AMPs did not affect their secondary structure, as proved by circular dichroism spectroscopy. The antimicrobial activity of the UPy-AMPs in solution was also retained. In addition, the incorporation of UPy-AMPs into a UPy-polymer (PCL<sub>2k</sub>-UPy) was stable and the resulting material was biocompatible. The addition of 4 mol% UPy-AMPs in PCL<sub>2k</sub>-UPy polymer samples protected the material against colonization by *E. coli* and (methicillin-resistant) *S. aureus*.

### CONCLUSION

The modular approach enables a stable but dynamic incorporation of the antimicrobial agents, allowing at the same time for the possibility to change the nature of the polymer (fouling/anti-fouling), as well as the use of AMPs with broad range activity, like the promising Synthetic Antimicrobial and Anti-biofilm Peptide SAAP-148.<sup>2</sup> Next, we aim to control cell adhesion by functionalizing UPy-units with the cell-adhesive peptide RGD sequence. Ultimately we aim to use such materials for *in situ* infection-free tissue engineering of vascular tissues, such as vascular grafts and heart valves.

### REFERENCES

1. Dankers P.Y.W. *et al.*, Nat. Mater. 4:568-74, 2005
2. de Breij A. & Riool M. *et al.*, Sci. Transl. Med., 2018

### ACKNOWLEDGMENTS

This work received funding from the Union's Seventh Framework Programme (FP/2007-2013) under Grant Agreement number 310389 (BIP-UPy). Furthermore, this work was supported by COST (European Cooperation in Science and Technology) Action iPROMEDAI (Project No. TD1305) and NWO NEWPOL grant SuperActive (Project No. 731.015.505) in collaboration with the Dutch Polymer Institute (DPI).

## Silicon Biosensors Examined with Surface Techniques: Molecular Arrangement and Composition, Antibody Orientation and Binding Stoichiometry

K. Gajos<sup>1</sup>, A. Budkowski<sup>1</sup>, P. Petrou<sup>2</sup>, V. Pagkali<sup>2</sup>, I. Raptis<sup>3</sup>, K. Awsiuk<sup>1</sup>, J. Rysz<sup>1</sup>, S. Kakabakos<sup>2</sup>

<sup>1</sup>M. Smoluchowski Institute of Physics, Jagiellonian University in Kraków, Poland

<sup>2</sup>INRaSTES, National Center for Sci. Research “Demokritos”, Greece

<sup>3</sup>INN, National Center for Sci. Research “Demokritos”, Greece

[katarzyna.gajos@doctoral.uj.edu.pl](mailto:katarzyna.gajos@doctoral.uj.edu.pl)

### INTRODUCTION

Optical biosensors, which enable a label-free, very sensitive real-time detection of many different molecules, are often based on functionalized silicon surfaces recognizing antigens by an antibody specific binding. To ensure the reliable and effective biosensors performance an uniform and high quality *biofunctionalization and assay protocols* are required. *Multi-step protocols* for immunosensors typically include: surface activation with organo-silanes, immobilization of probe molecules, blocking free sites with non-functional proteins and specific antigen – antibody binding reaction. Biosensor signal can monitor these stages, but it reflects only *cumulative* surface concentration of all different molecules. Therefore, a Time-of-Flight Secondary Ion Mass Spectrometry providing *molecular discrimination* is a powerful tool for characterization of multi-molecular overlayers on biosensing surfaces.

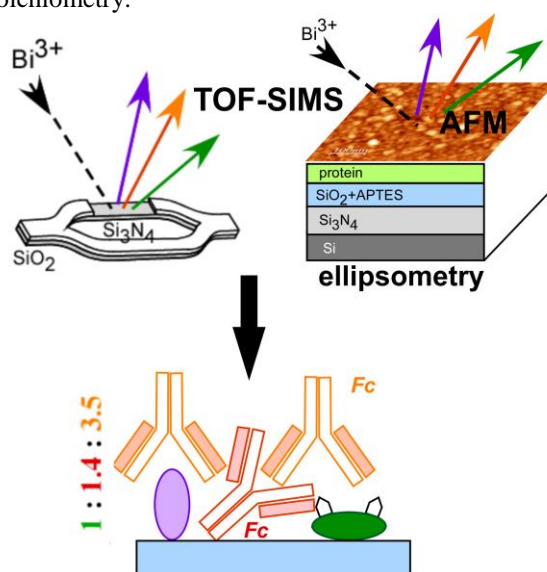
### EXPERIMENTAL METHODS

On-chip interferometric biosensors [1,2] and corresponding planar silicon biosensing surfaces [3,4] are examined after each of the successive steps of biofunctionalization and indirect immunoassay for determination of OchraToxin A (OTA) [2]. These subsequent steps involves: surface modification with (3-aminopropyl)triethoxysilane, immobilization of OTA-ovalbumin conjugate (probe), blocking free surface sites with bovine serum albumin, reaction with a mouse monoclonal antibody against OTA and finally, reaction with a goat anti-mouse secondary antibody. To determine molecular arrangement, composition and orientation in formed multi-molecular overlayers several surface since techniques are employed: Atomic Force Microscopy (AFM), Spectroscopic Ellipsometry and Time-of-Flight Secondary Ion Mass Spectrometry (TOF-SIMS) supported by multivariate data analysis (Principal Component Analysis - PCA).

### RESULTS AND DISCUSSION

A specific molecular arrangement is revealed by AFM, with a multi-component monolayer, which accommodates primary antibodies along with probe and blocking protein, to be finally covered by secondary antibodies [3]. Three novel perspectives of surface characterization are presented [2,3]: First, molecular composition of intermediate and final overlayers, expressed by component mass loadings of different proteins, is determined from TOF-SIMS combined with ellipsometry. Partial desorption of surface-bound probe and blocking protein upon primary immunoreaction is concluded. Second, taking into account this desorption,

binding stoichiometry of both antibodies in immune complexes formed onto the surface is determined, more accurately than estimation based on sensor response, since the last reflects only cumulative mass loading. Third, molecular orientation of immune-adsorbed primary (side-on) and secondary antibody (head-on), determined directly from Principal Component Analysis of TOF-SIMS data, corresponds well to their binding stoichiometry.



### CONCLUSION

The obtained results indicate the great importance of the step-by-step analysis with biomolecular discrimination of the adlayers formed onto biosensors during both functionalization and assay procedure to improve their performance.

### REFERENCES

1. K. Gajos, M. Angelopoulou, *et al.* Appl. Surf. Sci. 385(2016)529
2. K. Gajos *et al.* Appl. Surf. Sci. (2018) in press
3. K. Gajos *et al.*, Colloids Surf. B 150(2017)437
4. K. Gajos *et al.*, Appl. Surf. Sci. 410(2017)79

### ACKNOWLEDGMENTS

This work was supported by the EU funded project “FOODSNIFFER” (FP7-ICT8-318319) and financed by Polish National Science Center (NCN) under Grant 2016/21/N/ST5/00880.

## High-fidelity Control of Nanostructured Poly(ether-ether ketone) Surfaces by Directed Irradiation Synthesis Towards a Tunable Osseointegration

Ana Civantos<sup>1</sup>, Zak Koyn<sup>4</sup>, Jean Paul Allain<sup>1,2,3,4</sup>

<sup>1</sup>Department of Nuclear, Plasma, and Radiological Engineering, University of Illinois at Urbana-Champaign, USA

<sup>2</sup>Micro and Nanotechnology Laboratory, University of Illinois at Urbana-Champaign, USA

<sup>3</sup>Department of Bioengineering, University of Illinois at Urbana-Champaign, USA

<sup>4</sup>Energy Driven Technologies LLC (EDITEKK), Research Park (UIUC), USA

[ancifle@illinois.edu](mailto:ancifle@illinois.edu)

### INTRODUCTION

Although progress on surface modification of candidate implant materials has seen advances, high-fidelity control of enhanced osseointegration in bioactive scaffolds remains elusive<sup>1</sup>. Titanium (Ti) and its alloys have found broad application in dentistry and orthopaedic sectors. Recent work has also resulted in significant progress in surface modification of titanium-based materials enhancing bioactive properties<sup>2</sup>. However, there remain challenges such as ion leaching, inertness and radiopaque properties motivating progress in alternative material classes. One versatile and widely used substrate in orthopaedic surgery is poly-ether ether ketone (PEEK)<sup>3</sup>. These hard polymers offer intrinsic biocompatibility as well as improved mechanical properties and radiolucent behavior compared to Ti materials. Nevertheless, PEEK has some drawbacks such as reduced cell interaction resulting in lower osseointegration compared to Ti-based biomaterials. Surface modification approaches to induce enhanced cell proliferation and differentiation used for metal-based systems can be challenging to translate to hard polymers such as PEEK<sup>4</sup>. Therefore surface modification of PEEK that can introduce local morphology changes is desired<sup>5</sup>. In this work, Directed irradiation synthesis (DIS) is found to control the topography of PEEK with high-fidelity improving osteoconductivity.

### EXPERIMENTAL METHODS

PEEK polymer samples were modified using normal incidence argon (Ar<sup>+</sup>) ions at an energy of 1.0 keV at low fluences (denoted LPEEK) near 10<sup>17</sup> cm<sup>-2</sup> and higher fluences near 10<sup>18</sup> cm<sup>-2</sup> (HPEEK). Characterization consisted of: scanning electron microscopy (SEM), atomic force microscopy (AFM) and hydrophilicity evaluated by contact angle (CA). *In vitro* testing was performed using a preosteoblastic mouse cell line (MC3T3E1) after sterilizing the samples by EtOH 70% and UV exposure during 15 mins. Cell viability studied at 1, 4 and 7 days of cell cultures by Alamarblue assay (ThermoFisher), ALP content was quantified at 4 and 7 days through ALP Kit (Abcam) and cell morphology was performed through SEM evaluation and Actin and DAPI staining. Experiments were performed as triplicates using n=3 each condition. Data were expressed as mean ± standard deviation.

### RESULTS AND DISCUSSION

Cell attachment and proliferation of metabolic activity levels increased by a factor of two for HPEEK compared to control (untreated PEEK). Experiments

confirmed biocompatibility and positive cytotoxicity on DIS-modified samples. In addition, an increased cell differentiation was observed at 7 days for samples with DIS modification, showing ALP levels higher in both modified PEEKs. Indeed, HPEEK reached 3-fold greater ALP levels than unmodified PEEK which confirmed improved osteoconductivity properties in HPEEK samples compared to LPEEK and controls.

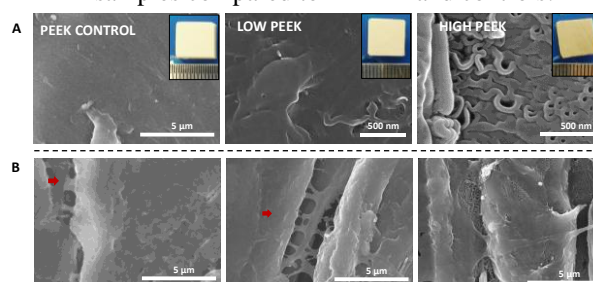


Fig. 1. SEM images of control and modified PEEK before (A) and after (B) 7 days of cell culture

Similarly, cell cytoskeleton images revealed developed actin structure compared to control PEEK which was confirmed by the total coverage of PEEK samples by MC3T3E1 cells at 7 days of cell culture. The increased osteoblast cell behavior towards a more developed cell interaction and cell differentiation in nanostructured PEEK samples confirming DIS as a potential surface modification to enhance the bioactivity of PEEK-based polymers for osseointegration modulation.

### CONCLUSION

DIS has demonstrated improved cell attachment, proliferation and differentiation of osteoblast cells by providing high-fidelity control of nanoscale modification of PEEK surfaces improving bone tissue regeneration. The ability to tailor-control the surface morphology with a single, scalable surface-modification approach can also open new applications for hard-polymer surface modification strategies.

### REFERENCES

- Rautray, T. R., Biomed Mater Res B Appl Biomater 93(2), 581-591 (2010).
- Allain, J. P., & Echeverry-Rendón, M. (2018). Hemocompatibility of Biomaterials for Clinical Applications (pp. 279-326), (2018)
- Najeeb, S., et al. J. Prosthodont Res, 60 (1), 12-19 (2016).
- Ma, R., & Tang, T. Int. J. Mol Sci, 15 (4), 5426-5445 (2014).
- Allain, JP *et al.* Selimovic, S. (Ed.). Book, Ch 2, CRC Press. 41-72, (2014).



## Effect of Topography and Chemical Cues of Biodegradable Polymeric Micro-Structured Replicas on Cellular Alignment and Proliferation

Paraskevi Kavatzikidou<sup>1</sup>, Despina Angelaki<sup>1,2</sup>, Lefki Chaniotaki<sup>1,3</sup>, Eleftheria Babaliari<sup>1,3</sup>, Anthi Ranella<sup>1</sup>, Emmanuel Stratakis<sup>1,2</sup>

<sup>1</sup>Foundation for Research and Technology - Hellas (FORTH), Institute of Electronic Structure and Laser (IESL)

<sup>2</sup>Department of Physics, University of Crete, Crete, Greece

<sup>3</sup>Department of Materials Science and Technology, University of Crete, Crete, Greece

[ekavatz@iesl.forth.gr](mailto:ekavatz@iesl.forth.gr)

### INTRODUCTION

Cells in general take decisions on their responses depending on the stimuli relative to their surrounding environment (cellular-substrate interface). The extracellular matrix provides the necessary cues at micro and nano-scale for the cell adhesion, orientation/alignment, and proliferation. In the nervous tissue, a complex multilayer environment, there are important features to be considered in order to design and develop a structure in terms of topography, morphology and chemistry. Ultrafast pulsed laser irradiation is considered as a simple and effective microfabrication method to produce structures controlling the structure geometry and pattern regularity<sup>1,2</sup>. Such structures characterised with an anisotropy discontinuous topographical nature could enhance neuronal growth and alignment<sup>3</sup>. Soft lithography has been successfully used to transfer well-defined micro-sized patterns from silicon to surfaces of biomaterials allowing the recreation of controlled microenvironments and an in depth study of the influence of surface properties on cell behavior<sup>4</sup>.

### EXPERIMENTAL METHODS

In this study, a series of micro-patterned silicon (Si) structures were fabricated by using the ultrashort laser irradiation at a range of fluences for linearly polarized light beam, resulting in three different roughnesses. Positive replicas on different concentrations of biodegradable polymer poly(lactide-co-glycolide) (PLGA, Mw40-75kDa in 65:35 ratio; ester terminated, Mw 50-75kDa; lactide:glycolide (75:25) and PDMS have been successfully reproduced via soft lithography. The morphological characterization of the polymeric replicas was performed by Scanning Electron Microscopy (SEM). The SEM images were used for the determination of the geometrical characteristics. The cytocompatibility evaluation of replicas with SW10s and N2a neuronal cell lines (30000 cells per well) and different time points (3 and 5 days) was assessed. Immunostaining protocols were used and assessed the cell viability (nucleus –DAPI), cell adhesion and alignment (Cytoskeleton-Phalloidin/actin), and Live /dead staining. A selection of the results are shown due to the limited space (PLGA 65:35 ratio, geometrical characteristics and Schwann cell proliferation).

### RESULTS AND DISCUSSION

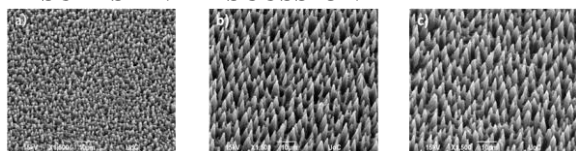
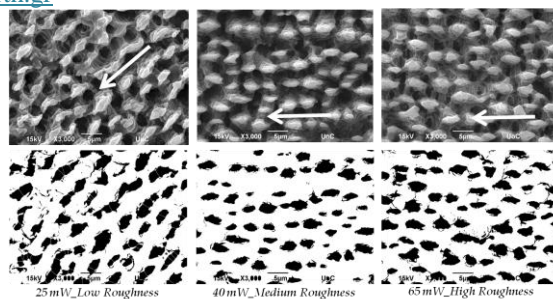


Fig. 1. SEM images [tilted view (a-Low, b-medium, c-high roughness)] of PLGA replicas.



Groups	Density [10(4) / mm(2)]	Height (h) (μm)	Width (b) (μm)	Aspect ratio (A)	Roughness ratio (r)
25mW_Low Roughness	7.18 ± 1.30	3.06 ± 0.40	2.93 ± 0.30	1.044	3.1
40mW_Medium Roughness	5.35 ± 0.25	4.34 ± 0.36	2.16 ± 0.31	2.005	5.0
65mW_High Roughness	4.69 ± 0.19	10.55 ± 1.10	4.68 ± 0.41	2.252	5.5

Fig. 2. SEM images of the PLGA replicas were processed by Fiji ImageJ, such as density and height (h) of spikes, aspect ratio [A = height (h) by radius of base of spikes] and roughness ratio ( $r = 1 + 2h/b$ , where b is the width of spikes).

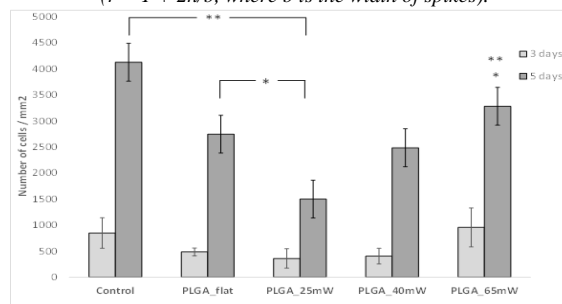


Fig. 3. Proliferation of Schwann cells (number of cells/mm<sup>2</sup>) cultured on the PLGA replicas (via live dead assay) at third and fifth day. The data were subjected to ANOVA with post-hoc Tukey HSD Test for multiple comparisons between the groups.

### CONCLUSION

All the topographies of the PLGA replicas supported SW10 cells' growth and proliferation up to 5 days. The high roughness replicas reported the highest cell number in both the time periods, followed by the medium roughness and the flat PLGA; while the lowest cell proliferation is shown at the low roughness replica. It is clear that these findings come in agreement with the previous work of our group on Si micro-structured substrates where the surface roughness did not influence the SW10 cell growth, but the surface morphology (anisotropic discontinuous pattern) played a key role for this response<sup>5</sup>.

### REFERENCES

- Stratakis, E. *et al.*, *Biomicrofluidics*, 5:013411, 2011.
- Ranella, A. *et al.*, *Acta Biomaterialia*, 6: 2711, 2010
- Simitzi, C. *et al.*, *ChemPhysChem Reviews*, 10.1002/cphc.201701175, 2018.
- Nikkhah, M. *et al.*, *Biomaterials*. 33:5230–5246, 2012.
- Simitzi, C. *et al.*, *Biomaterials*, 67:115-128, 2015.

### ACKNOWLEDGMENTS

This work was supported from funding by NFFA (EU H2020 framework programme).

## Formation and Physico-chemical Properties of Chitosan and Polyethyleneimine Containing LbL Films

Viktoryia Kulikouskaya, Kseniya Hileuskaya, Aliaksandr Kraskouski, Tsimafei Zhdanko, Vladimir Agabekov

Institute of Chemistry of New Materials of NAS of Belarus, Belarus

[kulikouskaya@gmail.com](mailto:kulikouskaya@gmail.com)

### INTRODUCTION

Surface modification by ultrathin films allows to significantly changing their properties, for example, wettability, biocompatibility, roughness, mechanical characteristics, etc. The Layer-by-Layer (LbL) self-assembly method, based on the alternating adsorption of oppositely charged polyelectrolytes, is promising technique for forming ultrathin coatings on the surface of various materials with nanometer precision<sup>1</sup>. The polyelectrolyte multilayer films are of interest for pharmaceutical industry, regenerative medicine and tissue engineering, in developing new drug delivery systems, for modification of implants due to prevent cell adhesion on them, as scaffolds for cells culturing.

### EXPERIMENTAL METHODS

Multilayer films were formed by alternating adsorption the oppositely charged components on the surface of hydrophilic silicon and quartz resonator. The synthetic polyelectrolyte polyethyleneimine (PEI) and the natural polysaccharide chitosan (Chit) were used as polycations, and polysaccharides dextran sulfate (DexS), pectin citrus (Pect), sodium salt of carboxymethyl cellulose (CMC) were chosen as polyanions. The regularities of LbL films formation were studied by quartz crystal microbalance technique in a liquid flow cell (QCM-200)<sup>2,3</sup>. The morphology of LbL films was studied by atomic force microscopy. Elastic modulus of the dried LbL films was determined by dynamic force spectroscopy<sup>4</sup>.

### RESULTS AND DISCUSSION

According to QCM data natural LbL-films (polysaccharides are used both as the polycation and the polyanion) display linear growth (Fig. 1a). The thickest films were formed by alternating adsorption of Chit and Pect ( $h_{\text{bilayer}} = 8.7 \pm 0.4$  nm), and the thinnest ones – from Chit and DexS ( $h_{\text{bilayer}} = 2.3 \pm 0.3$  nm). The thickness of (Chit/CMC)<sub>n</sub> film for the first bilayer was  $1.5 \pm 0.2$  nm, and from the second to the tenth was  $5.5 \pm 0.8$  nm, so the constant linear growth began from the second bilayer.

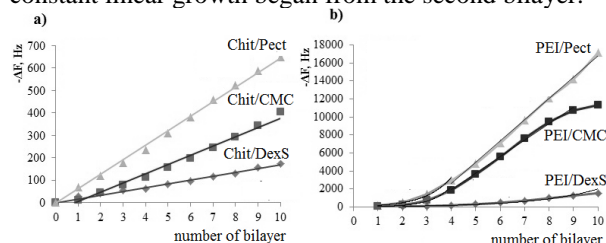


Fig. 1. Frequency shift upon alternative adsorption of component during LbL films formation

Mixed LbL films (synthetic polycation and natural polyanion) exhibit exponential growth (Fig. 1b). Films based on of PEI and DexS were characterized by the weakest exponential growth: the first bilayer thickness was  $1.8 \pm 0.3$  nm, and to the 10<sup>th</sup> bilayer the one

increased in ~20 times and reached  $38.3 \pm 2.8$  nm. For films based on Pect and CMC exponential growth was registered for the first four bilayers and then the film thickness was characterized by the linear growth.

The morphology of linearly grown natural LbL films is homogeneous and defect-free. For all polysaccharides bilayers roughness (Rms) was less than 0.5 nm, and for 4-bilayered systems didn't exceed 3.0 nm. Increase in the number of bilayers led to raise the film surface roughness only for (Chit/DexS)<sub>10</sub> ( $Rms = 30.4 \pm 6.2$  nm), while for (Chit/CMC)<sub>10</sub> and (Chit/Pect)<sub>10</sub> the one remained unchanged ( $Rms < 3.0$  nm). The morphology of mixed films are strongly depends on the number of bilayers and polyanion type. So, (PEI/DexS)<sub>n=1-4</sub> film is defect-free with  $Rms < 4$  nm. At the same time, (PEI/DexS)<sub>10</sub> system was characterized by the dramatic change in the morphology: the film became non-uniform with 20-70 nm "hollows". The PEI/CMC and PEI/Pect bilayers had an inhomogeneous surface with round shape aggregates, whose height reached 30 nm. (PEI/Pect)<sub>4</sub> film was characterized by the presence of separate prominents with diameter of  $1.0 \div 2.0$  μm and the height up to 80 nm. Further LbL assembly resulted in increasing the prominent height up to 1 μm.

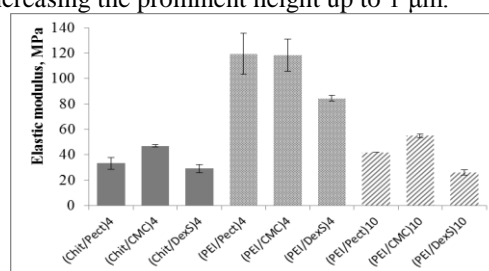


Fig. 2. The elastic modulus of LbL-films.

Natural LbL films are softer compared to mixed one (Fig. 2). The elastic modulus for 4-bilayered natural and mixed films is in the range of  $27 \div 47$  and  $87 \div 120$  MPa, respectively (Fig. 2). The increase in the number of bilayers from 4 to 10 for mixed films leads to the decrease in the elastic modulus by 2.2-3.2 times, while their values are almost identical to natural films (Fig. 2).

### CONCLUSION

So, natural LbL-films are characterized by the linear growth of the thickness and have defect-free surface. If Chit is substituted for the PEI in the multilayer system, the properties of the formed LbL films are significantly altered: the rigidity and surface roughness increases, the film growth acquires the exponential character.

### REFERENCES

- Borges J., *et al.*, Chem. Rev., 114:8883-8942, 2014.
- Hileuskaya K. S., *et al.*, Protection of Metals and Physical Chemistry of Surfaces, 54(1):48-53, 2018.
- Hileuskaya K., *et al.*, Phys. Proced., 40:84-92, 2013.
- Richert L., *et al.*, Biomacromol. 5:1908-1916, 2004.

## Nanostructured and Bifunctional Surfaces for Biomedical Applications

Claire Chattaway<sup>1</sup>, Sabrina Belbekhouche<sup>1</sup>, Filip E. Du Prez<sup>2</sup>, Sophie Demoustier-Champagne<sup>1</sup>, Karine Glinel<sup>1</sup>

<sup>1</sup>Institute of Condensed Matter & Nanosciences (Bio & Soft Matter), Université catholique de Louvain, Croix du Sud 1, box L7.04.02, B-1348 Louvain-la-Neuve, Belgium

<sup>2</sup>Polymer Chemistry Research Group, Department of Organic and Macromolecular Chemistry, Ghent University, Krijgslaan 281 S4, B-9000 Ghent, Belgium  
[claire.chattaway@uclouvain.be](mailto:claire.chattaway@uclouvain.be)

### INTRODUCTION

The development of nanostructured surfaces presenting multiple reactive chemical functions useful for subsequent immobilization of various compounds has been gaining increasing interest because of their potential uses for diverse applications, such as biosensing or development of model biological surfaces to control cellular processes. Among the many different reported approaches for tailoring surface properties of a material, self-assembled monolayers (SAMs) on gold appears as one of the most simple and versatile method. However, thiol-based SAMs present several drawbacks regarding to their stability.<sup>1</sup> Recently, we reported the use of thiolactone-based copolymers<sup>2</sup> as precursors to produce stable polythiol layers onto gold surfaces by aminolysis of the thiolactone ring.<sup>3</sup> A part of the thiol groups was involved in the formation of sulfur-gold bonds between the copolymer chains and the gold surface, while the other fraction remained free and available to immobilize thiolated derivatives through a cleavable disulfide bond. Herein, we propose two original strategies (routes 1 and 2), based on thiolactone copolymers, to design multifunctional gold surfaces.

### EXPERIMENTAL METHODS

Thiolactone-based copolymer was grafted onto gold surfaces using ethylenediamine for the aminolysis process. Carboxylic acid derivatives were grafted onto the free amino groups using EDC/sulfo-NHS chemistry. Thiolated dyes, used as model drugs were grafted on the free thiol groups through disulfide bonds, using chloramine-T as oxidative agent and further released in presence of DTT or L-glutathione used as reducing agent. Gold nanopillar arrays were prepared using electrodeposition within the nanopores of a polycarbonate template. A poly(acrylic acid) (PAA) layer was then spin-coated onto the surface and partially etched by air plasma. The top of the pillars was further functionalized with thiolactone copolymer and after dissolution of the PAA layer, the remaining substrate was covered with 11-mercaptopundecanoic acid.

### RESULTS AND DISCUSSION

**Route 1.** Macromolecular layers containing both free amine and thiol groups were successfully grafted on gold surfaces in a one-step procedure, using a thiolactone-based copolymer as precursor. Both free reactive groups present on the copolymer layers were further modified by thiolated and carboxylic derivatives in order to produce bifunctionalized surfaces (Fig. 1, left panel). The release on demand of the thiolated derivatives immobilized on these macromolecular thin films through disulfide bond cleavage under mild

reducing conditions was demonstrated, proving the redox-responsiveness of the layers.

**Route 2.** A set of nanofabrication and chemical grafting techniques were combined for preparing nanostructured surfaces made of gold nanopillars grafted with a chemical function A (e.g. thiol groups) on their top and distributed on a support functionalized by a reactive chemical function B (e.g. carboxylic acid groups) (Fig. 1, top right panel). The efficiency of this selective functionalization strategy was proved by revealing the presence of thiol groups on the surface through reaction with maleimide bearing gold nanoparticles (NPs). SEM picture (Fig. 1, bottom right panel) reveals that nanoparticles are only present on the top of the pillars, proving that the copolymer was selectively grafted on that part of the surface.

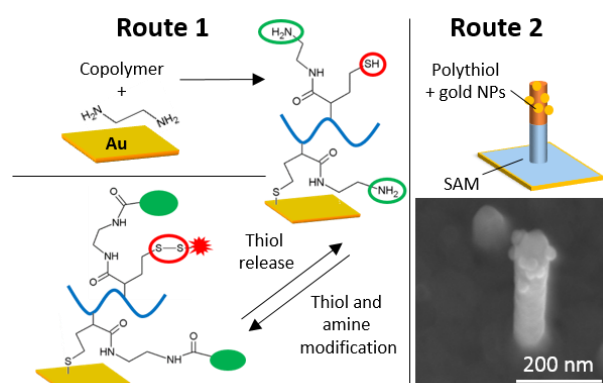


Fig. 1. Left panel: methodology (route 1) to elaborate bifunctionalized redox-responsive layers on gold surface; right panel: chemically patterned nanopillars obtained by route 2.

### CONCLUSION

The methodologies developed for the preparation of nanostructured and/or bifunctionalized redox-responsive layers should be advantageously used to produce bioactive surfaces with release properties.

### REFERENCES

- (1). Vericat C. *et al.*, PCCP. 7: 3258-3268, 2005.
- (2) Espeel P. *et al.*, J. Am. Chem. Soc. 133:1678-1681, 2011.
- (3) Belbekhouche S. *et al.*, ACS Appl. Mater. Interfaces. 6:22457-22466, 2014. hys. Res., Sect. B 196:81-88. 2002.

### ACKNOWLEDGMENTS

This work was supported by the Belgian Federal Science Policy (IAP program P7/05). CC benefits from a FRIA research fellowship provided by the F.R.S.-FNRS. KG is a Research Associate of the F.R.S.-FNRS.



## Cellular Responses under Static and Dynamic Conditions of Polymeric Micropatterned Substrates Fabricated via Ultrafast Laser Direct Writing

Eleftheria Babaliari<sup>1,2</sup>, Paraskevi Kavatzikidou<sup>1</sup>, Anna Mitraki<sup>1,2</sup>, Anthi Ranella<sup>1</sup>, Emmanuel Stratakis<sup>1,2</sup>

<sup>1</sup>Foundation for Research and Technology - Hellas (F.O.R.T.H.), Institute of Electronic Structure and Laser (I.E.S.L.), Heraklion, Crete, Greece

<sup>2</sup>Department of Materials Science and Technology, University of Crete, Heraklion, Crete, Greece  
[ebabaliari@iesl.forth.gr](mailto:ebabaliari@iesl.forth.gr)

### INTRODUCTION

Conventional cultures have been proven inadequate to provide sufficient levels of oxygen and nutrients to the interior of the scaffolds, and mechanical stimulation to the cells<sup>1</sup>. On the contrary, dynamic cultures realized with the aid of microfluidics reflect more appropriately the *in vivo* environment of cells in tissues such as the normal fluid flow within the body, consistent nutrient delivery, effective waste removal and mechanical stimulation due to fluid shear forces<sup>2,3</sup>. The purpose of the present work is to fabricate a novel microfluidic platform for the study of the combined effect of fluid shear forces and culture substrate morphology on cell proliferation and directionality<sup>4,5</sup>.

### EXPERIMENTAL METHODS

#### Microfluidic system

The microfluidic system is composed of a pressure controller, which is connected to a flow sensor and a chamber containing the microstructured substrates with the cells.

#### Fabrication of laser-microstructured substrates

- Yb:KGW laser (1026 nm)
- Substrate: PET coverslip

#### Dynamic and static cell cultures

Schwann (SW10) cells under static and flow conditions

### RESULTS AND DISCUSSION

#### Laser-microstructured substrates on PET coverslip

Figure 1 depicts the SEM images of PET coverslips that were ablated by the femtosecond laser at a constant fluence of 11.9 J/cm<sup>2</sup>, scan velocity of 7 mm/s and a  $x_{step}$  of 50  $\mu$ m.

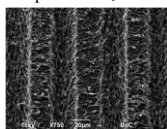


Fig. 1. SEM images of a laser-microstructured substrate, PET, with the geometry of lines.

#### UV-Vis measurements of laser-microstructured substrates

Increase of the absorption, in the region of 300–500 nm, in irradiated PET (lines) due to the presence of aromatic hydroxylated species produced during the photooxidation of PET.

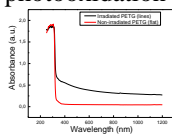


Fig. 2. UV-Vis measurements of irradiated PET [lines, (black color)] and non-irradiated PET [flat, (red color)].

#### Cell seeding of laser-microstructured substrates with SW10 cells

SW10 cells attached strongly and proliferated well in the lines. Moreover, cells appeared to be oriented along the direction of lines.

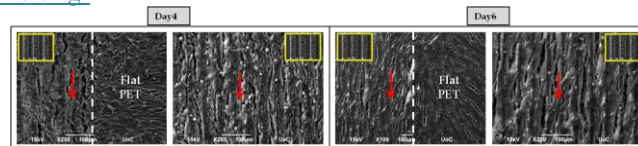


Fig. 3. SEM images of SW10 cells cultured on the lines at fourth and sixth day.

#### Fluorescent images of SW10 cells seeded on laser-microstructured substrates

The cytoskeleton of the cells was elongated along the direction of the lines whereas a random orientation observed on the flat PET.

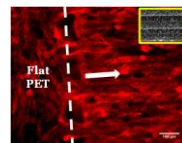


Fig. 4. Fluorescent images of SW10 cells cultured on the lines at fourth day.

#### Dynamic cell culture on PET coverslip and laser-microstructured substrates in the microfluidic system

By applying a flow rate of 50  $\mu$ l/min, SW10 cells appeared to be oriented along the direction of the lines and parallel to flow. Furthermore, cells seemed to be oriented parallel to flow on the flat PET.

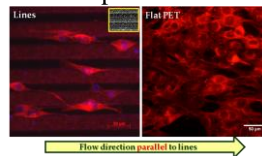


Fig. 5. Fluorescent images of SW10 cells cultured on the lines and on the flat PET when applying a flow rate of 50  $\mu$ l/min on the third day.

### CONCLUSION

A successful fabrication of polymeric micropatterned substrates was accomplished via ultrafast laser direct writing. Under static conditions, the cytoskeleton of the SW10 cells was elongated along the direction of the lines whereas a random orientation noticed on flat PET. Under flow conditions combined with the lines, cells appeared to be oriented along the direction of the lines and parallel to flow. Interestingly, cells appeared to be oriented parallel to flow on the flat area of PET.

### REFERENCES

- <sup>1</sup>Leclerc, E., et al. *Biomaterials* 27.4 (2006): 586
- <sup>2</sup>Gómez-Sjöberg, R., et al. *Analytical chemistry* 79.22 (2007): 8557
- <sup>3</sup>Mehling, M., et al. *Current opinion in Biotechnology* 25 (2014): 95
- <sup>4</sup>Stratakis, E., et al. *Biomicrofluidics* 5.1 (2011): 013411.
- <sup>5</sup>Ranella, A., et al. *Acta biomaterialia* 6.7 (2010): 2711

### ACKNOWLEDGMENTS

This work was supported from State Scholarships Foundation (IKY) (PhD Scholarship, «ESPA 2014-2020») and Onassis Foundation scholarship grant.

## New Hollow Core-shell Nanocapsules Facilitate Sustained Release of Immunomodulatory Drugs and Exhibit Adjuvant Properties

Anil Kumar Yamala<sup>2</sup>, Vinod Nadella<sup>3</sup>, Yitzhak Mastai<sup>4</sup>, Hridayesh Prakash<sup>4</sup>, Pradip Paik<sup>1,2\*</sup>

<sup>1</sup>School of Biomedical Engineering, Indian Institute of Technology (BHU), Varanasi 221 005, UP, India

<sup>2</sup>School of Engineering Sciences and Technology, University of Hyderabad, Hyderabad 500 046, TS, India

<sup>3</sup>School of Life Sciences, University of Hyderabad, Hyderabad 500 046, TS, India

<sup>4</sup>Department of Chemistry and the Institute of Nanotechnology, Bar-Ilan University, Ramat-Gan, 52900, Israel

[paik.bme@iitbhu.ac.in](mailto:paik.bme@iitbhu.ac.in), [ppse@uohyd.ac.ins](mailto:ppse@uohyd.ac.ins)

### INTRODUCTION

Significant efforts have been made over recent years to design suitable delivery materials for efficient loading as well as controlled / sustained release of drugs.<sup>1,2</sup> In the present study, we have synthesized pNAPA, new hollow polymeric nanocapsules and characterized their size, shape, *in vitro* cellular uptake and cytotoxicity in macrophages which play a significant role in the management of infection and cancer. Moreover macrophages are one of the main cells of body which respond to majority of pharmacological interventions and their stimulation is known to influence pharmacodynamics of drugs. We explored the pharmacological impact of pNAPA nanoparticles in modifying the response of macrophages towards SNP (physiological) and Interferon/Lipopolysaccharide (biological/pathological) inducers of NO in both HeLa epithelial cells and RAW macrophages cell lines. Our experiments demonstrated that pNAPA is a novel, biocompatible nanocarriers and hold potential of modifying immune response of macrophages particularly thus can be used as novel drug delivery cargoes for the management of various diseases.

### EXPERIMENTAL METHODS

Synthesis of N-acryloyl L-phenylalanine methyl ester monomer was carried out as per Einhorn modification of Shortens-Baumann reaction mechanism. Then hollow polymer NAPA nanocapsules by mini-emulsion polymerization technique. The internalization efficiency of these polymer nanocapsules RAW macrophages were used. Mitochondrial/metabolic activities of RAW macrophages and HeLa cells in response to nanocapsules was investigated by MTT assay. Encapsulating efficiency of nanocapsules for SNP was determined by UV-Vis spectroscopy. Nitric oxide production in macrophage culture supernatants was quantified by standard Griess reagent method.

### RESULTS AND DISCUSSION

This work presents for the first time the synthesis and development of a novel poly-N-acryloyl L-phenyl alanine methyl ester (pNAPA) nanocapsules of avg. size ca. 100-150 nm by mini-emulsion technique in regulating immunomodulatory drugs to the target for prolong action as adjuvant. pNAPA capsules are biocompatible and capable of encapsulating SNP at a rate of ~ 1.3  $\mu$ M per mg of capsules. These pNAPA-SNP nanoformulations while maintaining cellular homeostasis of macrophages also facilitated prolonged release of low level of NO and enhanced metabolic

activities of Th1 primed macrophages which is important for their immune response. Interestingly, pNAPA mediated skewing of naïve macrophages toward M1 phenotype potentially demonstrated its adjuvant action on macrophages. These results potentially suggested that pNAPA nanocapsules can serve as adjuvant for immune system while delivering the drugs for NO delivery. Thus, pNAPA nanocapsules could be used for the effective management of various infectious or tumor diseases where immunostimulation is paramount for treatment. Additionally, pNAPA nanocapsules hold the promise to support the potential clinical applications and innovative nano therapeutics.

### CONCLUSION

This report discloses a novel and biocompatible nano drug carrier, pNAPA nanocapsules, consisting of hollow core and a defined shell. This nano carrier exhibited attractive properties of SNP encapsulation and release of the same for sustained NO production by macrophages. In similar lines, pNAPA nanocapsule is efficient to release LNMA to block iNOS in the context of septic shock was shown rendering this novel nanosystem as promising NO-delivery vehicle for the sustained release of the drug thus highlighting its place in therapeutic settings. Extent of NO component loading is very high due to hollow structure. Release is sustained more than 90 h and highest ever reported. Further, our new pNAPA capsules and its NO formulation show a potential performance in cell stimulation at small molecular level and monitor cell signaling through sustained release of NO. Further, the novel hollow pNAPA capsules can be used for carrying other drugs to the targeted sides.

### REFERENCES

1. Van E. M. *et al.* Int. J. Pharm. 515: 132-164, 2016

### ACKNOWLEDGMENTS

Authors acknowledge financial awards of DST Fast-Track Grant for Young Scientist (Ref: SR/FTP/ETA-0079/2011) and UPE-II project (Ref: UH/UPE-II/28/2015/5669), DST PUSE-II, to Dr. Pradip Paik.

**DFT Modelling Studies of the LRRK2 Protein for Developing New Drug Treatments for Parkinson's Disease**

Jerry A. Darsey and Hetvi Shah

Centre for Molecular Design and Development &  
 Department of Chemistry  
 University of Arkansas at Little Rock  
 Little Rock, AR USA 72204  
[jadarsey@ualr.edu](mailto:jadarsey@ualr.edu)

**INTRODUCTION**

Parkinson's disease is a long-term degenerative disorder of the central nervous system that mainly affects the motor system. The cause of Parkinson's disease is generally unknown, but research has shown to involve both genetic and environmental factors. Parkinson's disease has affected about 6.2 million people in 2016 and resulted in more than 117,400 deaths globally<sup>1</sup>. Parkinson's disease typically occurs in people over the age of 60, of which about one percent are affected. Males are more often affected than females<sup>1,2</sup>. The most common gene mutation is said to be in the Leucine-rich repeat kinase 2 (LRRK2) gene, which provides instructions to make the LRRK2 protein. The functions that the protein carries out results in abnormalities, leading to Parkinson's disease. If a molecule binds to the active site of LRRK2 protein, it could lead to potential treatments<sup>3,4</sup>.

**METHODS**

The native structure of the LRRK2 enzymatic protein was determined. Seven molecules, that are said to bind the LRRK2, were identified and studied and their IC-50 values of each molecule was determined. Because there were ranges given for some molecules, three groupings were made: the lowest IC-50 value, the highest IC-50 value, and the average of the highest and lowest IC-50 value. This research conducted was to establish a correlation between the IC-50 values and DFT calculated values of the total energy, dipole moment, or HOMO/LUMO energy gap of each drug molecule with its binding to LRRK2 protein. The energy gap was established by subtracting the orbital energy of the highest occupied molecular orbital from the lowest unoccupied molecular orbital. The total energy, dipole moment, and HOMO/LUMO energy gap values determined from performing DFT molecular orbital modelling using the program, *Gaussian 09*.

**RESULTS AND DISCUSSION**

Plots were made of IC-50, 1/IC-50, and log IC-50 vs. total energy, HOMO/LUMO energy gap, and dipole moments. A strong correlation was found between 1/IC-50 and total energy, with the  $R^2$  value being 0.94. This is the first time, to these author's knowledge, that this correlation has been seen between IC-50 values and the DFT calculated total energy. This correlation was then used to find the IC-50 values for modifications to the known drug molecules for the treatment of Parkinson's, to determine if new potential drug molecules may perform better. Modelling was performed on new molecules in which the IC-50 values have not been experimentally measured. The 1/IC-50 vs. Total Energy

correlations was then used to develop these new potential drug treatments for Parkinson's disease.

**CONCLUSION**

In this study, it was found that there was a great correlation between the "1/IC50 (average and high) vs. the total energy," with the  $R^2$  or 0.94.

**REFERENCES**

1. National Parkinson Foundation: Believe in Better. Retrieved December 11, 2016, @ <http://www.parkinson.org/understanding-parkinsons/what-is-parkinsons>
2. Statistics on Parkinson's. (2016). @ [http://www.pdf.org/en/parkinson\\_statistics](http://www.pdf.org/en/parkinson_statistics)
3. Martin I., Kim J.W., Lee B.D., Kang H.C., Xu J.C., Jia H., Stankowski J., Kim M.S., Zhong J., Kumar M., Andrabi S.A., Xiong Y., Dickson D.W., Wszolek Z.K., Pandey A., Dawson T.M., Dawson V.L. Ribosomal protein s15 phosphorylation mediates LRRK2 neurodegeneration in Parkinson's disease. *Cell.*;157(2) pp. 472-85 (2014).
4. Gilligan, P. J., "Inhibitors of Leucine-Rich Repeat Kinase 2 (LRRK2): Progress and Promise for the Treatment of Parkinson's Disease". *Current Topics in Medicinal Chemistry*, 15 (10), pp. 927-938 (2015).

**ACKNOWLEDGMENTS**

The authors would like to thank the computational resources provided by the Centre for Molecular Design and Development and the Michael J. Fox Foundation for Parkinson's disease for funding part of this research.



## PEGylated Cationic/Anionic Nanogels with Gold Nanoparticles for Controlled Release of Anticancer Drugs

Angel Licea-Claverie<sup>1</sup>, Ivan Zapata-Gonzalez<sup>1</sup>, Lizbeth A. Manzaneres-Guevara<sup>1</sup>, Alejandra Gonzalez-Urias<sup>1</sup>, Irasema Oroz-Parra<sup>2,3</sup>, Alexei F. Licea-Navarro<sup>2</sup>

<sup>1</sup>Centro de Graduados e Investigación en Química/Instituto Tecnológico de Tijuana, Tijuana, B.C. México

<sup>2</sup>Departamento de Innovación Biomédica/CICESE, Ensenada B.C., México

<sup>3</sup>Facultad de Ciencias Marinas/Universidad Autónoma de Baja California, Ensenada, B.C., México

[aliceac@tectijuana.mx](mailto:aliceac@tectijuana.mx)

### INTRODUCTION

In this contribution a variation of the classical emulsion polymerization, called surfactant-free emulsion polymerization (SFEP) is presented as a method of choice for the preparation of stimuli-responsive nanogels envisioned for encapsulation and controlled release of drugs<sup>1</sup>. This methodology makes use of a specific type of macromers: methacrylate functionalized polyethyleneglycol (PEG-MA) with two goals in mind: to stabilize the emulsion process and to provide the nanogels with a PEGylated shell chemically attached to the crosslinked core. This methodology has been exploited previously to prepare temperature responsive polymers<sup>2</sup>, and in this contribution we present its application to prepare cationic and anionic, pH-responsive nanogels.

### EXPERIMENTAL METHODS

Figure 1 shows a scheme of the nanogels synthesis. One example is described: DEAEM (0.35 g, 1.889 mmol) was mixed with PEGMA with Mn: 1100 g/mol (0.15 g, 0.136 mmol), EGDMA crosslinker (7.48 x 10<sup>-3</sup> g, 0.037 mmol) and dissolved in 98 mL of deionized water at room temperature. The mixture was degassed before starting the polymerization at 85°C in a preheated oil bath and vigorously stirred. The initiator APS (0.0129 g, 0.0565 mmol) was added to the reaction vessel dissolved in 2 mL water. The polymerization process was allowed to continue for 1 h and was stopped by cooling. The resulting dispersions were purified via dialysis (MWCO: 12000-14000 Da) against deionized water. The nanogels were isolated by freeze drying.

### RESULTS AND DISCUSSION

It is well known that the tumor tissue shows lower pH values than the physiological one (7.4) and therefore pH-sensitive nanogels are strong candidates for drug delivery into tumors. In this work, two PEGylated nanogels were synthesized with different cross-linked cores: a cationic system with poly(*N,N*-diethylaminoethyl methacrylate) (PDEAEM) and an anionic system with poly(2-methacryloyloxy benzoic acid) (P2MBA). A surfactant free emulsion polymerization was carried out at different feed compositions. The synthetic conditions were adjusted to yield nanogels in sizes between 90 nm and 180 nm, resulting also in differences in their pH-responsive swelling behaviour. PDEAEM nanogels show swelling at pH < 7, while P2MBA nanogels show shrinkage at pH < 7. Cis-diamminedichloroplatinum (II) "Cisplatin" is one of most used antineoplastic drugs for various types of cancer, despite adverse side effects. In this work cisplatin was loaded in both types of nanogels, as

alternative to continue cisplatin use diminishing side effects.

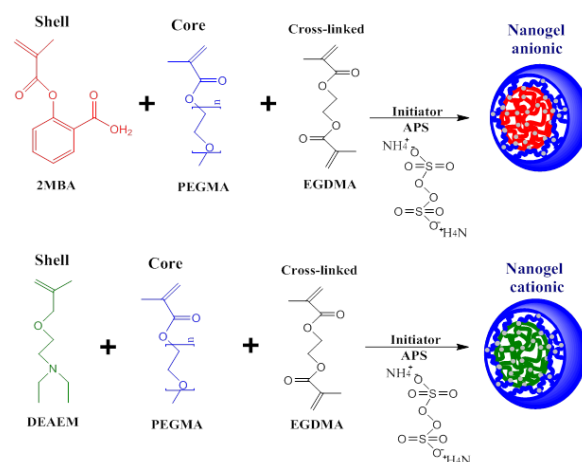


Fig. 1. Monomers used for the nanogels synthesis

Furthermore, 5-fluorouracil (5-FU) another first generation antineoplastic drug was loaded in PDEAEM core nanogels. Since there are no specific groups in 5-FU for strong interactions with the nanogels, gold nanoparticles (AuNP) were loaded with 5-FU, to increase 5-FU loadings. Table 1 show results on drug loadings. Results on pH-sensitive drug delivery and viability against different cell-lines will be presented at the meeting.

Table 1. Drug loadings in different PEGylated nanogels

Key	PEG:PDEAEM	D <sub>n</sub> (nm)	Loading (wt%)
NC2	80:20	148	25 <sup>b</sup>
NC2Au	80:20	172	43 <sup>c</sup>
NC3Au	85:15	157	51 <sup>c</sup>
NC4	55:45	121	42 <sup>b</sup>
NA455	63:37	93	33 <sup>d</sup>
NC51	85:15 <sup>a</sup>	111	30 <sup>d</sup>

a-P2MBA, b-5-FU, c-5-FU with AuNP, d-Cisplatin

### CONCLUSION

Cationic and anionic PEGylated nanogels are excellent candidates for loading and release of 5-FU and Cisplatin with potential application in anticancer therapy.

### REFERENCES

1. A. Kowalczyk, *et al.* Prog. Polym. Sci. 39, 43 (2014).
2. A. Serrano-Medina, *et al.* Int. J. Polym. Mater. Polym. Biomat. 67, 20 (2018).

### ACKNOWLEDGMENTS

Support by CONACYT Mexico through grants CB-2012-178709 and CB-2017-285419 is greatly appreciated.

## Curcumin Loaded 2-Ethyl-2-Oxazoline-grad-2-(4-Dodecyloxyphenyl)-2-Oxazoline Copolymer Nanoparticles with Excellent Chemical Stability and Bioavailability

Shubhashis Datta<sup>1</sup>, Annamária Jutková<sup>1</sup>, Petra Šrámková<sup>2</sup>, Lenka Lenkavská<sup>1</sup>, Veronika Huntošová<sup>1</sup>,  
Nadežda Petrenčíková<sup>2</sup>, Dušan Chorvát<sup>3</sup>, Pavol Miškovský<sup>1</sup>, Daniel Jancura<sup>1\*</sup>, Juraj Kronek<sup>2\*</sup>

<sup>1</sup>Center for Interdisciplinary Biosciences, Technology and Innovation Park, P. J. Šafárik University in Košice, Jesenná 5,  
041 54 Košice, Slovak Republic

<sup>2</sup>Polymer Institute of the Slovak Academy of Sciences, Dúbravská cesta 9, 845 41 Bratislava, Slovak Republic

<sup>3</sup>International Laser Centre, Iľkovičova 3, 841 04 Bratislava 4, Slovak Republic

[Juraj.kronek@savba.sk](mailto:Juraj.kronek@savba.sk)

### INTRODUCTION

Curcumin (CM) is recently recognized as a promising drug candidate in a large number of diseases such as cancer, neurodegenerative diseases, infectious diseases, and diabetes<sup>1,2</sup>. However, the application of CM in the therapeutic treatment has been limited due to its extremely low solubility and the fast degradation in aqueous solutions<sup>3</sup>. Therefore, various approaches such as conjugating CM with a polymer or encapsulating CM inside various nanomaterials including polymeric micelles, liposomes and silica nanoparticles were considered to increase the bioavailability of CM<sup>4</sup>. Among the possible polymeric candidates poly(2-oxazolines) (POx) are considered as the next generation polymers for drug delivery systems due to excellent biocompatibility, protein repellent behaviour, and low accumulation in organs during *in vivo* studies<sup>5-7</sup>.

In this work, we present a synthesis of a new gradient copolymer using the living cationic ring-opening copolymerization of hydrophilic 2-ethyl-2-oxazoline (EtOx) with lipophilic 2-(4-dodecyloxyphenyl)-2-oxazoline (DPOx). Prepared copolymers were used for self-assembly in aqueous solutions in the presence or absence of CM. Formed nanoparticles were studied with the respect to their stability, cytotoxicity, and cell uptake.

### EXPERIMENTAL METHODS

CM isolated from *Curcuma longa* was used for all experiments. Gradient copolymers were prepared by the living cationic polymerization of EtOx and DPOx in benzonitrile at 110°C for 24 h initiated by methyl 4-nitrobenzenesulfonate. Nanoparticles were prepared by solvent dependent dialysis method. Size and morphology of prepared nanoparticles were determined by dynamic light scattering (DLS) and cryo-SEM. Stability of CM encapsulated in micelles was determined by UV-Vis absorption spectroscopy. *In vitro* cytocompatibility of CM loaded and non-loaded nanoparticles were evaluated by MTT assay using two cancer (U87MG and HeLa) cell lines. Cell uptake was visualized by confocal laser-scanning microscopy (CLSM).

### RESULTS AND DISCUSSION

Cationic copolymerization of EtOx and DPOx provided gradient copolymer with the molar mass of 12 000 g mol<sup>-1</sup> with the dispersity of 1.26 demonstrating a living process of the copolymerization. Gradient copolymer was formed due to different rate of EtOx and DPOx consumption. Unloaded and CM-loaded nanoparticles

were prepared by dialysis method. Their size, morphology, loading capacity, and stability have been evaluated by means of DLS, cryo-SEM, and UV-Vis absorption spectroscopy. A diameter of nanoparticles was ranging from 50 to 350 nm and the drug loading capacity was found in the range from 12 to 22%.

It was already mentioned that the main drawback connected with the use of CM as a drug lies in rapid hydrolysis in an aqueous solution. UV-Vis absorption spectroscopy measurements of encapsulated CM showed that the micellar hydrophobic cavity composed of lipophilic polymer chains could effectively protect CM from degradation. It was shown that decrease of CM concentration after 1 h after dissolving in water was 80% while the decrease of protected CM concentration after 25 days was only 10%, 14%, and 18% dependently on the type of nanoparticles. CLSM images of two cancer (U87 MG and HeLa) cell lines treated with CM loaded nanoparticles proved the concentration dependent accumulation of CM within both kinds of cancer cells.

### CONCLUSION

The amphiphilic gradient copolymer synthesized in this work was capable of assembling in water to yield polymeric NPs that was successfully loaded with CM. Encapsulation of CM inside nanoparticles extremely enhanced stability of CM in aqueous environments. Moreover, *in vitro* experiments indicated a high cytocompatibility of CM loaded nanoparticles and a concentration dependent accumulation of CM loaded nanoparticles into U87MG and HeLa cells.

### REFERENCES

1. Goel A. *et al.* Biochem. Pharmacol. 75: 787-809, 2008
2. Li Y.Y. *et al.* Cancer Lett. 346: 197-205, 2014
3. Anand P. *et al.* Mol. Pharm. 4: 807-818, 2007
4. Naksuriya O. *et al.* Biomaterials 35: 3365-3383, 2014
5. Kronek J. *et al.* J. Mater. Sci. Mater. Med. 22: 1725-1734, 2011
6. Lowe S. *et al.* Polym. Chem. 6: 198-212, 2015
7. Wyfels L. *et al.* J. Control. Release 235: 63-71, 2016

### ACKNOWLEDGMENTS

The authors are thankful to the Slovak Grant Agency VEGA for the financial support in the project No. 2/0124/18 and the Slovak Research and Development Agency for financial support in the project No. APVV-15-0485.

## Dual Intracellular Targeting Nanosized Anticancer Drug Carriers with Intracellular Glutathione Responsiveness and Mitochondrial Targeting Activity

Yeon Su Choi, Han Chang Kang

Department of Pharmacy, The Catholic University of Korea, Bucheon, Gyeonggi-do 420-743, Republic of Korea  
[puristism@naver.com](mailto:puristism@naver.com)

### INTRODUCTION

Many researches have investigated intracellular thiol (e.g., glutathione)-triggered destruction of disulfide and mitochondria targeting because of quick release and selectively the delivered payloads in subcellular organelles<sup>1,2</sup>, respectively. In this study, the TMSPCL polymer composed of triphenylphosphonium (TPP) and poly( $\epsilon$ -caprolactone) (PCL) with multiple disulfide bonds (MSPCL) was selected. It is expected that TMSPCL polymer with multiple disulfide bonds will have mitochondrial targeting activity and accelerated release of payloads in their nanostructures when exposed to the thiol-rich cytosol. Thus, after constructing TMSPCL nanoparticles (NPs), their sizes and zeta-potentials were evaluated. Also, after loading a hydrophobic doxorubicin (DOX) into TMSPCL NPs, their physicochemical and biological characteristics were investigated for particle size, zeta-potential, drug loading capacity, in vitro cell killing effects, in vitro cellular uptake, and intracellular drug distribution.

### EXPERIMENTAL METHODS

To obtain MSPCL polymer, PCL<sub>0.5</sub> diols and the single disulfide-containing 3,3'-dithiodipropionic acid (DTPA) were alternatively connected by a conjugation reaction between to hydroxyl groups of PCL<sub>0.5</sub> diol blocks and two carboxylic acids of DTPA molecules. Two carboxylic acids at two ends of the synthesized MSPCL polymer were reacted with one hydroxyl group at one end of TPP by a coupling reaction and the resulting TMSPCL polymer was a triblock-type structure. To confirm their chemical structures and molecular weights, the polymers were examined by <sup>1</sup>H-NMR and GPC. The TMSPCL NPs were prepared to evaluate their physicochemical characteristic, material toxicity, therapeutic effects, and mitochondria targetability.

### RESULTS AND DISCUSSION

To achieve effective intracellular drug release and mitochondrial targeting from nanostructures, we designed MSPCL polymer synthesized by a coupling reaction between the PCL<sub>0.5</sub> diol and a single disulfide-containing dicarboxylic acid. The synthesized MSPCL polymer with approximately 7.5 disulfide bonds were further linked with TPP, resulting in TMSPCL polymer. The chemical structure of the TMSPCL polymer was confirmed by <sup>1</sup>H-NMR. The molar TPP ratio in the TMSPCL polymer was 1.86, and the results were converted to estimate the molecular weights (MW) of the TMSPCL (5745 Da) polymers. Using GPC, the additional MW analysis demonstrated that the number average MW ( $M_n$ ) of the TMSPCL polymer was 6880 Da (PDI 1.73), compared with the MW of MSPCL polymer was 5690 Da (PDI 1.71). In aqueous environments, the TMSPCL polymer was self-

assembled to construct positively-charged NPs below 350 nm because TPP moiety may have been placed on the outside of the NPs. The cytotoxicity of TMSPCL NPs was examined in MCF7 and MCF7/ADR-RES cell lines. The TMSPCL NPs represented slightly cytotoxicity at a high concentration (i.e., 500  $\mu\text{g mL}^{-1}$ ) in MCF7 and MCF7/ADR-RES cell lines because their cationic nature could induce some membrane damage and, ultimately, cell death. After a hydrophobic DOX was efficiently loaded in the hydrophobic compartments of the NPs, the formed DOX-loaded TMSPCL NPs (i.e., DOX@TMSPCL NPs) had approximately 180 nm in diameter and positive zeta-potential with loading content up to 13 wt%. In MCF7 and MCF7/ADR-RES cells, DOX@TMSPCL NPs represented approximately 3.2-fold and 175.4-fold higher cell-killing activities than free DOX, respectively. The DOX@TMSPCL NPs were efficiently internalized into MCF7 and MCF7/ADR-RES cells and then released DOX into the mitochondria.

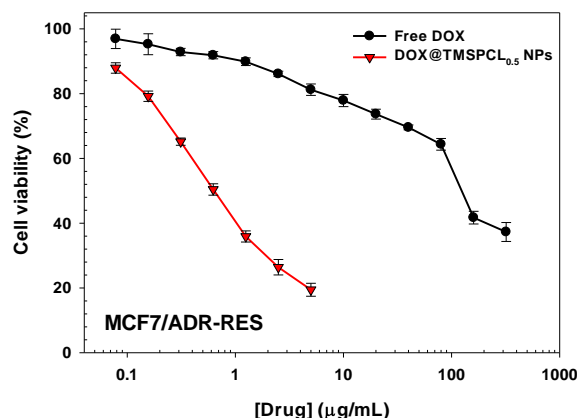


Fig. 1. In vitro cell killing effects of TMSPCL NPs in MCF7/ADR-RES cells.

### CONCLUSION

The TMSPCL polymer was designed and synthesized for intracellular quick drug release and mitochondria-targeting delivery of therapeutics. In aqueous environments, the spontaneous self-assembly of TMSPCL polymer formed its cationic NPs. The drug-loaded TMSPCL NPs had potential cell killing activity compared with free drugs, and their preferred accumulation occurred in the mitochondria. In conclusion, the TMSPCL NPs could have potential for subcellular-targeting carrier of therapeutic agents.

### REFERENCES

1. Cho D.Y. *et al.*, Adv. Funct. Mater. 25:5479-5491, 2015
2. Moon S.Y. *et al.*, RSC Adv. 6:15558-15576, 2016



## Controlled Release of Metformin Hydrochloride from Core-Shell Nanofibers with Fish Sarcoplasmic Protein

Sena Su<sup>1,2</sup>, Nalan S. Korkmaz<sup>2,3</sup>, Ulkugul Guven<sup>2,3</sup>, Mehmet S. Eroglu<sup>4</sup>, Nazmi Ekren<sup>5</sup>, Osman Kilic<sup>5</sup>, Faik N. Oktar<sup>6</sup>, Oguzhan Gunduz<sup>1,2</sup>

<sup>1</sup>Department of Metallurgical and Materials Engineering, Faculty of Technology, Marmara University, Turkey

<sup>2</sup>Advanced Nanomaterials Research Laboratory, Marmara University, Turkey

<sup>3</sup>Department of Biomedical Engineering, Faculty of Engineering, Yeditepe University, Turkey

<sup>4</sup>Department of Chemical Engineering, Faculty of Engineering, Marmara University, Turkey

<sup>5</sup>Department of Electrical Electronics Engineering, Faculty of Technology, Marmara University, Turkey

<sup>6</sup>Department of Biomedical Engineering, Faculty of Engineering, Marmara University, Turkey

[nalan\\_korkmaz@hotmail.com](mailto:nalan_korkmaz@hotmail.com)

[ulkugulen.058@gmail.com](mailto:ulkugulen.058@gmail.com)

### INTRODUCTION

Electrospinning is increasingly being used to produce nanoscaled structures from a wide range of biopolymer materials. The high surface area of ultra-thin fibers were produced by electrospinning makes them ideally suitable for various biomedical applications<sup>1,2</sup>. Electrospun nanofibers have received much attention due to fact that their unique topographical characteristics resemble major extra-cellular matrix (ECM) components in natural tissues.<sup>3</sup> Metformin Hydrochloride (MH) is a well-known drug used in the management of type 2 diabetes and also used to treatment of diabetic ulcers.<sup>4</sup> In this study biodegradable core-shell composite nanofibers with polylactic acid (PLA) as shell, MH and fish sarcoplasmic protein (FSP) containing Polyvinyl Alcohol (PVA) as core were prepared via coaxial electrospinning technique and characterized.

### EXPERIMENTAL METHODS

FSP was obtained from Atlantic bonito. PLA and PVA solutions, which contain MH and FSP at different ratios, were prepared and core-shell nanofibers were fabricated by coaxial electrospinning. Morphology of the composite nanofibers was observed using a scanning electron microscopy (SEM) and transmission electron microscopy (TEM). Wettability of electrospun nanofibers were characterized by contact angle (CA) measurements. Moreover, fourier transform infrared spectrometer (FTIR), differential scanning calorimetry (DSC) studies were used for analysis chemical composition and thermal characteristics of the nanofiber mats. Encapsulation and sustained release of MH in nanofibers were followed by UV spectroscopy. A cell culture test was performed in order to determine their cytotoxicity for wound dressing application.

### RESULTS AND DISCUSSION

The morphologies of the drug loaded core-shell electrospun nanofibers with different FSP concentration were observed by SEM and are displayed in Fig. 1. The characteristic picks of the polymers, FSP and MH were identified in the composite nanofibers. FT-IR spectra of the composite nanofiber, which contains 3 wt% FSP, were presented in Fig. 2 as an example. The drug and the protein were successfully encapsulated in the core polymer. In vitro drug release studies demonstrated that MH was sustained over a period of 21 days.

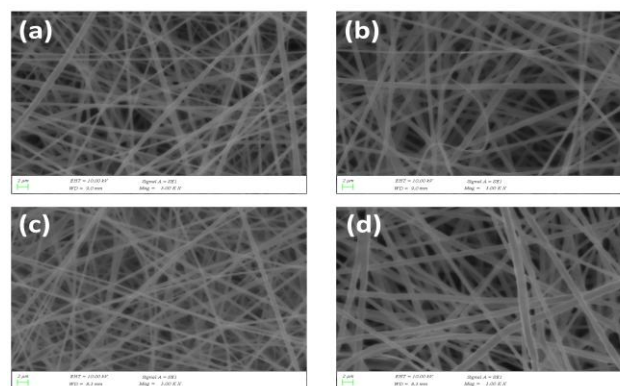


Fig. 1. SEM images of drug loaded core-shell nanofibers with (a) without FSP (b) 1 wt.% FSP (c) 3 wt.% FSP (d) 5 wt.% FSP

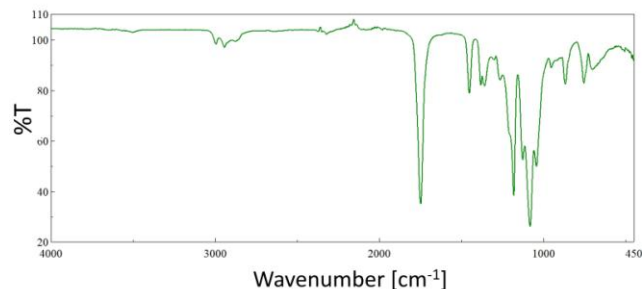


Fig. 2. FT-IR spectra of the nanofiber with 3 wt.% FSP

### CONCLUSION

Composite nanofibers containing drug and protein were successfully fabricated by using the coaxial electrospinning technique. This study revealed that the composite nanofibers had a good potential to be used in treatment of diabetic ulcers.

### REFERENCES

1. Bhardwaj N. *et al.*, Biotechnol. Adv. 28:325–347, 2010
2. Echegoyen Y. *et al.*, Trends Food Sci. Tech. 60:71-79, 2017
3. Choi J.S. *et al.*, Biomaterials 29: 587–596, 2008
4. Lee C. *et al.*, ACS Appl. Mater. Interfaces. 6: 10-17, 2014

### ACKNOWLEDGMENTS

This work is founded from Ministry of Development, project number: 2016K121280.

## Emulsion Technology for the Development of Bio-based Materials for Controlled Drug Delivery Applications

Chiara Setti<sup>1,2</sup>, Giulia Suarato<sup>1,3</sup>, Athanassia Athanassiou<sup>1</sup>, Ilker S. Bayer<sup>1</sup>

<sup>1</sup>Smart Materials, Istituto Italiano di Tecnologia, Via Morego 30, 16163 Genova, Italy

<sup>2</sup>Dipartimento di Informatica Bioingegneria, Robotica e Ingegneria dei Sistemi (DIBRIS),  
Universita Degli Studi di Genova, Via All'Opera Pia 13, 16145 Genova, Italy

<sup>3</sup>Drug Discovery and Development, Istituto Italiano di Tecnologia, Via Morego 30, 16163 Genova, Italy  
[chiara.setti@iit.it](mailto:chiara.setti@iit.it)

### INTRODUCTION

Emulsions have attracted a large interest in the pharmaceutical field, thanks to their thermodynamic stability, facile preparation, and ability in dispersing both lipophilic and hydrophilic compounds, thus enhancing their bioavailability<sup>1-2</sup>. As a result, they have found applications in encapsulating and delivering drugs with different physico-chemicals properties (hydrophilic, hydrophobic or amphiphilic), either alone or in combination, by oral, transdermal and parenteral routes<sup>3-6</sup>. In this context, we developed and investigated emulsions containing biopolymers, dispersed both in water and in oil phases, in order to obtain composite materials in the form of films or microbeads, able to load and deliver active agents in a controlled manner. Due to its biocompatibility and natural origin<sup>7</sup>, alginate was chosen as hydrophilic compound. For films fabrication, alginate was blended with a hydrophobic, biodegradable composite of starch and polycaprolactone (MaterBi<sup>®</sup>), while for microbeads formulation alginate was emulsified with a naturally derived hydrophobic material (beeswax).

### EXPERIMENTAL METHODS

*Films fabrication and characterization* Alginate-MaterBi<sup>®</sup> composite films were prepared by solvent casting and evaporation from respective emulsions, loaded with two model drugs, a hydrophilic eosin-based cutaneous antiseptic and the hydrophobic curcumin. The morphology of the dry films was characterized by SEM and AFM. Release studies were performed by using UV-visible spectroscopy. Human dermal fibroblasts adult (HDFa) were used to investigate the biocompatibility *in vitro* of the alginate-MaterBi<sup>®</sup> composite film extracts, by means of WST-1 assay and cell morphology analysis. All the measured values were expressed as mean  $\pm$  standard error of the mean (SEM). For *in vitro* biocompatibility tests One-way ANOVA followed by Bonferroni's post hoc test was used.

*Wax-incorporated emulsion alginate gel microbeads encapsulating natural active compounds* Alginate-Beeswax emulsions were prepared by ultrasonic emulsification of an hot aqueous solution in which sodium alginate, beeswax, and the natural active compounds were dispersed. The resulting emulsions were then extruded into calcium chloride solution (at 5°C) to obtain the gel beads. Emulsions droplet size distribution analysis was performed by optical microscopy measurements. Particle size distribution, surface topography and internal morphology of beads will be analysed by SEM and TEM. Release studies will be performed *in vitro* by means of UV-visible spectroscopy.

### RESULTS AND DISCUSSION

Morphological features investigated by SEM and AFM measurements indicated for the composite films a foam-like cellular surface and no macroscopic phase separation. Release studies demonstrated the ability of the composite film matrices to deliver the two model drugs individually or simultaneously in a sustained manner, due to the presence of MaterBi<sup>®</sup>. Moreover, drug release rates could be tuned by crosslinking of the alginate domains within the films by simple calcium salt solution immersion. Cell viability study demonstrated that the cells treated with the polymer extraction medium were healthy and had very strong proliferation levels comparable to the control ones ( $p < 0.05$ ). Preliminary optical microscopy investigation on alginate-beeswax emulsion gel beads demonstrated that increasing the amount of beeswax is possible to obtain smaller oil droplets, given the capability of the wax to act as an emulsifier. A more evident effect was obtained with the addition of the hydrophobic natural compound, the black cumin seed oil. SEM morphological analysis revealed for all the compositions a smooth surface rich in calcium residues, as reported by EDX analysis, indicating the presence of calcium alginate-based shell containing a core of beeswax.

### CONCLUSION

We demonstrated for the first time the ultrasonic-assisted self-emulsification between two biopolymers, MaterBi<sup>®</sup> and sodium alginate. The emulsions, stable for several days, were dried into composite solid films with varying MaterBi<sup>®</sup>/alginate fractions, which resulted biocompatible against HDFa cells. By tuning the component ratios and the calcium-crosslinking the films, loaded with two model drugs were able to release them in a controlled manner. In summary, our polymeric emulsion-based matrices can be proposed for a number of pharmaceutical applications, as potential wound care materials or in the area of hygienic packaging of certain pharmaceutical products.

### REFERENCES

1. Najjar, R. *et al.* *InTech* (2012)
2. Vikramjeet S. *et al.* *J Pharm Res* (2012)
3. Strickley, R. G. *et al.*, *Pharm Res* (2004)
4. Yu W. *et al.*, *Int J Pharm* (1993)
5. Collins-Gold, L.C *et al.*, *Adv Drug Deliv Rev* (1990)
6. Santos, P., *et al.*, *Skin Pharmacol Physiol* (2008)
7. Lee K.Y. *et al.*, *Prog Polym Sci* (2011)



## Amoxicillin-loaded Poly( $\epsilon$ -caprolactone)/poly(ethylene glycol) Biodegradable Electrospun Nanofibrous Mats for Wound Healing

Husam Younes<sup>1,2</sup>, Sandi Ali Adib<sup>1</sup>, & Shijimol Ma<sup>1</sup>

<sup>1</sup>Pharmaceutics & Polymeric Drug Delivery Research laboratory, College of Pharmacy, Qatar University, Doha, Qatar

<sup>2</sup>Office of Vice President for Research & Graduate Studies, Qatar University, Doha, Qatar

[husamy@qu.edu.qa](mailto:husamy@qu.edu.qa)

### INTRODUCTION

The ideal wound dressing should have a number of characteristics to enhance the wound healing process such as the provision of a moist environment to enhance healing, high porosity to enable good oxygen permeability and being a good barrier for protection of the wound from infection/dehydration, and offering broad-spectrum antimicrobial activity against bacterial infection<sup>1</sup>. Electrospinning (ES), as a new emerging technology, is currently considered as one of the best approaches for the preparation of three-dimensional biodegradable electrospun nanofibrous scaffolds (BENS) for use in wound healing and other tissue engineering applications as it enables better cells growth, and provides the cells with the mechanical signalling needed<sup>2,3</sup>. The purpose of this study therefore is to fabricate and characterize BENS prepared using the hydrophilic Poly (ethylene glycol) (PEG35000) with the hydrophobic Polycaprolactone (PCL) co-polymers and to compare the impact of loading them with Amoxicillin Trihydrate (AMX).

### EXPERIMENTAL METHODS

Blank and AMX-loaded BENS were fabricated using various weight percentage ratios of PEG35000 and PCL biodegradable polymers. Morphology of BENS were assessed using Scanning Electron Microscopy (SEM). Fourier Transform Infrared (FT-IR) Spectroscopy was used to identify the interaction between PEG35000 and AMX. Differential Scanning Calorimetry (DSC) was used to assess the crystallinity and thermal behaviour of the prepared BENS. The X-Ray Diffraction (XRD) analysis for the blank and drug loaded electrospun fibers was carried out to identify the changes in their crystalline pattern. The prepared BENS were also subjected to mechanical testing using Instron tensile tester. The *in vitro* antibacterial activity of the AMX-loaded BENS against common skin pathogens was also tested

### RESULTS AND DISCUSSION

Various weight percentage ratios of PCL75%: PEG25%, PCL50%: PEG25%, PCL25%: PEG75% in chloroform were prepared. The DSC and FT-IR analyses showed that the polymers and AMX structures were not affected by ES. The PCL75%: PEG25% mix resulted in the optimal mechanical strength and was further used for preparing the AMX-loaded BENS. The DCS, FT-IR and XRD studies confirmed the presence of amoxicillin in the BENS and its dispersion and transformation into its amorphous state. The *in vitro* antibacterial assay confirmed the efficiency of the drug loaded fibers against the common skin pathogens.

### CONCLUSION

Utilizing PCL and PEG polymers was successful and significantly enhanced the mechanical properties of the BENS and their antimicrobial activity. Our findings showed that PEG: PCL BENS have features that make them promising candidates for wound healing applications.

### REFERENCES

1. Andreu, V. *et al.* Materials, 8: 5154-5193, 2015.
2. Abdallah, O. *et al.* Pharma Nanotech, 4: 191-201, 2016.
3. Hassiba, A. *et al.* Nanomedicine, 11: 715-737, 2016.

### ACKNOWLEDGMENTS

This work was made possible by a UREP award [UREP 19-071-3-021] from the Qatar National Research Fund (a member of The Qatar Foundation). The statements made herein are solely the responsibility of the author(s).

## Multi-Compartment Collagen Devices as Modulators of Skin Fibrosis through Controlled Synergistic Dual Delivery of Anti-Fibrotics

João Coentro<sup>1,2</sup>, Dimitrios I. Zeugolis<sup>1,2</sup>

<sup>1</sup>Regenerative, Modular & Developmental Engineering Laboratory (REMODEL)  
National University of Ireland Galway (NUI Galway), Galway, Ireland

<sup>2</sup>Science Foundation Ireland (SFI) Centre for Research in Medical Devices (CÚRAM)  
National University of Ireland Galway (NUI Galway), Ireland

[j.quintascoentro1@nuigalway.ie](mailto:j.quintascoentro1@nuigalway.ie)

### INTRODUCTION

Fibrosis is a phenomenon characterised by the formation of excessive fibrous connective tissue, which can lead to the alteration of the dermis' architecture, while compromising the skin's function and its mechanical properties. This can cause a huge global burden on healthcare, with millions of patients suffering from cosmetic or even functional tissue/organ impairment, which considerably reduces their quality of life [1]. In order to treat this, Il-6 antagonists and decorin have been reported as potential anti-fibrotic therapeutics [2, 3]. Therefore, there is a need to develop multi-compartment systems, capable of delivering multiple bioactive agents in a controlled, safe and cost effective way. Although some technologies already succeed in doing this, usually they involve the use of multi-domain materials, which can raise concerns regarding cost of production, cytotoxicity and controllable release. Single domain systems seem a promising alternative that can address these issues. In this study it was hypothesized that multi-compartment crosslinked collagen type I systems can modulate skin fibrosis through the controlled synergistic dual delivery of an Il-6 antagonist and recombinant decorin. The main objectives so far were: to fabricate and characterise the collagen systems and to study the release profile of the loaded drugs in the developed system, while assessing the effect of these compounds on an *in vitro* fibrosis model.

### EXPERIMENTAL METHODS

Multi-compartment collagen-based systems were made as follows: solutions of dialyzed type I collagen at a concentration of 5 and 8 mg/ml were mixed with 10x PBS, after which they were neutralised and crosslinked with 1 and 2.5mM 4 arm-succinimidyl glutarate ester PEG (4 arm-PEG-SG), respectively. Through the use of a mould it was possible to create two separate compartments using both solutions, which were then incubated at 37°C for 18h. Hydrogels biophysical and biological characterisation: The systems were characterised through swelling assessment, collagenase degradation assay, rheological and compression tests.

The release of encapsulated drugs from the hydrogels was studied by HPLC and the effect of the delivered bioactive agents was assessed through proteomic analysis and imaging for fibrotic markers in an *in vitro* keloid model.

### RESULTS AND DISCUSSION

The biophysical and biological properties of these systems were found to be suitable for potential implantation in the skin *in vivo*, with adequate mechanical and biological resistance. A pilot study using FITC-dextran proved that the inner compartment was capable of promoting a sustained release over a long period of time (14 days), which was further confirmed with drug release assays using Il-6 antagonists and recombinant decorin, fitting the intended therapeutic release profile. Proteomic studies showed a decrease of endogenous collagen type I, TGF- $\beta$ 1 and  $\alpha$ -smooth muscle actin expression indicating reduced fibrosis.

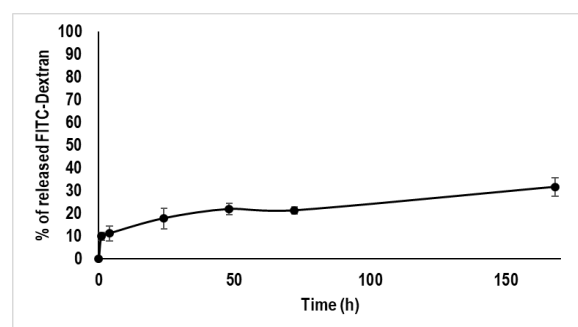


Fig. 1. Release profile of FITC-dextran from the system's inner compartment

### CONCLUSION

It was observed that this system is mechanically robust and stable *in vitro*, besides being an attractive dual drug delivery system considering its ability to release both drugs independently and ameliorating markers of fibrosis in an *in vitro* keloid model.

### REFERENCES

- [1] Chen *et al*, British journal of pharmacology, 158 (2009) 1196-1209.
- [2] Jarvinen *et al*, PNAS, 107 (2010) 21671-21676.
- [3] Desallais *et al*, Arthritis research & therapy, 16 (2014) R157.

### ACKNOWLEDGMENTS

This work was supported by Science Foundation Ireland and co-funded under the European Regional Development Fund (Grant Number 13/RC/2073).

## Polyvinylpyrrolidone/Ciprofloxacin-based Transparent Films and Electrospun Nanofibers as Potential Wound Care Dressings

Marco Contardi<sup>1,2</sup>, José A. Heredia-Guerrero<sup>1</sup>, Giovanni Perotto<sup>1</sup>, Paola Valentini<sup>3</sup>, Pier Paolo Pompa<sup>3</sup>, Raffaele Spanò<sup>4</sup>, Luca Goldoni<sup>4</sup>, Rosalia Bertorelli<sup>4</sup>, Athanassia Athanassiou<sup>1</sup>, Ilker S. Bayer<sup>1</sup> etc.

<sup>1</sup>Smart Materials, Istituto Italiano di Tecnologia, Via Morego 30, Genova 16163, Italy

<sup>2</sup>DIBRIS, University of Genoa, via Opera Pia 13, Genova 16145, Italy

<sup>3</sup>Nanobiointeractions and Nanodiagnostics, Istituto Italiano di Tecnologia, Via Morego 30, Genova 16163, Italy

<sup>4</sup>Department of Drug Discovery and Development, Istituto Italiano di Tecnologia, Via Morego 30, Genova 16163, Italy  
[marco.contardi@iit.it](mailto:marco.contardi@iit.it)

### INTRODUCTION

Nowadays, after-injury skin infections are one of the greatest challenges in the hospital environment in terms of health and costs management<sup>1-3</sup>. The total absence of skin coverage and the exudate production represent a perfect medium for bacterial growth, leading to a high risk of infections for the patients<sup>4</sup>. Moreover, the enhancement of infections due to antibiotic-resistant bacteria, such as *Pseudomonas aeruginosa*, require the development of innovative, effective, and cheap wound dressings<sup>5</sup>. Here, we reported a facile production of Polyvinylpyrrolidone<sup>6</sup>-based transparent films and electrospun nanofibers<sup>7</sup> loaded with an antibiotic, Ciprofloxacin (Cipro)<sup>8</sup>, and acetic acid (AcOH)<sup>9</sup>. The main goal of this work was to investigate the effect of the presence of Cipro and AcOH within the polymeric matrix by means of chemical, mechanical, and antibacterial characterizations. Lastly, the wound resorption ability of the polymeric matrices were considered, to assess their potential use *in vivo*.

### EXPERIMENTAL METHODS

Ciprofloxacin (Cipro) and Polyvinylpyrrolidone (PVP) powders were dissolved in water/acetic acid solutions containing 1, 5, 10 and 30% (v/v) AcOH in 10 mL of total volume. Films were easily produced by casting the solutions and by air drying for 3 days under an aspirated hood. Nanofibers were fabricated by means of a vertical electrospinning setup. The obtained samples were characterized via SEM, ATR-FTIR, TGA, water uptake capacity and mechanical tests and drug release studies. Antibacterial properties were investigated by inhibition zone assays on *Escherichia coli* and *Bacillus subtilis*. Preliminary *in vivo* tests were carried out using *in vivo* full-thickness excisional skin wound healing mice model.

All the measured values were expressed as mean  $\pm$  standard deviation of the mean.

### RESULTS AND DISCUSSION

As Cipro has low solubility in water and tendency to crystallize during solvent evaporation, by dispersing it in a proper ratio with AcOH and PVP we were able to obtain transparent films. In parallel, we fabricated free-beads nanofibers with diameters ranging between 450 and 250 nm. Furthermore, mechanical tests showed a plasticizer effect due to the presence of AcOH and Cipro, increasing the flexibility and handleability of the materials. Drug release studies were carried out, and a fast release profile was found both for films (from 6 to 12 minutes) and for nanofibers (2 minutes).

In the antibacterial analysis a synergic effect between AcOH and Cipro was highlighted. In the end, *in vivo* tests on C57BL/6J mice displayed good capacity to absorb exudate and dissolution rate of transparent antibiotic loaded films and nanofibers mats.

### CONCLUSION

PVP-based transparent films and nanofibers mats presented proper mechanical properties, fast release of Cipro, antibacterial effects, and capacity to absorb exudate, resulting highly suitable for designing new-generation of potential dressings for wound management and care.

### REFERENCES

1. Guest J.F. *et al.*, Int. Wound J. 14:322-330, 2017
2. Dreifke M.B. *et al.*, Mater. Sci. Eng. C 48:651-662 2015
3. Pereira R.F. *et al.*, Nanomedicine 8:603-621 2013
4. Vowden K. *et al.*, Br. J. Community Nurs. 8:4-13 2003
5. Boateng J. S. *et al.*, J. Pharm. Sci. 97:2892-2923 2008
6. Moura L. I. F. *et al.*, Acta Biomater. 9:7093-7114 2013
7. Rieger K. A. *et al.*, J. Mater. Chem. B 1:4531-4541 2013
8. Appelbaum P., Hunter P. *et al.*, Int. J. Antimicrob. Agents 16:5-15 2000
9. Haldstead F. D. *et al.*, Plos One 10:1371-1386 2015

## Partially-crosslinked, Co-complexed, Biomaterial Platforms for Potential Wound Healing Applications

Hillary Mndlovu, Pradeep Kumar, Thashree Marimuthu, Lisa du Toit, Yahya Choonara, Viness Pillay

Wits Advanced Drug Delivery Platform Research Unit,  
University of the Witwatersrand, Johannesburg, South Africa  
[674238@students.wits.ac.za](mailto:674238@students.wits.ac.za)

### INTRODUCTION

There are various experimental approaches in fabricating microplatforms for biomedical applications. However, there has been only minor alterations to the methods used to fabricate those microplatforms over the past decade. This led to recurring issues observed over a range of dressings such as the limited bioresorption of biomaterials leading to frequent need to change a dressing<sup>1</sup>. The freeze drying and lyophilisation approach has been widely used in preparation of various complex systems<sup>2,3</sup>. In this study the two approaches are combined with partial crosslinking of polymers into beads and then the pulverisation of the beads to improve both physical and mechanical properties of microplatforms for biomedical applications.

### EXPERIMENTAL METHODS

The approach made use of a four stepped method; partial-crosslinked polymers into soft beads, freeze drying, lyophilization and pulverization of beads into microparticles. Three formulations were prepared: partial-crosslinked alginate with calcium chloride, partial-crosslinked chitosan sodium triphosphate, and partial-crosslinked polyelectrolyte complex (PEC). Polymer solution droplets were poured into crosslinking reagents to form soft beads. The partial-crosslinked formulations were characterized along with their pristine counterpart via FTIR, XRD, BET-porosity analyser, DSC, TGA, NMR, UV-vis and SEM. The rheological properties of the hydrogel was analysed with the rheometer and the ElastoSens<sup>TM</sup> Bio<sup>2</sup> instrument while the degradation analyses was done in an incubator shaker.

### RESULTS AND DISCUSSION

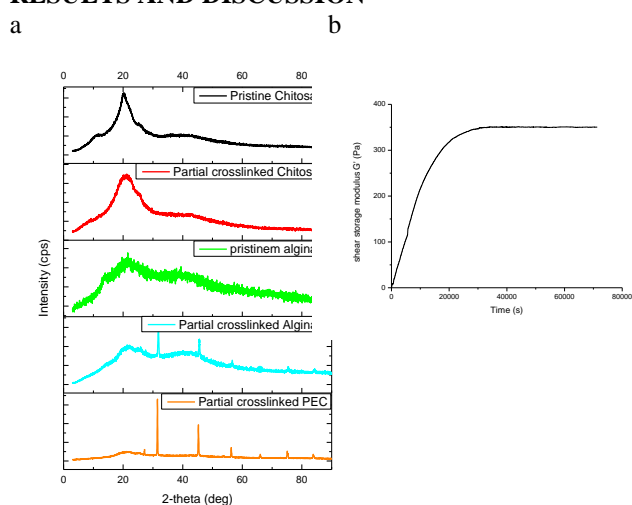


Fig. 1. (a) XRD diffractograms of the formulations, and (b) Kinetic gelling of the polyelectrolyte complex (37°C).

The degree of crosslinking test showed that 50% and 55% of chitosan and alginate were crosslinked, respectively. An instant gelling was observed during complexation (Fig. 1b). The complex hydrogel displayed an increased tensile strength compared to individual polymer hydrogels. Higher degree of porosity was aided by both lyophilisation approach and partial-crosslinking while the gelling and complexation of the pulverized polymers was abetted by the partial-crosslinking approach. The SEM-EDX analyse displayed a deposition of  $\text{Ca}^{2+}$ ,  $\text{Cl}^-$ ,  $\text{Na}^{2+}$ ,  $\text{O}_2$ , and Phosphorus around the complex, confirming presence of both crosslinked and uncrosslinked polymers. The present of the trace elements correlate with observations made on the diffractogram of the formulations (Fig.1a). The formulations displayed a retained thermal stability with increased water uptake. In 14 days, the partial-crosslinked formulations displayed a major increase in degradation with 59.2%, 90%, and 71% of the partial-crosslinked chitosan, alginate and the complex degradation, respectively. Pristine chitosan displayed minor degradation counterpart to its partial crosslinked counterpart whilst pristine alginate degradation was highly affected by its high water solubility. The partial-crosslinking may also improve the bioadhesivity, bioresorption, optimum drug entrapment and drug release of the complex system which may be beneficial in biomedical application.

### CONCLUSION

The increase in shear storage modulus over time confirmed both the instant gelling and ionic complexation of the polymers. The complex displayed improved physical properties such as water uptake, porosity, and thermal stability. The partial crosslinking aided the degradation of the complex over a reasonable period of time. This may eradicate the need for dressing changes. The presence of trace elements may assist in blood clotting situations and wound healing. This study shows promising approach in fabricating biocompatible, biodegradable and bioresorbable microplatforms for biomedical applications.

### REFERENCES

1. Pillay V. *et al.*, *Biomat. in Reg. Med. and the Immune System*, 209-223, 2015
2. Anisha, B.S., *et al.*, *Carbo. Pol.*, 92:1470-1476, 2013
3. Choi, Y. S., *et al.*, *J. of Mat. Sci.: Mat. in Med.*, 12:67-73,2001

### ACKNOWLEDGMENTS

The study was funded by the National Research Foundation (NRF)



## Biosynthetic Cellulose Based Hydrogels of Curcumin Encapsulated in Cyclodextrins as Wound Dressings

Abhishek Gupta<sup>1</sup>, Marek Kowalczyk<sup>2</sup>, Claire Martin<sup>3</sup>, Iza Radecka<sup>2</sup>

<sup>1</sup>School of Pharmacy, Faculty of Science and Engineering (FSE), University of Wolverhampton, U.K

<sup>2</sup>School of Biology, Chemistry and Forensic Science, FSE, University of Wolverhampton, U.K

<sup>3</sup>Department of Biological Sciences, Institute of Science and the Environment, University of Worcester, U.K

[a.gupta@wlv.ac.uk](mailto:a.gupta@wlv.ac.uk)

### INTRODUCTION

Curcumin (CUR) (diferuloylmethane) is a natural polyphenolic compound<sup>1</sup> well known as a wound healing agent<sup>2</sup>. Its antimicrobial activity ensues due to its ability to interact with an essential prokaryotic cell division initiating protein (FtsZ)<sup>3</sup>. The hydrophobicity of CUR limits its several biomedical applications but it can be overcome by microencapsulation of CUR in carriers like cyclodextrins (CDs) which are cyclic oligosaccharides. The current study demonstrates the production of biosynthetic cellulose based hydrogel dressings loaded with CUR inclusion complex (IC) with CDs and assessing their antimicrobial efficacy against *Staphylococcus aureus* (*S. aureus*).

### EXPERIMENTAL METHODS

IC of CUR with enhanced aqueous solubility was prepared by solvent evaporation (SE) method using hydroxypropyl beta-cyclodextrin (HPβCD) carrier. Supramolecular IC was characterised by FTIR. BC pellicles were synthesised and purified by the method reported previously<sup>4</sup>. Purified BC pellicles were padded dry (PD) and loaded with 5% aqueous solution of CUR-HPβCD under constant agitation overnight to obtain hydrogel formulations. This process was repeated by using freeze dried (FD) BC pellicles. Morphological studies were undertaken by SEM and antimicrobial activity of formulations was determined by disc diffusion assay using 8mm discs of the formulations and pure BC was used as a control. Zone of inhibition (ZOI) against *S. aureus* were measured at 24hrs.

### RESULTS AND DISCUSSION

Fully water soluble supramolecular IC of CUR-HPβCD (yellow in colour) was successfully synthesised. FTIR results revealed that due to the inclusion of CUR in HPβCD, the characteristic peaks of HPβCD appeared in the spectrum of IC (Fig 1). The characteristic peaks of CUR at 3504cm<sup>-1</sup> (O-H stretching), 1619cm<sup>-1</sup> (carbonyl C=O), 1591cm<sup>-1</sup> (aromatic C=C) were masked by HPβCD molecular vibrations (circled red, Fig 1). CUR peak at 1497cm<sup>-1</sup> (C=O and C=C vibrations) shifted to 1517cm<sup>-1</sup> in IC which could be due to complexation (circled blue, Fig 1). SEM results revealed the morphology of CUR and HPβCD changes to plate like structure in IC. IC gets physically entrapped in the BC fibre network during the loading process, as evident in the formulation SEM photomicrograph (Fig. 2). CUR has been proven to have antimicrobial effect against *S. aureus*<sup>1</sup>. Disc diffusion assay results in the present study (Fig. 3) revealed CUR-HPβCD-BC formulations (PD and FD) offer antimicrobial activity against the tested strain (*S. aureus*) at 24hrs. PD-BC loaded with IC showed higher antimicrobial activity compared to FD-BC hydrated with IC. This could be attributed to the higher uptake of drug by PD-BC compared to FD-BC.

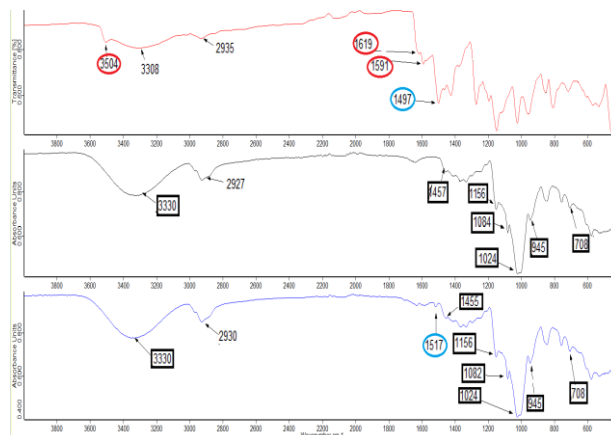


Fig. 1. FTIR results of: CUR (red); HPβCD (black) and IC (blue).

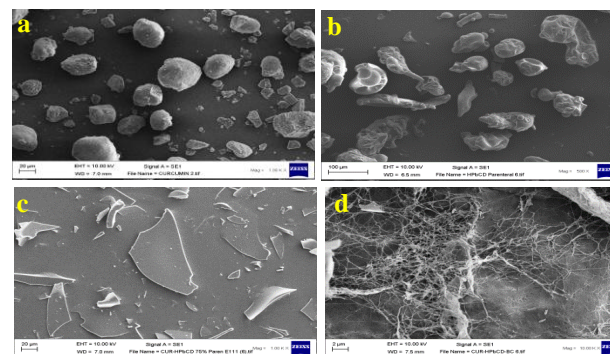


Fig. 2. SEM images (a) CUR (b) HPβCD (c) IC (d) CUR-HPβCD-BC formulation.

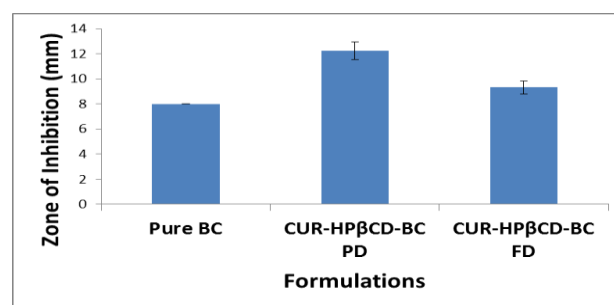


Fig. 3. A graph to represent ZOI for pure BC and hydrogel formulations against *S. aureus* (n=6; error bars=S.D.).

### CONCLUSION

This preliminary study confirms the potential use of antimicrobial CUR-HPβCD-BC hydrogels for wound management applications.

### REFERENCES

- Mun, S. *et al.*, *Phytomedicine*. 714:718-20, 2013.
- Akbik, D. *et al.*, *Life Sciences*. 1:7-116, 2014.
- Silva, A.C. *et al.*, *Trends in Food Science & Technology*. 74:82-72, 2018.
- Gupta A. *et al.*, *J. Microencap.* 725:734-33, 2016.



## Modification of Alginate-based Hydrogel for Therapeutic Applications Using Cold Atmospheric Plasma

Inès Hamouda<sup>1,2</sup>, Cédric Labay<sup>1,2</sup>, Maria Pau Ginebra<sup>1,2</sup>, Cristina Canal<sup>1,2</sup>

<sup>1</sup>Biomaterials, Biomechanics and Tissue Engineering Group, Dpt. Materials Science and Metallurgy, Technical University of Catalonia (UPC), c. Eduard Maristany 10-14, 08019 Barcelona, Spain

<sup>2</sup>Barcelona Research Center in Multiscale Science and Engineering, UPC, Spain

[ines.hamouda@upc.edu](mailto:ines.hamouda@upc.edu)

### INTRODUCTION

Cold plasmas are a source of a number of reactive species (ions, electrons, radicals, metastable molecules, UV/VIS radiation) that have been traditionally employed to modify the surface properties of biopolymers to tune their biological behaviour, usually at low pressures. With the development of Atmospheric Pressure Plasmas (APP) therapeutical applications have increased, and is attracting increasing attention. For instance, APP treatment has been shown to stimulate wound healing, and its effects seem to be related to the reactive oxygen and nitrogen species (RONS) they generate. Our preliminary data<sup>1</sup> have shown that APP and APP treated liquids are able to stimulate healthy bone cell proliferation. Due to their extraordinary capacity to absorb liquids, hydrogels are an attractive tool for drug delivery and tissue engineering applications<sup>2</sup>. In this work we want to evaluate, for the first time, the therapeutic effects of the reactive oxygen and nitrogen species (RONS) generated by APPs and contained within biocompatible alginate hydrogels. Therefore, the generation of RONS by APP in hydrogels will be quantified, and their *in vitro* cellular effects evaluated. Moreover, potential modifications in the bulk properties of the hydrogel will be evaluated following APP treatment in different conditions.

### EXPERIMENTAL METHODS

A natural alginate based hydrogel was treated with different types of APP jet (needle<sup>1</sup>, kINPen IND) and the effects of the plasma conditions such as gas flow distance to the sample or treatment time on the physical and chemical properties of the plasma-treated hydrogel were studied. Plasma effects on the hydrogel were monitored by FTIR, XPS and the behavior studied by rheology. RONS generated by APPJ such as H<sub>2</sub>O<sub>2</sub> and NO<sub>2</sub><sup>-</sup> were quantified by absorbance measurement using TiSO<sub>4</sub> and Griess reagent, respectively<sup>3,4</sup>. The *in-vitro* behavior was evaluated with human Mesenchymal stem cells and with osteoblasts.

### RESULTS AND DISCUSSION

The results showed that it is possible to generate different RONS in the polysaccharide-based hydrogel by APP treatment. Screening of different APP settings showed that the amount of RONS generated in the studied hydrogels results from the independent variation of the settings, and is highly dependant on the kind APP source employed. While an increase of plasma treatment time shows a progressive increase of [H<sub>2</sub>O<sub>2</sub>] and [NO<sub>2</sub><sup>-</sup>] with both APP sources studied, the absolute amount of RONS in the hydrogel can greatly vary depending on the plasma device used. Thus, APP treatment conditions were optimized in order to

maximize the amount of RONS. It is shown that the amount of RONS generated is some-fold lower than in APP-treated liquids (ie. Ringer) due to the modified reactivity caused by the presence of the biopolymer chains in solution. Chemical characterization of the hydrogels by FTIR and XPS revealed that the chemical polymer structure of the hydrogel APP treatment remains unchanged following APP treatment. Conversely, some minor changes in the rheological behaviour of the hydrogels before and after crosslinking have been recorded and are discussed in this work.

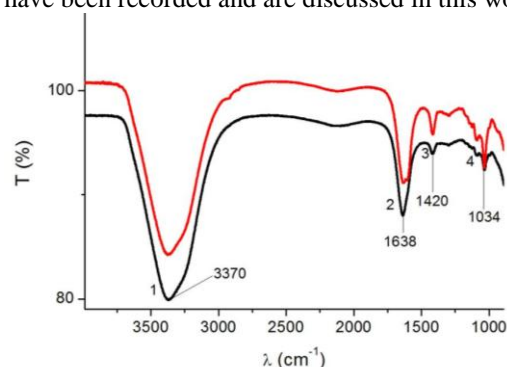


Fig. 1. FTIR spectra on an untreated (black line) and APP-treated (red line) alginate based hydrogel.

*In vitro* evaluation revealed an increase in the cell proliferation dependent on the dose of RONS introduced by APP in the hydrogels.

### CONCLUSION

Herein we highlighted that generation of RONS in a natural alginate-based hydrogel by APP is highly dependent on the treatment conditions employed. The treatment designed does not significantly modify the polymers' chemical properties and the *in vitro* results obtained provide interesting future prospects in views of wound healing and tissue engineering applications.

### REFERENCES

1. Canal, C. *et al.*, *Free Radic. Biol. Med.* 110, 2017.
2. El-Sherbiny, I. M. *et al.*, *Glob. Cardiol. Sci. Pract.* 2013, 38, 2013.
3. Giustarini, D. *et al.*, *Methods Enzymol.* 440, 361–380, 2008.
4. Eisenberg, G. *et al.*, *Ind. Eng. Chem. Anal. Ed.* 15, 327–328, 1943.

### ACKNOWLEDGMENTS

This project has received funding from the European Research Council (ERC) under the European Union's Horizon 2020 research and innovation programme (grant agreement No714793) and the financial support of MAT2015-65601-R project (MINECO/FEDER, EU).

## Monitoring of Matrix Remodeling during Living Cell Culture by Microrheological Measurements

Johanna Roether, Claude Oelschlaeger, Norbert Willenbacher

Institute for Mechanical Process Engineering and Mechanics, Applied Mechanics Group,  
Karlsruhe Institute of Technology, Germany

[Johanna.Roether@kit.edu](mailto:Johanna.Roether@kit.edu)

### INTRODUCTION

Viscoelastic response of a scaffold to cell-generated forces influences the in-vitro behaviour of the cells. Thus to understand cellular reaction, measurement of matrix local mechanical properties is of great importance. In this study, we have used hyaluronic acid (HA)<sup>1</sup>/collagen (Coll) based cryogel scaffolds for 3D cell culture. We were for the first time able to monitor changes in local viscoelastic properties in direct cell environment continuously using Multiple Particle Tracking (MPT) based microrheology. In combination with histologic staining, we gained a deeper insight in cell-matrix interactions.

### EXPERIMENTAL METHODS

MPT measurements were performed in cell-laden scaffolds by tracking the Brownian motion of inert beads, evenly distributed within the matrix. The resulting trajectories were transformed into mean square displacement traces from which local viscoelastic properties, i.e. storage modulus  $G'_{MPT}$  and loss modulus  $G''_{MPT}$  were calculated using the generalized Stokes-Einstein relation. As the tracer particles don't apply any force to cells and were proved to be non-cytotoxic, the MPT method is considered not to affect cell growth. Newly secreted fibers that contribute to matrix elasticity were identified by staining against fibronectin and other matrix proteins after 1, 3 and 8 days of cell culture.

### RESULTS AND DISCUSSION

Main results were that cryogel composition, local distribution of Coll and initial micromechanical properties affected cell behavior.

At low HA to Coll ratio, i.e. high Coll content, cells spread faster but proliferation rate was lower than in scaffolds with more HA. Cells adhered preferentially at locations with thick Coll fibers. When Coll was distributed homogeneously, cells adhered and spread more slowly than in networks with heterogeneous Coll distribution. But in latter, the degradation was accelerated. Continuous MPT monitoring showed that after 5 days  $G'_{MPT}$  was reduced by 80% of the initial local elastic modulus. Finally, we observed that in gels with low initial local elasticity, 3T3 cells produced higher amounts of fibronectin and additional Coll, compared to cells seeded in more rigid gels.

### CONCLUSION

In summary, the non-invasive characterization of matrix local mechanical and heterogeneity properties on microscale is possible by means of MPT measurements. Thus, our study serves as a window to a better understanding of matrix mechanical changes during cell culture on the length scale of single cell size.

### REFERENCES

<sup>1</sup> Oelschlaeger et al. (2016). *Biomacromol.* 17(2) p. 580-589.

### ACKNOWLEDGMENTS

We want to kindly acknowledge the support of Prof. Bastmeyer and Sarah Bertels, who contributed intensively for the cell culture experiments.

## Photocurable Polymer Materials for Innovative Hernia Repair

Mirosława El Fray

Poltiss sp z o.o., Al. Piastow 45, 71-311 Szczecin, Poland  
[office@poltiss.com](mailto:office@poltiss.com)

### INTRODUCTION

The inguinal or abdominal hernia is one of the most common problems related to the protrusion of an organ or the fascia of an organ through the wall of the cavity that normally contains it. To reinforce weakened tissue and avoid its over-stretching, non-degradable synthetic materials – usually polypropylene meshes are used. Recently, new biodegradable polymeric materials, which can be injected into weakened tissue and *in situ* polymerized were developed<sup>1</sup>. This approach can revolutionize the current hernia treatment procedures being easier, faster and safer. Here, we present the feasibility study toward injectable and photocurable materials concept for hernia repair on rabbit model.

### EXPERIMENTAL METHODS

New elastomeric materials were fabricated from patented formula of telechelic macromonomers<sup>2</sup>. The viscous liquids were exposed to 365 nm light irradiation for crosslinking *in situ in vivo* in rabbits to close the artificially fabricated hernia in abdominal wall. Hernia repair in rabbits was performed 2 months after artificial hernia fabrication. Skin and subcutaneous tissue were incised. Hernia was pushed back after tissue preparation. Viscous telechelic macromonomer was injected into hernia gate and irradiated with UV light for 5 min to create flexible film *in situ*. No sutures or other fixation was used to fix the implant. After hemostasis, the skin was closed with sutures. As a control, commercially available polypropylene mesh (PPM), DuraMesh™ (Sukol, 0.18 mm monofilament, 29 g/m<sup>2</sup>) was used. Semithin (4–6 μm) sections were stained with hematoxylin and eosin (HE) for cellular detail and morphology, and examined by light microscopy.

### RESULTS AND DISCUSSION

The artificially fabricated defect was regenerated and healthy tissue was build-up. Overall, the cellular response was similar between the new material and the PPM control. We did observe a trend towards higher eosinophil counts for the experimental material, as compared to control; however the differences were not significant. Importantly, the number of lymphocytes and macrophages counted was comparable for new material and the clinically used control, PPM. Importantly, no recurrence of hernia was noticed during the observation time and no adhesions were observed at sacrifice. Additionally, no complications were observed and all blood laboratory parameters were similar to the clinically utilized polypropylene mesh control group.

Likewise, analysis of cells in the hernia regions indicated a similar tissue response to new tested material and no significant differences between this material and the control. No inflammatory cells were detected in connective tissues and no sign of necrosis has been observed after one-month implantation.

### CONCLUSION

In this work, we provided a proof-of-concept of a viable clinical alternative to polymeric meshes for hernia repair by using an injectable viscous liquid turning out to the elastomeric solid upon the UV radiation. This solution is particularly important on developing new, minimally invasive protocols.

### REFERENCES

1. US 9,228,043 B2 (2016), PL 226421 (2017)
2. US 9,267,001 B2 (2016), PL216948 (2014), EP2712878 (2012)

## Construction of a Three Dimensional in Vitro Embryo Implantation Model Using Alginate Macroporous Scaffold

Dganit Stern<sup>1</sup>, Reuven Reich<sup>1</sup>, Tali Tavor-Re'em<sup>2</sup>

<sup>1</sup>Institute of Drug Research, School of Pharmacy, the Hebrew University, Jerusalem, Israel,

<sup>2</sup>Dept. of Pharmaceutical Engineering, Azrieli College of Engineering, Jerusalem, Israel

[talire@jce.ac.il](mailto:talire@jce.ac.il)

### INTRODUCTION

Implantation failure remains an unsolved obstacle in reproductive medicine and is a major cause of infertility in otherwise healthy women. Indeed, only about 20% of embryos transferred to the uterus, following in vitro fertilization (IVF), lead to the birth of a healthy infant. Due to obvious ethical restrictions there is an unmet need to establish an in vitro model that mimics the events in the uterine wall during the implantation process. The available two-dimensional models do not fully represent the event taking place at implantation.

### EXPERIMENTAL METHODS

Alginate scaffolds were prepared by a freeze-dry technique [1]. Endometrial cell lines, RL95-2 or HEC-1A, expressing high and low levels of Estrogen receptor- $\alpha$  (ER- $\alpha$ ), displaying receptive and non-receptive endometrial properties, respectively, were used. Cells were seeded into alginate scaffolds and cultured in sequential hormonal treatment, mimicking the menstrual cycle, i.e. one week priming of estrogen, following by two weeks of progesterone containing medium. Control media used: (a) 3 weeks in estrogen containing medium, (b) progesterone containing or (c) hormone-free media. E-cadherin mRNA expression levels were evaluated by qPCR. E-cadherin protein expression was evaluated by specific immuno-staining of cell constructs' thin cryo-sections, or by Western blot analysis. In order to evaluate cell constructs receptivity to trophoblast, JAR spheroids were seeded on top of 3 week-old cell constructs, and incubated for 24 h. Attachment of JAR spheroids to RL95-2 culture was evaluated by H&E staining. Statistical analysis: E-cadherin mRNA and protein comparison was performed by 2-way analysis of variance (ANOVA). Benferroni's post-hoc test was carried out to determine differences.  $P < 0.05$  was considered for statistical significance.

### RESULTS AND DISCUSSION

Cultivation under 3D conditions within macro-porous alginate scaffolds enabled long-term viability of the cells for at least 4 weeks. E-cadherin mRNA expression levels were shown to be significantly higher in 3-weeks old RL95-2 cell constructs, cultured in sequential hormonal treatment, compared to HEC-1A cells (Fig. 1A). E-cadherin immuno-staining revealed pronounced protein expression in RL95-2 cell constructs, compared to HEC-1A. These finding imply to the possible regulation of E-cadherin by ER- $\alpha$ . JAR spheroid attachment to 3-weeks old RL95-2 culture was confirmed by H&E staining, pointing out to the functionality of the implantation model (Fig. 2, left).

No such spheroid attachment was evident in HEC-1A (Fig. 2, middle). Moreover, transfection of HEC-1A cells with ER- $\alpha$  indicated restored capability of JAR spheroid adhesion (Fig. 2, right).

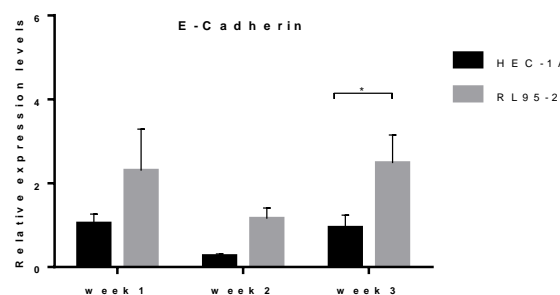


Fig. 1. Quantification of E-cadherin mRNA expression levels in cell constructs, evaluated by Real-Time PCR. \* -  $p < 0.05$ , 2-way ANOVA, Bonferroni's post-hoc test.

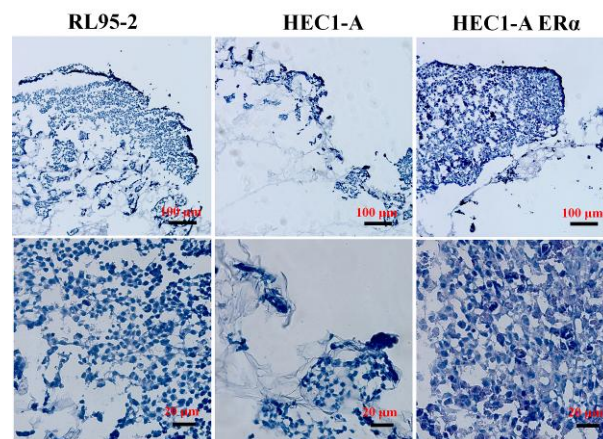


Fig. 2. JAR spheroid attachment to epithelial endometrial 3D culture models in alginate scaffolds. (Bars: Upper panel: 100 $\mu$ m; Lower panel: 20 $\mu$ m).

### CONCLUSION

Our 3D culture models within macro-porous alginate scaffolds enabled long-term culture of viable endometrial cells. These cultures may serve as a research model for studying the regulatory mechanism governing implantation process and evaluation of potential novel therapeutic strategy for regulating implantation defects and restoring the ability to implant embryos in patients with repeated implantation failure.

### REFERENCES

1. Shaoiro L, Cohen S., Biomaterials 18:583-90, 1997  
References must be numbered. Keep the same style.

### ACKNOWLEDGMENTS

This study was funded by Azrieli College of Engineering (DS).



## Engineered Substrates with Site-specific Immobilized Laminin for Neural Stem Cells

Daniela Barros<sup>1,2,3</sup>, Paula Parreira<sup>1,2</sup>, Joana Furtado<sup>2,4</sup>, Frederico Ferreira-da-Silva<sup>2,4</sup>, Andrés J. García<sup>5,6</sup>, M. Cristina L. Martins<sup>1,2,3</sup>, Isabel Freitas Amaral<sup>1,2,7</sup>, Ana Paula Pêgo<sup>1,2,3,7</sup>

<sup>1</sup>IS - Instituto de Investigação e Inovação em Saúde, Universidade do Porto (UPorto), Portugal; <sup>2</sup>INEB - Instituto de Engenharia Biomédica, UPorto, Portugal; <sup>3</sup>ICBAS - Instituto de Ciências Biomédicas Abel Salazar, UPorto, Portugal;

<sup>4</sup>IBMC - Instituto de Biologia Molecular e Celular, UPorto, Portugal; <sup>5</sup>Parker H. Petit Institute for Bioengineering and Biosciences, Georgia Institute of Technology, Atlanta, Georgia, USA; <sup>6</sup>George W. Woodruff School of Mechanical Engineering, Georgia Institute of Technology, Atlanta, Georgia, USA; <sup>7</sup>FEUP - Faculdade de Engenharia, UPorto, Portugal

[daniela.barros@ineb.up.pt](mailto:daniela.barros@ineb.up.pt)

### INTRODUCTION

Laminin (Ln) is a heterotrimeric glycoprotein with multi-bioactive domains involved in the modulation of neural stem cell (NSC) and neuronal cell behavior, including cell adhesion and viability, axonal extension, as well as synapse function and stability. Previous attempts to immobilize Ln into biomaterial-based matrices were limited to non-specific immobilization approaches, which may compromise the exposure of crucial Ln bioactive epitopes, as those interacting with cell surface receptors and with other extracellular matrix (ECM) molecules. To control the immobilization and the conformation of full-length recombinant human Laminin (rhLn), here we explore an affinity-based approach in which a recombinant human fragment of an ECM component (rhX), with high affinity to a specific site in the Ln triple  $\alpha$ -helical coiled-coil, was explored to ensure the site-selective immobilization of rhLn on both 2D model surfaces (self-assembled monolayers (SAMs)) and within protease-sensitive PEG-based hydrogels. The bioactivity of the proposed substrates was assessed using human neural stem cells (hNSCs).

### EXPERIMENTAL METHODS

The selected fragment (rhX) was produced in the *E. coli* BL21(DE3) strain and purified by affinity chromatography. Its bioactivity was assessed by both solid-binding assay and surface plasmon resonance. The selective functionalization of rhX N-terminal amine with a thiol-PEG-succinimidyl glutaramide (HS-PEG-SGA) was conducted under optimized conditions and characterized by SDS-PAGE and mass spectrometry. Mixed SAMs of EG4 (non-fouling substrate) and MonoPEGylated rhX were prepared and their ability to mediate immobilization of rhLn-521 evaluated using a Quartz Crystal Microbalance. The ability of MonoPEGylated rhX-bound rhLn-521 to promote the cell adhesion of H9-derived NSCs was then assessed. After cell adhesion, cells were incubated with Calcein AM and cell adhesion per square centimeter quantified measuring the total fluorescence intensity and the total cell number. For the formation of PEG-based hydrogels, 4-arm PEG-maleimide macromers were functionalized with MonoPEGylated rhX, which was then conjugated with Ln and cross-linked into a hydrogel by addition of a cysteine-flanked MMP-sensitive peptide in the absence or presence of hNSCs.

### RESULTS AND DISCUSSION

The produced rhX fragment (purity > 90%) showed high affinity both to mouse Ln-111 ( $K_D = 0.98$  nM) and rhLn-521 ( $K_D = 0.54$  nM). Selective N-terminal PEGylation of rhX yielded predominantly MonoPEGylated rhX. Peptide mapping further confirmed the N-terminal PEGylation of the fragment. The resultant MonoPEGylated rhX retained a high affinity to mouse Ln-111 ( $K_D = 3.36$  nM) and rhLn-521 ( $K_D = 1.58$  nM). The immobilization of MonoPEGylated rhX on SAMs led to an efficient immobilization of rhLn-521 (638 ng/cm<sup>2</sup>) with retention of bioactivity, as shown by the ability of affinity-bound rhLn-521 to support hNSC adhesion. The tethering of MonoPEGylated rhX to 4-arm PEG maleimide and subsequent conjugation with Ln did not compromise hydrogel formation, either in the absence or presence of cells. Furthermore, the Ln-functionalized hydrogels were able to support the viability and the neuronal differentiation of hNSCs (Fig. 1).

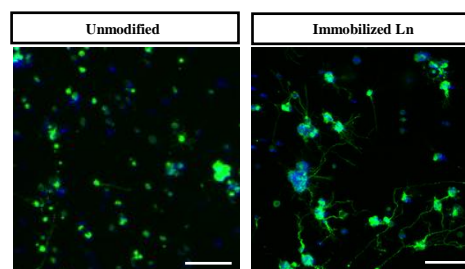


Fig. 1. hNSCs (H9 hESC-Derived) differentiation within PEG-based hydrogels – unmodified or immobilized Ln (100  $\mu$ g/mL). Cells were seeded as single cells ( $4 \times 10^6$  cells/mL) and cultured under neuronal differentiation conditions for 14 days. Scale bar = 80  $\mu$ m.

### CONCLUSION

The present work demonstrates the potential of the rhX fragment to control the immobilization of Ln into biomaterial-based matrices. The two Ln-functionalized substrates were able to support hNSC adhesion. Moreover, the protease-sensitive hydrogel containing affinity-bound Ln was shown to support hNSC viability and neuronal differentiation. Although here we explored the applicability of Ln-functionalized hydrogels in the context of nervous tissue, these platforms can also be applied in other disease contexts, due to the affinity of the produced rhX fragment for different laminin isoforms.

### ACKNOWLEDGMENTS

This work was supported by Portuguese by FCT/Ministério da Ciência, Tecnologia e Inovação and by FEDER funds through COMPETE 2020 (POCI-01-0145- FEDER-007274). D Barros PhD studies were funded by FCT PhD Programs and Programa Operacional Potencial Humano (POCH), specifically by the BiotechHealth Program (Doctoral Program on Cellular and Molecular Biotechnology Applied to Health Sciences).



## Electrospinning of Non-Ionic Cellulose Ether Nanofibers with Silver Nanoparticles having Antibacterial Activity

Ashwini Wali<sup>1,2</sup>, Satish R. Inamdar<sup>2</sup>, Manohar V. Badiger<sup>1</sup>

<sup>1</sup>Polymer Science and Engineering Division, CSIR-National Chemical Laboratory, Dr. Homi Bhabha Road, Pune 411008, India

<sup>2</sup>Department of Chemical Engineering, Vishwakarma Institute of Technology, Bibwewadi, Pune 411037, India  
[ac.wali@ncl.res.in](mailto:ac.wali@ncl.res.in)

### INTRODUCTION

Electrospinning is a simple, cost-effective, and reproducible process where in both synthetic and natural polymers can be used. This process utilizes the electrostatic forces to draw the fibers from the droplet formed at the tip of spinneret. It has been found to be attractive for various applications in biomedical engineering, filtration, protective clothing, catalysis reactions and sensors<sup>1</sup>. Non-ionic cellulose ethers namely Ethyl hydroxyl ethyl cellulose (EHEC) is an important polysaccharide which finds applications as thickening/rheology control agents in paints, cosmetics, detergents and oil recovery. This polymer is non-toxic, biocompatible, biodegradable which finds applications in biomedical field as well<sup>2</sup>. Poly (vinyl alcohol) (PVA) is a semi-crystalline hydrophilic polymer. It is a highly biocompatible and non-toxic polymer with good thermal and mechanical properties having high water solubility. It has a wide range of applications in medical, cosmetic, food, pharmaceutical and packaging industries. Inorganic metals like silver nanoparticles (AgNP's) being safe are used with various polymers as antibacterial and disinfectant agents. As the silver particle size approaches the nano-level, the total surface area becomes increasingly larger with respect to its volume and also the antibacterial efficiency is increased. We are the first to report on electrospinning of EHEC nanofibers for biomedical applications.

### EXPERIMENTAL METHODS

#### Materials:

Ethyl hydroxyl ethyl cellulose (EHEC) was obtained from Akzo-Nobel Functional Chemicals AB, Sweden with trade name as Bermocoll E411 FQ. The molecular weight is 1200Kg/mol with about 7000 anhydro glucose units (AGU). Polyvinyl alcohol (PVA), cold water soluble with degree of polymerization is 0.6 and 89% hydrolyzed was obtained from S.D Fine Chemicals, Boisar, India. Silver nitrate, AR grade was purchased from Thomas Baker. Distilled water was used throughout the experiments.

#### Preparation of EHEC/PVA/AgNP's blend solutions:

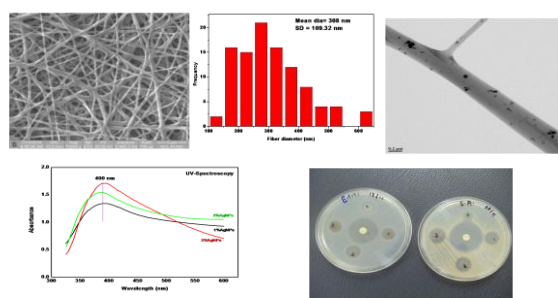
The EHEC/PVA with 10 % (w/v) was dissolved in double distilled water under stirring for 8 h. A known quantity of AgNO<sub>3</sub> was mixed in this solution under magnetic stirring for 1 h at room temperature with various Ag content (1, 2, and 3 wt %) and kept under UV light for 30 minutes to undergo photo polymerization.

#### Electrospinning of EHEC/PVA/AgNP's blend nanofibers:

The blend solution was taken in a plastic syringe with a blunt needle having 8 mm diameter connected to a syringe pump to control the solution flow rate. The applied voltage was adjusted to 25 kV. Fibers were collected on plate collector having an aluminium foil placed at a 15 cm distance from the needle tip.

#### Characterization:

The morphology of the nanofibers were studied using Scanning Electron Microscopy quanta 200 3D dual beam ESEM FEI, Finland. The size of the Ag-NPs in nanofibers were determined using TEM FEI, TECNA IG2 F30 instrument operated at an accelerated voltage of 200 kV. X-ray diffraction was done on a Rigaku Micromax-007HF diffractometer operating at 40 kV and 30 mA.



Thermal analysis was performed in the temperature range from 30 to 900 °C at a controlled heating rate of 10 °C min<sup>-1</sup>. The antibacterial activity were investigated on these nanofibers by the disc diffusion method using *S. Aureus* (NCIM No: 2079) and *E. Coli* (NCIM No:2065).

### RESULTS AND DISCUSSION

The SEM images revealed the morphology of the nanofibers and the average diameter was in the range of 300-350 nm. The size of the silver nanoparticles was 10-20 nm. The UV-spectrometry results confirmed the presence of Ag nanoparticles at 400nm. XRD also confirmed the presence of silver at 19.2, 28, 32 and 47 ° respectively. TGA increased the degradation temperature from 250 to 270°C. The antibacterial effect was observed in gram positive and gram negative bacteria. The zone of inhibition increased as the concentration of silver nanoparticles increased.

### CONCLUSION

The EHEC/PVA/AgNP nanofiber mats exhibiting good tensile strength could be effectively used in tissue engineering as cost effective wound dressing materials.

### REFERENCES

1. Md. Shahidul Islam. *et al.*, Colloids and Surfaces A: Physicochem. Eng. Aspects. 436:279–286, 2013
2. Ashwini Wali. *et al.*, Carbohydrate Polymers.81:175-182, 2018

### ACKNOWLEDGMENTS

A.Wali acknowledges CSIR-Delhi for the SRF fellowship with award number 31/11(822)2013-EMR-I and CSIR-NCL for providing all the research facilities.

## Collagen-based Devices as Multi Cargo Delivery Vehicles for Tendon Treatments

Eugenia Pugliese<sup>1,2</sup>, Yves Bayon<sup>3</sup>, Dimitrios Zeugolis<sup>1,2</sup>

<sup>1</sup>Regenerative, Modular & Developmental Engineering Laboratory (REMODEL), National University of Galway, Ireland

<sup>2</sup>Centre for Research in Medical Devices (CURAM), National University of Galway, Ireland

<sup>3</sup>Medtronic, Sofradim Production, France

[eugenia.pugliese@nuigalway.ie](mailto:eugenia.pugliese@nuigalway.ie)

### INTRODUCTION

Biomaterial-based approaches are valid alternatives to tissue graft in tendon regeneration but have often failed to completely recapitulate native tendon composition and mechanical properties<sup>1</sup>. Cell-mediated therapies, specifically with bone marrow mesenchymal stem cells (BMSCs) may potentially recover native tendon function, if stem cells survival, localization and differentiation towards tenogenic lineage is attained<sup>2</sup>. To this end, collagen type I hydrogels cross-linked to different extents with poly-ethylene glycol succinimidyl succinate (PEG-SS) will be fabricated to encapsulate BMSCs and direct their differentiation towards tenogenic lineage, while providing controlled release of biomolecules for tendon treatments.

### EXPERIMENTAL METHODS

Commercially available (Medtronic) porcine collagen type I was used to fabricate collagen hydrogels at a final concentration of 5 mg/mL and cross-linked with 4 and 8 arms PEG-SS, molecular weight of 10, 20 and 40 kDa and varying concentrations of 0, 0.1, 0.5, 1 and 2.5 mM. Cross-linking efficiency was tested through free amines assay (TNBSA) and collagenase degradation; mechanical properties were measured through compression test. One-way analysis of variance was performed to compare multiple groups and differences were considered to be significant at a level of  $p \leq 0.05$ .

### RESULTS AND DISCUSSION

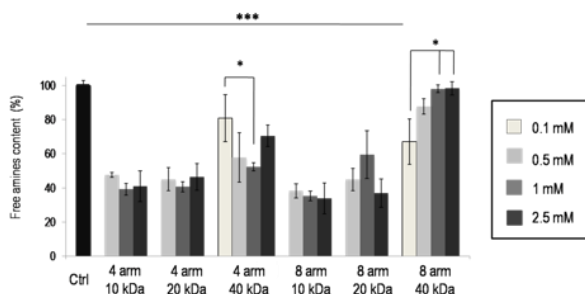


Fig. 1. Free amines (TNBSA) assay for the detection of free amines residual after cross-linking.

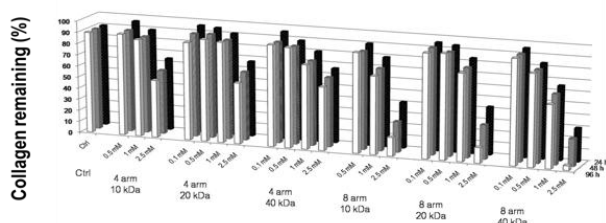


Fig. 2. Collagen remaining (%) over the time (4 days) in collagenase type II buffer (50 U/mL).

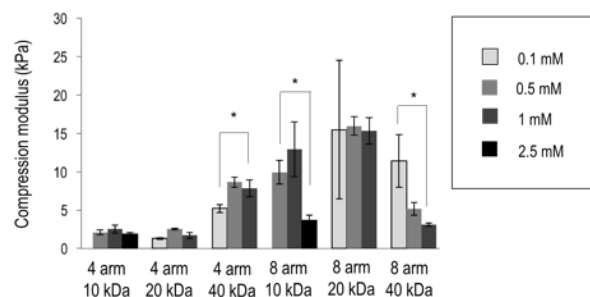


Fig. 3. Compression modulus resulting from compression test, 100 % deformation, 8 mm/min speed.

Collagen type I hydrogels were successfully cross-linked with varying concentration of PEG-SS; specifically, hydrogels cross-linked with 0.5 and 1 mM of 4 and 8 arms, 10 and 20 kDa PEG-SS showed approximately 50 % reduction of free amines compared to non-cross-linked hydrogels and approximately 20% degradation in collagenase type II buffer. Results from the compression tests showed that all cross-linked hydrogels have a compression modulus in the range of 1-15 kPa, making them suitable for BMSCs encapsulation. 4 and 8 arm PEG-SS 10 and 20 kDa will be furthered biologically tested to assess the influence of varying stiffness as a function of the different PEG-SS concentrations, arms and molecular weight on BMSCs differentiation into tenogenic lineage and the controlled release of biomolecules.

### CONCLUSION

Collagen hydrogels cross-linked with 4 and 8 arm, 10 kDa and 20 kDa PEG-SS are the most crosslinked and the most resistant over the time to the action of collagenase type II. All cross-linked hydrogels are in the range of expected stiffness for soft materials. The BMSCs differentiation toward tenogenic lineage and the controlled release of biomolecules for tendon treatment will be assessed as a function of the different extent of PEG-SS cross-linking.

### REFERENCES

1. Gaspar D. *et al.*, Adv Drug Deliv Rev, 2015
2. Spanoudes K. *et al.*, Trends in Biotechnology, 2014

### ACKNOWLEDGMENTS

This project has been funded by the European Union, Horizon 2020 Programme, under the Marie Skłodowska-Curie Actions, Innovative Training Networks, Grant Agreement 676338

## Design of a Novel Microfeatured Poly(Glycerol Sebacate) Methacrylate (PGSM) Scaffolds for Corneal Regeneration

Iris C Becerril-Rodriguez, Sheila MacNeil, Frederik Claeysens

Department of Materials Science and Engineering, Kroto Research Institute, University of Sheffield, United Kingdom  
[icbecerrilrodriguez1@sheffield.ac.uk](mailto:icbecerrilrodriguez1@sheffield.ac.uk)

### INTRODUCTION

Limbal epithelial stem cells (LESCs) culture has reached the point of development that allows its adequate use in tissue engineering. However, the survival of the cells after transplantation in the host tissue has not been successful<sup>1</sup>. The main challenge is the development of a safe and efficient carrier that delivers cells to specific sites and ensures their survival. Previous biomaterials used in corneal regeneration lack a proper limbal stem cell (niche) microenvironment that can offer physical protection to stem cells<sup>2,3</sup>. The microenvironment improves cell survival after transplantation and mimics the characteristics of the corneal limbus<sup>4,5</sup>.

The poly (glycerol sebacate) (PGS) is a biocompatible, biodegradable, bioresorbable, and inexpensive elastomer. Due to its physicochemical and mechanical characteristics is a useful polymer for working with soft tissue, such as the cornea<sup>6</sup>.

### EXPERIMENTAL METHODS

Synthesis of PGSM is carried out by the polycondensation of sebacic acid and glycerol. Methacrylate groups have been added to the PGS molecule to obtain an additional level of control over its strength, degradation, crosslinking density and elongation. Two variants of PGSM scaffolds were synthesized, each with different methacrylation percentages: 50% methacrylated PGSM high internal phase emulsions (HIPEs), and 30% methacrylated transparent PGSM scaffolds. Diphenyl (2,4,6-trimethylbenzoyl) phosphine oxide / 2-hydroxyl-2-methyl propiophone) was used as a photoinitiator at a concentration of 1% w/w for UV curing. The software used for design the microfeatured scaffold was Solidworks.

The characterization of PGS and PGSM molecules was carried out by ATR-FTIR, TGA, and GPC analysis. The scaffold morphology was observed through SEM and confocal light microscopy.

### RESULTS AND DISCUSSION

We have designed and produced a novel microfeatured poly (glycerol sebacate) methacrylate (PGSM) implantable outer rings with well-defined niches, whose 3D shape can be modified as required. This is the first report of microfeatured PGSM scaffolds for corneal regeneration. The stem cell pockets are expected to improve healing of the cornea through re-epithelization, increase survival through physical protection, and efficiently deliver stem cells to their destination. The Figure 1 shows the microfeatured scaffolds and its design.



Fig. 1. a) Scaffold template design in Solidworks, b) 50% methacrylated PGSM high internal phase emulsions (HIPEs), c) 30% methacrylated transparent PGSM scaffolds.

FTIR-ATR analysis confirmed the addition of methacrylate groups, and GPC analysis determined an average molecular weight of 20,000 Da. The scaffold morphology was observed through SEM, its analysis confirmed that we obtained a porous scaffold. Confocal light microscopy was used for analysing the cell distribution through the scaffold structure.

### CONCLUSION

PGSM shows high biocompatibility, tuneable degradation, mechanical and physical surface properties, making it an ideal candidate for soft-tissue applications. Previous results obtained from our research group suggest that these microfeatured PGSM-based scaffolds will improve limbal stem cell survival after implantation in the host tissue.

### REFERENCES

1. Sehic A. *et al.*, Journal of Functional Biomaterials. 6, 863-888, 2015.
2. Levis HJ. *et al.*, Biomaterials. 34: 8860-8868 2013.
3. Ortega I. *et al.*, Journal of visualized experiments. 91:1-11, 2014.
4. Chee K. *et al.*, Clinical and Experimental Ophthalmology 34:64-73 2006.
5. Li W. *et al.*, Cell Research. 17:26-36, 2007.
6. Yia, Y. *et al.*, Polymer Chemistry, 7: 2553-2564, 2016

### ACKNOWLEDGMENTS

This work is supported by grants from the National Science and Technology Council in Mexico (CONACyT) and the University of Sheffield.

## Design and Characterization of Synthetic Biodegradable Films for Tendon Tissue Engineering

Sofia Ribeiro<sup>1,2</sup>, Vit Novacek<sup>1</sup>, Emanuel M. Fernandes<sup>4,5</sup>, Manuela E. Gomes<sup>4,5</sup>, Rui L. Reis<sup>4,5</sup>, Yves Bayon<sup>1</sup>, Dimitrios I. Zeugolis<sup>2,3</sup>

<sup>1</sup>Medtronic, Sofradim Production, Trevoux, France

<sup>2</sup>Regenerative, Modular & Developmental Engineering Laboratory (REMODEL)  
National University of Ireland Galway (NUI Galway), Galway, Ireland

<sup>3</sup>Science Foundation Ireland (SFI) Centre for Research in Medical Devices (CÚRAM)  
National University of Ireland Galway (NUI Galway), Ireland

<sup>4</sup>3B's Research Group – Biomaterials, Biodegradables and Biomimetics, University of Minho  
Headquarters of the European Institute of Excellence on Tissue Engineering and Regenerative Medicine,  
Guimarães, Portugal

<sup>5</sup>ICVS/3B's – PT Government Associate Laboratory, Braga/Guimarães, Portugal  
[sofia.ribeiro@medtronic.com](mailto:sofia.ribeiro@medtronic.com)

### INTRODUCTION

Biodegradable polymers have been studied and applied in biomedical field, such as tissue engineering applications.<sup>1</sup>

To repair soft tissue, it is vital to ensure that the biomaterial is able to mimic the complex elasticity of the native tissue. Huge efforts have been invested into the development and design of appropriate elastomeric biomaterials to match the tissue of choice.<sup>2</sup>

It has been demonstrated that substrate stiffness has a huge influence on cellular growth, differentiation, motility and phenotype maintenance.<sup>3</sup> The goal of the present study is to characterize extensively a set of polymeric films with variable mechanical profiles.

### EXPERIMENTAL METHODS

Absorbable polyesters made from different combination of monomers, such as lactic acid, glycolic acid, trimethylene carbonate, dioxanone &  $\beta$ -caprolactone, were selected for their physico-chemical intrinsic properties. Even though the selected polymers have similar chemistry they show different mechanical and degradation properties (Fig. 1).

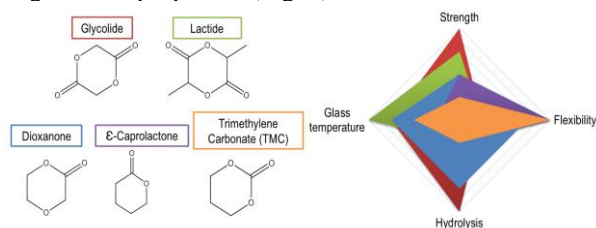


Fig. 1- Monomers selected (Glycolide, Lactide; Dioxanone,  $\epsilon$ -Caprolactone and Trimethylene Carbonate) and the representation of their intrinsic properties.

The films were manufactured by compressing moulding using a thermal presser and then characterized by scanning electron microscopy (SEM), differential scanning calorimetry (DSC), nuclear magnetic resonance spectroscopy (NMR) and Fourier transform infrared spectroscopy (FTIR).

The mechanical properties of the films were assessed by dynamic mechanical analysis (DMA) in dry and wet conditions and also by atomic force microscopy (AFM). Initial *in vitro* assays were performed using human dermal fibroblasts (hDFs) and human adipose stem cells (hASCs) to assess the cell cytocompatibility and proliferation of the films.

### RESULTS AND DISCUSSION

It was possible to successfully produce polymeric films using a large range of polyesters using a thermal presser. Chemical analysis was used to trace the chemical profile for each polymer. The selection performed lead to materials with very distinct profiles, regarding their crystallinity content and degradation rate.

The mechanical properties of the materials were analysed regarding at their macro level by DMA at 37°C in a PBS bath. The results show that the developed films have a storage modulus range from 0.1 up to 2.6 GPa.

The 2D and 3D surface topographies of the upper side of the films were imaged using AFM. The root mean square deviation values of the surface roughness and the material's stiffness at a micro-level were also analysed. The results obtained are within the range intended for tendon tissue repair.

Biological assays showed good cell adhesion, cell proliferation and cell viability.

### CONCLUSION

Overall the selection of polymers gives us good options for a potential tendon repair scaffold. The film's mechanical properties are within the described elastic modulus range, 0.4 to 1.2GPa, depending on function and anatomic location of the tendon.<sup>4,5</sup>

In the future, their bio-instructive properties (eg. phenotype maintenance, cell differentiation) will be screened.

### REFERENCES

1. Nair L. et al., Prog. Polym. Sci. 32:762-798, 2007
2. Chen Q. et al., Prog. Polym. Sci. 38 :584-671, 2013
3. McMurray R. et al., Nat. Mat. 10 :637-644, 2011
4. Baldino L. et al., Br. Med. Bull. 117 : 25-37, 2016
5. Maganaris C. et al., J. Physiol. 521 : 307-313, 1999

### ACKNOWLEDGMENTS

This work received funding from H2020-MSCA-ITN-2015 - Tendon Therapy Train - Project N° 676338. It has also been supported from Science Foundation Ireland and the European Regional Development Fund (Grant Agreement Number: 13/RC/2073).



## Melt Compounded Polymer Nanocomposite for the Production of 3D Printing Scaffold in Regenerative Medicine

Marco Scatto<sup>1</sup>, Maria Bastianini<sup>2</sup>, Michele Sisani<sup>2</sup>, Paolo Scopece<sup>1</sup>, María Cámara Torres<sup>3</sup>, Ravi Sinha<sup>3</sup>, Ainhoa Egizabal Luzuriaga<sup>5</sup>, Carlos Mota<sup>3</sup>, Alessandro Patelli<sup>4</sup>, Lorenzo Moroni<sup>3</sup>

<sup>1</sup>Nadir S.r.l., c/o Campus Scientifico Università Ca' Foscari Venezia, Via Torino 155b, 30172 Mestre (VE), Italy,

<sup>2</sup>Prolabin & Tefarm S.r.l., Via dell'Acciaio 9, 06134 Perugia Italy,

<sup>3</sup>MERLN Institute for Technology-Inspired Regenerative Medicine, Maastricht University, Universiteitsingel 40, 6229ER, Maastricht, the Netherlands.

<sup>4</sup>Department of Physics and Astronomy, Padova University, via Marzolo 8 35122 Padova, Italy

<sup>5</sup>Fundación Tecnalia Research and Innovation, Health Division, Parque Científico y Tecnológico de Gipuzkoa, Mikeletegi Pasealekua 2. E-20009 Donostia-San Sebastián, Spain

[scatto@nadir-tech.it](mailto:scatto@nadir-tech.it)

### INTRODUCTION

Additive manufacturing (AM) represents a valuable alternative to traditional processing methods in the manufacture of various products such as scaffold for regenerative medicine. AM techniques showed unique capabilities for fabricating complex structures, with precisely controlled physical characteristics, facile tunable biological functionality, mechanical properties and easily customizable architecture. In this work, we show the use of synthetic Layered Double Hydroxide (LDH), Zirconium phosphate (ZrP) intercalated with antibiotics, and reduced Graphene Oxide (rGO) in polymer composite produced with Melt Compounding Technology assisted by Twin Screw Extruder. The modification of polymeric compounds is a custom business activity and well suits biomedical application (devices, Long-Term Implantable Polymers, Bioresorbable Polymers). The biological activity of polymeric compounds was originated from antibiotic organic guest anions intercalated in interlayer region of LDH or ZrP filler. The intercalation of guest antibiotic anions into LDHs or ZrPs also permits to chemically stabilize them through electrostatic interactions, to physically protect them from external harsh conditions (i.e. temperature, oxygen, UV rays and humidity) and to controllably release them out of the inorganic lattice upon anion exchange reaction [1]. Also reduce Graphene Oxide is able to provide biological activity in terms of cell growth and cell differentiation [2].

### EXPERIMENTAL METHODS

During the production of Polymer Nanocomposite with Melt compounding technology, a Co-rotating Twin Screw Extruder (D=11mm; L/D=40mm) localized in Nadir Lab was used with the following raw materials: Bioresorbable copolymer, Poly(ethyleneoxide)/poly(butylene terephthalate) 300PEOT55PBT45 (PolyVation B.V.); Synthetic Layered Double Hydroxide (LDH) and Zirconium phosphate (ZrP) intercalated with antibiotics provided by Prolabin & Tefarms; Reduced Graphene Oxide (rGO) provided by Abalonyx. Temperature profile, screw rate, screw profile, feed rate have been optimized during polymer nanocomposite production. These nanocomposites have been characterized morphologically with XRD evaluation, mechanically (tensile test with ISO 527 and compressive test with ISO 604), and biologically in terms of their potential antibacterial bioactivity and cytocompatibility.

### RESULTS AND DISCUSSION

We have prepared melt compounded nanocomposite at different loadings of LDH intercalated with ciprofloxacin, ZrP intercalated with gentamicin and rGO. The rheology of the nanocomposites has been measured and their extrudability through a 400 µm and a 250 µm extrusion needles has been demonstrated. In particular, the biocidal activity has been carried out against *Staphylococcus epidermidis* and *Pseudomonas aeruginosa* both identified as bacteria responsible for septic scaffolding failure. Moreover, cytotoxicity of neat processed polymer was evaluated according to the standard ISO10993- part 5 biological evaluation of medical devices Human mesenchymal stromal cells (hMSCs) adhesion, proliferation and morphology was analyzed on 2D films with different concentrations of LDH, ZrP and rGO.

The nanocomposites didn't show any toxic response to hMSCs. Cell culture studies showed good cellular adhesion and proliferation, thus confirming the biocompatibility of the manufactured nanocomposites. Nanocomposites with Gentamicin were more active against *Staphylococcus epidermidis* than against *Pseudomonas aeruginosa*. Nanocomposites with Ciprofloxacin were more active against *Pseudomonas aeruginosa* than against *Staphylococcus epidermidis*. Nanocomposites with rGO concentrations of 10 and 15 wt% also showed biocidal activity against both bacterial strains.

### CONCLUSION

The polymeric nanocomposites developed in this work can be a useful feedstock for AM scaffolds fabrication for tissue regeneration applications. Melt compounded bioresorbable nanocomposites can improve scaffold performance by tuning and optimizing shape complexity, mechanical properties and cell growth.

### REFERENCES

- [1] M. Scatto, M. Sisani, AIP Conference Proceedings, 1779, 2016
- [2] Rodriguez Losada N. *et al.*, Conference Society for Neuroscience, Washington, November 2014

### ACKNOWLEDGMENTS

This research is co-funded by the H2020 Project – FAST "Functionally Graded Additive Manufacturing Scaffolds by Hybrid Manufacturing" (NMP07, GA n. 685825).



## Stimuli Responsive Homoarm and Miktoarm Stars – the Influence of Composition on Phase Transition and Morphology

Anna Mielańczyk<sup>1</sup>, Maria Kupczak<sup>1</sup>, Małgorzata Burek<sup>2</sup>, Łukasz Mielańczyk<sup>3</sup>, Olesya Klymenko<sup>3</sup>, Ilona Wandzik<sup>2</sup>, Dorota Neugebauer<sup>1</sup>

<sup>1</sup>Department of Physical Chemistry and Technology of Polymers, Faculty of Chemistry, Silesian University of Technology, Poland

<sup>2</sup>Department of Organic Chemistry, Bioorganic Chemistry and Biotechnology, Faculty of Chemistry, Silesian University of Technology, Poland

<sup>3</sup>Department of Histology and Embryology, School of Medicine with the Division of Dentistry in Zabrze, Medical University of Silesia, Poland

[anna.mielanczyk@polsl.pl](mailto:anna.mielanczyk@polsl.pl)

### INTRODUCTION

Poly(2-hydroxyethyl methacrylate) (PHEMA) and poly(*N,N'*-dimethylaminoethyl methacrylate) PDMAEMA are functional polymers frequently used for the production of smart materials in the industrial and medical fields<sup>1</sup>. Moreover, PDMAEMA due to the presence of aliphatic tertiary amine groups, exhibits pH- and thermoresponsiveness, which creates an opportunity for potential application as stimuli-responsive drug delivery systems. The presented research covers the results of physicochemical and morphological characterization of series of amphiphilic stimuli-responsive homoarm and miktoarm stars. The polymers were obtained by combination of atom transfer radical polymerization (polymethacrylic arms), coordination-insertion ring opening polymerization (polyester arm) and click reaction<sup>2</sup>.

### EXPERIMENTAL METHODS

**The physicochemical characterization.** <sup>1</sup>H NMR spectra of the synthesized polymers solutions in DMSO-d<sub>6</sub>, D<sub>2</sub>O were collected on Varian Inova 600 MHz spectrometer. Molecular weights (*M<sub>n</sub>*, *M<sub>w</sub>*) and dispersity (*Đ*) indices were determined by size exclusion chromatography (SEC, 1100 Agilent 1260 Infinity), PS standards, THF as a solvent. UV-vis spectroscopy (Thermo Scientific Evolution 300) was used to determine the cloud point temperatures (*T<sub>CP</sub>*). Optical absorbances of polymers in aqueous solutions (1 mg/mL) were measured at 500 nm at temperature ranging from 5 to 80°C with a heating rate of 2°C/min. The hydrodynamic diameters (*D<sub>h</sub>*) of particles in water and PBS solutions were measured by DLS at r.t. and *T<sub>CP</sub>*. Samples were placed in PMMA cell after dilution (1 mg/mL) with water/PBS and measured at 25°C or above *T<sub>CP</sub>* ± 0.1°C.

**The morphological characterization.** Transmission electron microscopy analysis of polymers was performed with use of FEI Tecnai G2 Spirit BioTWIN transmission electron microscope (TEM) at 120 kV. Topography analyzes were performed by the use of atomic force microscope (AFM) Bioscope Catalyst (Veeco/Digital Instruments) equipped with a NanoScope V controller. Experiments were performed with two types of silicon nitride cantilevers Scan Asyst-Fluid+ and MSNL - A (Bruker Nano Inc.) with typical tip diameter of 20 nm and 2 nm, respectively.

### RESULTS AND DISCUSSION

A series of the well-defined five-armed PDMAEMA, PHEMA and P(DMAEMA-*co*-HEMA) homoarm stars, as well as PDMAEMA<sub>5</sub>PCL and PDMAEMA<sub>5</sub>PLA miktostars were obtained and characterized. Considering the aqueous solutions of star-shaped (co)polymers, *T<sub>CP</sub>* values of their solutions in PBS increased with increasing DMAEMA content. The particle sizes of star-shaped copolymers measured in water were smaller (113-335 nm) than those measured for corresponding copolymers in PBS (493-970 nm) at *T<sub>CP</sub>*. Moreover, copolymers exhibited lower *D<sub>h</sub>* values than homopolymers of HEMA and DMAEMA. This effect was more pronounced in PBS solutions. AFM analysis showed that the star-shaped PHEMA, PDMAEMA and miktoarm PDMAEMA<sub>5</sub>PCL exhibited tendency to create mono- and multilayers with some interesting structures on the surface. Whereas, TEM analysis revealed that five-arm PDMAEMA creates cylindrical nanostructures above the determined *T<sub>CP</sub>* instead of globules.

### CONCLUSION

The composition of arms influenced on both, the *T<sub>CP</sub>* and *D<sub>h</sub>* values. The presence of salt in polymeric solutions affects their phase transition, increasing *T<sub>CP</sub>* values and sizes of aggregates/globules formed during the process. The AFM and TEM analyses allowed to investigate changes in polymers morphology related to their composition and thermoresponsive behavior. The ability of tailoring the shape of the self-assembled nanostructures, combined with their responsivity to stimuli, will be further investigated in order to yield polymeric materials dedicated to biomedical applications.

### REFERENCES

1. Menglian W. *et al.*, Polym. Chem. 8:127-143, 2017.
2. Mielańczyk A. *et al.*, submitted to Polym. Chem.

### ACKNOWLEDGMENTS

The authors gratefully acknowledge financial support from the National Science Center, Decision No DEC-2016/23/D/ST5/01312. TEM and AFM analyses were performed using equipment financed by the Silesian Biofarma program supported by POIG.02.03.01-24-099/13 grant.

## Hyaluronan-Based Nanogels as Trojan Horse: Chasing Intracellular Pathogens

Elita Montanari<sup>1</sup>, Chiara Di Meo<sup>1</sup>, Tommasina Coviello<sup>1</sup>, Patrizia Mancini<sup>2</sup>, Luciana Mosca<sup>3</sup>, Pietro Matricardi<sup>1</sup>

<sup>1</sup>Department of Drug Chemistry and Technologies, Sapienza University of Rome, Italy

<sup>2</sup>Department of Experimental Medicine, Sapienza University of Rome, Italy

<sup>3</sup>Department of Biochemical Sciences, Sapienza University of Rome, Italy

[elita.montanari@uniroma1.it](mailto:elita.montanari@uniroma1.it)

### INTRODUCTION

A number of pathogens (e.g. *S. aureus*) are able to invade and persist in a range of cell types (e.g. keratinocytes)<sup>1</sup>; this adaptation may offer protection from the immune response and be a factor in treatment failure due to the inability of the antibiotics to target intracellular microorganisms. The incorporation of antimicrobials into hyaluronan-cholesterol nanogels (NHs)<sup>2</sup> represents a novel paradigm in the delivery of therapeutics against intracellular pathogens. Indeed, a major receptor for hyaluronan (HA) is CD44 and it is highly expressed on the surface of a number of host cells (e.g. keratinocytes<sup>3</sup>, activated macrophages, fibroblasts) and it is heavily involved in HA endocytosis.

### EXPERIMENTAL METHODS

In order to generate NHs, HA carboxyl groups were functionalised with a small hydrophobic molecule, cholesterol. Sterile and antibiotics-loaded NHs were achieved using an autoclave (121°C, 20 min). Mean diameter, size distribution, PDI and  $\zeta$ -pot were studied with Zetasizer instrument. TEM and AFM micrographs of free NHs were performed in dry and liquid state. Loading efficiency (LE%) and drug release of antibiotics-loaded NHs were checked through spectrometry and spectroscopy analyses. Cell viability of human keratinocytes (HaCaT) and human dermal fibroblasts (HDF) was studied after incubation with free and loaded NHs. MIC of free and loaded NHs was evaluated, firstly, against planktonic *S. aureus* and *P. aeruginosa*, secondly, against the intracellular pathogens. Finally, the internalisation kinetics and the intracellular fate of NHs were studied with flow cytometry and fluorescent microscopy in HaCaT cells.

### RESULTS AND DISCUSSION

NHs can be achieved (Fig. 1) and loaded with a fast one-step sterile cycle using an autoclave.

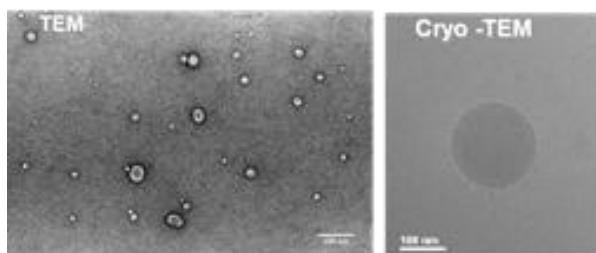


Fig.1. TEM and Cryo-TEM micrographs of NHs.

Loaded-NHs do not affect viability of HaCaT or HDF (conc. < 500  $\mu$ g/mL) over 48 h and display the same MIC values as free LVF against planktonic *S. Aureus* and *P. aeruginosa* (Fig. 2)<sup>4</sup>.

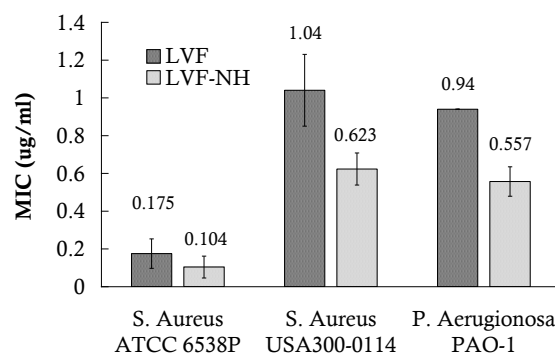


Fig. 2. MIC against planktonic bacteria.

However, intracellularly, the antibacterial activity of LVF was highly enhanced by NHs. As we demonstrated that NHs co-localise with lysosomes of cells (HaCaT) (Fig.3)<sup>5</sup> and it is known that free LVF predominantly accumulates in the cytosol, these results strongly suggest that NHs may be able to change the intracellular fate of LVF from cytosol to lysosomes, thereby targeting the intracellular pathogens.

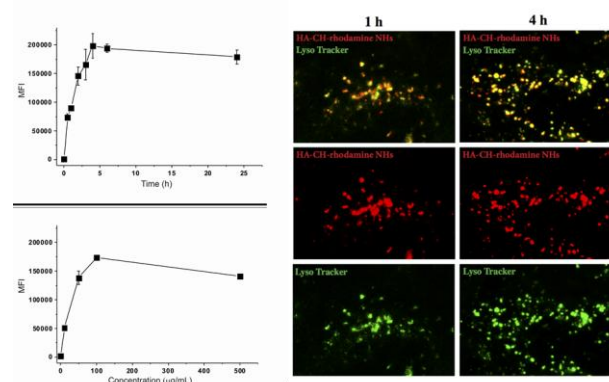


Fig. 3. NHs internalisation kinetics and co-localisation with lysosomes in HaCaT.

### CONCLUSION

This research demonstrates that I) lysosomal formulations may be more effective against *S. aureus* and *P. aeruginosa* once they are taken up by a cell II) the sub-cellular targeting may be essential for targeting such intracellular pathogens, opening new avenues for HA-based NHs treatments of persistent skin infections.

### REFERENCES

1. Kintarak S *et al.* Infect Immun.,72:5668-75, 2004
2. Montanari E *et al.* Macromol. Biosci.,13:185-94, 2013
3. Tammi R *et al.* J. Biol. Chem.,276:35111, 2001
4. Montanari E *et al.* Eur. J. Pharm. Biopharm.,87:518-523, 2014
5. Montanari E. *et al.*, Adv. Healthc. Mat.,submitted

## Anisotropic Thermoresponsive Nanofibers for Engineering Extracellular Matrix-rich Living Substitutes

Andrea De Pieri<sup>1,2,3</sup>, Alexander Gorelov<sup>4</sup>, Yuri Rochev<sup>3,5</sup>, Dimitrios I. Zeugolis<sup>2,3</sup>

<sup>1</sup>Proxy Biomedical Ltd., Coilleach, Spiddal, Galway, Ireland

<sup>2</sup>Regenerative, Modular & Developmental Engineering Laboratory (REMODEL)

National University of Ireland Galway (NUI Galway), Galway, Ireland

<sup>3</sup>Science Foundation Ireland (SFI) Centre for Research in Medical Devices (CÚRAM)

National University of Ireland Galway (NUI Galway), Galway, Ireland

<sup>4</sup>School of Chemistry, University College Dublin Dublin, Ireland

<sup>5</sup>School of Chemistry, National University of Ireland Galway (NUI Galway), Galway, Ireland

[andrea.depieri@proxybiomedical.com](mailto:andrea.depieri@proxybiomedical.com)

### INTRODUCTION

Tissue engineering by self-assembly is a technique that consists of growing cells on surfaces made of thermoresponsive polymers. This technique allows for the production of contiguous cell sheets by simply lowering the temperature below the polymer's low critical solution temperature. In this approach cell-cell junctions and deposited extracellular matrix (ECM) remain intact, which provides a better cell localisation at the site of injury [1]. However, these systems lack the possibility to introduce topographical cues, that are fundamental for the organisation of many types of tissues. Moreover, the fabrication of ECM-rich cell sheets would be highly desirable. This limitation could be overcome by inducing macromolecular crowding (MMC) conditions during the culture period [2]. Herein we venture to fabricate aligned electrospun thermoresponsive nanofibres to sustain the growth and detachment of ECM-rich cell sheets in the presence of a MMC microenvironment.

### EXPERIMENTAL METHODS

Poly-N-isopropylacrylamide (pNIPAm) and 85% N-isopropylacrylamide/15% N-tert-butylacrylamide (pNIPAm/NTBA) copolymer were used. To create aligned nanofibers, the polymers were electrospun and collected on a mandrel rotating at 2000 rpm. Fibres diameter and orientation were assessed through scanning electron microscopy (SEM). Human adipose derived stem cells (hADSCs) were treated with media containing macromolecular crowders to enhance matrix deposition. Cell metabolic activity, proliferation, viability and morphology were assessed and immunocytochemistry was conducted in order to estimate matrix deposition and composition. Cell detachment was performed by decreasing the temperature of culture to 10°C for 20 minutes.

### RESULTS AND DISCUSSION

The electrospinning process resulted in the production of pNIPAm and pNIPAm/NTBA fibres in a diameter range from 1 to 2 µm and an overall alignment of 80% (Fig. 1 A). However, the pNIPAm fibres were unstable in wet conditions; therefore they were not suitable for cell culture experiments. On the contrary, the pNIPAm/NTBA fibres maintained their state and morphology in wet conditions up to 14 days. Cell viability, proliferation and metabolic activity revealed that hADSCs were able to grow on the thermoresponsive pNIPAm/NTBA scaffold.

The cells were able to align on the fibres after 3 days (Fig. 1 B) and they were able to detach as an intact cell sheet in presence of MMC (Fig. 1 C). Moreover, it was demonstrated that MMC, by a volume extrusion effect, enhances Collagen type I deposition, which is one of the main components of the ECM (Fig. 2). Collectively the pNIPAm/NTBA thermoresponsive fibres were able to sustain growth and detachment of ECM-rich cell sheets.

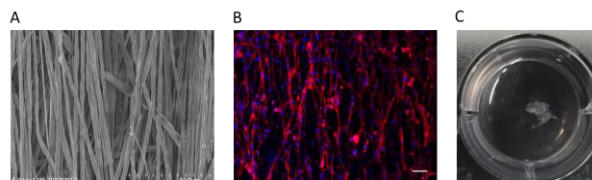


Fig. 1. SEM image of the pNIPAm/NTBA fibres (A). hADSC aligned on the fibres after 3 days in culture (B) and detached as an intact cell sheet in the presence of MMC after 7 days (C)

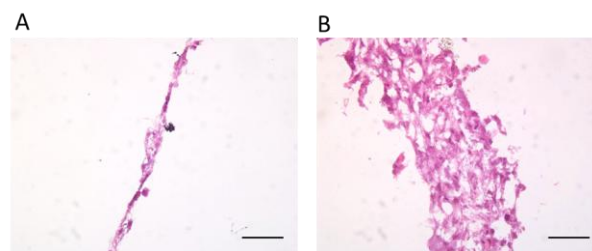


Fig. 2. H/E staining of hADSC cell sheets cultured without (A) and with (B) the presence of MMC.

### CONCLUSION

Herein, we fabricated thermoresponsive electrospun fibres for ECM-rich cell sheet tissue engineering. By recapitulating the hierarchical organised structure of native tissues like tendons, we aim to improve the development of supramolecular assembled tissue substitute based on the principle of *in vitro* organogenesis

### REFERENCES

1. Yang et al., Biomaterials. ;28: 5033-5043, 2007
2. Satyam. et al., Adv Mater. 26: 3024-3034, 2014

### ACKNOWLEDGMENTS

The authors would like to thank the Tendon Therapy Train-H2020-MSCA-ITN-2015-ETN (Grant no: 676338) and Science Foundation Ireland (SFI) Centre for Research in Medical Devices (CÚRAM) (Grant no: 13/RC/2073) for providing financial support to this project.



## UV, Vis- Reactive Natural Polymer Derivatives and Stabilization of Protein Drugs

Tae-il Son<sup>1\*</sup>; Shin-Woong Kim<sup>1</sup>; Jae-Won Kim<sup>1</sup>; Seung-Hyun Noh<sup>1</sup>; Yoshihiro Ito<sup>2,3</sup>

<sup>1</sup>Department of Systems Biotechnology, Chung-Ang University, Anseong-si, Gyeonggi-do 456-756, Republic of Korea

<sup>2</sup>Nano Medical Engineering Laboratory, RIKEN, 2-1 Hirosawa, Wako, Saitama 351-0198, Japan

<sup>3</sup>Department of Computational Intelligence and systems Science, Interdisciplinary Graduate School of Science and Engineering Tokyo Institute of Technology, 4259 nagatsuda-cho, Midori-ku, Yokohama, 226-9501, Japan

[tisohn@cau.ac.kr](mailto:tisohn@cau.ac.kr)

### INTRODUCTION

Medical materials are used to diagnose and treat diseases, and to replace damaged body parts or promote regeneration. Such materials should not elicit any side effects or an immune rejection response. Moreover, they should be able to sustain the function of materials without degradation for appropriate periods according to the therapeutic purpose. Natural polymers that have been extracted from plants or animals, or have been generated by biosynthesis, have low immune rejection responses and excellent biocompatibility, and can be applied to various medical fields. To immobilize drugs using natural polymer, photo-immobilization method has been designed. For photo-immobilization, photo-reactive functional group should be introduced to natural polymer. According to purpose of application, you could choose one of the photo-reactive functional group. Natural polymers include collagen, alginate, chitosan, and hyaluronic acid; such polymers have been used to improve cell affinity and tissue adhesion, and have been used in coating materials for implants and stents, as corneas, and in drug delivery systems.



Fig. 1. Immobilization of protein drugs

### EXPERIMENTAL METHODS

Various types of photo-reactive Natural Polymer derivatives have been prepared, e.g., UV-reactive chitosan derivatives. LM-O-CMC was prepared according to depolymerization method and carboxymethylated method. Az-P-LM-O-CMC was prepared with 4-phosphonobutyric acid and 11-azido-3,6,9-trioxaundecan-1-amine. To evaluate protein immobilization, Natural Polymer solution containing FITC-BSA was cast onto a titanium plate. The samples were covered with a photomask and UV irradiation was carried out. After washing, the samples were observed by fluorescence microscopy. To characterize titanium surfaces coated with each sample, water contact angle measurement was carried out. To test protein release, a Human BMP-2 ELISA Kit was used. The protein release test was carried out according to the concentration of Natural Polymer and the number of coated layers.

### RESULTS AND DISCUSSION

Az-P-LM-O-CMC was prepared by coupling 4-phosphonobutyric acid and 11-azido-3,6,9-trioxaundecan-1-amine. Phosphonate groups form

coordination bonds with titanium in the same way, and azido groups facilitate protein immobilization. Through micropatterning, Az-P-LM-O-CMC is suggested that the azido group have the ability to immobilize protein. Water contact angle was confirmed that on hydrophilic surfaces, cell adhesion and growth are improved. Photo-crosslinking via azido groups affects the hydrophilicity of the titanium surface. Protein release test was verified that the drug release rate could be controlled by adjusting the number of layers. Cytotoxicity was confirmed that Az-P-LM-O-CMC did not affect the viability of cells.

### CONCLUSION

The medical applications of photo-reactive natural polymers vary depending on whether they are reactive to UV or visible light. Differences in the photo-curing ratio, degradation time, etc., depend on the light source. Therefore, photo-reactive natural polymers can be selected and used depending on their intended purpose.

- UV-reactive natural polymers can be used to coat medical devices such as titanium implants, dressing foam, etc., to improve the devices. For example, Az-LMC, Az-Gel, and Az-HA have been used to coat titanium surfaces. They are UV-reactive and can be used for drug-immobilization. As a result, biocompatible and drug-releasing titanium devices can be prepared, which can be used in orthopedic or oral implants. Protein immobilization was identified with fluorescence microscopy using micropatterning. Protein release tests revealed that the rate of protein release could be controlled by adjusting the number of coated layers. Biocompatible UV-reactive natural polymers could be coated onto titanium and simultaneously used to immobilize BMP-2. The significant disadvantage of implants is the long period of time required for osseointegration, and UV-reactive natural polymers is expected to be a good coating material for implants.
- Visible-light-reactive natural polymers have even wider applicability than UV-reactive natural polymers. It has been reported that UV light can cause skin cancer and genetic mutations, and can weaken the immune system. Therefore, visible light is considered safer for use in the human body. Visible light-reactive natural polymers can usually be used to heal wounds or prevent adhesion. For example, F-LM-O-CMC, F-Alg and F-Gel can be used as wound-healing agents. Their photo-reactive property can be used to photo-immobilize drugs or growth factors. Photo-immobilized drugs or growth factors are released slowly during the healing period, thereby helping effective wound healing.

### REFERENCES

- [1] Kim EH. *Macromolecular Res.* 2016; 24:99-103.
- [2] Jeong JH. *JIEC.* 2016; 34:33-40.

## Synthesis of Naturally-derived Star-shaped Polymers through ATRP Methods with Diminished Catalyst Concentration

Izabela Zaborniak, Paweł Chmielarz

Department of Physical Chemistry, Rzeszow University of Technology, Poland  
[i.zaborniak@stud.prz.edu.pl](mailto:i.zaborniak@stud.prz.edu.pl)

### INTRODUCTION

Naturally-derived star-like polymers based on tannic acid and quercetin were received for the first time by the two-step synthesis. Initially, brominated biomolecules-based macroinitiators were synthesized by the transesterification reaction with 2-bromoisobutryl bromide. Subsequent, a naturally-occurring star-shaped polymers with a polar core and hydrophobic poly(*tert*-butyl acrylate) (*PtBA*) side arms were synthesized through low ppm atom transfer radical polymerization (ATRP) methods including electrochemically mediated atom transfer radical polymerization (*e*ATRP).

ATRP allows to prepare polymers characterized by narrow molecular weight distribution (MWD) and control over molecular weight (MW) [1].

Quercetin is considered as a strong antioxidant because of its ability to scavenge free radicals and bind transition metal ions [2]. Tannic acid, like quercetin, is an effective natural antioxidant [3] with a wide range of applications. Biopolymers based on quercetin and tannic acid are widely used in pharmaceutical industry [4,5] and as antifouling and antimicrobial polymer coatings [6,7].

### EXPERIMENTAL METHODS

**Materials:** Tannic acid (TA) was purchased from Alfa Aesar. Quercetin (QC, >95%), 2-bromoisobutryl bromide (BriBBR, 98%), *N*-methyl-2-pyrrolidone (NMP, >99%), dichloromethane (DCM, >99.9%), sodium hydrogencarbonate (NaHCO<sub>3</sub>, >99.7%), magnesium sulfate (MgSO<sub>4</sub>, >99.5%), tetrahydrofuran (THF, >99.9%), methanol (MeOH, >99.8%), tetrabutylammonium perchlorate (TBAP, >98%), copper(II) bromide (Cu<sup>II</sup>Br<sub>2</sub>, 99.9%) were purchased from Aldrich. *N,N*-Dimethylformamide (DMF, 99.9%) was purchased from Acros. Tris(2-pyridylmethyl)amine (TPMA) were prepared according to references [8].

**Analysis:** Products of synthesis were analysed by <sup>1</sup>H NMR and GPC. <sup>1</sup>H NMR spectra in CDCl<sub>3</sub> and DMSO were measured in a Bruker Avance 500 MHz spectrometer. Monomer conversion and theoretical number-average molecular weight ( $M_{n,th}$ ) were received from NMR analysis. MWs and MWDs were acquired by Viscotek T60A GPC.

### RESULTS AND DISCUSSION

Macroinitiators based on quercetin and tannic acid structure were synthesized by the transesterification reaction with 2-bromoisobutryl bromide (Fig. 1) [9]. The chemical structure of QC-Br and TA-Br was confirmed by <sup>1</sup>H NMR. In the both cases degree of substitution of the hydroxy groups was determined by the area ratio of the methyl protons derived from 2-bromoisobutryl bromide to aromatic protons. Naturally-derived polymers with a tannic acid and quercetin core and *PtBA* side chains through low ppm

ATRP methods were received (Fig. 1). The reaction was characterized by the first-order kinetic relationship.

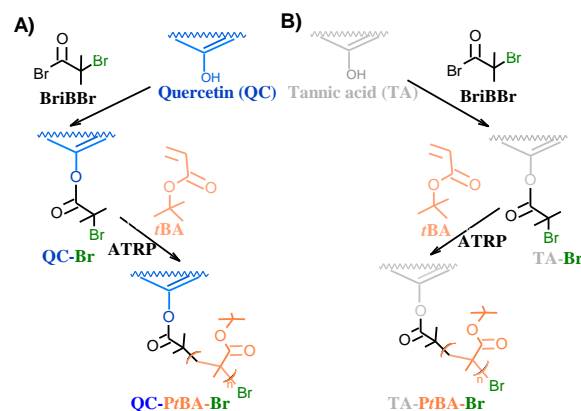


Fig. 1. Synthesis of QC-*PtBA*-Br (A) and TA-*PtBA*-Br (B)

The achieved polymers were characterized by narrow molecular weight distribution. The naturally-derived star-like polymers have been synthesized for the first time using ppm levels of Cu<sup>II</sup> complex. The chemical structure of the received QC-*PtBA*-Br and TA-*PtBA*-Br pseudo-star-shaped polymers was confirmed by <sup>1</sup>H NMR spectroscopy.

### CONCLUSION

Naturally-derived macromolecules were synthesized based on a new strategy including the synthesis of a quercetin- and tannic acid-based cores with 2-bromoisobutryl bromide as initiation molecules, and grafting of the *PtBA* arms of the biomolecules-based moiety by low ppm ATRP methods. The results of GPC, and <sup>1</sup>H NMR prove the successful preparation of the star-shaped polymers. These new polymer materials have potential applications as key elements of biologically active thin films in tissue engineering and as drug delivery systems.

### REFERENCES

- Chmielarz P. *et al.*, Prog. Polym. Sci. 69:47-78, 2017
- D'Andrea G. *et al.*, Fitoterapia 106:256-271, 2015
- Gulcin I. *et al.*, Arab. J. Chem. 3:43-53, 2010
- Kim B.-S. *et al.*, Chem. Commun. 28:4194-4196, 2009
- Liu F. *et al.*, Soft Matter 10: 9237-9247, 2014
- Pranantyo D. *et al.*, Biomacromolecules 16:723-732, 2015
- Bozic M. *et al.*, Carb Polym 89:854-864, 2012
- Park, S. *et al.*, Angew. Chem. Int. Ed. 54:2388-2392, 2015
- Chmielarz P. *et al.*, Beilstein J. Org. Chem. 13:2466-2472, 2017

### ACKNOWLEDGMENTS

Financial support from DS.CF.16.001, DS./M.CF.17.004 and DS./M.CF.xx.xxx is gratefully acknowledged.



## Fluorescence, Mechanical and Swelling Properties of Chitosan-genipin and Chitosan-genipin-PVP Hydrogels

Durda Vukajlovic, Oana Bretcanu, Julie Parker, Katarina Novakovic

School of Engineering, Newcastle University, United Kingdom

[D.Vukajlovic2@newcastle.ac.uk](mailto:D.Vukajlovic2@newcastle.ac.uk)

### INTRODUCTION

Chitosan (Cht) is an extensively studied biomaterial due to its biocompatibility and biodegradability. The addition of genipin (Gen) to chitosan hydrogels produces crosslinks which strengthen the hydrogel network and, as an added bonus, induces fluorescence. At the same time, genipin, a natural agent extracted from Gardenia fruit, has significantly lower toxicity compared to other currently used substances.<sup>1</sup> Polyvinylpyrrolidone (PVP) has been added to the hydrogels to further aid water absorption and enhance pore dispersion. The aim of this work is to determine the effect of genipin and PVP on the fluorescence, mechanical and swelling properties of chitosan-genipin and chitosan-genipin-PVP hydrogels, relevant to prospective medical applications.

### EXPERIMENTAL METHODS

Hydrogels were prepared by mixing known amounts of chitosan, genipin and PVP solutions of defined concentrations. Sample composition is labelled in respect to the molar ratio of the components. Fluorescence intensity measurements were performed in situ, to follow polymerization of the hydrogels over 24 h at 37°C. A UV-VIS spectrophotometer (BMG LabTech, FLUOstar Omega Microplate Reader), Vision Plate™ 24 Well microplate, and excitation and emission wavelengths of 550 nm and 650 nm, respectively, were used. Data was collected every hour for each sample.

Compression tests were carried out employing a Tinius Olsen machine using a 5 N load cell. Following synthesis, hydrogel samples were immersed in pH 7 for a week prior to the tests. Hydrogels along with the buffer were transferred to the petri dish and compressed. Compressive strength and compressive modulus were calculated.

Swelling tests were carried out following hydrogel synthesis (37°C, 24h). pH 2 buffer was used as a medium and the change in volume of the hydrogel was recorded optically every 15 min over 24 h employing a specially designed experimental set up.<sup>2</sup> The volume of each gel at specific times was calculated using ImageJ and compared to the initial volume of the sample.

### RESULTS AND DISCUSSION

General trends anticipated in hydrogels composed of crosslinked chitosan are captured. Mechanical properties improve with the increasing amount of genipin in the samples while an increase in swelling in acidic medium is proportional to a decrease in the amount of crosslinker present. An increase in the genipin:chitosan ratio leads to an increased compressive strength and compressive modulus. An acidic environment causes protonation and repulsion between the chitosan chains, and swelling of the chitosan hydrogels, however, the abundance of genipin leads to

the opposite effect and shrinking of the samples. Added PVP is demonstrated to enhance swelling by absorbing the aqueous medium.

On the other hand, fluorescence intensity measurements display more complex trends. While initially (0-10 h) an increase in crosslinking density correlates with an increase in fluorescence, fluorescence intensity values for fully polymerised gels (after 24 h) do not necessarily correspond to the actual number of crosslinks present in the samples due to a quenching effect. This is best observed in samples with high crosslinking density. (Interestingly, the presence of PVP decreases the observed quenching (Fig. 1)).

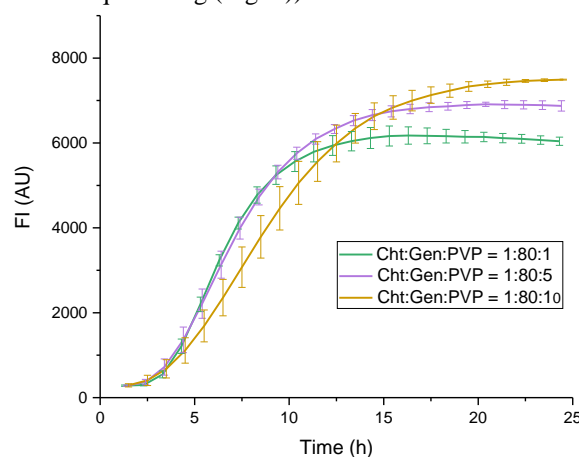


Fig. 1. Fluorescence intensity measurement for chitosan-genipin-PVP samples

### CONCLUSION

In this study chitosan hydrogels (with and without PVP), crosslinked with genipin are investigated. Mechanical properties, swelling in acidic medium as well as fluorescence of samples were recorded and analysed. The effect of fluorescence quenching is studied in detail. While an increase in genipin in chitosan hydrogels results in increasing mechanical strength this cannot be captured via fluorescence intensity measurements above a certain amount of crosslinker used due to fluorescence quenching caused by high crosslinking density. PVP is shown to contribute to the mechanical properties of the hydrogels and as a result alters fluorescence intensity.

### REFERENCES

- Muzzarelli R. A. A. *et al.*, *Mar Drugs*. 13:7314-38, 2015
- Marin *et al.*, *Chem. Eng. J.* 327:889-97, 2017

### ACKNOWLEDGMENTS

This work was supported by UK Engineering and Physical Sciences Research Council (EPSRC) grant number EP/N033655/1, NUORS Award and CEAMIPS funding.

## RGD-functionalized Hydrogels to Deliver Factors Secreted by Human Mesenchymal Stem Cells in Spinal Cord Injury

Emanuele Mauri<sup>1</sup>, Pietro Veglianese<sup>2</sup>, Monica Sani<sup>3</sup>, Alessandro Sacchetti<sup>1</sup>, Filippo Rossi<sup>1</sup>

<sup>1</sup>Department of Chemistry, Materials and Chemical Engineering "Giulio Natta", Politecnico di Milano, Milan, Italy

<sup>2</sup>Department of Neuroscience, IRCCS Mario Negri Institute for Pharmacological Research, Milan, Italy

<sup>3</sup>CNR Institute of Chemistry of Molecular Recognition, Milan, Italy

[emanuele.mauri@polimi.it](mailto:emanuele.mauri@polimi.it)

### INTRODUCTION

Many treatments have been proposed to counteract the neuropathological evolution of spinal cord injury. Among them, the use of human mesenchymal stem cells (hMSCs) appears as a promising approach<sup>1</sup>. However, the systemic hMSCs administration presents several limitations in therapeutic efficacy due to the reduced number of living and active cells in the target site. To overcome this critical aspect, we have proposed the design of a functionalized hydrogel as a 3D biomimetic tool to host and sustain hMSCs. Specifically, the uncleavable junctions of bioactive components, such as arginine-glycine-aspartic acid (RGD) tripeptide, and the extracellular matrix (ECM) deposition offer a better-quality niche where hMSCs can maintain a healthy state over time, proliferate and deliver paracrine factors.

This rationale and the use of a new hMSCs loading procedure on lyophilized hydrogels showed increased stem cells viability and density in *in vitro* studies, and *in vivo* experiments highlighted the diffusion of the stem cells from hydrogels towards the injury site able to immunomodulate the pro-inflammatory condition and promote pro-regenerative effects *in situ*.

### EXPERIMENTAL METHODS

#### Synthesis of RGD-functionalized hydrogel

RGD was functionalized with azide group and polyacrylic acid carboxyl groups were modified with alkyne moiety. Click reaction occurred between RGD and the polymer to create a stable and uncleavable linker. The resulting RGD-polymer reacted with carbomer, polyethylene glycol and agarose in a microwave-assisted reaction to give rise to the 3D hydrogel scaffold<sup>2</sup>. The latter was lyophilized and sterilized, resulting in a sponge-like hydrogel.

#### Cell loading and ECM deposition within hydrogel

hMSCs were suspended in growth medium and directly added to the sponge-like RGD-hydrogel.

The ECM deposition was performed letting grow hMSCs for 14 days, within the hydrogel; then the scaffold was lyophilized. Released ECM was quantified by Sirius Red staining protocol.

#### Cell density and viability

*In vitro* hMSCs density and survival were determined by analysing confocal images of living cells stained with calcein and the cell differentiation was assessed by Real Time PCR, performing the gene expression for osteogenic, chondrogenic and adipogenic lineage. *In vivo* experiments were performed in adult mice, positioning hMSCs loaded hydrogel in the injured area and tracking the viable cells stained with 5-6-carboxyfluorescein diacetate N-succinimidyl ester using a stereomicroscope. FACS and mRNA analyses were performed to evaluate the hMSC paracrine effect.

### RESULTS AND DISCUSSION

The use of a hydrogel with RGD and a pre-constituted ECM deposited by hMSCs (Fig. 1A, red line) appeared as an effective strategy to increase cell adhesion, viability and density for at least 21 days after the seeding, than the use of an unmodified 3D scaffold (Fig. 1A, black line). The almost totally of hMSCs showed a healthy spindle shape morphology (Fig. 1B) 1 day after encapsulation with a significantly higher long-lasting cell density compared to unmodified hydrogel (Fig. 1C).

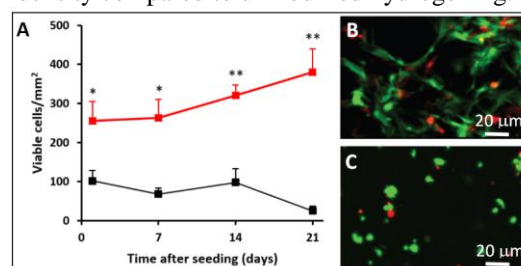


Fig. 1. hMSCs viability and morphology *in vitro*. A: cell viability profiles; B: hMSCs in RGD-hydrogel+ECM; C: hMSCs in unmodified hydrogel.

Moreover, the synthesized material preserved hMSC stemness, confirming that a potential pleiotropic effect is maintained for a multi-therapeutic approach. *In vivo* studies demonstrated the efficient hydrogel implantation (Fig. 2) and the release of cellular factors in the injured site, which were able to increase and/or convert M2 macrophages, promoting a proregenerative environment that represents a relevant outcome in SCI<sup>3</sup>.

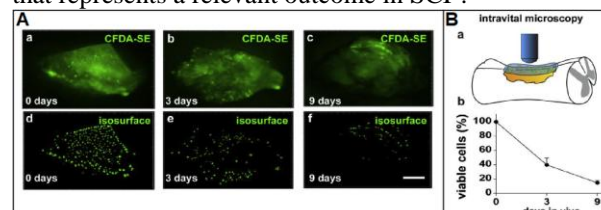


Fig. 2. hMSCs viability in functionalized hydrogel *in vivo*. A: intravital acquisition up to 9 days; B: hMSCs viability trend.

### CONCLUSION

The proposed functionalized hydrogels ensure improved hMSCs adhesion and viability, thanks to the combination of RGD motif and ECM deposition. Their *in vivo* application promotes oriented delivery of paracrine factors for treating the spinal cord injured site.

### REFERENCES

- Silva N. A. *et al.*, Progr. Neurobiol. 114:25-57, 2014
- Sacchetti A. *et al.* Tetrahedron Lett. 55:6817-6820, 2014
- Caron I. *et al.*, Biomaterials 75:135-147, 2016

### ACKNOWLEDGMENTS

Author's research is supported by Ministry of Health.

## Polymer Assisted Housing of Actives for Designed Release

Munmaya K. Mishra

Altria Client Services LLC, Research, Development & Regulatory Affairs

601 E. Jackson Street, Richmond, VA 23219, USA;

[munmaya.mishra@altria.com](mailto:munmaya.mishra@altria.com)

### INTRODUCTION

Controlled release is a term referring to the presentation or delivery of active ingredients in response to time or stimuli (such as pH, enzymes, light, magnetic fields, temperature, ultrasonic, osmosis, electronic control, etc.) at a desired site. The control (or more appropriately designed or defined) release of actives can be achieved via encapsulation-immobilization<sup>1</sup> of the same. This talk will focus on our work in the area of encapsulation - immobilization of a flavor ingredient by a variety of techniques including controlled polymerization<sup>2</sup>, coacervation<sup>3</sup>, cocrystallization-complexation<sup>4</sup>, capsules<sup>5</sup>, emulsification<sup>6</sup>, inclusion complexation<sup>7</sup>, porous materials<sup>8</sup>, supercritical CO<sub>2</sub> assisted impregnation<sup>9</sup>, etc. for controlled release applications. As an example the atom transfer radical polymerization of menthyl acrylate<sup>2</sup> was performed in a controlled / living manner. The pyrolysis of poly-(menthyl acrylate) released flavor compounds and provided an alternative route to synthesize poly (acrylic acid) with controlled structures. In another approach we had prepared porous structures<sup>8</sup> using hot melt reactive extrusion blending of chitosan (up to ~40%) and poly (acrylic acid) PAA without any process additives. The carboxylic groups of PAA interacted with the amine groups of chitosan during the melt process, and the system exhibited good melt flow. The infrared spectroscopic data confirmed the existence of a complex formation and possible hydrogen bonding between chitosan and PAA during the melt process. Scanning electron microscopy micrographs indicated that chitosan was well-dispersed in the PAA blends. Similarly we had prepared porous fibers using a novel polymer blend comprising a hydrophobic poly(vinyl acetate) (PVAC) and a hydrophilic poly(acrylic acid) (PAA) in a single step by melt spinning process. The fibers melt-spun from the polymer blends of 40 - 60% PVAC with PAA making the remainder of 100% consisted of a honeycombed, porous fiber structure with some internal cell to cell interconnectivity. These porous structures are capable of housing active ingredients for later use. As a different technique we had used near-critical and supercritical CO<sub>2</sub> to facilitate the impregnation of flavors such as, vanillin and l-menthol, into cellulose acetate<sup>9</sup> (up to ~10 wt% vanillin or l-menthol impregnated into CA fiber as verified by gravimetric, TGA, and TGA/MS analyses). SEM analysis of the CA fiber showed that the fiber did not undergo structural changes for this impregnation process. These studies will be further elaborated during this talk.

### REFERENCES

1. M. Mishra (Ed); *Handbook of Encapsulation Controlled Release*; 2015, CRC Press, Boca Raton, USA
2. S. Liu, M. Mishra, P. Lipowicz, B. Duan: 2015, *US Patent* 9185925; M. Mishra, K. Paine, J. Paine III, S. Liu: 2015, *US Patent* 9089162; S. Liu and M. Mishra; *Macromolecules*, 40, 867 (2007)
3. T. Sengupta, M. Mishra, W. Sweeney, D. Fernandez: 2013, *US Patent* 8356606; T. Sengupta, D. Fernandez, M. Mishra, W. Sweeney, S-S. Yang: 2015, *US Patent* 9167847
4. B. Duan, M. Mishra, P. Lipowicz, S. Liu: 2013, *US Patent* 8361236; M. Mishra, S. Liu, D. Kellogg: 2013, *US Patent* 8541401
5. M. Mishra, J. Fournier, K. Paine: *US Patent Application* 20060144412
6. T. Sengupta, M. Mishra, D. Fernandez, W. Sweeney, T. Howell: *US Patent Application* 20120045553
7. M. Mishra, S. Wrenn, J. Fournier: 2014, *US Patent* 8864909
8. M. Mishra, H. Yu, J. Molnar, V. Baliga: *Des. Monom. and Polym.*; 12, 273 (2009); S. Jeung and M. Mishra; *Int'l. J. of Polym. Mater.*; 60, 102 (2011)
9. M. McHugh, G. Karles, D. Gee, J. Banyasz, Z. Shen, M. Mishra: 2012, *US Patent* 8201564; Z. Shen, G. Huvard, S. Warriner, M. McHugh, J. Banyasz, M. Mishra: *Polymer*, 49, 1579 (2008)

## Unravelling Mechanical Properties of Biopolymer Films by means of Force Spectroscopy

Jagoba Iturri, Maria Sumarokova, Andreas Weber, José Luis Toca-Herrera

Institute for Biophysics, Dept. of NanoBiotechnology, BOKU University of Natural Resources and Life Sciences, Vienna, Austria

[jagoba.iturri@boku.ac.at](mailto:jagoba.iturri@boku.ac.at)

### INTRODUCTION

The use of diverse biopolymers as active coatings/films opens a broad range of possibilities for the development of new promising interfaces. These, might be employed in a number of applications with both biomedical and biotechnological purposes.

This is the case of well-known Fibronectin, which contains the RGD (Ala-Gly-Asp) aminoacid sequence, extensively employed for the specific recognition of extracellular integrins in cell attachment processes<sup>1</sup>. Another example, with a certainly more limited usage so far, would be that of Mucin. Mucin is a main component of body mucous barriers, in charge of the first barrier faced by drugs or drug delivery systems prior to absorption. Such trapping of foreign substances takes place mainly via steric and adhesive forces<sup>2</sup>. The presence of these type of interactions highlights how, besides the chemical features in both cases, studying the role played by their respective mechanical properties at the nanoscale might turn of great interest. Thus, mechanics-related factors can shed light on understanding their final activity and performance.

### EXPERIMENTAL METHODS

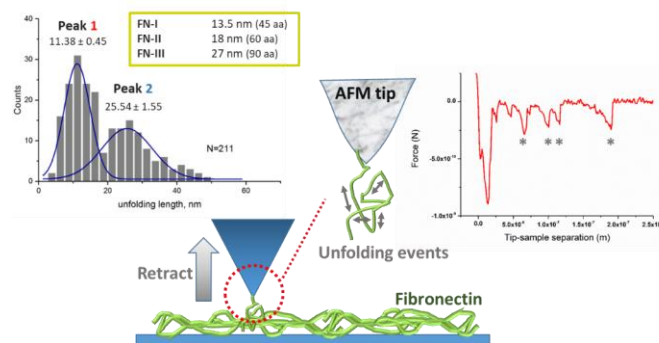
In this work, we have used Atomic Force Microscopy (AFM, Nanowizard III, JPK) in Force Spectroscopy mode to study, via nanoindentation, the specific/nonspecific adhesion and the unfolding properties of commercial porcine mucin and fibronectin coatings, under different experimental conditions. Measurements were performed by varying factors such as the loading rate and the residence time (also called Dwell time) of the AFM-tip on the biopolymer layer, or even environmental conditions as the pH of the bulk. These studies were complemented by means of Quartz Crystal Microbalance with Dissipation (QCM-D) (quantification of the mass bound) and both Optical and Fluorescence Microscopy, for the monitoring of cell culture studies.

### RESULTS AND DISCUSSION

In general terms, adhesion between silicon nitride tips and biopolymer films increased with the loading rate, delivering similar values for residence times of 1 and 2 seconds. Moreover, the adhesion force did not vary with the loading rate for contact time of 0 s.

In the particular case of Fibronectin, the unfolding of its domains also depended of the Dwell time (no unfolding events were observed for zero residence time). Applied loads of 2 nN were able to stretch the fibronectin layer up to 200 nm and to unfold the three fibronectin domains, which were similar for a Dwell time of 1 and 2 s. However, the unfolding length increased with loading rate: below  $2.5 \mu\text{m s}^{-1}$  the obtained lengths matched the value of *FN I* (13.5 nm), while for higher

speeds the measured values corresponded to the lengths of *FN II* (18 nm) and *FN III* (27 nm). Extensively, the use of living cells instead of pyramidal indenters as measuring probes allowed for the quantification of the formed cell-fibronectin interaction.



In turn, Mucin films showed a clear interplay between the chemistry of the indenting probe and the adhesion obtained. As proven, controlled treatment of the protein layer with different pH values (7.4 and 2) can revert the wetting conditions of the biopolymer and induce changes in its properties. Additional tests by dipping experiments and cell seeding confirmed these results.

### CONCLUSION

This work points out the utilization of the atomic force microscope technique beyond its usual employment in order to investigate another type of basic questions related to materials physics, chemistry, and biology. Here, evaluation of the mechanical properties of the above mentioned biopolymers, employed as scaffold-forming materials, offered a more complete physicochemical characterization of the systems under study and a scaling of their properties at the nanoscale into their final performance at higher scale ranges.

### REFERENCES

1. Iturri J. *et al.*, Sci. Rep. 5:9533, 2015
2. Oh, S. *et al.*, Eur. J. Pharm. Biopharm. 96:477-483, 2015

### ACKNOWLEDGMENTS

Authors thanks the Erasmus Iamonet Program for financial support, as well as the Austrian Science Fund (FWF) project number P29562-N28. Authors also thank Jacqueline Friedmann, Amsatou Andorfer-Sarr, Alberto Moreno-Cencerrado (BOKU) and Maria Maeres (TU Berlin) for technical support.



## How a Minute Addition of a Vitamin Can Enhance Polyethylene for Young and Active Patients

Daniel Delfosse<sup>1</sup>, Reto Lerf<sup>1</sup>, Peter Munger<sup>2</sup>

<sup>1</sup>Innovation & Technology, Mathys Ltd Bettlach, Switzerland

<sup>2</sup>Clinical Affairs, Mathys Ltd Bettlach, Switzerland

[reto.lerf@mathysmedical.com](mailto:reto.lerf@mathysmedical.com)

### INTRODUCTION

The 2<sup>nd</sup> generation of a vitamin E enhanced highly cross-linked polyethylene (VEPE) was introduced with the promise that a minute addition of vitamin E will maintain the high wear resistance of the 1<sup>st</sup> generation highly cross-linked polyethylene (HXLPE) but provide vastly improved stability against oxidation.

The first VEPE was introduced for hip arthroplasty in 2007 as E1-poly (Biomet Inc., Warsaw, IN) using an infusion process to add the vitamin E. In 2009, vitamys (Mathys Ltd Bettlach, Switzerland) was the second VEPE in clinical application – and the first using a blending technique to add 0.1 wt.-% vitamin E. In the meantime, many orthopaedic companies have followed the example of Mathys, introducing their own brands of a blended VEPE. Still today, VEPE is regarded as a novel material with good pre-clinical data, short-term clinical follow-up and unknown potential side effects. It is therefore of utmost importance to follow the clinical results with these early patients very closely.

### EXPERIMENTAL METHODS

#### Pre-clinical investigation:

Mechanical properties were measured using tensile, Charpy impact and small punch testing. Wear resistance was determined using a hip simulator. All tests were performed with vitamys (cross-linked at different doses) and compared to standard polyethylene. To determine the long-term stability, all tests were repeated with material that was subjected to accelerated aging.

#### Clinical evidence:

With the first clinical introduction of vitamys in the RM Pressfit hip cup (Fig. 1), several clinical studies were started, either initiated by the company or by independent medical investigators. In addition, the registry data was analysed using the latest published reports or separate ad hoc reports from the Registry.



Fig. 1. The RM Pressfit vitamys cup

### RESULTS AND DISCUSSION

#### Pre-clinical investigation:

While the mechanical and tribological properties of standard polyethylene deteriorated quickly during aging, the properties of vitamys were not influenced by artificial aging even for times equivalent to 40 years in vivo.

#### Clinical evidence:

Clinical follow-up data for the RM Pressfit vitamys cup is already available in a number of publications<sup>1-5</sup>. The vitamys VEPE material has shown excellent short to mid-term clinical follow-up. The revision rates of the RM Pressfit vitamys hip cup are low, even lower than the average hip cup from the national registry data. There is a clear difference in wear rate between vitamys VEPE and standard polyethylene. The head penetration in the vitamys material is significantly slower (after the initial creep phase) than in the UHMWPE (Fig. 2). The wear rate of this VEPE material in vivo is around 0.02 mm/year<sup>5</sup>. This compares favourably to a review article<sup>6</sup> that determined the linear in vivo head penetration for conventional polyethylene and 1<sup>st</sup> generation HXLPE as 0.137 and 0.042 mm/year.

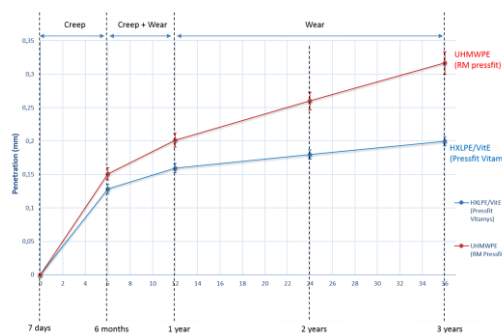


Fig. 2. In vivo head penetration for vitamys and UHMWPE<sup>5</sup>

### CONCLUSIONS

1. VEPE has a short-term advantage for THA compared to standard polyethylene: Because of the lower wear rate, larger articulation diameters are allowed, thus reducing the dislocation risk for the patient.
2. VEPE also has a long-term advantage compared to standard polyethylene: Due to the stabilization with vitamin E, the properties of VEPE do not deteriorate in the oxidative environment within a patient.
3. No potential side effects have been discovered at 7y of clinical follow-up.
4. A minute addition to a well-known bio-polymer may open a new field of applications. For hip arthroplasty, especially young and active patients will profit from it.

### REFERENCES

1. Beck M. *et al.*, in K. Knahr (Ed.): Total Hip Arthroplasty, 21-31, 2012
2. Halma J.J. *et al.*, J Arthroplasty 30:615-21, 2015
3. Scemama C. *et al.*, Int. Orthop. 2016
4. Wyatt M. *et al.*, Hip Int. 27:368-72, 2017
5. Rochcongar G. *et al.*, JBJS Am. 100:107-14, 2018
6. Kurtz S. *et al.*, Clin Orthop Relat Res 469:2262-77, 2011



## New Thermoplastic Polyurethane Elastomers for Biomedical Applications: Synthesis and Characterization

Andrzej Puszka<sup>1</sup>, Magdalena Rogulska<sup>1</sup>, Pavel N. Yakushev<sup>2</sup>, Vladimir Bershtein<sup>2</sup>

<sup>1</sup>Maria Curie-Skłodowska University, Faculty of Chemistry, Department of Polymer Chemistry, Gliniana 33, 20-614 Lublin, Poland

<sup>2</sup>Ioffe Institute, 26 Politekhnicheskaya str., 194021 St.-Petersburg, Russia  
[andrzej.puszka@umcs.pl](mailto:andrzej.puszka@umcs.pl)

### INTRODUCTION

Polyurethanes are a versatile class of polymers with substantial strength, toughness and elasticity and they can be widely used in a variety of applications in such areas as protecting coatings, elastomers, adhesives, foams, membranes, medical implants, biomaterials, etc. Thermoplastic polyurethane elastomers (TPUs) are copolymers usually composed of alternating soft segments derived from aliphatic polyether, polyester or polycarbonate diols and hard segments formed from aromatic diisocyanates (usually 1,1'-methanediylbis(4-isocyanatobenzene) (MDI)) or aliphatic diisocyanates (mostly 1,1'-methanediylbis(4-isocyanatocyclohexane) and short-chain diols (predominantly butane-1,4-diol (BD)). TPUs with polyether soft segments and aliphatic diisocyanates are characterized by better low-temperature properties and hydrolytic resistance than TPUs with polyester soft segments, but they are liable to oxidation. Improved oxidative resistance and hydrolytic stability are shown by TPUs with polycarbonate soft segments. Because of their combination of excellent biostability and biocompatibility and their high tensile strength and modulus, they are preferred as biopolymers for long-term implantation. Moreover, biomedical TPUs have been used as catheters, heart valves, heart assist devices, infusion pumps, blood-contacting materials, wound dressings. The purpose of this paper was to synthesize and characterize new TPUs based on two diisocyanates, i.e. aromatic MDI and aliphatic 1,6-diisocyanatohexane (HDI), newly obtained unconventional aliphatic-aromatic chain extender 2,2'-methylenebis[(4,1-phenylene)methylene-sulfanediyl]diethanol (diol E) and poly( $\epsilon$ -caprolactone) diol (PCL) of  $\overline{M}_n = 2000\text{g/mol}$  as the soft segment.

### EXPERIMENTAL METHODS

Reduced viscosities ( $\eta_{\text{red}}$ , dL/g) of 0.5 % polymer solution in 1,1,2,2-tetrachloroethane with a weight ratio of 1:3 were measured in an Ubbelohde viscometer at 25°C. Fourier transform infrared (FTIR) spectra were obtained with a Perkin-Elmer 1725 X FTIR spectrophotometer using thin films. Thermogravimetric analysis (TGA) was performed on a MOM 3427 derivatograph (Paulik, Paulik and Erdey, Hungary) at a heating rate of 10°C/min in air, in the range of 20-1000°C. Differential scanning calorimetry (DSC) thermograms were obtained using a NETZSCH 204 calorimeter in the range of -100-200°C. The reported transitions were taken from first or second heating scans at a heating/cooling rate of 10°C/min. Glass transition temperatures ( $T_g$ 's) for the polymer samples were taken as an inflection point on curves of heat-capacity changes. Melting temperatures ( $T_m$ 's) were read at

endothermic-peak maxima. Dynamic mechanical analysis (DMA) of both series of these TPUs has been performed in the tensile mode using a Dynamic Mechanical Spectrometer DMS 6100 and a Workstation Exstar 6000 (Seiko Instruments, Japan). The experiments were carried out at frequencies of 0.1, 1 and 10 Hz, at heating rate  $dT/dt = 3\text{ K/min}$ , over the temperature range from -120<sup>0</sup> to 120<sup>0</sup>C. Mechanical loss modulus  $E''$ , dynamic (storage) modulus  $E'$ , and mechanical loss factor  $\tan\delta = E''/E'$  as functions of temperature were measured. Polyurethane hardness was measured by the Shore A/D method on a Zwick 7206/H04 hardness tester at 23°C; values were taken after 15 s. Tensile testing was performed on a Zwick/Roell Z010 tensile-testing machine according to Polish Standard PN-81/C-89034 at the speed of 100 mm/min at 23°C; the tensile test pieces 1 mm thick and 6 mm wide (for the section measured) were cut from the pressed sheet. Press moulding was done with a Carver hydraulic press (USA) at 80–130°C under 10–30 MPa pressure.

### RESULTS AND DISCUSSION

The resulting TPUs were colorless high-molar-mass materials. Their structures were confirmed by FTIR analysis. The DSC analysis showed that all TPUs have partially crystalline structure, but a greater tendency for crystallization was revealed by TPU based on HDI. These polymers showed tensile strength in the range of 12.3-32.4 MPa and elongation at break in the range of 300-750%. In both series, increased hard-segment content resulted in increased  $T_g$ , hardness, modulus of elasticity and tensile strength, whereas elongation at break decreased. The polymers based on diol E compared with those based on diol H showed much higher hardness, tensile strength, modulus of elasticity but smaller elongation at break. All the synthesized TPUs exhibited a relatively good thermal stability, their  $T_1$  were in the range of 255-315°C. The increase of hard-segment content in the polymers caused some reduction in  $T_1$ ,  $T_5$  and  $T_{10}$ .

### CONCLUSION

The resulting TPUs were colorless, transparent, high-molar-mass materials. Their properties depended largely on type of diisocyanate used for synthesis.

### ACKNOWLEDGMENTS

The research has received partial funding from the People Programme (Marie Curie Actions) of the Seventh EU Framework Programme FP7 under REA grant agreement PIRSES-GA-2013-612484 – NanoBioMat (Nanostructured Biocompatible/Bioactive Materials).

## Selection of the Sterilization Method for an Implantable Device for Therapeutics Delivery

Radosław A. Wach, Alicja K. Olejnik, Agnieszka Adamus-Włodarczyk

Faculty of Chemistry, Institute of Applied Radiation Chemistry, Lodz University of Technology, Poland

[wach@mitr.p.lodz.pl](mailto:wach@mitr.p.lodz.pl)

### INTRODUCTION

Surgical implants intended to deliver therapeutics should fulfil essential requirements, such as mechanical and chemical stability in physiological environment during treatment of a disease or during their lifespan, and then explanted or gradually degraded. In order to guarantee proper functioning of such system, especially in the case of complex configuration or multifunctional tasks, e.g. active medical devices, besides selection of biomaterials and involved manufacturing processes, the designer should also consider potential sterilization method. Academia scientist involved in early stage development of a system delivering therapeutics often ignore possible detrimental effect of sterilization on material properties or functioning of the device, though the sterilization is critically needed when it comes to commercialization of the new device.

Validation of selected sterilization technique in terms of its effectiveness, reliability and reproducibility is the prerequisite the manufacturer is requested to demonstrate to the notifying authorities in order to prove microbiological safety of the new device.<sup>1</sup>

The manufacturer intended to distribute medical products within EU should follow regulations specified in directives of 90/385/EEC, 93/42/EEC, 98/79/EC with regards to sterilization, and further, the guidance of ISO standards. Reduction of the bioburden on and in the device to Sterility Assurance Level to  $10^{-6}$  is required.

### EXPERIMENTAL METHODS

The theoretical approach to selection of potentially applicable sterilization methods was based on the knowledge of properties of the polymeric materials composed the device of bio-electronic implant intended for delivering therapeutics from genetically engineered cells stimulated by light, the complexity of its design and presence of sensitive components or subsystems.<sup>2</sup> The device should be provided sterile for cells loading.

### RESULTS AND DISCUSSION

Approach to selection of a sterilization technique should begin on screening materials, components or systems included in the implant device. If all of these can withstand high temperature, a dry hot air (160-200°C) or moisturised air (steam, 121 or 134°C) methods may be the first choice. The methods are very reliable and easy to control. The complex shapes and inner elements are also heated, thus the device is entirely sterilized. The method is in principle restricted for thermoplastics, an unsuitable for biodegradable polymers. However, high degree of crystallinity of polymeric materials with high melting temperature may reduce potential negative effects of thermal treatment. Encompassed electronics exclude thermal methods, as well as presence of optically functional polymers – opacity may occur.

As only low-temperature methods are acceptable, radiation may be considered – its reliable and relatively inexpensive. Either electron beam or gamma rays are highly penetrable and provide sterility of the entire implant, not only its surface, which is especially appropriate for complicated shapes or highly porous materials. Many polymers may be sterilized by radiation, even some biodegradable ones. Nevertheless, the delivered energy may cause polymer degradation, which (if not compensated by crosslinking) reduces applicability of this method. Besides, radiation induces deterioration of electronics (thermal annealing may restore its operation).

Plasma - hydrogen peroxide may be considered, and applied as effective surface sterilization method. One should take under consideration rise of the temperature (40-60°C) and pressure changes during the process, and altered surfaces not resistant to highly oxidative environment, that may influence optical properties. In general, it can be applied to electronic systems.

The other option is ethylene oxide sterilization, commonly utilized of polymers and combined materials. The method can be applied for optics and electronics. Beside temperature rise (30-65°C) and rapid pressure changes, dissolution of the gas (highly toxic) in the polymer and possible chemical reactions with it should be considered.

If the multicomponent implantable system cannot be sterilized by a single method due to incompatibility of various material and components, the common practice is to separately apply different sterilization processes for each material and assembly the device under aseptic environment (aseptic processing).

### CONCLUSION

The course of selection of potentially applicable sterilization methods for developed implantable bio-electronic device for therapeutics delivery was presented. Validation of these methods will be done experimentally, according to specific ISO guidance, evaluating possible alternation of physical and chemical properties of the implant, and followed by biocompatibility and functional assessment.

### REFERENCES

1. Wach R.A. *et al.*, *Wojskowa Farmacja i Medycyna* 2: 185-190, 2009
2. Michel F. and Folcher M., *Porto Biomed. J.* 2: 145-149, 2017

### ACKNOWLEDGMENTS

This work has received funding from the European Union's H2020 research and innovation programme under grant agreement No 720694, 'Optogenerapy'. Cooperation with Prof. M. Folcher and his team of ETH Zurich Switzerland is acknowledged.

## A Green and Simple Process to Develop Conductive Polyurethane Foams for Biomedical Applications

Valentina Caba<sup>1,2</sup>, Laura Borgese<sup>1</sup>, Silvia Agnelli<sup>1</sup>, Laura E. Depero<sup>1</sup>

<sup>1</sup>Department of Mechanical and Industrial Engineering, University of Brescia, Italy

<sup>2</sup>Ferrari srl, Italy

[v.caba@unibs.it](mailto:v.caba@unibs.it)

### INTRODUCTION

In the last years, electrically conductive polymers have shown great potential for biomedical applications. Elastomeric polymer composites may be used as biosensor electrodes<sup>1</sup>. In particular, elastomeric polyurethane (PU) has high potential due to its versatility and biocompatibility. It can be realized in compact or porous layers, called films and foams respectively, depending on the process. The purpose of this study is to develop electrically conductive elastomeric PU foam suitable as electrode for biomedical applications. Compared to conductive films, breathable foam has the advantage that could be used also for long time application electrodes. Conductive PU foam is obtained *via* a water-based green process.

### EXPERIMENTAL METHODS

Elastomeric PU is obtained by mixing water PU dispersions with cross-linkers, followed by drying process by evaporation. Foams are obtained by mechanical frothing from the same mixture used for films. Paper transfer casting process is used to realize both films and foams for testing.

Dispersions containing polyether, polyester, and polycarbonate and a mixture of them are considered. The effects of the addition with micrometric size metal-based particles, at various contents, are investigated and compared to those obtained with carbon based nano-fillers. Surface resistivity is measured on the paper side of the layers according to the two-point probes method, with a potentiostat. Mechanical and breathability tests are performed. Aging test in simulated sweat is tested.

### RESULTS AND DISCUSSION

The role of the different reagents used and of the process steps is tested measuring surface resistivity of films. The target for application in electrostimulation devices is to obtain a surface resistivity lower than 300  $\Omega$ . For this purpose, several types of micrometric-size metal particles are used. A comparison is made among composites with 50wt% particles, i.e. above the percolation threshold. It is found that filler type affects the conductivity of the material, regardless of all the other reagents used, and that the highest conductivity is obtained with silver coated glass particles (SP). Nanofillers are also considered in order to reduce the amount of conductive filler. However, experimental tests are still being carried out to improve the dispersion of the particles. The effect of filler loading in foams is tested in comparison with films. Percolation threshold of electrical conductivity of SP filled films is about 45%<sup>2</sup>, and in the range from 50 to 65% for SP filled foams (Fig. 1). As expected, considering the porosity of the foam, it is less conductive than the corresponding film, even if the filler is well dispersed over the whole material (Fig. 2).

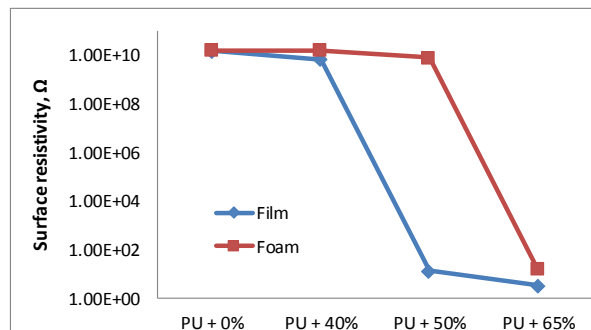


Fig. 1. Surface resistivity of PU films and foams with different loading of silver coated glass particles.

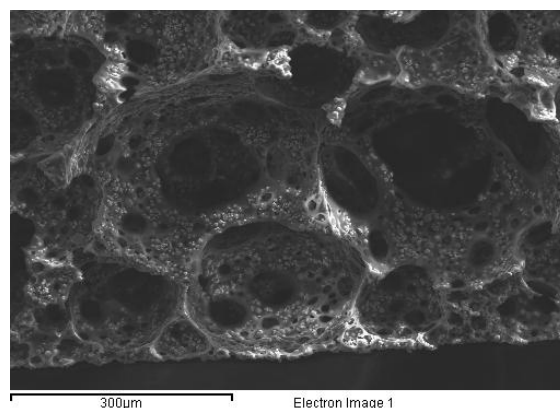


Fig. 2. Scanning electron microscopy image of cut section of foam sample with 65wt% silver coated glass particles.

The aging tests performed on foam filled with silver coated copper in acid and basic sweat solution revealed a change in conductivity respect to the one with SP filler. Mechanical characterization reveals that conductive polyurethane foam has elongation at break about 20% less than the foam without SP filler. The tensile strength at break does not change significantly. Breathability tests on foams demonstrated higher permeability to water vapour than films.

### CONCLUSION

In this work conductive elastomeric polyurethane foams are obtained from water formulations, with an easy and green process. Electrical and mechanical properties are determined. Aging stability and breathability are checked. Further studies to verify biocompatibility are ongoing. The results show that this material can be potentially applied in the biomedical field for electrostimulation devices.

### REFERENCES

- Chen, Y.-H. *et al. Sensors* **14**, 23758–23780 (2014).
- Caba, V., *Res. Rev. J Mat. Sci. Res. Rev. J Mat. Sci* **5**, (2017).



## In vitro and In vivo Biodegradability of Soybean Oil and Polylactic Acid (PLA) Blended Films

Elvan Akyol<sup>1</sup>, R. Seda Tıgılı Aydın<sup>2</sup>, Baki Hazer<sup>1</sup>

<sup>1</sup>Chemistry Department, Bulent Ecevit University, Turkey

<sup>2</sup>Biomedical Engineering Department, Bulent Ecevit University, Turkey

[elvan.akyol@hotmail.com](mailto:elvan.akyol@hotmail.com)

### INTRODUCTION

The purpose of this research is to understand and characterize in vitro and in vivo biodegradability of different forms of soybean oil and PLA (Polylactic acid) blend films<sup>1</sup>. In this study, the effect of soybean oil inclusion on hydrolytic degradation of polylactic acid (PLA) was investigated both in vitro and in vivo.

### EXPERIMENTAL METHODS

We have transformed lactic acid to Polylactic acid with ring-opening polymerization and distilled with styrene. Types of soybean oil were commercial soybean oil (SOYA), epoxy soybean oil (ESO) and epoxidized soybean oil. The polymeric soybean oil (PSO) was prepared due the auto-oxidation according to previously reported procedure in the literature<sup>2</sup>. Epoxy soybean oil has been produced from commercial soybean oil with usage of formic acid and hydrogen peroxide. PLA/oil blends were prepared in chloroform in order to achieve 2, 7, 14, and 20% (w/w) oil in blends. These blends films were characterized with the usage of FT-IR, GPC, TGA, SEM and tensile test. In vitro biodegradation studies were assessed for 8 weeks period. Selected samples were implanted in Sprague Dawley rabbits and in vivo biodegradability of samples were evaluated after 4 weeks.

### RESULTS AND DISCUSSION

SOYA blended PLA membranes show the lowest degradation rates by bulk degradation after 4 weeks in vitro. Approximately twofold high percentage weight losses of all membranes were obtained after 4 weeks of degradation in vivo in comparison with in vitro data.

Table 1. In vitro biodegradability after 8 weeks

Blend Films	Mw loss % (kDa)	Weight Loss %	T <sub>max</sub> (°C)
PLA	60.4	7.8	356.3
PLA-PSyox-14	68.1	6.6	347.6
PLA-Sy 14	59.3	5.0	349.3
PLA-ESO-14	39.7	7.2	318.2

Table 2. In vivo degradation data of polymer blend films after 4 weeks

Blend Films	Mw loss % (kDa)	Weight Loss %	T <sub>max</sub> (°C)
PLA	70.3	68.7	364.1
PLA-PSyox-14	72.6	68.5	308.3
PLA-Sy 14	68.9	47.3	358.4
PLA-ESO-14	58.7	49.1	315.3

T<sub>max</sub>: Temperature at maximum degradation rate (DTG curve)

Drastic morphological changes were observed on surface of degraded membranes in vivo with large pores, cracks, fissures and large cavities (Fig. 2).

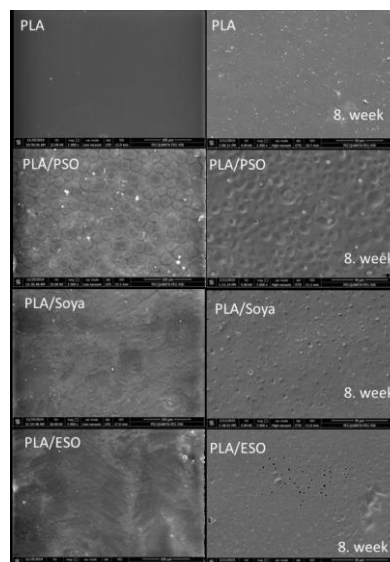


Fig. 1. SEM images of PLA-Soybean oil blend films after 8 Weeks of in vitro degradation

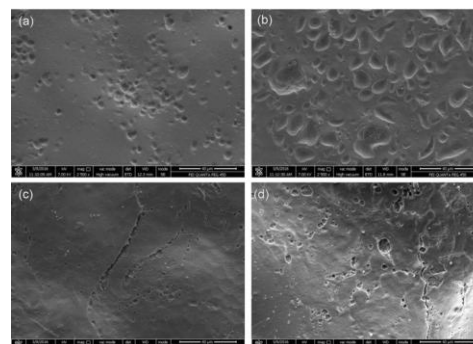


Fig. 2. SEM images of data of (a)PLA, (b) PLA/PSO, (c) PLA/SOYA and (d) PLA/ESO after 4 weeks of in vivo degradation

### CONCLUSION

Results concluded that soybean oil blend films can be used to produce many products such as packing materials, plastic containers and bottles with their biodegradable nature. Moreover, results showed controllable degradation profiles which encourage the use of soy bean oil based materials as biomaterials for several biomedical applications.

### REFERENCES

1. R. Seda Tıgılı Aydın et al., J. of American Oils Chemists' Society. 3:413-424, 2017
2. B. Hazer, J Polym Environ 22:200-208,2011

### ACKNOWLEDGMENTS

The authors would like to thank financial supports of Turkish Scientific Research Council (TÜBİTAK) (Grant Number: 213M375) and Bulent Ecevit University Research Fund (Grant Number: 2014-39971044-02).

## Enhancing Pseudoislet Biofunctionality using Microparticle Technology

Ajile Abdulhusein (Elttayef)<sup>1</sup>, Catriona (Kelly)<sup>2</sup>, Ying (Yang)<sup>1</sup>

<sup>1</sup>Guy Hilton Research Centre/Keele University, UK

<sup>2</sup>Ulster University/Stratified Medicine, UK

[y.yang@keele.ac.uk](mailto:y.yang@keele.ac.uk)

### INTRODUCTION

Pseudoislets (PIs) are aggregates of islets cells that mimic primary islets of Langerhans. Central necrosis hampers the biofunctionality of PIs, due to a shortage of nutrient and oxygen diffusion the PI core. This is particularly true for PIs > 150  $\mu\text{m}^1$ . We hypothesise that construction of 'vents' by incorporating microparticles into the centre of PIs will prevent cell residence at the centre of PIs thereby permitting nutrients/oxygen to diffuse to the core. Additionally, loading of these microparticles with anti-necrotic or anti-apoptotic drugs may further enhance the viability and functionality of PIs<sup>2,3</sup>. This study aimed to synthesis and characterise gelatin microparticles (GMs) and assess their impact on the biofunctionality of PIs.

### EXPERIMENTAL METHODS

The BRIN-BD11 rat pancreatic  $\beta$ -cell line was cultured in suspension for up to 7 days to generate PIs. Two cell seeding densities, 32,000 and 64,000 cells/PI were used. 40  $\mu\text{m}$  GMs were produced from Gelatin A in water-in-oil emulsion and crosslinked with 5% glutaraldehyde for 6 hours. The neat GMs or GMs loaded with IL-10 and anti-IL-1 $\beta$  (100 ng/mL and 5  $\mu\text{g}/\text{mL}$  respectively) were incorporated to PIs at a concentration of 25-50 GMs/PI. The cell viability of the PIs was assessed using cell counting kit-8 (CCK-8) and lactate dehydrogenase (LDH). Insulin release from PIs was evaluated after stimulation with 16.7 mM glucose for 20 minutes. One-way ANOVA with multiple comparisons was performed to determine statistical significance. P-values ( $P < 0.05$ ) were considered as significant. All statistical analyses were performed using GraphPad Prism 7.

### RESULTS AND DISCUSSION

The incorporation of GMs into PIs resulted in enhanced cell viability regardless the cell seeding density. In addition, the viability of PIs increased 11-15% when IL-10 was added to media for both cell seeding densities compared with PIs without GMs or those free of IL-10. Similarly, adding anti-IL-1 $\beta$  directly to media improved the viability of PIs by 13-14% compared with control (PIs free of GMs). Loading of the two cytokines into GMs protected the cytokines from degradative processes and achieved sustained-release of the anti-inflammatory drug from GMs. Incorporating the drug-loaded GMs to PIs resulted in a synergistic effect that enhanced PI biofunctionality. These PIs showed increased cell viability by 30% at a cell seeding density of 32,000 cells/PI and 25% at a cell seeding density of 64,000 cells/PIs with GMs loaded with IL-10 compared with control (Fig. 1). Similarly, the viability was elevated by 40% at a cell seeding density of 32,000 cells/PI and 20% at the cell seeding density of 64,000 cells/PIs with GMs loaded with anti-IL-1 $\beta$  compared

with control at day 7. The cellular LDH released from the PIs showed a decline when GMs loaded with IL-10 were incorporated into the PIs regardless of the seeding density used. Similar data was observed with the use of anti-IL-1 $\beta$ . Ultimately, the biofunctionality of PIs over a one-week culture period was improved in term of insulin production, which was increased by 1.5-fold when IL-10 was loaded onto GMs and by 1.6-fold when anti-IL-1 $\beta$  was loaded onto the GMs.

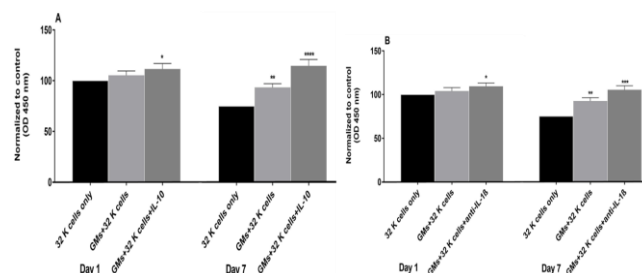


Fig. 1. PI viability following incorporation of GMs loaded with IL-10 and anti-IL1 $\beta$  at seeding densities of 32,000 cells/PIs (A) and 64,000 cells/PIs (B)

### CONCLUSION

The incorporation of GMs into the centre of large PIs was successfully achieved in this study. Thus GMs facilitated the creation of voids or blocked cells from being located in the centre of PIs. Loading GMs with anti-inflammatory cytokines protected cytokine degradation and resulted in sustained, slow release. The synergetic effect of microparticles and sustained drug release on the biofunctionality of PIs has been achieved. Overall, the inclusion of anti-inflammatory or anti-apoptotic agents bound to GMs appears to be an effective strategy to enhance cell survival and improve the functionality of PIs.

### REFERENCES

- Luther MJ. *et al.* Biochem Biophys Res Commun. 8(12): 4278–84, 2012.
- Shi M. *et al.* Control Release Off J Control Release. Soc.125(1):196-205.2011
- MacGregor RR, *et al.* Am J Physiol - Endocrinol Meta. 1;290(5):E771–9. 2006.

### ACKNOWLEDGMENTS

Funding for this project was provided by the Iraqi Ministry of higher education and scientific research.



## Unraveling the Structural Changes of Alginate-Based Microspheres *In Vitro* and *In Vivo* Using Confocal Raman Microscopy

Z. Kroneková<sup>1</sup>, M. Pelach<sup>1,2</sup>, P. Mazancová<sup>1</sup>, L. Uhelská<sup>1</sup>, L. Kleščíková<sup>1</sup>, D. Treľová<sup>1</sup>, F. Rázga<sup>1</sup>, V. Némethová<sup>1</sup>, E. Majková<sup>2</sup>, P. Šiffalovič<sup>2</sup>, V. Raus<sup>1,3</sup>, D. Chorvát<sup>4</sup>, J. J. McGarrigle<sup>5</sup>, M. Omami<sup>5</sup>, D. Isa<sup>5</sup>, S. Ghani<sup>5</sup>, J. Oberholzer<sup>5</sup>, I. Lacík<sup>1</sup>

<sup>1</sup>Polymer Institute SAS, Dúbravská cesta 9, 845 41 Bratislava, Slovakia

<sup>2</sup>Institute of Physics SAS, Dúbravská cesta 9, 845 11 Bratislava, Slovakia

<sup>3</sup>Institute of Macromolecular Chemistry, AS CR, Heyrovsky Sq. 2, 162 06 Prague 6, Czech Republic

<sup>4</sup>International Laser Center, Ilkovicova 3, 841 04 Bratislava, Slovakia

<sup>5</sup>Department of Surgery, University of Illinois at Chicago, 840 South Wood Street, Chicago, IL 60612, USA

[zuzana.kronekova@savba.sk](mailto:zuzana.kronekova@savba.sk)

### INTRODUCTION

Encapsulation of insulin producing cells in non-covalently crosslinked microspheres represents a next-generation functional treatment for type 1 diabetes. Alginate based microspheres have been extensively studied in this respect, but no clinical therapy has been approved to date.<sup>1</sup>

The physico-chemical properties of alginate-based microspheres including the structure characterized by the spatial distribution of polymers directly influence their immunoprotective properties and overall *in vivo* performance. To understand the results from transplantation of encapsulated cells and to identify correlations between the response of the immune system and the structure of the microspheres additional data on microsphere structure before and more importantly after the explantation are critically needed.<sup>2</sup> We have recently demonstrated that confocal Raman microscopy (CRM) is non-invasive, label-free analytical method that is sufficiently sensitive and applicable to explanted microspheres.<sup>3</sup>

In this study, CRM was used to unravel the structural changes of alginate microbeads and the three-component (SA-SCS/PMCG) microcapsules before and after transplantation.

### EXPERIMENTAL METHODS

**Chemicals:** High viscosity sodium alginate (SA, high M-content) was supplied by ISP Alginates (Girvan, Ayrshire, UK), UP-LVG from Novamatrix (Sandvika, Norway), sodium cellulose sulfate (SCS) from Across Organics (New Jersey, NJ, USA), poly(methylene-co-guanidine) hydrochloride (PMCG) from Scientific Polymer Products Inc. (Ontario, NY, USA). NaCl, BaCl<sub>2</sub>·2H<sub>2</sub>O, CaCl<sub>2</sub>·2H<sub>2</sub>O, were purchased from MikroCHEM (Slovakia).

**Microsphere preparation:** Alginate microbeads of higher and of lower heterogeneity, and three-component SA-SCS/PMCG microcapsules were prepared as described in<sup>3</sup>.

**Confocal Raman Microscopy:** Microcapsules were placed into an in house-designed holder and covered with respective storing solution. Raman spectra were collected using Witec UHTS300 spectrometer equipped with the Witec alpha 300 R+ confocal microscope using 785 nm laser line for excitation and immerse objective (Zeiss 20x, N.A. 1) focused at the equatorial microsphere cross-section. The baseline correction was performed for all spectra. Subsequently the peaks were fitted with Gauss functions (Witec Project plus).<sup>3</sup>

### RESULTS AND DISCUSSION

The two types of microspheres were subjected to various storing solutions as well as implanted intraperitoneally into C57bl/6 mice to analyze the environment influence on their structure. To characterize these structural changes, both qualitative and quantitative modes of evaluation have been used.<sup>3</sup> The model microspheres behaved differently with respect to changes in spatial distribution of polymers depending on the microsphere environment. While the heterogeneous character of alginate microbeads changed to the homogeneous one upon implantation, the three-component microcapsule retained its heterogeneous structure. Moreover, the homogeneous character of spatial alginate distribution in the microbead was independent on the initial degree of heterogeneity. Applying the quantitative modes of evaluation the real concentrations of the components in both types of microspheres were assessed. Thus, the information about the microenvironment cells would encounter upon their encapsulation was obtained.

### CONCLUSION

The obtained CRM data provide invaluable information about the structure and structural changes of two different microsphere types used for cell encapsulation. These results help us to better understand how the *in vivo* environment impacts the immunoprotective properties and performance of the hydrogel biomaterials, which should facilitate rational optimization of the encapsulation systems.

### REFERENCES

- Desai T., Shea, L. D., Nat. Rev. Drug Discov. 16: 367–350, 2017
- Rokstad A.M. *et al.*, Adv. Drug Deliv. Rev. 67-68: 111-130, 2014
- Kroneková Z. *et al.*, *Sci. Rep.* 8:1637, 2018

### ACKNOWLEDGMENTS

This research was supported by the JDRF Grant No. 2-SRA-2014-288-Q-R, the Chicago Diabetes Project, and also by the Slovak Research and Development Agency under contract numbers APVV-14-0858 and APVV-15-0641, the VEGA Grant Agency project no. 2/0124/18 and no. 2/0059/16. FR thanks to the *SASPRO Program* No. 0057/01/02).

## Targeting Cellular Organelles with Therapeutic Fluorescent Nanoparticles

Diana Costa, João A. Queiroz and Carla Cruz

CICS-UBI- Health Sciences Research Centre, University of Beira Interior, Covilhã, Portugal  
[dcosta@fcsaude.ubi.pt](mailto:dcosta@fcsaude.ubi.pt)

### INTRODUCTION

Researchers still hold for the development of viable non-viral delivery systems able of cell targeting and therapeutic action. Not only targeting nucleus and evolution in gene therapy protocols is relevant, but targeting other organelles as lysosomes and mitochondria become imperative to consolidate emerging and innovative therapeutics.<sup>1-3</sup> The conception of ligands and fluorescent probes that can target a specific organelle while ensuring cell viability is a priority in the formulation of advanced delivery systems. The conjugation of these compounds with biopharmaceutical based vectors leads to organelle targeting and, therefore, enhanced therapeutic efficacy.<sup>4</sup> In line with this, new targeting approaches need to be considered in order to instigate the development in the therapies centred in the nucleus, lysosomes and mitochondria.

### EXPERIMENTAL METHODS

AcridTriamine, NaphTripodal, QuinTriamine and [16]phenN<sub>2</sub> have been synthesized as described elsewhere.<sup>5</sup>

*Formulation of BSA or pDNA nanoparticles.* 5 µg of pDNA or BSA, 120 µg of CaCl<sub>2</sub> and 7.5 µL of fluorescent compound were mixed. This solution was gently added dropwise to 255 µL of Na<sub>2</sub>CO<sub>3</sub> solution. The pellet contained the nanoparticles. The morphology of the systems was evaluated by Scanning Electron Microscopy and the size and zeta potential by Dynamic Light Scattering.<sup>5</sup>

*In vitro transfection studies.* HeLa cells were transfected with BSA or pDNA nanoparticles. After transfection, mitochondrial and cytosolic cellular fractions were separated using adequate commercially available kits. The levels of BSA and p53 proteins were quantified by the bicinchoninic acid method and p53 pan ELISA kit, respectively.

### RESULTS AND DISCUSSION

*Sub-cellular localization.* The intracellular localization of the fluorescent compounds was assessed by confocal microscopy. QuinTriamine colocalizes with the lysosomes, while AcridTriamine and NaphTripodal are localized in the cytoplasm of MCF-7 cells. None of the compounds localize in the nucleus.

*Characteristics of Ligand/Plasmid DNA or BSA nanoparticles.* pDNA nanoparticles are oval or spherical in shape and present diameters higher than 170 nm but lower than 340 nm. [16]phenN<sub>2</sub> based nano carriers are the ones showing the lowest sizes. Considering the surface charges, all the systems exhibit positive zeta potential values, what can enhance the ability to permeate the negatively charged cellular membranes. The cytotoxicity profile of the developed vectors was evaluated through the MTT colorimetric

assay in fibroblast, HeLa and MCF-7 cells. All systems were found to be biocompatible. For all ligands studied, BSA nanoparticles present large sizes when compared with the corresponding pDNA based systems.

*Targeting of cellular organelles.* The cellular uptake and internalization of nanoparticles have been examined by the quantification of compound fluorescence intensity in the cellular fractions of HeLa cells. AcridTriamine and NaphTripodal are found in the cytosol, while QuinTriamine was detected in the lysosomes. Higher levels of [16]phenN<sub>2</sub> can be quantified in the mitochondria.

*Quantification of proteins.* The presence of BSA and the expression of p53 protein after cell transfection mediated by the developed vectors were investigated. Incubation with AcridTriamine, NaphTripodal, QuinTriamine and [16]phenN<sub>2</sub>/BSA systems in HeLa cells results in the presence of BSA in the cytosol, lysosomes and mitochondria, respectively. This confirms the specific targeting ability of fluorescent carriers. Transfection mediated by AcridTriamine or NaphTripodal/pDNA results in the expression of p53 protein in the cytosol.<sup>5</sup> When QuinTriamine is present, p53 is also produced but in less extent. No p53 is produced when [16]phenN<sub>2</sub> based pDNA vectors mediate the transfection of HeLa cells. This ligand targets mitochondria and, due to a different genetic code from the nucleus, no p53 protein expression occurs.<sup>5</sup>

### CONCLUSION

The fluorescent compounds can localize in one of the cellular fractions: cytosol, lysosomes or mitochondria. When the ligands are incorporated into nanoparticles they confer targeting ability to the carrier. BSA can be found in the various organelles and p53 protein can also be expressed, except for [16]phenN<sub>2</sub> based pDNA vectors. This work is a great contribution for the design of targeted drug and gene delivery systems.

### REFERENCES

1. Vankayala R. *et al.*, Adv. Funct. Mater. 25:5934-5945, 2015.
2. Weissig V. Methods Mol. Biol. 1265:1-11, 2015.
3. Piao S. *et al.*, Ann N Y Acad. Sci. 1371:45-54, 2016.
4. Santos J. *et al.*, Colloids Surf. B 121:129-140, 2014.
5. Costa D. *et al.*, Biomacromolecules 18:2928-2936, 2017.

### ACKNOWLEDGMENTS

D. Costa and C. Cruz acknowledge the FCT program contract IF/01459/2015 and IF/00959/2015, respectively, supported by Fundo Social Europeu e Programa Operacional Potencial Humano. The work was supported by FCT (project FCOMP-01-0124-FEDER-041068).

## Cold Atmospheric Plasma Generation and Quantification of Reactive Oxygen and Nitrogen Species in Biocompatible Hydrogels

Cédric Labay<sup>1,2</sup>, Ines Hamouda<sup>1,2</sup>, Maria-Pau Ginebra<sup>1,2</sup>, Cristina Canal<sup>1,2</sup><sup>1</sup>Biomaterials, Biomechanics and Tissue Engineering Group, Dpt. Materials Science and Metallurgy, Technical University of Catalonia (UPC), Escola d'Enginyeria Barcelona Est (EEBE), c/ Eduard Maristany 10-14, 08019 Barcelona, Spain<sup>2</sup>Barcelona Research Center in Multiscale Science and Engineering, UPC, Spain  
[cristina.canal@upc.edu](mailto:cristina.canal@upc.edu)**INTRODUCTION**

Plasma medicine is an emergent field focusing on the application of cold atmospheric pressure plasma (APP) for therapeutic purposes. APP is a totally or partially ionized gas containing ions, electrons, radicals, metastable molecules, UV/VIS radiation. It has been described effective in the stimulation of wound healing, in sterilization and in selective cancer treatment<sup>1</sup>. Plasma treatment of liquids can produce highly reactive oxygen and nitrogen species (RONS) such as hydroxyl radical ( $\cdot\text{OH}$ ), peroxides ( $\text{H}_2\text{O}_2$ ), nitrites ( $\text{NO}_2^-$ ), peroxyxynitrite ( $\text{ONOO}^-$ ) or superoxide ( $\text{O}_2^-$ ) among others<sup>2</sup>, that may readily modify essential biomolecules in cells. These RONS have in fact been associated with the biological effects of APP, although the exact mechanisms still remain unclear.

Hydrogel delivery systems can provide spatial and temporal control over the release of various therapeutic agents. Given the expanding field of plasma medicine, it is the aim of this work to investigate the potential of hydrogels for generation and delivery of APP-generated RONS to tissues. To that aim it is essential to suitably adapt methods for measurement of RONS in liquids to hydrogels.

**EXPERIMENTAL METHODS**

Different hydrogels (alginate, alginate-gelatine, carboxymethylcellulose) prepared in a range of concentrations have been treated with different APP jets<sup>1</sup> prior to crosslinking. Different APP conditions have been evaluated (ie. time, gas flow, distance to the sample). Quantification of  $[\text{H}_2\text{O}_2]$  and  $[\text{NO}_2^-]$  has been performed reacting the treated biopolymers with  $\text{TiSO}_4$  and Griess reagent, respectively<sup>2</sup>. Ringer's saline has been employed as control for the determination of RONS generated by APP. Cell adhesion & proliferation has been evaluated up to 72h in the treated hydrogels.

**RESULTS AND DISCUSSION**

One of the novel assets of this work rests upon the adaptation and optimization of the methods to quantify RONS usually employed in plasma-treated liquids to different hydrogels. This is a challenging issue due to the potential interactions of the usual probes for the different RONS with the hydrogel chains. Herein, by using different types of APP, and of hydrogels we demonstrate that the concentration of RONS generated in hydrogels is in general several-fold lower than in liquids. This can be attributed to the reactivity of the biopolymer chains which decrease the mean free-path of the different RONS with respect to their behaviour in liquids.

The concentration -for instance- of  $\text{H}_2\text{O}_2$  or  $\text{NO}_2^-$  can be tuned by the modulation of the APP working conditions. This will be a crucial feature to be able to control the dose of RONS in the hydrogel-based biomaterials and thus its therapeutic effects.

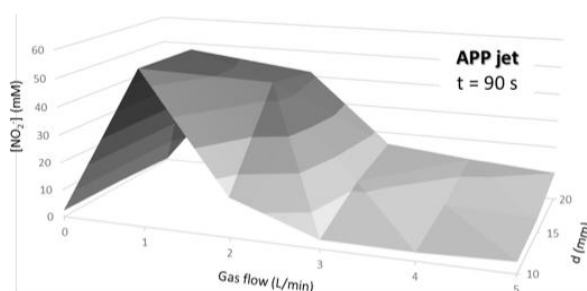


Fig. 1. Influence of gas flow and distance to the sample in  $[\text{NO}_2^-]$  generated in 0.5% alginate hydrogels by APP.

The potential impact of this is shown by the enhanced cell proliferation in contact with the APP-treated hydrogels.

**CONCLUSION**

We have been able to successfully adapt methods for measurement of RONS to hydrogels. The reactivity of APP with hydrogels greatly depends on the plasma device employed but also on the kind of hydrogel employed and its concentration.

This is a first step towards the use of hydrogels in plasma medicine, to deliver APP generated RONS to the target site. As shown by the cell viability, this can find applications in tissue engineering.

**REFERENCES**

1. Canal C. *et al.*, Free Rad. J. Biol. Med. 110:72-80, 2017
2. Bruggeman P.J. *et al.*, Plasma Sources Sci. Technol. 25:053002, 2016

**ACKNOWLEDGMENTS**

This project has received funding from the European Research Council (ERC) under the European Union's Horizon 2020 research and innovation programme (grant agreement No714793) and the financial support of MAT2015-65601-R project (MINECO/FEDER, EU).

## Identification of Hematopoietic Stem Cells Microparticles from Cord Blood Transplants

Damianos Sotiropoulos<sup>1</sup>, Angeliki Xagorari<sup>1</sup>, Marina Geroussi<sup>2</sup>, Antonia Sioga<sup>3</sup>, Dimitris Bougiouklis<sup>1</sup>,  
Anagnostis Argiriou<sup>2</sup>, Achilles Anagnostopoulos<sup>1</sup>

<sup>1</sup>Public Cord Blood Bank of Thessaloniki, Department of Hematology-BMT unit,  
"G.Papanicolaou" Hospital, Thessaloniki, Greece

<sup>2</sup>Institute of Applied Biosciences – Centre for Research and Technology Hellas, Thessaloniki, Greece

<sup>3</sup>Medical School, Aristotle University of Thessaloniki, Department of Histology-Embryology and Anthropology,  
Thessaloniki, Greece  
[dsotiro@otenet.gr](mailto:dsotiro@otenet.gr)

### INTRODUCTION

Microparticles (MPs) are small bilayered membrane vesicles, which can transfer bioactive molecules such as lipids, growth factors, microRNAs. Umbilical Cord Blood Transplant Units (UCB) has been established as a source of Hematopoietic Stem Cells (HSC) in allogeneic transplantation. MicroRNAs (miRNAs) are short non-coding RNA chains that regulate gene expression displaying important regulatory roles in many cellular processes. We have reported herein monitoring of miRNAs containing CD34+ microparticles (MPs) as a candidate parameter of the UCBs.

### EXPERIMENTAL METHODS

Cord blood units (CBUs) (n=37) were processed using the Sepax automated method (Biosafe). After processing, cryopreservation was performed using 10% DMSO in a controlled rate freezer (IceCube, Sy-lab). Adjusted variables of the CBUs included their net volume, the absolute number of CD34+ per graft and their viability as determined by flow cytometry. Mononuclear cells were seeded in semisolid cultures in the presence of a cocktail of growth factors for colony forming unit growth. The MPs were isolated after centrifugation of the plasma and their number was determined after incubation with Annexin V (AnnV+) and CD34 antibody by flow cytometry. Electron microscope photographs were obtained, after the appropriate preparation for TEM. CD34+ specific MPs as well as CD34+ cells isolation with immunomagnetic beads has been performed through MiniMACS columns (Miltenyi). Total RNA, including miRNA, was extracted from CD34+ and MPs using the miRNeasy Micro kit and miRNeasy Serum/Plasma kit (Qiagen), respectively. Samples' concentration was assessed by Qubit fluorimeter (Thermo Fisher scientific) and cDNA synthesis was achieved using miScript II RT kit (Qiagen). Quantitative Real Time PCR was performed to assess the presence of selected miRNAs in CD34+ and MPs in five independent donor samples (miScript SYBR Green PCR kit, Qiagen). Statistical analysis was done using t-test, Pearson's and Spearman's depending on the normality of the distribution of variables

### RESULTS AND DISCUSSION

The AnnV+/CD34+MPs during post-processing (51,38±37,87) decreased compared to the number of pre-processing AnnV+/CD34+MPs (57,7±51,2). The number of AnnV+/CD34+MPs (pre-processing vs. post-processing) has statistically significant mean positive correlation ( $p < 0,000$ , Spearman's rho = 0,696) whereas the number of post-processing CD34 cell per unit was not statistically significant. The number of post-processing AnnV+/CD34+MPs was positively correlated to the number of BFUe pre- and post-processing ( $p < 0,037$ ;  $r = 0,344$  and  $p < 0,003$ ;  $r = 0,474$  respectively). The post-processing AnnV+/CD34+MPs has positive correlation to the number of CFU-GM pre- and post-processing ( $p < 0,015$ ;  $r = 0,396$  and  $p < 0,036$ ;  $r = 0,347$  respectively).

Molecular analysis of post-processing CD34+ cells and MPs was identified the presence of microRNA 106b, 221, 224, 517c, 518a, 519d, 520h. miRNAs 517c and 520h were detected in low levels. miRNAs 106b, 221, 224, 518a, 519d were very low or undetectable. Additionally, a different profile was observed in cell lines meaning a line specificity of the selected miRNAs.

### CONCLUSION

In this project we have detected and identified microparticles of hematopoietic stem cells. The procedure of purification is very effective. We have proved that they carry microRNAs, indicating a possible role in cell to cell interactions. Their use as carriers for treatment compounds is under investigation.



## Synthesis and Self-Assembly of Amphiphilic Block Copolymers from Bio-based Hydroxypropyl Methyl Cellulose and Poly(L-lactide)

Aijing LU, Suming LI

Institut Européen des Membranes, UMR CNRS 5635, Université de Montpellier, France

[aijing.lu@etu.umontpellier.fr](mailto:aijing.lu@etu.umontpellier.fr)

### INTRODUCTION

Micelles self-assembled from amphiphilic block copolymers attracted great interest for controlled delivery of hydrophobic drugs and DNA.<sup>1</sup> Bio-based hydroxypropyl methyl cellulose (HPMC) and poly(L-lactide) (PLA) are widely used in the biomedical and pharmaceutical fields due to their biodegradability and biocompatibility<sup>2,3</sup>. In this work, amphiphilic block copolymers composed of PLA as hydrophobic block and HPMC as hydrophilic block were synthesized and characterized, and their self-assembly properties were studied to evaluate their potential as drug carrier.

### EXPERIMENTAL METHODS

#### 1. Synthesis of HPMC-PLA diblock copolymers

Amino terminated PLA (PLA-NH<sub>2</sub>) with DP of 10, 20, 30 and 40 was synthesized by ring opening polymerization of L-lactide using 3-(Boc-amino)-1-propanol as initiator and Sn(Oct)<sub>2</sub> as catalyst, followed by deprotection with trifluoroacetic acid. HPMC with Mw of 8000 was obtained by acid depolymerization. HPMC-PLA was then synthesized by reductive amination of PLA-NH<sub>2</sub> and aldehyde terminated HPMC, using sodium triacetoxyborohydride as reducing agent. The copolymers were characterised by <sup>1</sup>NMR, DOSY-NMR, FT-IR, GPC, etc.

#### 2. Self-assembly of HPMC-PLA diblock copolymers

Copolymer micelles were prepared by dissolution in water. The size of micelles was determined by using Anton Paar Litesizer, and the morphology by TEM. The critical micelle concentration (CMC) of copolymers was determined with F-7000FL spectrophotometer, using pyrene as fluorescence probe.

### RESULTS AND DISCUSSION

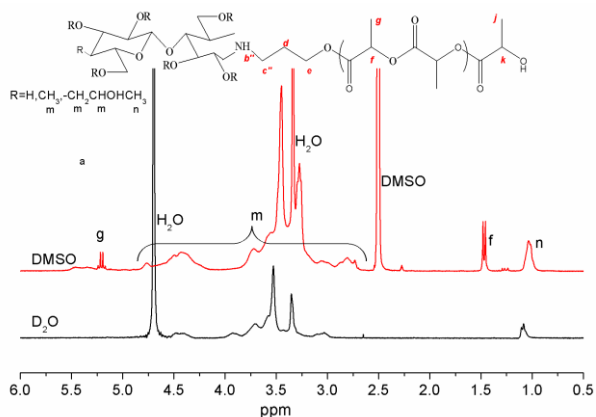


Fig. 1. <sup>1</sup>H NMR spectrum of HPMC-PLA in DMSO-*d*<sub>6</sub> and D<sub>2</sub>O

Fig. 1 shows the <sup>1</sup>H NMR pattern of HPMC8K-PLA<sub>40</sub> in DMSO-*d*<sub>6</sub> and D<sub>2</sub>O. The signals g and f belong to the methyl and methine protons of PLA block, and signals m and n belong to methyl and methylene of HPMC.

Both components are present in DMSO, but the signals belonging to PLA are not detected in D<sub>2</sub>O. This is due to the fact that the copolymer self-assembled to form micelles, and only the signals of the hydrophilic shell are detected.

Table 1. Size and PDI of HPMC-PLA micelles

Sample	Size (nm)	PDI
HPMC8k-PLA <sub>10</sub>	171.6±3.4	0.25
HPMC8k-PLA <sub>20</sub>	191.0±1.7	0.17
HPMC8k-PLA <sub>30</sub>	215.8±1.7	0.15
HPMC8k-PLA <sub>40</sub>	212.2±2.4	0.26

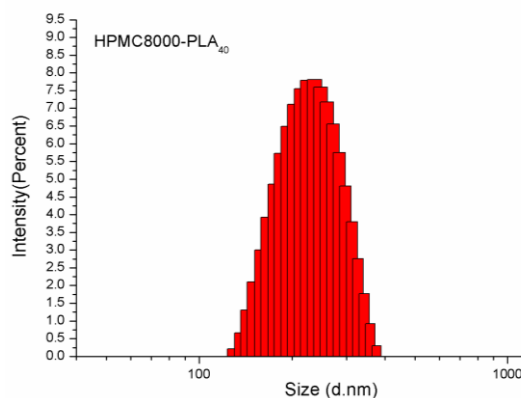


Fig. 2. Size distribution of HPMC-PLA block copolymer

The diameter of micelles was determined by using DLS (Fig. 2). It increases from 171.6 nm for HPMC8k-PLA<sub>10</sub> to 212.2 nm for HPMC8k-PLA<sub>40</sub>. The PDI is narrow, ranging from 0.15 to 0.26. TEM shows that micelles are spherical in shape, and low CMC values are obtained.

### CONCLUSION

HPMC-PLA block copolymers with various PLA block lengths were synthesized by reductive amination of PLA-NH<sub>2</sub> and HPMC. The copolymers self-assembled in water to yield spherical micelles with low CMC. Thus bio-based and amphiphilic HPMC-PLA copolymers could be promising as carrier of hydrophobic drugs.

### REFERENCES

- Nicolas J. *et al.* Chem. Soc. Rev.,42:1147-1235, 2013
- Siepmann J. *et al.* Advanced Drug Delivery Reviews.48: 139-157, 2001
- Castro-Aguirre E. *et al.* Advanced Drug Delivery Reviews. 107:333-366, 2016

### ACKNOWLEDGMENTS

This study was supported by the CHINA SCHOLARSHIP COUNCIL.



## Avidin-functionalized Gellan Gum as Modular Hydrogel for 3D Cell Culture

Christine Gering<sup>1</sup>, Jenny Parraga<sup>1</sup>, Janne T. Koivisto<sup>1,2</sup>, Jenni Leppiniemi<sup>2</sup>, Vesa Hytönen<sup>2</sup>, Minna Kellomäki<sup>1,2</sup>

<sup>1</sup>BioMediTech Institute and Faculty of Biomedical Sciences and Engineering, Tampere University of Technology, Tampere, Finland

<sup>2</sup>BioMediTech Institute and Faculty of Medicine and Life Sciences, University of Tampere, Tampere, Finland  
[christine.gering@tut.fi](mailto:christine.gering@tut.fi)

### INTRODUCTION

Hydrogels have for long been a promising class of materials for tissue engineering applications<sup>1,2</sup>. Essentially, hydrogels form a scaffold-like support structure for cells and provide an aqueous environment, which mimics natural tissues. Regenerative medicine exploits hydrogels for cell delivery, but they also allow research on cells for disease modelling and cell biology. Although most hydrogel materials are biocompatible, they are also biologically relatively inert.

To combat this situation, various approaches have been described in the literature to functionalize hydrogels with an abundance of bioactive molecules through the means of various chemical strategies. Direct covalent coupling strategies limit the functionalized polymer to one, relatively narrow target application. Indirect modification with proteins that can selectively bind certain compounds offers an alternative approach<sup>3</sup>. Due to its superior affinity and specificity, the avidin-biotin binding has been exploited for many diverse biochemical applications<sup>4</sup>. Hydrogel containing covalently coupled avidin would allow for the convenient and flexible modification with biotin-labelled compounds, for example the peptide sequences.

Here, we propose a modular hydrogel material that requires no further chemical functionalization steps. The base material is avidin-conjugated gellan gum (GG), which can be modified in situ through the addition of biotinylated compounds. GG is a polysaccharide, which has recently been proposed as a suitable tissue engineering material<sup>5,6</sup>. GG hydrogels have been used for 2D and 3D cell culture but satisfying cell response have not been achieved without functionalization.

### EXPERIMENTAL METHODS

Commercial GG was purified to substitute counterions with sodium (NaGG). NaGG was functionalized with charge-neutralized chimeric avidin via carbodiimide conjugation. Elution analysis with surfactant confirmed that the avidin is bound to the polymer network and not merely entrapped or physically adsorbed. Fluorescence titration with biotinylated fluorescein (b5F) was performed to determine the activity and concentration of avidin. The mechanical properties of the different hydrogels were examined with compression testing of unconstrained samples and uniaxial loading using Bose BioDynamic ElectroForce Instrument 5100. Human fibroblasts (WI-38) were cultured over three days encapsulated in NaGG-avd (941 000 cells/mL) and plated on top (63 000 cells/cm<sup>2</sup>) with addition of biotinylated RGD or fibronectin. The constructs were LIVE/DEAD® stained and the microscope images were analysed with ImageJ.

### RESULTS AND DISCUSSION

The structural and mechanical properties of NaGG-avd after functionalization were analyzed. Avidin remained active, as proven by fluorescence titration using a biotinylated dye (b5F). The fluorescence intensity of b5F is quenched in presence of avidin, thus the amount of avidin can be estimated and the ability of avidin to bind biotin is confirmed. A functionalization degree between 9 and 15% was achieved between different batches.

Self-supporting gel samples could be created from the functionalized NaGG using ionic crosslinking method with the bioamine spermidine<sup>6</sup>, as well as calcium chloride solution. The gels had a fracture strength of 6.4±1.2 kPa and a fracture strain of 36.5±5.5% relative strain when formed with spermidine.

Cell culture with fibroblasts showed high viability of the cells with over 80% live cells in 3D, while in 2D lower viability was achieved and clustering of the cells was observed.

### CONCLUSION

In conclusion, a tuneable base material with modification sites was created. GG was functionalized with the protein avidin and the conjugation was shown to perturb neither the hydrogel characteristics of gellan gum, nor the biotin-binding capabilities of avidin.

The functionalized hydrogel was successfully applied to culture fibroblasts in 3D. The presented approach offers a simple, yet flexible solution for hydrogel materials that can support encapsulated cells and provide a native environment. Desired factors, such as RGD, can be tethered to the hydrogel in situ. In the future, we aim to increase the functionalization degree and test the suggested material with various cell types and biotinylated factors.

### REFERENCES

1. Tibbitt M.W. and Anseth K.S., *Biotechnol. Bioeng.* 103:655-663, 2009.
2. Tirrell D.A. and Langer R., *Nature*, 428:487-492, 2004.
3. Hermanson G.T., "Bioconjugate Techniques" (3rd ed.) 2013.
4. Livnah O. et al, *Proc. Natl. Acad. Sci. U. S. A.* 90:5076-5080, 1993.
5. Prajapati V.D. et al, *Carbohydr. Polym.* 93:670-678, 2013.
6. Koivisto J.T. et al, *Biomed. Mater.* 12:25-14, 2017.

### ACKNOWLEDGMENTS

We wish to thank the Human Spare Parts project of Tekes – the Finnish Funding Agency for Innovation, for funding this project.

### 3D Cell-laden Collagen Villi Model for Mimicking Intestinal Villus Epithelium and Capillary

WonJin Kim, Minseong Kim, Gi Hoon Yang, JaeYoon Lee, Miji Yeo, YoungWon Koo, JiUn Lee, HaeRi Kim, GeunHyung Kim\*

Department of Biomechatronic Engineering, Sungkyunkwan University (SKKU), Suwon, Republic of Korea  
[joshbass@skku.edu](mailto:joshbass@skku.edu)

#### INTRODUCTION

3D cell culture within 3D structures provides cells more physiological conditions including cell-to-cell and cell-to-substrate interactions and suitable biochemical signaling compared to conventional 2D cell culture.<sup>1</sup> To date, 3D cell-printing technology for obtaining a 3D cell-laden structure has been studied in tissue engineering applications.<sup>2-4</sup> However, a realistic villi model using cell-laden bioink with both the biocompatibility and mechanical strength to achieve villus structure has not been developed. Furthermore, 3D villi model requires vascularization to perform their specific functions.<sup>5</sup> Here, we developed a human intestinal villi model including vascularization using a cell-printing technique. Human umbilical vein endothelial cells (HUVECs)-laden collagen bioink and epithelial cells (Caco-2)-laden collagen bioink were printed using core-shell nozzle to mimic the anatomical human villi structure. The vascularized 3D villi structure showed appropriate geometry.

#### EXPERIMENTAL METHODS

##### *Fabrication of cell-laden hydrogel model*

Porcine tendon collagen type-I was used as the cell carrier hydrogel. The collagen was mixed with Caco-2 cells (bioink-I), and HUVECs (bioink-II) at a density of  $1 \times 10^7$  cells/mL. TA was mixed with the bioinks for collagen cross-linking. The bioinks were printed using a dispensing system with a 3-axis printing system and core-shell nozzle (core outer diameter (OD) = 410  $\mu$ m, and shell OD = 810  $\mu$ m) to achieve the 3D vascularized villi model. The bioink II was extruded at the core nozzle, and the bioink I was extruded in the shell nozzle.

##### *Fluorescence imaging*

The 3D vascularized villi models were exposed to 0.15 mM calcein AM and 2 mM ethidium homodimer-1 for 1 h in an incubator. The stained specimens were visualized under a confocal microscope.

#### RESULTS AND DISCUSSION

Before fabricating the Caco-2/HUVEC-laden villi model, we fabricated villi structure using collagen solution without cells (core) and bioink-I (shell) to mimic a mono-layer epithelium of human villi architecture. As shown in the live/dead image (Fig. 1(a)), the epithelia cells developed a mono-layer of epithelium after 14 days of fabrication.

Then, the bioink-I and -II ejected from the core-shell nozzle can be printed to fabricate the vascularized villi structures. As shown in figure 1(b), we can obtain a Caco-2/HUVEC-laden intestinal villi array, which is similar to the actual geometry of the human gastrointestinal tract. A single villus showed high aspect ratio (height/diameter), as shown in the SEM and optical images (Fig. 1(c)).

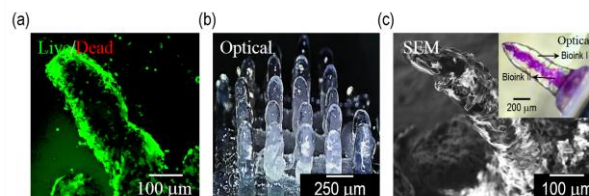


Fig. 1. (a) Live/dead image of Caco-2 laden mono-layer epithelium. (b) Optical images of a 3D vascularized villi model. (c) SEM and optical images of the fabricated villus structure

#### CONCLUSION

In this study, we fabricated 3D vascularized villi model using Caco-2-laden/HUVEC-laden bioinks. The HUVECs were located in the core region and the Caco-2 cells were located in the shell region completely after fabrication. The villi structure fabricating technique can be a strong technique to mimic complex tissue engineering scaffolds.

#### REFERENCES

1. Sung J. H. *et al.*, Lab Chip 11:389-392, 2011
2. Markstedt K. *et al.*, Biomacromolecules 16:1489-1496, 2015
3. Rutz A. L. *et al.*, Adv. Mater. 27:1607-1614, 2015
4. Zhu K. *et al.*, Adv. Func. Mater. 27:1605352, 2017
5. Di Fiore M. S. Atlas of human histology. No. C/611.0181F. 1979

#### ACKNOWLEDGMENTS

This study was supported by a grant from the Ministry of Trade, Industry & Energy (MOTIE, Korea) under Industrial Technology Innovation Program (No. 10063541: Development of bioceramic 3D printing materials and low temperature (<40°C) process customized by implant sites) and was supported by a fund by Research of Korea Centers for Disease Control and Prevention.

## Development of Novel Injectable Hydrogels for Osteochondral Regeneration

Luis García-Fernández<sup>1,2</sup>, Marta Olmeda-Lozano<sup>3</sup>, Blanca Vázquez-Lasa<sup>1,2</sup>, Julio San Román<sup>1,2</sup>

<sup>1</sup>Biomaterials Group/Institute of Polymer Science and Technology, Spanish National Research Council (ICTP-CSIC), Spain

<sup>2</sup>Centro de Investigaciones Biológicas en Red, Bioingeniería, Biomateriales y Nanomedicina (CIBER-BBN), Spain

<sup>3</sup>University Hospital Infanta Elena, Spain

[luis.garcia@csic.es](mailto:luis.garcia@csic.es)

### INTRODUCTION

Osteochondral tissue presents a very complex morphology that result in the development of complex treatments. On one side, articular cartilage is an avascular tissue that lines the ends of bones in diarthrodial joints, serves to support and acts as a shock absorber and facilitates joint's motion in low friction<sup>1</sup>. On the other side, the bony layer is comprised of a variety of cell population, inorganic compounds, extracellular matrix (ECM) and other components designed to provide mechanical support to the body<sup>2</sup>. The osteochondral tissue comprises the interface between bone and cartilage and is a gradual transition in which the key constituents of each tissue undergo an exchange in predominance.

In this work, we developed a novel injectable natural polymer-based system for osteochondral regeneration.

### EXPERIMENTAL METHODS

**Design of an injectable hydrogel:** We developed a semi-Interpenetrating Polymer Network (semi-IPN) based on two natural products: hyaluronic acid (HA) and gelatin crosslinked using oxidized dextran.

The hydrogel was also loaded with different anti-inflammatory drugs (dexamethasone and naproxen) in order to improve the cartilage regeneration.

The gelation time for different concentrations of gelatin, HA and dextran was determined to optimize the composition.

**Physical characterization:** Swelling and degradation of the different hydrogels were studied in phosphate buffer saline medium at 37°C.

The release of dexamethasone and naproxen was followed by UV in the same conditions.

**Biological characterization:** Cytotoxicity and cell adhesion was determined using MTT and Alamar blue assays respectively. These assays were performed on osteoblast and chondrocyte cells.

### RESULTS AND DISCUSSION

The hydrogels present a gelation time of 35 min, this time is enough for their manipulation before the *in vivo* injection.

The hydrogels present a low swelling rate due to their preparation in wet condition, and a degradation time correlated to their composition (Fig. 1).

Naproxen-loaded hydrogels present the low degradation rate and the hydrogels complete degrade after 7 days.

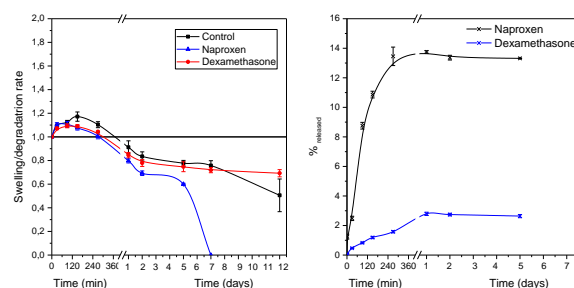


Fig. 1. Swelling/degradation rate of the hydrogels and release of dexamethasone and naproxen.

Dexamethasone-loaded hydrogels and not loaded hydrogels present a degradation time higher than 12 days. The release of naproxen and dexamethasone (Figure 1) increased during the first day and then it stabilized. The low values of release are due to the low solubility of the different drugs in aqueous medium.

*In vitro* test (Fig. 2) showed that the hydrogels do not present cytotoxicity and allow the cell growth and proliferation on their surface with both cell lines.

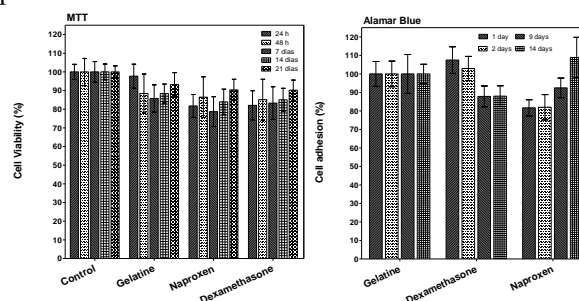


Fig. 2. Cytotoxicity and cell adhesion determined by MTT and Alamar Blue on chondrocytes.

### CONCLUSION

We prepared different hydrogels based on natural polymers and loaded with different anti-inflammatory drugs for their use as injectable hydrogels for osteochondral regeneration.

The hydrogels present an adequate gelation time for their use as injectable hydrogels and allow cell adhesion and proliferation.

These properties make our hydrogels good candidates for their use in osteochondral regeneration.

### REFERENCES

- [1] Moutos Franklin T., *et al.*, Nature Materials 6:162, 2007
- [2] O'Keefe Regis J., *et al.*, Tissue Engineering. Part B, Reviews 17:389-392, 2011



## Wet Electrospinning and *in situ* Biofunctionalization of Degradable Multiblock Copolyester

Peter Sobolewski, Julia Bukala, Karolina Stepień, Rahul Sahay, Mirosława El Fray

Division of Biomaterials and Microbiological Technologies  
Faculty of Chemical Technology and Engineering  
West Pomeranian University of Technology Szczecin  
17 Piastów Ave, Szczecin 70-311, Poland  
[psobolewski@zut.edu.pl](mailto:psobolewski@zut.edu.pl)

### INTRODUCTION

Characteristic features of biological soft tissues include hierarchical organization, nonlinear elasticity, anisotropy, and a low Young's modulus (on the order of 1 MPa). Electrospinning is a popular approach for generating scaffolds for tissue engineering soft tissue; however, the traditional flat or rotating collectors struggle to reconstitute the properties of extracellular matrix (ECM) of soft tissues. An alternative approach uses a coagulation bath as the collector (wet electrospinning), which yields biomimetic, highly porous scaffolds composed of coiled fibers and can allow for *in situ* biofunctionalization.<sup>1,2</sup> However, to-date this methodology has been under-studied, particularly regarding the influence of process parameters on fiber and construct morphology. Here we utilize this method to electrospin degradable thermoplastic elastomer, poly(butylene succinate - dilinoleic succinate) (PBS-DLS), and we examine the influence of process parameters, such as polymer concentration, flow rate, and applied voltage, on the morphology of obtained constructs.

### EXPERIMENTAL METHODS

PBS-DLS, with 70:30 wt% ratio of hard to soft segments, was prepared *via* two step-process, melt transesterification and polycondensation, using succinic acid (SA), 1,4-butanediol (1,4-BD), and dimer linoleic diol (DLA-OH, Pripol™ 2033), with Ti(BuO)<sub>4</sub> as catalyst, as described previously.<sup>3</sup> Polymer solutions for the electrospinning were prepared in chloroform, ranging from 20 to 30% w/v. Process parameters studied included: the polymer solution flow rate (0.5 mL/hr to 4 mL/hr), applied voltage (9 kV and 14 kV), and the size (5 to 20 cm) and composition of the collector dish (glass or metal). Temperature (RT) and distance from the collector (15 cm) were fixed. The coagulation bath was filled to a depth of 1 cm with 96% ethanol or 95% ethanol with 1 mM NaOH and 5 mg/mL dopamine for *in situ* biofunctionalization. The morphology of obtained fibrous constructs was assessed using Keyence Laser Scanning Microscope (LSM), model VK-9710K. Contact angle measurements were performed using Krüss DSA100 goniometer.

### RESULTS AND DISCUSSION

We were able to electrospin degradable thermoplastic elastomer PBS-DLS into ethanol bath (wet collector) and obtain coiled, 3D fibrous constructs. Increasing flow rate from 0.5 mL/hr to 4 mL/hr resulted in an increase in fiber diameter from 7 μm to 19 μm and a decrease in coil diameter from 640 μm to 230 μm. Increasing the applied voltage from 9 kV to 14 kV, at

a fixed flow rate of 2 mL/hr, did not affect fiber diameter, but also resulted in reduced size of fiber coils from 320 μm to 180 μm. Importantly, the two parameters were synergistic (Fig. 1): combining 4 mL/hr flow rate with 14 kV applied voltage yielded 13 μm fibers and 70 μm coils.

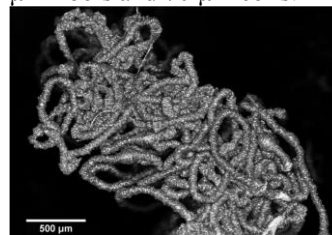


Fig. 1. LSM micrograph of electrospun PBS-DLS (25% w/v in chloroform, 3 mL/hr, 14 kV, EtOH bath)

The size and composition of the collector dish had a negligible effect. Further, we were able to carry out *in situ* biofunctionalization of the obtained PBS-DLS fibrous constructs by adding dopamine (and NaOH) to the bath, resulting in a shift from superhydrophobic character to highly hydrophilic (Fig. 2).



Fig. 2: Water contact angle (after 30 s) of electrospun PBS-DLS (25% w/v in chloroform, 3 mL/hr, 14 kV) Left: 96% EtOH bath. Right: 95% EtOH with 1 mM NaOH and 5 mg/mL dopamine

### CONCLUSIONS

We have successfully adapted the wet electrospinning process and *in situ* biofunctionalization to electrospin degradable thermoplastic elastomer PBS-DLS. We systematically examined the role of the electrospinning process parameters on fibrous construct morphology. (Micro)mechanical testing of obtained constructs, as well as cell viability and cell infiltration tests are on going.

### REFERENCES

1. Yokoyama Y. *et al.*, Mater Lett. 63(9–10):754–6, 2009.
2. Taskin MB. *et al.*, ACS Appl Mater Interfaces. 8(25):15864–73, 2016.
3. Liverani L. *et al.*, Eur Polym J 81:295-306, 2016.

### ACKNOWLEDGMENTS

The project was financially supported by National Science Centre, Poland, under the HARMONIA scheme (UMO2014/14/M/ ST8/00610). The authors have no financial conflicts.

## Mechanical and *in vitro* Properties of PLA/Bioactive Glass Composites

Inari Lyyra<sup>1</sup>, Katri Leino<sup>1</sup>, Terttu Hukka<sup>2</sup>, Minna Kellomäki<sup>1</sup>, Jonathan Massera<sup>1</sup>

<sup>1</sup>BioMediTech Institute and Faculty of Biomedical Sciences and Engineering,  
Tampere University of Technology, Finland

<sup>2</sup>Laboratory of Chemistry and Bioengineering, Tampere University of Technology, Finland  
[inari.lyyra@tut.fi](mailto:inari.lyyra@tut.fi)

### INTRODUCTION

Composites of bioactive glass and biodegradable polymers are easily machined to different shapes (screws, plates, scaffolds) and promote bone regrowth.<sup>1</sup> Their dissolution rate can be easily tailored and they can be doped with ions for example enhancing vascularization or inhibiting inflammation.<sup>1</sup> However, the fast degradation and high water content of some bioactive glass leads to thermal degradation of the polymer during extrusion. New composite rods of bioactive silicate or phosphate glasses and polylactide (PLA) were processed and immersed in TRIS buffer for 40 weeks. The objectives were to assess the release of ions from the glasses and their potential for osteogenesis and the impact of the glasses on the PLA degradation.

### EXPERIMENTAL METHODS

Medical grade PLDLA (L/DL ratio 70/30, Evonik Industries AG, Darmstadt, Germany) was co-extruded into 2mm diameter rods with silicate glass 13-93 (10, 30 and 50 wt-% loading) and phosphate glass Sr50 (10, 25 and 35 wt-% loading). The 7 cm rods were immersed in TRIS buffer for up to 40 weeks. The buffer solution was changed every two weeks. The pH, ion release (using ICP-OES), water uptake, mechanical properties (3-point bending) and the dispersion of the glass particles (125-250 µm) and CaP formation (EDX/SEM) were studied.

### RESULTS AND DISCUSSION

#### pH results

The PLA alone did not lead to any change in pH indicating that the material is stable. PLA/13-93 composite, however, induce a rise in pH during the first two weeks of immersion before stabilizing. This can be attributed to leaching of ions from glass particles at the materials surface, initially and within the bulk (lower mobility) later on. PLA/Sr50 composites induce a decrease in pH for immersion up to 2 weeks which then leveled off. This can be attributed to the fast glass dissolution. Furthermore, the high release of phosphate is known to lead to a pH decrease. In both composites the pH changes were loading dependent. The higher the glass content the more pronounced was the pH change.

#### Water uptake

The water uptake was high for the PLA/Sr50 (20-65 %), compared to the PLA/13-93 composites (4-25 %). This can be attributed to the faster dissolution rate and congruent dissolution as well as the known tendency of phosphate glasses to be hydroscopic. The water uptake increased with increasing immersion time and glass content. The pure PLA did not seem to absorb any water up to 10 weeks.

#### Ion release

Upon PLA/13-93 immersion, all the ions present in the glass are released in the buffer solution in a non-congruent manner. The release of Na and K are lower than typically seen when immersing the glass alone. These ions seem to be trapped inside the polymer matrix. The PLA/Sr50 dissolves congruently, as expected. Overall, the phosphate glass released a higher amount of ions into the solution compared to silicate glasses. As for the pH and water uptake, the ion release is a function of the glass content.

#### Mechanical properties – three-point bending

Adding bioactive glass decreased the stress at maximum load. The decrease increased with increasing glass load and was independent of glass composition. The mechanical properties of the composites decreased with increasing immersion time. This is attributed to the pores formed upon glass dissolution. In pure PLA there was no change in mechanical properties for up to 10 weeks.

#### EDX/SEM

At 10 weeks there was some 13-93 left in the composites, but the Sr50 had been almost completely dissolved and formed a CaP reactive layer as shown in Fig. 1.

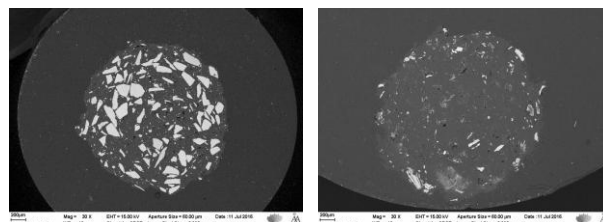


Fig. 1. SEM images of the composites cross section with (left) silicate and (right) phosphate glass particles, at 10 weeks in TRIS.

### CONCLUSION

Composites of PLA and bioactive glasses can be co-extruded without altering either of the materials. Increasing glass content led to increased water uptake, ion release, and a decrease in mechanical properties. This study introduces new processable bioactive glass-polymer composites with tailored ion release and potential for inducing osteogenesis and antimicrobial properties to be used in bone tissue engineering.

### REFERENCES

- Misra S. K. *et al.*, *Biomacromolecules*. 7:2249-2258, 2006

### ACKNOWLEDGEMENTS

The authors acknowledge the Academy of Finland, Jane and Aatos Erkkö foundation and the TUT foundation for financial support.



## PHBV Based Bone Tissue Engineering Scaffolds Doped with Diatom Shells

Ali Deniz Dalgic<sup>1</sup>, Deniz Atila<sup>1</sup>, Ayten Karatas<sup>2</sup>, Aysen Tezcaner<sup>1,3</sup>, Dilek Keskin<sup>1,3</sup>

<sup>1</sup>Department of Engineering Sciences, Middle East Technical University, Ankara, Turkey

<sup>2</sup>Department of Molecular Biology and Genetics, İstanbul Technical University, İstanbul, Turkey

<sup>3</sup>BIOMATEN, Center of Excellence in Biomaterials and Tissue Engineering Research Center, Ankara, Turkey

[deniz.dalgic@metu.edu.tr](mailto:deniz.dalgic@metu.edu.tr)

### INTRODUCTION

The importance of silicone (Si) on osteogenesis of bone related cells was approved in terms of proliferation, alkaline phosphatase activity, matrix deposition levels, and osteocalcin synthesis<sup>1</sup>. One of the natural sources of Si is biosilica shells of diatoms. Poly(3-hydroxybutyrate-co-3-hydroxyvalerate) PHBV is a biocompatible and biodegradable polymer obtained from bacterial source and PHBV based scaffolds were reported to be used as bone scaffolds<sup>2</sup>. Polycaprolactone (PCL) is a widely used, highly biocompatible polymer that has strong mechanical properties<sup>3</sup> and used to improve stability of PHBV fiber structure. In this study, wet electrospinning method was used to develop diatom shell doped 3D fibrous scaffold from PHBV and PCL polymers and osteogenic potential of scaffold was investigated by in vitro studies.

### EXPERIMENTAL METHODS

#### Characterization of diatom shells and scaffold

Chemical composition of diatom shells was analysed with X-ray Photoelectron Spectroscopy (ESCA). Morphology of shells and scaffold was observed under scanning electron microscope (SEM).

#### Wet electrospinning

PHBV/PCL polymer solution (14%) was prepared in hexafluoroisopropanol (HFIP) and diatom shells (20:1, Polymer:Shell, wt:wt) were electrospun within the polymer solution. Solution was delivered at a rate of 3ml/h with a syringe pump from 18cm distance into an ethanol bath under high voltage (13kV).

#### In vitro cell viability analysis

Human osteosarcoma cell line (Saos-2) was used in in vitro studies. Alamar blue assay was conducted to evaluate cell viability.

#### Statistical Analysis

One-way analysis of variance test was applied with Tukey's multiple comparison. Differences were considered statistically significant for  $p < 0.05$ .

### RESULTS AND DISCUSSION

Chemical composition of diatom shells was determined by ESCA (Table 1). The main structure of diatoms Si and O elements showed highest percentages with traces of Al and Ca. The adventitious carbon was formed during the analysis and was not included in shell composition.

Table 1. Surface element composition (%) of diatom shells

Composition (%)	O	Si	C	Al	Ca
	63.2	23.1	11.1	1.9	0.7

SEM images show that diatom are pure and successfully embedded in fibers after electrospinning (Fig. 1).

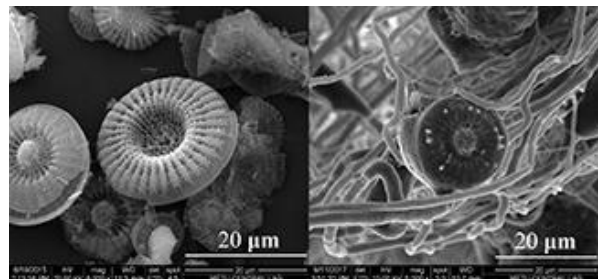


Fig. 1. SEM images of purified diatom shells (Left) and diatom shell doped fibers (Right)

Diatom shells concentration effect on Saos-2 cell proliferation was evaluated by alamar blue assay and optimum shell concentration that induces cell proliferation was determined (Fig. 2).

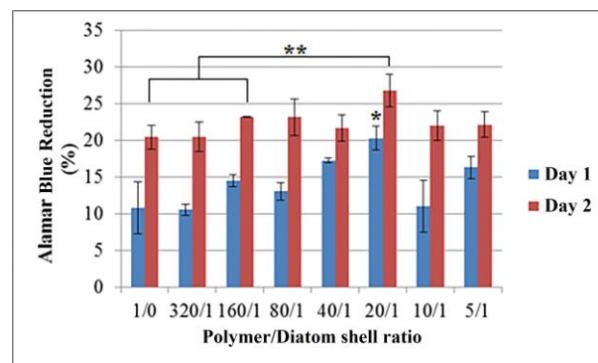


Fig. 2. Percent alamar blue reduction of Saos-2 cells proliferated on scaffolds with different diatom shell concentration

### CONCLUSION

Diatom shells were electrospun as in their original size for the first time to be doped into a 3D electrospun scaffold. The optimum polymer/shell concentration was determined and diatom shells doped scaffold showed induced Saos-2 cell proliferation.

### REFERENCES

- Jugdohsingh R. et al., *J Nutr Health Aging*, 11:99–110, 2007
- Sombatmankhong K. et al., *Polymer*, 48:1419–27, 2007
- Song H. et al., *Key Eng Mater*, 342-343:265-268, 2007

### ACKNOWLEDGMENTS

This work has been supported by grants from the Scientific and Technical Research Council of Turkey, project no: TUBITAK-215M893.

## PCL Fibers' Porosity Impact on Cells Attachment and Proliferation for Tissue Engineering

Sara Metwally, Joanna Karbowniczek, Adam Gruszczyński, Piotr K. Szewczyk, Urszula Stachewicz

International Centre of Electron Microscopy for Materials Science, Faculty of Metals Engineering and Industrial Computer Science, AGH University of Science and Technology, Poland

[metwally@agh.edu.pl](mailto:metwally@agh.edu.pl)

### INTRODUCTION

Electrospinning is a popular technique used extensively for advanced tissue engineering scaffolds. Poly ( $\epsilon$ -caprolactone) (PCL) fiber scaffolds shown promising results to support osteoblast cells growth for improved bone regeneration [1]. Porosity of scaffolds and individual fibers are very important for cell attachment, growth and proliferation [2,3]. The aim of the study is verifying cell attachment to porous and non-porous fibers via observation of filopodia morphology using advance microscopy techniques.

### EXPERIMENTAL METHODS

#### Material

PCL was dissolved in chloroform and mixture of chloroform and dimethylsulfoxide (DMSO) in ration 90:10 v/v to produce a polymer concentration of 12% wt. in solution, for electrospinning of non-porous and porous fibers, respectively. Using electrospinning set-up EC-DIG (IME Technologies, Netherlands) we applied 14 kV to the stainless needle keeping the constant distance of 20 cm to the collector and the polymer solution flow rate at  $0.5 \text{ ml} \cdot \text{h}^{-1}$ .

#### Cell culture

Before cell seeding, fiber scaffolds were sterilized with UV light for 30 min. Human osteoblast-like cells (MG-63) were seeded in a density of  $2 \times 10^4 \text{ cell/cm}^2$  and cultured in DMEM culture media supplemented with 10% FBS, 1% amino acids, 1% glutamine and 2% penicillin streptomycin, for 3 days in a temperature of  $37^\circ\text{C}$  and humidity of 95% in 5%  $\text{CO}_2$  atmosphere.

#### Microscopy

PCL fibers and scaffolds with cells were characterized using scanning electron microscope (SEM, Merlin Gemini II, Zeiss) and fluorescence microscopy (Inverted light microscope IB-100, Delta Optical). Prior fluorescence imaging samples were stained with 50% HOECHST solution in PBS for 30 min. and rinsed in PBS afterwards. The structure of scaffolds and cells integration with fibers was investigated with 3D tomography based on SEM with focused ion beam (FIB-SEM).

### RESULTS AND DISCUSSION

PCL fibers were successfully produced using different polymer solvents. Addition of DMSO resulted in pores formation on PCL fibers. The microscopy investigations showed that porosity of PCL fibers increased cell attachment and proliferation in comparison to non-porous fibers. Moreover, porosity of fibers influenced cell morphology and grow by filopodia formation and wrapping around fibers as shown in Fig. 1. This porosity increased the cells integration as the filopodia have more edges to attach, allowing cells easier

migration in scaffolds. Additionally, 3D tomography results gave possibilities to verify in details cell attachment mechanism to fibers with porosity and without.

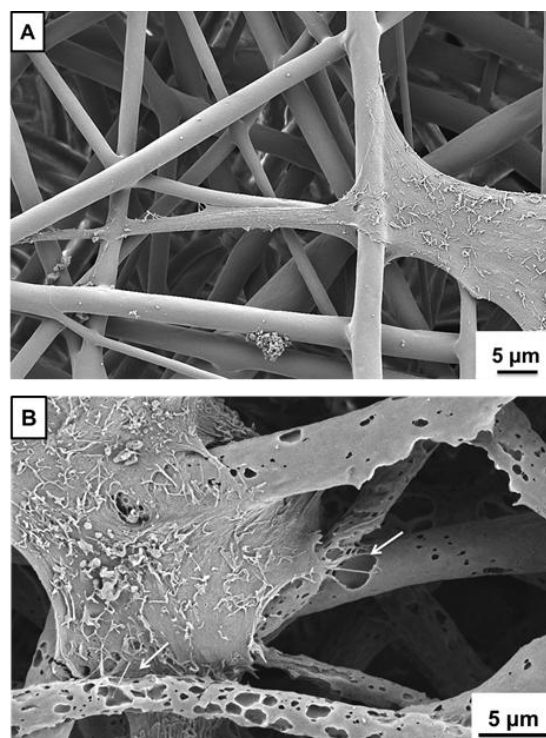


Fig. 1. SEM micrographs of filopodia integration with PCL fibers A) without porosity, B) with porosity, after 3 days of cell culture.

### CONCLUSION

Cells attachment and proliferation are strongly affected by PCL fibers morphology. Microscopy studies shown increased cells proliferation on porous in comparison to non-porous PCL fibers. In summary, the hierarchical roughness within tissue scaffolds favors cells proliferation, confirming a potential in bone regeneration.

### REFERENCES

1. Wang J. *et al.*, J. Biomed. Mater. Res. A. 93(2): 753-762, 2009
2. Ma P.X. *et al.*, J. Biomed. Mater. Res. 46(1): 60-72, 1999
3. Stachewicz U. *et al.*, Mater. Sci. Eng. C. 2017, *in pres.* doi.org/10.1016/j.msec.2017.08.076

### ACKNOWLEDGMENTS

The study was conducted within the funding SONATA 8 project granted by National Science Centre in Poland NO. 2014/15/D/ST5/02598

## Formation of 3D Porous Scaffolds Based on Pectins for Tissue Engineering

Aliaksandr Kraskouski<sup>1</sup>, Alexandr Zhura<sup>2</sup>, Kseniya Hileuskaya<sup>1</sup>, Viktoryia Kulikouskaya<sup>1</sup>, Stanislau Tratyak<sup>2</sup>, Vladimir Agabekov<sup>1</sup>

<sup>1</sup>Institute of Chemistry of New Materials, NAS of Belarus, Belarus

<sup>2</sup>Belarusian State Medical University, Belarus

[aleks.kraskovsky@gmail.com](mailto:aleks.kraskovsky@gmail.com)

### INTRODUCTION

Highly porous 3D scaffolds made of biopolymers are of great interest in tissue engineering applications<sup>1,2</sup>. Creation of biocompatible and biodegradable carriers, to which mesenchymal stem cells (MSCs) show high adhesion without loss of its functional properties<sup>3</sup>, is one of the most rapidly progressing fields of regenerative medicine. Natural biopolymers, such as polysaccharides, are promising materials for tissue regeneration<sup>4</sup>. The aim of this work was to produce biodegradable porous pectin-based scaffolds using freeze-drying method.

### EXPERIMENTAL METHODS

To form the scaffolds, 3% pectin (high methoxylated (Pect-HM), low methoxylated (Pect-LM) or amidated (Pect-A)) solutions, containing glycerol, were poured into 35 mm plastic Petri dishes, frozen and freeze-dried for 8 hours. Glycerol was used as a porogen, the pectin:glycerol weight ratio was 6:1. The dried scaffolds were cross-linked with solution of calcium chloride in 75% ethanol for 1 hour, washed with 75% ethanol twice and 96% ethanol once for 10 min. The pectin:CaCl<sub>2</sub> weight ratio was 1:1 and 1:10. The scaffolds were then dried at 50°C. The morphology of the scaffolds was studied using scanning electron microscope (SEM) (JEOL, JCM-6000Plus, Japan). Samples were covered by platinum and SEM images were made with resolution 200 µm. The density and porosity of the scaffolds were determined by liquid displacement method<sup>2</sup> with ethanol as the displacement liquid.

### RESULTS AND DISCUSSION

SEM images showed the interconnected porous structure of prepared "sponge-like" scaffolds with pore size of 70,0±21,0 µm in case of Pect-LM and Pect-A, and 123,0±21,0 µm in case of Pect-HM. The obtained scaffolds were soluble in water and physiological media. To increase the stability of the obtained scaffolds, pectin chains were cross-linked with Ca<sup>2+</sup>. It has been determined that after cross-linking the porous structure of the scaffolds was preserved (Fig. 1). However, for Pect-HM scaffold the decrease in the pore size depending on the concentration of Ca<sup>2+</sup> was shown. Thus, the pore size was 84,0±31,0 and 54,0±14,0 µm for the pectin:CaCl<sub>2</sub> ratio of 1:1 and 1:10 respectively. The Pect-A scaffolds had a non-uniform structure compared with homogeneous structure of Pect-HM and Pect-LM scaffolds: at SEM images cavities were observed (Fig. 1c). The density of the initial and cross-linked scaffolds was about 30,0-37,0 mg/cm<sup>3</sup>, except for the Pect-HM scaffold, whose density was about 44,0 mg/cm<sup>3</sup> upon pectin:CaCl<sub>2</sub> ratio of 1:10. The porosity of all prepared scaffolds was 80-95 %. It has been found

that the increase in the concentration of calcium chloride leads to the increase in the porosity of the materials. The scaffolds based on Pect-LM were less porous.

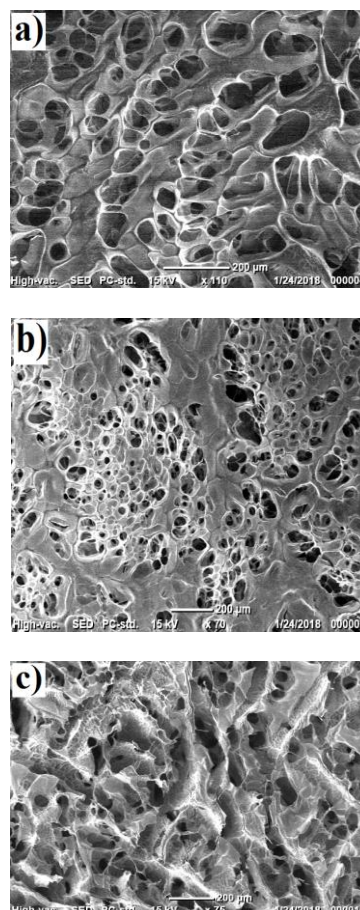


Fig. 1. SEM images of the scaffolds based on Pect-HM (a), Pect-LM (b) and Pect-A (c). The pectin:CaCl<sub>2</sub> weight ratio was 1:1.

All porous scaffolds showed adhesion of 70-80% rat stem cells while culturing in Dulbecco medium during 3 hours. The stem cells were viable and didn't lost ability to growth.

### CONCLUSION

The biocompatible porous scaffolds based on pectins, cross-linked with calcium chloride, were obtained using freeze-drying method. The prepared scaffolds may be appropriate for tissue engineering applications.

### REFERENCES

1. Ninan N. *et al.*, Carbohydr. Polym. 98:877-885, 2013.
2. Kaczmarek B. *et al.*, Polym. Test. 65:163-168, 2018.
3. Liu Zh.-M. *et al.*, Macromol. Biosci. 10:1043-1054, 2010.
4. Coimbra P. *et al.*, Int. J. Biol. Macromol. 48:112-118, 2011.



## Melt Processing and Characterization of Tricalcium phosphate filled Polybutylene adipate-co-terephthalate / Polymethyl methacrylate Composites for Biomedical Applications

Ravichandran Kandaswamy, Girija Bheemaneni

Department of Rubber and Plastics Technology, Anna University, India

[ravi@mitindia.edu](mailto:ravi@mitindia.edu)

### INTRODUCTION

Polybutylene adipate-co-terephthalate (PBAT) is a biodegradable thermoplastic aliphatic-aromatic random copolyester having low modulus and stiffness, but has high flexibility and toughness and gaining importance in medical applications<sup>1</sup>. The flexibility and toughness of this polymer makes it ideal for blending with another polymer that have high modulus and strength, but are very brittle. The most significant reason for blending PBAT as the flexible complement to other polymers is it will preserve biodegradability; as long as both copolymers can degrade, the blended copolymer will also degrade. Polymethyl methacrylate (PMMA) is a brittle polymer and has a good degree of biocompatibility with human tissues and prominently used in artificial lenses, bone and dental applications, but has limited bioactivity<sup>2</sup>. Blending PBAT with PMMA reduces the brittle nature of PMMA. To enhance the bioactivity of the polymer, ceramic particles can be introduced into the polymer matrices which improves the bioactive property. One such material is tricalcium phosphate (TCP) which are biodegradable and biocompatible. In this present work, PBAT/PMMA/TCP composites were fabricated and characterized for its tensile and bioactivity properties.

### EXPERIMENTAL METHODS

**Materials:** PBAT resin Ecoflex F BX 7011 BASF, PMMA resin Sumiplex ME from Sumitomo Chemicals and tricalcium phosphate from Loba Chemie were used for preparing composites. The chemicals used for cytotoxicity assay was purchased from cell clone, India. 3-(4,5-dimethylthiazol-2-yl)-2,5-diphenyltetrazolium bromide (MTT) assay, Dulbecco's modified Eagle's medium (DMEM), Phosphate buffered saline (PBS) pH 7.4, distilled water and all other chemicals used for the preparation of SBF solution were purchased from Sigma Aldrich, India and used without any purification. Squamous epithelial cells extracted naturally from the recipients during the experiment.

**Fabrication of PBAT/PMMA/TCP composites:** PBAT and PMMA was melt blended in 50:50 wt. % ratio using Brabender Plasticoder at 200°C at 30 rpm and 70 rpm screw speed for 10 min. The developed blend were filled with (1, 3, 5 and 7 wt. %) tricalcium phosphate filler. Composite sample sheets of thickness 1mm were prepared by compression moulding at mould temperature 150°C. The composites were characterized for FTIR, water absorption and soil burial test. Tensile properties were measured using as per ASTM D 638 using Tinius Olsen-UTM at a cross-head speed 50 mm/min. Hardness were measured as per ASTM D2240 using Durometer Shore A hardness tester. Bioactivity of the composites were measured by immersing the samples into the freshly prepared SBF solution for 7 days at 37°C and then dried in oven at 40°C for 4h and examined under Scanning Electron Microscopy SEM (SEM-JEOL JSM 850) and

Elemental analysis by Energy dispersive Analysis of X-ray (EDAX) for the confirmation of the calcium phosphate layer formation on the surface of the composites. MTT (3-[4, 5-dimethylthiazol-2-yl]-2, 5 diphenyltetrazolium bromide; thiazolyl blue) was used to evaluate the cytotoxicity nature of the samples. The squamous epithelial cells were isolated aseptically from six healthy volunteers and then, cells were dissolved in 1x PBS and centrifuged at 3000rpm for 10min. The cells were mixed with DMEM. Different concentrations (265mg, 539mg, 766mg, and 1040mg) of composites were added to the 10,000 cells of squamous epithelial cells contain eppendorf and incubate for 2hrs. After incubation the reaction mixture was removed by centrifugation and 100µl of MTT ((5mg/mL) was added to cell pellet contains eppendorf and incubated for 2hrs. After incubation, MTT was removed by centrifugation. Finally, 300µl of DMSO was added to the each tube and dissolve the final product formazan. The colored solution was transferred into 96 well culture plates. The absorbance was measured at 570nm using Bio-Rad Colorimeter.

### RESULTS AND DISCUSSION

FTIR spectrum of PBAT/PMMA blend show peak at wave number 2951 cm<sup>-1</sup> due to C-H stretching which obtained in between 2961 cm<sup>-1</sup> for PBAT and 2926 cm<sup>-1</sup> for PMMA respectively. The peak for C=O of ester group was observed at 1720 cm<sup>-1</sup> for the blend similar to 1713 cm<sup>-1</sup> and 1737 cm<sup>-1</sup> for PBAT and PMMA respectively. The appearance of peak at 1273 cm<sup>-1</sup> was considered to be due to C-O stretching which was shifted from the 1267 cm<sup>-1</sup> position observed in the spectrum of PBAT. Addition of filler into the blend matrix increases the tensile strength and hardness. In-vitro bioactivity of the composites was evaluated by examining the deposition of hydroxyapatite on the surface after soaking in SBF fluid, which confirmed by SEM and EDAX for the formation of the calcium phosphate layer. Soil burial test of the composites at 10, 20, 30, 40, 50 and 60 days, exhibits more fragments than the individual polymers. Water absorption of the composites in PBS, tap water and distilled water is less than 2%. The MTT assay cytotoxicity test of the composites does not release toxic elements into the medium containing squamous epithelial cells.

### CONCLUSION

PBAT/PMMA/TCP was physically blended and shows an improvement in tensile properties Bioactivity nature was confirmed by the formation of calcium phosphate layer. Cytotoxicity test of the composites does not release toxic elements into the medium containing squamous epithelial cells and the composites can be used suitably for biomedical applications.

### REFERENCES

1. Fukushima K. *et al.*, J. Polym. Res. 20:302, 2013
2. Park J.B. Ann. Biomed. Eng. 20(6):583, 1992

## Tuning the Mechanical Properties of Alginate-Peptide Hydrogels

Guy Ochbaum<sup>1</sup>, Ronit Bitton<sup>1,2</sup>

<sup>1</sup>Department of Chemical Engineering, Ben-Gurion University of the Negev, Beer-Sheva 84105, Israel

<sup>2</sup>Ilse Katz Institute for Nanoscale Science and Technology, Ben-Gurion University of the Negev, Beer-Sheva 84105, Israel  
[ochbaumg@post.bgu.ac.il](mailto:ochbaumg@post.bgu.ac.il)

### INTRODUCTION

The challenge in development of surrogate ECMs is to design and prepare synthetic materials capable of influencing cell differentiation, survival and migration through both biochemical interactions and mechanical cues. Current effort in the engineering of synthetic ECM has focused on installing molecular features (peptides) within insoluble scaffolds, either by self-assembly or through covalent modifications of polymer. Apart from inflicting bioactivity, incorporating biomolecules a tissue engineering scaffold may also cause a change in its physical properties, which will indirectly lead to a change in its bioactivity, as hierarchical structural organization and mechanical properties have been shown to affect cellular response to them.

Alginate, a polysaccharide that gels in the presence of divalent ions has been used as an artificial bio-surrounding similar to the natural Extra Cellular Matrix; Covalent bonding peptides to alginates is routinely used tailor alginate's biofunctionality. Here, we investigate the possibility of tuning the mechanical properties of alginate-peptide gels by altering the sequence of the covalently bound peptide.

### EXPERIMENTAL METHODS

We present a systematic investigation of the effect of three RGD-containing peptides, G<sub>6</sub>KRGDY, A<sub>6</sub>KRGDY and V<sub>6</sub>KRGDY, on the physical properties of alginate hydrogels. Characterization of these hydrogels was done by using Small angle X-ray scattering (SAXS) and rheology.

### RESULTS AND DISCUSSION

Alginate/peptide hybrids were prepared by two methods: 1) Covalent binding of the peptide to the alginate backbone (such hybrids were designated 'alginate-peptide'), and 2) direct mixing of peptide and alginate solutions (such hybrids were designated 'alginate + peptide').

Frequency sweep scans of the all the samples (Figure 1) are characteristic of a gel. Comparing storage modulus G' (i.e. gel stiffness) of alginate+peptide gels to that of Alginate-peptide gels shows that for the A<sub>6</sub>KRGDY and V<sub>6</sub>KRGDY peptides, the storage modulus of the alginate-peptide gels was an order of magnitude higher than that of the alginate+peptide gels. In the case of the alginate/G<sub>6</sub>KRGDY gels the G' of alginate-G<sub>6</sub>KRGDY gel was also higher than that of the alginate+G<sub>6</sub>KRGDY gel, yet the differences between the last two is much smaller.

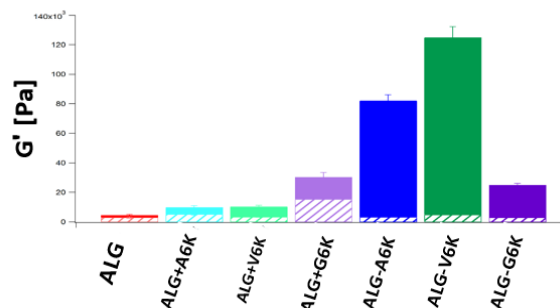


Fig. 1. Trend for the storage modulus at  $\omega = 10$  rad/s during frequency sweep test in water (Solid) and PBS (patterns).

Kratky plots of the SAXS data obtained from alginate peptide gels (Fig. 2) show a peak, representing the presence of frozen inhomogeneities in the gel network followed by a straight line characteristic of worm-like chains. The differences between the scattering curves suggest the origin to the differences in the gels' stiffness are the differences between their cross-linked zones.

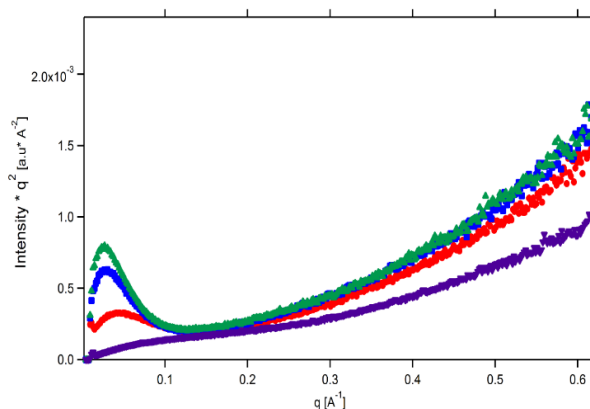


Fig. 2. Kratky plots for alginate gels. Alginate (●), alginate-A<sub>6</sub>KRGDY (■), alginate-V<sub>6</sub>KRGDY (▲) and alginate-G<sub>6</sub>KRGDY (▼) formed by covalent binding.

### CONCLUSION

Our results showed that the ability of peptides to self-assemble in aqueous solutions (i.e. the peptide sequence) is an important factor in tuning the mechanical properties of alginate/peptide gels. Therefore, a detailed structural analysis of the conjugated architecture in solution can be used as a tool to tailor the properties of alginate/peptide hybrid hydrogels.



## Double-Layered Polymer Scaffolds Fabricated by Combination of Electrospinning and Thermally Induced Phase Separation

Patrycja Domalik-Pyzik, Anna Morawska-Chochół, Jan Chłopek

Department of Biomaterials and Composites, Faculty of Materials Science and Ceramics,  
AGH University of Science and Technology, Krakow, Poland  
[pdomalik@agh.edu.pl](mailto:pdomalik@agh.edu.pl)

### INTRODUCTION

For many years now, vascular grafts made of synthetic polymers have been successfully used for the replacement of large diameter blood vessels. However, such synthetic grafts are not suitable for small diameter ( $id < 6$  mm) blood vessels due to increased risk of intimal hyperplasia and thrombus formation<sup>1</sup>. Hence, tissue engineering approach, in which small vessels could be regenerated on the basis of 3D scaffolds, seems a promising alternative. To resemble the structure of a native blood vessel that consists of three distinct layers, researchers work on the development of various multi-layered scaffolds. With increasing interest in electrospinning many of those attempts are based on spinning layers of different polymers<sup>2</sup>. However, this results in production of only one type of microstructure, usually with low porosity. Highly porous scaffolds can be produced using thermally induced phase separation – simple and cost-effective method, but not without disadvantages. Increased porosity is beneficial in terms of cell penetration but it also comes with poor mechanical properties. Compromise can be achieved by using both methods<sup>3</sup>.

In this study small calibre vascular scaffolds, with double-layered structure, were fabricated by combining electrospinning (ES) and thermally induced phase separation (TIPS).

### EXPERIMENTAL METHODS

The inner layer of the proposed scaffold was produced by electrospinning polycaprolactone (PCL) solution (5 wt% in chloroform:methanol 2:1). The porous outer layer was produced using the TIPS method: polylactide solution (2.5 wt% in dioxane) was poured into the moulds containing electrospun PCL tubes. The moulds were placed in a  $-80$  °C refrigerator for 6 h and freeze-dried for 96 h. Microstructure of the scaffolds (porosity, pore and fibre diameter and orientation) was characterized with scanning electron microscopy and ImageJ software. Mechanical properties including tensile strength, Young's modulus, compliance and suture retention strength were evaluated using universal testing machine Zwick 1435.

### RESULTS AND DISCUSSION

We have proposed a method for fabrication of small calibre vascular scaffolds that uses both: electrospinning and thermally induced phase separation and results in double-layered structure of the scaffold.

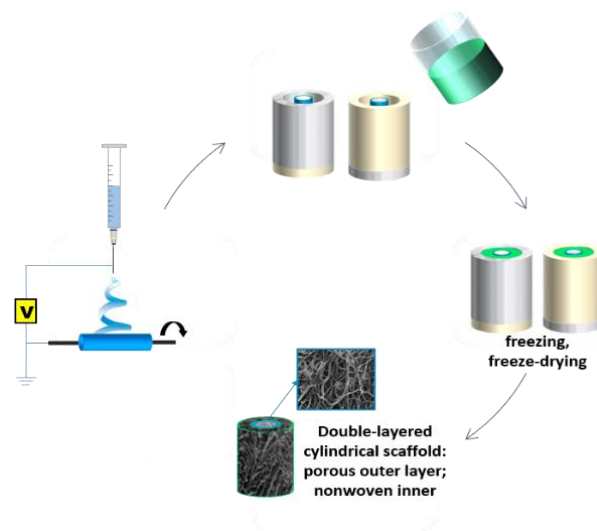


Figure 1 shows scheme of the scaffold preparation process. Nonwoven PCL tubes were produced by electrospinning. Different materials (stainless steel and Teflon) used for the construction of the moulds (e.g. inner shaft and bottom plate made of PTFE, outer cylinder made of SS) used in the TIPS method allowed to create temperature gradient and resulted in different pores orientation of the scaffolds outer layer. Mechanical properties of the double-layered scaffolds matched parameters of the native vessels.

### CONCLUSION

Asymmetric construction of the proposed scaffolds resembles structure of a native blood vessel and creates different conditions for growth and proliferation of EC and SMC. Utilisation of such simple manufacturing methods like electrospinning and freeze-drying as well as use of medically verified biodegradable polymers (PLA and PCL) opens possibilities for further modifications.

### REFERENCES

1. Lin JH. *et al.* Material Letters. 190:201-204, 2017.
2. McClure MJ. *et al.* Acta Biomater. 6(7):2422-33, 2010.
3. Domalik-Pyzik P. *et al.* Eng Biomater. 120:2-7, 2013.

### ACKNOWLEDGMENTS

This research was financed by the Dean grant No. 15.11.160.019 of Faculty of Materials Science and Ceramics, AGH University of Science and Technology.

## Development of Cryopreserved Cell-laden Scaffold Using a Cell Printing System Supplemented with Low-temperature Processing Method

JaeYoon Lee<sup>1</sup>, Minseong Kim<sup>1</sup>, Gi Hoon Yang<sup>1</sup>, Miji Yeo<sup>1</sup>, WonJin Kim<sup>1</sup>, JiUn Lee<sup>1</sup>, YoungWon Koo<sup>1</sup>, Hae Ri Kim<sup>1</sup>, YoungEun Choe<sup>2</sup> and GeunHyung Kim<sup>1\*</sup>

<sup>1</sup>Department of Biomechatronic Engineering, Sungkyunkwan University, South Korea

<sup>2</sup>Department of New Material Engineering, Chosun University, Gwangju, South Korea

[dlwodbsdbs@gmail.com](mailto:dlwodbsdbs@gmail.com)

### INTRODUCTION

One of the specific issues of ideal wound healing scaffold should be prepared in short period. Because rapid healing could prevent the possibility of infection, scar and irreversible loss of damaged tissue<sup>1</sup>. Premade and preserved scaffold is one of the solution for this issue. In this study we fabricate a cryopreserved cell-laden scaffold with hollow structure.

### EXPERIMENTAL METHODS

We used coaxial nozzle for dispensing cell and cell preservation solution in the core region, and gelatin methacrylate (GelMA) in the shell region for structure support and rapid gelation. To obtain optimum processing conditions, various low temperatures from -5°C to -30°C were applied to the working stage. In addition, the rapid temperature change during processing was a critically important parameter affecting initial cell viability. To reduce this effect, we used various cooling temperature before the cell-laden solution was printed onto low-temperature plate.

### RESULTS AND DISCUSSION

Following 2 weeks of cryopreservation, the cells (osteoblast-like-cells or human adipose stem cells) in the scaffold showed good viability (over 90%), steady growth, and similar mineralization to that of a control scaffold fabricated using a conventional cell-printing process without cryopreservation.

### CONCLUSION

In this study, an innovative cell printing process supplemented with a microfluidic channel, a core/shell nozzle, and low temperature working stage was proposed to obtain a cell-laden collagen scaffold for cryopreservation. By controlling various processing factors, such as the temperature of microfluidic channel, working plate temperature, flow rates in core and shell region, and nozzle moving speed, a porous cell-laden scaffold (core: cell-laden collagen/DMSO, shell: GelMA) with high cell viability could be successfully fabricated.

### REFERENCES

1. Karlsson, J. O., & Toner, M. (1996). Long-term storage of tissues by cryopreservation: critical issues. *Biomaterials*, 17(3), 243-256.

### ACKNOWLEDGMENTS

This study was supported by a grant from the Ministry of Trade, Industry & Energy (MOTIE, Korea) under Industrial Technology Innovation Program (No. 10063541: Development of bioceramic 3D printing materials and low temperature (<40 °C) process customized by implant sites) and was supported by a fund by Research of Korea Centers for Disease Control and Prevention.

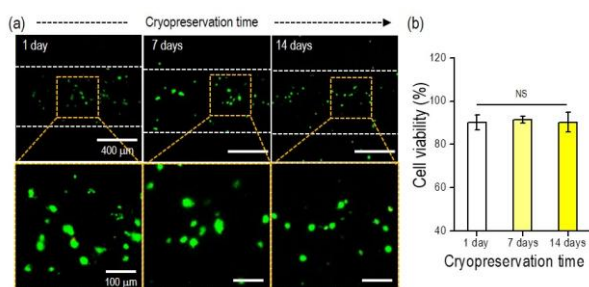


Fig. 1. (a, b) Cell viability analyzed by live (green)/dead (red) assay of the scaffolds cryopreserved for 1, 7, and 14 days. NS means statistical non-significance.

## Plasma Modification of PCL Fiber Mats and the Possibility of a Graded Functionalization

Sarah Oehmichen<sup>1</sup>, Anna Lena Hoheisel<sup>2</sup>, Steffen Sydow<sup>1</sup>, Nadeschda Schmidt<sup>3</sup>, Birgit Glasmacher<sup>2</sup>, Peter Behrens<sup>3</sup>, Henning Menzel<sup>1</sup>

<sup>1</sup>Institute of Technical Chemistry, TU Braunschweig, Germany

<sup>2</sup>Institute for Multiphase Processes, Leibniz Universität Hannover, Germany

<sup>3</sup>Institute for Inorganic Chemistry, Leibniz Universität Hannover, Germany

[oehmichen@tu-braunschweig.de](mailto:oehmichen@tu-braunschweig.de)

### INTRODUCTION

For tissue engineering applications, in particular for an application as a cell instructive implant, electrospun fiber mats have to be functionalized in a way that they release for example signalling proteins with a gradient. Therefore, concepts for the generation of graded surface properties on such fiber mats has gained a lot of interest in the recent years<sup>1</sup>.

### EXPERIMENTAL METHODS

#### Plasma modification of PCL fiber mats

Poly( $\epsilon$ -caprolactone) (PCL) fiber mats were prepared by electrospinning as described previously.<sup>2</sup> A plasma oven was used to modify the fiber mats. First experiments were performed with a plasma power of 8 to 80 W and a treatment time of 1 to 60 s. To generate a wettability gradient a mask technique was used, where the mask was moved stepwise. Ultrapure water was used to determine the contact angle (CA). Three samples were measured per plasma program and three drops of ultrapure water measured on each mat.

#### Immobilization of nanoparticles

To immobilize polymer based chitosan-tripolyphosphat (CS/TPP)<sup>2</sup> and inorganic nanoporous silica nanoparticles (NPSNP)<sup>2</sup> the plasma modified fibers were incubated in the nanoparticle suspension and dried after washing<sup>2</sup>. The immobilization was proved by confocal laser scanning microscopy (CLSM) and scanning electron microscopy (SEM).

### RESULTS AND DISCUSSION

#### Plasma modification of PCL fiber mats

The influence of power and duration of the plasma treatment on the wettability of the sample surface was investigated. The contact angles decrease with power and treatment time increasing (Fig. 1). With higher intensity of treatment (e.g. 30 W\_30 s) it is possible to obtain a completely wettable surface (CA = 0°).

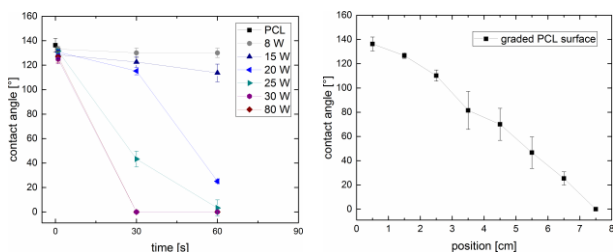


Fig. 1. CA as a function of plasma power and time (left) and progression of the CA of a PCL fibre mat treated with mask technique (1 cm corresponds to an increase in irradiation time of 15 s, right).

Using a mask technique, i.e. after 15 s of irradiation with 20 W the mask was moved by 1 cm, a surface with

graded wettability was produced. Fig. 1 shows the gradient along the sample, from the hydrophobic starting material at 0.5 cm ( $CA_{0.5\text{ cm}} = 136^\circ$ ) to a hydrophilic surface at 7.5 cm ( $CA_{7.5\text{ cm}} = 0^\circ$ ). These trends correspond well to the work of PITT<sup>3</sup> and CANTINI<sup>4</sup>.

#### Immobilization of nanoparticles

The immobilization of the CS/TPP-NP (Fig. 2a) and the NPSNP was proven by microscopic methods. The inorganic nanoparticles can be clearly identified in the SEM image (Fig. 2b). However, the CSS/TP NP transform into a homogeneous films, which is not clearly detectable by SEM. Therefore, fluorescently labelled CS/TPP NP in combination with CLSM were used to prove the functionalization (Fig. 2a).

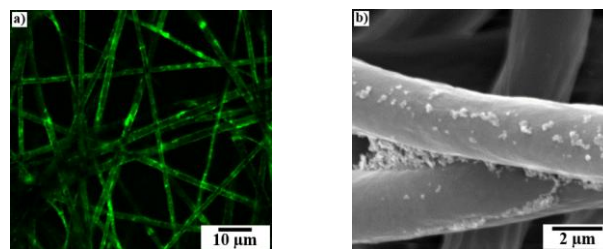


Fig. 2. a) CLSM image of CS/TPP nanoparticles; and b) SEM image of NPSNPs immobilized on plasma modified (30W\_60s) PCL fiber mat.

### CONCLUSION

It was shown that plasma treatment changes the wettability of PCL fiber mats depending on the plasma power and treatment time. With this knowledge and the use of a mask, a gradient from a hydrophobic to a hydrophilic surface can be generated. We are also able to immobilize two types of nanoparticles, which are potential drug release systems<sup>2</sup>. Thus, the methodology might be used to prepare implants, which can release drugs in a spatially and temporally graded way.

### REFERENCES

1. Khang G., Biosurface and Biotribology 1:202-213, 2015
2. de Cassan D., et al., Colloids Surf. B Biointerfaces in press, 2017
3. Pitt W.G., J. Colloid Interface Sci. 113:223-227, 1989
4. Cantini M. et al., Biomater. Sci. 1:202-212, 2013

### ACKNOWLEDGMENTS

This research project has been supported by DFG Research Unit FOR 2180 „Graded Implants for Tendon-Bone Junctions“. We also want to thank Robert Hänsch for CLSM measurements.

## Fabrication of Fibrous 3D Collagen Scaffold Mimicking Extracellular Matrix Using Electrohydrodynamic Jet Process for Tissue Regeneration

Minseong Kim<sup>1</sup>, Gi Hoon Yang<sup>1</sup>, JaeYoon Lee<sup>1</sup>, Miji Yeo<sup>1</sup>, WonJin Kim<sup>1</sup>, YoungWon Koo<sup>1</sup>, JiUn Lee<sup>1</sup>, HaeRi Kim<sup>1</sup>, YoungEun Choe<sup>2</sup>, and GeunHyung Kim<sup>1\*</sup>

<sup>1</sup>Department of Biomechatronic Engineering, College of Biotechnology and Bioengineering, Sungkyunkwan University (SKKU), Suwon, Republic of Korea

<sup>2</sup>Department of Material Science and Engineering, Chosun University, Gwangju, Korea

[hshomuboy@gmail.com](mailto:hshomuboy@gmail.com)

### INTRODUCTION

Collagen, the main component of extracellular matrix (ECM), plays a role as cell attachment, migration and differentiation of tissue. Thereby, collagen has been used to produce structures similar with topological structure to ECM in tissue engineering.<sup>1</sup> However, fabricating structures similar with ECM by using collagen is necessary to use a high toxic solvent.<sup>2</sup> Therefore, the cell survival rate is low and it has limitation to apply in tissue engineering due to fabricating only in two dimensional (2D) mat structures. To solve these problems, Kim et al. selected low toxic materials and fabricated three dimensional (3D) fibrous collagen scaffolds by electrohydrodynamic (EHD) jet process. In order to use pure collagen with low electrical conductivity, it was mixed with high conductive polymers to form EHD jet process so that fibrous collagen scaffolds were fabricated by dissolving high conductive polymers. To ensure the stability of the fabrication process, various parameter studies (flow rate, electric field, height, feeding speed etc.) were conducted. When nerve cells were cultured on the fabricated 3D fibrous collagen scaffolds, 2D fabricated collagen mats and solid free-form process go higher cell activation and differentiation results than structures with similar topological structures. Through this, 3D fibrous collagen scaffolds may play a potential role in future nerou-regenerative medicine.

### EXPERIMENTAL METHODS

In the study, type-I collagen from porcine tendon was obtained from Bioland Inc. (Matrixen-PSP; Bioland Inc., Cheonan, South Korea). Poly(vinyl alcohol) (Mn = 89,000 – 98,000 g/mol) and poly(ethylene oxide) (Mn = 900,000 g/mol) were purchased from Sigma-Aldrich Co. (St. Louis, USA).

A printing speed of 5 mm/s was controlled using a three-axis printing system (DTR3-2210 T-SG, DASA Robot, Seoul, South Korea). The power supply (SHV 300RD-50K; Convertech, Seoul, South Korea) was used to provide the electric field. The EHD jet process used ethanol as a target medium with a grounded copper plate. After EHD jet processing, the collagen 3D fibrous structure were cross-linked by using 50 mM EDC solution in ethanol for 1 h at room temperature. The collagen structures were washed three times with distilled water in a 4 h interval at 37°C, and were freeze-dried at –76°C for 12 h.

To ensure the stability of the fabrication process, various parameter studies (flow rate, electric field, height, feeding seed etc.) were conducted. Also, nerve cells (PC12) were cultured on the fabricated 3D fibrous

collagen scaffolds to check higher cell migration and differentiation.

### RESULTS AND DISCUSSION

To fabricate cylindrical struts consisting of micro/nanofibrous bundles of collagen, we used a previously described EHD jet process.<sup>3,4</sup>

We observed the effects of various electric field intensities, feeding flow rate of the collagen solution and distance between nozzle and ground. Based on the various process parameters study result, the optimal processing condition could be selected to successfully achieve a controllable mesh structure consisting of collagen microfibers.

To demonstrate its feasibility as a biomedical scaffold, cellular activities on the 3D fibrous collagen structure were assessed *in vitro* test. We determined cell-seeding efficiency, metabolic activities, and performed a fluorescence analysis.

### CONCLUSION

In this study, a novel fibrous scaffold that consisted of collagen was manufactured and assessed by using and electrohydrodynamic jet process supplemented with ethanol. In the study, a reasonable processing window for the various processing parameters, including electric field, processing height, flow rate, and even nozzle diameters, was selected. By selecting optimal processing conditions, we produced a multi-layered collagen structure consisting of cylindrical struts entangled with micro/nanofibrous collagen. The collagen fibrous scaffold exhibited significantly higher cell-seeding efficiency and metabolic activities compared with the control. These results suggest that the 3D fibrous collagen scaffold described may be useful in soft tissue regeneration.

### REFERENCES

1. G. A. Di Lullo et al., *J. Biol. Chem.* 277:4223-4231
2. J. A. Matthews et al., *Biomacromolecules*, 3:232-238
3. M. Kim et al., *Langmuir*, 30: 8551-8557
4. M. Kim et al., *Chem. Eng. J.* 279:317-326, 2015

### ACKNOWLEDGMENTS

This study was supported by a grant from the Ministry of Trade, Industry & Energy (MOTIE, Korea) under Industrial Technology Innovation Program (No. 10063541: Development of bioceramic 3D printing materials and low temperature (<40 °C) process customized by implant sites) and was supported by a fund by Research of Korea Centers for Disease Control and Prevention.



## Production of the GO-doped PLA-based nanofibers and investigation of their electrical properties

Sertan Ozen<sup>1,2</sup>, Mehmet Onur Aydogdu<sup>1,3</sup>, Zeynep Ruya Ege<sup>1,4</sup>, Sümeyye Cesur<sup>1,3</sup>, Umit Kemalettin Terzi<sup>5</sup>, Hayriye Korkmaz<sup>5</sup>, Nazmi Ekren<sup>1,5</sup>, Faik Nüzhet Oktar<sup>1,6</sup>, Osman Kilic<sup>7</sup>, Beyhan Kilic<sup>8</sup>, Oguzhan Gunduz<sup>1,9</sup>

<sup>1</sup>Advanced Nanomaterials Research Laboratory, Marmara University, Turkey

<sup>2</sup>Department of Electrical and Electronic Engineering, Master of Science, Institute of Pure and Applied Sciences, Marmara University, Turkey

<sup>3</sup>Department of Metallurgical and Materials Engineering, Institute of Pure and Applied Sciences, Marmara University, Turkey

<sup>4</sup>Department of Biomedical Engineering, Faculty of Engineering, Istanbul University, Turkey

<sup>5</sup>Department of Electrical and Electronic Engineering, Faculty of Technology, Marmara University, Turkey

<sup>6</sup>Department of Bioengineering, Faculty of Engineering, Marmara University, Turkey

<sup>7</sup>Department of Electrical and Electronics Engineering, Faculty of Engineering, Marmara University, Turkey

<sup>8</sup>Department of Electrical Engineering, Yıldız Technical University, Turkey

<sup>9</sup>Department of Metallurgical and Materials Engineering, Faculty of Technology, Marmara University, Turkey

[ozensertan@gmail.com](mailto:ozensertan@gmail.com)

### INTRODUCTION

Graphene is a two-dimensional (2-D) sheets consisted by thin layers of pure carbon. Due to its exceptional electrical, mechanical, thermal and barrier properties, it has been a very popular material and already used in various applications [1]. Its Young modulus is 1 Tpa and ultimate strength is nearly 130 GPa[2]. Therefore, graphene can be promising for developing strong nano materials. Additionally, composite materials also have ability to combine beneficial features of different materials in one final product. Therefore, using a polymeric material together with graphene can enable production of the composite graphene nanofibers. In this study graphite was oxidized by the Hummer's method in order to obtain excess amount of graphene. By reducing of Graphite oxide (GO) with hydrazine, Reduce Graphene Oxide (rGO) was fabricated.

Fibers was tailored using coaxial electrospinning method to obtain amplified features such as high mechanical properties and thermal stability. As a difference from the current studies, natural BHA which was obtained from bovine bone used instead of synthetic HA.

### EXPERIMENTAL METHODS

GO was obtained by Hummer's Method. rGO was obtained by reduction procedure with Hydrazine. Poly(lactic acid (PLA) was prepared in chloroform. BHA was dissolved in Tetrahydrofuran (THF). rGO was dissolved in Dimethylformamide (DMF) with %1 and %0.5 ratio. PLA/rGO PLA/BHA/rGO nanofibers were produced by CES method. Fiber morphology were examined using scanning electron microscope (SEM). In order to evaluated of chemical differentiations of nanofibers fourier transform infrared spectrometer (FT-IR) spectra were recorded. Tensile tests of fibers were carried out. Electrical properties such as permittivity, dielectric loss and alternating current conductivity of the rGO containing nanofibers were analyzed. Cell culture test will be performed in order to determine their cytotoxicity and analyse the biocompatibility of the scaffolds.

### RESULTS AND DISCUSSION

GO and rGO that obtained by the Hummer's method were given by SEM images in Fig. 1(a,b).

The morphologies of the rGO reinforced electrospun composite nanofibers also were given by SEM at Fig. 1(c,d). Electrical properties were displayed in Fig. 2.

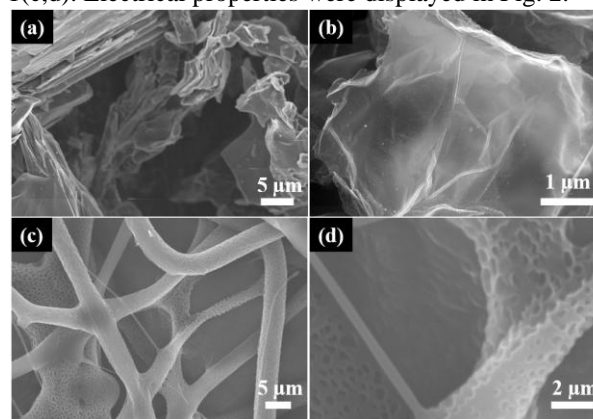


Fig. 1. SEM images of (a) GO (b) rGO (c)PLA/BHA/rGO (d) PLA/BHA/ high magnification.

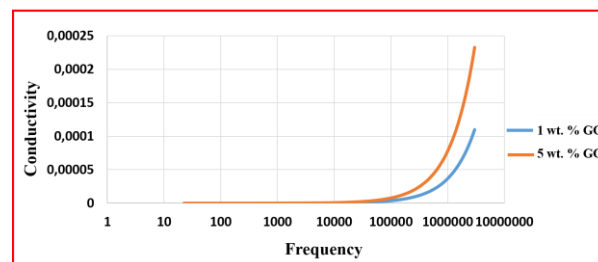


Fig. 2. AC conductivity curves of scaffolds with different GO ratios.

### CONCLUSION

PLA/BHA/rGO nanofibers were produced via CES technique. The stiffness and electrical properties of electrospun PLA/BHA/rGO composite nanofiber mats increased with the increase of rGO content. rGO based nanofiber can be potential to be used for tissue engineering.

### REFERENCES

- Novoselov K. et al., Proceed Natl Acad Sci., 102, 10451, 2005
- Lee, C. et al., Hone, J. Sci., 321, 385–388, 2008.

### ACKNOWLEDGMENTS

This work is founded from Ministry of Development, project number: 2016K121280.

## Fabrication and Antibacterial Activity of Films Based on Pectin-Ag Nanocomposites

Kseniya Hileuskaya<sup>1</sup>, Aliaksandr Kraskouski<sup>1</sup>, Alena Ladutska<sup>2</sup>, Galina Novik<sup>2</sup>, Vladimir Agabekov<sup>1</sup>

<sup>1</sup>Institute of Chemistry of New Material of National Academy of Sciences of Belarus, Belarus

<sup>2</sup>Institute of Microbiology of National Academy of Sciences of Belarus, Belarus.

k\_hilevskay@mail.ru

### INTRODUCTION

The worldwide escalation of bacterial multi-drug resistant to conventional medical antibiotics is a serious concern for modern medicine and veterinary. One of the promising approaches for overcoming bacterial resistance is the use of metallic nanoparticles, for example silver nanoparticles (AgNPs). It is known that AgNPs exhibit very strong antimicrobial activity. Nowadays, polymer-inorganic composite materials such as silver-containing thin films could be an answer to drug-resistant bacteria. Another effective way is the use of silver nanoparticles-antibiotic combinations<sup>1</sup>. In this paper, we describe the preparation and properties of polymer films based on the pectin-Ag nanocomposite and their use as a carrier for kanamycin (KAN).

### EXPERIMENTAL METHODS

Pectin-Ag nanocomposites based on pectins with different degrees of esterification and amidation (Citrus, DE 71%, Mv~141000; Amid, DE 32%, CA 18%, Mv~120000; Classic, DE 35-42%, Mv~89000) were synthesized by the "green chemistry" method<sup>2</sup>. The pectin:Ag weight ratio in the reaction mixture was 25:1, the silver concentration was 2,0 mM. The films were prepared by a casting evaporation technique from aqueous polymer solutions: premixed the pectin-Ag nanocomposite hydrosol with 3% solution of polyvinyl alcohol (PVA, Mw~30000, 66000 and 145000). The glycerol was used as a plasticizer in the weight ratio of PVA:glycerol=2:1. Antibiotic-containing films were prepared by adding a solution of kanamycin (15 mg/ml) to the mixture of pectin-Ag nanocomposite and PVA. The mixture was poured into the 90 mm Petri dishes and dried at 50 °C for 18 hours. The final concentration of kanamycin in the films was 1 mg/cm<sup>2</sup>. The kanamycin release from the films in physiological solution (0.9% NaCl) at 37 °C was investigated. Antibacterial activity against test strains of *B. pumilus*, *B. subtilis*, *E. coli*, *Ps. aeruginosa* was studied by well diffusion methods.

### RESULTS AND DISCUSSION

The resulting films had a smooth uniform morphology, a color from orange-yellow to brown-red and were stable to sterilization by 70% ethanol. The mass of obtained films was ~ 0.5 g and the thickness - 44-60 μm. The presence of surface plasmon resonance (SPR) band in the region of 424-445 nm in the absorption spectra of films indicates the presence of Ag<sup>0</sup> nanoparticles. In comparison with the initial hydrosols (λ<sub>max</sub> = 410-415 nm), a shift of the SPR maximum of films to the long-wave region was observed. This shift was caused by changes in the AgNPs environment. The entrapped kanamycin in the pectin-Ag/PVA films did not reduce its bioavailability and allowed

prolonging release in physiological saline of 0.9% NaCl pH 5.5 up to 180 min. The release rate of KAN from the films was essentially independent of the PVA molecular weight and the nanocomposite type.

It was found that the obtained films exhibited antibacterial activity against selected strains (Fig. 1). The type of nanocomposite affected the activity of the films, which did not depend on the PVA molecular weight. Thus, the largest growth-inhibiting effect for films based on Ag-Citrus nanocomposite was observed (Fig. 1a).

Regardless of the type of nanocomposite used and the PVA molecular weight an increase in inhibition zones for KAN-containing films compared to the initial films was shown. The films based on Ag-Amid nanocomposite had the highest antibacterial activity against *B. subtilis* among the all studied KAN-containing films (fig. 2).

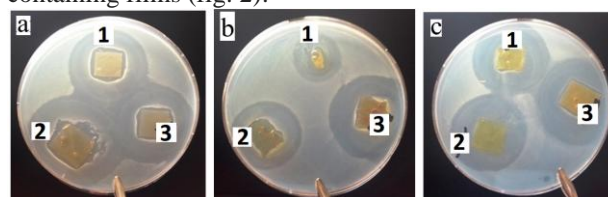


Fig. 1 Inhibition zones of the films based on Ag-Citrus (a), Ag-Classic (b) and Ag-Amid (c) nanocomposite against *B. subtilis*. The PVA molecular weight was 30000 (1), 66000(2) and 145000 (3).

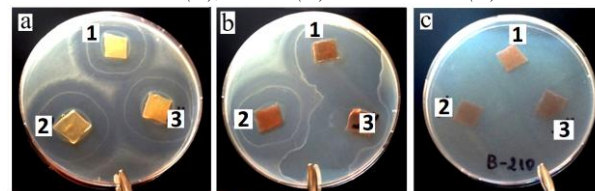


Fig. 2 Inhibition zones of the KAN-containing films based on Ag-Citrus (a), Ag-Classic (b), Ag-Amid (c) nanocomposite against *B. subtilis*. The PVA molecular weight was 30000 (1), 66000(2) and 145000 (3).

### CONCLUSION

Thus, the films based on Ag-pectin nanocomposites can be used to entrap kanamycine, prolong its release and enhance its antimicrobial effect.

### REFERENCES

1. Allahverdiyev A.M. et al., Expert Rev. Anti Infect. Ther. 9(11):1035-52, 2011
2. Al-Muhanna M.K.A. et al., Colloid J. 77(6): 677-684, 2015

### ACKNOWLEDGMENTS

This work was supported by Belarusian Republican Foundation for Fundamental Research (project BRFFR X16-057).

## Alginate of *Azotobacter* Origin

Elizaveta Akoulina<sup>1,2</sup>, Andrej Dudun<sup>1</sup>, Anton Bonartsev<sup>2</sup>, Vera Voinova<sup>2</sup>, Garina Bonartseva<sup>1</sup>

<sup>1</sup>Research Center of Biotechnology RAS, Russia

<sup>2</sup>Faculty of Biology, M.V.Lomonosov Moscow State University, Russia

[akoulinaliza@gmail.com](mailto:akoulinaliza@gmail.com)

### INTRODUCTION

Alginates (ALG) are polyuronic acids which are consisted of monomers of  $\alpha$ -L-mannuronic acid and  $\beta$ -D-guluronic acid.<sup>1</sup> Usually they can be obtained from brown seaweeds but also can be produced by certain bacteria such as *Pseudomonas sp.* and *Azotobacter sp.* In case of bacterial biosynthesis their structure (ratio of residues and molecular weight) can be controlled by regulating growth conditions of strain-producer.<sup>2</sup>

### EXPERIMENTAL METHODS

**The object of study.** In this work the following strains were used: *A. chroococcum* 7B, *A. chroococcum* 12BS (with enhanced slime production), *A. agile* 12, and *A. indicum* 8, all isolated from soddy-podzolic soils of the Moscow region. Bacterial cultures were cultivated in solid Ashby's medium or in liquid Burk's medium.<sup>2</sup>

**Determination and isolation of ALG in culture media.** In order to break capsules and to decrease the viscosity of the solution 10 mL of 0.1M EDTA solution and 10 mL of 1.0 M NaCl were added to 100 mL of culture media. After that the samples were centrifuged for 30 min at 4500 g. The pellet was separated, washed with water and lyophilised. To collect the ALG the supernatant was supplemented with a threefold volume of isopropanol or ethanol. The pellet was collected by centrifugation (20 min at 4000 g), lyophilised and dissolved in 0.9% NaCl. This procedure was repeated three times. The pellet was then lyophilised. The process resulted in water-soluble dry sodium ALG. All experiments and measurements were performed in triplicate.

**Determination of ALG viscosity.** The molecular weight (MW) of ALG was determined by viscosimetry. The specific viscosity was calculated according to the formula:

$$\eta_{sp} = (t - t_0)/t_0,$$

where  $t_0$  is the flow time of the solvent and  $t$  is the flow time of the polymer solution. The molecular weight was calculated according to

the Mark-Houwink equation<sup>4</sup>  $[\eta] = K(M)^a$  with the following coefficients:  $K = 7.3 \times 10^{-5}$ ;  $a = 0.92$ ;

$$[\eta] = 7.3 \times 10^{-5} \times (M)^{0.92},$$

where  $M$  is the molecular weight and  $[\eta]$  is viscosity.

### RESULTS AND DISCUSSION

It was shown that during cultivation by all strains in solid media or liquid media biomass yield was increased (Fig. 1) but amount of alginate was slightly fallen. The molecular weight of alginate was also decreased (Fig. 2). Both observations can be explained by alginate lyase activity.<sup>3</sup>

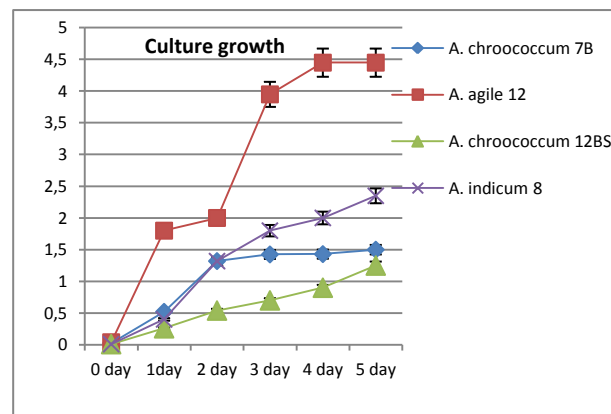


Fig. 1. Dynamics of biomass production of tested strains

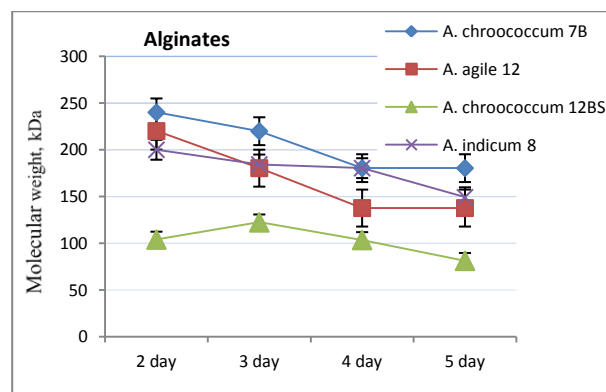


Fig. 2. Dynamics of MW of ALG produced by tested strains

### CONCLUSION

Thus, we obtained ALG by biosynthesis with different strains of *A. sp.* and under different growth terms. And it was shown that yield of ALG depended on time of biosynthesis process that was accompanied by decrease in MW of biopolymer. Further we plan to investigate correlation between alginate lyase activity and MW of alginate itself.

### REFERENCES

1. Pena, C., Galindo, E., Buchs, J., Proc. Biochem.Soc.46 (1): 290–297, 2011.
2. Bonartseva G. A. *et al.* Appl Biochem and Microbiol, 53(1):52–59, 2017.
3. Trujillo-Roldn M. A. *et al.*, Appl Microbiol Biotechnol, 60:733–737, 2003.
4. Usov, A.I., Usp Khim, 68(11):1051–1061, 1999.

### ACKNOWLEDGMENTS

This work was supported by Russian Science Foundation, project # 17-74-20104.



## Fabrication and Characterization of PLA/SA/HA Composite Nanofiber by Electrospinning for Bone Tissue Engineering Applications

Sumeyye Cesur<sup>1,2</sup>, Nazmi Ekren<sup>3</sup>, Osman Kilic<sup>4</sup>, Faik N. Oktar<sup>5,1</sup>, Dilek Bilgic Alkaya<sup>6</sup>, Serap Ayaz Seyhan<sup>6</sup>, Zeynep Ruya Ege<sup>1,7</sup>, Oguzhan Gunduz<sup>1,2</sup>

<sup>1</sup>Advanced Nanotechnology Laboratory, Marmara University, Istanbul

<sup>2</sup>Department of Metallurgy and Material Engineering, Faculty of Technology, Marmara University, Istanbul

<sup>3</sup>Department of Electric and Electronic Engineering, Faculty of Technology, Marmara University, Istanbul

<sup>4</sup>Department of Electric and Electronic Engineering, Faculty of Engineering, Marmara University, Istanbul

<sup>5</sup>Department of Bioengineering, Faculty of Engineering, Marmara University, Istanbul

<sup>6</sup>Department of Analytical Chemistry, Faculty of Pharmacy, Marmara University, 34668 Istanbul, Turkey

<sup>7</sup>Department Biomedical Engineering, Faculty of Engineering Istanbul University, Turkey

[sumeyye-cesur@hotmail.com](mailto:sumeyye-cesur@hotmail.com)

### INTRODUCTION

Electrospun ultrafine fibres fabricated from biodegradable polymers are mostly functional as tissue engineering scaffolds for regenerating a variety of body tissues. Biopolymers like polyesters, polyvinyl alcohol, polyethylene oxide, and polylactic acid (PLA) have been in effect electrospun into micro- and nanofiber mats<sup>1</sup>. Because of these, it is widely used in variety of biomedical applications. Sodium alginate (SA) has anti-bacterial, hydrophilicity and biocompatibility. For these reasons, SA is used various applications such as environmental, clinical, biomedical and other areas<sup>2</sup>. Main mineral constituent to human bones and teeth is hydroxyapatite (HA). It is biocompatible, non-toxic, and also bioactive<sup>3</sup>. In this study, fabrication of biodegradable and biocompatible features composite nanofibers for bone tissue engineering applications was aimed.

### EXPERIMENTAL METHODS

Firstly, Polylactic acid (PLA)/sodium alginate (SA) emulsion was prepared as following. 8wt.% PLA was prepared by dissolving in 20ml chloroform. 3wt.% Twin 80 was added to PLA solution. Different amount of SA as 0.8wt, 1wt.%, 1.2wt.% and 2wt. % were dissolved in distile water for 10min. 1ml of SA solution was added to 8wt.% PLA solution and this mixture was stirred to obtain uniform emulsion. This procedure was repeated for different amount of SA. Then, SA/PLA nanofibers were fabricated by emulsion electrospinning procedures at different flow rate and voltage. After then, HA was obtained from orange spiny oyster seashell (*Spondylus Barbatus*) by hot-plate method. In hot-plate method, seashell was washed, dried, crushed and ball milled until a powder of 100µm particles size was obtained. Raw powders were stirred at 80°C for 15min on a hotplate. Powders are calcined at 800°C for 4h to obtain material that has similar properties with HA. This solution that contains 1.2wt.% SA and 8wt.% PLA in 10ml was prepared again and 2wt.% HA was added to this solution. SA/PLA/HA nanofibers were fabricated by electrospinning. Physical characterization of emulsions was performed by viscometer, surface tension, electrical conductivity and density. Mechanical properties of nanofibers were characterized by tensile test. Morphology of obtained nanofibers was examined by scanning electron microscopy (SEM) and infrared spectra were performed by Fourier transform infrared spectroscopy (FTIR) to scrutinize chemical structure characterization. Wettability of electrospun nanofibers

were characterized by contact angle (CA) measurements. Differential scanning calorimetry (DSC) studies were used for analysis chemical composition and thermal characteristics of the nanofiber mats. The crystalline phases of HA was analyzed by powder X-Ray Diffraction (XRD).

### RESULTS AND DISCUSSION

The morphologies of the PLA/SA electrospun nanofibers with different SA concentration were observed by SEM (Fig. 1). Mechanical properties of composite nanofibers were characterized by tensile test (Fig. 2). Compared with the pure PLA nanofiber, the elongation at break of PLA/SA composite nanofiber was obviously higher. In addition to this, the elongation at break of PLA/SA/HA composite nanofiber was obviously the lowest.

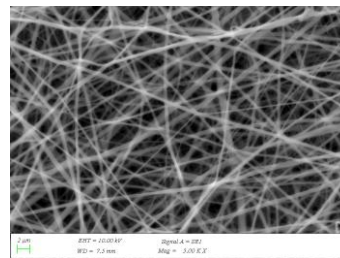


Fig. 1. SEM images of PLA/SA composite nanofibers.

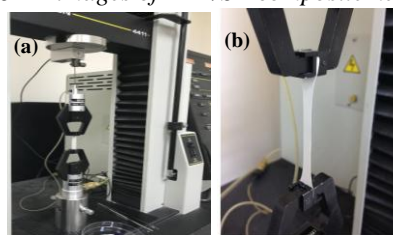


Fig. 2. (a) and (b) Photographs of the tensile test experimental set-up.

### CONCLUSION

Composite nanofibers containing PLA/SA and PLA/SA/HA were successfully fabricated by using the electrospinning technique. Physical, mechanical, chemical and morphological tests showed possibility for usage in tissue engineering and this will be supported by in-vitro analysis.

### REFERENCES

1. Abdalkarim S.Y.H. *et al.*, Cellulose 24:2925–2938, 2017
2. Xu W. *et al.*, J Mech Behav Biomed Mater. 65:428-438, 2017
3. Rujitanapanich S. *et al.*, Energy Procedia. 56:112-117, 2014.

### ACKNOWLEDGMENTS

This study has been founded by Ministry of Development, Turkey; project no:2016K121280.



## Sonochemical Synthesis of Nanoparticles of Bioactive Molecules for Their Direct Embedding into Polymeric Surfaces

Paulina Chytrosz, Monika Golda-Cępa, Andrzej Kotarba

Faculty of Chemistry, Jagiellonian University, Poland

[paulina.chytrosz@student.uj.edu.pl](mailto:paulina.chytrosz@student.uj.edu.pl)

### INTRODUCTION

Nanomaterials have become a new group of materials with wide range and variety of applications, starting with material engineering through food technology ending with medicine. Nanometric materials often exhibit properties dissimilar to their bulk equivalents because of the increase in the surface area, unsaturated sites, quantum effects etc. Different properties are specially manifested in terms of superior activity of nanoparticles when compared to the bulk material. A huge interest in nanotechnology led to the growth of novel synthesis methods to produce a variety of nanostructured materials. At present, the sonochemistry is one of the promising and efficient technique for synthesis not only inorganic nanoparticles, but also organic ones.<sup>1,2,3</sup> The use of this method can be particularly interesting for the nanoparticles made of bioactive compounds, i.e. antibiotics, vitamins, enzymes. The sonochemical method can provide foundations for the preparation of therapeutic, bioactive and even self-cleaning surfaces.

### EXPERIMENTAL METHODS

An aqueous solution treated with high intensity ultrasounds causes phenomenon called acoustic cavitation. Application of such powerful radiation causes weakening of the chemical bonds between bioactive molecules. The clue of this process is to produce bubbles by acoustic cavitation. The applied frequency of 20 kHz induces nucleation, growth and collapse of these bubbles which is graphically shown in Fig. 1. Collapsing bubbles create so called 'hot spots' (extremely high, localized pressure and temperature – hundreds bar and thousands K)<sup>4</sup> which are directly responsible for the chemical effects of ultrasound. The bubbles collapse takes time in the range of nanoseconds and extremely high cooling rates (10 K/s). These conditions allow the synthesis of nanostructured materials of various chemical nature. However, different substances need specific reaction parameters including time, power, solvent and concentration.

### RESULTS AND DISCUSSION

Different compounds are produced by sonochemical synthesis: enzymes, diet supplements, medicines. First reports regarding the feasibility of such synthesis appeared in 2012 with the publication of A. Gedanken<sup>1</sup> where  $\alpha$ -amylase nanoparticles formation upon sonochemical method is reported, followed by successful formation of tetracycline nanoparticles<sup>2</sup>, vitamin B<sub>12</sub>, and penicillin<sup>3</sup>. All the produced nanoparticles reached the size in the range 30 nm – 100 nm. Formation of NPs increased the activity and bioavailability of the drugs, moreover the depth of tissue penetration was significantly improved.

The sonochemical method does not affect the chemical structure of bioactive substances as confirmed by spectroscopic methods. It was found, that the final size range of sonochemically-obtained nanoparticles depends strongly on the time of synthesis and concentration of the starting solution. Such synthesis allows simultaneous formation and embedment of nanoparticles into porous surfaces e.g. modified polymers<sup>5</sup>. In the case of antibiotic (tetracycline, gentamycin) antibacterial coatings were sonochemically produced by embedding nanoparticles into the polymer surface. Such systems led to control drug release.

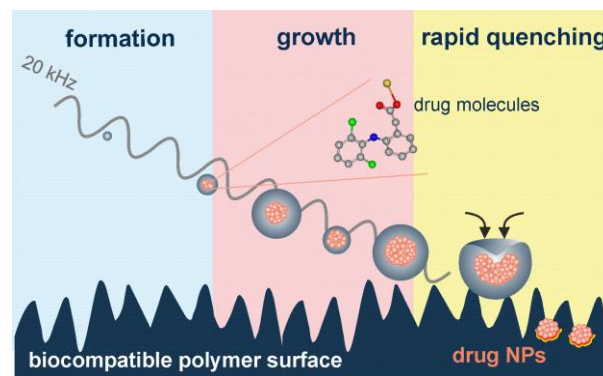


Fig. 1. Graphical scheme of the stages taking place during sonochemical embedment of nanoparticles of bioactive molecules into the surface of a polymer film.

### CONCLUSION

Sonochemical synthesis is a powerful method for the production of nanostructured materials made of biologically active substances. No changes in chemical structure, activity and bioavailability of such nanoparticles upon sonochemical synthesis were observed. By controlling the ultrasonic bath parameters during the functionalization of polymeric biomaterial surfaces the in-site release of bioactive molecule from NPs can be controlled.

### REFERENCES

1. Meridor D. *et al.*, Ultrason Sonochem 20(1):425-431 2013
2. Grinberg O. *et al.*, J. Mater. Chem. B 3:59-64 2015,
3. Yariv I. *et al.*, Int. J. Nanomed 10:3593-3601 2015
4. Hinman J.J. *et al.*, Top. Curr. Chem 375(1):59-95 2017
5. Gedanken A., Ultrason Sonochem 14:418-430 2007

### ACKNOWLEDGMENTS

The financial support of the project is provided by Faculty of Chemistry, Jagiellonian University grant no. K/DSC/004566.

## The New Inorganic/organic Cone Cement Based on Si Doped Alpha TCP

Ewelina Cichoń, Aneta Zima, Joanna Czechowska, Anna Ślósarczyk

Department of Ceramics and Refractories/Faculty of Material Science and Ceramics,  
AGH University of Science and Technology, Poland  
[ecichon@agh.edu.pl](mailto:ecichon@agh.edu.pl)

### INTRODUCTION

Treatment of large bone defects, caused by trauma as well as tumor or cyst resection, is a big challenge for modern medicine. Various types of grafts have been used to restore damaged bone. Autografts have been considered as the gold standard because of less risk of rejection. However, application of autografts is associated with significant drawbacks including increased surgery time, donor site pain, risk of wound infection and insufficient availability. Also for large size defects the use of allogenic and autologous bone is not an optimal option. To avoid the mentioned complications in clinical practice, various synthetic biomaterials are used to fill bone losses. Calcium phosphate bioceramics (CaPs) are excellent implant materials for bone repair and regeneration because their chemical composition is similar to the inorganic components of natural bone. Calcium phosphate bone cements (CPCs) represent a unique advantage over sintered bioceramics which do not reveal surgical handiness [1]. However, their mechanical and rheological properties as well as degradation rate are not satisfying. Therefore, a lot of research has been carried out on improving these properties of CPCs. A commonly used approach is an addition of polymers to liquid or solid phases of cements [2-6]. The aim of this study was to determine the effect of hydroxypropyl methylcellulose (HPMC) on the properties of inorganic/organic bone cements based on  $\alpha$ -tricalcium phosphate ( $\alpha$ -TCP) and Si doped  $\alpha$ -TCP (Si- $\alpha$ -TCP).

### EXPERIMENTAL METHODS

The solid phase of obtained cements consisted of the highly reactive undoped  $\alpha$ -tricalcium phosphate or  $\alpha$ -TCP doped with 0.1 wt.% or 0.3 wt.% of Si. Initial powders were synthesized by the wet chemical method. As the source of silicon - 98% silicon tetraacetate (Sigma-Aldrich) was used. Hydroxypropyl methylcellulose (HPMC) was added to powder phase in the amount of 0.5 wt.% or 1 wt.%. As a liquid phase the 2 wt.%  $\text{Na}_2\text{HPO}_4$  solution was used. The setting times of the prepared samples were measured according to ASTM C266-08. The physicochemical properties of the obtained cement type materials such as: phase composition (XRD, D-2 Phaser, Bruker), porosity (MIP, Auto Pore IV, Micromeritics) and compressive strength (Universal testing machine, Instron) were determined.

### RESULTS AND DISCUSSION

The addition of HPMC to cements based on undoped  $\alpha$ -TCP noticeably increased its final setting time from about 12 minutes to almost one hour. The negative effect of the polymer on the final setting time decreased with the introduction of silicon into the  $\alpha$ -TCP structure.

The XRD analysis of Si- $\alpha$ -TCP powders revealed no secondary phases apart from the  $\alpha$ -TCP phase (Fig. 1).

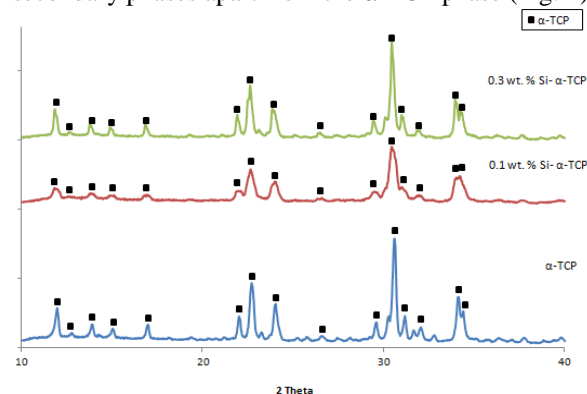


Fig. 1 X-ray diffractogram of the  $\alpha$ -TCP and Si doped  $\alpha$ -TCP.

XRD analysis of selected bone cements seven days after setting showed the presence of two crystalline phases:  $\alpha$ -TCP and hydroxyapatite. The study has also shown that silicon doping accelerates the hydrolysis of  $\alpha$ -TCP to hydroxyapatite.

Polymer addition and silicon modification of  $\alpha$ -TCP affected on the formation of mesopores in studied materials. The obtained microstructure may be useful to achieve the controlled release of biological active molecules which can be introduced during the cement preparation.

### CONCLUSION

Introduction of HPMC to the solid phase of CPCs allowed to obtain inorganic/organic bone cements. Cements on the basis of 0.3 wt.% silicon doped  $\alpha$ -TCP revealed the most favorable setting times. These cements set in less than 30 minutes which gives promising perspectives for their use in medicine. Cements doped with silicon exhibited higher porosity if compared to not-doped ones. On the other hand, the addition of HPMC reduced the porosity, most likely by filling pores in the cement. The obtained cements showed the compressive strength from  $1.5 \pm 0.7$  MPa to  $6.8 \pm 1.0$  MPa. Developed cement-type materials require further research.

### REFERENCES

1. Khairoun I. *et al.*, J Biomed Mater Res, 60:4, 2002
2. Bohner M. *et al.*, Biomaterials, 26:13, 2005
3. Ding S. J. *et al.*, Tissue Eng Part A, 16:7, 2010
4. Palmer I. *et al.*, J Biomed Mater Res B Appl Biomater, 104:2, 2016
5. Seyedlar, R. *et al.*, Carbohydr Polym., 99, 2014
6. An, J. *et al.*, J Biomed Mater Res A, 104:5, 2016

### ACKNOWLEDGMENTS

This work was supported by the Faculty of Materials Science and Ceramics AGH University of Science and Technology - Project No.11.11.160.617 (2018).

## Electrospun Multilayer Nanofiber Based Intelligent Drug Delivery and Release System

Zeynep Ruya EGE<sup>1,2</sup>, Faik Nüzhet Otkar<sup>2,3</sup>, Aydın Akan<sup>4</sup>, Dürdane Serap Kuruca<sup>5</sup>, Betül Karademir<sup>6</sup>, Gökçe Erdemir<sup>7</sup>, Sümeyye Cesur<sup>2,8</sup>, Oguzhan Gunduz<sup>2,8</sup>

<sup>1</sup>Department of Biomedical Engineering, Faculty of Engineering, Istanbul University, Turkey

<sup>2</sup>Advanced Nanomaterials Research Laboratory, Marmara University, Turkey

<sup>3</sup>Department of Bioengineering, Faculty of Engineering, Marmara University, Turkey

<sup>4</sup>Department of Biomedical Engineering, Faculty of Engineering and Architectural, Katip Celebi University, Turkey

<sup>5</sup>Department of Basic Medical Sciences, Faculty of Medicine, Istanbul University, Turkey

<sup>6</sup>Department of Biochemistry, Faculty of Medicine, Marmara University, Turkey

<sup>7</sup>Institute of Aziz Sancar Experimental Medicine Research, Faculty of Medicine, Turkey

<sup>8</sup>Department of Metallurgical and Materials Engineering, Faculty of Technology, Marmara University, Turkey

[zruyadeveli@gmail.com](mailto:zruyadeveli@gmail.com)

### INTRODUCTION

Polymeric nanomaterials are noted in biomedical applications due to their advanced ability to cell penetrating, drug delivering, and long sustained drug releasing capacity<sup>1,2</sup>. Electrospinning (ES) is the ideal method for the production of polymeric nanofibers. Indocyanine Green (ICG), which has recently attracted attention both in terms of diagnosis and treatment. After intravenous injection, the blood circulation life of ICG is rather short. This is a disadvantage in targeted drug delivery studies<sup>3</sup>. In this study, by loading of ICG at core, interface and shell of the biodegradable polymer nanofibers poly(lactic acid) (PLA) and poly caprolactone (PCL) acts via coaxial electrospinning method (CES). ICG has been portabilized and stabilized. The pH sensitive release was examined and characterized.

### EXPERIMENTAL METHODS

ICG was obtained from Acros Organics. The polymer solutions of PLA and PCL were prepared in the DCM:DMF and DMF:THF solvents at a ratio of 4:1 and 1:1, respectively. ICG (1mg/ml) was dissolved in methanol. Mono (polymer-ICG) and multilayer (polymer-polymer-ICG) nanofibers were produced by CES method with different combinations. Loaded ICG was visualized by confocal microscopy. Fiber morphologies were examined with Scanning Electron Microscope (SEM). In order to evaluate of chemical differentiations of nanofibers fourier transform infrared spectrometer (FT-IR) spectra were recorded. Tensile tests of fibers were carried out. pH sensitive ICG release analyzes were performed. Cell uptake analyses and cytotoxicity test were performed.

### RESULTS AND DISCUSSION

ICG loaded nanofibers morphologies were given by SEM images in Fig. 1. It is also shown by the confocal image that the fibers tubes are loaded with ICG linearly Fig. 1d. The characteristic peaks were obtained from nanofiber mat. The characteristic peaks were obtained from multi layer composite electrospun nanofiber mat that containing PLA, PCL and ICG by FT-IR at Fig 2. In vitro pH-sensitive release studies demonstrated, that ICG release from multilayer nanofiber were successfully at the acidic condition.

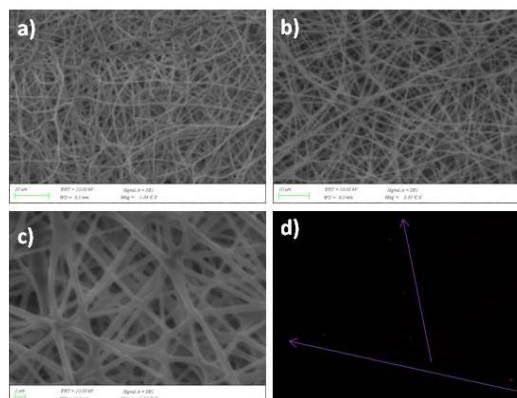


Fig. 1. SEM images of ICG loaded (a) PLA/ICG (b) PLA/PCL/ICG (c) PLA/ICG/PCL (d) confocal image of ICG in nanofiber

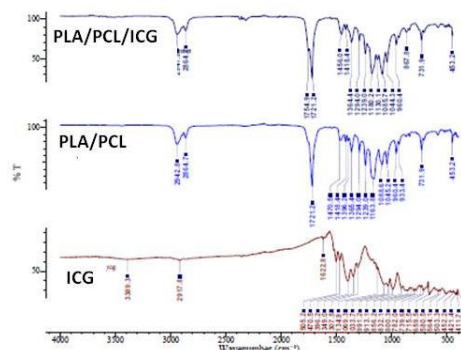


Fig. 2. FT-IR spectra of the nanofibers

### CONCLUSION

ICG loaded nanofibers were produced via CES technique. This study revealed that composite nanofibers can be used as a nanoprobe for the cancer cell imaging.

### REFERENCES

1. Zhaohui T. *et al.*, Prog. Polym. Sci., 60, 86–128, 2011.
2. Bazylińska U. *et al.*, Colloids Surf., A: Phys. Eng. Asp., 442, 42–49, 2014.
3. Schaafsma B.E., J. Surgical Oncology, 104, 323–332, 2011.

### ACKNOWLEDGMENTS

This work is funded from TUBITAK, project number: 217M028.



## Melt Compounded Biocompatible Thermoplastic Polyurethane (TPU) for the Engineering of 3D printed Aortic Heart Valve Ring: Design, Fabrication, Testing and Simulation

Emanuele Gasparotti<sup>1</sup>, Emanuele Vignali<sup>1</sup>, Giorgio Soldani<sup>2</sup>, Paola Losi<sup>2</sup>, Marco Scatto<sup>3</sup>, Simona Celi<sup>1</sup>

<sup>1</sup>BioCardioLab, Bioengineering Unit, Fondazione Toscana Gabriele Monasterio, Massa, Italy

<sup>2</sup>Biomaterial Laboratory, Institute of Clinical Physiology CNR, Massa, Italy

<sup>3</sup>Nadir S.r.l., c/o Campus Scientifico Università Ca' Foscari Venezia, Via Torino 155b, 30172 Mestre (VE), Italy  
[emanuele.gasparotti@ftgm.it](mailto:emanuele.gasparotti@ftgm.it)

### INTRODUCTION

Heart diseases, including valve pathologies, are the leading cause of death worldwide. The principal requirements for heart valve replacement are an efficient function and long-term durability without the need for anticoagulation, coupled with the ability to be accommodated in many different types of patient. In recent years the combination of additive manufacturing (AM) techniques and the development of advanced polymeric materials, opened new scenarios for polymeric heart valves (PHVs). In this context, much attention has been given on thermoplastic polyurethanes (TPUs) considering their physio-chemical properties and versatility in processing, coupled with improved biocompatibility and stability. In our previous studies [1], a silicone based TPU has been employed to fabricate vascular grafts which revealed a calcification and thrombogenicity reduction after animal testing. In this work, we realize an innovative polymer compound based on TPU and silicone with biological activity as feedstock for Fused Deposition Method (FDM) 3D printer to realize of custom polymeric heart valves ring.

### EXPERIMENTAL METHODS

During the production of Polymer Nanocomposite with melt compounding technology, a co-rotating twin screw extruder localized in Nadir Lab has been used. TPU biocompatible polymer has been chosen as polymer matrix for heart valve ring. This polymer has been melt compounded with an innovative filler able to provide antimicrobial properties and anticalcification effect. Finally, the composites have been tested:

**Biological testing** – In vitro tests have been carried out to evaluate the calcification by infrared analysis and SEM [2]. The antimicrobial activity has been assessed by a standard disc diffusion method with *S. aureus*.

**Mechanical testing** – A 3D printer has been adopted to fabricate dog bone specimens for tensile tests, according to ASTM D1708 standard. To investigate the mechanical characteristics variation depending on the fabrication technique, three different infill fiber angles have been used: 0°, 45° and 90°. Uniaxial tensile tests have been carried out through a custom traction machine. On the basis of experimental data, a Finite Element (FE) simulation of the ring radial crimping has been imposed. The areas of maximum stress and deformation have been investigated. Finally, a valve ring prototype has been realized via AM. The extruder temperature was kept constant at 225°C and the layer thickness at 0.2 mm.

### RESULTS AND DISCUSSION

Several melt compounded TPUs with different loading of anticalcification additives and antimicrobial agents have been prepared. Tensile stress behavior up to 100% deformation is independent from the filament orientation, as no significant difference emerged between the three specimen categories (Fig. 1a). The 0° specimens have exhibited higher stresses at rupture (Table 1). The FE simulation of the ring compression has revealed maximum deformations of 17%, which assures the hypothesis of purely elastic deformation (Fig. 1b).

TPU samples presented significantly less formation of calcification compared to bovine pericardium, the standard material for biological heart valve.

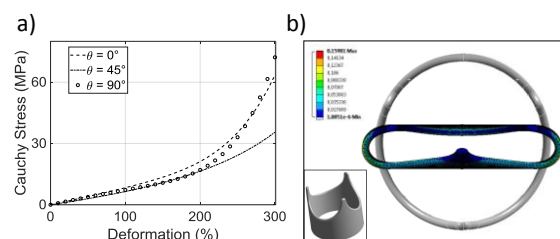


Fig. 1. a) Stress-strain average curves, b) FE simulation result: deformed and undeformed shape.

Table 1. Tensile test results (mean ± standard deviation)

	0°	45°	90°
Ultimate Stress (MPa)	59,7±17,3	42,5±3,1	12,3±2
Ultimate Strain (%)	307±39,6	330±11,2	183±39,3
Stress @50% (MPa)	4,6±0,76	3,3±0,27	3,9±0,55
Stress @100% (MPa)	8,4±1,2	6,7±0,5	7,3±0,6

### CONCLUSION

AM fabrication of custom PHVs has been analysed. Melt compounded biocompatible TPU composites can improve heart valves performance by tuning and optimizing shape complexity, mechanical and biological properties. The mechanical properties assessment has demonstrated that AM is a valid approach to fabricate rings with reliable elastic characteristics. A high level of micro-structure customization in terms of compound loadings is assured.

### REFERENCES

- [1] Soldani G., Losi P., et al. Biomaterials. 2010 Mar;31(9):2592-605
- [2] Bernacca G.M., Mackay T.G., Wheatley DJ., J Heart Valve Dis. 1992 Sep;1(1):115-30.

### ACKNOWLEDGMENTS

This research was supported by Regional ValveTech project funding from Regione Toscana.



## Comparison of PCL, PLC70:30, PLC85:15, PLG82:18 as a Matrix for Biodegradable X-rays Visible Composites

Zaneta Górecka, Emilia Choińska, Wojciech Świąszkowski

Faculty of Materials Science and Engineering, Warsaw University of Technology, Poland

[gorecka.zaneta@gmail.com](mailto:gorecka.zaneta@gmail.com)

### INTRODUCTION

Manufacturing of fiducial markers (FM) from biodegradable materials supersedes a further surgical intervention connected with removing them from implantation site. One of types of materials for this application are composites with thermoplastic matrix. These types of materials can be used in 3D manufacturing, like Fused Deposition Modelling (FDM), to fabricate various shapes of devices.

Synthetic thermoplastic biodegradable polymers, mainly aliphatic polyesters such as polyglycolide (PGA), polylactide (PLA), poly( $\epsilon$ -caprolactone) (PCL), their copolymers and blends have been widely investigated to utilize in tissue regeneration as scaffolds that provide the necessary support for cells and tissues. They undergo degradation by random hydrolytic cleavage of ester bonds in vivo. They can also be used as contrast devices e.g. in X-ray computed tomography imaging, if some radiopaque component is added.<sup>1-4</sup> Advantage of use of synthetic polymers in manufacturing of medical devices is repeatable large-scale production with controlled properties.

The aim of this study was the comparison of different commercially available thermoplastic biodegradable polymers as a matrix for X-rays visible composites.

### EXPERIMENTAL METHODS

PCL, P[LLAcoCL] with a molar ratio of 70 to 30 (PLC70) and 85 to 15 (PLC85) and P[LLAcoGA] with a molar ratio of 82 to 18 (PLG82) were used as the matrix of composites. BaSO<sub>4</sub> and HAp (were used as fillers of composites. Composite materials 80:10:10 (polymer:BaSO<sub>4</sub>:HAp) were prepared by solvent casting technique and then extruded to fabricate 1mm in diameter rods used in the following experiments: degradation experiment in PBS and material characterisation by means of  $\mu$ CT, TGA, DSC, GPC, SEM, contact angle measurements and mechanical tests in various conditions.

### RESULTS AND DISCUSSION

Obtained results showed the difference in degradation profile of materials. The highest water absorption was for matrix PLG82. It caused immediate decrease of average molecular weight and undesired swelling of material. Water absorption for both P[LLAcoCL]-based materials was similar, however faster mass loss of PLC70 was observed. For PLC70-based material strong change in T<sub>g</sub> and  $\Delta H$  was observed during degradation. T<sub>g</sub> decreased from 27°C to -19°C.

SEM observations of surface after 20 weeks of degradation did not show any significant differences from not incubated material. Nevertheless, the decrease of water contact angle was observed for all copolymer-based materials. Profiles of radiographs of PCL-, PLC70- and PLC85-based materials during degradation

were stable. Only for PLG82 decrease in radiopaque properties occurred. Profile of PLG82-based composite showed also the increase of diameter of degraded rods.

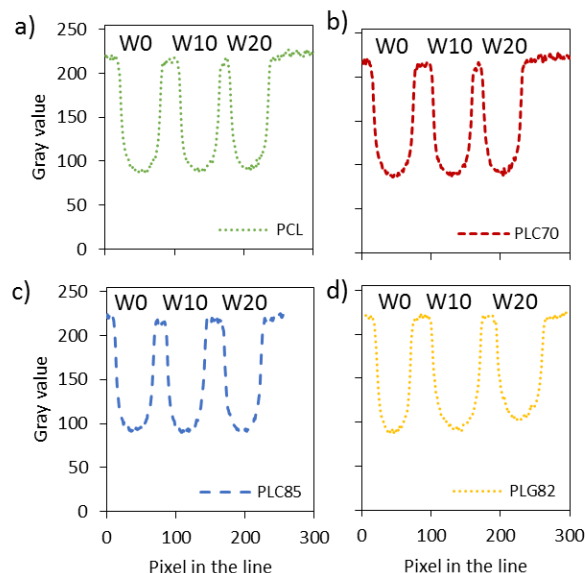


Fig. 1. Profiles of radiographs of all investigated materials after 0, 10 and 20 weeks of degradation

Despite the fact that the degradation process occurred in all materials – the radiographs' profiles were stable. However, there were changes in mechanical properties which play a significant role of device stability.

### CONCLUSION

The results obtained by wide range of analytical techniques suggest the application of PCL- and PLC70-based composites as promising materials systems for long term innovative biodegradable fiducial markers for X-ray based medical imaging. Moreover, PCL matrix can be used when very long time of monitoring is required.

### REFERENCES

1. No, Y. J *et al.*, J. Biomed. Mater. Res. B 103.7:1465-1477, 2015;
2. Samuel R. *et al.*, RSC Adv. 5:102: 84125–84133, 2015;
3. Nottelet B. *et al.*, Eur. J. Pharm. Biopharm. 97:350–370, 2015;
4. Gorecka Z, *et al.* J. Mater. Chem. B. 4:5700-5712, 2016.

### ACKNOWLEDGMENTS

This study was supported by the National Center for Research and Developments in Poland (STRATEGMED1/233624/4/NCBR/2014, project MENTOREYE).

## Multiphase Hydrogel System Modified with Graphene Oxide and Hydroxyapatite for Cartilage Tissue Engineering – Preliminary Study

Martyna Hunger, Patrycja Domalik-Pyzik, Jan Chłopek

Department of Biomaterials and Composites, Faculty of Materials Science and Ceramics,  
AGH University of Science and Technology, Krakow, Poland

[hunger@agh.edu.pl](mailto:hunger@agh.edu.pl)

### INTRODUCTION

Cartilage is an avascular tissue nourished by diffusion from synovial fluid or subchondral bone. Lack of vascularity significantly reduces its regenerative potential; therefore conventional methods of cartilage treatment are less effective than tissue engineering approaches. Seeking new treatment options for diseased cartilage is nowadays particularly important due to the risks associated with civilization diseases and increasing number of osteoarticular system traumas and injuries<sup>1</sup>. Hydrogel-based scaffolds can constitute a promising solution for cartilage regeneration because of their biodegradability and biocompatibility. Among them, chitosan-based hydrogels present one of the most favourable properties that can be further tailored by introducing appropriate modifying phases, thus creating composite systems<sup>2,3,4,5</sup>.

The aim of this research was to fabricate composites based on chitosan (CS) and poly(ethylene glycol) (PEG), modified with graphene oxide (GO) and hydroxyapatite (HAp). The influence of the amount and the type of the modifying phases on the physicochemical properties of the obtained materials, as well as their potential for use in cartilage tissue engineering were evaluated.

### EXPERIMENTAL METHODS

Chitosan (Acros Organics, MW=100,000-300,000), tannic acid (TAc; 88% POCH S.A.), poly(ethylene glycol) (PEG; Acros Organics, MW=400), graphene oxide (ITME, Poland), and hydroxyapatite (MKN-HXAP, 12  $\mu\text{m}$ ) were used as received. CS solution in 5% lactic acid was mixed with PEG (0-80% w/w of CS). Next, different amounts of GO (0-3% w/w of CS) and HAp (0-30% w/w/ of CS) were added and homogenised by sonication. After 24h, TAc (0-20% w/w of CS) was introduced gradually with continuous mixing on a magnetic stirrer. As prepared solutions were casted onto Petri dishes and dried in ambient conditions for 72h in order to obtain polymer and composite films. Porous scaffolds were prepared by freeze-drying in a 24-well plates (freezing temperature -80°C).

Microstructural (digital microscope, SEM), structural (FTIR-ATR), thermal (DSC), mechanical (static tensile test) and surface (wettability) properties of the obtained materials were evaluated.

### RESULTS AND DISCUSSION

The degree of deacetylation (DD) is one of the key parameters characterizing chitosan and affecting its physicochemical and biological properties. The DD of the CS used in this study was verified by titration method (with 0.1 M NaOH), and equalled 84%.

In the first step, screening was done to find the optimal concentration of TAc (a crosslinking and antioxidant agent) and PEG400 – for improved wettability. It was observed that the addition of tannic acid improves the mechanical properties when compared to chitosan only films. While – as expected – PEG addition was beneficial in terms of surface properties. Moreover, addition of 20% (w/w) PEG also improves mechanical properties. Finally, 20% (w/w) and 20% (w/w) of TAc and PEG400, respectively were chosen for further studies where various amounts of GO and HAp were tested.

When used separately, GO and HAp had contradictory effects on mechanical properties. With the increase of GO content, tensile strength also increased, while the more HAp was used, the more brittle was the material. Their simultaneous addition allowed to customize the properties. Favourable apatite-like formation was observed in case of the samples with higher HAp content. Moreover, there were some evidences that GO can act as a crosslinking agent.

### CONCLUSION

The designed multiphase systems combines beneficial properties of chitosan hydrogels, tannic acid, poly(ethylene glycol), graphene oxide, and hydroxyapatite. This research is a first step towards development of a novel gradient scaffolds for cartilage tissue engineering. Further studies are necessary to investigate in more detail the biological properties of the proposed material solution.

### REFERENCES

1. Armiento A.R., *et al.*, Acta Biomater, 2018, 65, 1-20
2. Naahidi S., *et al.*, Biotechnol Adv, 2017, 35, 530-544
3. Oryan A., Sahviah S., Int J Biol Macromol, 2017, 104, 1003-1011
4. Wang J. *et al.*, Materials, 2015, 8(12): 8097–8105
5. Ma S., *et al.*, Polymer, 2016, 98, 516-535

### ACKNOWLEDGMENTS

The authors would like to thank the National Centre for Research and Development, Poland for providing financial support to this project (STRATEGMED 3/303570/7/NCBR/2017).

Joanna Jagiełło and Dr. Ludwika Lipińska from the Institute of Electronics Materials Technology (ITME) in Warsaw are gratefully acknowledged for providing graphene oxide. Dr. Kinga Pielichowska (AGH-UST) is acknowledged for excellence in DSC measurements.

## Biopolymers for Advanced Medical Applications Based on Polyhydroxyalkanoates (PHAs) Derived from Polyolefin Waste Materials

Brian Johnston<sup>1</sup>, David Hill<sup>1</sup>, Marek Kowalczyk<sup>1,2</sup>, Iwona Kwiecień<sup>2</sup>, Jennifer Gonzalez Ausejo<sup>3</sup>, Iza K. Radecka<sup>1</sup>

<sup>1</sup>School of Sciences, Faculty of Science and Engineering, University of Wolverhampton, Wolverhampton, WV1 1SB, UK

<sup>2</sup>Centre of Polymer and Carbon Materials, Polish Academy of Sciences, M. Curie-Skłodowskiej 34, 41-819 Zabrze, Poland

<sup>3</sup>Universitat Jaume I Castelló de la Plana, Castellón, Spain.  
[b.johnston@wlv.ac.uk](mailto:b.johnston@wlv.ac.uk)

### INTRODUCTION

Increasing levels of plastic pollution around the world means that alternatives to petro-chemical plastics are urgently required. Polyhydroxyalkanoates (PHAs) are a group of biocompatible, non-toxic and biodegradable plastics that are produced by bacteria and they could be used as a synthetic plastic replacement<sup>1</sup>. The main factors limiting the widespread usage of PHAs are the high production costs and expensive chemical processing<sup>2</sup>. In this study chemical processes were used to breakdown waste plastics into waxes which were then metabolized by bacteria into PHAs. These products were then analyzed at the molecular level and can be applied for 3D printing of advanced biomaterials.

### EXPERIMENTAL METHODS

Oxidized polyethylene wax (O-PEW) and non-oxidized polyethylene wax (N-PEW) were used as carbon sources for PHA biosynthesis<sup>1,3,4</sup>. The O-PEW was obtained from PE thermal degradation and N-PEW were formed using pyrolysis<sup>1,3</sup>. These waxes were metabolized by *Cupriavidus necator* H16 in a bioreactor for 48 hours to make PHAs. Fermentation was in both nitrogen rich and nitrogen-limited media supplemented with either O-PEW or N-PEW. The biopolymers produced were analyzed using FTIR, NMR, GPC, TGA and electrospray ionisation tandem mass spectrometry (ESI-MS/MS) to assess structure<sup>1,4</sup>. HEK293 and WI-38 cells were used for toxicity tests.

### RESULTS AND DISCUSSION

The accumulation of PHAs varied from 20% to 40 % (wt/wt) of dry biomass in both growth media. When TSB was supplemented with O-PEW, bacteria produced PHA which contained 3-hydroxybutyrate and up to 3 mol % of 3-hydroxyvalerate and 3-hydroxyhexanoate co-monomeric units<sup>4</sup>. The ESI-MS/MS enabled PHA characterization when the content of 3-hydroxybutyrate was high and the appearance of other PHA repeating units was low<sup>4</sup>. When N-PEW was used, the PHA formed contained 3-hydroxybutyrate (HB) with 11 mol% of 3-hydroxyvalerate (HV) units<sup>1</sup>. MTT assays demonstrated human cells were successfully grown on 3D printed PHA-blend scaffolds for seven days, with no signs of toxicity, further illustrated by SEM observation.

### CONCLUSION

O-PEW and N-PEW could be a promising carbon source for PHA production. The PHAs formed can be applied to novel biomaterials for medical applications without toxic or hazardous consequences.

### REFERENCES

- Johnston, B., Jiang, G., Hill, D., Adamus, G., Kwiecień, I., Zieba, M., Sikorska, W., Green, M., Kowalczyk, M and Radecka, I. (2017) The Molecular Level Characterization of Biodegradable Polymers Originated from Polyethylene Using Non-Oxygenated Polyethylene Wax as a Carbon Source for Polyhydroxyalkanoate Production. *Bioengineering* 2017, 4, 73; doi:10.3390/bioengineering4030073.
- Jiang, G., Hill D.J., Kowalczyk, M., Johnston, B., Adamus, G., Irorere, V. and Radecka, I. (2016) Carbon Sources for Polyhydroxyalkanoates and an Integrated Biorefinery. *International Journal of Molecular Sciences* 17 (7):1157, doi: 10.3390/ijms17071157.
- Guzik, M., Kenny, S., Duane, G., Casey, E., Woods, T., Babu, R., Nikodinovic-Runic, J., Murray M. and O'Connor, K. (2014). Conversion of post consumer polyethylene to the biodegradable polymer polyhydroxyalkanoate. *Applied Microbiology Biotechnology*; 98, 4223-4232, doi: 10.1007/s00253-013-5489-2.
- Radecka I., Irorere V., Jiang G., Hill D., Williams C., Adamus G., Kwiecień M., Marek A.A., Zawadiak J., Johnston B. and Kowalczyk M. (2016) Oxidized Polyethylene Wax as a Potential Carbon Source for PHA Production. *Materials*, 9 (5), 367; doi:10.3390/ma9050367.
- Gonzalez Ausejo, J., Sánchez-Safont, E., Maria Lagarón, J., Balart, R., Cabedo, L., and Gamez-Perez, J. (2017) Compatibilization of poly(3-hydroxybutyrate-co-3-hydroxyvalerate)-poly(lactic acid) blends with diisocyanates. *Journal of Applied Polymer Science*; doi: 10.1002/app.44806.

### ACKNOWLEDGMENTS

Funded by the Research Investment Fund, University of Wolverhampton (Wolverhampton, UK). Partial financial support from the European Regional Development Fund Project EnTRESS No 01R16P00718 and M ERA.NET "Pelargodont" project under Horizon 2020 is gratefully acknowledged.

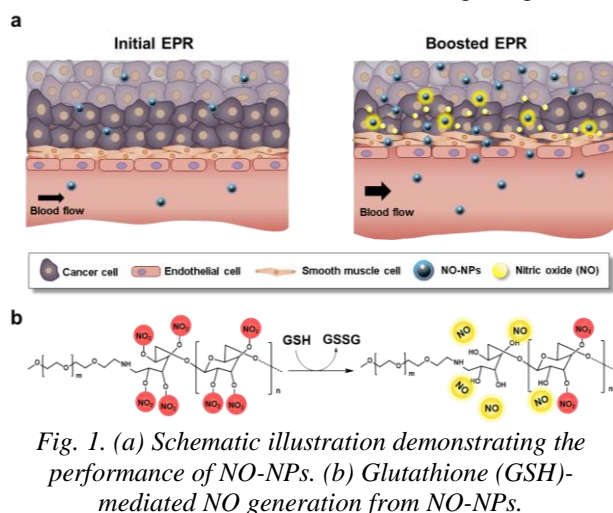
## Nitric Oxide-Generating Bioreducible Polymeric Nanoparticles for Site-Specific Vasodilation in Tumour Tissue

Hyewon Ko, Jae Hyung Park

Department of Health Sciences and Technology, Sungkyunkwan University, Republic of Korea  
[tizi9057@gmail.com](mailto:tizi9057@gmail.com)

## INTRODUCTION

In recent years, nanomedicines have been considered as a potential alternative to the conventional chemotherapy since they can selectively accumulate in tumour tissue through enhanced permeability and retention (EPR) effect<sup>1</sup>. However, they have rarely been successful in clinical trials because of the lower passive targeting efficiency in human<sup>2,3</sup>. To surmount the limited drug delivery efficacy of the nanocarriers, we designed the polymeric nanoparticles to induce vasodilation using nitric oxide (NO)<sup>4</sup>. NO is a gas transmitter which can dilate blood vessels, but the application of NO has been limited due to an extremely short half-life (1 s) and high reactivity<sup>5</sup>. In this study, NO-generating nanoparticles (NO-NPs) was developed which can release NO in response to reductive environment so that they can induce site-specific vasodilation adjacent to tumour tissue, leading to an increase the vessel permeability and enhanced tumour accumulation of drugs (Fig. 1).



## EXPERIMENTAL METHODS

Poly(ethylene glycol)-*b*-nitrate dextran (PEG-*b*-NO-Dex), which forms NO-NPs in aqueous condition, was prepared by modification of the hydroxyl groups of Dex into nitro esters. Doxorubicin-loaded NO-NPs (DOX-NO-NPs) were prepared by dialysis method. Briefly, DOX dissolved in chloroform was added to PEG-*b*-NO-Dex solution, and the mixture was dialyzed and lyophilized to obtain DOX-NO-NPs. The changes in *in vivo* tumour blood flow was quantified using 3D ultrasound Doppler and visualized using laser speckle contrast imaging system. *In vivo* biodistribution of DOX was evaluated by quantifying DOX content in tumours and major organs using fluorescence spectrophotometer by subtracting autofluorescence of each organ.

## RESULTS AND DISCUSSION

The amphiphilic PEG-*b*-NO-Dex could spontaneously self-assembled and form NO-NPs in aqueous solution. The NO-NPs were disassembled via a hydrophobic to hydrophilic transition by generating NO in response to GSH, a compound abundant at the intracellular level of tumour tissue. The tumour blood flow was quantitatively analysed and the results showed that 1.3-fold increase in vascularity compared to initial level when NO-NPs were systemically administered to tumour-bearing mice, whereas saline-treated groups did not show any significant difference (Fig. 2a,b). The same tendency of tumour vasculature was observed in laser speckle contrast imaging (Fig. 2c). Also, we investigated DOX distributions to investigate the effect of NO on drug delivery efficacy. DOX content in tumour tissue in DOX-NO-NPs-treated group was 5.4-fold and 1.5-fold higher than free DOX or DOX-control NPs treated groups, respectively (Fig. 2d). These results suggested that NO-NPs could induce tumour-specific vasodilation and boost EPR effect to enhance the drug accumulation at the target site, leading to improved therapeutic efficacy.

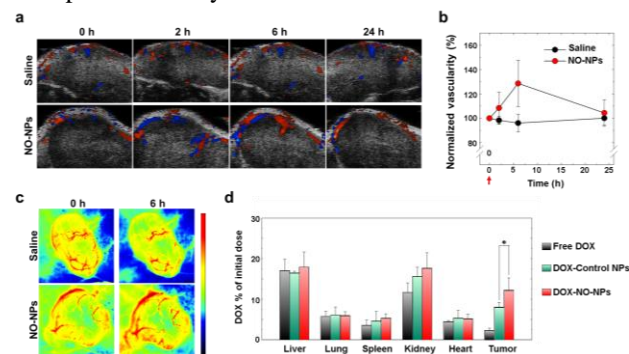


*Fig. 2. (a) Power Doppler images for tumour vascularity. (b) Quantitative analysis of changes in tumour vascularity. (c) Representative laser speckle images of tumour tissue. (d) DOX distribution in major organs and tumour lysate.*

## CONCLUSION

In this study, we developed the polymeric nanoparticles which can release NO and anticancer drug simultaneously with GSH-responsive release behaviour. Owing to these specific characteristics, they could successfully induce an increase in tumour blood flow and vascular permeability. Overall, NO-NPs can be considered as potential EPR-boosting drug delivery carriers for better antitumor efficacy outcomes.

## REFERENCES

- Jain R.K. *et al.*, Nat. Rev. Clin. Oncol. 7:653-664, 2010
- Shi J. *et al.*, Nat. Rev. Cancer 17:20-37, 2017.
- Nichols J.W. *et al.*, J. Control. Release 190:451-464, 2016.
- Fang J. *et al.*, Adv. Drug Delivery Rev. 63:136-151, 2011.
- Miller M.R. *et al.*, Br. J. Pharmacol. 151:305-321, 2007.



## Chitosan-matrix Hydrogels Modified with Graphene Additives – Variations in Physicochemical Properties

Karolina Kosowska, Patrycja Domalik-Pyzik, Jan Chłopek

Department of Biomaterials and Composites, Faculty of Materials Science and Ceramics,  
AGH University of Science and Technology, Poland  
[kosowska@agh.edu.pl](mailto:kosowska@agh.edu.pl)

### INTRODUCTION

Three-dimensional polymer networks, characterized by high-water content are called hydrogels. Those interesting materials can be tailored to serve as scaffolds for tissue engineering, hence they constitute an important class of biomaterial group. Bearing in mind that the material for tissue regeneration must be biocompatible, chitosan (CS), a natural polymer with many beneficial properties<sup>1</sup>, has been selected. Chemical cross-linking is a commonly used method for hydrogel fabrication; however organic cross-linking agents like glutaraldehyde can be toxic<sup>2</sup>. That is why in our work, we decided to prepare CS hydrogels using non-toxic and environmentally friendly materials. Graphene oxide (GO), reduced graphene oxide (rGO) and tannic acid (TAc) were applied instead of commonly used cross-linkers. Moreover, we synthesized different rGOs using non-toxic agents, like: L-ascorbic acid (AAc), green tea extract (GT) and grape extract (GE). We also attempted to obtain gradient composite materials based on CS hydrogels modified with GO and rGO.

### EXPERIMENTAL METHODS

GO was prepared from graphite by the modified Marcano method (ITME, Poland)<sup>3</sup>. The reduction of GO was carried out by three methods: (1) 0.3 g of AAc (Avantor Performance Materials Poland S.A.) was added to aqueous dispersion of GO (0.01 mg/ml) under stirring. Next, NaOH (Avantor) solution was dripped to adjust the pH to 9-11. The system was sonicated for 1 h, heated to 70°C, and kept under stirring for 2 h. After cooling down, rGO was centrifuged, washed with distilled water and freeze-dried. (2) 20 g of GO powder was added to 200 ml of GT extract (40 g of leaves (Gunpowder, Richmond) brewed in 335 ml of distilled water), the next steps were as in (1). (3) GO reduction was performed as previously, using grape extract (135 g of grapes in 335 ml of water).

GO (1.5 wt.%) and three types of “green” synthesized rGO (1.5 wt.%) were tested as cross-linkers for chitosan. Briefly, dispersion of GO or rGO was added to 4.7% (w/v) CS (Acros Organics) solution in 5% acetic or lactic acid (Avantor), with or without TAc (5%; Sigma-Aldrich). After 24 h, homogenous solutions were casted onto Teflon dishes and dried for 96 h at RT. Materials were characterized by ATR, XPS, XRD, DSC and SEM. In addition, wettability, degradation in PBS (37°C) and bioactivity (SBF) were investigated.

### RESULTS AND DISCUSSION

The results of XRD and XPS were used to assess the degree of reduction of GO. D-spacing of GO and rGOs were calculated using Bragg's equation – for GO, rGO\_AAc, rGO\_GT and rGO\_GE it was: 0.77, 0.39,

0.35 and 0.37 nm, respectively. The second determinant of the degree of the reduction was the C/O atomic ratio derived from the XPS data. They showed that AAc was the most effective reducing agent – C/O atomic ratio increased from 0.78 for GO to 1.88 for rGO\_AAc. For rGO\_GT and rGO\_GE, the shift was lower: 1.10 and 1.07, respectively. Next, we investigated the relationship between the type of the nanoparticles and the properties of chitosan-based composites (Table).

Sample	T <sub>g</sub> [°C]	ICr [%]	Contact angle [°]	Deg. time
CS	163.0	0.0	109.9	1 day
CS/GO	186.2	4.7	102.8	3 days
CS/rGO_AAc	180.0	23.9	75.7	90 days
CS/rGO_GT	175.7	39.1	91.5	3 days
CS/rGO_GE	167.5	47.1	98.1	3 days

Reduction of GO by AAc, under alkaline conditions, caused electrostatic repulsion between exfoliated graphene sheets. In the composite system, mobility of chitosan chains was affected due to the strong physical interactions with rGO\_AAc sheets. As a consequence, thermal and chemical stability (up to 90 days in PBS) of chitosan were improved. Moreover, only CS/rGO\_AAc samples were found to be hydrophilic. For those reasons, rGO\_AAc was selected for further research on the optimization of the hydrogels properties. The change of the solvent from acetic acid to lactic acid and the addition of TAc improved mechanical properties of the CS composites. Their bioactivity was confirmed using *in vitro* assay (SBF incubation).

### CONCLUSION

All of the demonstrated “green” methods of reducing GO were effective and can be adopted on a large scale. Uniform distribution of rGO\_AAc and self-assembled character of composite hydrogel components allowed to exploit the potential of graphene nanofillers for tissue engineering applications.

### REFERENCES

1. LogithKumar R. *et al.*, Carbohydr. Polym. 151:172-188, 2016
2. Takigawa T. *et al.*, J. Occup. Health. 48:75-87, 2006
3. Boguslawski J. *et al.*, Photonics Res. 3:119-125, 2015

### ACKNOWLEDGMENTS

The authors would like to thank the National Centre for Research and Development, Poland for providing financial support to this project (STRATEGMED3/303570/7/NCBR/2017). J. Jagiełło and Dr. L. Lipińska from the Institute of Electronics Materials Technology (ITME) in Warsaw are gratefully acknowledged for providing graphene oxide.

## A Study on the Degradation Properties of Pectin/Chitosan Scaffold

Maryna Lazouskaya, Viktoryia Kulikouskaya, Vladimir Agabekov

Institute of Chemistry of New Materials of NAS of Belarus, Belarus

[lozovskaya.marina@rambler.ru](mailto:lozovskaya.marina@rambler.ru)

### INTRODUCTION

In recent years, scaffolds of polyelectrolyte complexes (PEC), based on chitosan (CS) with various anionic polyelectrolytes, such as alginates, carrageenans, gelatin, etc<sup>1-2</sup>, have attracted increasing attention for tissue engineering application due to its porous structure and beneficial biological properties<sup>3</sup>. PEC, based on chitosan and pectin (Pec), have properties that overcome the limitations of individual polymers (stability, mechanical strength, sustained release of the substance, included in the PEC matrix, degradation rate)<sup>4-5</sup>. Degradation of scaffolds for tissue engineering is the key parameter: scaffolds should degrade as new tissue formation takes place<sup>6</sup>.

### EXPERIMENTAL METHODS

To produce scaffolds of pectin/chitosan polyelectrolyte complex (Pec:CS PEC), 5 mg/ml solution of chitosan in 1% acetic acid was added drop vice into 5 mg/ml water solution of pectin under vigorous shaking on the vortex. The volume ratio Pec:CS varied in the range 1:1, 1:1.5, 1:2. The resulting gel-like complexes were left for a while to complete the formation of PEC and later freeze-dried for 8h. Degradation behavior was investigated by exposing to media of different pH and ionic strength: 0.09% NaCl, H<sub>2</sub>O, Dulbecco's phosphate buffered saline (PBS) with weight loss determination within a month at 37°C.

### RESULTS AND DISCUSSION

Pec:CS PEC possess interconnected porous structure with pore size about 100 μm (Fig. 1). Such highly porous structure is favorable for tissue engineering as it meets the needs for the mass transfer of large numbers of cells.

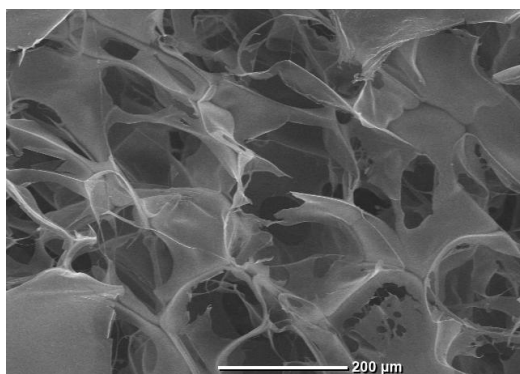


Fig. 1. SEM image of Pec:CS=1:1

The degradation profiles of Pec:CS PEC in different media were studied. Fig. 2 shows that the largest weight loss is observed in water and reaches more than 80% after 1 hour, while in NaCl and PBS weight loss is around 50-60% after 1 month (Fig. 2).

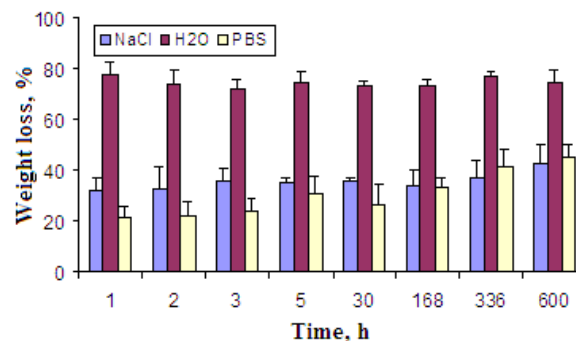


Fig. 2. Weight loss of Pec:CS=1:1 within a month incubation in different media at 37°C.

For samples with different Pec:CS volume ratio, weight loss increase with increasing amount of chitosan (Fig. 3). Apparently, this is due to the washing out of unreacted chitosan from the PEC network, as amount of ionized groups of CS is higher than that of Pec ( $4,66 \cdot 10^{-3}$  against  $0,53 \cdot 10^{-3}$  mol per 1g).

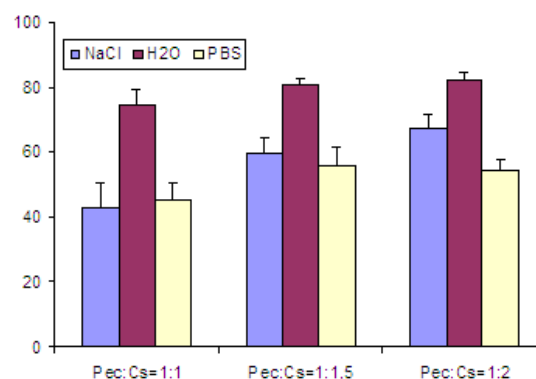


Fig. 3. Weight loss of Pec:CS for samples with different Pec:CS ratio after a month incubation in different media at 37°C.

### CONCLUSION

In the present study pectin/chitosan polyelectrolyte scaffolds were investigated for degradation behaviour. It was demonstrated that such scaffold degradation is favourable for tissue engineering application.

### REFERENCES

1. Inamdar N, Mourya V. K. Chitosan and anionic polymers – complex formation and application Edited by Ashotosh Tiwari. Polysaccharides: development, properties and application. Nova Science Publishers, Inc., 2010, 15:333-377.
2. Hamman J. H., Mar. Drugs, 8:1305-1322, 2010.
3. Martino A. D., Biomaterials, 26:5983-5990, 2005.
4. Morris G. A., et al., Biotechnol. Genet. Eng. Rev., 27:257-284, 2010.
5. Pandey S., et al., J. Young Pharm., 5:160-166, 2013.
6. Vacanti J. P, Langer R., Mol. Med., 354:32-34, 1999.

## Moldable Hyaluronic Acid Hydrogel Based on Dynamic Chemistry as Skin Regenerative Material

Liyang Shi<sup>1</sup>, Yannan Zhao<sup>2</sup>, Jöns Hilborn<sup>1</sup>, Jianwu Dai<sup>2</sup>, Dmitri. A. Ossipov<sup>1</sup>

<sup>1</sup>Division of Polymer Chemistry, Department of Chemistry-Ångström, Uppsala University, Uppsala, SE 751 21, Sweden

<sup>2</sup>Center for Regenerative Medicine, State Key Laboratory of Molecular Developmental Biology, Institute of Genetics and Developmental Biology, Chinese Academy of Sciences, Beijing, P. R. China

[liyang.shi@kemi.uu.se](mailto:liyang.shi@kemi.uu.se)

### INTRODUCTION

Skin defect is one of the most common diseases in the clinical. Despite of the self-healing abilities of skin in small wound case, the regenerations for large and full-thick skin defects are still big challenging. Polymeric biomaterial mediated regenerative methods provide cost-effective solutions for the treatment of skin defect. Hydrogels formed by hyaluronic acid (HA) is one promising biomaterial candidate since HA is involved in inflammation, granulation, and reepithelialization wound healing processes in the body.<sup>1</sup> It is reported that the hydrazone-crosslinked HA hydrogel could significantly improve the reepithelialization in vivo.<sup>2</sup> However, this covalently HA hydrogel inherently lack moldable and self-healing properties, resulting in easily structure collapse under force-loaded environment in vivo. In this study, we developed a dynamic HA hydrogel based on bisphosphonate-silver coordination bonds, and applied it for wound healing.

### EXPERIMENTAL METHODS

HA was firstly modified with maleimide (Mal) group with 1-ethyl-3-(3-dimethylaminopropyl) carbodiimide (EDC) coupling reaction to obtain Mal functionalized HA (HA-Mal). Then bisphosphonate (BP) groups was linked on HA backbone using chemoselective “click” reaction between thiolated bisphosphonate and HA-Mal. The hydrogel was formed by simple mixing two hydrogel precursors, AgNO<sub>3</sub> solution and BP functionalized HA (HA-BP) solution. The self-healing properties were confirmed by microscope observations and rheological tests. For animals’ studies, we applied our hydrogel on the rat full-thick skin defect models for 10 days, and elevated the skin regeneration using percentage of remaining wound size and histological observation.

### RESULTS AND DISCUSSION

HA was successfully modified with BP group using NMR spectrum analysis. The degree of modification of HA with BP groups was evaluated to be ≈20%, based on the integral of the two protons adjacent to the BP bridging carbon normalized to the integral of acetamide protons on HA backbone. HA-BP/Ag<sup>+</sup> hydrogel could be formed in several seconds after mixing HA-BP solution and silver ions solution. One pieces of HA-BP/Ag<sup>+</sup> hydrogel enabled to shape into different shapes. Moreover, two cut pieces hydrogels could self-heal together in 30 seconds without any external stimulus, and the storage modulus of healed hydrogel showed no decrease comparing with that of pre-cutting one. Animal experiments showed the HA-BP/Ag<sup>+</sup> hydrogel can significantly decrease wound remaining rate and promote the thickness of regenerated epidermis as compared with the group without hydrogel treatment.

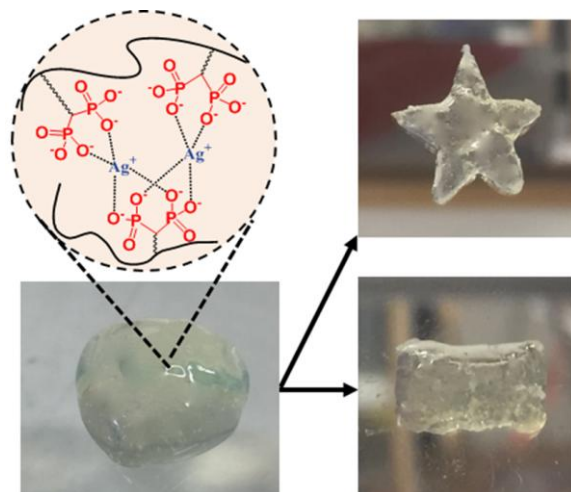


Fig. 1. Images of HA-BP/Ag<sup>+</sup> hydrogel and schematics for its crosslinking. The hydrogel can be shaped into various shapes.

### CONCLUSION

We develop a novel HA hydrogel based on dynamic coordination bonds between bisphosphonate and metal ions. The novel hydrogel shows self-healing and moldable properties, and abilities to promote skin regeneration in full-thick skin defect model. These results demonstrated moldable HA-BP/Ag<sup>+</sup> hydrogel is a promising skin regenerative material with ability to fill irregular-shaped defects.

### REFERENCES

1. Shi L. *et al.*, Adv. Healthcare Mater. 2017: 1700973.
2. Kirker K. R. *et al.*, Biomaterials 2002, 23: 3661-3671.

### ACKNOWLEDGMENTS

The authors acknowledge the funds from “Biodesign” Project in EU, Key Research Program of the Chinese Academy of Sciences (Grant No. ZDRW-ZS-2016-2) and Youth Innovation Promotion Association CAS (2016096) Project in China. L.S thanks China Scholarship Council.

## Preparation and Characterization of Polyurethane-based Multifunctional Bone Cements

Klaudia Ordon, Kinga Pielichowska

Faculty of Material Science and Ceramics, AGH University of Science and Technology, Poland  
[ordon@agh.edu.pl](mailto:ordon@agh.edu.pl)

### INTRODUCTION

The number of orthopedic surgeries which are performed using bond cements is still growing nowadays. It is connected with a much more active lifestyle and it contributes to increase people's life expectancy. Currently, in clinical practice during hip or knee prosthetic implantation are often used in order to stabilize the endoprosthesis acrylic bone cements mainly using poly(methyl methacrylate) (PMMA). Acrylate bone cements are used in the same form from the late 1950s, when for the first time they were used by Charnley. All cements of this type - commercially available - are two-component systems composed of powder and liquid component. After mixing these two components, the polymerization of methyl methacrylate (MMA) and solidification of the bone cement. This is connected with a significant increase of the cement mass temperature, which may lead us to thermal necrosis of the circumfluent tissues and to the possibility of the monomer leakage which is toxic for tissues. That may lead to chemical necrosis of the tissues. In addition, acrylic bone cements usually show poor adhesion to the bone tissue and lack of the bioactivity [1,2]. In the light of the problems presented the main goal of the research is to create and characterize new biodegradable, biocompatible and bioactive bone cements. Potential alternative for currently used acrylate cements are polyurethanesaccharides. Polyurethanes (PU) are widely used in different biomedical applications because of their good mechanical properties and biocompatibility. Polyurethanes offer the possibility of building various structural elements in respect of chemical structure, also biodegradable. They bid making injectable systems and provide functionalization in order to improve conditions for adhesion and cell proliferation. Furthermore, polyurethanes in biomedical using allow obtaining materials with a broad mechanical properties' spectrum [3]. The amendment of mechanical properties can be achieved among others by spatial crosslinking polyurethane with a multifunctional crosslinker, such as for example starch or other polysaccharides. Combination of these two groups of biocompatible polymers - PUs and polysaccharides - could give the possibility of fabrication of a new class of materials with wide range of properties, dedicated to the bone cements applications.

### EXPERIMENTAL METHODS

In the first stage of the work characterization of all used raw materials was performed, followed by elaboration of a method for obtaining polymer bone cements based on polyurethanesaccharides with the addition of bioceramics. Polyurethane based materials were obtained in a two-step bulk polymerization procedure [4].

Poly(ethylene glycol) (PEG) with average molar mass 2000 and 1,6-hexamethylene diisocyanate (HDI) were used in stoichiometric amount. 1,4-butanediol (BDO) and starch were used as a chain extender. Before starting the synthesis of bone cement, PEG was dried under vacuum at the temperature of 110°C. Hydroxyapatite (HAp) was incorporated into the melted prepolymer and stirred. Next, mixture of BDO and starch in proper amount was incorporated. Samples were prepared with both HAp and without HAp. The main methods used for of obtained bone cement characterization there were DSC, TG, FTIR, X-ray and SEM. The assessment of the mechanical properties (e.g. tensile strength, hardness) was also performed.

### RESULTS AND DISCUSSION

This work reports on the preparation and characterization of polyurethane-based bone cements. Based on the results obtained, structure/property relationships can be established. It was found that the obtained materials constitute a preliminary basis for obtaining a new generation of multifunctional polyurethane-based bone cements.

### CONCLUSION

We have developed polyurethane bone cements containing polysaccharides and bioactive ceramic. The structure of the obtained polyurethanes was confirmed by FTIR technique. The obtained materials are characterized by the promising properties and have a high potential for their further use in surgery as multifunctional polyurethane-based bone cements.

### REFERENCES

1. Dunne N., Clements J., Joint Replacement Technology 2:212-256, 2014
2. Vaishya R., Cjauhan M. et. al., J. Clin. Orthop. Trauma 4:157-163, 2013
3. Marzec M., Kucińska-Lipka J. et. al., Mater. Sci. Eng., C 80:736-747, 2017
4. Pielichowska K., Nowak M. et. al., Appl. Energy 162:1024-1033, 2016

### ACKNOWLEDGMENTS

Authors are grateful to the Polish National Science Centre for financial support under the Contract No. UMO-2016/22/E/ST8/00048.



## Design of Poly $\epsilon$ -caprolactone /zein Blends for Delivery of Essential Oils as Antimicrobial Biomaterials

Binh Thi Thanh Phan<sup>1,2</sup>, Christopher Lovell<sup>2</sup>, Wolfgang H. Goldmann<sup>3</sup>, Aldo R. Boccaccini<sup>1</sup>

<sup>1</sup>Institute of Biomaterials, Friedrich-Alexander University Erlangen - Nuremberg, Germany

<sup>2</sup>Lucideon Ltd., Queens Road, Stoke-on-Trent, United Kingdom

<sup>3</sup>Department of Biophysics, Friedrich-Alexander University Erlangen - Nuremberg, Germany  
[binh.tt.phan@fau.de](mailto:binh.tt.phan@fau.de)

### INTRODUCTION

Essential oils (EOs) are recognized as one of the most effective natural agents to kill bacteria and prevent biofilm formation. Despite the high interest in the application of EOs in modern biomaterials, significant challenges remain due to their unique properties. Herein, we report the development of antimicrobial biomaterials, using biodegradable poly  $\epsilon$ -caprolactone (PCL) and natural corn protein - zein, to deliver and control the release of selected essential oils. The combination of PCL and zein improve the overall biodegradability and mechanical properties for biomedical applications<sup>1,2</sup>.

### EXPERIMENTAL METHODS

PCL ( $M_w = 80\ 000$ ), zein and essential oils (cinnamon bark oil, peppermint oil) were purchased from Sigma-Aldrich. PCL and PCL/zein films were dissolved in acetone-ethanol (2:1 v/v), followed by an addition of one of the essential oil, then casting on Petri dishes by the solvent-casting method. The contents of zein and EOs were varied to investigate the effect of zein and EOs on the properties of resulting films.

The morphology of the films was observed by SEM. The encapsulation efficiency and release of essential oils were quantified by Gas chromatography – Mass Spectrometry (GC-MS). The physical properties were tested by tensile tests, water uptake, FTIR and mass loss in Phosphate Buffered Saline (PBS). The biological activity was evaluated by the well-established agar diffusion Halo-Optical Density test and cytotoxicity assay.

### RESULTS AND DISCUSSION

The blend films were highly porous due to the solvent evaporation, resulting in a lower Young's modulus. The addition of zein significantly increased the hydrophilicity indicated by the water-uptake but decreased the stiffness of the films.

The essential oil - encapsulation efficiency of the films was more than 60%. No change in mechanical properties was observed in the films with the 5w/w% content of essential oils. In contrast, the Young's modulus slightly reduced in the films with 10 - 15w/w% content of cinnamon bark oil. The biologic tests showed good antimicrobial activity against both *S. carnosus* and *E.coli* with the presence of cinnamon bark oil of  $\geq 5w/w\%$  and was found to be more effective against Gram-positive than Gram-negative bacteria.

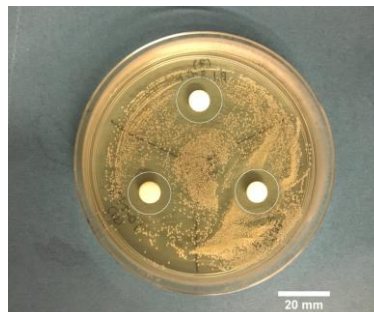


Fig. 1. Agar-diffusion images of the blends with 5w/w% cinnamon bark oil against *S. carnosus*.

Scale bar = 20 mm.

The films containing peppermint oil also suppressed the growth of bacteria, but were much less effective than those of cinnamon bark oil. The release of essential oils was quick during the first 6h, and prolonged depending on the loading amount of the essential oil. However, a higher concentration of essential oils exhibited a higher cytotoxicity.

### CONCLUSION

The solvent-casting method resulted in highly porous structure. The addition of zein improved the hydrophilicity of PCL polymer matrices. Thus, the degradation of the blends was increased, indicated by the mass loss of the films in PBS buffer. The polymeric matrices were able to highly encapsulate the essential oils during the preparation. The Halo test indicated potent antimicrobial activity of cinnamon bark oil against both Gram-positive and Gram-negative bacteria. The peppermint oil required a higher content to prevent the growth of bacteria, but it had lower toxicity than the cinnamon bark oil. This research presents a new biopolymer system of essential oils with highly effective antibacterial activity promising for coating implants.

### REFERENCES

1. Martínez-Abad A. *et al*, Food Control 34(1):214-220, 2013
2. Fereshteh Z. *et al*, Materials Science and Engineering: C 54: 50-60, 2015.

### ACKNOWLEDGMENTS

The authors would like to thank the HyMedPoly Programme (Grant no: 643050) funded by the European Union's Horizon 2020 research and innovation programme for providing financial support.

## The Influence of the Solvent Type on the Structure of Thermosensitive Chitosan Hydrogels Containing Graphene Oxide

Katarzyna Pieklarz, Michał Tylman, Zofia Modrzejewska

Faculty of Process and Environmental Engineering, Lodz University of Technology, Poland

[katarzyna.pieklarz@edu.p.lodz.pl](mailto:katarzyna.pieklarz@edu.p.lodz.pl)

### INTRODUCTION

In recent years, the development of nanotechnology sciences has been observed, focusing mainly on the study of carbon nanostructures, such as graphene oxide. The main reason for this trend is the possibility of using nanoparticles in medicine and biomedical engineering. Nanoparticles can be used in clinical practice for the treatment, for example, neurodegenerative diseases, cancerous diseases and medical diagnostics<sup>1,2,3</sup>.

The above scientific tendencies caused that the aim of the research is creation of a new generation of thermosensitive chitosan gels containing graphene oxide (Fig. 1) for biomedical applications, for example for damage regeneration bone tissue. In addition, the study concerns the analysis of the effect of the solvent type on the structure gels.

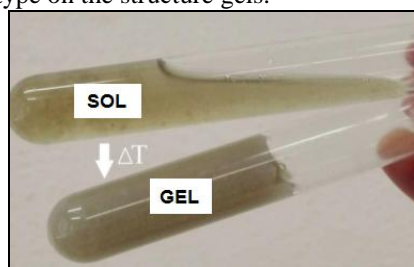


Fig. 1. Thermosensitive chitosan hydrogels containing GO

### EXPERIMENTAL METHODS

Chitosan from crab shells with low viscosity of a degree of deacetylation SD ~ 79.5% and molecular weight of 86 kDa and lactic and hydrochloric acid at a concentration of 0.1 M were used for preparation of hydrogels. The nanocomponent used was graphene oxide. Sodium  $\beta$  – glycerophosphate was used as a neutralizing and buffering agent.

The structure of hydrogels was investigated by using Fourier Transform Infrared spectroscopy. The FTIR spectrum was recorded over the range 400 – 4000  $\text{cm}^{-1}$ .

### RESULTS AND DISCUSSION

For chitosan lactate gels (Fig. 2), changes are observed in the band range corresponding to O-H vibrations whose intensity increases with increasing GO concentrations and for bands for 1080 wave numbers and overlapping bands 980  $\text{cm}^{-1}$  and 950  $\text{cm}^{-1}$  – the intensity decreases. There are no changes in the amine band.

For chitosan chloride gels (Fig. 3) the intensity of bands O-H vibrations decreases with the increase in GO concentration. There are significant changes in the amine band - the intensity of bands at 1660 wave number decreases, while the band of 1520  $\text{cm}^{-1}$  disappears. This demonstrates the involvement of these groups in reaction with GO, especially amino groups.

Changes are also observed in the band characteristic for saccharide structure, with the increase GO, the intensity of the 2 major bands for the wave numbers 1080  $\text{cm}^{-1}$  and 980  $\text{cm}^{-1}$  decreases, a small arm for the wave number 1100  $\text{cm}^{-1}$  (1150  $\text{cm}^{-1}$ ) and the band for the wave number 900  $\text{cm}^{-1}$  become clearer.

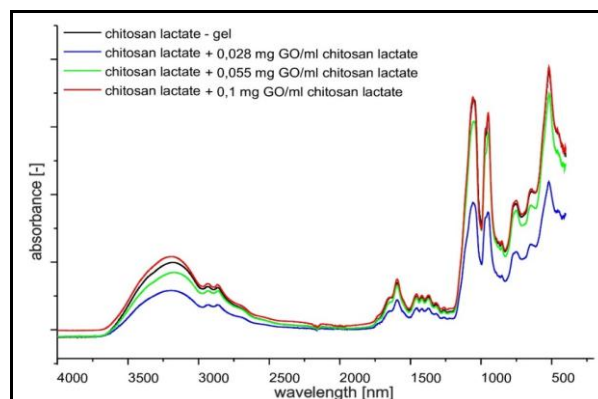


Fig. 2. FTIR spectra of chitosan lactate gels with GO

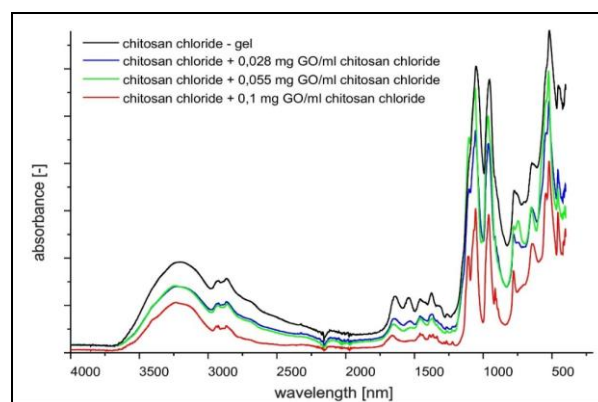


Fig. 3. FTIR spectra of chitosan chloride gels with GO

### CONCLUSION

Chitosan gels formed at physiological body temperature can contain nano-ingredients in their structure. The chosen direction of research is innovative and is the basis for further experiments using other carbon nanostructures. Thermosensitive gels prepared with the use of chitosan salts and GO can be an interesting material as scaffolds for in tissue engineering.

### REFERENCES

1. Bao R-Y. *et al.*, Carbohydr. Polym. 155:507-515, 2017
2. Kumar S. *et al.*, ACS Appl. Mater. 40:26431-26457, 2016
3. Murthy S.K., Int. J. Nanomedicine 2:129-141, 2007

## Tumour Microenvironment-Recognizable Polymeric Conjugate for Cancer Immunotherapy

Jung Min Shin, Seok Ho Song, Jae Hyung Park

School of Chemical Engineering, College of Engineering, Sungkyunkwan University  
[jmabcd@skku.edu](mailto:jmabcd@skku.edu)

### INTRODUCTION

Antigen specific CD8<sup>+</sup> cytotoxic T lymphocytes (CTLs) play significant roles in immunological rejection in cancer immunotherapy. Most tumours, however, are not removed by the immune system because they have self-antigens, which are not recognized as nonself by CTLs. In this work, we hypothesized that “foreignizing” target tumour cells by delivering foreign antigen specifically into the tumour cells using tumour microenvironment-recognizable polymeric conjugate might result in immunological rejection by a nonself-antigen reactive CTLs.

### EXPERIMENTAL METHODS

Tumour microenvironment-recognizable Polymeric conjugate (PEG-pep-HA-OVA) conjugate was prepared by using reductive amination and EDC/NHS chemistry. Fluorescein isothiocyanate (FITC) and Cy5.5 near-infrared dye-labelled PEG-pep-HA-OVA conjugates were used for further experiments.

Cellular uptake behaviour of polymeric conjugate was monitored in HPV-16 E7-expressing mouse cervical cancer model (TC-1) cells for 3hr. *In vitro* antigen presentation and CTL-mediated TC-1 killing effect were investigated using flow cytometry. *In vivo* biodistribution and anti-tumour efficacy of conjugate were carried out to evaluate *in vivo* effect of polymeric conjugate using TC-1 tumour-bearing mice.

### RESULTS AND DISCUSSION

In this study, we demonstrated PEG-pep-HA-OVA as a promising agent for cancer immunotherapy. The OVA contents in PEG-pep-HA-OVA conjugate are 13.2 wt.% calculated using BCA assay. Cellular uptake behaviour image suggested that tumour microenvironment-recognizable PEGylation of the conjugate facilitated its uptake by CD44<sup>+</sup> TC-1 tumour cells in MMP9 abundant condition (Fig. 1). *In vivo* antigen presentation was observed with OVA-vaccinated mice model showing about 10-fold higher amount of OVA antigen presentation than free OVA protein when we treat PEG-pep-HA-OVA conjugate. Tumour volume of OVA-vaccinated mice model did not significantly increase when treated with PEG-pep-HA-OVA conjugate implying antitumor effect of the tumour microenvironment-recognizable polymeric conjugate (Fig. 2).

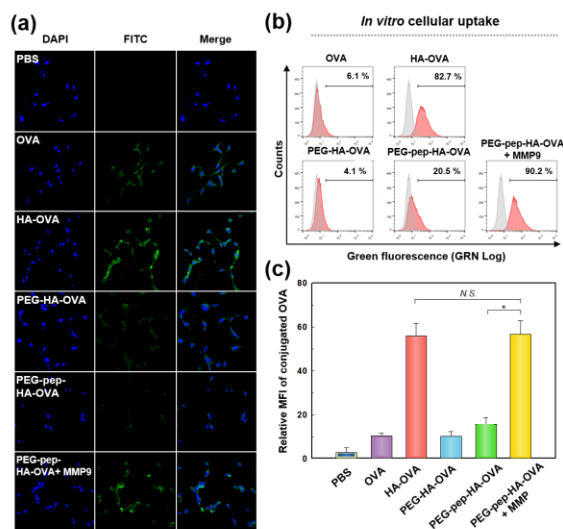


Fig. 1. Tumour microenvironment-recognizable cellular uptake of behaviour of polymeric conjugate. (a) Representative confocal microscopic image. (b) Flow cytometry analysis.

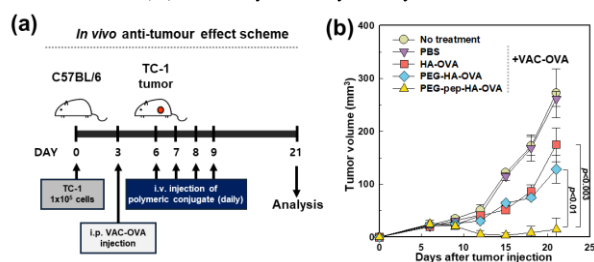


Fig. 2. *In vivo* immunotherapeutic efficacy of the tumour microenvironment-recognizable polymeric conjugate. (a) *In vivo* anti-tumour effect scheme. (b) Anti-tumour effect. Error bars represent the standard deviation ( $n = 3$ ).

### CONCLUSION

Herein, we revealed that tumour microenvironment-recognizable polymeric conjugate can targeting tumour site and generating antitumor effect by cause immune rejection against tumours that present foreign antigen. These results demonstrated that the polymeric conjugates bearing foreign antigen are promising cancer immunotherapeutic agents by foreignizing tumour cells.

### REFERENCES

1. P. Friedl. *et al.*, Nat. Rev. Immunol. 5:532-545, 2005
2. L. Fong. *et al.*, Annu. Rev. Immunol. 18:245-273, 2000
3. H.Y. Yoon. *et al.*, J. Control. Release, 199:98-105, 2015



## Synthesis and Characterization of Drug Loaded PVA/ $\beta$ -Tri Calcium Phosphate Powders for Bone Engineering Applications

Aysenur Topsakal<sup>2,1</sup>, Nazmi Ekren<sup>3,1</sup>, Osman Kilic<sup>4,1</sup>, Faik N. Oktar<sup>5,1</sup>, Mahir Mahirogullari<sup>6,1</sup>, Oguzhan Gunduz<sup>2,1</sup>

<sup>1</sup>Metallurgy and Material Engineering/ Advanced Nanotechnology Laboratory, Marmara University, Istanbul

<sup>2</sup>Department of Metallurgy and Material Engineering, Faculty of Technology, Marmara University, Istanbul

<sup>3</sup>Department of Electric and Electronic Engineering, Faculty of Technology, Marmara University, Istanbul

<sup>4</sup>Department of Electric and Electronic Engineering, Faculty of Engineering, Marmara University, Istanbul

<sup>5</sup>Department of Bioengineering, Faculty of Engineering, Marmara University, Istanbul

<sup>6</sup>Department of Orthopedics and Traumatology, Memorial Hospital, Istanbul

[topsakalaysenur@gmail.com](mailto:topsakalaysenur@gmail.com)

### INTRODUCTION

$\beta$ -tricalcium phosphate [ $\beta$ - $\text{Ca}_3(\text{PO}_4)_2$ ] ( $\beta$ -TCP) powders are commonly applied in biomedical fields due to biocompatibility and osteoconductivity<sup>1</sup>. Poly(vinyl alcohol) (PVA) is semi-crystalline hydrophilic polymer that has good chemical and thermal stability. Also PVA is biocompatible and non-toxic polymer<sup>2</sup>. Different chemical routes among, which solid state and wet precipitation are conventional methods, can be used to synthesize  $\beta$ -TCP. These routes have different advantages and disadvantages. Wet chemical precipitation is simple for experimental operation and has low operation temperature and high purity products at a reasonable cost but sometimes incomplete reaction and sedimentation cause changing of stoichiometries<sup>3</sup>. Production of drug loaded PVA/ $\beta$ -Tri calcium phosphate powders for bone tissue engineering was aimed.

### EXPERIMENTAL METHODS

$\beta$ -TCP powders were synthesis by reaction of calcium nitrate tetra-hydrate ( $\text{Ca}(\text{NO}_3)_2 \times 4\text{H}_2\text{O}$ ) with diammonium hydrogen phosphate ( $(\text{NH}_4)_2\text{HPO}_4$ ). 150mL of 0.4mol ( $\text{Ca}(\text{NO}_3)_2 \times 4\text{H}_2\text{O}$ ) solution with pH=4 and 150mL of 0.6mol ( $(\text{NH}_4)_2\text{HPO}_4$ ) solution with pH=8.2 were prepared at room temperature. ( $\text{Ca}(\text{NO}_3)_2 \times 4\text{H}_2\text{O}$ ) was added into ( $(\text{NH}_4)_2\text{HPO}_4$ ) solution by dropwise to produce white precipitate. 10 ml of %1 wt. PVA solution was prepared by dissolving with water at 120°C and added to solution. Throughout the mixing process, the pH of the system was maintained at pH=9 by adding of ammonia solution (25%). Dispersion characteristics were improved by the washing of synthesized precipitate with distilled water and 100% ethanol. The suspension was filtered in a filter glass with application of mild suction. After filtration compact, sticky filter cake was dried at 80°C for 24h. The as-dried powders were crushed by using mortar and pestle. After the production process, surface morphology of obtained powders were examined by scanning electron microscopy (SEM) and infrared spectra were performed by Fourier transform infrared spectroscopy (FTIR) to scrutinize chemical structure characterization. After the production and characterization process, rifampicin as drug was loaded to produced PVA/ $\beta$ -TCP powders. 1 mg rifampicin was dissolved in 1 ml methanol and 2 mg PVA/ $\beta$ -TCP powder was added to this solution. After the mixing process for 24, drug loaded powder<sup>\*\*\*\*</sup> was obtained and spectral analysis was made.

### RESULTS AND DISCUSSION

FTIR spectrum of powders was prepared with pH= 9 was indicated in Figure 1. The FTIR spectrum shows absorption peaks in the range of 1100-950  $\text{cm}^{-1}$  attributed to P-O vibrations in  $\text{Ca}_3(\text{PO}_4)_2$ . In addition to this, broad absorption band at 3200–3600 $\text{cm}^{-1}$  indicates O-H stretch in alcohol (PVA)<sup>4</sup>.

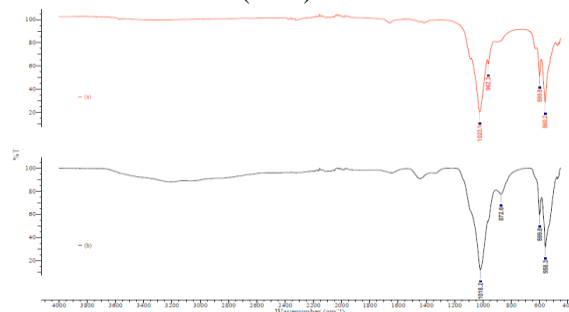


Fig. 1. FTIR spectrum of (a) commercial  $\beta$ -TCP (Sigma) and (b) PVA/ $\beta$ -TCP powders.

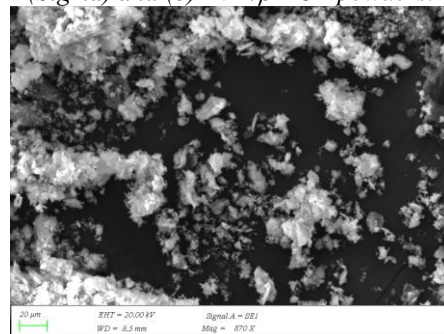


Fig. 2. SEM image of PVA/ $\beta$ -TCP powders.

Surface morphology of powders was observed by SEM as shown in Fig. 2. Powders show granular and crystalline structures.

### CONCLUSION

PVA/ $\beta$ -TCP powders were successfully synthesized through wet precipitation process. The wet precipitation is a low cost method for production of  $\beta$ -TCP. Moreover, produced PVA/ $\beta$ -TCP powders can be used in bone tissue engineering applications.

### REFERENCES

1. Mirhadi B., *et al.*, Process and Appl. Of Ceram., 5:193-198, 2011
2. Mohammadi Y., *et al.*, The Int. Jour. of Art. Org., 30:204-211, 2007.
3. Ghosh R., *et al.*, Mater. Sci. Eng. C, 67:345-352, 2016
4. Grigoravičute I., *et al.*, Adv. Powd. Tech., 28:2325-2331, 2017.

### ACKNOWLEDGMENT

This study has been founded by Ministry of Development, Turkey; project no: 2016K121280.



## Photo-crosslinkable 'Nature-inspired' Synthetic Polymers for Adipose Tissue Regeneration

Liesbeth Tytgat<sup>1,2</sup>, Marica Markovic<sup>3,4</sup>, Taimoor Qazi<sup>5</sup>, Heidi Ottevaere<sup>1</sup>, Hugo Thienpont<sup>1</sup>, Aleksandr Ovsianikov<sup>3,4</sup>, Peter Dubrue<sup>2</sup>, Sandra Van Vlierberghe<sup>1,2</sup>

<sup>1</sup>Brussels Photonics (B-PHOT) – Department of Applied Physics and Photonics, Vrije Universiteit Brussel, Belgium

<sup>2</sup>Polymer Chemistry & Biomaterials Group – Centre of Macromolecular Chemistry (CMAc) – Department of Organic and Macromolecular Chemistry, Ghent University, Belgium

<sup>3</sup>Institute of Materials Science and Technology, Technische Universität Wien, Austria

<sup>4</sup>Austrian Cluster for Tissue Regeneration, Austria

<sup>5</sup>Julius Wolff Institute, Charité – Universitätsmedizin Berlin, Germany

[ltytgat@b-phot.org](mailto:ltytgat@b-phot.org)

### INTRODUCTION

Gelatin-based materials are frequently used for various tissue engineering applications due to their excellent cell-interactive characteristics<sup>1</sup>. Animal-derived gelatin is often used to fabricate 3D scaffolds for adipose tissue engineering applications<sup>2</sup>. However, the concerns associated with the use of animal-derived materials have emerged through the last two decades due to batch to batch variations and the risk of pathogen transmittance. We hypothesize that recombinant collagen I peptide (RCP) (Cellnest<sup>TM</sup>, Fujifilm) could be a promising alternative to solve the issues associated with gelatin from animal origin. The main difference between both materials is that RCP contains a higher number of cell-interactive arginine-glycine-aspartic acid (RGD) tripeptides within its backbone compared to gelatin. In the present work, both materials have been functionalized with methacrylamide functionalities to introduce photo-crosslinkable moieties. Subsequently, the hydrogel building blocks have been processed via UV polymerization in the presence of a photo-initiator in hydrogel films and their adipose tissue regeneration potential has been evaluated. Next, two-photon polymerization (2PP) was applied to produce 3D microscaffolds.

### EXPERIMENTAL METHODS

Gelatin B and RCP were modified using 2.5 and 1 equivalents methacrylic anhydride (MA) respectively to obtain methacrylamide-modified derivatives (GEL-MOD with a degree of substitution (DS) of 97% and RCP-MOD with a DS of 90%). The materials developed were characterized in depth via (HR-MAS) <sup>1</sup>H-NMR spectroscopy, swelling and gel fraction experiments as well as rheology. Furthermore, the biocompatibility of the hydrogel building blocks was evaluated by monitoring the metabolic activity of encapsulated adipose tissue-derived stem cells (ASC-TERT). 3D scaffolds were fabricated via 2PP (780 nm).

### RESULTS AND DISCUSSION

After modification, RCP-MOD contained 1.6 times more photo-crosslinkable functionalities compared to GEL-MOD. The DSC results showed that the physical crosslinking behavior of RCP-MOD was hampered due to the higher number of photo-crosslinkable groups that disturbed the triple helix formation. The results of the gel fraction and HR-MAS <sup>1</sup>H-NMR spectroscopy experiments indicated an efficient crosslinking resulting in a gel fraction exceeding 90% for both materials.

Furthermore, storage modulus  $G'$  of the chemically crosslinked RCP-MOD was comparable with GEL-MOD (i.e. 6 kPa). The water uptake capacity of RCP-MOD was lower compared to GEL-MOD, which was anticipated since RCP-MOD has 20% more hydrophobic functionalities including leucine and 24% less hydrophilic moieties such as aspartic acid than GEL-MOD. There are various reports in literature which indicate that GEL-MOD is biocompatible<sup>1,3</sup>. The cell encapsulation experiments with ASC-TERT cells showed that RCP-MOD hydrogels are also biocompatible. Furthermore, RCP-MOD and GEL-MOD could be processed via 2PP into 3D scaffolds<sup>4</sup>.

### CONCLUSION

The physico-chemical properties, the biocompatibility and the processing potential of RCP-MOD are comparable with those of animal-derived GEL-MOD indicating that RCP-MOD is an attractive alternative that can be used for adipose tissue engineering applications.

### REFERENCES

1. Yue, K. *et al. Biomaterials* **73**, 254–271 (2015).
2. Van Nieuwenhove, I. *et al. Acta Biomater.* **63**, 37–49 (2017).
3. Van Nieuwenhove, I. *et al. Carbohydr. Polym.* **161**, 295–305 (2017).
4. Van Hoorick, J. *et al. Biomacromolecules* **18**, 3260–3272 (2017).

### ACKNOWLEDGMENTS

Liesbeth Tytgat would like to thank FWO for providing her a PhD fellowship and Fujifilm Manufacturing Europe B.V. for providing Cellnest.

## Evaluation of the Degradation Process of Scaffolds Fabricated by Compression Molding with Particulate Leaching

Anna Wiśniewska, Aneta Liber-Kneć

Faculty of Mechanical Engineering, Division of Applied Mechanics, Cracow University of Technology, Poland  
[wisniewska.anna@student.pk.edu.pl](mailto:wisniewska.anna@student.pk.edu.pl)

### INTRODUCTION

The scaffold used in tissue engineering for cells deposition is one of the key factors in tissue reconstruction [1-3]. Biodegradable materials are often used to make scaffolds, which disappear in time, and their place is occupied by rebuilding tissue. Obtaining a scaffold with appropriate features i.e. architecture, mechanical properties, is determined by the choice of material and the method of scaffold's preparation [3]. The aim of the work was to make porous scaffolds from biodegradable polymers (polylactide (PLA) and polyhydroxyalkanoate (PHA)) using polymer compression molding with porogen leaching and to evaluate the structure of the scaffolds before and after the material degradation process.

### EXPERIMENTAL METHODS

In order to obtain a porous structure, the polymer granules with porogen in a 4:1 weight ratio were mixed. Two kinds of porogen were used: sugar crystals and sodium chloride crystals, resulting in obtain 4 different types of porous scaffolds. Mixed polymer granules and porogen were placed in a metal mold, heated and then pressed. The resulting roll-shaped specimens were cut into discs and then placed in hot water to remove porogen by leaching. Next, the open porosity and the apparent density of the obtained scaffolds by the hydrostatic method were determined. Their structure, using a stereoscopic microscope SteREO Discovery V8, was also evaluated. Then an analysis of the pores size distribution was made by creating histograms for the parameters tested (equivalent pore size, shape factor, pore surface area). After preliminary observation of the structure, the scaffolds were incubated in Ringer's solution at 37°C for 18 months. During this period the process of degradation was checked by measuring the scaffold's mass changes and incubation fluids conductivity changes. After the incubation, reassessment of the scaffolds structure was made.

### RESULTS AND DISCUSSION

The use of sugar crystals as porogen resulted in a pores diameter distribution, which was close to the Gaussian distribution with a predominance pore diameter 400-700 [μm]. Whereas the use of sodium chlorine as porogen resulted in more varied equivalent diameter values, in the range 100-1300 [μm].

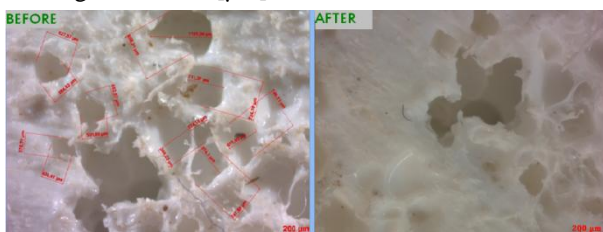


Fig. 1. The surface of the scaffold made from mixture PLA with sugar crystals before and after degradation.

After incubation increase of the pore size and loss of spherical shape have been observed (Fig. 1-2).

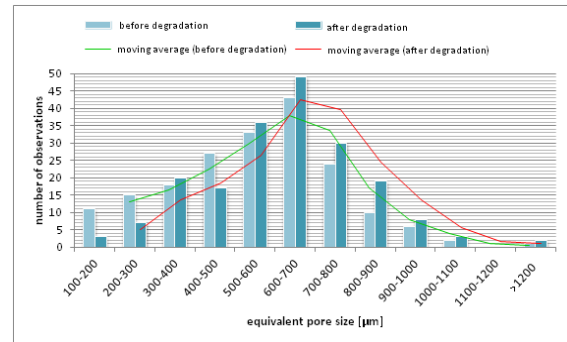


Fig. 2 Histogram of equivalent pore diameter for scaffolds made from mixture PHA with sugar crystals

After incubation decrease of the value of apparent density and increase in the open porosity of the obtained scaffolds were observed. With incubation time, the conductivity of the incubation fluids increased and the weight of the scaffolds decreased. All these changes indicate the progressive degradation of scaffolds. The largest loss in mass and relatively high conductivity was characterized by scaffolds based on PHA and sodium chloride. These observations indicate that it underwent the fastest degradation process.

### CONCLUSION

Based on the results of the tests, it can be stated that the polymer casting method with porogen leaching allows for the production of scaffolds with differentiated distribution of pores. The use of sugar crystals results in more spherical shaped pores that are more suitable for cell adhesion and growth. The scaffolds made from both PLA and PHA, for production of which sugar crystals were used, should fulfill their role in fibrous tissue regeneration, thanks to appropriate pore size (over 500 [μm]) [3]. PHA and sodium chloride scaffolds are also suitable for use in fibrous tissue engineering. All types of produced scaffolds have been found to be suitable for use in bone tissue regeneration, wherein the best are scaffolds made from PLA and sodium chloride crystals [1-3]. This type of scaffold is also most suitable for application in fibro-cartilaginous tissue engineering.

### REFERENCES

1. Dutta R. C., et al.: *Competent Processing Techniques for Scaffolds in Tissue Engineering*, Biotechnol. Adv., 35(2): 240-250, 2017.
2. Weigel T., et al.: *Design and preparation of polymeric scaffolds for tissue engineering*, Expert Rev. Med. Devices, 3(6): 835-851, 2006.
3. Dziadek M., et al.: *Wybrane metody otrzymywania porowatych rusztozań w inżynierii tkankowej*, Acta Bio-Optica et Informatica Medica Inżynieria Biomedyczna, vol. 20, no. 4, p. 193-203, 2014.

## Antibacterial Nanofibrous Wound Dressing Material by Electrospinning Method

Eda Yeniay<sup>1,2</sup>, Leyla Öcal<sup>1,2</sup>, Esra Altun<sup>1,2</sup>, Faik N. Oktar<sup>1,3</sup>, Nazmi Ekren<sup>1,4</sup>, Osman Kilic<sup>1,5</sup>, Oguzhan Gunduz<sup>1,6</sup>

<sup>1</sup>Advanced Nanomaterials Research Laboratory, Department of Metallurgical and Materials Engineering, Marmara University, Turkey

<sup>2</sup>Department of Metallurgical and Materials Engineering, Master of Science, Institute of Pure and Applied Sciences, Marmara University, Turkey

<sup>3</sup>Department of Bioengineer, Faculty of Engineer, Marmara University, Turkey

<sup>4</sup>Department of Electrical- Electronics Engineering, Faculty of Technology, Marmara University, Turkey

<sup>5</sup>Department of Electrical- Electronics Engineering, Faculty of Technology, Marmara University, Turkey

<sup>6</sup>Department of Metallurgical and Materials Engineering, Faculty of Technology, Marmara University, Turkey

[yeniyeda@gmail.com](mailto:yeniyeda@gmail.com)

### INTRODUCTION

Antibacterial wound dressing materials are very useful materials for accelerating the wound healing process. In this study, antibacterial nanofibrous wound dressing material was fabricated from mixing of Poly-lactic acid (PLA) /Starch (St) /Chitosan (Ch) /Zinc Oxide (ZnO) by electrospinning method. Starch was used to increase cell viability. Ch is obtained by alkaline deacetylation of chitin that is the principal exoskeleton component in crustaceans<sup>1</sup>. ZnO has been used to enhance antibacterial properties of the antibacterial nanofibrous wound dressing material because of its unique antimicrobial feature.

### EXPERIMENTAL METHODS

#### 1. Solution Preparation

Poly-lactic acid (PLA) solution was prepared by dissolving as 10 wt% in Dichloromethane (DCM) and Dimethylformamide (DMF) (70:30). Chitosan was dissolved with a mixture of acetic acid and ethanol (90:10 wt ratio) and was stirred with the magnetic stirrer for 3 hours at ambient temperature (23°C). Starch (5 wt%) was dissolved with a Dimethylsulfoxide (DMSO) and added to the PLA/Cs mixture. Finally ZnO added to PLA/Cs/St mixture as 1 wt%.

#### 2. Electrospinning Method

The electrospinning method is a method for obtaining nanofibrous scaffolds. For this study 10 mL plastic syringe loaded with solutions and syringe was inserted into the programmable syringe pump, the flow rate was adjusted as 10 ml/h. The working distance was set to 20 Mm and 28 kV was applied to obtain nanofibrous scaffolds.

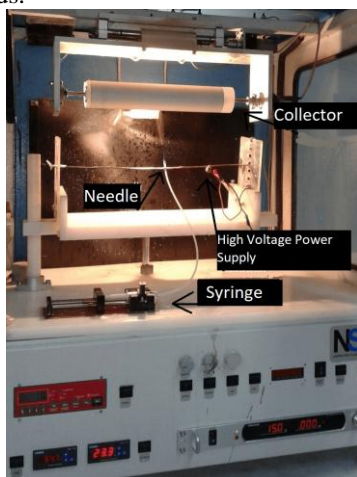


Fig. 1. Digital image of electrospinning device

### RESULTS AND DISCUSSION

The morphology of the electrospun nanofibrous wound dressing material was characterized by a Scanning Electron Microscope (SEM)<sup>2</sup>. As can be seen in Fig. 2, all the samples including St and ZnO have frequent nanofiber texture. Also, St is seemed as bead form in the nanofibrous structure, next to Zn particles.

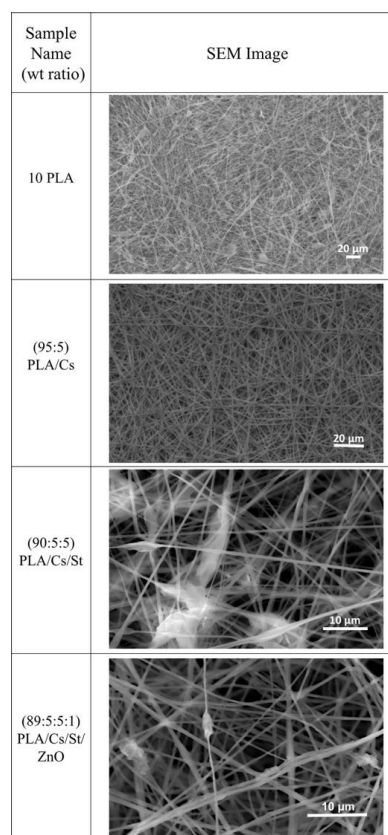


Fig. 2. SEM images of nanofibrous samples

### CONCLUSION

In the present study, an antibacterial nanofibrous wound dressing material were successfully prepared from mixed Poly-lactic acid (PLA) /Starch (St) /Chitosan (Ch) /Zinc Oxide (ZnO) solution by electrospinning method. Considering the antimicrobial properties, the wound dressing materials seem very promising for biomedical engineering studies.

### REFERENCES

1. P. Fernandez-Saiz, J.M. Lagaron, M.J. Ocio: Food. Hydrocolloid, 2009
2. Komur et al. BioMed Eng OnLine, 10.1186/s12938-017-0334-y, 2017.



## Study the Schiff-base Reaction in the Alginate-gelatin Hydrogels

Zahra Emami<sup>1</sup>, Morteza Ehsani<sup>1</sup>, Mojgan Zandi<sup>1</sup>, Reza Foudazi<sup>2</sup>

<sup>1</sup>Department of Biomaterials, Iran Polymer and Petrochemical Institute, Tehran, Iran

<sup>2</sup>Department of Chemical and Materials Engineering, New Mexico State University, Las Cruces

[z.emami@ippi.ac.ir](mailto:z.emami@ippi.ac.ir)

### INTRODUCTION

Hydrogels are an important class of biomaterials which are widely used in biomedical applications such as tissue engineering and drug delivery systems. Among different biopolymers, alginate and gelatin are two polymers commonly used because of their nontoxicity, biocompatibility, and biodegradability. Alginate can be oxidized by sodium periodate, in which aldehyde groups are generated in its backbone. The aldehyde functional groups react with amine groups in gelatin through Schiff-base reaction,<sup>1</sup> and form a crosslinked hydrogel. Generally, oxidized alginate have been crosslinked by gelatin in the presence of either borax or phosphate buffer saline (PBS). In this work, we investigate the effect of these two buffers on the properties of the prepared hydrogels.

### EXPERIMENTAL METHODS

5 wt.% aqueous solution of sodium alginate (Sigma Aldrich Co.) was prepared. Then, the required values of sodium meta periodate were added while stirring under dark condition at room temperature. After quenching the reaction and filtering the oxidized alginate, the sample was frozen and lyophilized.

The hydrogels were prepared by mixing oxidized alginate and gelatin in the presence of 0.1 M phosphate buffer saline (PBS) or 0.1 M borax. To this end, equal volume of 15% oxidized alginate in each buffer and 15% gelatin in distilled water were mixed and incubated at 37°C overnight.

Attenuated total reflectance Fourier transform infrared (ATR-FTIR) spectrometer (Bruker Equinox, Germany) equipped with a Golden Gate single reflection ATR-FTIR attachment was used to evaluate the functional groups of hydrogels. Additionally, swelling analysis was carried out through immersing hydrogels in water at 37°C and recording the water uptake with time.

### RESULTS AND DISCUSSION

Aldehyde groups in oxidized alginates can react with amine groups in gelatin via Schiff base linkages to form hydrogel. To confirm a successful Schiff-base reaction, FT-IR spectra of prepared hydrogels was studied as shown in Fig. 1. In both samples the peak at 1735 cm<sup>-1</sup> which is related to aldehyde groups is disappeared and a new peak at 1620 cm<sup>-1</sup> is observed related to C=N double bond.<sup>2</sup> Therefore, the imine bond formed and the alginate and gelatin has formed a crosslinked structure. Additionally, the intensity of peak at 1620 cm<sup>-1</sup> for sample prepared in borax media is lower than the one prepared in PBS media, and a new peak at 1133 cm<sup>-1</sup> is present in the sample prepared in borax media. This peak is related to C-N bond and shows that borax can convert C=N to C-N bond, thus, decreases the intensity of peaks related to C=N bonds.

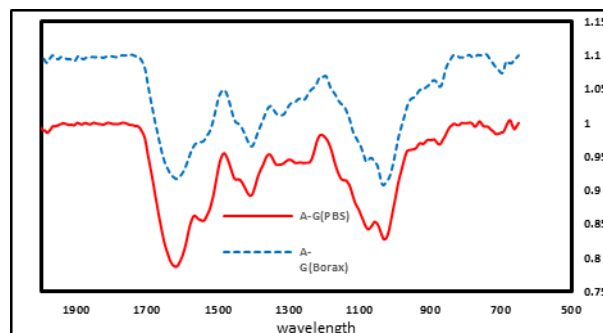


Fig. 1. FT-IR spectra of prepared hydrogels

Swelling analysis of the sample shows that hydrogels prepared in PBS media were dissolved in water after 12 hours, while the hydrogel prepared in borax media can swell until 48 hours and then they start to degrade. Imine bonds in the hydrogel prepared in PBS can be hydrolysed in presence of water. Due to the conversion of the C=N bond to C-N in hydrogels prepared in borax media, the hydrolysis reaction is slowed down and the hydrogel can swell.

### CONCLUSION

Although the phosphate buffer saline or borax are not main part of Schiff-base reaction but presence of them can affect on progress of the Schiff-base reaction and final bonds in prepared hydrogels.

### REFERENCES

1. B. Balakrishnan. *et al.*, *Biomaterials*, 26:3941–3951, 2005.
2. H. Baniasadi *et al.*, *J. Biomater. Appl.*, 31:152–161, 2016.



## The Comparison of Crosslinking Methods of Bicomponent PCL/gelatin Electrospun Nanofibres

Judyta Dulnik, Paweł Sajkiewicz

Laboratory of Polymers and Biomaterials, Institute of Fundamental Technological Research,  
Polish Academy of Sciences, Poland

[jdulnik@ippt.pan.pl](mailto:jdulnik@ippt.pan.pl)

### INTRODUCTION

In our laboratory, we optimized the method of obtaining bicomponent nanofibres made of polycaprolactone (PCL) with an addition of gelatin, through electrospinning from a green, cheap and safe for the operator solvent system – a mixture of acetic and formic acid (Fig. 1a)<sup>1</sup>. Unfortunately, further *in vitro* biodegradation studies showed fast biopolymer leaching from the fibres. With loss of gelatin in the fibre structure and on its surface, the biofunctionality of a material decreases. It is reflected in its hydrophilicity, and as well as morphology and can be observed in scanning electron microscopy (SEM) images (Fig. 1b)<sup>2</sup>. The solution to this predicament is crosslinking of gelatin within the fibre. We decided to investigate a set of different chemical crosslinking methods. Our main concerns were that the methods were as much low toxic as possible and had innovative potential.

### EXPERIMENTAL METHODS

Four crosslinking agents were chosen: 1-ethyl-3-(3-dimethylaminopropyl) carbodiimide hydrochloride (EDC), genipin, 1,4-butanediol diglycidyl ether (BDDGE) and transglutaminase. For each, a set of different concentrations and times were tested on a material with PCL to gelatin ratio 7:3 electrospun from acetic acid/formic acid (AA/FA) mixture solution. Crosslinked materials underwent then a 24 h biodegradation test in phosphate buffer saline in 37°C. To determine the crosslinking effectiveness and the changes of fibres' morphology, all samples, both right after crosslinking and after biodegradation test, were subjected to SEM imaging, as well as weight measurement to assess gelatin mass loss.

### RESULTS AND DISCUSSION

Depending on the crosslinking agent used the results differed significantly. Our two main assessment criteria were: not less than 85% of gelatin mass left and maintained morphology after 24h in 37°C PBS. The main observations were:

- Both EDC/NHS and genipin were able to keep gelatin content within the satisfactory range (85% and up), with the use of relatively low crosslinking agent concentrations (1,25‰ /0,425‰ and 2‰ respectively).
- With the use of BDDGE, only high concentrations and long periods of time yield dependable good results of maintaining gelatin content.
- Transglutaminase, even in high dose, failed to adequately prevent gelatin loss or fibres morphology to deteriorate (fig. 1d).

- Only the materials crosslinked in EDC/NHS maintained satisfactory morphology after 24h biodegradation test. Fibres were smooth and not fused together (Fig. 1c).
- The most cost and time effective method was the use of EDC/NHS, as it required extremely small concentrations of compounds and a good result can be achieved in a couple of hours.

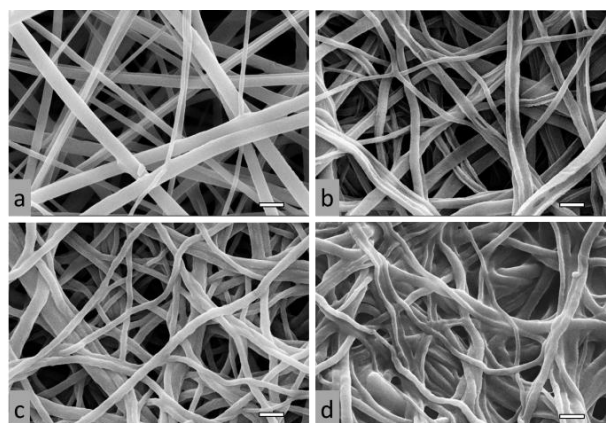


Fig. 1. SEM images of PCL/gelatin 7:3 nanofibres electrospun from AA/FA solvent mixture: a) untreated sample, b, c, d - samples after 24h in 37°C PBS, b) untreated sample with apparent linear groove-like sites remaining after gelatin leaching, c) sample crosslinked with EDC/NHS, d) sample crosslinked with transglutaminase; marker 1μm.

### CONCLUSION

Based both on the effectiveness of preserving gelatin within the fibre, as well as maintaining as close morphology as possible to the untreated nonwoven material, EDC/NHS method of crosslinking PCL/gelatin nanofibres was chosen as the best from the tested group. Further, comprehensive research is planned to optimize the method including mechanical testing, prolonged biodegradation and cellular studies.

### REFERENCES

1. Denis, P. *et al.*, *Int. J. Polym. Mater. Po.* 64:354-364, 2015
2. Dulnik J. *et al.*, *Polym. Degrad. Stabil.* 130:10-21, 2016

### ACKNOWLEDGMENTS

This work was funded by the Polish National Science Center (NCN) under the Grant No.: 2015/17/N/ST8/02027.

## Polymers for 3D Printing for Head and Neck Applications

Sibylle Voigt<sup>1</sup>, Gabriele Grimm<sup>2</sup>, Katja Otto<sup>1</sup>, Astrid Enkelmann<sup>1</sup>, Uwe Brick<sup>3</sup>, Matthias Schnabelrauch<sup>2</sup>, Gerlind Schneider<sup>1</sup>

<sup>1</sup>ENT Department, Jena University Hospital, Germany

<sup>2</sup>INNOVENT e.V. Technologieentwicklung, Germany

<sup>3</sup>burms, Germany

[sibylle.voigt@med.uni-jena.de](mailto:sibylle.voigt@med.uni-jena.de)

### INTRODUCTION

Medical devices made from soft materials for head and neck applications (septal buttons, epitheses, ear molds and ITE's) are usually produced using a negative mold for subsequent casting, which is a long and material-consuming process. Additive manufacturing (3D printing) is faster and more flexible, so a new flexible and printable material should be developed. Prior to the polymerization, the material should be liquid with low viscosity, and should have a fast curing time by near UV or short-wavelength visible light. After curing, the material should be flexible with a low shore hardness and sufficient mechanical strength, but also biocompatible.

### EXPERIMENTAL METHODS

A UV-curable multicomponent acrylate/methacrylate elastomer was developed. With a DLP printer (Miicraft+, Young Optics Europe, Jena), test specimens were printed with a voxel size of about 50  $\mu\text{m}$ , followed by chemical and thermal post-treatment. The specimens were evaluated and tested with regard to handling, material properties and surface quality. Further, biocompatibility testing was performed using viability assays (WST-1, LDH) on established cell lines (HeLa, MC3T3-E1), both by direct cell cultivation of the test specimens (direct contact assay) and by dilution test. Besides, various surface coatings were tested.

### RESULTS AND DISCUSSION

All printed specimens made from the multicomponent acrylate/methacrylate elastomer could be printed with sufficient precision and surface finish for the intended applications. The printed specimen showed lower elasticity than routinely applied medical devices made of soft materials, as well as a significantly higher brittleness or lower tear strength, but the material is suitable for the intended applications.

The cultivation of the cells by dilution test and the direct cultivation of the test specimens with cells showed a high viability. A heat treatment of the specimens led to an increased viability of the cells. The comparison of the chemically post-treated surface coatings showed no differences.

### CONCLUSION

It could be shown that the developed printable material can be surface-treated and is suitable for the applications in the head and neck area. Methacrylate-based materials should undergo thermal post-treatment with a defined washing procedure which minimizes the amount of monomers with acrylate/methacrylate groups and thus achieves higher cytocompatibility. However, it was not possible to provide an "exclusive" printable soft and flexible material for use in an additive manufacturing process that can accommodate all of the requirements mentioned above. Further investigations and modifications are necessary.

## Assessment of Antibacterial Behavior of Some Polymer Composites Used for 3D Printing

Dan Batalu<sup>1</sup>, Anamaria Bunesu<sup>1</sup>, Marcela Bucur<sup>2,3</sup>, Luminita Marutescu<sup>2,3</sup>, Mariana Carmen Chifiriuc<sup>2,3</sup>, Petre Badica<sup>4</sup>

<sup>1</sup>Materials Science and Engineering Faculty, University Politehnica of Bucharest, Romania

<sup>2</sup>Faculty of Biology, University of Bucharest, Romania

<sup>3</sup>The Research Institute of the University of Bucharest – ICUB, Romania

<sup>4</sup>National Institute of Materials Physics, Magurele, Romania

[dan\\_batalu@yahoo.com](mailto:dan_batalu@yahoo.com)

### INTRODUCTION

Polymeric materials are gaining large attention for medical engineering applications, such as biodegradable screws, knee or shoulder implants, dentistry, ophthalmology, orthoses, esthetic implants and others. Some of the most frequently involved polymeric materials are poly(vinyl chloride) – PVC, ultrahigh molecular weight polyethylene (UHMWPE), silicone, polyester, nylon, polyurethane (PUR), Poly L Lactic Acid (PLLA), polyglycolide (PGA), polydioxanone (PDS), etc.<sup>1,2</sup>. However, the number of polymers used for 3D printing is increasing constantly, and new materials including composites are tested<sup>3</sup>. In our work, we tested composite polymers added with powders for increasing their antibacterial behavior against different bacterial cells, for envisioned medical applications based on 3D printing.

### EXPERIMENTAL METHODS

Commercial PLA was added with 1% of antibacterial powder. The added polymers were 3D printed in small squares of 10x10 mm<sup>2</sup> and 3 mm thickness, and tested against two bacterial reference strains, traceable to the ATCC (American Type Culture Collection), i.e. *Escherichia coli* ATCC 25922 and *Staphylococcus aureus* ATCC 25923.

### RESULTS AND DISCUSSION

The antibacterial activity of pristine and added PLA samples was tested in dynamic, by assessing the number of viable cell counts of bacterial cells grown on the respective materials at different time intervals. Both pristine and added PLA samples show a good inhibitory activity of bacterial growth, installed after 2 h of incubation and increasing in intensity after 4 and respectively 24 h (Fig. 1). If the pristine polymer exhibited a slightly more intensive activity against *S. aureus* after 2 h, the added PLA shows a more constantly linear and homogenous behaviour against both Gram negative *E. coli* and Gram positive *S. aureus* strains (Fig. 1, green arrow). This behaviour represents an important advantage, allowing the obtaining of a large-spectrum and controlled antibacterial effect. The early occurrence of the inhibitory effect upon the bacterial growth could prevent the development of bacterial biofilms on the surface of medical devices.

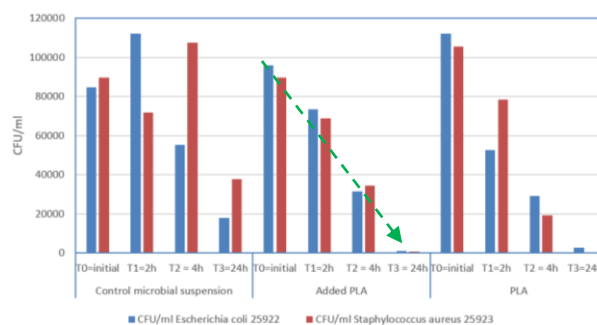


Fig. 1. Antibacterial behaviour of pristine and added PLA.

### CONCLUSION

Polymers with antibacterial behaviour are important for medical applications, such as implants or self-cleaning tools/instruments, considering that microbial biofilms are one of the most important causes of chronic infections and implants failure. Also, the persistence of microbial cells on different surfaces could represent an important source of contamination in different environments, from hospitals, to pharmaceutical, food industry and drinking water network. The 3D printing has numerous applications in the medical field, hence a search for new composite materials with controlled properties is necessary. In this study we show that new additions to PLA can improve the antibacterial behaviour of the obtained composite materials. Further experiments are necessary for optimization of the composite materials.

### REFERENCES

- Buddy D.R. *et al.*, Biomaterials Science. An Introduction to Materials in Medicine, 1996.
- Upender V. *et al.*, Int. J Polym Mater Po, 67:78-85, 2018.
- Seyeon H. *et al.*, J. Electron Mater, 44:771-777, 2015.

### ACKNOWLEDGMENTS

This work was supported by a grant of the Romanian National Authority for Scientific Research and Innovation, CCCDI-UEFISCDI, project number 74/2017 COFUND-M-ERA.NET II-BIOMB, within PNCDI III.

## Acetylcholinesterase from *Eisenia Foetida* as Biosensor for Pesticides

Erika Flores-Loyola<sup>1</sup>, Magdalena Galindo-Guzman<sup>2</sup>, Selene Sepulveda-Guzman<sup>3</sup>

<sup>1</sup>Facultad De Ciencias Biologicas, Universidad Autonoma De Coahuila, Mexico

<sup>2</sup>Facultad de Agricultura y Zootecnia, Universidad Juarez del Estado de Durango, Mexico

<sup>3</sup>Facultad de Ingenieria Mecanica y Electrica, Universidad Autonoma de Nuevo Leon, Mexico

[erika-flores@uadec.edu.mx](mailto:erika-flores@uadec.edu.mx)

### INTRODUCTION

Organophosphates are among the most used and toxic pesticides in agriculture in Mexico due to their high activity, low bioaccumulation and relatively fast degradation when it is in the environment<sup>1</sup>. Despite this, some amounts of pesticides are transferred to water through draining from the fields surface, which can produce series of toxic effects in aquatic organisms and human beings<sup>2</sup>.

The toxicity mechanism of organophosphate pesticides (OP) is based in the acetylcholinesterase (AChE) inhibition, by irreversible phosphorylation, producing acetylcholine accumulation and therefore a malfunction of the nervous system.

AChEs from insects are especially susceptible to this effect<sup>3</sup>. *Eisenia Foetida* (*E. Foetida*) is a very sensitive organism against OP. This is why they have been used as living sensors for the presence of this substances<sup>4</sup>. As a defence mechanism, *E. Foetida* produces enzymes AChE to degrade those. Thus, it is possible to use these organisms to extract AChE in order to assay the presence of OP in low concentrations<sup>5</sup>. Therefore, in this work, an enzymatic concentrated of acetylcholinesterase was prepared from *E. foetida*. The inhibitory effect of commercial organophosphate pesticides as malathion, diazinon, methamidophos and dimethoate on its enzymatic activity was evaluated, as well as its selectivity when using organochlorine, carbamate and pyrethroid pesticides. Acetylcholinesterase activity was measured using indoxyl acetate as chromogenic substrate.

### EXPERIMENTAL METHODS

The OP effect on the activity of a dried raw enzymatic extract of AChE from *E. Foetida* was studied. 5 mg of AChE enzymatic extract was added in 1 mL of OP solutions from 1-10 mg/L at 25°C for 20 min; after that 0.4 mL of 0.1 M sodium phosphate buffer and 100 µL of 0.05 M indoxyl acetate in methanol (aqueous solution 5%) were added. Absorbance was measured after 20 minutes in a Genesys 10 UV scanning spectrophotometer at 670 nm. OP's were commercially acquired (malathion, diazinon, dimethoate, metamidophos). Also, as a control, a carbamate (carbofuran), a pyrethroid (cipermetrine) and an organochlorinated (endosulfan) pesticide were used. The inhibition degree of OP on the AChE was also determined by amperometric detection through the immobilization of AChE on a mixture of graphene/polyaniline, which was supported on a glassy carbon electrode. Cyclic voltammetry was carried out in a Basi-Epsilon potentiostat/galvanostat at room temperature in a standard three electrode cell with a platinum counterelectrode and an Ag/AgCl reference

electrode. The AChE on the modified electrode was incubated for 20 min with 50 µl of pesticide (10 mg/L) and then transferred to a cell containing 50µl of indoxyl acetate 0.05 M in phosphate buffer 0.1 M, pH 7.5. A potential sweep of 0-1000 mV, and a sweep speed of 100 mV/s were used.

### RESULTS AND DISCUSSION

All organophosphosphate pesticides tested, in concentrations between 1-10 mg/L, decreased acetylcholinesterase activity (36 % on average). On the other hand carbamates only slightly inhibited the enzymatic activity (16 %) and organochlorines and pyrethroids showed little or no significant inhibitory effect (1-5 %) for any tested concentrations. This is because the different mode of action of each group of pesticides. For this reason, the activity of the AChE is not significantly affected and this remain catalyzing the decomposition of indoxyl acetate even in the presence of pesticides with chemical groups different to organophosphates, which is indicative of acetylcholinesterase selectivity against this specific type of inhibitors.

Results of amperometric analysis showed a higher sensibility of the AChE biosensor allowing the detection of concentrations up to 0.01 ppm.

### CONCLUSION

Results indicated the raw AChE extract effectively detect the inhibition generated by the presence of OP as an absorbance diminishing was observed with the increasing concentration of OP. The enzymatic activity remains almost inalterable in the presence of non-organophosphate pesticides, as in the case of cipermetrine and endosulphan, indication of the selectivity of AChE to the OP detection in concentrations as low as 1 mg/L through spectroscopic detection and up to 0.01 ppm through the use of an amperometric transduction method.

### REFERENCES

1. Sharma D. *et al.*, 2010. *Talanta*. 82:1077-89, 2010.
2. Kilany A. Y. *et al.*, *ILCPA*. 17:236-248, 2014.
3. Qiaolin L. *et al.*, *Talanta*. 156-157: 34-41, 2016.
4. Gambi N., *et al.*, *Comp. Biochem. Physiol. C*. 145: 678-685, 2007.
5. Villatte F., *et al.*, *Biotechniques*



***In vitro* Bioactivity and Long-term Hydrolytic Degradation of Poly( $\epsilon$ -caprolactone)/bioactive Glass Composites**

Michał Dziadek, Barbara Zagrajczuk, Katarzyna Cholewa-Kowalska

Department of Glass Technology and Amorphous Coatings, AGH University of Science and Technology, Poland  
[dziadek@agh.edu.pl](mailto:dziadek@agh.edu.pl)**INTRODUCTION**

Biomaterials for bone tissue engineering applications should degrade progressively at a rate matching the regeneration of new bone *in vivo* to allow full restoration of native tissue structure and functions<sup>1</sup>. The degradation behaviour of the materials should vary based on target applications, namely material form (e.g. scaffold, barrier membrane) and implantation site.

The direct bone bonding ability through the formation of a bone-like hydroxyapatite (HAp) phase on the material surface without an intermediate layer of modified tissue is the main advantage of the so-called bioactive glasses<sup>2</sup>. Moreover, reactions on the material surface could induce the release of critical concentrations of soluble Si, Ca, P and Na ions, which can lead to favourable intracellular and extracellular responses, actively stimulating bone formation<sup>3</sup>. Such bioactive glasses belong to the group of osteoinductive biomaterials. The evaluation of the biomaterial bioactivity usually refers to the identification of the HAp layer on its surface in a living organism (*in vivo*) or in simulated body environment (*in vitro*)<sup>2</sup>. The so-called simulated body fluid (SBF) was developed by Kokubo and has been the most widely used solution for *in vitro* bioactivity tests recently<sup>4</sup>. However, SBF cannot simulate physiological conditions in a living body completely, because it only substitutes inorganic part of blood serum. Therefore, in the literature, attempts to substitute SBF with the commercially available cell culture media, i.a. HEPES-free Dulbecco's Modified Eagle Medium (DMEM) solution, have been reported<sup>4</sup>. Apart from the inorganic part of blood serum, this solution contains also the organic component (vitamins, amino acids, etc.). Moreover, DMEM can be supplemented with foetal bovine serum (FBS), containing additional organic species, such as proteins, to obtain complete growth medium for certain cell lines. The medium can be carbonate buffered as the test is performed in a 37°C incubator under a humidified atmosphere of 95% air and 5% CO<sub>2</sub>, which better simulates the *in vivo* environment<sup>4,5</sup>.

**EXPERIMENTAL METHODS**

In the present work, the effect of content (12 and 21 vol.%), size (<3  $\mu\text{m}$ , <45  $\mu\text{m}$ ) and chemical composition (silica-rich and calcium-rich) of gel-derived bioactive glass particles from the SiO<sub>2</sub>-CaO-P<sub>2</sub>O<sub>5</sub> system on the *in vitro* bioactivity and long-term degradation behaviour of PCL-based, solvent-cast composite films was investigated. Calcium phosphate layer forming ability was assessed in SBF and DMEM supplemented with 10% FBS. The samples were examined with SEM/EDX and ATR-FTIR methods. The changes in the concentration of Ca, P, Si in the SBF and DMEM during film incubation were analysed using ICP-OES method. Degradation kinetics of composites

was examined by incubation them in phosphate buffer saline (PBS) up to 15 months. Degradation process was monitored by measuring pH. Weight changes, surface morphology, chemical composition (SEM/EDX), degree of crystallinity, melting temperature (DSC), and tensile properties of the samples were examined after 1, 3, 6, 9, 12, and 15 months of incubation in PBS.

**RESULTS AND DISCUSSION**

Obtained composite films showed excellent *in vitro* bioactivity, as evidenced by the formation of calcium phosphate (CaP) layer on their surfaces upon immersion in SBF and DMEM. However, kinetics of bioactivity process strongly depended on the type of the medium used. The layer of amino acids and proteins, derived from cell culture medium, on the surfaces of composites created barrier that inhibited release the ions on the one hand, while increased nucleation density of calcium phosphates, affecting the morphology of formed CaP layers on the other. We showed that kinetics of bioactivity process of composite films could be easily modulated with the use of different contents and chemical compositions of fillers.

The results showed that modification of PCL matrix with bioactive glass particles accelerated its degradation. We proved that the degradation rate of composites could be controlled and optimized for bone regeneration, in particular by using bioactive fillers causing different calcium phosphate layer forming ability on the surfaces of composites, depending on particle size and chemical composition.

**CONCLUSION**

We have presented new opportunities to design and obtain multifunctional composites with tunable degradation and bioactivity kinetics that can meet complex requirements of bone tissue engineering.

**REFERENCES**

1. Larrañaga A, et al. (2014) Polym Degrad Stab 110:121–128.
2. Łączka M, et al. (2016) Ceram Int 42:14313–14325.
3. Hench LL (2009) J Eur Ceram Soc 29:1257–1265.
4. Lee JTY, et al (2011) Acta Biomater 7:2615–2622.
5. Rohanová D, et al (2014) J Mater Chem B 2:5068–5076.

**ACKNOWLEDGMENTS**

This work was supported by the National Science Centre, Poland Grant No. 2015/17/N/ST8/00226 (MD). Michał Dziadek acknowledges financial support from the National Science Centre, Poland under doctoral scholarship (2017/24/T/ST8/00041). Supported by the Foundation for Polish Science (FNP).

## Surface Charge Controlled Cell Proliferation on Electrospun Polyvinylidene Fluoride Fibers

Piotr K. Szewczyk<sup>1</sup>, Sara Metwally<sup>1</sup>, Joanna Karbowniczek<sup>1</sup>, Adam Gruszczyński<sup>1</sup>, Mateusz Marzec<sup>2</sup>, Andrzej Bernasik<sup>2,3</sup>, Urszula Stachewicz<sup>1</sup>

<sup>1</sup>International Centre of Electron Microscopy for Materials Science and Faculty of Metals Engineering and Industrial Computer Science, AGH University of Science and Technology, Poland

<sup>2</sup>Academic Centre for Materials and Nanotechnology, AGH University of Science and Technology, Poland

<sup>3</sup>Faculty of Physics and Applied Computer Science, AGH University of Science and Technology, Poland

[pszew@agh.edu.pl](mailto:pszew@agh.edu.pl)

### INTRODUCTION

Electrospinning is widely used to produce nanofibers, especially for biomedical engineering [1,2]. One of the important parameters in electrospinning that controls surface properties of produced polymer fibers is voltage polarity [3,4]. Within this study we want to control surface charges on Polyvinylidene Fluoride (PVDF) fibers by alternating voltage polarity during electrospinning. Next, we verify cell responses to the obtained surface potential on electrospun polymer fibers.

### EXPERIMENTAL METHODS

#### Electrospinning

(PVDF,  $M_w = 275000$  g mol<sup>-1</sup>, was dissolved in solution of Acetone and Dimethylacetamide (DMAc), in ratio of 1:1 to produce a solution with polymer concentration of 22% wt. This solution was used for electrospinning using EC-DIF apparatus with climate control system. The applied voltage to the nozzle was  $\pm 15$  kV. The distance to the collector was kept at 18 cm. Other parameters were as follows: flow rate 1.5 ml h<sup>-1</sup>,  $T = 25^\circ\text{C}$  and  $H = 60\%$ .

#### Cell culture

Osteoblast-like cells (MG-63) were seeded in a density of  $2 \times 10^4$  cells/cm<sup>2</sup> on fiber meshes sterilized with UV light. We used medium consisted of 10% FBS, 1% amino acids, 1% glutamine and 2% of penicillin streptomycin. Cells were kept for 3 days in culture at temperature of 37°C, humidity of 95% and atmosphere contained 5% CO<sub>2</sub>.

#### Microscopy

Scanning electron microscope (SEM) and was used to evaluate fibers morphology and to investigate cell proliferation and attachment to fibers. Additionally, Focused Ion Beam Scanning Electron Microscopy technique (FIB-SEM) allowed us to prepare 3D reconstructions of cell attachment to the PVDF fibers.

#### Surface characterization

Surface chemistry of PVDF fibers was verified using grazing angle X-ray photoelectron spectroscopy (XPS) and surface potential was measured using Kelvin Probe Force Microscopy (KPFM).

### RESULTS AND DISCUSSION

Electrospinning of PVDF nanofibers resulted in fibers with similar morphology and average fiber diameter for sample produced with positive voltage polarity  $1.39 \mu\text{m} \pm 0.58 \mu\text{m}$  and for fibers electrospun with negative

voltage polarity  $1.37 \mu\text{m} \pm 0.57 \mu\text{m}$ . Contact potential difference obtained from KPFM resulted in  $-1.23 \pm 0.32$  V and  $-2.09 \pm 0.85$  V for PVDF fibers produced with negative and positive voltage polarity respectively. The XPS results indicated that for electrospun PVDF fibers with negative voltage polarity applied to the needle 42.5 at.% of fluorine groups were present at the surface and 45.9% fluorine groups were found in the PVDF fibers electrospun with positive voltage polarity. The PVDF fibers with higher surface potential (-1.23V) were produced with negative voltage polarity during electrospinning and led to enhanced cell proliferation and attachment as presented in Fig. 1.

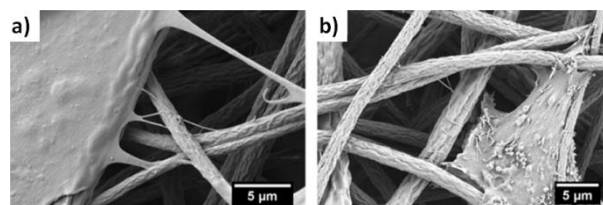


Fig. 1. SEM images of cells attached to electrospun PVDF fibers showing their attachment via filopodia to a) less negatively charged fibers, b) more negatively charged fibers.

### CONCLUSION

Alternating voltage polarity during electrospinning allowed modification of surface potential of PVDF fibers. XPS results suggested the reorientation of electronegative F<sup>-</sup> to the surface once the positive charges were applied to the electrospun PVDF solution. Thus lower surface potential on PVDF fibers was caused by higher content of F<sup>-</sup> at the surface. In summary lower surface potential obtained with negative voltage polarity resulted in enhanced cell proliferation and better attachment to the fibers.

### REFERENCES

- [1] Vasita, R.; Katti, D. S. *Int. J. Nanomedicine* **2006**, *1* (1), 15–30.
- [2] Venugopal, J.; Ramakrishna, S. *Appl. Biochem. Biotechnol.* **2005**, *125* (3), 147–157.
- [3] Tong, H.-W.; Wang, M. *Biomed. Mater.* **2010**, *5* (5), 54110.
- [4] U. Stachewicz, C. A. Stone, C. R. Willis, and A. H. Barber, *J. Mater. Chem.*, **2012**, *22* (43), 22935.

### ACKNOWLEDGMENTS

The study was conducted within the funding from SONATA 8 project granted by National Science Centre in Poland, No 2014/15/D/ST5/02598.

## Solution Blow Spun Poly-L-Lactic Acid/Ceramic Fibrous Composites

Michał Wojasiński<sup>1</sup>, Joanna Latocha<sup>1</sup>, Paweł Sobieszuk<sup>1</sup>, Tomasz Ciach<sup>1,2</sup>

<sup>1</sup>Faculty of Chemical and Process Engineering, Division of Biotechnology and Bioprocess Engineering, Warsaw University of Technology, Poland

<sup>2</sup>Central Laboratory of Advanced Materials and Technology CEZAMAT, Warsaw, Poland  
[michal.wojasinski.dokt@pw.edu.pl](mailto:michal.wojasinski.dokt@pw.edu.pl)

### INTRODUCTION

Since the electrospinning, the most popular method for production of fibers for medical purposes, exhibits low throughput, the solution blow spinning (SBS) gathered a lot of attention nowadays. SBS allows production of fibers in the nanometer and submicrometer range of fiber diameter. This process was described also as a method for production of composite fibers with reinforcements like: carbon nanotubes, nanobioactive glass, zirconium, etc<sup>1</sup>. Use of poly-L-lactic acid (PLLA) polymer with bioactive ceramics like  $\beta$ -tricalcium phosphate, hydroxyapatite or any other calcium phosphate particles allows production of polymer/ceramic fibrous structure, with properties promoting bone cells adhesion and growth. What is more, the lack of the requirement of specific and dangerous equipment to provide a driving force (like high voltage in electrospinning), SBS fibers can be collected on a variety of surfaces, including a surface of living tissue<sup>2,3</sup>. This feature can become more important since 3D printed biomedical scaffolds getting popular. Their surface, may require modification for improving integration with tissues by enhancing cells adhesion and cells proliferation.

The aim of this work is to present a robust method for PLLA/ceramic composite fibrous mats production. SBS mats can be applied on the surface of any bone tissue implant.

### EXPERIMENTAL METHODS

For production of SBS composite mats the poly-L-lactic acid (Biomer L9000, Mw>200kDa) was used as a matrix, and three ceramics:  $\beta$ -tricalcium phosphate ( $\beta$ TCP), hydroxyapatite nanoparticles (nHAp) (both Sigma Aldrich), and hydroxyapatite nanoparticles modified with phosphatidylcholine (nHAp-PC, self-synthesized, in continuous reactor)<sup>4</sup> were used as reinforcements. Polymer was dissolved in chloroform:acetone (3:1v/v mixture) in 6%w/w concentration and each ceramic was added (separately) in 1:3 ratio to polymer and mixed by ultrasounds for 5 minutes. Fibers were produced using previously described SBS system<sup>5</sup>.

Ceramic aggregates were investigated by scanning electron microscopy (SEM) to measure their sizes. Composites were examined by SEM to analyze their morphology, reinforcement distribution in fibers, fibers sizes, and pore sizes, gravimetric method to evaluate volumetric porosity, goniometer to analyze water contact angle, FTIR spectroscopy and Alizarin Red staining (ARS) to indicate presence of minerals, and cytotoxicity test (XTT, L929 cell line) and cell proliferation test (MG63 cell line) to evaluate

cytotoxicity of the materials and enhancement of bone cell's proliferation.

### RESULTS AND DISCUSSION

SEM analysis indicated that  $\beta$ TCP and nHAp-PC create aggregates with sizes from a few to about 50 $\mu$ m, whether nHAp aggregates are less than 40 $\mu$ m in size. Nevertheless, all aggregates were incorporated in SBS fibers. From all proposed reinforcements, nHAp distributes the most uniformly within fibers. This feature allows uniform cell adhesion and proliferation in further tests. Regardless of ceramic used in fibers production, all mats were composed of fibers with mean fiber diameter of about 200 nm. Addition of ceramics did not affect the volumetric porosity (about 90%) and water contact angle (about 110°). FTIR analysis indicates peaks typical for each ceramic in each type of fibrous composites, and ARS shows presence of calcium minerals within whole structure of the mats. All above described results show that SBS mats can incorporate three types of ceramics without significant decrease of material's structural properties. Cytotoxicity XTT test on L929 cell culture according to ISO 10993 standard indicates no cytotoxic response (>80% cell viability, in comparison to negative control). Results of MG63 cells proliferation on the surface of the composite fibrous mats in comparison to plain PLLA fibers is greater (according to SEM, fluorescence and laser confocal microscopy).

### CONCLUSION

SBS composite PLLA/ceramic fibrous mats applicable on various surfaces can be successfully and robustly produced. What is more, presented mats can be used as the scaffolds themselves.

### REFERENCES

1. Daristotle J.L. *et al.*, ACS Appl. Mater. Inter. 8:34951-34963, 2014
2. Medeiros E.S. *et al.*, J. Appl. Polym. Sci. 133:2322-2330, 2009
3. Behrens A.M. *et al.*, ACS Macro. Lett. 3:249-254, 2014
4. Wojasiński M. *et al.*, Pol. J. Chem. Technol. 16:43-50, 2014
5. Wojasiński M. *et al.* Colloid Polym. Sci. 293:1561-1568, 2015

### ACKNOWLEDGMENTS

Authors acknowledge funding: "Innovative polymer composites for filling bone defects"-INPOLYBOND. NCBR/EC, Smart Growth Operational Program for 2014-2020 of European Regional Development Fund, (POIR.04.01.04.00-0133/15).



## Cefuroxime Axetil Loaded PHBV/PCL Electrospun Scaffolds for Bone Tissue Engineering

Ali Deniz Dalgıç<sup>1</sup>, Deniz Atıla<sup>1</sup>, Ayten Karataş<sup>2</sup>, Ayşen Tezcaner<sup>1,3</sup>, Dilek Keskin<sup>1,3</sup>

<sup>1</sup>Department of Engineering Sciences, Middle East Technical University, Ankara, Turkey

<sup>2</sup>Department of Molecular Biology and Genetics, İstanbul Technical University, İstanbul, Turkey

<sup>3</sup>CoE BIOMATEN, Center of Excellence in Biomaterials and Tissue Engineering, Ankara, Turkey

[atila.deniz@metu.edu.tr](mailto:atila.deniz@metu.edu.tr)

### INTRODUCTION

Osteomyelitis is termed as infection of bone caused by microorganisms, which is hard to treat by systemic antibiotic administration<sup>1</sup>. Local release of cefuroxime axetil (CA), an antibiotic with broad spectrum hold promise for treating this disease<sup>2</sup>. Poly (hydroxyl butyrate co-hydroxy valerate) (PHBV) is a natural thermoplastic copolyester synthesized by blue-green algae<sup>3</sup>. Poly( $\epsilon$ -caprolactone) (PCL) is a flexible polyester; and thus, generally used for tuning brittleness in blends<sup>4</sup>. Electrospinning is a simple technique to form fibers from polymeric solutions or blends under high electrical voltage<sup>5</sup>. In this work, CA loaded electrospun PHBV/PCL scaffolds were prepared and characterized for their potential as a local antibiotic delivery system for both treating infection and supporting bone regeneration at the defect site.

### EXPERIMENTAL METHODS

PHBV and PCL with different weight ratios (9/1, 8/1, 7/1) were dissolved in 1,1,1,3,3,3-Hexafluoro-2-propanol (HFIP) solvent with a 14% total polymer concentration. CA powder was added into this solution. PHBV was also electrospun separately as a control group under the same conditions. Electrospinning was performed by using an ethanol bath as a collector for 3-dimensionality under 18 kV electrical voltage at a distance of 12 cm from the syringe nozzle with a flow rate of 4 ml/hr. Morphological characterizations were conducted by scanning electron microscopy (SEM). Pore size distribution and porosity were determined by mercury porosimeter combined with helium pycnometer.

### RESULTS AND DISCUSSION

Initially, only-PHBV solutions were electrospun and monitored via SEM; however, the cracks and breaks were observed within the fibrous structures (Fig. 1a). Since PCL is a flexible polymer PCL was also added in gradually increased amounts to the polymer solution to modulate the brittleness of PHBV and reduce fractures (Fig 1b-d). SEM images showed that cracking of fibres was reduced (Fig. 1b and c) and almost removed (Fig. 1d). After optimization study for electrospinning, pore size of the fabricated PHBV/PCL:7/3 fibrous meshes varied between 5 and 200  $\mu\text{m}$ . Porosity of the scaffolds was measured as 75.85% which was suitable for cell infiltration and proliferation.

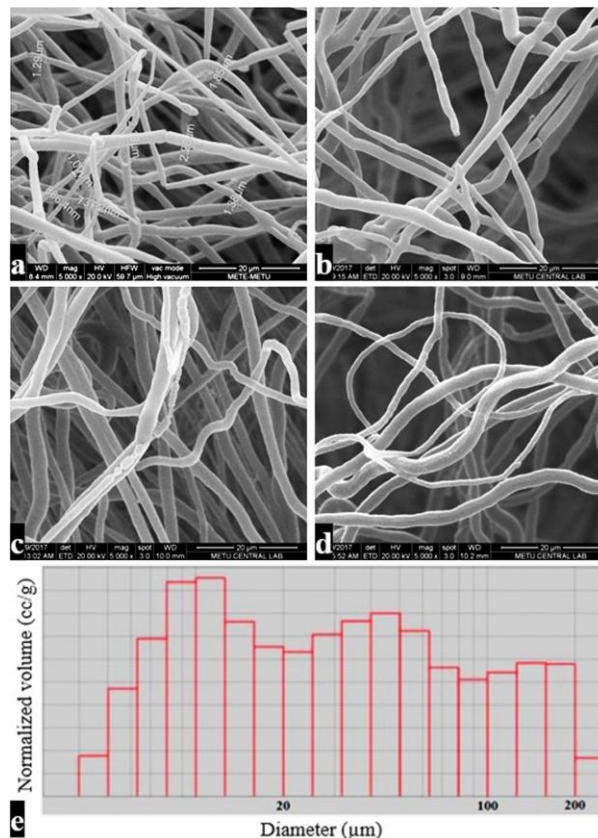


Fig. 1. SEM images of electrospun PHBV (a) and PHBV/PCL fibres with the ratios of 9/1 (b), 8/2 (c), and 7/3 (d) Pore size distribution of PHBV/PCL:7/3 fibres(e) (Magnifications: 5000X; Scale bars: 20  $\mu\text{m}$ ).

### CONCLUSION

CA loaded electrospun PHBV/PCL scaffolds were prepared first time for tissue engineering applications. Further characterizations of scaffolds (mechanical tests, *in vitro* release study, cell culture studies, etc.) are under study.

### REFERENCES

1. Ellington J.K. *et al.*, J Orthop Res. 24:87-93, 2006
2. Nandi S.K. *et al.*, Ceram. Int. 35:3207-3216, 2009
3. Correia D.M. *et al.*, Polym Eng Sci. 54:1608-17, 2014
4. Kosorn W. *et al.*, J. Biomed. Mater. Res. B. 105:1141-50, 2017
5. Meng W. *et al.*, J Mater Sci Mater Med. 19:2799-807, 2008

### ACKNOWLEDGMENTS

This work has been supported by grants from the Scientific and Technical Research Council of Turkey, project no: TUBITAK-215M893.



## Controlled Delivery of bFGF and TGF- $\beta$ 1 via Polymeric Nanoparticles within Hybrid Hydrogels for Articular Cartilage Tissue Engineering

Milad Fathi Achachelouei<sup>1</sup>, Nihal Engin Vrana<sup>2</sup>, Erhan Bat<sup>1,3</sup>, Dilek Keskin<sup>1,4,5</sup>, Aysen Tezcaner<sup>1,4,5</sup>

<sup>1</sup>Department of Biomedical Engineering, Middle East Technical University, Turkey

<sup>2</sup>Inserm UMR 1121, University of Strasbourg, France

<sup>3</sup>Department of Chemical Engineering, Middle East Technical University, Turkey

<sup>4</sup>Department of Engineering Science, Middle East Technical University, Turkey

<sup>5</sup>BIOMATEN, METU, Center of Excellence in Biomaterials and Tissue Engineering, Turkey

[milad.achachelouei@metu.edu.tr](mailto:milad.achachelouei@metu.edu.tr)

### INTRODUCTION

Several approaches have been developed for engineering of cartilage, each with its own pros and cons. Poly (ethylene glycol) (PEGDMA) is a good candidate as a photocrosslinkable 3D scaffold for encapsulation of various cells due to its tailor-made characteristic such as adjustable crosslinking degree, but due to its synthetic nature it lacks bioactive molecules and migration of cells is limited inside the scaffold. Silk fibroin as a natural polymer has shown good mechanical strength, biocompatibility and can be mixed with other polymers to form hybrid hydrogels.<sup>1</sup> Basic fibroblast growth factor (bFGF) and transforming growth factor  $\beta$ 1 (TGF- $\beta$ 1) has positive effect on proliferation and chondrogenic differentiation of human mesenchymal stem cells (hMSC), respectively.<sup>2</sup> In this study a hybrid physically cross-linked silk fibroin and chemically photocrosslinked PEGDMA containing bFGF and TGF- $\beta$ 1 loaded PLGA nanoparticles and dental pulp stem cells (DPSC) was developed for cartilage tissue engineering.

### EXPERIMENTAL METHODS

#### Synthesis of Hybrid Hydrogel

PEGDMA has been synthesized using 4000Mn PEG, triethylamine and methacryloyl chloride under argon gas and degree of crosslinking was determined using <sup>1</sup>H-NMR. Silk fibroin has been isolated from silk cocoons with final concentration of 8%. Hybrid hydrogels were formed by gelating silk fibroin using probe sonicator followed by photocrosslinking with different concentrations and ratios with PEGDMA in the presence of irgacure D-2959 under 365nm UV lamp. Mechanical properties of hydrogel were investigated with compression test using 10 N load cell and applying ANOVA with Tukey post hoc test.

#### Preparation of Nanoparticles

Nanoparticles were produced using double emulsion solvent evaporation method. Briefly, aqueous solutions containing bFGF or TGF- $\beta$ 1 were probe sonicated with the PLGA polymer in DCM to form first emulsion. The second emulsion was formed by probe sonicating the first emulsion in PVA solution. The organic solvent was then evaporated by stirring the solution for 5 hours at room temperature. Nanoparticles were collected through centrifugation. Morphology of nanoparticles was determined by scanning electron microscopy (SEM) and size distribution was determined using Image J program. Encapsulation efficiency of nanoparticles for bFGF and TGF- $\beta$ 1 and release profile of growth factors in PBS at 37°C were determined using ELISA kits.

### In vitro studies

DPSCs were isolated from human pulp tissue with enzymatic digestion. DPSCs were encapsulated in hydrogels with bFGF and TGF- $\beta$ 1 loaded nanoparticles. Cell viability was studied using Alamar blue assay. Live/dead assay was also carried out using calcein-AM and propidium iodide dyes and the images were taken using confocal microscopy.

### RESULTS AND DISCUSSION

<sup>1</sup>H-NMR result has shown 75% metacrylation degree for PEG. Compression moduli of hydrogels (n=4) varied between 95.7 $\pm$ 17.2 kPa and 333.1 $\pm$ 14.9 kPa depending on the composition and ratio of silk fibroin and PEGDMA (Fig. 1A). SEM analysis showed that nanoparticles had round morphology with a mean diameter of 774.7 $\pm$ 264 nm (Fig. 1B).

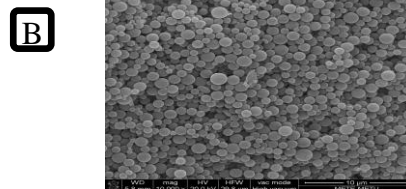
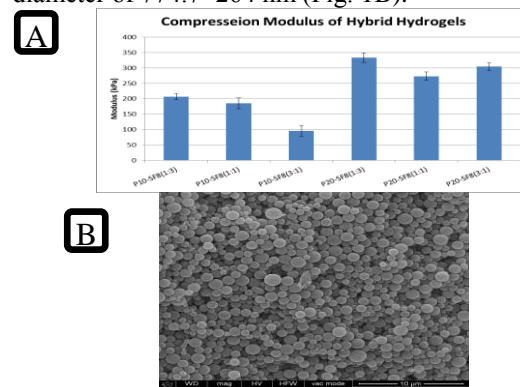


Fig. 1A. Compression modulus of hybrid hydrogels (e.g. 10 %PEGDMA + 8% Silk fibroin with 1 to 3 volume ratio: P10-SF8 (1:3)). Fig. 1B. SEM analysis for nanoparticles morphology (scale bar = 10  $\mu$ m).

### CONCLUSION

In this study a hybrid hydrogel with tunable mechanical properties that provides a suitable environment for cell encapsulation has been developed. Hydrogel system together with growth factor loaded nanoparticles and DPSCs hold potential for cartilage tissue engineering applications.

### REFERENCES

- Xiao W. *et al.*, Acta Biomater. 7:2384-2393, 2011
- Ng F. *et al.*, Blood. 112:295-307, 2008

### ACKNOWLEDGMENTS

This work has been supported by grants from the Horizon 2020 PANBioRA (760921) and Center of Excellence in Biomaterials and Tissue Engineering (BIOMATEN).

## Various Approaches to the *in vitro* Bioactivity Evaluation of the Polymer-Ceramics Composites for Bone Tissue Engineering

Barbara Zagrajczuk, Michal Dziadek, Agata Flis, Katarzyna Cholewa-Kowalska, Maria Laczka

Dept. of Glass Technology and Amorphous Coatings, Fac. of Mat. Sci. and Ceramics,  
AGH University of Science and Technology, Mickiewicza Ave. 30, 30-059 Krakow, Poland  
[b.zagrajczuk@gmail.com](mailto:b.zagrajczuk@gmail.com)

### INTRODUCTION

Bioglasses are the ceramic materials that are characterized by the ability to create permanent and stable bond with bone tissue, and also can stimulate it to faster regeneration<sup>1</sup>. A biomaterial bioactivity can be defined as a potential to the bone-like apatite formation on its surface in a physiological conditions, what is important in forming bonds between bioactive material and regenerated bone tissue. An incorporation of the bioglass particles into the polymer matrix creates a possibility of obtaining new materials with controlled and enhanced biological performance. Bioglasses can be obtain by melting method or sol-gel process. Gel-derived bioglasses exhibit higher bioactivity than melted ones due to their high surface area and lower temperature processing, resulting in retaining SiOH groups on the surface. The aim of the study was to evaluate the bioactive properties of the polymer-ceramics composites containing bioactive glass particles of various chemical compositions, as materials for bone tissue engineering. Detailed bioactivity study concerning materials behavior in different testing conditions and trial of a quantitative bioactivity evaluation have been performed.

### EXPERIMENTAL METHODS

Bioactive glasses from the SiO<sub>2</sub>-CaO and the SiO<sub>2</sub>-CaO-P<sub>2</sub>O<sub>5</sub> systems were fabricated with the sol-gel technique. Particular glasses from both systems were differing in the molar CaO/SiO<sub>2</sub> ratio in the range of 1/4 to 3/2, which determined the type of created Si groups Q<sup>n</sup> (n - number of bridging oxygen ions in Si nearest environment). Then, bioglass powders were sieved to particle size <45µm and incorporated into polymer (PLGA) matrix in order to obtain composite films (2D forms) and scaffolds (3D forms). 2D materials were obtained by a solvent casting method, whereas 3D forms by the solvent casting and the particulate leaching (SCPL) technique. Obtained composite materials were tested for the surface properties (2D) and mechanical properties (2D and 3D). *In vitro* bioactivity, described as the ability to form apatite layer at the materials surface in contact with incubating solution, was tested in different incubation conditions (static, dynamic and semi-dynamic), in simulated body fluid (SBF) solution, for 3,7 and 14 days of incubation. Bioactivity was evaluated qualitatively with the SEM microscopy coupled with EDS analysis, and FTIR-ATR spectroscopy. Moreover, the ICP-OES analysis of the post-incubation SBF samples have been made in order to evaluate changes in the particular elements (Ca and P) concentrations. In addition, a semi quantitative bioactivity evaluation was performed with the ICP-OES method.

### RESULTS AND DISCUSSION

All of the obtained glasses formed white powders. 2D composite films appeared to have the glass particles spread uniformly in the polymer matrix. Water contact angle and roughness measurements indicated significant differences between top and bottom surfaces of the films. In addition significant differences in microstructures between these two sides have been observed in the SEM microphotographs.

*In vitro* bioactivity evaluation indicted that all of the tested composite materials were bioactive. The rate of apatite layer formation was dependant on the chemical composition of glass particles. More disrupted network structure of the glasses with higher CaO/SiO<sub>2</sub> ratio resulted in higher solubility and the same time faster CaP rich layer formation during immersion in simulated body fluid<sup>2</sup>. Differences in the CaP-rich layer formation rates, morphologies and Ca/P ratios amongst different incubation conditions have been observed both in the 2D and 3D composite materials. Dynamic and semi-dynamic incubation conditions favoured faster apatite layer formation. That was also confirmed by the ICP-OES analysis, which has indicated different patterns and dynamics of ions migrations in the SBF fluid between particular experimental routes.

### CONCLUSION

Our study confirmed that chemical composition of gel-derived bioglasses used as composite modifiers affects the bioactivity of composite materials. Moreover, the selected experimental conditions have a large influence on the bioactivity process assessment. Conducting the experiment in dynamic conditions imply faster CaP layer formation.

### REFERENCES

1. Hench L.L. *et.al.*, Life Chem. Rep. 13:187–241, 1996.
2. Elgayar I. *et.al.*, J. Non-Cryst. Solids 351:173–183, 2005.

### ACKNOWLEDGMENTS

This work was supported by the National Science Centre Poland Grant nos. 2014/13/B/ST8/02973 (ML) and 2017/25/N/ST8/01593 (BZ).

## Alginate-based Hydrogels Modified with Graphene Oxide for Cartilage Regeneration

Klaudia Ordon, Aleksandra Lach, Monika Skoczeń, Kinga Pielichowska

Faculty of Material Science and Ceramics, AGH University of Science and Technology, Poland  
[ordon@agh.edu.pl](mailto:ordon@agh.edu.pl)

### INTRODUCTION

Hydrogels are three-dimensional networks composed of hydrophilic polymers characterized by high ability to absorb and retain water [1-3]. Water absorption is an important property influencing mechanical properties of the material, its biocompatibility and ability to release drugs inside the organism. In order to maintain the consistence of hydrogels materials in aqueous media and prevent their dissolution they are subjected to crosslinking process. As a result of this process ionic or covalent crosslinks are formed [2]. Hydrogels generally are structurally similar to the macromolecular-based components in the body, therefore can often be delivered via minimally invasive administration [6].

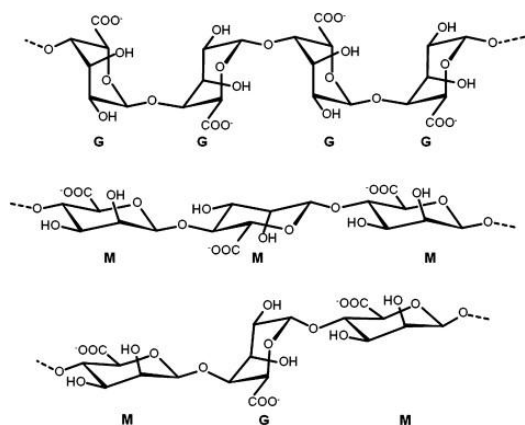


Fig. 1. Chemical structures of M-block, G-block, and alternating block in alginate [6].

One of the most versatile natural materials known to form hydrogels is alginate. Alginate is linear unbranched polysaccharide derived from brown algae that contains the repeating units of 1,4-linked  $\alpha$ -L-guluronic acid (G) and  $\beta$ -D-mannuronic acid (M) (Fig. 1) [3,5,6]. Alginate hydrogels have reversible gelling properties in solutions aqueous. These properties relate to the ionic interactions between divalent cations, such as calcium, magnesium, barium and carboxylic acid moieties on the guluronic acid residues. Since crosslinked ionically alginate during the gelling process does not damage cells and is considered as biocompatible, there has been a great deal of interest in the use of alginate hydrogels for cell encapsulation, drug delivery and tissue regeneration. Although conducted studies have reported promising results, there is still limited control over the swelling ratios and degradation profiles of ionically crosslinked alginate hydrogels, which is likely due to the uncontrollable loss of divalent cations into the surrounding environment [3]. The aim of this work was to obtain hydrogels based on sodium alginate for tissue engineering applications, showing good mechanical properties, bioactivity and a compact structure.

### EXPERIMENTAL METHODS

Sodium alginate was ionically crosslinked by treatment with a calcium chloride solution. For this purpose, sodium alginate was dissolved in distilled water, and in the calcium chloride solutions of various concentrations. Then, hydroxyapatite HAp and graphene oxide GO were introduced into the chosen solutions. The obtained hydrogels were then investigated towards mechanical properties including compressive tests, morphological analysis, wettability, rheological analysis, bioactivity and biodegradation tests.

### RESULTS AND DISCUSSION

The preliminary results show that the hydrogels based on an alginate, and graphene oxide as well as hydroxyapatite can be obtained and then characterized. These hydrogels were subjected to an extensive physicochemical characterization to highlight the impact of GO and HAp on bioactivity and biomechanical outcome. It was found that modification of alginate with HAp and GO leads to significant changes in hydrogel properties.

### CONCLUSION

The observations indicated that the changes of calcium and sodium alginate as well as GO i HAp concentration have significant impact on the morphology and mechanical properties of the cross-linked structure. The obtained hydrogel composites have a potential to be used in different biomedical applications, including tissue engineering and regenerative medicine due to excellent biocompatibility, bioactivity, stability and appropriate mechanical properties. Prospective research for these materials includes the in vivo studies.

### REFERENCES

- Espona-Noguera A., Ciriza J. et al., *Int J Biol Macromol.* 107:1261-1269, 2018
- Pazdan K., Pielichowska K. et al., *Engineering of Biomaterials* 126: 31-39, 2014
- Jeon O., Bouhadir K.H. et al., *Biomaterials* 30:2724-2734, 2009
- Huang Q., Liu S. et al., *J. Mater. Sci. Technol.* 33:821-826, 2017
- Kaklamani G., Cheneler D. et al., *J. Mech. Behav. Biomed. Mater.* 36:135-142, 2014
- Lee K.Y., Mooney D.J., *Prog. Polym. Sci.* 37: 106-126, 2012

### ACKNOWLEDGMENTS

Authors are grateful to the The National Center for Research and Development (NCBiR), Poland, for financial support of project No STRATEGMED3/303570/7/NCBR/2017.

## Electron-crosslinked Gelatin Hydrogels Mineralized Enzymatically for Bone Regeneration

Stefanie Riedel<sup>1,2</sup>, Karolina Mazur<sup>3</sup>, Danny Ward<sup>4</sup>, Lorna Ashton<sup>5</sup>, Stefan G. Mayr<sup>1,2</sup>, Timothy E.L. Douglas<sup>6,7</sup>

<sup>1</sup>Leibniz Institute of Surface Engineering (IOM), Leipzig, Germany

<sup>2</sup>Division of Surface Physics, University Leipzig, Germany

<sup>3</sup>Cracow University of Technology, Poland

<sup>4</sup>Biological and Life Science Dept., Lancaster University, United Kingdom

<sup>5</sup>Chemistry Dept., Lancaster University, United Kingdom

<sup>6</sup>Engineering Dept., Lancaster University, United Kingdom

<sup>7</sup>Materials Science Institute (MSI), Lancaster University, United Kingdom

[t.douglas@lancaster.ac.uk](mailto:t.douglas@lancaster.ac.uk)

### INTRODUCTION

Hydrogels are used increasingly as biomaterials for tissue regeneration. One advantage is ease of incorporation of biologically active molecules, including alkaline phosphatase (ALP), the enzyme responsible for the mineralization of bone tissue with calcium phosphate (CaP) *in vivo* by cleaving phosphate from organophosphates such as glycerophosphate (GP). Mineralization of hydrogels with CaP leads to mechanical reinforcement and promotion of cell attachment and proliferation. Hydrogels consisting of proteins such as gelatin have the advantage of offering binding sites to cells to improve their adhesion. Gelatin requires crosslinking to stabilise it at body temperature. Gelatin can be crosslinked and simultaneously sterilized by electron irradiation. In this study, gelatin hydrogels containing ALP were mineralized with CaP by incorporation of ALP during hydrogel formation and incubation in a solution of calcium glycerophosphate (CaGP), which served as a source of calcium ions and ALP substrate.

### EXPERIMENTAL METHODS

Gelatin hydrogels were prepared from type I gelatin solution 8 mg/ml in ddH<sub>2</sub>O. ALP was added at 0, 1.25 or 2.5 mg/ml. The gelatin-ALP solution swelled for 1h at room temperature and was then heated to 37°C, poured into desired moulds under stirring and allowed to polymerize at 6°C for 12 h. For electron irradiation, samples were placed in sealed airtight bags containing N<sub>2</sub> and irradiated under cooling with electrons by a linear electron accelerator (MB10-30MP; Mevex, Ontario, Canada) with doses of 5, 10, 15 20 and 40 kGy in steps of 5 kGy. Samples were incubated in ddH<sub>2</sub>O or 0.1 M CaGP (50043) for 7 days. After mineralization compressive modulus was determined. To determine the ratio of mineralized material, the samples were weighed in the hydrated state and then dried for 24 h at 60°C. The % of dry mass can then be calculated by the ratio of the weight in the dried state and the weight in the hydrated state. SEM, FTIR and Raman were performed after drying.

### RESULTS AND DISCUSSION

Dry mass percentage and compressive modulus (Fig. 1) increased with increasing ALP concentration. Increasing radiation dose to 10 kGy increased dry mass percentage and compressive modulus markedly. SEM (Fig. 2) revealed formation of CaP deposits in hydrogels containing ALP. FTIR and Raman spectra (not shown)

demonstrated the presence of phosphate peaks characteristic for CaP in samples containing ALP.

### CONCLUSION

ALP incorporated into gelatin hydrogels formed by electron irradiation retained biological activity and induced CaP formation, especially at doses  $\geq 10$  kGy.

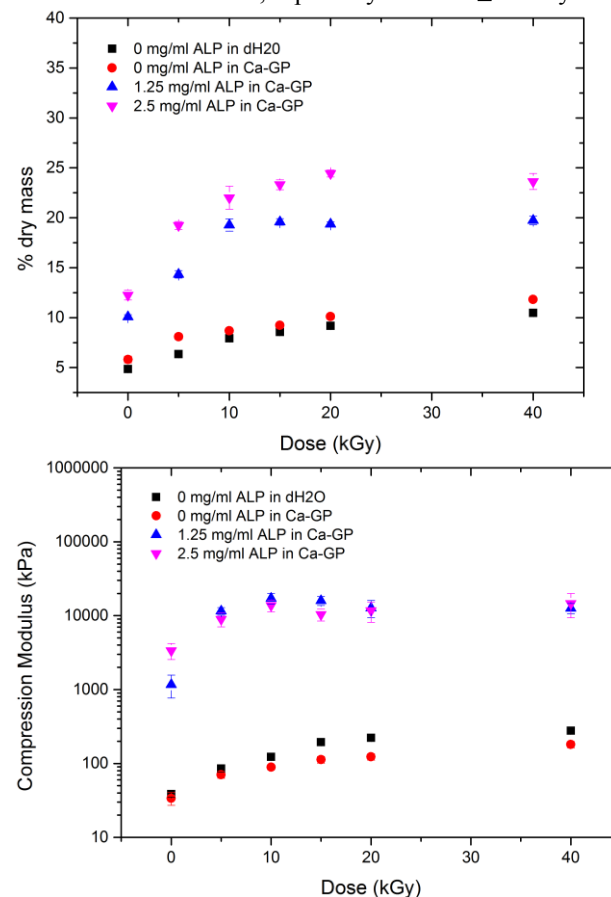


Fig. 1. Dry mass percentage (top) and compressive modulus (bottom) of hydrogels after 7 d mineralization.

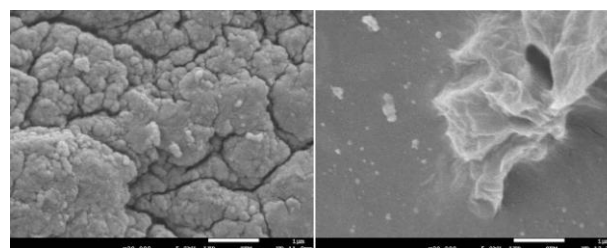


Fig. 2. SEM of hydrogels after mineralization (7 d)  
Left: 2.5 mg/ml ALP in Ca-GP.  
Right: 0 mg/ml ALP in ddH<sub>2</sub>O.



## $\beta$ -TCP/PHO Biocomposites for Bone Tissue Engineering

Ewelina Cichon<sup>1</sup>, Katarzyna Harażna<sup>2</sup>, Maciej Guzik<sup>2</sup>, Aneta Zima<sup>1</sup>, Anna Ślósarczyk<sup>1</sup>

<sup>1</sup>Department of Ceramics and Refractories/Faculty of Material Science and Ceramics, AGH University of Science and Technology, Poland

<sup>2</sup>Jerzy Haber Institute of Catalysis and Surface Chemistry, Polish Academy of Science, Poland  
[ecichon@agh.edu.pl](mailto:ecichon@agh.edu.pl)

### INTRODUCTION

Materials that can be used in the field of bone tissue engineering must be biocompatible and nontoxic. They should also exhibit adequate mechanical properties, such as compressive strength, stiffness and hardness [1]. Natural bone tissue consist of inorganic (apatite) and organic (mainly collagen) parts. The last one forms the principal organic matrix and ensures bone elasticity. Calcium phosphates (CaPs) such as hydroxyapatite (HA) and beta tricalcium phosphate ( $\beta$ -TCP), due to their similarity to mineral component of natural bone, are widely used in orthopaedy and dentistry [2,3]. Up to now many studies have been carried out in the field of bioceramic/polymer biomaterials for bone tissue engineering, however, to the best of our knowledge, none of the previous research have considered the use of bioceramics and medium chain length bacterial derived polyester – poly-3-hydroxyoctanoate (PHO). Both components are fully biocompatible, thus enabling generation of composite material that not only will support bone regeneration (thanks to  $\beta$ -TCP) but also will nourish the developing tissue (thanks to degradation of PHO to its oligomers (R)-3-hydroxyfatty acids).

### EXPERIMENTAL METHODS

$\beta$ -TCP powder was obtained by the wet chemical method. Ceramic samples were prepared by consequent uniaxial pressing at 100 MPa and sintered at temperature over 1000°C.  $\beta$ -TCP phase purity was confirmed by X-ray diffraction (XRD). Bioceramic tablets were polymer-coated by immersion using 2,5%; 5% or 10% (w/v) solutions of PHO in ethyl acetate (symbol of material: 2,5PHO; 5PHO; 10PHO). Microstructure and chemical composition in microareas were analysed by scanning electron microscopy (SEM) and X-ray energy dispersive microanalysis (EDX). Measurements of contact angle of water were carried out for  $\beta$ -TCP and PHO materials.

### RESULTS AND DISCUSSION

SEM observations confirmed that all of ceramic specimens were successfully coated with polymer. In the sample 2,5PHO ceramic grains were visible through the thin layer of polymer (Fig. 1). In the case of 5PHO and 10PHO ceramic surfaces were completely covered with polymer and the layer thickness was about 30 and 240  $\mu$ m, respectively (Fig. 2). EDS studies revealed high carbon content on the surface of the composites. Bioceramic  $\beta$ -TCP samples revealed contact angle of  $35,60 \pm 6,74^\circ$ , whereas for PHO this value was  $98,63 \pm 8,28^\circ$ .

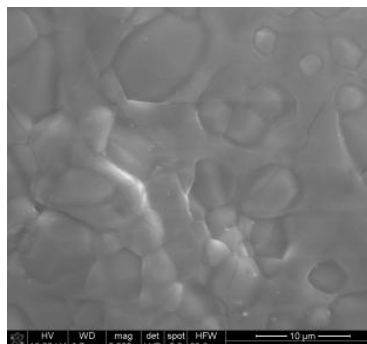


Fig. 1. Microstructure of 2,5PHO sample.

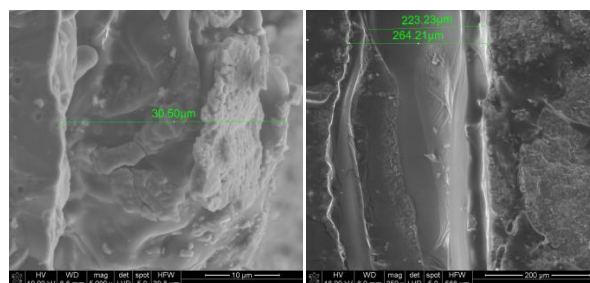


Fig. 2. Fractures of 5PHO and 10PHO samples with indicated thickness of the polymer layer.

### CONCLUSION

In this study  $\beta$ -TCP tablets were coated with PHO in order to obtain  $\beta$ -TCP/PHO biocomposites – potential biomaterials for bone tissue engineering. Materials were successfully prepared by immersion of ceramic samples in homogeneous polymer solutions. The thickness of the PHO layer depended on the concentration of the initial polymer solution. The surface of  $\beta$ -TCP revealed hydrophilicity, while PHO was hydrophobic. Obtained organic-inorganic composites require further research.

### REFERENCES

1. Bedian L. *et al.*, Int J Biol Macromol. 98:837-846, 2017
2. Lu J. *et al.*, RSC Adv. 8(4):2015-2033, 2018
3. Ng J. *et al.*, Tissue Eng Part B Rev. 23(5):480-493, 2017

### ACKNOWLEDGMENTS

Research funded by The National Centre for Research and Development, grant Lider no. LIDER/27/0090/L-7/15/NCBR/2016 and Faculty of Materials Science and Ceramics AGH University of Science and Technology - Project No.11.11.160.617 (2018). KH acknowledges the support of InterDokMed project no. POWER.03.02.00-00-I013/16.

## Polymeric Orthopaedic Textiles Ultrasonically Coated with Bioactive Nanoparticles and their Stability in Human Body Simulated Environment

Julia Rogowska-Tylman<sup>1,2</sup>, Bartosz Woźniak<sup>1</sup>, Agnieszka Chodara<sup>1,2</sup>, Sylwia Dąbrowska<sup>1</sup>, Robert Mrugas<sup>3</sup>, Witold Łojkowski<sup>1</sup>

<sup>1</sup>Laboratory of Nanostructures, Institute of High Pressure Physics, Polish Academy of Sciences, Warsaw, Poland

<sup>2</sup>Faculty of Materials Science and Engineering, Warsaw University of Technology, Warsaw, Poland

<sup>3</sup>Ortholigaments Ltd., Poland

[juliaRT@labnano.pl](mailto:juliaRT@labnano.pl)

### INTRODUCTION

Bio-properties of calcium phosphate ceramics such as hydroxyapatite (HA)  $\text{Ca}_{10}(\text{PO}_4)_6(\text{OH})_2$ , mainly their ability for implant fixation and solubility, have been studied extensively over the years. The results have shown their stable adhesion with the adjacent bone tissue, in conditions in which mechanical stability is not always ideal [1,2]. In this study we have shown that hydroxyapatite produced in IHPP PAS offers several advantages, such as a nanocrystalline structure similar to that of bone, along with documented characteristics of biocompatibility and reliability in the establishment of in vivo osseointegration [3,4]. We have demonstrated that nanoHA deposited on polymeric fibers, when used as orthopaedic implant, will provide gradual release of calcium ions into the phosphate buffered saline (PBS) environment. The future bone-bonding properties of a material were additionally evaluated by examining the ability of apatite formation on its surface in a simulated body fluid (SBF).

### EXPERIMENTAL METHODS

Two grades of hydroxyapatite nanopowders were synthesized by IHPP PAS, Poland (GoHAP type III – SSA 186.3 m<sup>2</sup>/g, density 2.93 g/cm<sup>3</sup>, size 15±1 nm and GoHAP type I- SSA 242.4 m<sup>2</sup>/g, density 2.89 g/cm<sup>3</sup>, size 8±1 nm) [4]. Ultrasonic coating method was used for surface modification of the materials [5]. Coating stability and activity was tested by immersion in phosphate buffered saline (PBS) and simulated body fluid (SBF) at 37°C on laboratory shaker (100rpm). During immersion test pH and medium conductivity was closely monitored.

### RESULTS AND DISCUSSION

As a result of ultrasonic wave induced nearby the textile substrate homogenous nanohydroxyapatite coatings of 200-350nm thickness were obtained on polymeric fibers. Scanning Electron Microscopy imaging revealed that nHA particles cover fibers but do not interfere with the structure or porosity of the base material. The coating stability test revealed that the coating dissolution in PBS was slow and nHA was present on fibers surface even after 30 days of immersion in both media. Moreover, the immersion in SBF medium caused calcium phosphate crystals formation on the fibers structure. Morphology of the resulted structures varied depending on nHA type used.

### CONCLUSION

The novel method of nHA deposition on the polymeric fibers can serve as an alternative for currently known orthopaedic implants modification solutions. It can also enhance the bone regeneration process in bone/implant interface region. Material testing revealed good stability and bioactivity of the deposited nHA coating. Moreover, the immersion test of the in vivo bone bioactivity prediction in SBF can reduce the number of animals used in and the duration of future animal experiments.

### REFERENCES

1. T. J. Webster, C. Ergun, R. H. Doremus, R. W. Siegel, R. Bizios, Enhanced functions of osteoblasts on nanophase ceramics, *Biomaterials* Vol.21, Issue 17, 2000, Pages: 1803–1810.
2. D. Predoi, R. A. Vatasescu-Balcan, I. Pasuk, M. Costache, R. Trusca, Calcium phosphate ceramics for biomedical applications, *Journal of Optoelectronics and Adv. Materials* 10(8), Pages: 2151-2155.
3. D. Smolen, T. Chudoba, I. Malka, A. Kedzierska, W. Łojkowski, W. Świeszkowski, K. J. Kurzydłowski, Highly bio-compatible, nanocrystalline hydroxyapatite synthesized in a solvothermal process driven by high energy density microwave radiation, *Int J Nanomedicine*. 2013; 8: 653–668.
4. S. Kuśnieruk, J. Wojnarowicz, A. Chodara, T. Chudoba, W. Łojkowski, Influence of hydrothermal synthesis parameters on the properties of hydroxyapatite nanoparticles, *B. J. Of Nanotech.*, Vol.7, 2016, Pages: 1586-1601.
5. Polish Patent PL226891: Method for producing bone implant and the bone implant, granted by Polish Patent Office on 29.09.2017.

### ACKNOWLEDGMENTS

This work is supported by the polish National Centre for Research and Development (NCBR) project: NANOLIGABOND(POIR.04.01.02-00-0016/16) *Artificial tendons and ligaments fixation to bone tissue using nanotechnological approach.*

## Enzymatically mineralized gellan gum/alginate porous scaffolds for bone and cartilage regeneration

Krzysztof Pietryga<sup>1</sup>, Violeta Rodriguez<sup>2</sup>, Véronique Larreta-Garde<sup>2</sup>, Elżbieta Pamuła<sup>1</sup>

<sup>1</sup>Department of Biomaterials and Composites, Faculty of Materials Science and Ceramics, AGH University of Science and Technology, Kraków, Poland

<sup>2</sup>Errmece, University of Cergy-Pontoise, Cergy-Pontoise, France  
[pietryga@agh.edu.pl](mailto:pietryga@agh.edu.pl)

### INTRODUCTION

Mineralization of hydrogel materials with calcium phosphate (CaP) can improve bioactivity and adapt hydrogels to bone regeneration [1]. Hydrogels can be enzymatically mineralized by incorporation of an enzyme - alkaline phosphatase (ALP) and incubation in calcium glycerophosphate (CaGP). The ALP will use the CaGP as a substrate, cleaving the phosphate and thereby increasing its local concentration, enabling precipitation of CaP [2]. Ceramic phase presence in hydrogel leads to a number of advantages including improved mechanical properties, bioactivity and affinity to biologically active molecules [3]. The study is aimed to develop a method for fabrication of porous hydrogel materials for bone and cartilage defects treatment based on enzymatic mineralization of gellan gum/alginate (GGA) mixtures.

### EXPERIMENTAL METHODS

Porous polysaccharide scaffolds were prepared by freeze drying 10% w/v paste obtained by mixing gellan gum and alginate (weight ratio 3:1) and 2 mg/ml ALP with water, followed by incubation in 1% CaCl<sub>2</sub> for 30 min. Mineralization was carried out by incubation in 0.1 M CaGP for 1, 3 and 7 days. Scaffolds were characterised by optical (VHX-5000, Keyence) and scanning electron (Gemini SEM 300, Zeiss) microscopes. Activity of released and entrapped within the scaffold ALP was measured by para-nitrophenyl phosphate (pNPP) assay. Presence of mineral phase after mineralization was confirmed by EDX (Bruker) and FTIR (ATR mode, Bruker Tensor 27). Progress of mineralization was assessed by FTIR and increase in dry mass percentage. Rheological properties (storage and loss moduli, G' and G'', respectively) were evaluated in 1 Hz oscillation mode (MRC 301, Anton Paar).

### RESULTS AND DISCUSSION

CaCl<sub>2</sub>-crosslinked hydrogel scaffolds with interconnected pores of size around 200 µm were obtained (Fig. 1 A1, A2). Incorporated ALP remained active inside hydrogel allowing enzymatic mineralization, although more than 50% of ALP was released within 24 h (data not shown). SEM images showed mineral precipitates with crystal size <100 nm on the scaffolds surface (Fig. 1 B2). GGA material was mineralized gradually over time and increase of 30% dry mass was obtained on day 7 (Fig 1 C). Increase in scaffold G' and G'' after mineralization was observed (Fig. 1 D) and it was positively correlated with average content of mineral phase. CaP creation was confirmed by FTIR by presence of characteristic peaks related to phosphate groups at 1050, 570 and 600 cm<sup>-1</sup> (Fig. 1 E).

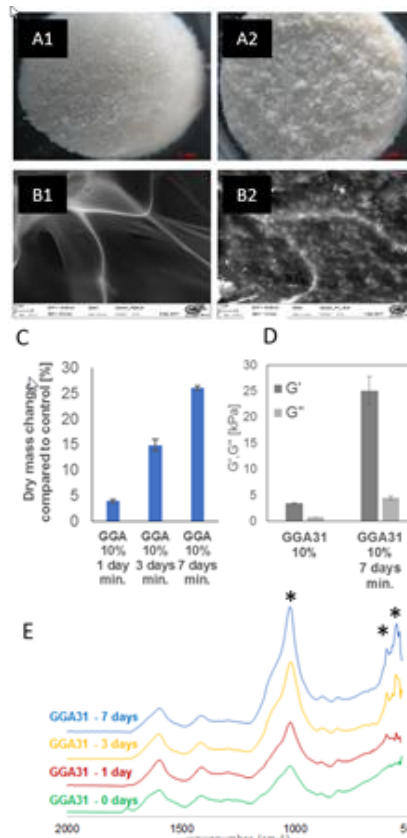


Fig. 1. Macroscopic appearance (A) and microstructure (B) of non-mineralized (A1, B1) and mineralized (A2, B2) GGA scaffolds; dry mass changes after GGA mineralization for 1, 3, and 7 days (C); G' and G'' moduli of GGA before and after 7-day mineralization (D); FTIR-ATR spectra of GGA mineralized for 0, 1, 3 and 7 days.

### CONCLUSION

Highly mineralized GGA scaffolds were produced by three-step procedure: 1) freeze-drying of GGA/ALP paste, 2) crosslinking of resulting sponges with calcium ions and 3) incubation in CaGP. The scaffolds were characterized by homogenous distribution of fine CaP crystals and improved mechanical properties as compared to non-mineralized scaffolds.

### REFERENCES

- [1] Legeros RZ. 1991; Calcium Phosphates in Oral Biology and Medicine. vol 15
- [2] Douglas, T.E., Messersmith, P.B., et al., 2012. Macromolecular bioscience, 12(8), pp.1077–1089.
- [3] Boyan, B. et al., 2003. Eur Cell Mater, 6(24), pp.22–27.

### ACKNOWLEDGMENTS

K.P. acknowledges European Society for Biomaterials for Racquel LeGeros Award (2017), which supported his stay at Errmece, University of Cergy-Pontoise, France.

## Assessment of Cytocompatibility of PLLA/PLLATMC Scaffolds Prepared by Low-cost 3D Printing

Jakub Marchewka, Bartosz Mielan, Elzbieta Pamula, Jadwiga Laska

Faculty of Materials Science and Ceramics, AGH University of Science and Technology, Poland

[jmar@agh.edu.pl](mailto:jmar@agh.edu.pl)

### INTRODUCTION

Damages of bone and cartilage tissue related to communication and sport accidents are still a substantial medical problem in which application of polymeric scaffolds is one of the most effective therapeutic procedures<sup>1,2</sup>.

3D printing is nowadays one of the most promising methods used to prepare polymeric scaffolds for tissue regeneration<sup>3</sup>. The structure of these products including shape, dimensions and infill is precisely designed by computer model so they could be well-matched to the specific medical application. Reduction of the costs may be achieved using equipment developed by open-source RepRap project and freeware GNU GPL software.

Poly(L-lactide) (PLLA) and poly(L-lactide-co-trimethylene carbonate) 15/85 (PLLATMC) are proposed to prepare blends with various mechanical properties processed by fused deposition modelling (FDM). The most crucial aspect of the potential application of the produced scaffolds in tissue engineering is the *in vitro* assessment of their cytocompatibility.

### EXPERIMENTAL METHODS

RepRapPro Mendel (RepRapPro, UK) was applied as a commercially available 3D FDM printer based on RepRap project. Blender, Slic3r and Pronterface as a package of freeware software were used to design the computer model and to optimize and control the printing process.

PLLA and PLLATMC were purchased from BioMatPol, Poland and their blends were prepared by screw extrusion. Blends of PLLA and PLLATMC with the weight ratio of the two polymers 80:20 and 30:70 were used to prepare scaffolds. The filament of the 80:20 blend was processed with the standard printer configuration while the 30:70 material was processed in the form of a granulate needed profoundly modified printer construction based on our own design.

The scaffolds were sterilized by soaking in 70% ethanol and UV irradiation. 50,000 human osteoblast-like MG 63 cells (European Collection of Cell Cultures, UK) were seeded on each scaffold and cultured up to 14 days at 37°C in a humidified air atmosphere containing 5% of carbon dioxide. Proliferation of the cells was measured quantitatively after 7 and 14 days culture using alamarBlue test and viability was assessed after 1, 3, 7 and 14 days using LIVE/DEAD test. Cells were also examined after haematoxylin and eosin (H&E) staining under optical microscopy (Keyence VHX-900F) after 7 and 14 days. AlamarBlue tests were conducted after transfer of the scaffolds to the new plates.

### RESULTS AND DISCUSSION

Scaffolds were printed as cylinders with the height of 1.0 mm and the diameter of 15.0 mm built of four layers in 0°/60°/120° orientation. Two series were prepared using the two different compositions - 80:20 (A) and 30:70 (B) among which four porosities, namely 35% (A1 and B1), 45% (A2, B2), 55% (A3, B3) and 65% (A4, B4), were obtained.

The cell proliferation on 30:70 PLLA:PLLATMC scaffolds after 14 days (Fig. 1B) was higher than on 80:20 ones (Fig. 1A), however the relative changes between 7 and 14 days were lower. Porosity had no significant effect on the cell growth in neither material.

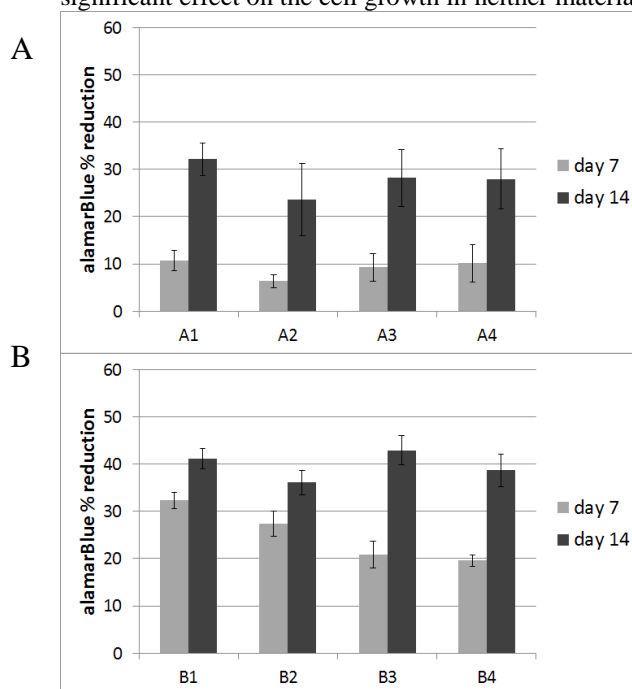


Fig. 1. Viability of MG 63 cells cultured on PLLA:PLLATMC blends 80:20 (A) and 30:70 (B) with porosity of 35% (A1, B1), 45% (A2, B2), 55% (A3, B3) and 65% (A4, B4).

### CONCLUSION

PLLA:PLLATMC blends with various compositions could be processed using standard or modified RepRap printer. Differences in cells proliferation and viability depend mainly on the material composition and less on the structure of the scaffold. The scaffolds may be considered as materials for tissue engineering.

### REFERENCES

- Chan B.P., Leong K.W., Eur. Spine J., 17, 467-479, 2008.
- Bartolo P.J. *et al.* [in:] Virtual Prototyping & Bio Manufacturing in Medical Applications, Springer, 149-170, 2008.
- Hutmacher D.W., J. Biomater. Sci. Polym. Ed., 12(1), 107-124, 2001.



## Preparation of Microspheres with Different Topologies for Cell Culture in Tissue Engineering

Bartosz Mielan, Małgorzata Krok-Borkowicz, Elżbieta Pamuła

Department of Biomaterials and Composites, Faculty of Materials Science and Ceramics,  
AGH University of Science and Technology, Kraków, Poland

[barmie@agh.edu.pl](mailto:barmie@agh.edu.pl)

### INTRODUCTION

Microspheres (MS) are an alternative way to conduct cell cultures. They may be used to create material-cell constructs and organize them into more complex tissue-like structures, according to a novel tissue engineering approach called *bottom-up* [1]. Particularly promising are MS made of resorbable polymers like poly(L-lactide-*co*-glycolide) (PLGA) due to their ability to degrade over time [2]. Oil-in-water emulsification with solvent evaporation is quite a simple method to obtain MS in a lab-scale. It is possible to modify emulsification process by addition of different solvents into oil phase to design tailored diameter, shape and surface microstructure of created MS. Some authors suggest using hydrocarbons due to their low boiling point, which results in their accelerated evaporation during MS formation [3]. Also PLGA shows low solubility in hydrocarbons, which gives opportunity to create pores in formed MS.

The purpose of this study was to obtain both nonporous and porous PLGA MS, i.e. MS1 and MS2, respectively, and study their microstructure and biological properties as cell carriers in *bottom-up* tissue engineering.

### EXPERIMENTAL METHODS

MS were obtained by oil-in-water emulsification. PLGA (85:15,  $M_n = 100$  kDa,  $M_w = 210$  kDa) was dissolved in 7.5% wt/vol dichloromethane (DCM) to produce MS1 or in mixture of DCM and hexane at a ratio 9:1 to produce MS2. Respective oil phases were added drop by drop into water phase containing poly(vinyl alcohol) (PVA) placed on magnetic stirrer (1000 rpm for MS1 and 500 rpm for MS2) for 24 h. PVA concentration was 2% for MS1 and 0.1% for MS2. After formation MS were collected, washed 5 times and dried at 37°C. Measurement of MS diameter and microstructure observation were conducted with optical microscopy (Keyence VHX-900F) and scanning electron microscopy (Nano Nova SEM 200), respectively. MG-63 osteoblast-like cells were cultured either in the extracts from MS (obtained by incubation 60 mg MS in 2 ml medium for 24 h at 37°C) or on the MS in static conditions (48-well plates) at 37°C in 5% CO<sub>2</sub> atmosphere. Live-dead staining (calcein AM/propidium iodide) and Alamar Blue assay were conducted on days 1, 3 and 7 to assess usefulness of produced MS.

### RESULTS AND DISCUSSION

MS1 had diameter of  $156 \pm 49$   $\mu\text{m}$  while MS2  $213 \pm 78$   $\mu\text{m}$ . They showed considerable differences in morphology. MS1 produced with the use of DCM only were smooth with regular shape (Fig. 1A), while those produced with DCM/hexane mixture were porous (Fig. 1B). The median size of pores of MS2 was 8  $\mu\text{m}$ .

Biological tests proved that extracts of MS were not cytotoxic for MG-63 cells, however cell growth was inhibited on porous MS2 as compared to smooth MS1 (Fig. 1 C,D).

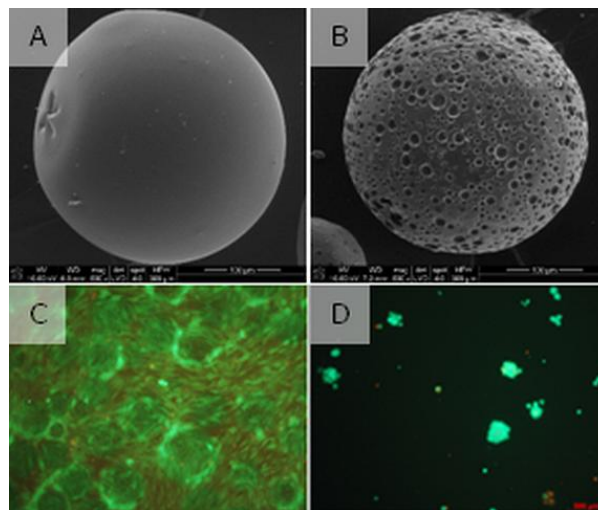


Fig. 1. SEM microphotographs (A,B) and MG-63 cell cultured for 7-day stained live-dead (C,D) on MS1 – smooth, obtained from DCM oil phase (A,C) and MS2 – porous, obtained from DCM/hexane oil phase (B,D).

### CONCLUSION

It is possible to modify microstructure of MS by controlling synthesis conditions and addition of hexane to DCM oil phase. Addition of hexane allows to fabricate MS with median pore size of 8  $\mu\text{m}$  and rough, porous surface. Although such MS were found not cytotoxic for cells as shown by MG-63 cell culture in the extracts, they supported the cells to lower extent as compared to smooth MS1.

### REFERENCES

- [1] B. Schon, G. J. Hooper, and T. B. F. Woodfield, "Modular Tissue Assembly Strategies for Biofabrication of Engineered Cartilage," *Ann. Biomed. Eng.*, vol. 45, no. 1, pp. 100–114, 2017.
- [2] F. Ramazani *et al.*, "Strategies for encapsulation of small hydrophilic and amphiphilic drugs in PLGA microspheres: State-of-the-art and challenges," *Int. J. Pharm.*, vol. 499, no. 1–2, pp. 358–367, 2016.
- [3] M. R. Kim, S. Lee, J. Park, and K. Young, "Golf ball-shaped PLGA microparticles with internal pores fabricated by simple O / W emulsion w," *Chem. Commun.*, vol. 46, pp. 7433–7435, 2010.

### ACKNOWLEDGMENTS

This study was financed from National Science Center, Poland (UMO-2016/21/D/ST8/0185).

## Poly lactide Based Nanocomposites Reinforced with Graphene Oxide for Bone Surgery Implants

Nerea Uriarte Losada<sup>1,2</sup>, Bartosz Mielan<sup>2</sup>, Barbara Szaraniec<sup>2</sup>, Elżbieta Pamuła<sup>2</sup>, Jan Chłopek<sup>2</sup>

<sup>1</sup>Institute of Biomedical Engineering, Faculty of Engineering, Mondragon University, Spain

<sup>2</sup>Department of Biomaterials and Composites, Faculty of Materials Science and Ceramics, AGH University of Science and Technology, Krakow, Poland

[szaran@agh.edu.pl](mailto:szaran@agh.edu.pl)

### INTRODUCTION

The worldwide incidence of bone disorders is growing exponentially, especially in populations where aging is coupled with unhealthy habits. High regenerative capacity of bone allows most of bone injuries to heal automatically. However, in the case of large bone defects surgical procedures are required. They use different mechanisms and devices to ensure proper bone healing [1]. There are several bone tissue engineering (BTE) approaches available currently, e.g. various bone-grafts or orthopaedic implants, but unfortunately all of them have some disadvantages [2]. Considering this, in the last decade, attention has been focused on biodegradable nanocomposites, which are expected to better interact with biological tissues. That is why this project aimed to evaluate polylactide (PLA) based nanocomposites reinforced with graphene oxide (GO) as a possible novel material for bone surgery implants. When considering a new biomaterial, it is especially important to assess its biocompatibility. All materials intended to use in contact with biological tissues must perform with an appropriate host response, without causing any adverse effect within the organism. In nanocomposite systems, such as the one developed in this study, one of the key factors affecting material biocompatibility is the type and the amount of nanoadditive used [3]. The first step in evaluation of biological properties of potential biomaterials is their assessment in contact with cells in culture to exclude potential cytotoxicity. Thus in this study we analyse behaviour of developed composites in contact with bone cells.

### EXPERIMENTAL METHODS

PLA (PuraSorb PL38, Purac), GO (ITME) and dichloromethane (DCM, Avantor) were used to manufacture five nanocomposites with GO concentration of 0 wt.%, 0.2 wt.%, 0.5 wt.%, 1 wt.% and 3 wt.%. The GO suspensions in PLA solution in DCM were homogenised using magnetic stirrer and sonication and subsequently casted into glass Petri dishes. Next, they were stored in a vertical ventilation fume hood for a day at a room temperature, ensuring the solidification of PLA/GO nanocomposite foils. Surface properties, i.e. roughness (contact profilometer, Hommel Tester) and wettability (goniometer, DSA10 Krüss) of the specimens were examined before and after immersion test (phosphate buffered saline (PBS) for 6 weeks, at 37°C). To examine cytocompatibility of the PLA/GO nanocomposites, MG63 osteoblast-like cells were seeded on the samples at concentration 25000 cells/cm<sup>2</sup> and cultured under 5% CO<sub>2</sub> atmosphere at 37°C for 7 days. Alamar Blue assay and live-dead test (both from Sigma Aldrich) were performed

after 1, 3 and 7 days of culture to analyse viability and proliferation of the cells.

### RESULTS AND DISCUSSION

Roughness of the nanocomposites was increased as compared to that of the pure polymer (Ra=0.22 and Ra=0.11 for PLA/3GO and PLA, respectively). After incubation in PBS PLA roughness did not change, while that on the nanocomposites increased by about 30% due to material degradation. Wettability of all tested materials was similar and was in the range of 70-80°, both before and after incubation in PBS.

Cell seeding efficiency on all materials was the same as shown by the reduction of Alamar Blue on day 1 (Fig. 1). On day 3 cell proliferation was higher on all PLA/GO nanocomposites than on reference PLGA. The same tendency was observed on day 7. The cells cultured on PLA/0.5GO showed the highest viability. This may suggest that MG63 osteoblast-like cells exhibit the highest affinity towards the sample with a middle amount of GO, i.e. 0.5wt%.

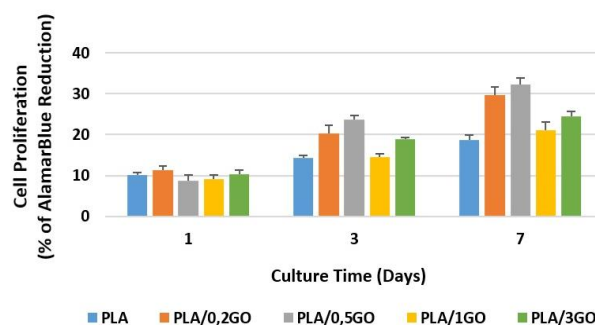


Fig. 1. Viability of MG63 cells cultured on the surface of PLA and PLA/GO nanocomposites.

### CONCLUSION

PLA/GO nanocomposites might be considered for bone surgery implants. As shown in the preliminary studies, addition of graphene oxide in the amount of 0.2 to 3wt% does not adversely affect cytocompatibility of the developed nanocomposites. Their higher roughness may be favourable for cells in culture.

### REFERENCES

- [1] V.Campana G.Milano, E.Pagano et al. J Mat Sci: Mat Med, 10 (2014) 2445-2461
- [2] M.M.Stevens Materials Today (2008) 18-25
- [3] Y.Wang, S.Wua, X.Zhao, Bio-Med Mat Eng 24 (2014) 2007-2013

### ACKNOWLEDGMENTS

This research was financed by the Dean grant No. 15.11.160.182 of Faculty of Materials Science and Ceramics, AGH University of Science and Technology.

## Structuring of Surfaces Dedicated for the Integration with the Cardiovascular Tissue

Klaudia Trembecka-Wójciga<sup>1</sup>, Roman Major<sup>1</sup>, Jurgen Marcus Lackner<sup>2</sup>, Bogusław Major<sup>1</sup>

<sup>1</sup>Institute of Metallurgy and Materials Science Polish Academy of Science, Poland

<sup>2</sup>Joanneum Research Forschungsges mbH, Institute of Surface Technologies and Photonics, Functional Surfaces, Austria  
[k.trembecka@imim.pl](mailto:k.trembecka@imim.pl)

### INTRODUCTION

Engineering of biomaterials requires a thorough understanding of cell-material interaction. The work concerns the surface modification of the material with its destination in the regeneration of the cardiovascular system. Biomaterials dedicated for direct blood contacting require the design of fully atrombogenic surface which do not adverse interact with any blood components<sup>1</sup>. This represents a really complex task due to a variety of processes occurring within this interface including plasma protein adsorption, cell adhesion, and activation followed by thrombus formation<sup>2</sup>. One of the promising methods to improve atrombogenic properties of materials is in vivo delivering of the anticoagulant drugs using polymer based micelles<sup>3</sup>. The work focused on surface modification in form of channels to improve cell-material integration. Surfaces were finally modified with polymer coating in form of micelles with anticoagulant drugs.

### EXPERIMENTAL METHODS

In the frame of the work, the Ti substrate was modified in the form of the patterns made by laser interference lithography technique. To improve tissue-PU integration, multilayer polyelectrolyte films were considered as final functional coatings in the form of polymer structures-micelles delivering the anticoagulant drugs. Microstructure and topography of migration channels were characterized using Atomic Force Microscopy. Cell – material interactions were described. For the analysis Hematopoietic Stem Cells were used in order to analyse cell adhesion, proliferation and differentiation towards endothelium. To analyse heamocompatybility properties of drug delivering coatings clinically used tester was used (Impact-R).

### RESULTS AND DISCUSSION

Surface structuration in form of channels has direct influence on endothelial cells behaviour. Scanning laser confocal microscopy (CLSM) confirmed the regular distribution of channels on substrates (Fig.1). The oriented cell growth on channelled surfaces was observed (Fig. 1). Channels distribution had direct influence on cell density and formation of cell junctions. Surface modification by polyelectrolyte coating with micelles has direct influence on heamocompatibility properties of materials (Fig. 2). Anticoagulant drug release causes changes in blood component activation. After 7 days of presence of micelles with drug on surface the amount of adhered platelets and leukocytes to the surface was smaller than for 1 day of incubation. Crosslinking the coating by NHS/EDC causes weaker drug release through polymer coating.

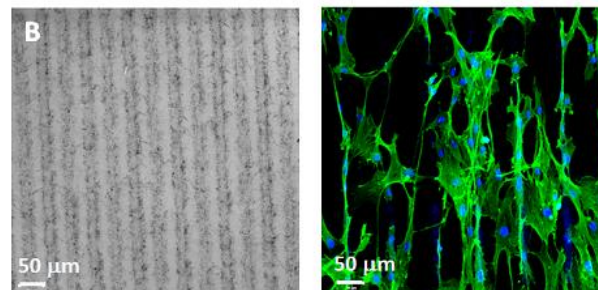


Fig. 1. Migration channels on surface elaborated (on the left) and endothelial cell response on channelled surfaces (on the right).

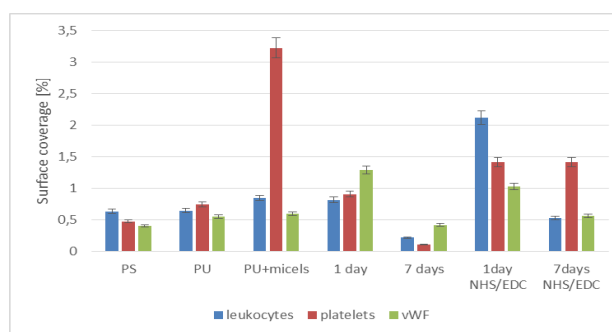


Fig. 2. Surface analysis by CLSM after Impact-R test. Analysis done after 1 and 7 days after micelles with anticoagulant drugs incubation on PU substrate.

### CONCLUSION

Controlled time release of the anticoagulant drug from micelles causes reduction of platelets and leukocytes adhesion to the surface and adsorption of von Willebrand factor. Surface modification in form of channels by laser ablation technique causes oriented cell growth on substrates and promotes cell – material integration.

### REFERENCES

- Sanak M. *et al.* Bull. Pol. Acad. Sci. Tech. Sci. 58(2):317-22, 2010
- Yi P. *et al.* Mater. Sci. Eng. C 59:669–76, 2016
- Ramesh CV. *et al.*, Int J Pept Protein Res. 45(4):386-90, 1995

### ACKNOWLEDGMENTS

The work was prepared under the project "Functional carbon based coatings on titanium substrate, modified by laser ablation designed for the integration with cardiac tissue and ultimately inhibit the blood clotting process" of the Polish National Centre of Science No. 2016/21/N/ST8/00186



## Chemoselective Functionalization of Hydrogels for Tunable pH-sensitive Drug Delivery

Emanuele Mauri, Alessandro Sacchetti, Filippo Rossi

Department of Chemistry, Materials and Chemical Engineering "Giulio Natta", Politecnico di Milano, Milan, Italy  
[emanuele.mauri@polimi.it](mailto:emanuele.mauri@polimi.it)

### INTRODUCTION

In the last decades, the development of controlled drug delivery systems has attracted considerable attention in biochemical and therapeutic treatments<sup>1-2</sup>. The synthesis of hydrogels as devices functionalized through cleavable linkers gives the opportunity to produce vehicles capable to tune drug release in targeted conditions, also maintaining the drug level within a desired range for a sustained period of time. However, respect to the good results obtained with antibodies and peptides, several critical aspects are related to the fact that drug release from 3D matrices is mostly driven by very quickly pure diffusion mechanism. In this work, we propose the microwave-assisted synthesis of hydrogels functionalized with pH-sensitive linkers, ester and hydrazone, and the study of multiple tunable delivery of rhodamine B (RhB) conjugated with the functionalized polymeric network. RhB choice was due to its resemblance to many hydrophilic analgesic and anti-inflammatory drugs.

### EXPERIMENTAL METHODS

#### Hydrogels synthesis

Polymeric functionalization occurred on polyethylene glycol (PEG) chains. To synthesize the final hydrogels with ester cleavable linkers (ACPEG-e hydrogels), PEG reacted with RhB acid chloride through esterification reaction; whereas hydrogels with hydrazone functionality (ACPEG-h hydrogels) were obtained using PEG modified aldehyde<sup>2</sup> reacting with RhB hydrazine derivative. NMR and FT-IR analyses were performed to characterize the obtained products. Hydrogel synthesis occurred via polycondensation reaction between the carboxyl groups of carbomer and hydroxyl groups of PEG, PEG grafting RhB and agarose.

#### RhB release studies

Release experiments of RhB from hydrogels were performed at 37°C, at pH 7.4 and 8.5; the released amount was measured by UV spectroscopy at 570 nm and determined referring to the standard calibration curve for RhB.

### RESULTS AND DISCUSSION

The efficient synthesis of hydrogel modified with cleavable linkers was confirmed by NMR, FT-IR and rheological studies. The RhB release profiles from ACPEG-e and AC-PEG-h hydrogels were performed at conditions that mimic the classic *in vivo* environment and at basic pH, typical of some diseases like colon.

The percentage of released RhB is defined as the ratio between the released amount and the total amount linked to the polymeric scaffold. The comparison of the release profiles associated to ester (♦ blue at pH=7.4; ♦ red at pH=8.5) and hydrazone (▲ blue at pH=7.4; ▲ red at pH=8.5) functionalization and the sample with

RhB only physically entrapped within 3D network (● black at pH=7.4 and pH=8.5) shows that drug release is prolonged for a much longer period in the functionalized hydrogels (Fig. 1A, B). A linear plot of these release profiles at both pH illustrates a double diffusion regime with different slopes<sup>3</sup>. The transition and duration of the two regimes depends on the nature of the functionalization. These regimes probably correspond to: (i) ester/hydrazone bonds present at the interface hydrogel/water that could be easily cleavable and (ii) ester/hydrazone bonds present in the inner core (Fig. 1C, D).

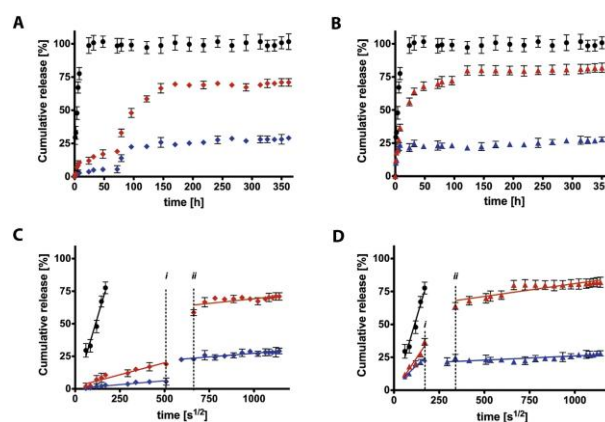


Fig. 1. A: *In vitro* RhB release profile delivered from unmodified hydrogel (●) and ACPEG-e at pH 7.4 (♦, blue) and at pH 8.5 (♦, red). B: *In vitro* RhB release profile from unmodified hydrogel (●) and ACPEG-h at pH 7.4 (▲, blue) and at pH 8.5 (▲, red). C: The slope of RhB release from unmodified hydrogel (●), ACPEG-e at pH 7.4 (♦, blue) and at pH 8.5 (♦, red) against the square root time representative of the Fickian diffusion coefficient. D: The slope of RhB release from unmodified hydrogel (●), ACPEG-h at pH 7.4 (▲, blue) and at pH 8.5 (▲, red) against the square root time representative of the Fickian diffusion coefficient.

### CONCLUSION

Microwave-assisted hydrogels composed by PEG modified with ester or hydrazone groups grafting RhB allow to tune the release of the drug load upon different physiological pH conditions. Moreover, our method of synthesis yields sterile polymeric networks in absence of organic solvent and by-products.

### REFERENCES

1. Perale G. *et al.* J.Control. Release 159:271-280, 2012
2. Gunce E. *et al.* Biomater. Sci. Eng. 3:370-380, 2017
2. Mauri E. *et al.* Polym. Adv. Technol. 26:1456-1460, 2015
3. Mauri E. *et al.*, Mat. Sci. Eng. C 61:851-857, 2016

### ACKNOWLEDGMENTS

This work was supported by Bando Giovani Ricercatori Ministry of Health.



## The Content of Collagen in Collagen-polyester Material and Hemostatic Research

Chun-Hui Huang, Yi-Ting Wang, Pei-Ni Huang, Hsiao-Cheng Yen

R&D Department/HANBIOMEDICAL INC., Taiwan  
[han.biomedical008@gmail.com](mailto:han.biomedical008@gmail.com)

### INTRODUCTION

Collagen plays an important role in the hemostatic process. When collagen exposes in wounds, it rapidly aggregates and activates platelets. It also indirectly causes fibrinogen and tissue fluid to react with thrombin and form blood fibrin<sup>1</sup>. However, the cost of a collagen-based pad is relatively higher than other pads for wound handling. In this study, we used a novel method to produce 1% collagen polyester nonwoven fabric, and measure the hemostasis performance as well as tissue repair outcome in comparison with collagen-free pad. The results showed that the 1% collagen pad can significantly reduce the time of hemostasis. We conclude that the pad of 1% collagen polyester nonwoven fabric is better than other collagen-free pad in terms of hemostasis and wound healing, and it also a cost effective way for wound handling.

### EXPERIMENTAL METHODS

The pad of 1% collagen polyester nonwoven fabric was produced, and the collagen content was measured and calculated by optical-density (OD) of hydroxyproline. The hemostatic effect was tested by SD rats. Total six SD rats are equally divided into test-group and control-group. After the process of anesthesia, rats were underwent the muscle-incision surgery. The right femoral artery of rats were punctured with 24G needle<sup>3</sup>. To stanch bleeding, the wounds of test-group are covered with 1% collagen-polyester non-woven fabric; and the wounds of control-group are covered with CSD<sup>®</sup> polyester non-woven fabric (40×40×2mm). We record the duration of time until the hemostasis was completed<sup>3</sup>. Student's t-test is used as a statistical analysis ( $\alpha=0.05$ ) to analyze the data of experiment.

### RESULTS AND DISCUSSION

The result shows that the collagen nonwoven fabric pad contained 1±0.4% collagen which was matched the pre-set goal of the pad. The hemostatic time of test-group and control-group were 53.00±8.88 and 137.66±11.01 seconds, respectively. The p-value calculated was 0.037. The results showed that 1% collagen-polyester pad exhibited a much better performance of hemostasis than collagen-free pad. Even though the collagen content was only 1%, the effect of enhancing platelet aggregation as well as accelerating the formation of blood clot were achieved.

sample	collagen-polyester non-woven fabric	CSD <sup>®</sup> polyester non-woven fabric
1	46	125
2	50	145
3	63	143
mean±SD	53.00±8.88	137.66±11.01

*Table 1. Hemostatic effect experiment (P=0.037)*

The duration of time until the bleeding is stopped. The sample is considered as no hemostatic effect if still bleeding after 90 seconds. Student's t-test is used as a statistical analysis ( $\alpha=0.05$ ) to analyze the data of experiment.

### CONCLUSION

This study showed that 1% collagen-polyester pad had better efficacy of hemostasis than collagen-free pad. Also, 1% of collagen pad is cost effective for wound handling. Further studies is undergoing, more data will be present soon.

### REFERENCES

References must be numbered. Keep the same style.

1. Farndale, R. et al. *J. Thromb. Haemost.* 2(4): 561-573, 2004
2. Reddy, G. et al. *Clinical biochemistry.* 29(3): 225-229, 1996
3. Ersoy, G. et al. *Advances in therapy.* 24(3): 485-492, 2007

### ACKNOWLEDGMENTS

We would like to thank Mackey Memorial Hospital and Dr. Chin-Lung Chang for providing support to this project.

## Nanocapsules Based on Amphiphilic Polysaccharides as Nanocarriers for Biomedical Applications

Małgorzata Janik<sup>1</sup>, Joanna Szafranec<sup>1,2</sup>, Mikel Felipe<sup>1</sup>, Szczepan Zapotoczny<sup>1</sup>

<sup>1</sup>Department of Physical Chemistry and Electrochemistry, Faculty of Chemistry, Jagiellonian University, Poland

<sup>2</sup>Department of Pharmaceutical Technology and Biopharmaceutics, Faculty of Pharmacy, Jagiellonian University Medical College, Poland

[mal.janik@uj.edu.pl](mailto:mal.janik@uj.edu.pl)

### INTRODUCTION

Numerous biopolymeric materials have been applied for fabrication of carriers of bioactive compounds enabling site-specific targeting or serving as contrast agents in imaging techniques. Chemical modification of biopolymers is a way to obtain great tools to form functionalized vehicles. Much of them have been designed to encapsulate lipophilic therapeutic substances as number of therapeutics exhibit poor solubility in water.<sup>1</sup>

The aim of this research was to obtain amphiphilic polysaccharide derivatives that can be used to prepare nanoscale carriers for lipophilic drugs applicable in theranostics. The idea of preparation focused on core-shell type nanocapsules.<sup>2,3</sup>

### EXPERIMENTAL METHODS

#### Fabrication of nanocapsules

Hydrophobic derivatizations of the ionic polysaccharide (hyaluronic acid, HA) were realised by attachment of alkyl (C12) or fluorinated (FC10) chains using appropriate primary amines through EDC/NHS coupling to the polymer carboxylic groups.<sup>4</sup> Then the adipic acid dihydrazide (AAD) serving as a linker was reacted with such hydrophobically modified polymer for subsequent attachment of biotin. Each polymer was purified by dialysis and freeze-dried.

Nanocapsules were obtained directly in ultrasound-assisted emulsification process. The solution of a given polysaccharide derivative was mixed with an oil phase. The mixture was firstly homogenized using vortex shaker and then sonicated in the ultrasonic bath.<sup>5</sup>

#### Instruments

Elemental analysis, ATR-FTIR and NMR spectroscopies were used to characterize the obtained polymer derivatives. The TNBS assay was used to detect and calculate the number of free amines and the degree of substitution by AAD. The HABA/AVIDIN assay was performed to determine the degree of substitution of biotin. Dynamic light scattering (DLS) measurements were performed to determine size distribution of the nanocapsules and their zeta potential. The emulsions stability was tested using an optical analyzer Turbiscan on the basis of turbidity measurements. Field emission scanning electron microscope was used for imaging of the capsules.

#### Cytotoxicity assay

The cytotoxicity of the obtained materials was evaluated *in vitro* by Neutral Red Uptake (NRU) assay. Cells were treated with different concentrations of derivatives of polysaccharide. Quantitative analysis of

cytotoxicity was determined by spectrophotometric measurements.

### RESULTS AND DISCUSSION

Degree of substitution of each HA derivative was not exceeding 8% to avoid the increase of toxicity and hydrophobicity.

All synthesized polysaccharide derivatives were able to stabilize oil droplets. The obtained milky emulsions were found to contain capsules of hydrodynamic diameters in 200–500 nm range. After few days of storage both at 25°C and 4°C no visual signs of any macroscopic oil droplets were seen that could have been the result of the disintegration of the capsules. The measured absolute values of zeta potential did not change during prolonged storage indicating their good stability over time. Efficiency of stabilization was additionally confirmed by turbidity measurements and optical observations. Samples were compared to the blanks for the emulsions of oil phase obtained at the same conditions but without any stabilizer. Milky-like emulsion tended to coalesce, regardless the storage conditions. Also, the initial zeta potential value of blanks after sonication was equal to  $-53.3 \pm 1.8$  mV, after several days it was changing gradually towards zero.

Cytotoxicity assays of polysaccharides showed no symptoms of toxicity and qualified nontoxic polysaccharides for further research.

### CONCLUSION

The presented results indicated that the obtained polysaccharide derivatives are functional and promising materials for fabrication of nanocarriers containing liquid oil cores. The capsules formed in a surfactant-free method were found to be effectively stabilized by hydrophobically modified hyaluronic acid. It was also shown that the capsules are stable for a long time. Moreover, the obtained carriers were found to be non-cytotoxic and their interactions with cells did not influence the proliferation.

### REFERENCES

- Loftsson, T., *et al.*, J. Pharm. Pharmacol., 62:1607-1621, 2010.
- Larsson M. *et al.*, Prog. Polym. Sci., 38:1307-1328, 2013.
- Lalush I. *et al.*, Biomacromolecules, 6:121-130, 2005.
- Toriyabe N. *et al.*, Biol. Pharm. Bull., 34:1084-1089, 2011.
- Szafranec, J., *et al.*, Nanoscale, 9:18867–18880, 2017.

### ACKNOWLEDGMENTS

M. J. gratefully acknowledges the financial support of the Polish Ministry of Science and Higher Education within the “Diamentowy Grant” Programme, grant agreement no. 0154/DIA/2016/45.

## Study on the Influence of pH upon the Doxorubicine Loading in Core/multilayer Shell Microcapsules of BSA Gel/polyelectrolyte Complexes pectin/chitosan/hyaluronic Acid

Violeta Pașcalău<sup>1</sup>, Codruta Pavel<sup>1</sup>, Alina Pinteă<sup>1</sup>, Cecilia Cristea<sup>2</sup>, Eموke Pall<sup>3</sup>, Nicodim Fit<sup>4</sup>, Horea Chicinas<sup>1</sup>, Traian Marinca<sup>1</sup> and Catalin Popa<sup>1</sup>

<sup>1</sup>Department of Materials science and engineering /Technical University of Cluj-Napoca, Romania

<sup>2</sup>Department of Analytical Chemistry/"Iuliu Hațieganu" University of Medicine and Pharmacy Cluj-Napoca, Romania

<sup>3</sup>Clinical Department/University of Agricultural Sciences and Veterinary Medicine of Cluj-Napoca, Romania

<sup>4</sup>Clinical and Paraclinical Department/University of Agricultural Sciences and Veterinary Medicine of Cluj-Napoca, Romania

[violeta.pascalau@stm.utcluj.ro](mailto:violeta.pascalau@stm.utcluj.ro)

### INTRODUCTION

Hyaluronic acid (HA) is a linear polysaccharide widely distributed throughout connective, epithelial and neural tissues. It is composed of two alternating units of D-glucuronic acid and N-acetyl-D-glucosamine. HA can be easily used as a self-assembly inducer because of its biocompatibility and biodegradability. In addition, it has a strong affinity to cell-specific surface markers overexpressed on the surface of many types of cancer cells, such as glycoprotein CD44 and receptor for HA-mediated motility<sup>1,2</sup>.

Doxorubicin (DOX) is among the most effective chemotherapeutics used in treating cancers<sup>3</sup>. However, its use can be severely limited by its renal, hepatic and, most important, cardiac toxicity<sup>4</sup>.

With regard to anticancer drug delivery, prolonged drug release is of major importance, thus HA-associated microparticles have been widely proposed as antitumor drug carriers<sup>5</sup>. HA-microparticles are not only able to tune the release of the active agent, but can also promote targeted delivery of the antitumor drug<sup>6</sup>.

Our approach is based on the microencapsulation technology for drug loading, administration, and release of Dox using BSA gel/pectin/chitosan/hyaluronic acid core-shell microcapsules.

### EXPERIMENTAL METHODS

In our work the encapsulation of Dox has been performed in the preformed microcapsules by a diffusion process from solution, in two different pH media, 4.5 and 6.8, respectively.

FTIR, X-ray diffraction, Thermal analysis, CLSM and SEM techniques were used for microcapsules analysis and emphasize the Dox encapsulation.

Evaluation of Encapsulation efficiency (%) and Loading efficiency (%) of the active agent was studied by UV-Vis spectrophotometry, using a quantitative method, based on calibration curve for the two types of loaded microcapsules, in order to establish the loading mechanism of Dox in microcapsules.

The Dox release profile from microcapsules was performed into an acidic medium, similar to that existing in the tumoral environment.

For the evaluation of the biocompatibility of Dox encapsulated microcapsules, we investigated the microcapsules effect on Hepatocellular Hep3B cells and on mesenchymal stem cells cultures with MTT and Alamar Blue viability assays.

### RESULTS AND DISCUSSION

Results regarding the Encapsulation efficiency (%) and the Loading efficiency (%) of the active agent in microcapsules in pH 4.5 and pH 6.8 solutions, provide information about the mechanism of the encapsulation process.

The *in vitro* release profile of Dox from microcapsules in an acidic medium leads the way for further tests of sustained Dox delivery in anticancer therapy.

The results of the biocompatibility evaluation of Dox encapsulated microcapsules on Hepatocellular carcinoma Hep3B cells and mesenchymal stem cells cultures, respectively are recommending the system for the targeted delivery of Dox.

### CONCLUSION

The results of synthesis and characterization of Dox microencapsulated carriers containing hyaluronic acid in the polyelectrolyte complex formed with chitosan in the shell's outer layer represent a good premise for targeted delivery of anticancer drug.

### REFERENCES

1. Dosio F. *et al.*, Adv. Drug Deliver. Rev. 97:204–236, 2016.
2. Laurent T.C., Fraser J.R.E., FASEB J. 6:2397–2404, 1992.
3. Gurav D.D. *et al.*, Colloid Surface B 143:352–358, 2016.
4. Takemura G. *et al.*, Prog. Cardiovasc. Dis. 49:330–352, 2007.
5. Zhang P., *et al.*, Colloid Surface B 142: 223–229, 2016.
6. Karbownik M.S., Nowak J.Z., Pharmacol. Rep. 65:1056–1074, 2013.

### ACKNOWLEDGMENTS

This work was supported by a grant of the Romanian Minister of Research and Innovation, CCCDI – UEFISCDI, project number PN-III-P1-1.2-PCCDI-2017-0221/59PCCDI/2018 (IMPROVE), within PNCDI III.

## Nanocapsules Based on Chitosan Carboxylate and Poly(N-Vinylpyrrolidone-*alt*-Itaconic Anhydride) - A Promising Alternative for the Basal Cell Carcinoma Treatment

Delia Mihaela Rata<sup>1</sup>, Anca Niculina Cadinoiu<sup>1</sup>, Leonard Ionut Atanase<sup>1</sup>, Luiza Madalina Gradinaru<sup>3</sup>, Marcel Popa<sup>1,2</sup>

<sup>1</sup>Department of Biomaterials, "Apollonia" University of Iași, România

<sup>2</sup>Academy of Romanian Scientists, Romania

<sup>3</sup>"Petru Poni" Institute of Macromolecular Chemistry, Romania

[iureadeliamihaela@yahoo.com](mailto:iureadeliamihaela@yahoo.com)

### INTRODUCTION

Basal cell carcinoma (BCCs) are the most prevalent form of skin cancer, accounting for 70% - 80% of all diagnosis, can grow rapidly, causes destruction or damage in a large region (mainly nose and ear) of tissue, and rarely causes metastasis to the lymph nodes, lung, bone, and liver<sup>1</sup>. Conventional chemotherapy applied to these conditions shows non-specific targeting, and high doses of anticancer drugs affect both normal and tumour cells and leads to the fast development of cellular resistance causing toxic effects on the entire body. New therapeutic strategies based on nanoparticulates systems could be a promising solution to address these problems because can be designed to achieve prolonged circulation times, greater stability, and decreased toxicity to normal tissues<sup>2</sup>. This study reports the preparation of new nanocapsules based on a natural polymer, chitosan carboxylate and a synthetic one, poly (N-vinylpyrrolidone-*alt*-itaconic anhydride) [(poly(NVPAl)] using an interfacial condensation technique. The important advantage of this preparation method is given by the fact that the interfacial condensation does not require any kind of cross linking agents that are usually toxic and difficult to remove from the synthesized products.

### EXPERIMENTAL METHODS

Acetone, dimethylsulfoxide (DMSO), 5-Fluorouracil (5-FU), hexane and surfactants (Tween 80, Span 80) were purchased from Sigma-Aldrich. Chitosan carboxylate (CC) with different degree of carboxylation (between 5-80%) and poly (NVPAl) have been synthesized and characterized in our laboratory. Nanocapsules based on CC and poly (NVPAl) were prepared by the interfacial condensation reaction. In a beaker were placed 10 ml of DMSO, 500 mg copolymer has been added under magnetic stirring. After complete dissolution of the copolymer, 15 ml acetone was added under continuous stirring. Separately, they were introduced in another flask 50 ml of water solution, in which a specific amount of CC, but with different degree of carboxylation were dissolved at 40°C. In both organic and water phase were added surfactants in order to assure the round shape of the capsules. The copolymer solution has been added drop-wise into the aqueous solution of CC, under continuous magnetic stirring. The obtained nanocapsules were washed with water and acetone and finally dried. An important parameter considered in this study was the influence of the number of carboxyl groups on CC chain on the physico-chemical, morphological and biological characteristics of the nanoparticles. Nanocapsules structural characteristics were evaluated with a Digilab Scimitar

FTS 2000 FTIR spectrometer. Nanocapsules diameter and surface morphology has been evaluated by DLS and by Scanning Electron Microscope (SEM). The swelling degree in solutions that mimicking biological fluids (PBS, pH 7.4), has been determined by gravimetric method. Finally, has been studied the encapsulation capacity of 5-FU into nanocapsules and their *in vitro* skin permeation.

### RESULTS AND DISCUSSION

FTIR spectroscopy confirmed the reaction between the anhydride groups of poly (NVPAl) and the amino functional groups of the CC with the formation of amide groups. The mean diameter of the obtained nanocapsules ranged from 150 to 250 nm. The nanocapsules have a spherical shape and present relatively low dimensional polydispersity. (Fig. 1)

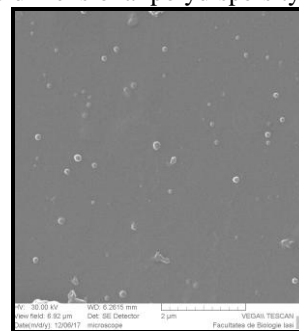


Fig. 1. Scanning electron microscopy (SEM)

The swelling degree of the nanocapsules in alkaline medium (pH 7.4) varied between 1500-2900% and depended on the degree of carboxylation. The encapsulation efficiency of 5-FU in the capsules was between 43% and 59%, and the amount of drug released from nanocapsules varied between 0.3-0.45 g 5-FU/1g nanocapsules.

### CONCLUSION

The preliminary findings in this research are encouraging and have potential application in treatment of BCCs.

### REFERENCES

1. Severino P. *et al.*, Clin. Transl. Oncol., 15:417–424, 2013.
2. Barreto J.A. *et al.*, Adv. Mater., 23: H18-H40, 2011.

### ACKNOWLEDGMENTS

„This work was supported by a grant of Ministry of Research and Innovation, CNCS - UEFISCDI, project number PN-III-P4-ID-PCE-2016-0613, within PNCDI III”.



## Aptamer-Functionalized Liposomes - A New Attempt to Treat Basal Cell Carcinoma

Anca-Niculina Cadinoiu<sup>1</sup>, Delia-Mihaela Rață<sup>1</sup>, Leonard-Ionuț Atanase<sup>1</sup>, Marcel Popa<sup>1,2</sup>

<sup>1</sup>Department of Biomaterials, “Apollonia” University of Iași, România

<sup>2</sup>The Academy of Romanian Scientists, România

[jancaniculina@yahoo.com](mailto:jancaniculina@yahoo.com)

### INTRODUCTION

More than one out of every three new cancers is a skin cancer, and the large majority are basal cell carcinomas (BCC). This cancer is usually caused by a combination of cumulative and intense, occasional sun exposure<sup>1,2</sup>. Even if for the treatment of skin cancers many drug-loaded systems have been studied in the literature, at the best of our knowledge, no studies have been performed concerning the use of functionalized liposomes with specific ligands easily recognizable by the receptors of the tumoral cells, for the targeted therapy of BCC. This therapy is a treatment that targets the cancer's specific genes, proteins, or the tissue environment that contributes to cancer growth and survival and blocks the growth and the spread of cancer cells while limiting damage to healthy cells. Therefore, the objective of the present study was to obtain a new formulation based on aptamer-functionalised liposomes for topical delivery of 5-fluorouracil (5-FU), as an anticancer drug widely used in the treatment of BCC.

### EXPERIMENTAL METHODS

The liposomes were prepared by film hydration method. Briefly, PC, CHOL and DSPE-PEG-MAL, in different molar ratio, were dissolved in chloroform in a round-bottomed flask. After dissolution, the solvent was evaporated under reduced pressure at room temperature in a rotary evaporator, leading to the formation of a thin and homogeneous film of lipids on the surface of the flask. The film obtained was then hydrated using 5 mL of 5-FU aqueous solution in phosphate buffered saline (pH = 7.4) at room temperature. The size of liposomes was reduced by multiple extrusion steps through polycarbonate membranes with a final pore size of 200 nm. Unencapsulated 5-FU was removed by centrifugation using a membrane ultrafiltration filter. To obtain the liposomes functionalized with AS1411, thiol-terminated. AS1411 was conjugated to liposomes via the formation of a thioether linkage. The conjugation efficiency between AS1411 and liposomes was determined spectrophotometrically by measuring the concentration of the collected unconjugated aptamer after the ultrafiltration of the products.

Size and polydispersity index (PDI) of the obtained liposomes were determined by dynamic light scattering (DLS). The zeta potential was measured by laser doppler micro-electrophoresis at 25°C after dilution in the hydration medium to an appropriate counting rate. The 5-FU encapsulation efficiency was spectrophotometrically (NanoDrop One Spectrophotometer from Thermo Scientific) studied after the destruction of liposomes in the presence of Triton X-100. The release of 5-FU was evaluated *in vitro* using static Franz diffusion cells with artificial membranes.

### RESULTS AND DISCUSSION

The new aptamer-functionalised liposomes were designed to improve therapeutic effects of 5-FU administration by eliminating a series of secondary, undesired effects, determined by the classical administration, and to improve health condition of people with BCC.

AS1411 conjugation increased liposome size, suggesting that the presence of an additional hydrophilic molecule on the liposomal surface increased the hydrodynamic radius. As expected, the negatively charged DNA aptamer reduced the surface potential of the liposomes.

The drug encapsulation efficiency was directly proportional to the initial drug concentration in the hydration solution and was between 0.05 and 4.5%.

Vertical Franz diffusion cells with artificial membranes were used to evaluate of *in vitro* release of 5-FU. The membrane separates the donor compartment, containing the drug-loaded liposomes from the receptor compartment filled with the collection medium (PBS, pH 7.4, 32 ± 1°C). The receptor fluid was thoroughly stirred during the entire experiment. After elapsed times 0.2 mL of the receiving solution was withdrawn and replaced with an equal volume of pre-thermostated fresh medium. Sink conditions were maintained throughout the experiment. The concentrations of drug in the receiver medium were determined by UV-Vis spectroscopy. The cumulative amount released per unit area was calculated from the concentration of drug in the receiving medium and plotted as a function of time. After 24 hours only a small amount of drug, between 8 and 12%, was released.

### CONCLUSION

The results obtained were satisfactory and will be the basis for new tests to prove the effectiveness of these formulations in the treatment of BCC.

### REFERENCES

1. Ersu B., in Basal Cell Carcinoma, V. Madan (ed), InTech, 2012
2. Rubin A.I. *et al.*, N. Engl. J. Med. 353:2262-9, 2005

### ACKNOWLEDGMENTS

„This work was supported by a grant of Ministry of Research and Innovation, CNCS - UEFISCDI, project number PN-III-P4-ID-PCE-2016-0613, within PNCDI III”.

## Chitosan-g-Poly(Glycidyl Methacrylate) Microparticles as Sustained Drug Delivery System for Oral Administration

Silvia Vasiliu<sup>1</sup>, Stefania Racovita<sup>1</sup>, Ionela Gugoasa<sup>2</sup>, Marcel Popa<sup>2,3,4</sup>, Anca Cadinoiu<sup>4</sup>

<sup>1</sup>Functional Polymers Department, “Petru Poni” Institute of Macromolecular Chemistry, Iași, România

<sup>2</sup>Faculty of Chemical Engineering and Environmental Protection, “Gheorghe Asachi” Technical University, Iași, România

<sup>3</sup>Academy of Romanian Scientists, Bucuresti, România

<sup>4</sup>Department of Biomaterials, “Apollonia” University of Iași, România  
[jancaniculina@yahoo.com](mailto:jancaniculina@yahoo.com)

### INTRODUCTION

For pharmaceutical and medical purposes the grafted chitosan (CH) copolymers can be obtained by several methods<sup>1,2</sup>. Chitosan-g-poly(acrylic acid) particles and microparticles of polyacrylamide-g-chitosan crosslinked with glutaraldehyde were prepared to encapsulate indomethacin, hydrophilic drugs or sensitive proteins and nifedipine<sup>3,4</sup>. Also, the graft chitosan copolymers have potential to be used in dialysis<sup>5</sup> and present interesting properties for wound healing and cardiovascular applications<sup>6</sup>. The aim of this work consists in the synthesis of the new porous polymer carriers based on chitosan-g-poly(glycidyl methacrylate) in order to obtain the drug delivery systems for potential applications in the treatment of infectious diseases.

### EXPERIMENTAL METHODS

The microparticles based on glycidyl methacrylate (GMA) and mono, di and triethylene glycol dimethacrylate (EGDMA, DEGDMA and TEGDMA) labeled G microparticles were prepared by aqueous suspension polymerization method<sup>7-9</sup>.

The microparticles based on GMA-EGDMA-CH, GMA-DEGDMA-CH and GMA-TEGDMA-CH, labeled C microparticles were obtained through the same procedure with few modifications: (1) the aqueous phase was formed by a solution of PVA and chitosan (1.5 wt %); (2) in the aqueous phase a second free radical initiator ammonium persulfate (APS) is used to create radicals on polysaccharide chains. The CH/monomers ratio was 1:23 (w/w). For all experiments the organic / aqueous phase ratio was 1:9. The copolymerization reactions were conducted under N<sub>2</sub> atmosphere for 8h at 78°C and 1h at 90°C with a stirring rate of 360 r.p.m. The G and C microparticles were washed with hot water and then were extracted with methanol. Finally, the microparticles were dried under vacuum at 50°C for 48 h and sieved.

### RESULTS AND DISCUSSION

G and C microparticles were synthesized by suspension polymerization technique. Scanning electron microscopy (SEM) shows that both G and C microparticles have a spherical shape and porous structures. The addition of the polysaccharide in the reaction medium leads to the modification of microparticles morphology. The average diameters of C microparticles are smaller than that of G microparticles leading to the idea that chitosan has two roles: (a) as reactant alongside GMA and dimethacrylic monomers and (b) as suspension stabilizer in combination with PVA. Also the dimension of the pores on the surface of

microparticles was smaller than in the case of G microparticles. The increase of the chain length of dimethacrylic ester leads to the synthesis of microparticles characterized by an increase in surface roughness. These morphological differences between G and C microparticles were also observed with Atomic Force Microscopy technique (AFM). The chloramphenicol hemisuccinate sodium salt (CPh) loaded microparticles were prepared during the preparation of microparticles by the suspension polymerization techniques with specification that CPh was dissolved in aqueous phase solution. The quantity of drug loaded was calculated from the total amount of chlorine presented in CPh microparticles determined by elemental analysis. The CPh presence in microparticles structure was confirmed by elemental analysis, FT-IR spectroscopy, SEM and AFM analysis. The presence of CPh does not alter the porous structure and shape of microparticles. To elucidate the drug transport mechanism involved in the release process of CPh from microparticles, various models were applied: Higuchi, Korsmeyer-Peppas and Baker-Lonsdale models. The most appropriate model was selected based on the highest value of the correlation coefficient (R<sup>2</sup>).

### CONCLUSION

Porous microparticles of chitosan-g-poly(glycidyl methacrylate) were obtained by grafting chitosan onto crosslinked networks based on GMA and dimethacrylic monomers using a simple and efficient method namely suspension polymerization technique. The study of the drug release versus time indicates that chitosan incorporation in the structure of GMA microparticles leads to the preparation of the sustained drug release system that can be used for oral administration of antibiotics in the treatment of infectious diseases.

### REFERENCES

1. Romskevic T. *et al.*, Chemija 8:33-38, 2007
2. Sun T. *Et al*, Eur. Polym. J. 39 :189-192, 20032
3. Kumbar S. G. *et al.*, J. Appl. Polym. Sci. 87 :1525-1536, 2003
4. Jayakumar R. *et al.*, Carbohydr. Polym. 62 :142-158, 2005
5. Li Y. *Et al*, Polym. Int. 52:285-290, 2003
6. Chung T. W. *Et al*, Biomaterials 23:4803-4809, 2002
7. Lungan M. A. *et al.*, Carbohydr. Polym. 104:213-222, 2014
8. Lungan M. A. *Et al.*, Carbohydr. Polym. 125 :323-333, 2015
9. Cigu T. A. *et al.*, Eur. Polym. J. 82 :132-152, 2016

## Poly(ethylene glycol) methyl ether acrylate Grafted Chitosan Micro and Nanoparticles with Potential Applications in Ophthalmology

Corina-Lenuta Savin<sup>1,2</sup>, Delia Mihaela Rata<sup>3</sup>, Marcel Popa<sup>1,3,4</sup>, Christelle Delaite<sup>2</sup>, Gerard Riess<sup>2</sup>, Catalina Anisoara Peptu<sup>1</sup>

<sup>1</sup>Department of Natural and Synthetic Polymers, Faculty of Chemical Engineering and Environmental Protection, "Gheorghe Asachi" Technical University of Iași, România

<sup>2</sup>Laboratoire de Pétrochimie et d'Ingénierie Macromoléculaires Institut J.B. Donnet, Université de Haute Alsace, Mulhouse France

<sup>3</sup>Department of Biomaterials, "Apollonia" University of Iași, România

<sup>4</sup>Academy of Romanian Scientists, Bucuresti, Romania

[iureadeliamihaela@yahoo.com](mailto:iureadeliamihaela@yahoo.com)

### INTRODUCTION

The present work proposes a method for obtaining micro/nanoparticles with potential applications in ocular drug delivery. Although chitosan as it is, is one of the most used natural polymers for drug delivery due to its valuable properties (biodegradability, biocompatibility, muco-adhesiveness, etc.) we consider appropriate to functionalize it with poly(ethylene glycol) acrylate methyl ether for obtaining chitosan with improved solubility. Synthetic poly(ethylene glycol) acrylate methyl ether (PEG-A) have been grafted on chitosan via Michael addition<sup>1,2,3</sup>. The final aim is to prepare nanoparticles with potential applications in ophthalmology.

### EXPERIMENTAL METHODS

Chitosan derivatives and their modification degree have been analysed by NMR and FTIR. The nanoparticles have been prepared by double crosslinking in reverse emulsion<sup>4,5</sup> using sodium tripolyphosphate or sodium sulphate (ionic crosslinking) and glutaraldehyde (covalent crosslinking), the process being optimized through the modification of certain reaction parameters (polymer ratio, stirring rate, crosslinker amount, etc.). The particles with optimal characteristics (in terms of morphology, water swelling degree) have been analysed from the point of view of the capacity of inclusion/release of specific drugs (levofloxacin).

### RESULTS AND DISCUSSION

This study highlights the way of obtaining micro/nanoparticles based on natural chitosan chemically grafted with synthetic poly(ethylene glycol) methyl ether acrylate through Michael addition<sup>1,2,3</sup>. Chitosan has been successfully functionalized (grafted) with PEG-A, the analyses showing a grafting degree of 16 %. Micro and nanoparticles present a spherical shape and a relative high dimensional polydispersity (Fig. 1 and Fig. 2).

The nanoparticles showed a relative high swelling degree (700÷1000%) which explained the high drug loading efficiency. The *in vitro* release results are encouraging, showing that the amount of levofloxacin released in 24 hours is closed to the maximum dose usually administered in patients with ocular infections.

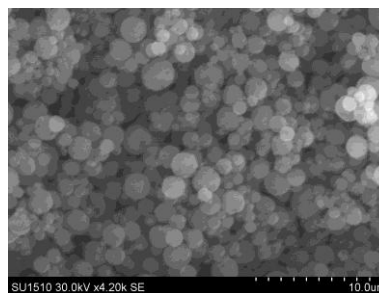


Fig. 1. Poly(ethylene glycol) methyl ether acrylate grafted chitosan micro/nanoparticles crosslinked with sodium tripolyphosphate (SEM image)

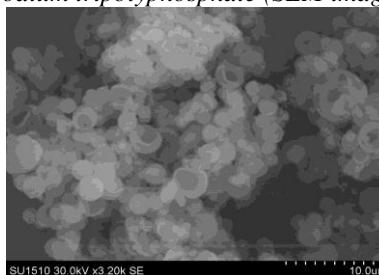


Fig. 2. Poly(ethylene glycol) methyl ether acrylate grafted chitosan micro/nanoparticles crosslinked with sodium sulphate (SEM image)

### CONCLUSION

Chitosan has been successfully grafted with PEG derivative and the micro/nanoparticles can be a reliable solution for the treatment of ocular infections. Further investigations including *in vivo* tests for testing their ability to release other ophthalmic drugs and intraocular bio distribution of micro/nanoparticles are envisaged.

### REFERENCES

1. Guiping Ma *et al.*, Int. J. Bio. Macro.molec, 45:499–503, 2009.
2. Jing H. *et al.*, Carbohydr. Polym. 83 :270-276, 2011
3. Hitoshi S. *et al.*, Biomacromolecules, 4 :1250-1254, 2003
4. Andrei G. *et al.*, Int. J. Pharm. 493 (2015).
5. Sofia A. Papadimitriou *et al.*, Int. J. Pharm. 430 :318– 327, 2012

### ACKNOWLEDGMENTS

This work was supported by a grant of the Romanian National Authority for Scientific Research and Innovation, CNCS/CCCDI – UEFISCDI, project number PN-III-P2-2.1-BG-2016-0175, within PNCDI III (project number 20/2016).

## Microcapsules Consisting of a BSA Gel Core and a Multilayer Shell of Polysaccharides Polyelectrolite Complexes with the Outer Layer Containing Hyaluronic Acid

Codruta Pavel, Violeta Pascalau, Alina Pinte, Horea Chicinas, Florin Popa and Catalin Popa

Department of Materials Science and Engineering /Technical University of Cluj-Napoca, Romania

[codruta.pavel@stm.utcluj.ro](mailto:codruta.pavel@stm.utcluj.ro)

### INTRODUCTION

Development of targeted and controlled drug delivery system is increasingly explored in anticancer therapy, in order to maintain a therapeutic optimal drug concentration, as higher concentration cause toxic side effects, while lower ones are ineffective<sup>1</sup>.

Microencapsulation is an innovative technology that can be used for drug loading, administration, and release<sup>2</sup>. Both natural and synthetic polymers can be assembled in microcapsules for controlled drug delivery, but those made of natural polymers show the advantage of biocompatibility and biodegradability<sup>3</sup>.

One of the chemical strategies in designing drug carriers for delivery anticancer agents uses Hyaluronic acid, which is biocompatible, biodegradable, nontoxic, non-immunogenic and interacts by the ligand-receptor mechanism with receptors overexpressed on many tumours cells<sup>4,5</sup>.

We propose the development, based on previous studies<sup>6</sup>, of novel core-shell microcapsules of BSA gel with polyelectrolite complex multilayer shell of natural polysaccharides with opposite charges, pectin, hyaluronic acid and chitosan respectively, as carriers for an antitumor active agent, to be used in cancer therapy.

### EXPERIMENTAL METHODS

A sacrificial CaCO<sub>3</sub> template method was used in order to obtain microcapsules with a BSA gel core and a layer-by-layer deposition technique of polyelectrolite complexes formed between pectin/chitosan in the inner layers and hyaluronic acid/chitosan in the outer layers of the shell.

The following techniques: FTIR, X-ray diffraction, Thermal analysis, Confocal laser scanning microscopy and Scanning electron microscopy were used for the physical - chemical characterization of microcapsules.

In the first step, the protein component is co-precipitated in sacrificial porous microtemplates. In the second step, these microtemplates are coated using electrostatic interactions or hydrogen bonding as the driving force for multilayer build-up. Third, the sacrificial dissolved microtemplates are removed through the semipermeable polyelectrolyte shell, the protein remaining in the core of the capsules.

### RESULTS AND DISCUSSION

Spherical micron - size microcapsules were obtained, confirmed by the physical - chemical analyses.

The electrostatic interaction between the opposite charges of pectin, hyaluronic acid and chitosan are the driving force for the synthesis of all types of hydrogels, calcium cross-linked pectin and pectin/chitosan, chitosan/hyaluronic acid, respectively polyelectrolite complex forming the multilayered shell onto the CaCO<sub>3</sub>/BSA microtemplate, finally resulting in the BSA gel microcapsules suitable for drug encapsulation. All the components are natural and may take advantage of the already proved biocompatibility and non-toxicity.

### CONCLUSION

Spherical micron – size microcapsules were obtained, with structures that were confirmed by physical-chemical analyses. Hyaluronic acid was introduced into the outer layer of the shell in order to use the synthesized microcapsules as carriers in targeted anticancer therapy.

### REFERENCES

1. Gurav D.D. *et al.*, Colloid Surface B 143:352–358, 2016.
2. Haroun A.A. and El-Halawany N.R. IRBM 31:234–241, 2010.
3. Cassano R. *et al.*, React Funct Polym 72:446–450, 2012.
4. Fumagalli G. *et al.*, Drug Discov Today 21(8):1321-1329, 2016.
5. Wang X. *et al.*, J Control Release 193:139–153, 2014.
6. Paşcalău V. *et al.*, J Biomater appl 30(6):857-872, 2016.

### ACKNOWLEDGMENTS

This work was supported by a grant of the Romanian Minister of Research and Innovation, CCCDI – UEFISCDI, project number PN-III-P1-1.2-PCCDI-2017-0221/59PCCDI/2018 (IMPROVE), within PNCDI III.



## Control of Paclitaxel Release from 3D Matrices Produced by Electrospinning

Konstantin Kuznetsov<sup>1</sup>, Alena Stepanova<sup>1,2</sup>, Olga Novikova<sup>1</sup>, Ren Kvon<sup>3</sup>, Irina Romanova<sup>2</sup>, Andrey Karpenko<sup>1</sup>, Evgeny Pokushalov<sup>1</sup>, Alexander Karaskov<sup>1</sup>, Pavel Laktionov<sup>1,2</sup>

<sup>1</sup>“E. Meshalkin National medical research center” of the Ministry of Health of the Russian Federation, Russia

<sup>2</sup>Institute of Chemical Biology and Fundamental Medicine, Novosibirsk, Russia

<sup>3</sup>Boreskov Institute of Catalysis SB RAS, Novosibirsk, Russia

[lakt@niboch.nsc.ru](mailto:lakt@niboch.nsc.ru)

### INTRODUCTION

Neointima growth in the places of vascular stent installation, treatment of abdominal and pelvis adhesive disease, as well as a number of other clinical states require methods to prevent local cell proliferation. Thus, approaches for long-term delivery of anti-proliferative drugs into the surroundings of implantable medical devices in dosages inhibiting cell growth are still demanded. Use of materials releasing cell-growth inhibitors can provide a solution. Here we describe the release of paclitaxel (PTX) from polycaprolactone-based 3D matrices in depend on the composition of electrospinning solution, surrounding medium and present the data of PTX cytotoxicity against artery wall myocytes.

### EXPERIMENTAL METHODS

Human myocytes (HM) were isolated from the media of internal carotid artery segments, obtained after excision of pathological tortuosity. HM were cultivated in IMDM culture medium with 10% FBS, at 37°C, 6% CO<sub>2</sub> and characterized using anti-desmin, myosin and  $\alpha$ -SMA antibodies. PTX toxicity was studied in vitro using MTT Cell Proliferation Assay Kit. Tritium-labelled PTX was prepared by tritium exchange as previously described<sup>1</sup>. Matrices were produced from the solution of polycaprolactone (PCL) with human serum albumin (HSA) in hexafluoro-2-propanol with unlabelled and H<sup>3</sup>-labelled PTX using custom designed electrospinning system supplied with 30 kV high voltage power supply from Spellman Co. The radioactivity of H<sup>3</sup>-PTX released into PBS or human serum was measured using Liquid Scintillation Analyzer. Chemical composition of the surface layer was studied using XPS.

### RESULTS AND DISCUSSION

It was shown that cells isolated from artery express myosin and  $\alpha$ -SMA antigens and thus could be classified as HM. MTT assay demonstrated 50% growth inhibition of HM by PTX concentrations of at least 400 ng/ml, whereas at least 100 $\times$  lower concentration of PTX was required for comparable inhibition of HeLa growth. This indicates the low boundary for PTX concentration necessary to prevent HM growth *in vivo*. H<sup>3</sup>-labelled PTX with radioactivity 1,5 mCi/ml in methanol (approx 5  $\mu$ g/ml), free from any contaminants was used in the study. Matrices from PCL with HSA (10:1, w:w) and PTX with radioactivity of 25.000 cpm/cm<sup>2</sup> were produced by electrospinning as described<sup>2</sup>. The speed of PTX release from fibers into the serum was higher than for PBS, and was dependent on the PTX concentration in the outside medium.

The main portion of PTX was released during the first few days (Fig. 1).

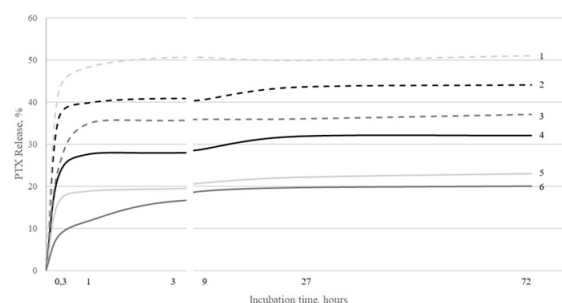


Fig. 1. Time-dependence of PTX release from different 3D matrices, %. **1** – PCL+10% HSA+3% DMSO in serum; **2** - PCL+10% HSA in serum; **3** - PCL+10% HSA+6% DMSO in serum; **4** - PCL+10% HSA in PBS; **5** - PCL+10% HSA+3% DMSO in PBS; **6** - PCL+10% HSA+6% DMSO in PBS.

XPS demonstrated that PTX is over-represented in the surface layer of fibers in comparison to its central volume by a factor of almost 1.000 $\times$ . Introduction of 3-6% DMSO into the polymer solution for electrospinning decreased the speed of PTX release and the overall released amount, as well as increased the exposure of HSA in the surface layer of the fibers. PTX release was shown to depend from the redistribution of PTX between fiber surface-bound and free HSA.

### CONCLUSION

Introduction of HSA, which interacts with PTX<sup>3</sup>, and DMSO, which is a good PTX solvent in basic solution for electrospinning, resulted in two-phase PTX release kinetics necessary for long term cytostatic effect of 3D matrices on surrounding cells. Markedly, cytostatic concentration of PTX for human myocytes was higher than for tumour cells, demanding that to achieve toxicity the concentration of PTX should exceed 0,2  $\mu$ g/mg of 3D matrix.

### REFERENCES

1. Sidorov V.N. *et al.*, Patent SU 1823961 A3.
2. Chernonosova V.S. *et al.*, Polym. Adv. Technol. 28: 819-827, 2017.
3. Purcell M. *et al.*, Biochim Biophys Acta. 1478: 61-68, 2000.

### ACKNOWLEDGMENTS

The study was supported by a grant from the Russian Science Foundation №17-75-30009.

## Preparation and Characterization of Liposomal Curcumin

Katsiaryna Dubatouka, Vladimir Agabekov

Institute of Chemistry of New materials NASB, Belarus

[d\\_katerina@tut.by](mailto:d_katerina@tut.by)

### INTRODUCTION

Curcumin is a polyphenolic compound which is widely used to treat many types of diseases, including cancers<sup>1</sup>. It has poor solubility in water solutions, low bioavailability and high systemic elimination. Liposomes (closed spherical particles, built of lipid bilayers) can be used in order to solve these problems due to its safety, ability to solubilize hydrophobic compounds, and preserve them from elimination and destruction in blood<sup>2,3</sup>.

The purpose of this study was to obtain liposomal curcumin using combination of the thin film hydration and sonication methods, characterize liposomes in size, zeta potential, incorporation efficiency and release profile of curcumin in water in order to choose the best formulation for further using in biomedicine.

### EXPERIMENTAL METHODS

Liposomes (LipCur) were prepared by the thin film hydration method from the mixture of egg phosphatidylcholine (Sigma), cholesterol (Acros Organics) and curcumin (Fluka) in chloroform. The solvent was removed under vacuum on a rotary evaporator (IR-1M2, Russia), distilled water was added, then the mixture was stirred for 30 minutes and sonicated (35 kHz, Bandelin Electronic, Germany) for 30 minutes. Free curcumin was separated from liposomal curcumin by centrifugation (HERMLE Z36HK, Germany) at 18000 rpm for 45 min at 4°C (3 times). Obtained liposomes were lyophilized. The mean diameter size and zeta-potential were measured using dynamic light scattering in a photon correlation spectrometer (Zetasizer NanoZS, Malvern, UK). The concentration of curcumin in liposomes was determined photometrically at 430 nm (Solar CM 2203, Belarus). The incorporation efficiency (IE) was calculated from the following equation:  $IE (\%) = (\text{concentration of curcumin in liposomes} / \text{total concentration of curcumin}) \times 100\%$ . The stability studies were performed at 4°C and 37°C during 7 days. In vitro release of curcumin from liposomes was determined in water.

### RESULTS AND DISCUSSION

The mean diameter, zeta potential and incorporation efficiency for formulations with ratio liposomes:curcumin from 1:0.01 to 1:0.05 (wt.) are shown in Table 1. Zeta potential characterizes stability of the formulations and its surface charge. Combination of the thin film hydration and sonication methods allows getting stable and small unilamellar liposomes. Size and of zeta potential of LipCur was in range from 35 to 52 nm and from -36.4 to -22.9 mV.

The stability studies performed at 4°C and 37°C during 7 days were shown no significant difference in size and zeta potential for LipCur formulations. Incorporation efficiency was increased from 1.29 for LipCur(1:0.01) to 24.12 % for LipCur(1:0.05) and optimal ratio for liposomal curcumin was 1:0.04 (IE 23.49 %).

Table 1. Characteristics of the liposomal curcumin

Formulations (liposomes: curcumin, wt)	Diameter, nm	Zeta potential, mV	Incorporation efficiency (IE), %
1:0.01	52±6	-22.9±0.8	1.29±0.09
1:0.02	36±4	-36.4±0.7	5.96±0.31
1:0.03	43±5	-26.8±0.5	18.46±0.77
1:0.04	39±4	-23.3±0.7	23.49±0.84
1:0.05	35±4	-30.1±0.6	24.12±0.83

Fig. 1 shows the release of curcumin from liposomes in water at 37°C for two formulations. After 8 hours incubation 3.3 and 18.9 % of curcumin was released from LipCur(1:0.04) and LipCur(1:0.03) respectively and increased up to 72.6 and 78.9 % for 7 days.

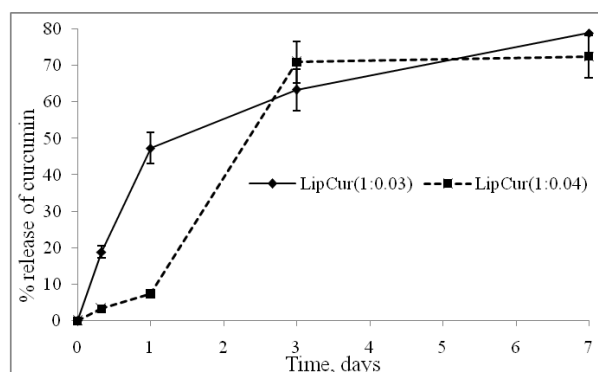


Fig. 1. Release of curcumin from liposomes in water at 37°C for LipCur(1:0.03) and LipCur(1:0.04).

Low rate of curcumin release from liposomes shows stability of LipCur formulations and low degradation of lipid bilayer under those conditions and can be used in biomedicine.

### CONCLUSION

It was obtained and characterized stable negatively charged liposomal curcumin with size ~40 nm and incorporation efficiency ~24 % with low release rate during 7 days up to ~73 %.

### REFERENCES

- Feng T. *et al.*, Int. J. of Nanomedicine. 12:6027-6044, 2017
- Pandelidou M. *et al.*, J. Nanosci.Nanotechnol. 11: 1259-1266, 2011
- Mahmud M. *et al.*, PLoS ONE 11 (12): e0167787

## Polysaccharides-based Capsules Loaded with Magnetic Nanoparticles

Elżbieta Gumieniczek-Chłopek<sup>1,2</sup>, Joanna Odrobińska<sup>2</sup>, Czesław Kapusta<sup>1</sup>, Szczepan Zapotoczny<sup>2</sup>

<sup>1</sup>Faculty of Physics and Applied Computer Science, AGH University of Science and Technology, Poland

<sup>2</sup>Faculty of Chemistry, Jagiellonian University, Poland

[elzbieta.gumieniczek@student.uj.edu.pl](mailto:elzbieta.gumieniczek@student.uj.edu.pl)

### INTRODUCTION

Nanomedicine using materials, procedures and tools of nanotechnology may lead to novel approaches in solving biomedical problems. Important and dynamically developing field concerns fabrication of nanosystems for controlled delivery of active substances. Additional encapsulation of superparamagnetic nanoparticles within such nanocarrier structure broadens their applicability in e.g.: magnetic resonance imaging, magnetic drug delivery, iron deficiency therapy and hyperthermia treatment<sup>1</sup>. Core-shell capsules were shown to be formed using hydrophobically modified biopolymers that can anchor into the oil cores stabilizing the capsules without necessity of using low molecular weight surfactants that are commonly undesirable in biomedical applications.<sup>2</sup> Encapsulation of superparamagnetic iron oxide nanoparticles (SPION) inside the oil core of such capsule provide magnetic properties of the whole carrier.

### EXPERIMENTAL METHODS

SPION were synthesised by the thermal decomposition of iron (III) oleate. The metal-oleate complex was prepared by reacting anhydrous iron chloride (III) and sodium oleate in solution of deionized water, n-hexane and ethanol. The resulting solution was heated to 60°C and kept at that temperature for 5 hours. The resulting dark hydrophobic phase was separated in separatory funnel, washed with deionized water and heated to 40°C to evaporate hexane. Iron (III) oleate was then dissolved in solution of octadecene and oleic acid. The reaction was carried out in anaerobic atmosphere with incessant stirring and increasing temperature. When the mixture reached 318°C it was kept at this temperature for 45 minutes. The resulting solution was cooled to room temperature, washed with ethanol and separated from unreacted residues by sonication in hexane and centrifugation.<sup>3</sup> The obtained iron oxide nanoparticles were investigated by light scattering and zeta potential measurements, Mössbauer spectroscopy, magnetometry, X-ray diffraction, infrared spectroscopy and Scanning Tunnelling Electron Microscope (STEM).

Amphiphilic chitosan derivative (CChit-C12) containing quaternary ammonium and N-dodecyl groups was synthesized in two stage according to the modified procedure described previously<sup>4</sup>, using the 50% excess of glycidyltrimethylammonium chloride. Quality and substitution degree of obtained product was investigated by Nuclear Magnetic Resonance (NMR), elemental analysis and conductometric titration. Preparation of the capsules was based on self-assembly of chitosan derivate on the dispersed oil cores containing SPION. The capsules were obtained in emulsification process (supported by vortex shaker and

30 minutes of ultrasonication) of CChit-C12 (1 g/L in 0.15M NaCl) and oleic acid with SPION dispersed mixture<sup>2</sup>. Physicochemical properties and stability of the capsules were examined by light scattering and zeta potential measurements and Scanning Tunnelling Electron Microscope (STEM).

### RESULTS AND DISCUSSION

Hydrodynamic average size of obtained SPION were found to be in the range of 80 nm. Mössbauer spectroscopy and X-ray diffraction revealed maghemite structure of the particles, while magnetometry studies confirmed their superparamagnetic properties<sup>5</sup>. Infrared spectroscopy confirmed coating of SPION by oleic acid. STEM imaging present spherical shape and similar size of the magnetic nanoparticles.

NMR, elemental analysis and conductometric titration studies revealed degree of substitution of chitosan by quaternary ammonium to be ca. 60%, whereas degree of substitution by N-dodecyl groups was 2%<sup>6</sup>. Hydrodynamic average size and zeta potential of the prepared chitosan-based capsules templated on magnetic oil core were found to be around 500 nm and +28 mV, respectively. STEM imaging approved spherical shape of the capsules, size and presence of iron oxide nanoparticles inside the oleic core structure.

### CONCLUSION

Chitosan-based capsules templated on oleic core containing magnetic nanoparticles were fabricated in a facile emulsification procedure. The synthesized SPION were soluble in oil enabling its efficient encapsulation in the capsules' cores. The obtained capsules are promising carriers of bioactive compounds that may be targeted using magnetic field.

### REFERENCES

1. Hola K., Markova Z., Zoppellaro G., Tucek J, Zboril R., *Biotechnol. Adv.*, 33, 1162, 2015
2. Szafraniec J., Janik M., Odrobińska J., Zapotoczny S., *Nanoscale*, 7, 5525, 2015
3. Leszczyński B, PhD thesis, 2016
4. Karczewicz A., et al., *Colloids Surfaces B Biointerfaces* 109, 307, 2013
5. Berkowitz A.E., Schuele W.J., Flanders P.J., *J.Appl.Phys.*, 39, 1261, 1968
6. Bulwan M., Zapotoczny S., Nowakowska M., *Soft Matter*, 5, 4726, 2009

### ACKNOWLEDGMENTS

E.G.Ch. has been partly supported by the EU Project POWR.03.02.00-00-I004/16

## Click-Nanohydrogels Based on Riboflavin-modified Hyaluronan

Nicole Zoratto, Giuliana Manzi, Elita Montanari, Tommasina Coviello, Pietro Matricardi and Chiara Di Meo\*

Department of Drug Chemistry and Technologies, Sapienza University of Rome, Italy

[chiara.dimeo@uniroma1.it](mailto:chiara.dimeo@uniroma1.it)

## INTRODUCTION

Since the last decade, hydrogel nanoparticles (also known as nanogels, NHs) have been considered one of the most promising nanostructured drug delivery systems for the targeted and controlled/responsive delivery of therapeutic and/or diagnostic agents. Indeed, these nano-carriers show unique physico-chemical properties that combine the characteristics of hydrogels (soft consistency, high water content and low interfacial tension with water and biological fluids) with those of the nanosized drug delivery systems. These unique properties make NHs more similar to living tissues than other classes of synthetic nano-carriers. In the past, highly hydrophilic and biocompatible polysaccharide-based NHs have been already developed, showing to be promising systems for drug delivery applications<sup>1-4</sup>. In this work an innovative NH based on hyaluronan (HA) and a riboflavin derivative (Rfv) was developed by using a “click-chemistry” reaction<sup>5</sup>.

## EXPERIMENTAL METHODS

Tetrabutylammonium hyaluronan (HA<sup>TBA+</sup>) was able to react with propargylbromide in order to obtain HA-propargyl derivatives (HA-Prop) capable to link azide-derivatives in the presence of Cu(I) as catalyst (Huisgen 1,3-dipolar “click” cycloaddition). For this purpose, the azide derivative of tetrabutrate riboflavin (Rfv-N<sub>3</sub>) was synthesised and linked to HA-Prop (Fig. 1). The resulting amphiphilic product (HA-c-Rfv) was able to form NHs in aqueous environment after suitable treatments. For instance, the recently proposed autoclaving process (121°C, 20 min)<sup>3</sup> represents a fast one-step method for achieving sterile and drug loaded NHs. A number of drugs (e.g. piroxicam, dexamethasone and paclitaxel) have been loaded into NHs by treating the dry drug film in the presence of the HA-c-Rfv aqueous suspension at 121°C for 20 min. Moreover, HA-c-Rfv bearing free alkyne groups were further functionalised with PEG-N<sub>3</sub> chains in order to obtain pegylated- NHs.

## RESULTS AND DISCUSSION

HA with several MW and different propargyl and riboflavin derivatisation degrees were investigated. The resulting nano-systems showed a mean diameter in the range of 200-300 nm and ζ-potential of -30/40 mV, depending on the polymer MW and derivatisation degree; NHs showed high stability at physiological pH; the freeze-drying process was also assessed with the aim to store NHs as freeze-dried powder that can be quickly re-hydrated in aqueous solvents (Fig. 2); for this purpose, the addition of a suitable cryo-protectant was necessary to retain the NHs properties (size and PDI).

HA-c-Rfv NHs are particularly suitable for loading and delivering hydrophobic drugs, having at least one aromatic ring (e.g. piroxicam, dexamethasone and paclitaxel<sup>5</sup>) (Fig. 2). Indeed, it is assumed that the drug molecules can be located in the lipophilic core (where the Rfv moieties are), interacting through hydrophobic forces and π-π stacking interactions with the aromatic rings of Rfv. The polymeric HA-propargyl backbone, partially linked to Rfv was capable to react with other functionalising molecules bearing an azide group, suitable for passive or active targeting: for instance, PEG-N<sub>3</sub> has been linked to NHs in order to improve the drug delivery to the targeted site of action *in vivo*<sup>5</sup>.

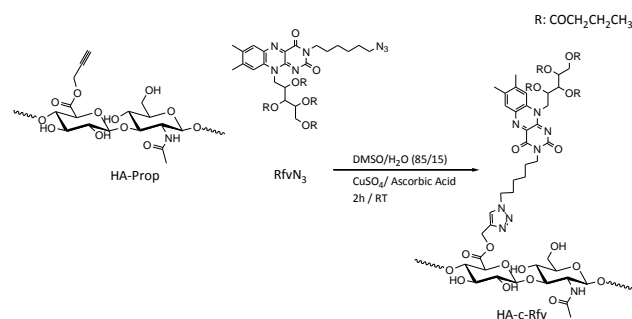


Fig. 1. Click reaction between HA-Prop and Rfv-N<sub>3</sub><sup>5</sup>.

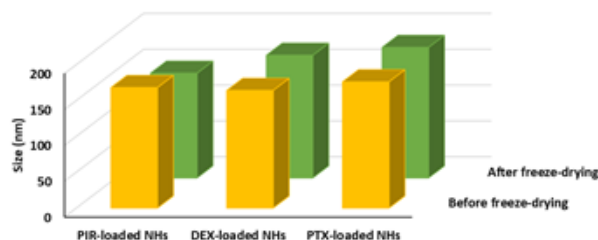


Fig. 2. Size of drug-loaded NHs.

## CONCLUSION

In this work, innovative NHs based on HA and Rfv linked by a “click chemistry” reaction have been developed. These NHs show good dimensions, high stability and an excellent drug loading capability. Moreover, by using suitable conditions, it is possible to have NHs with free alkyne groups that can be easily used for further functionalization.

## REFERENCES

1. D'Arrigo G *et al.* Eur. J. Pharm. Biopharm. 87:208-16, 2014
2. Montanari E *et al.*, Macromol. Biosci. 13:1185-94, 2013
3. Montanari E *et al.* J Mat. Sci.:Mat. Med. 26:32, 2015
4. Di Meo C *et al.* Carbohydr. Polym. 115:502-09, 2015
5. Manzi G *et al.* Carbohydr. Polym, 174:706-15, 2017



## Dexamethasone-loaded Bioreducible Branched Polyethyleneimine for Enhanced Nonviral Transfection

Sang Jun Park, Han Chang Kang

Department of Pharmacy, The Catholic University of Korea, Bucheon, Gyeonggi-do 14662, Republic of Korea  
[psj910417@gmail.com](mailto:psj910417@gmail.com)

### INTRODUCTION

Dexamethasone (DEX) is an anti-inflammatory drug and has interesting activities for accelerating nuclear translocation and dilating nuclear pores, resulting in effective nuclear delivery of biologics as well as chemical drugs. To effectively deliver plasmid DNA (pDNA) into the nucleus, this study selected DEX and its loaded polycation. Especially, the reducible polycation (RPC) was synthesized from the low molecular weight (LMW) branched polyethyleneimine (bPEI) via thiolation and oxidation<sup>1</sup>. Hydrophobic DEX was loaded into internal hydrophobic compartments of hydrophilic RPC, resulting in DEX@RPC. After complexing pDNA with DEX@RPC, the resultant DEX@RPC/pDNA complexes were investigated in terms of size, zeta-potential, cytotoxicity, gene condensation ability, transfection efficiency, cellular uptake, and nuclear uptake.

### EXPERIMENTAL METHODS

For synthesis of RPC, primary amines of bPEI<sub>0.8kDa</sub> were thiolated by 2-iminothiolane hydrochloride in DPBS (pH 7.0-7.4) for 24 h at room temperature (RT). Then DMSO and L-cysteine hydrochloride monohydrate were added to the aforementioned solution, and DMSO-induced oxidative polymerization of thiolated bPEI<sub>0.8kDa</sub> was conducted for 24 h at RT. Finally, RPC was obtained after dialyzed and then lyophilized. After forming RPC/pDNA complexes and DEX@RPC/pDNA complexes, their size and zeta-potential were evaluated by a zetasizer. For gene condensation, the complexes were evaluated by a gel retardation assay. Transfection efficiency and cytotoxicity of the complexes were evaluated by a luciferase assay and an MTT assay in MCF7 and HeLa cell lines.

### RESULTS AND DISCUSSION

When DEX@RPC was complexed with pDNA at weight ratio (WR)  $\geq 2$ , the sizes of the DEX@RPC/pDNA complexes were below 100 nm in diameter. The WR-dependent size pattern of the DEX@RPC/pDNA complexes was similar to that of the RPC/pDNA complexes used as the control polyplexes. The zeta-potentials of DEX@RPC/pDNA complexes were approximately 22 mV at WR 2 and reached approximately 40 mV at  $5 \leq WR \leq 10$ . Although RPC/pDNA complexes had slightly different patterns in zeta-potentials, their zeta-potentials were within approximately 30-50 mV of the same WR range. RPC and DEX@RPC were completely protected and condensed pDNA after forming their polyplexes. To evaluate decomplexation of pDNA from the polyplexes, WR 5 was used. In a thiol-depleted condition (i.e., 0 mM of DTT), heparin-induced pDNA release from the RPC/pDNA complexes was represented at lower

concentrations of heparin than that from DEX@RPC/pDNA complexes. The results indicate that DEX@RPC/pDNA complexes have more colloidal stability than RPC/pDNA complexes. However, when using a thiol-rich environment (i.e., 20 mM of DTT) mimicked to the cytosolic environment, thiol-triggered degradation of disulfide bonds in RPC and DEX@RPC caused faster release of pDNA from their polyplexes than those in a thiol-depleted condition.

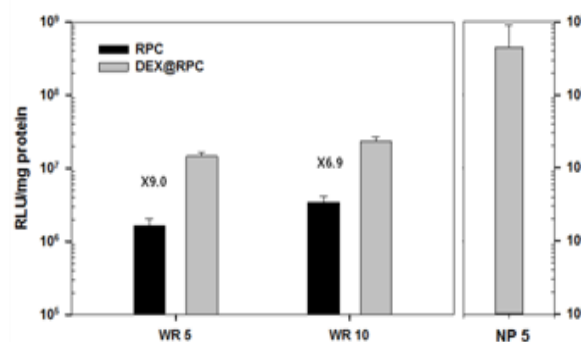


Fig. 1. In vitro gene transfection efficiency of RPC/pDNA complexes and DEX@RPC/pDNA complexes in MCF7 cells.

In MCF7 and HeLa cells, RPC/pDNA complexes and DEX@RPC/pDNA complexes did not show remarkable cytotoxicity. However, DEX@RPC/pDNA complexes showed 7-9-fold and 2-12-fold higher luciferase expression than RPC/pDNA complexes in MCF7 and HeLa cells, respectively. The results were caused by DEX-induced more nuclear uptake of pDNA in DEX@RPC/pDNA complexes than RPC/pDNA complexes.

### CONCLUSION

Hydrophobic DEX was physically loaded into internal hydrophobic compartments in a hydrophilic RPC. The resultant DEX@RPC were complexed with pDNA, forming DEX@RPC/pDNA complexes. The polyplexes showed higher gene expression and higher pDNA delivery in the nucleus compared to DEX-free polyplexes. Thus, DEX-loaded polycation could be potential gene carriers through effective nuclear pDNA delivery.

### REFERENCES

- Kang H. C. *et al.*, Biomaterials 32:1193-1203, 2011
- Echeverria P. C. *et al.*, Mol. Cell. Biol. 29(17):4788-4797, 2009

## Effective Cytotoxic Efficacy of Doxorubicin-loaded Reducible Polycation to Cancer Cells

Dong U Ju, Kitae Ryu, Han Chang Kang

Department of Pharmacy, The Catholic University of Korea, Bucheon, Gyeonggi-do 14662, Republic of Korea  
[dongwoo0420@nate.com](mailto:dongwoo0420@nate.com)

### INTRODUCTION

Doxorubicin (DOX) is a hydrophobic anticancer drug. To make its therapeutic effects, DOX binds to DNA and the resultant DOX-bound DNA interferes the action of topoisomerase II and prevents DNA replication<sup>1</sup>. However, DOX has severe side effects such as cardiac toxicity. Thus, drug delivery systems have been considered to reduce its side effects and improve its therapeutic efficacy.

In this study, we used reducible polycation (RPC) having branched low molecular weight poly(ethylene imine) (bPEI) with disulfide linkage as a doxorubicin delivery carrier. Hydrophilic RPC has hydrophobic spaces inside for carrying a hydrophobic drug. In addition, the disulfide bonds inside the RPC can be cleaved by glutathione in the intracellular environment. Thus, the study prepared DOX-loaded RPC (DOX@RPC) and investigated their physicochemical and biological properties as a drug delivery carrier.

### EXPERIMENTAL METHODS

#### Synthesis of Reducible Polycation (RPC)

RPC were synthesized as previously reported<sup>2</sup>. Briefly, 2-iminothiolane was added into bPEI<sub>0.8kDa</sub> for thiol formation, and then DMSO was added for oxidation.

#### Preparation of DOX-loaded RPC (DOX@RPC)

DOX and RPC were dissolved in DMSO and stirred for 24 h. The RPC-DOX mixture solution was dialyzed against deionized water (DIW) for 48 h using a dialysis tube (molecular weight cut-off of 3.5kDa), followed by filtering with a syringe filter (0.45 μm). The resultant DOX@RPC was obtained after lyophilization.

#### Measurement of DOX content in DOX@RPC

Loading contents and efficiencies of DOX in DOX@RPC were measured as previously reported<sup>3</sup>. DOX@RPC was dissolved in DIW (5 mg/mL) and exposed to 10 mM DTT for 1 h at 37°C. After that, the suspension was centrifuged at 15000 rpm for 3 h, and the extracted DOX was dissolved in DMSO. The absorbance at 501 nm was monitored with a microplate reader (SpectraMax M5, Molecular Devices, Sunnyvale, CA, USA).

#### Cytotoxicity test of DOX@RPC

MCF7 and MCF7/ADR-RES (an adriamycin resistance cell line of MCF7) cells were seeded in 96-well plates with  $5 \times 10^3$  cells/well and cultured for 24 h prior to the addition of DOX, DOX-HCl and DOX@RPC. The cells were exposed to different concentrations of the drug solution for 24 h. MTT solution (5 mg/mL) was treated to each well. After 4 h of incubation, formazan crystal was dissolved with DMSO and the absorbance of the solution was measured at 572 nm.

### RESULTS AND DISCUSSION

RPC was synthesized by auto-oxidation of DMSO and the molecular weight of RPC was 9.8 kDa via the

viscosity measurement. When aiming for targets 10 wt% DOX in DOX@RPC<sub>9.8kDa</sub>, the actual DOX loading contents obtained 4.2% and the loading efficiency is 39%.

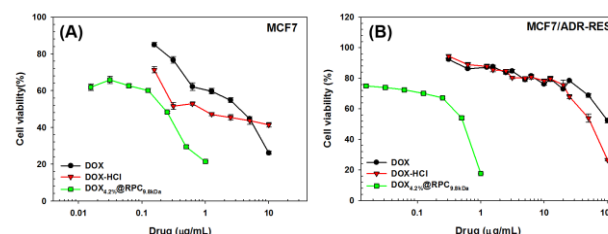


Fig. 1. Cytotoxicity test of DOX, DOX-HCl, and DOX<sub>4.2%</sub>@RPC<sub>9.8kDa</sub> in (A) MCF7 cells and (B) MCF7/ADR-RES cells.

MTT assay was performed on MCF7 cells and MCF7/ADR-RES cells (Fig. 1). Each cell was treated with DOX (a hydrophobic form), DOX-HCl (a hydrophilic form), and DOX<sub>4.2%</sub>@RPC<sub>9.8kDa</sub>. The IC<sub>50</sub> values of DOX, DOX-HCl, and DOX<sub>4.2%</sub>@RPC<sub>9.8kDa</sub> in MCF7 cells were 3.5 μg/mL, 0.9 μg/mL, and 0.2 μg/mL, respectively. In addition, the IC<sub>50</sub> values of DOX, DOX-HCl, and DOX<sub>4.2%</sub>@RPC<sub>9.8kDa</sub> in MCF7/ADR-RES cells were above 100 μg/mL, 55.7 μg/mL, and 0.5 μg/mL, respectively. In MCF7 cells, the killing effect of DOX<sub>4.2%</sub>@RPC<sub>9.8kDa</sub> was 17-fold and 4.5-fold higher than that of DOX and DOX-HCl, respectively. Especially, in MCF7/ADR-RES cells, DOX<sub>4.2%</sub>@RPC<sub>9.8kDa</sub> had 185-fold and 111-fold more therapeutic effects than DOX and DOX-HCl, respectively. Due to detouring an efflux pump route of DOX using DOX@RPC, the designed DOX@RPC represented effective cell killing ability via disulfide breakage in glutathione-rich cytosol, and overcome the activation of P-glycoprotein efflux pump<sup>4</sup>.

### CONCLUSION

By using RPC as a hydrophilic drug carrier with hydrophobic internal compartments, hydrophobic anticancer drugs could be effectively delivered into cells. Beyond DOX, Drug@RPC for other hydrophobic drugs could be effective anticancer nanodrugs in drug-sensitive cells as well as drug-resistant cells.

### REFERENCES

1. Thorn C. F. *et al.*, Pharmacogenet Genomics. 21:440-446, 2011
2. Kang H. *et al.*, Biomaterials. 32:1193-1203, 2011
3. Cho H. *et al.*, Macromol. Biosci. 14:1483-1494, 2014
4. Goren D. *et al.*, Clin. Cancer Res. 6:1949-1957, 2000

## Evaluation of the *in vitro* Response of Keratinocytes and Fibroblasts to Collagen-hydroxyethyl Cellulose Matrices with Incorporated Collagen-gelatin Microspheres

Justyna Kozłowska<sup>1</sup>, Natalia Stachowiak<sup>1</sup>, Anna Bajek<sup>2</sup>, Alina Sionkowska<sup>1</sup>, Lukasz Kazmierski<sup>2</sup>

<sup>1</sup>Department of Chemistry of Biomaterials and Cosmetics, Faculty of Chemistry, Nicolaus Copernicus University in Toruń, Poland

<sup>2</sup>Department of Tissue Engineering, Chair of Urology, Faculty of Medicine, Ludwik Rydygier Collegium Medicum in Bydgoszcz, Nicolaus Copernicus University in Toruń, Poland

[justynak@chem.umk.pl](mailto:justynak@chem.umk.pl)

### INTRODUCTION

Penetration into the skin is a key element in dermal reactions, be it to xenobiotics, to drugs, or to other active compounds<sup>1</sup>. Nowadays, the extremely rapid development of microparticulate systems used in many branches of science, especially in medicine and pharmacy, is observed<sup>2</sup>. Among microparticles, microsphere is one of the most promising for active substance delivery system. In this work, the innovative structure, namely microspheres incorporated into 3D polymer matrix was prepared and it can be considered as a dual delivery platform for dermatological or cosmetic applications.

Materials used in dermatology, pharmacy and cosmetology should be characterized by biocompatibility and non-toxicity, and biopolymers, such as collagen, gelatin and hydroxyethyl cellulose are known for their unique properties suitable for these applications<sup>3</sup>. Therefore, in this study collagen and hydroxyethyl cellulose were selected as a bulk of matrices and by incorporating of collagen-gelatin microspheres some properties of matrices, such as *in vitro* release performance, were modified. Obtained materials were loaded with pot marigold (*Calendula officinalis*) flower extract and the *in vitro* response of keratinocytes and fibroblasts was studied.

### EXPERIMENTAL METHODS

Collagen (col) type I was obtained in our laboratory from fish scales of *Esox lucius*<sup>4</sup>. Collagen-gelatin (col-gel) microspheres were prepared by water-in-oil emulsion described by Kawai et al. with some modifications<sup>5</sup>. To prepare microspheres-loaded matrices, col-gel microspheres (0.15 g) were mixed with 30 ml collagen suspension (0.5% w/v) and hydroxyethyl cellulose (0.15 g), and magnetically stirred for 30 min. Then, mixture was frozen and lyophilized. After lyophilisation, matrices were cross-linked using a cross-linking mixture EDC/NHS and they were frozen and lyophilized again. Collagen-hydroxyethyl cellulose matrices incorporating collagen-gelatin microspheres were named col/hec (col-gel).

Before loading the *Calendula officinalis* flower extract onto the microspheres-loaded matrices assays were performed to establish its cytotoxic concentration according to ISO 10993-5. Then, col/hec (col-gel) matrices were loaded with the extract, their cytotoxicity and biological activity were evaluated again using MTT assay. Additionally, an MTT assay assessing viability of cells adhered to col-gel microparticles was performed.

The biological property – cytotoxicity – was determined using fibroblast cell line (3T3) and keratinocytes cell line.

### RESULTS AND DISCUSSION

Fig. 1 shows the microstructure of a polymer matrix with incorporated microspheres. The prepared 3D matrices have a porous structure and microspheres have spherical shape.

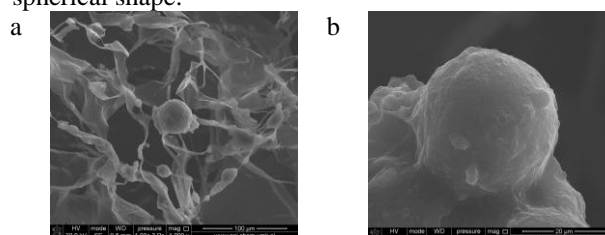


Fig. 1. SEM of EDC/NHS crosslinked col/hec matrix containing col-gel microspheres: a)  $\times 1000$ ; b)  $\times 5000$

*Calendula officinalis* flower extract below 1% resulted in higher cell viability than in the range of 1-2%. When keratinocytes and fibroblasts were exposed to microspheres loaded matrices with 0.1% and 0.5% extract, the viability was greater. These results were supported by light microscopy.

### CONCLUSION

We developed a novel delivery system for controlled release of a pot marigold flower extract that might be helpful in treating chronic skin wounds or in other dermatological and cosmetic applications.

### REFERENCES

- Schaefer H. et al., Skin Penetration in: Textbook of Contact Dermatitis, Rycroft R.J.G et al. (Eds.), Springer, Berlin, Heidelberg, 2001
- Tomic I. et al., Int. J. Pharm. 505:42-51, 2016
- Mogoşanu G.D. et al., Pharmaceutical Natural Polymers: Structure and Chemistry in: Handbook of Polymers for Pharmaceutical Technologies: Structure and Chemistry, Thakur V.K. et al. (Eds.), Scrivener Publishing LLC Wiley, USA, 2015
- Kozłowska J. et al., Int. J. Biol. Macromol. 81:220-227, 2015
- Kawai K. et al., Biomaterials 21: 489-499, 2000

### ACKNOWLEDGMENTS

Financial support from the National Science Centre (NCN, Poland) Grant No UMO-2016/21/D/ST8/01705 is gratefully acknowledged

## Effect of Assembly pH and Ionic Strength of Chitosan/Casein Multilayers on Benzydamine Hydrochloride Release

Maria Marudova<sup>1</sup>, Antoaneta Marinova<sup>1</sup>, Asya Viraneva<sup>1</sup>, Sotir Sotirov<sup>1</sup>, Bissera Pilicheva<sup>2</sup>, Ivan Bodurov<sup>1</sup>, Ivanka Vlaeva<sup>3</sup>, Ginka Exner<sup>1</sup>, Yordanka Uzunova<sup>2</sup>, Temenuzhka Yovcheva<sup>1</sup>

<sup>1</sup>Faculty of Physics and Technology, University of Plovdiv "Paisii Hilendarski", Bulgaria

<sup>2</sup>Faculty of Pharmacy, Medical University – Plovdiv, Bulgaria

<sup>3</sup>Faculty of Economics, University of Food Technologies - Plovdiv, Bulgaria

[marudova@uni-plovdiv.net](mailto:marudova@uni-plovdiv.net)

### INTRODUCTION

Layer-by-layer polyelectrolyte multilayers (LLPEMs) are of great interest as drug delivery systems, because of the possibilities for precise control of their structure and properties<sup>1</sup>. Depending on the assembly conditions and the type of polyelectrolytes, the LLPEMs can be either impermeable or permeable to small molecules (such as drugs) and behave as elastic solids or soft and swellable membranes<sup>2</sup>. The present study deals with the effect of assembly pH and ionic strength on the swelling and drug release of chitosan/casein LLPEMs, built-up on precharged polylactic acid (PLA) substrates. All monitored parameters depend on both pH and ionic strength, which could be attributed to the charge density of the LLPEM together with the screening effect of the counterions, controlling the drug diffusion process.

### EXPERIMENTAL METHODS

The PLA substrates were casted from 2% chloroform solutions and dried until reaching constant weight. Just prior to the deposition, the substrates were charged positively by means of a point-to-plane three-electrode corona discharge system. Casein/chitosan LLPEMs were formulated by alternative substrate dipping into 1% casein solution with pH 8 and 1% chitosan solutions with different pH – 4.0, 5.0, and 5.5. The ionic strength for both solutions varied between 10 mM and 1000 mM. After each chitosan layer the LLPEMs were immersed in 1% benzydamine hydrochlorid (BH) solution and hold there for 30 min. The LLPEMs' water content and swelling were determined. The BH release was investigated by monitoring UV-absorbance at 308 nm. Atomic Force Microscopy (AFM) revealed the LLPEMs surface topography.

### RESULTS AND DISCUSSION

The BH release kinetics is presented in Fig. 1.

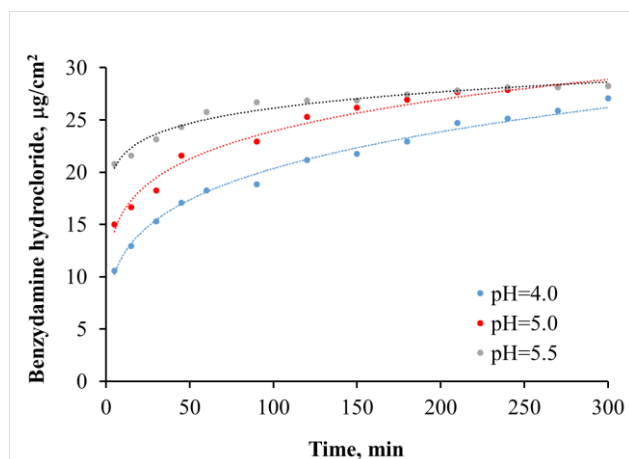


Fig. 1. BH release kinetics at different pH

The experimental data obey the power law model. For comparative purposes, a period of 24 h was chosen for BH release. The maximum quantity of BH was released by the LLPEMs designed with chitosan solution of pH 4, although the release rate was the slowest. Assembly ionic strength increase from 10 mM to 100 mM results in increased BH release. However, further increase to 1000 mM causes the released BH decrease. This observations are suggested to result from differences in the density and diffusion constant of LLPEMs designed at different pH and ionic strength. Chitosan charge density at low pH (4.0) is high. The LLPEMs in this case possess very strong binding capacity, causing slow BH release rate. At increasing pH the charge density drops, which results in higher release rates. The ionic strength is expressed in different screening effect, which control the chitosan/casein electrostatic interactions as well as the LLPEMs density. At ionic strength, 10 mM the drug amount is low, since the high LLPEMs dense hindering the drug penetration. At too high ionic strength, the LLPEMs become too loose and the drug entrapment into the LLPEMs becomes very difficult. The explanation above is based on the swelling and surface topography investigations. The swelling and the surface roughness are the highest at pH 5.5, which indicates very loose structure. Hence, the diffusion coefficient in this case is the highest and the drug release is fastest.

### CONCLUSION

- The pH at which the LLPEMs were design affects the drug binding capacity and its release rate. At low pH the electrostatic interactions are strong, the binding capacity becomes very high, resulting in slow release rate. At too high pH, the structure is too loose and does not facilitate the drug molecules anchoring;
- According to our study, the best balance between density and binding capacity was achieved at ionic strength of 100 mM.

### REFERENCES

1. Vilela C., *et al.*, *Expert Opin Drug Del.* 14(2):189-200, 2017.
2. Mertz G., *et al.*, *Colloids Surf A Physicochem Eng Asp.*, 415:77-85, 2012.

### ACKNOWLEDGMENTS

This study was funded by Bulgarian National Scientific Fund, Project No DFNI B-02/7.



## Chitosan/Poly(lactic acid) Blends as Drug Delivery Systems

Maria Marudova, Tsvetan Yorov, Sotir Sotirov

Faculty of Physics and Technology, University of Plovdiv "Paisii Hilendarski", Bulgaria  
[marudova@uni-plovdiv.net](mailto:marudova@uni-plovdiv.net)

### INTRODUCTION

In the recent years, there has been a growing interest in biodegradable polymers for tissue engineering and medical treatment applications, especially in the field of controlled drug delivery, mainly due to their controlled biodegradability and the excellent biocompatibility<sup>1</sup>.

In the present work the possibilities for immobilization and controlled release of a model drug salicylic acid (SA) from chitosan/poly(lactic acid) (Ch/PLA) blend films are studied. The release kinetics of the model drug into saline was interpreted in the context of already existing models<sup>2,3</sup> and important functional parameters of the polymer matrix have been defined. The release behaviour is addressed to some structural and physico-chemical characteristics of the investigated system.

### EXPERIMENTAL METHODS

Low molecular weight chitosan and poly(DL-lactic acid) were used to cast blend films with different weight ratios. SA in 1% concentration (based on the solution weight) was immobilized in all types of blend films. The film water content and water capacity were determined by standard methods. The specific interactions between the SA and the Ch were characterized by FT-IR spectroscopy in the range from 600 cm<sup>-1</sup> to 2000 cm<sup>-1</sup>. The structural state of the immobilized in the Ch/PLA blends SA was determined by the method of differential scanning calorimetry (DSC) in the temperature range from 0°C to 300°C during heating at rate 10°C/min. The salicylic acid release kinetics was tested in saline solution at 37° C and atmospheric pressure for 5 days. The amount of the released SA was determined by UV-spectroscopy at 296 nm. The Weibull and Higuchi kinetic models were used for fitting of the experimental kinetic curves and model parameters were determined using non-linear regression software.

### RESULTS AND DISCUSSION

The hydrophobic properties of the Ch/PLA matrix are characterized by the evaluation of water content and water capacity. A linear dependence between the water content and the Ch content in the matrix is observed, while the highest water capacity is detected at Ch/PLA ratio 5:5, which is associated with clearly expressed porous structure of the blend, visualized by SEM.

New bands in FT-IR spectra of SA/polymer systems are observed and are associated with polyelectrolyte complex formation between the Ch and the SA.

One of the basic factors affecting drug release is the structural state of the drug in the matrix. It is proved by DSC method that the SA is in completely amorphous state.

A typical release kinetics curve of salicylic acid in saline is presented on Fig. 1.

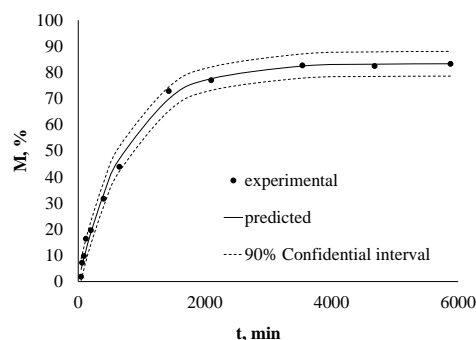


Fig. 1. Kinetics curve of salicylic acid in saline

A rapid drug release is observed at the beginning of the process, and then a saturation region is reached. The Weibull model is applied to the experimental results. Determining the parameters of the model, it becomes clear that the smallest released quantities are observed at concentrations with a predominant PLA content. This is due to the good barrier properties and the hydrophobic structure of PLA, which prevent drug dissolution in the matrix. In matrices with equal ratio between the polymers, the released amount is greatest, the probable cause being the strongly expressed porous structure. In Ch matrices, the release rate is slightly lower due to the specific interactions between chitosan and salicylic acid and the formation of polyelectrolyte complexes that are poorly soluble.

### CONCLUSION

- The model drug SA has been immobilized successfully in amorphous state in all Ch/PLA matrices.
- FT-IR analysis has shown a specific interaction between Ch and SA, resulting in the formation of polyelectrolyte complexes.
- The release kinetics of the SA from chitosan/poly(lactic acid) matrix is subordinated to the Higuchi and Weibull models.
- The release can be controlled by changes in the proportion between Ch and PLA. It is governed by the hydrophobic nature of the PLA and the complexes formed between Ch and SA.

### REFERENCES

1. Wang W. *et al.*, Mater. Sci. Eng. C. 46:514–520, 2015.
2. Harris Shoaib M. *et al.*, Pak. J. Pharm. Sci., 19(2):119-124, 2006.
3. Chinh N, *et al.*, J. Appl. Polym. Sci., 133(16), 2016.

### ACKNOWLEDGMENTS

This study was funded by Bulgarian National Scientific Fund, Project No DFNI B-02/7.

## Poly lactide as Drug Carrier in Composite Implant

Agnieszka Skórska-Stania<sup>1</sup>, Agnieszka Jelonek<sup>1</sup>, Monika Brzychczy-Włoch<sup>2</sup>

<sup>1</sup>Faculty of Chemistry, Jagiellonian University, Poland

<sup>2</sup>Department of Microbiology, Jagiellonian University Poland

[agnieszka.skorska-stania@uj.edu.pl](mailto:agnieszka.skorska-stania@uj.edu.pl)

### INTRODUCTION

Poly lactide (PLA) is one of the most commonly used biodegradable polymers. In the human body environment, PLA undergoes hydrolytic degradation, decomposes into oligomers, followed by lactic acid monomers. It shows a relatively good biocompatibility and mechanical strength, which depend on molecular weight, contribution of stereoisomers of lactic acid and its production techniques. PLA is widely used in medical applications like tissue engineering, wound managements and drug delivery systems<sup>1</sup>.

The studies concerned a ceramic-polymer composite with a core consisting of hydroxyapatite or biphasic calcium phosphates (BCP). Poly(D,L-lactide) (PDLLA) was used as a coating material for ceramic granules to improve their mechanical strength as well as the adhesion of the granules to each other and to the cavity walls. Additionally, PDLLA was also a matrix for the incorporation of a drug such as clindamycin. During polymer degradation process the antibiotic was gradually released to the implantation place. The composite implant was designed to meet the necessary requirements for biomaterials<sup>2</sup>.

The main objective of these studies was to permit an evaluation of the amount of drug released from implant.

### EXPERIMENTAL METHODS

Poly(D,L-lactide) used in the following work was obtained using zirconium catalyst at the Center of Polymer and Carbon Materials of the Polish Academy of Sciences in Zabrze. The molar mass (Mw) of PDLLA was 88.85 kDa, whereas the mass dispersion (Mw/Mn) was 1.85.

The first step of our investigation was the analysis of degradation profile of PDLLA coatings on microgranules of hydroxyapatites and on those of biphasic calcium phosphates. For this purpose, implants were incubated in phosphate buffer at pH 7.4 for about 7 weeks at 37°C. The pH change occurring during this degradation was also observed. It is worth to notice, that it was impossible to quantify the amount of released clindamycin by using spectroscopic methods.

In order to check if the amount of antibiotic released from PDLLA matrix is sufficient to inhibit the growth of microorganism, the disc-diffusion method was applied. *Staphylococcus aureus* ATCC 25923 was the reference strain. The samples of clindamycin released from the PDLLA cover were collected for each group of microgranules to phosphate buffer after 1, 2, 3, 4, 5, 6 and 7 days. The experiment was repeated three times for each sample.

The following tests were performed: E-test and DA disc, in order to check the activity of clindamycin hydrochloride against the bacterial strain. E-test allows the determination of MIC (Minimal Inhibitory

Concentration) or minimum concentration of antibiotic that inhibits bacterial growth<sup>3</sup>. In this method, on an agar matrix with the analyzed strain culture, a narrow strip is applied. The strip is saturated with an antibiotic in such a way, that the concentration of antibiotic increase lengthwise along the strip. After about 24 hours, the result of the E-test allows to determine the degree of resistance of a strain to a given drug. The DA (2µg) disc is control of a model antibiotic on the analyzed strain and provides information if this strain is sensitive to applied antibiotic.

### RESULTS AND DISCUSSION

PDLLA coating of hydroxyapatite microgranules degrades under *in vitro* conditions causing insignificant change in pH – 0,51±0.03 during 51 days of experiment. Similarly, *in vitro* degradation of BCP microgranules and their polymeric layer also does not cause a significant change in pH (0,59±0.09) during whole experiment. The degradation rate for PDLLA layer on hydroxyapatite granules was 8±1% and on BCP granules – 3±1 %. This kind of degradation ensured the mechanical strength of the whole implant and also the release of active substances from it.

The E-test showed that the MIC is 0.064 mg/l, which is in agreement with EUCAST standard from 2015: MIC for clindamycin and *Staphylococcus aureus* is equal or smaller than 0.25 mg/l. Result of the DA 2µg disc was 29 mm, where, according to the EUCAST guidelines, the strain is sensitive if the zone of inhibition of growth is equal or greater than 22 mm<sup>3</sup>.

Clindamycin incorporated in the PDLLA matrix shows a bactericidal effect in the required period of time, *i.e.* 7 days, so the initial concentration of antibiotic was chosen correctly.

### CONCLUSION

Poly(D,L-lactide) coating is a proper matrix for the antibiotic incorporation. It is assumed that release time of the therapeutic drug dose is required to prevent post-operative infections.

Received results confirmed potential clinical applications of the implant during orthopaedic surgery as a drug carrier. Obviously, the final determination of the application capacity of the designed implant will be possible after biological tests including *in vivo* tests.

### REFERENCES

1. Hamad K. *et al.* – eXPRESS Polymer Letters 9:435–455, 2015
2. Jelonek, A. PhD thesis, Jagiellonian University, 2013
3. European Committee on Antimicrobial Susceptibility Testing Breakpoint tables for interpretation of MICs and zone diameters Version 5.0, valid from 2015-01-01 Smith G. *et al.*, J. Biomech. 2:5-11, 2011

## Development and Characterization Minocycline Loaded Chitosan Nanoparticles for Local-drug-delivery

Victor Martin<sup>3</sup>, Catarina Santos<sup>1,2</sup>, Marta Alves<sup>2</sup>, Lúcia Gonçalves<sup>3</sup>, Isabel C. Ribeiro<sup>3</sup>, Ana Bettencourt<sup>3</sup>

<sup>1</sup>ESTSetubal, CDP2T, Instituto Politécnico de Setúbal, Campus IPS, 2914-508 Setúbal, Portugal

<sup>2</sup>CQE, Instituto Superior Técnico, Universidade de Lisboa, Av. Rovisco Pais, 1049-001 Lisboa, Portugal

<sup>3</sup>Research Institute for Medicines (iMed.Ulisboa), Faculty of Pharmacy, Universidade de Lisboa, Av. Prof. Gama Pinto, 1649-003 Lisbon, Portugal

[catarina.santos@estsetubal.ips.pt](mailto:catarina.santos@estsetubal.ips.pt)

### INTRODUCTION

Periodontitis is an inflammatory disease of gums involving the degeneration of periodontal ligaments, creation of periodontal pocket and resorption of alveolar bone [1]. Believes that dynamic interactions between bacterial factors and host response with genetic and environmental aspects are considered as the primary cause for tissue destruction in periodontitis [1].

Treatment of periodontitis is highly complex and can benefit from local drug delivery approaches. Local targeting can improve the therapeutic outcomes by achieving factors like site-specific delivery, low dose requirement, reduction in gastrointestinal side effects and decrease in dosing frequency [2].

The aim of the study was to develop a novel local drug delivery system composed of minocycline and chitosan. Minocycline is a broad-spectrum antibiotic that has many advantages over other antibiotics, e.g., both anti-inflammatory as well as antimicrobial properties and negligible or no phototoxicity which make a good candidate for the treatment of periodontitis [1].

Chitosan due to its biocompatibility, biodegradation, low toxicity, simple and reproducible preparation methods is a promising candidate as a carrier of nano and micro-particulate drug delivery systems [2].

### EXPERIMENTAL METHODS

The Chitosan nanoparticles (NPs) were prepared using an ionic gelation technique previously optimized in our laboratory [3]. Briefly, NPs were prepared using the following solutions: Chitosan (Low Molecular weight - 50 to 190kDa, deacetylation above 92%, Aldrich) 1 mg/mL at pH 5.5; Tween 80 2% (Polysorbate, Merck) sodium tripolyphosphate (TPP) 1 mg/mL at pH 7.5; minocycline hydrochloride (MH, kindly provided by Atral Cipan, Portugal) (2mg/mL). NPs without the drug (blank) were also prepared.

The morphology, size and compositions, of minocycline loaded chitosan nanoparticles (MH-NPs) were characterized by transmission electron microscopy (TEM).

The drug encapsulation efficiency (EE%) and *in vitro* drug release (dialysis membrane method) were assessed. Antibiotic quantification was conducted by spectrophotometry (350 nm).

### RESULTS AND DISCUSSION

The MH-NPs were spherical shape with nanometric size, as illustrated by TEM micrographs (Fig. 1). The encapsulation of MH did not change significantly the properties in terms of Zeta Potential (Table 1).

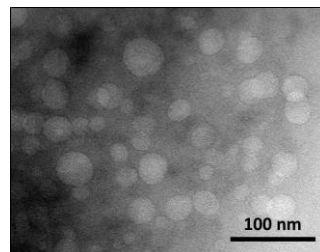


Fig. 1. Transmission electron micrograph of MH-NPs

Table 1. Evaluation of particle zeta potential and drug encapsulation.

Formulation	ZP (mV)	EE (%)
Blank NPs	20±1	-
MH-NPs	23±1	19.2±3.6

ZP – zeta potential; EE% (expressed as the percentage of antibiotic encapsulated in particles reported to the initial amount of antibiotic used for NPs preparation).

The EE (%) values proved to be adequate to obtain concentrations of the drug higher than  $0.305 \pm 0.050$  µg/mL just after 30 min of release.

The release assays also showed a controlled released of the encapsulated antibiotic in comparison to the free drug during a 4h period. An initial burst during the first hour was followed by a slower rate release, which is consistent with a biphasic profile suitable for targeting local periodontics infections.

### CONCLUSION

In summary, minocycline loaded chitosan nanoparticles were successfully synthesised using a simple ionic gelation technique.

All NPs prepared in this study had particle size in a nanometer range and positive values of zeta potential. The results of the *in vitro* release study suggested that MH-NPs are suitable for the treatment of periodontics infections.

### REFERENCES

1. Parag M. Khatri, *et al.* J Adv Pharm Technol Res. 3 (1): 75–79, 2012.
2. Sunil A. Agnihotri, *et al.* J of Control Release 100: 5–28, 2004.
3. Cadete A, *et al.* Eur J Pharm Sci.;45 (4):451–8, 2012.

### ACKNOWLEDGMENTS

The CQE/IST and iMed.Ulisboa authors would like to thank Fundação para a Ciência e Tecnologia (FCT) for the funding under the contract UID/QUI/ 00100/2013 and UID/DTP/04138/2013, respectively.

## Polymer-clay Nanocomposites with Antibacterial Activity

Alicja Rapacz-Kmita<sup>1</sup>, Maciej Mikołajczyk<sup>2</sup>, Barbara Szaraniec<sup>1</sup>, Marta Ludwicka<sup>1</sup>, Ewa Stodolak-Zych<sup>1</sup>

<sup>1</sup>Faculty of Materials Science and Ceramics, AGH University of Science and Technology, Krakow, Poland

<sup>2</sup>Division of Microbiology, The University Hospital in Krakow, Poland

[kmita@agh.edu.pl](mailto:kmita@agh.edu.pl)

### INTRODUCTION

Clays, including montmorillonite (MMT), can be successfully used in drug delivery systems<sup>1,2</sup>, due to their great capability to intercalate active substances into the interlayer spaces. Drugs may be released then in a sustainable way, which influences the efficiency and quality of therapeutic treatment. Based on these characteristics, clays can be further used not only in a direct drug delivery, e.g. oral dosing, but in the manufacturing of most advanced forms, that uses drug delivery, such as polymer-clay nanocomposites for applications, where antibacterial activity is desired. The aim of this study was to investigate the antibacterial properties and physical properties of polylactide films filled with montmorillonite, which was intercalated with gentamicin and neomycin.

### EXPERIMENTAL METHODS

Biologically pure montmorillonite (MMT) with the trade name Veegum®F (R.T. Vanderbilt Inc., USA) was used in the study. MMT was intercalated with aminoglycoside antibiotics (gentamycin, neomycin), and then was used to obtain the nanocomposite PLA films (INGEO 3251D, Natureworks, USA) with antibacterial properties. Drug intercalation was carried out in a water suspension at 50°C for 24 h, and nanocomposite films were obtained by casting, using dichloromethane as solvent (the fraction of intercalated MMT was 2% by weight). The obtained foils were tested for: contact angle, surface roughness, mechanical tensile strength as well as for antibacterial properties, considering the different surface roughness of the film, resulting from the method of preparation. Antibacterial tests were performed against *Escherichia coli* Gram-negative bacteria (ATCC 25922) using a disk diffusion method to determine diameters of zones inhibiting bacterial growth around nanocomposite film discs.

### RESULTS AND DISCUSSION

Nanocomposite films showed a hydrophilic character with simultaneous regularity of the higher contact angle for the rougher side, and the addition of drug intercalated MMT to PLA did not significantly changed the wettability (Tab. 1). In turn, tensile strength and Young's modulus decreased for the films with the addition of montmorillonite with an antibiotic (Tab. 2).

Table 1. Contact angle of nanocomposite films

Film		Contact angle $\theta$ [°]
PLA/MMT	↑	81,45±3,20
	↓	75,10±3,12
PLA/MMT+G	↑	80,96±5,18
	↓	68,40±2,97
PLA/MMT+N	↑	83,65±5,33
	↓	77,40±5,32

Table 2. Mechanical properties of nanocomposite films

Film	$R_m$ [MPa]	$\varepsilon F_{max}$ [%]	E [GPa]
PLA/MMT	40,34±2,46	1,43±0,13	3,06±0,21
PLA/MMT+G	32,89±3,05	1,83±0,16	2,61±0,35
PLA/MMT+N	33,02±2,98	1,70±0,36	2,64±0,09

The basic PLA/MMT composite films showed no antibacterial activity, regardless of the contact type with the bacterial culture, (rough vs. smooth side), and no zones of inhibition of bacterial growth were noticed (Tab. 3). For the composite films filled with MMT intercalated with gentamicin or neomycin, both composite materials exhibited antibacterial activity and the occurrence of inhibition zones of the growth of Gram-negative bacteria was evident. Moreover, in both cases, a tendency for larger zones of inhibition to appear around the film discs, which were placed with the smooth side towards the bacterial culture was noticed. The rough surface provided on average half the diameters of the inhibition zones, as well as, what is characteristic - irregular/elliptical shapes. It can therefore be assumed that the appearance of larger zones of inhibition around the smooth surfaces of the film is the result of a better adhesion of the smooth side of the film to the bacterial culture on agar.

Table 3. Diameters of inhibition zones of *E. coli* growth around composite film discs (avg. of 6 measurements)

Film	Diameter of inhibition zone [mm]	
	Rough surface	Smooth surface
PLA/MMT	0	0
PLA/MMT+G	8,0	19,0
PLA/MMT+N	7,6	15,3

### CONCLUSION

Addition of montmorillonite intercalated with antibiotics to the polylactide matrix provided the possibility of obtaining composites with antibacterial properties. The presence of inhibition zones of *E. coli* growth around the PLA/MMT+G and PLA/MMT+N composite films clearly indicates that the interaction of the antibiotic with both the clay carrier and polymer matrix did not affect its bactericidal effect.

### REFERENCES

- Rapacz-Kmita A. *et al.*, Mater. Sci. Eng. C 70:471-478, 2017
- Golubeva O.Y. *et al.*, Appl. Clay Sci. 112-113:10-16, 2015

### ACKNOWLEDGMENTS

This study was performed within the framework of funding for statutory activities of AGH University of Science and Technology in Cracow, Faculty of Materials Science and Ceramics (11.11.160.617).



## Multifunctional Porous Membranes with Antibacterial Properties

Ewa Dzierzkowska<sup>1</sup>, Ewa Stodolak-Zych<sup>1</sup>, Maciej Mikołajczyk<sup>2</sup>, Marcin Gajek<sup>3</sup>, [Alicja Rapacz-Kmita](mailto:kmita@agh.edu.pl)<sup>3</sup>

<sup>1</sup>Department of Biomaterials and Composite Materials, Faculty of Materials Science and Ceramics, AGH University of Science and Technology, Krakow, Poland

<sup>2</sup>Division of Microbiology, The University Hospital in Krakow, Krakow, Poland

<sup>3</sup>Department of Ceramics and Refractories, Faculty of Materials Science and Ceramics, AGH University of Science and Technology, Krakow, Poland

[kmita@agh.edu.pl](mailto:kmita@agh.edu.pl)

### INTRODUCTION

Fibrous membranes are potential carrier materials for pharmacologically active substances i.e. antibiotics. This type of membranes can be for example used during implantation procedure, due to their high absorbability allowing them to absorb blood. This clinical observation brings numerous benefits: it purifies the implantation field, fills undeveloped space and the presence of fibrous structure provides a scaffold for incoming cells<sup>1</sup>. Additionally, a proper modification of fibrous membranes at the stage of their preparation allows to obtain an antibacterial functionality. For this purpose, drugs are added to the fiber-forming solution or filled with a porous form of fiber<sup>2</sup>.

In this work, a bioresorbable polymer polylactide (PLA), known as biomedical material, was used and fibrous membranes were formed by electrospinning method. The fibers were modified by introducing gentamycin (GM) into the spinning solution during the manufacturing process. The first group of membranes was PLA/GM fibers obtained in a traditional way - on a steel collector. The second group of membranes was wet spun porous PLA/GM fibers.

Microstructure of fibrous membranes was observed using electron microscopy (SEM/EDS) and confocal microscope. The fiber diameters and their basic physicochemical parameters (contact angle, surface energy) were estimated. The presence of GM into polymer fibers was tested against both Gram-positive and Gram-negative bacteria. Drug release was monitored by changing of analytical ion concentration and parallel studies were conducted in contact with Gram-positive bacteria.

### EXPERIMENTAL METHODS

Commercial polymer: PLA (Carbochem), was used in the experiment. Mixture of dichloromethane (DCM) and dimethylformamide (DMF) was used as the solvent (all the solvents from Avantor). The precipitating reagent was polyvinylpyrrolidone (PVP) (Across), and the spinning solution were doped 5% wt. of gentamycin (Polfa). Ethanol or methanol were used as a coagulant bath (Avantor).

The fibrous membranes were air dried and then vacuumed for 48h. Microstructure of membranes was observed under scanning electron microscope (Nova NanoSEM) and confocal microscope (Olympus LEXT). Other features of membrane were tested during wettability test and surface free energy calculation (Kruss 15 DSA), drug release (ICP-ES), and durability in *in vitro* condition (PBS/3msc/37°C). Multilevel carrier membranes were tested for agar-based method.

Pure (unmodified) polymer membranes were used as references in all tests.

### RESULTS AND DISCUSSION

PLA fibers were characterized by a smaller fiber diameter (200-600 nm) compared to fibers modified with gentamycin (fiber diameter 0.8-1.2 μm) (Fig. 1). The presence of pores increases the fiber diameter to 1.7 μm. At the same time, the higher was the porosity of the fibers, the greater their wettability (over 80%). The addition of gentamycin increased the hydrophilicity of the fiber, reducing the surface free energy, however the influence of gentamycin was more pronounced in porous fibers. Membranes composed of porous PLA/GM were degrading faster, releasing gentamycin. This translated into better antibacterial activity in a shorter period (48 hours).

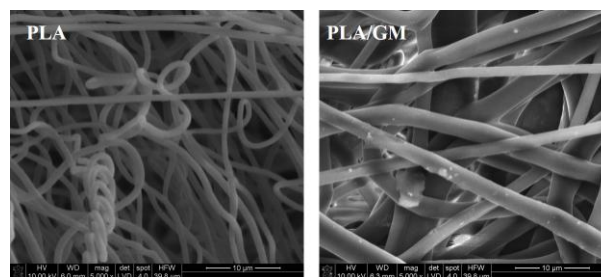


Fig. 1. Microstructure of membrane materials modified by drug (gentamycin)

### CONCLUSION

The fibrous membranes obtained by electrospinning method can be modified in a wide range at the manufacturing stage: by introducing pharmacologically active substances i.e. antibiotics into them or improving fibers porosity. Thus, such membranes are an interesting alternative to other drug carriers: microcapsules, sponge or scaffolds.

### REFERENCES

1. Dimitriou R. *et al.*, BMC Med. 10: 81-105, 2012
2. Hassanin A. *et al.*, Adv. Mater. Res. 894:364-368, 2014

### ACKNOWLEDGMENTS

This study was performed within the framework of funding for statutory activities of AGH University of Science and Technology in Cracow, Faculty of Materials Science and Ceramics (11.11.160.182).

## Novel Temperature Responsive Nanocapsules for Anti-aging Skin Care Applications

Sergiy Grishchuk, Liudmyla Gryshchuk

Institut fuer Verbundwerkstoffe GmbH (Institute for Composite Materials), Erwin-Schroedinger-Straße 58,  
67663 Kaiserslautern, Germany  
[sergiy.grishchuk@ivw.uni-kl.de](mailto:sergiy.grishchuk@ivw.uni-kl.de)

### INTRODUCTION

Since beginning of 1990<sup>th</sup> big attention is paid for the development of skin care products containing polymeric nanocapsules (NCs) with active ingredients in the core. This is related to the several benefits of NCs compared to other common carriers like liposomes, solid lipid particles, polymeric micro- and nanoparticles, such as lower amount of polymer, higher loading capacity, protection from degradation and improvement of stability of active substances and reduction of their irritant effect, increased efficiency of skin care formulations, tailored penetration of NCs into the skin and controlled release rate of active ingredients<sup>1,2</sup>.

Currently there is a strong need for novel functional products that realize skin thermal comfort, skin anti-ageing and skin natural antimicrobial control. These should have both an increased efficiency and cost-benefits compared to the currently available products. A recently developed innovative nano-encapsulation technology<sup>3</sup> makes use of specific materials' in situ self-assembly capabilities which opens pathways to fulfil these needs.

The present work is aimed at the modification of a natural protein by small bio-based aromatic molecules (alone and in combination with amino acids) for nano-encapsulation of natural anti-aging compounds resulting in temperature responsive NCs for potential application in anti-ageing cream formulations. This research was focused on the investigation of response of new NCs to the skin surface (32°C) and nominal human body (36.6°C) temperatures depending on the modification.

### EXPERIMENTAL METHODS

Bio-based small aromatic compounds bearing various reactive groups such as carboxylic acid chloride, aldehyde, and primary hydroxyl groups were used alone and/or in combination with amino acids for modification of a protein. Weight related protein/modifier ratios of 1/0.25, 1/0.5, and 1/0.75 were investigated. Bio-liquefied wheat bran was used as active ingredient for encapsulation. Encapsulation procedure (trade secret) was supported by approved for skin care surfactants and additives.

Particle size distribution and  $\zeta$ -potential of developed NC-dispersions diluted in ultra-pure water were determined at 25, 32 and 36.5 °C by dynamic light scattering technique using Zetasizer Nano ZS from Malvern and compared to those of NCs based on non-modified protein. All dispersions were stabilized at desired temperature for 10 min prior to the measurement. Five records were collected for each measurement for the determination of respective average values.

### RESULTS AND DISCUSSION

Representative results are shown in Fig. 1.

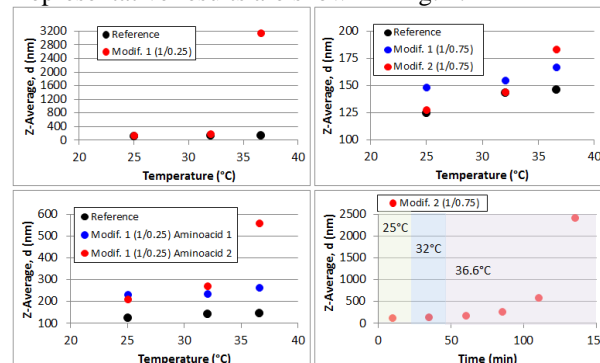


Fig. 1. Influence of type and amount of modifier as well as time on the average particle size of NCs at 25, 32 and 36.6°C

Due to modification of shell-building protein with small aromatic compounds, NCs with mostly lower polydispersity index (PDI), slightly bigger average size ( $d$ ), and similar  $\zeta$ -potential values ( $\zeta$ ) were formed. Slight influence of modifier type and amount on the increase of " $d$ " and "PDI" at 32°C guarantying still efficient penetration of NCs into the skin and obvious one at 36.6°C (required for better release of the active component in the skin layers), whereas no significant influence on " $\zeta$ ", was observed. At the same time, longer holding time at both skin and body temperature resulted in continuous increase of " $d$ " and "PDI". This is, probably, related to different level of  $\pi$ - $\pi$  stacking of aromatic units at 25°C and their disassembly at higher temperatures.

### CONCLUSION

NC-dispersions with high potential for skin care applications with temperature responsive release profile could be developed thanks to the used modifications.

### REFERENCES

1. Grumezescu A.M. (2016): Nanobiomaterials in Galenic Formulations and Cosmetics: Applications of Nanobiomaterials. Elsevier Science. 460 pp.
2. Dragicevic, N.; Maibach, H. I. (2016): Percutaneous Penetration Enhancers Chemical Methods in Penetration Enhancement: Nanocarriers. Springer Berlin Heidelberg. 384 pp.
3. Patent WO2013120856 A1, 2013

### ACKNOWLEDGMENTS

SKHINCAPS project has received funding from the European Union's Horizon 2020 research and innovation programme under grant agreement No 685909.

## Electrosprayed Chitosan Micro/Nanoparticles for Drug Delivery Applications

Badriya Baig<sup>1</sup>, Yaser E. Greish<sup>2</sup>, Amr Amin<sup>1</sup>

Departments of <sup>1</sup>Biology, and <sup>2</sup>Chemistry, United Arab Emirates University, UAE  
[y.afifi@uaeu.ac.ae](mailto:y.afifi@uaeu.ac.ae)

### INTRODUCTION

Since the emergence of Nanotechnology, all the attention has centered upon utilizing it to its best abilities. Tackling problematic medical issues through nanotechnological approach has seen an increasing demand among the research community, in particular oncologists as cancer remains one of the top causes of death worldwide (1). Multifunctional biocompatible nanoparticles (NPs) furnish a new perspective into drug delivery system compensating the usual anti-cancer drug shortcomings such as low solubility, bioavailability and absorption. As well as, using NPs for directly delivering the anticancer drugs to the tumor site maximize the efficiency of drug delivery. The well-known chitosan nanoparticle been chosen to be fabricated via electrospray method. Electrospray has been reported to generate reproducible polymer particles along with the ability to manipulate the particle size by changing the fabrication parameters such as working distance, flow rate, voltage and polymer concentration (2). The generated nanoparticles are to be loaded with therapeutic agents such as metformin and vismodegib as well as targeting agent, that is EpCAM monoclonal antibody.

### EXPERIMENTAL METHODS

An electrospray technique (Fig. 1) was used to prepare chitosan micro and nanoparticles. Chitosan with two different molecular weights were used in the current study. Moreover, the effect of varying the applied voltage, the feeding rate, and the spinning distance on the structure and morphology of the prepared chitosan particles were studied. Chitosan particles were electrosprayed into a grounded solution of a sodium tripolyphosphate as a cross-linking agent. The electrosprayed particles were washed, dried and characterized for their structure, and morphology using FTIR, TGA and SEM techniques in order to optimize the conditions that are needed to prepare chitosan particles with a homogeneous particle size distribution.

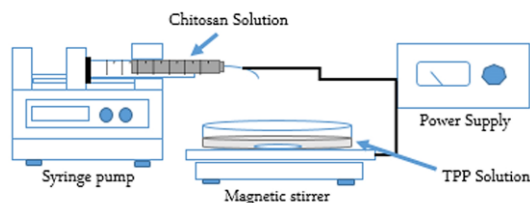


Fig. 1. Electrospray setup

### RESULTS AND DISCUSSION

Fig. 2 shows the FTIR spectra and TGA thermograms of the chitosan particles made by electrospraying low and high molecular weight chitosan solutions at pre-determined electrospray conditions. Both figures indicate phase purity of the particles without signs of degradation of chitosan by the effect of the applied high

voltage of electrospray. Pure chitosan of both molecular weights were also shown for comparison.

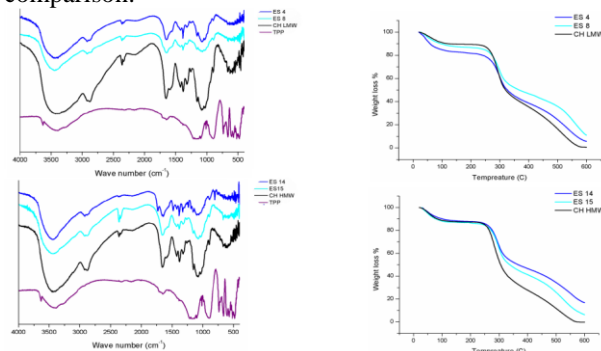


Fig. 2. FTIR spectra and TGA thermograms of chitosan-coated magnetite NPs

Fig. 3 shows SEM micrographs of micro- and nanoparticles made from low (A,B) and high (C,D) molecular weight chitosan solutions. All samples showed spherical morphology of the particles with variable size that largely depends on the electrospray conditions. Agglomerates of the particles are due to the drying of the particles after their formation. It is evident that higher molecular weight chitosan solutions produced smaller size particles, which could be related to their higher viscosity.

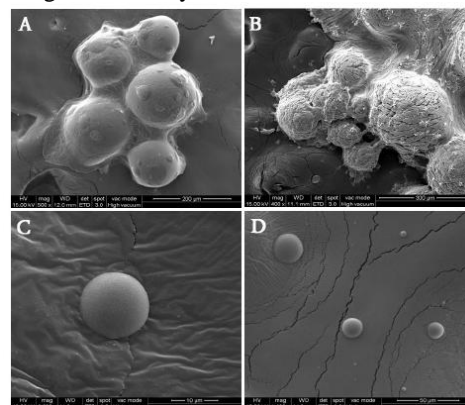


Fig. 3. SEM micrographs of chitosan-coated magnetite NPs

### CONCLUSION

Chitosan micro and nanoparticles with a homogeneous size distribution were successfully prepared and characterized using an electrospray technique.

### REFERENCES

- Ghadi et al. *Caspian J. Intern Med.* 2014; 5:156-161
- Zhang et al. *Int J. Pharm.* 2010; 397: 211-217

### ACKNOWLEDGMENTS

The author acknowledges the funding provided by the UAE University as part of the Zayed Centre of Health Sciences (grant 31R049).



## Controlled Growth Factor Release by Nanoparticulate Multilayer Systems for Graded Implants

Steffen Sydow<sup>1</sup>, Dominik de Cassan<sup>1</sup>, Yvonne Roger<sup>2</sup>, Julius Sundermann<sup>3</sup>, Heike Bunjes<sup>3</sup>, Andrea Hoffmann<sup>2</sup>, Henning Menzel<sup>1</sup>

<sup>1</sup>Institute of Technical Chemistry, TU Braunschweig, Germany

<sup>2</sup>Clinic of Orthopedics, MH Hannover, Germany

<sup>3</sup>Institute for Pharmaceutical Technology, TU Braunschweig, Germany

[s.sydow@tu-braunschweig.de](mailto:s.sydow@tu-braunschweig.de)

### INTRODUCTION

Functional implants between complex tissues e.g. at a bone-tendon-junction are still an unsolved medical problem. Spatial gradients along the implant could improve the situation. Besides gradients in the mechanical properties, the release of growth factor proteins in a graded way would be a significant progress. For generation of such gradients a combination of nanoparticles as a drug carrier immobilized by the Layer-by-Layer method (LbL) is focussed.<sup>1</sup>

### EXPERIMENTAL METHODS

#### Preparation of nanoparticles

Nanoparticles were prepared from aqueous solution by ionotropic gelation of chitosan (CS) or chitosan derivatives and sodium tripolyphosphate (TPP) as described previously.<sup>2</sup> Particle diameter and zeta-potential were characterized via dynamic light scattering (DLS). Growth factors like BMP-2 and TGF- $\beta$ 3 could be encapsulated into the nanoparticles by mixing during the formation process.

#### Multilayer formation

Nanoparticle coatings on silicon wafers as reference material and on modified electrospun Poly( $\epsilon$ -caprolactone) (PCL) fiber mats were prepared by LbL using a dip-robot and alginate, chondroitin sulfate or hyaluronic acid as polyanions.<sup>3</sup> The resulting films were proven by confocal laser scanning microscopy (CLSM), atomic force microscopy (AFM) and scanning electron microscopy (SEM).

### RESULTS AND DISCUSSION

#### LbL formation of multilayer

Nanoparticles with a well-defined particle size and zeta potential have been obtained after particle formation. The cationic nanoparticles were coated on silicon as a model surface by LbL-technique with different polyanionic interlayers. A linear increase in layer thickness with the number of dipping cycles is observed (Fig. 1).<sup>4</sup> Varying the dipping depth resulted in a concentration gradient on the substrate.

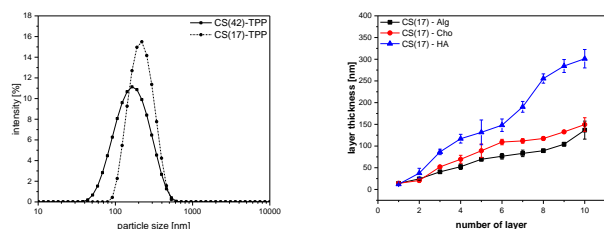


Fig. 1. Particle Size distribution of CS/TPP nanoparticles measured by DLS (left) and ellipsometric film thickness of multilayer films of CS/TPP nanoparticles and various polyanions (right).

By Transferring the multilayer system to modified PCL fibers the construction of multilayers is also possible.<sup>3</sup> Using nanoparticles prepared of different fluorescently labelled Chitosan derivatives the fibers are completely coated. By using alginate as an interlayer a multilayer system is observable because of electrostatic interactions (Fig. 2a).

#### Encapsulation of growth factor proteins

Nanoparticles based on chitosan provide an excellent approach for drug delivery applications<sup>2</sup>. Bone morphogenetic protein 2 (BMP-2) and transforming growth factor beta 3 (TGF- $\beta$ 3) were successfully incorporated with an efficiency over 90%. The release from particles and multilayer systems on PCL fiber mats was investigated by an enzyme linked immunosorbent assay (ELISA).

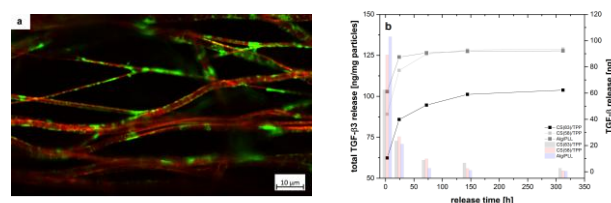


Fig. 2 a) CLSM image of CS/TPP nanoparticles and b) release profile of different chitosan and alginate nanoparticles loaded with transforming growth factor beta 3 (TGF- $\beta$ 3).

### CONCLUSION

It was shown that the combination of nanoparticles obtained by ionotropic gelation as drug release system with the LbL-technique could be an effective method to generate tailored multilayer systems. The encapsulation and release of growth factors like BMP-2 or TGF- $\beta$ 3 were successfully proven by enzyme assays. We are also able to immobilize these nanoparticles systems onto electrospun fiber mat surfaces, which might be used as a first step to prepare spatially implants.<sup>3</sup>

### REFERENCES

- Poth N. et al., *Biomolecules*, 5:3-19, 2015.
- Wang J. J. et al, *Int. J. Nanomedicine*, 6:765-774, 2011.
- de Cassan D. et al., *Colloids Surf. B Biointerfaces*, 163:309-320, 2018.
- Sydow S. et al., submitted.

### ACKNOWLEDGMENTS

This research project has been supported by DFG Research Unit FOR 2180 „Graded Implants for Tendon-Bone Junctions“. We also want to thank Robert Hänsch for CLSM measurements.



## Gentamicin Loaded Poly(d,l-lactide-co-glycolide) Nanoparticles as Drug Delivery Carriers

Katarzyna Reczyńska<sup>1</sup>, Anna-Maria Tryba<sup>1</sup>, Krzysztof Pietryga<sup>1</sup>, Juergen M. Lackner<sup>2</sup>, Elżbieta Pamuła<sup>1\*</sup><sup>1</sup>AGH University of Science and Technology, Faculty of Materials Science and Ceramics, Department of Biomaterials and Composites, Al. Mickiewicza 30, 30-059 Kraków, Poland<sup>2</sup>JOANNEUM RESEARCH Forschungsgesellschaft mbH MATERIALS - Institute of Surface Technologies and Photonics, Laser and Plasma Processing, Leobner Straße 94, 8712 Niklasdorf, Austria  
corresponding author: [epamula@agh.edu.pl](mailto:epamula@agh.edu.pl)**INTRODUCTION**

Resorbable nanoparticles are versatile drug delivery systems. Poly(d,l-lactide-co-glycolide) (PLGA) nanoparticles can be loaded with antibiotics [1], anticancer drugs [2] or other biologically active molecules [3]. One of the biggest advantages of PLGA drug carriers is that degradation rate of the polymer depends on co-monomer ratio [4]. Thus by selection of PLGA type it is possible to control the kinetics of drug release and to adjust nanoparticles for specific needs. In this study we aim to obtain PLGA nanoparticles loaded with gentamicin (Gent) providing required doses of the drug. Such nanoparticles can be further used as suspension in water or in hydrogels or attached on the surface of metallic implants to provide antibacterial properties or treat tissue infections.

**EXPERIMENTAL METHODS**

PLGA nanoparticles loaded with gentamicin (Gent) were fabricated using emulsification/solvent evaporation method. PLGA copolymers of different d,l-lactide to glycolide monomer ratios (50:50, 75:25 and 85:15, Corbion, Purac) mixed with 5% or 10% w/w Gent were dissolved in dichloromethane (DCM) at 1.67% concentration. 6 ml of PLGA/DCM solution was then added dropwise into ice-cold 15 ml of 4% polyvinyl alcohol (PVA, Mowiol 4-88, Sigma-Aldrich) aqueous solution and homogenized using ultrasound probe (3 min, 40% amplitude). As prepared nanoemulsion was stirred using magnetic stirrer for 24 h until complete evaporation of DCM. Then, nanoparticle suspension was collected and purified by repeated centrifugation (15000 rpm, 20 min, 4°C) and rinsing with UHQ-water. Nanoparticles were freeze-dried for 24 h and stored at 4°C.

The size and morphology of prepared nanoparticles were determined using atomic force microscopy (AFM) and dynamic light scattering (DLS). Drug loading efficiency was determined spectrophotometrically using OPA assay. Drug release studies were performed with nanoparticles suspended in PBS using Amicon tubes (MWCO 14 kDa). The tubes were placed on mechanical stirrer and incubated at 37°C for up to 1 month. The amount of Gent released to PBS was determined using OPA assay.

**RESULTS AND DISCUSSION**

Fabricated PLGA nanoparticles were spherical in shape (Fig. 1A) and their size determined by DLS method was between 120-180 nm (Fig. 1B). All types of nanoparticles were very uniform in size with polydispersity index below 0.3.

Gent loading efficiency was around 55-75%. The initial burst release of Gent was present in all types of PLGA nanoparticles, however significant differences were observed in longer time periods between PLGA nanoparticles of different monomer ratios. PLGA 50:50 nanoparticles degraded faster than PLGA 75:25 and 85:15, what resulted in enhanced release of Gent.

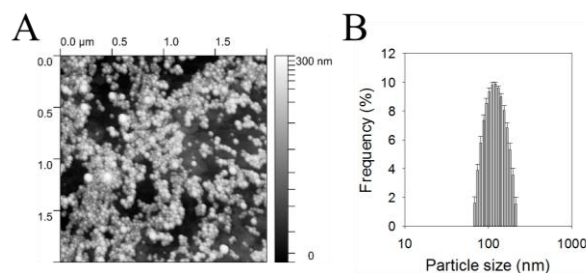


Fig. 1. PLGA 85:15 nanoparticles: (A) AFM image, (B) particle size distribution.

**CONCLUSION**

PLGA nanoparticles of uniform size distribution and high Gent loading efficiency were fabricated using emulsification/solvent evaporation method. Degradation rate of nanoparticles and in consequence drug release behavior were determined by PLGA composition (ratio of DL-lactide to glycolide co-monomers). It is possible to adjust the properties of PLGA nanoparticles to precisely control drug release kinetics.

In the future, PLGA nanoparticles can be used alone as injections (for localized drug delivery), suspended in hydrogels or utilized for modification of various polymeric, ceramic or metallic implants.

**REFERENCES**

1. Posadowska, U., M. Brzywczy-Włoch, and E. Pamuła, *Gentamicin loaded PLGA nanoparticles as local drug delivery system for the osteomyelitis treatment*. Acta of bioengineering and biomechanics, 2015. **17**(3).
2. Tabatabaei Mirakabad, F.S., et al., *A Comparison between the cytotoxic effects of pure curcumin and curcumin-loaded PLGA-PEG nanoparticles on the MCF-7 human breast cancer cell line*. Artificial cells, nanomedicine, and biotechnology, 2016. **44**(1): p. 423-430.
3. Mody, N., et al., *Dendrimer, liposomes, carbon nanotubes and PLGA nanoparticles: one platform assessment of drug delivery potential*. Aaps Pharmscitech, 2014. **15**(2): p. 388-399.
4. Lu, L., C.A. Garcia, and A.G. Mikos, *In vitro degradation of thin poly (DL-lactic-co-glycolic acid) films*. Journal of Biomedical Materials Research: An Official Journal of The Society for Biomaterials, The Japanese Society for Biomaterials, and The Australian Society for Biomaterials, 1999. **46**(2): p. 236-244.

**ACKNOWLEDGMENTS**

This study was supported by M.ERA.NET project "SPD-BioTribo"

## Characterization of compound loading into polymer nanospheres for dermal applications

Rose Soskind<sup>1,2</sup>, [Bozena B. Michniak-Kohn](mailto:michniak@pharmacy.rutgers.edu)<sup>1,2,3</sup>

<sup>1</sup>Center for Dermal Research, <sup>2</sup>Ernest Mario School of Pharmacy, <sup>3</sup>New Jersey Center for Biomaterials  
Rutgers, The State University of New Jersey, Piscataway, NJ 08854

[michniak@pharmacy.rutgers.edu](mailto:michniak@pharmacy.rutgers.edu)

### INTRODUCTION

Biodegradable polymers that can self-assemble into nano-sized structures define an important platform for topical drug delivery system carriers. Furthermore, dermal drug delivery offers several advantages over routes of delivery including avoidance of hepatic first pass effect, increased patient compliance and avoidance of gastro-intestinal issues.

In this study, it was found that TyroSpheres, developed at the New Jersey Center for Biomaterials at Rutgers University, provide highly effective nano-sized structures for lipophilic compound encapsulation. These nanoparticles have been shown to deliver drugs preferentially to the upper skin layers, thus having the promise of increased medical efficacy and safety of drugs for treating skin disorders.

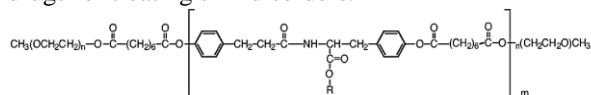


*Fig. Tyrosine-derived polymer used as a component of the TyroSpheres*

Preliminary studies with TyroSpheres conducted with the antioxidants quercetin and vitamin E (as  $\alpha$ -tocopherol) and the immunosuppressant tacrolimus have demonstrated significant differences in drug loading capacity into TyroSpheres. These drugs were loaded into TyroSpheres in order to address stability and irritation issues and to evaluate delivery of these compounds to the skin layers *in vitro*. Dynamic light scattering showed that the size of nanospheres in solution was about 40-45 nm, with low variation based on a poly-dispersity index of <0.2 observed throughout these studies. The hydrodynamic size remained consistent after leaving the nanospheres at 25°C for 30 days. Transmission electron microscopy images confirmed the presence of nanosphere structures. Although quercetin has a smaller molecular weight than vitamin E and tacrolimus, it was found to have a much lower maximum loading of about 5% weight/weight for initial drug feed, versus vitamin E and tacrolimus which had greater than 50% weight/weight loading. Fourier-transform infrared spectra demonstrated spectral changes between empty and drug-loaded TyroSpheres, indicating the occurrence of polymer-drug interactions. TyroSpheres loaded with varying drug concentrations will be further explored in *in vitro* drug release, skin permeation, and cell irritation studies. Results of these studies will be applied to developing topically applied TyroSphere formulations for treating a variety of skin disorders, including atopic dermatitis and alopecia areata, both of which are currently associated with a low quality of life and limited treatment options.

## Edible Biopolymers Films and Coatings Prepare from Cactus Mucilage and Whey Protein

Jolanta E. Marszalek, Erika Flores Loyola, Jorge A. De La Rosa Martínez

Facultad De Ciencias Biológicas, Universidad Autónoma De Coahuila, Mexico

[jolamar@yahoo.com](mailto:jolamar@yahoo.com)

### INTRODUCTION

Replacing the oil-based packaging materials with biobased films and coatings gives not only competitive advantage due to more sustainable and greener preparation, but also addresses the concerns regarding the disposal of synthetic plastic.<sup>1</sup> Bioplastics generated from renewable agricultural products are readily degraded after their disposal. In addition, these bio-based materials can be used as edible coatings to extend life of produce and decrease amount of food waste. The success of an edible coating strongly depends on its barrier property to moisture, oxygen, and CO<sub>2</sub>. Several edible coatings based on cellulose, casein, zein, soy protein, and chitosan, have shown such desirable characteristics.<sup>2</sup> The nopal *Opuntia ficus indica* is the most widespread *Opuntia* in the world.<sup>3</sup> The mucilage from *Opuntia ficus indica* is an interesting and promising material with emulsifying properties.<sup>4</sup> Chemical composition of this mucilage is a complex mixture of polysaccharides including D-galactose, L-arabinose, D-xylose, and L-rhamnose and D-galacturonic acid.<sup>5</sup> The average molecular weight is between  $2.3 \cdot 10^4$  and  $4.3 \cdot 10^6$  Da.<sup>5</sup> The composition and rheological characteristics of *Opuntia* mucilage allow its potential use as edible films, degradable plastic biofilms<sup>6</sup>, flexible and rigid packaging materials. On the other hand edible films and coatings based on whey proteins show great potential for oxygen-sensitive products especially when used with nanofiller that improves its barrier properties.<sup>9</sup> Here we report polymer coatings based on bend of nopal mucilage and whey protein both form natural source from local area.

### EXPERIMENTAL METHODS

The nopal cladodes were collected in June from 2- to 3-year-old plants growing in Torreon, Coah, MX. To extract mucilage 600gr of cactus was washed and cut into small pieces, then placed in 3L of water and left for 24hr. Next the liquid was filtered and stored at 4°C. The mucilage content was determined to be 0.27%. Whey protein was obtained as by product of panela cheese production. The whey base was centrifuged for 15 minutes at 10000 rpm at 4°C and then frozen to separate remaining fat (0.34%). Films were cast in Petri dish from the unmodified solutions and mixes of the two solutions in various ratios. The films were dried overnight in an oven at 45°C. Coating on the fruit was made by dipping the fruit in coating solution for 30 s, the excess coating was drained and the coated fruit were dried for 30 min at 20°C. After the coating process, fruit was stored at 5°C for 10 days. The films were analysed by IR spectroscopy and microscopy. Fruit was analysed in regards to firmness, colour and appearance.

### RESULTS AND DISCUSSION

The preliminary results show that the prepared films give a good coverage of the surface. They have good adherence thus a coating of Teflon needs to be used to allow detachment for further analysis. IR analysis of the mucilage and whey films shows broad peak 2400-3500cm<sup>-1</sup> from NH, OH stretch. In mucilage film other stretching vibration band 1606 cm<sup>-1</sup> is due to asymmetric stretching of the carboxylic C=O double bond. A 1515 cm<sup>-1</sup> is of phenolic -OH and -C=O stretching of carboxylates. A 1380 cm<sup>-1</sup> band could be stretching vibration of -COO. Mixed film shows bands reflecting both materials.

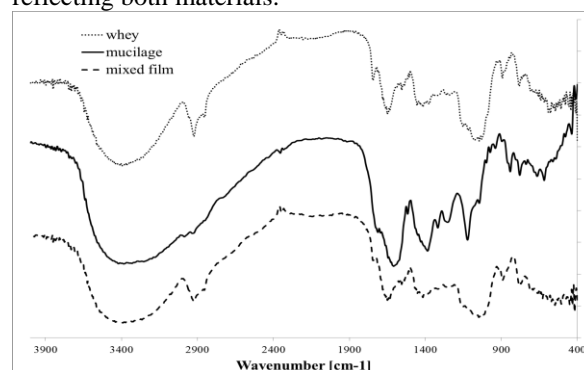


Fig. 1. IR of films prepared from mucilage, whey and mixture 1:9, mucilage : whey.

When the fruit was covered with protecting coating the firmness increased by about 50% similar as seen by Del-Valle.<sup>7</sup> This difference in firmness was sustained in subsequent days proving that these coatings are good candidates for application as edible coating.

### CONCLUSION

Mucilage from nopal could represent a good option for the development of biodegradable films and edible coatings in countries, such as Mexico, where nopal is highly produced at low cost, constituting a processing alternative for nopal, and a source of economic resources for low income communities. The films have good film forming properties and can be modified in regard to their flexibility and permeability. Combination with whey protein the properties change and present additional option as an edible coating. Fruit coating showed to improve their firmness and sustain color over the storage period.

### REFERENCES

1. Vartiainen, J. *et al.* Mater. Sci. Appl.5:708-718, 2014
2. Lin, D. *et al.* Compr. Rev. Food Sci. Food Saf.6: 60-75, 2007
3. Ingles, P. *et al.* In Cacti biology and uses; Nobel, P. S., Ed.; UNIVERSITY OF CALIFORNIA PRESS: Berkeley, Los Angeles, London, 2002; pp 163–183.
4. Medina-Torres, L. Food Hydrocoll.14:417-424, 2000
5. Medina-Torres, L.; *et al.* Carbohydr. Polym 52:143-150, 2003
6. Espino-Diaz, M. *et al.* J. Food Sci.75: 347-352, 2010
7. Del-Valle, V. *et al.* J. Food Chem.91: 751–756, 2005
9. Schmid, M. *et al.* Front. Mater 4: 1–15, 2017

## Synthesis of Poly(Lactic-co-Glycolic Acid) Based Biomaterials and Study of Wettability of Their Films

Muhammad Ayyoob, Xin Yang, Young Jun Kim\*

Department Chemical Engineering, Sungkyunkwan University, South Korea  
[mayyoob@skku.edu](mailto:mayyoob@skku.edu), [\\*youngkim@skku.edu](mailto:*youngkim@skku.edu)

### INTRODUCTION

Poly(D,L-lactide-co-glycolide) (PLGA) based copolymer is one of the most widely investigated biomaterials. PLGA has gain considerable attention of researchers due to its tailored biodegradability, bioresorption, biocompatibility, non-toxic and controllable degradation profile by means of monomer ratios. High molecular weight PLGA usually synthesized via ring opening copolymerization of lactide and glycolide diesters<sup>1</sup>. But synthesis of lactide and glycolide from oligomers of lactic acid and glycolic acid is a complex, multistep and costly process<sup>2</sup>. Direct esterification is a suitable alternative synthetic route but not well established yet due to poor thermal stability of PLGA<sup>3</sup>. In the present work, a series of high molecular weight PLGA copolymer were synthesized and characterized for thermal transition properties, NMR spectroscopic studies and hydrophobicity of PLGA films.

### EXPERIMENTAL METHODS

#### Materials

Glycolic acid, chloroform, tetrahydrofuran(THF), tin(II) chloride dihydrate and methanesulfonic acid were purchased from Sigma Aldrich, Korea. DL-lactic acid 85% to 90% aqueous solution procured from Alfa Aesar. HFIP was purchased from Fluorochem Ltd., UK.

#### Synthesis of copolymer

PLGA was synthesized with different monomer compositions of LA:GA, as 90:10, 80:20, 70:30, 60:40 and 50:50. In a typical synthesis procedure, pre-determined moles of glycolic acid and DL-lactic acid were added to 250 ml three-neck flask, equipped with a mechanical stirrer and a vacuum line. The reaction mixture was dehydrated for four hours at 120°C, then raised to 140 to 160°C. SnCl<sub>2</sub>·2H<sub>2</sub>O and MSA (1:1 MSA:SnCl<sub>2</sub>·2H<sub>2</sub>O) were also added to the reaction mixture at this stage. After predefined reaction time, the reaction was stopped by taking out flask from the oil bath, the polymer was taken out of from the flask characterized.

#### Characterization

The inherent and intrinsic viscosities of the PLGA were determined at 30°C, with 0.5 dl/g in chloroform or THF. The viscosity average molecular weight was calculated, using Mark-Houwink constants of K and α. For thermal properties differential scanning calorimetry (DSC) using DSC Q20, TA Instruments and thermogravimetric analysis (TGA) using TGA7, Perkin-Elmer analyser. <sup>1</sup>H nuclear magnetic resonance (NMR) spectroscopy was performed in order to determine the molar ratios PLGA copolymers. Deuterated chloroform (CDCl<sub>3</sub>) was used as a solvent for <sup>1</sup>H-NMR spectroscopy and performed at Bruker NMR 400mhz.

#### Film preparation and Water contact angle measurement of PLGA copolymers

Polymer films were prepared via solvent casting in chloroform with 1g/10 ml concentration. The solution was poured into a glass petri dish and kept at room temperature for 3 days. Films were then further dried under vacuum at 30°C for 24 hours. Water contact angle was measured using an imaging camera CAMLN-13S2M-CS made by “Point Grey” USA and distilled water. Films pasted on the glass slides by a double-sided adhesive tape prior to measurements.

### RESULTS AND DISCUSSION

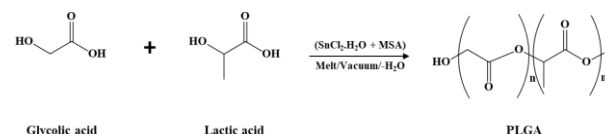


Fig.1. Synthesis Scheme of PLGA Copolymers

PLGA copolymers were synthesized as described in synthesis scheme in Fig. 1. All synthesis and characterization results are presented in Table 1.

Table 1. Synthesis of PLGA and Properties of Copolymers.

PLGA	Time	$\eta^*$	$M_v$	$T_g$	WCA	Film Thickness	$P_{GA} = I_G / (2I_L + I_G)$
LA/GA	(Hrs)	(dl/g)	(g/mol)	(°C)	(degree)	(mm)	% GA Unit
100/0	48	0.83	130,000	70	85.9	0.10	16.7
90/10	20	0.57	79,000	55	73.3	0.11	22.1
80/20	20	0.45	58,000	51	72.0	0.18	31.9
70/30	48	0.81	125,000	48	69.0	0.12	31.9
60/40	20	0.47	77,000	48	66.8	0.15	N/D
50/50	20	0.56	61,000	44	61.0	0.17	55.5
50/50**	120	0.85	133,000	N/D	N/D	N/D	61.3

\* intrinsic viscosity

\*\* at 140 oC for 120 hours, all other synthesize at 165 oC for several hours.

Viscosity average molecular weight was determined using Mark-Houwink's constants of K and α from Kenley's equation:

$$[\eta] = (1.07 \times 10^{-4}) M_v^{0.761} \quad (1)^{4,5}$$

### CONCLUSION

High molecular weight PLGA was synthesized via direct esterification under mild conditions. At maximum, 133k g/mol. molecular weight was achieved in 120 hours at 140°C. Hydrophobicity decreased with an increase of glycolic acid molar ratio.

### REFERENCES

1. Ao Q. G. *et al.* Polymer J. 34:786-793, 2002
2. Yin H. *et al.* J Appl Polym Sci. 41566:1-6, 2015
3. Lan P. *et al.* J Appl Polym Sci 92:2163-8, 2009
4. Ouyang C. *et al.* Polym Bull. 67:793-803, 2010
5. Richard A K. *et al.* Macromolecules. 20:2398-403

### ACKNOWLEDGEMENT

This work was supported by the Technology Innovation Program, (Contract number: 10077004, “Development of high-strength/bio-resorbable polyglycolic acid-based block copolymers and their reinforced composite with a tensile strength of 120 MPa or higher for spinal fixation” funded by the Ministry of Trade, Industry & Energy of Korea.



## Controlled Degradation Time of Polylactide and Polypropylene

Ewelina Niedzielska, Anna Masek

Department of Chemistry, Institute of Polymer and Dye Technology, Lodz University of Technology, Poland  
[ewelina.niedzielska@edu.p.lodz.pl](mailto:ewelina.niedzielska@edu.p.lodz.pl)

### INTRODUCTION

Currently, polymeric materials are widely used in many sectors of the economy. Almost half of the polymers are used for the production of packaging. The most common for this purpose are conventional polymers such as polyethylene, polypropylene or polystyrene. These materials, despite their excellent properties, after use, they do not decompose in the natural environment, contributing for the generation of waste. The solution to the problem may be the use of biodegradable polymers that are environmentally friendly and consumer friendly. The processing and usage characteristics of polymers from renewable sources are comparable with the characteristics of polymers of petrochemical origin.

### EXPERIMENTAL METHODS

The aim of our work was to conduct accelerated UV ageing of extruded polylactide (Ingeo™ biopolymer 4043D, NatureWorks, USA) and polypropylene samples, comparison and examination of the impact of the degradation process on their properties. We performed FTIR spectral analyzes. We carried out a color change test, measurement of contact angle and measurement of Vicat's softening temperature. We made the surface analysis using SEM and a stereoscopic microscope.

#### UV ageing

We installed samples of PP and PLA in the Atlas 2000 UV device. A single measurement lasted 360 minutes and consisted of two alternating segments: daily (duration: 240 min., T= 60°C, intensity: 0.7 W / m<sup>2</sup>) and night time (duration: 120 minutes, T= 50°C, without UV radiation). The ageing time was up to 800h.

### RESULTS AND DISCUSSION

The value of the  $dE^*ab$  coefficient allows to determine influence ageing on the color of the polymer. On the graph (Fig. 1) we showed change color of the  $dE^*ab$  coefficient for PLA and PP samples changes after 800h UV ageing.

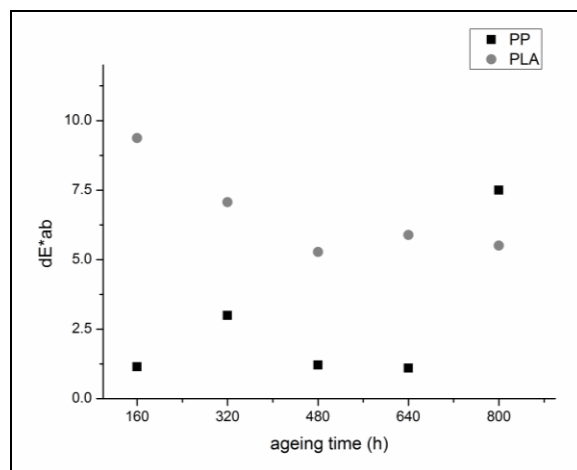


Fig. 1. Coefficient  $dE^*ab$  of polylactide PLA and polypropylene PP samples after 800h UV ageing

### CONCLUSION

Poly lactide could be successfully used as a packaging material for food or disposable products. Production of biodegradable packaging it could help to solve the global storage problem to a significant extent and waste disposal.

### ACKNOWLEDGMENTS

This study was supported by the National Centre for Research and Development (NCBR) project: LIDER/32/0139/L-7/15/NCBR/2016.

## The Influence of Soft Segments on Properties of New Segmented Polyurethanes Based on Cycloaliphatic Diisocyanate

Andrzej Puszka

Maria Curie-Skłodowska University, Faculty of Chemistry, Department of Polymer Chemistry,  
Gliniana 33, 20-614 Lublin, Poland

[andrzej.puszka@umcs.pl](mailto:andrzej.puszka@umcs.pl)

### INTRODUCTION

The purpose of this article was the synthesis and characterization of new segment polyurethanes derived from a cycloaliphatic diisocyanate, i.e. 1,1'-methanediybis(4-isocyanatocyclohexane) (HMDI, *Desmodur W*<sup>®</sup>) and a non-conventional chain extender, i.e. 2,2'-methylenebis[(4,1-phenylene)methylene-sulfanediy]diethanol (diol E). Soft segments were poly(oxytetramethylene) diol of  $\overline{M}_n=1000$ g/mol (PTMO-1000) and 2000g/mol (PTMO-2000), poly(hexamethylene carbonate) diol of  $\overline{M}_n=860$ g/mol (PWH-860), polycarbonate diol of  $\overline{M}_n=2000$ g/mol (WD-2000, *Desmophen C2200*<sup>®</sup>) and poly( $\epsilon$ -caprolactone) diol of  $\overline{M}_n=2000$ g/mol (PCL-2000). Using the method of catalyzed single-stage polyaddition in the alloy and the above substrates, segmental polyurethanes with a ~50 wt% of hard segments content were obtained. Designations of the synthesized polymers were as follows: TPU derived from PTMO-1000: P1, PTMO-2000: P2, PWH-860: W1, WD-2000: W2, PCL-2000: K.

### EXPERIMENTAL METHODS

Attenuated total reflection Fourier transform infrared (ATR-FTIR) spectra were obtained with a FTIR TENSOR 27 (Bruker) spectrophotometer using thin films. Spectra were recorded from 4,000 to 600  $\text{cm}^{-1}$  averaging 32 scans with a resolution of 4  $\text{cm}^{-1}$ . Refractive index was measured at 23°C by using Conbest Abbe's Refractometer Type 325 instrument according to method A of European Standard EN ISO 489:1999. 1-Bromonaphthalene was applied between the sample film and the prism shield. TG was performed with a Netzsch STA 449 F1 Jupiter thermal analyzer (Germany) in the range 40-700°C in helium (gas flow=20 $\text{cm}^3/\text{min}$ ) and a t the heating rate of 10°C/min. Sample masses of about 10 mg were used. All measurements were taken in  $\text{Al}_2\text{O}_3$  crucibles (with mass about 160 mg) and as a reference empty  $\text{Al}_2\text{O}_3$  crucible was employed. DSC thermograms were obtained with a Netzsch 204 calorimeter (Günzburg, Germany) in the range of -100–200°C. The reported transitions were taken from first and second heating scans. The scans were performed at the heating/cooling rate of 10°C/min under nitrogen atmosphere (flow = 30  $\text{cm}^3/\text{min}$ ). Sample masses of about 10 mg were used. Glass-transition temperatures ( $T_g$ s) for the polymer samples were taken as the inflection point on the curves of the heat-capacity changes. All DSC measurements were taken in aluminum pans with pierced lid (mass of 40  $\pm$  1 mg). As a reference, empty aluminum crucible was applied. The ultraviolet-visible (UV-VIS) spectra of the compression-molded sheets of the SPURs were determined by a UV-2550 (Shimadzu, Kioto, Japan)

UV spectrophotometer at a scanning rate of 200 nm/min in the range of 200–900 nm. The hardness of the SPURs was measured by the Shore A/D method on a Zwick 7206/H04 hardness tester (Germany) at 23°C. The values were taken after 15s. Tensile testing was performed on a Zwick/Roell Z010 tensile-testing machine according to Polish Standard PN-81/C-89034 at the speed of 100 mm/min at 23°C; the tensile test pieces 1 mm thick and 6 mm wide (for the section measured) were cut from the pressed sheet. Press moulding was done with a Carver hydraulic press (USA) at 80–130°C under 10–30MPa pressure. The single lap-shear strength of the polymers to copper plate, 100 mm x 25 mm x 1.5 mm, was measured in accordance with Polish Standard PN-EN 1465:2009 by using a Zwick/Roell Z010 (Germany). The adhesive joint, 12.5 mm x 25 mm x 0.2 mm, was prepared by pressing the polymer between the ends of two copper plates (prepared according to PN-EN-13887:2005), and then leaving them under a pressure of 30 MPa to cooling to room temperature. Next, plates were fixed by tensile-testing machine clips and underwent tensile testing at speed of 2 mm/min at 23°C.

### RESULTS AND DISCUSSION

The polymers obtained were colorless, transparent materials with transmittance values from 71.2 to 88.0% (at 800nm), which varied depending on the soft segment used. DSC analysis showed that the polymers obtained were amorphous with glass transitions temperatures ( $T_g$ ) ranging from -76°C to 28°C. The lowest value of  $T_g$  and thus the best microphase separation was shown by the P2. Polymers with polycarbonate soft segments had  $T_g$  values at the border of elastomers and plastomers. All TPUs were characterized by relatively good thermal stability (temperatures of 1% of the mass loss were in the range of 248-271°C), wherein the least stable being the polymer with a polycaprolactone soft segment (K). The remaining polymers showed similar thermal stability. The tensile strengths were in the range of 8.75-51.2 MPa; elongations at break 275-525% and the modulus of elasticity were in the range of 0.34-54.8 MPa. The hardness of the obtained polymers ranged from 55-94°Sh (scale A) and 16-48°Sh (scale D). Of all TPUs, both the highest tensile strength and hardness had the polymer obtained with WD-2000 as a soft segment. The obtained TPUs also showed adhesions to copper in the range of 3.26-13.86 MPa and refractive indexes values in the range of 1.516-1.531.

### CONCLUSION

The study showed that the type of soft segments used for the synthesis of TPUs had a significant effect on the properties of the polymers.

## Physicochemical and Biological Properties of Biomimetic Hydrogel Materials for Tissue Engineering Application

Adriana Gilarska<sup>1,2</sup>, Joanna Lewandowska-Łańcucka<sup>1</sup>, Maria Nowakowska<sup>1</sup>

<sup>1</sup>Faculty of Chemistry, Jagiellonian University, Gronostajowa 2, 30-387 Kraków, Poland

<sup>2</sup>Faculty of Physics and Applied Computer Science, AGH University of Science and Technology, Mickiewicza 30, 30-059 Kraków, Poland

[adriana.gilarska@vp.pl](mailto:adriana.gilarska@vp.pl)

### INTRODUCTION

Design and research of polymeric hydrogel materials increased their potential in biomedical applications and enabled the development of significant advances in tissue engineering<sup>1</sup>. Hydrogels exhibit the ability to swell, biocompatibility, high content of water and flexibility. These properties make them suitable materials as scaffolds for tissue regeneration<sup>2</sup>.

This work presents the results of our study on biomimetic injectable hydrogel materials for tissue engineering application. Components of hydrogels were the biopolymers – collagen, chitosan and hyaluronic acid that are commonly used for that purpose<sup>3,4</sup>, due to their presence in many mammalian tissues (collagen, hyaluronic acid) and structural similarity to natural glycosaminoglycans (chitosan)<sup>5</sup>.

### EXPERIMENTAL METHODS

Collagen/chitosan and collagen/chitosan/hyaluronic acid hydrogels were obtained. The crosslinking agent in these systems was genipin. Various concentration of crosslinking agent (2, 10 and 20 mM) as well as different content of biopolymers were tested.

Swelling and degradation properties of developed structures were determined. Obtained materials were also characterized by FTIR spectroscopy, contact angle measurements (wettability) and SEM imaging (microstructure). Cytotoxicity testing of hydrogel materials was studied using the MG-63 cell line and the Alamar Blue assay. Cell morphology was examined by SEM observations.

The results were expressed as a mean  $\pm$  standard deviation. Statistical significance was calculated using the one-way Analysis of Variance (ANOVA) with Tukey's honestly significant difference post hoc test and Student's t-test.

### RESULTS AND DISCUSSION

Optimization of hydrogels composition showed that physicochemical properties of these materials depend on the concentration of genipin and the hyaluronic acid amount. All hydrogels tested are the hydrophilic materials and show high swelling ratio. These properties are significant for tissue engineering applications. Hydrogels with the highest genipin concentration (20 mM) exhibited compact structures and prolonged degradation. Content of hyaluronic acid in studied structures influences on degree of the wettability. Preliminary biological studies demonstrated that obtained materials are biocompatible and can support the proliferation of MG-63 cell line, that is very important considering their potential biomedical applications.

### CONCLUSION

Genipin-crosslinked hydrogels based on biopolymers – collagen, chitosan and hyaluronic acid were obtained. Significant properties for scaffolding design such as swelling, wettability, degradation, morphology and biocompatibility were investigated. The results of our study demonstrated that chemically crosslinked hydrogels synthesized from collagen, chitosan and hyaluronic acid can be promising and worth attention materials for the scaffold preparation and regeneration of small tissue defects.

### REFERENCES

1. Dhandayuthapani B. *et al.*, Int. J. Polym. Sci. 2011, 290602, 2011
2. Kopecek J. *et al.*, Biomaterials, 28(34):5185–5192, 2007
3. Sionkowska A. *et al.*, Int J. Biol. Macromol. 89:442-448, 2016
4. Fiejdasz S. *et al.*, Biomed. Mater. 8, 035013, 2013
5. Lewandowska K. *et al.*, J. Mol. Liq. 220:726-730, 2016

### ACKNOWLEDGMENTS

JL-Ł acknowledges the financial support of National Science Centre, Poland, grant 2016/21/D/ST5/01635.

## Barrier Properties of Bilayer Films of FucoPol and Chitosan

Ana Rita Ferreira<sup>1</sup>, Vítor Alves<sup>2</sup>, Isabel Coelhoso<sup>1</sup>

<sup>1</sup>LAQV-REQUIMTE, Dep. Química, FCT, Universidade NOVA de Lisboa, Portugal

<sup>2</sup>LEAF – Linking Landscape, Environment, Agriculture and Food, ISA, Universidade de Lisboa, Portugal  
[imrc@fct.unl.pt](mailto:imrc@fct.unl.pt)

### INTRODUCTION

Polysaccharides have been widely used for edible and/or biodegradable films development. FucoPol is a fucose-rich exopolysaccharide produced by the bacterium *Enterobacter*<sup>1</sup>. FucoPol films have been reported to be transparent, with brown tone, hydrophilic with high permeability to water vapor and good barrier properties to gases (CO<sub>2</sub> and O<sub>2</sub>)<sup>2</sup>. Chitosan is derived from chitin, which is the most abundant natural amino polysaccharide in nature. Improvement in mechanical properties, better performance in terms of water vapor permeability and lower water solubility have been reported for blends and bilayer films of chitosan with starch, pectin or alginate<sup>3</sup> comparing to chitosan stand-alone films.

In this context, the aim of the present study is to develop bilayer films of chitosan and FucoPol and characterize them in terms of their barrier properties to O<sub>2</sub> and CO<sub>2</sub>, envisaging their potential use in food and biomedical applications.

### EXPERIMENTAL METHODS

Bilayer films were prepared by a two-step coating technique. Firstly, a FucoPol solution (1.5% w/w) with citric acid (50% w/w) was cast onto a Teflon petri dish and dried at 30 °C until a firm but still adhesive surface was obtained. Then, a chitosan solution (1.5% w/w) with glycerol (50% w/w) and citric acid (50% w/w), was cast on the top of FucoPol film and both layers were dried at 30 °C during 24 h<sup>4</sup>. The gas permeability tests were carried out using a stainless steel cell with two identical chambers separated by the film. The permeability was evaluated by pressurizing one of the chambers (feed) up to 0.4 bar, with pure gas, either carbon dioxide (99.998%) or oxygen (99.999%) (Praxair, Spain), followed by the measurement of the pressure change in both chambers over time, using two pressure transducers (JUMO, Model 404327, Germany). The temperature was maintained constant at 30°C, using a thermostatic bath (Julabo, Model EH, Germany). The permeability was calculated by Eq.1, using five independent measurements:

$$\frac{1}{\beta} \left( \frac{\Delta p_0}{\Delta p} \right) = P \frac{t}{\delta} \quad (1)$$

where  $\Delta p$  (mbar) is the pressure difference between feed and permeate compartment,  $P$  (mol/msPa) is the gas permeability,  $t$ (s) is the time,  $\delta$ (m) is the film thickness and  $\beta$  is the geometric parameter of cell.

### RESULTS AND DISCUSSION

The oxygen permeability of the FucoPol, chitosan and the bilayer films are one order of magnitude lower than their carbon dioxide permeability values (Table 1).

Bilayer films presented a significantly higher barrier to O<sub>2</sub> than the control films, with an O<sub>2</sub> of 0.47x10<sup>-16</sup> mol/msPa. In any case, the values are always bellow 1 barrer, which is equal to 3.34 x 10<sup>-16</sup> mol/msPa. Regarding the barrier behavior to CO<sub>2</sub>, bilayer films presented a permeability of 5.8x10<sup>-16</sup> mol/msPa, which is significantly lower from that of chitosan films. Comparing the FucoPol/chitosan bilayer with synthetic polymer LDPE, it is perceived significantly higher barrier properties, both to O<sub>2</sub> and to CO<sub>2</sub>. However, the barrier properties of the bilayer are still lower than that of ethylene vinyl alcohol (EVOH) films, one of the better gas barriers, with permeability to O<sub>2</sub> of 0.24x10<sup>-16</sup> mol/msPa.

Table 1. O<sub>2</sub> and CO<sub>2</sub> permeability

Film	O <sub>2</sub> (10 <sup>-16</sup> mol/msPa)	CO <sub>2</sub> (10 <sup>-16</sup> mol/msPa)	Ref.
FucoPol	1.93	6.5	[4]
Chitosan	2.35	15.0	[4]
Bilayer	0.47	5.8	[4]
HDPE	2.20	35.5	[5]
EVOH 29	0.24	0.165	[6]

### CONCLUSION

Bilayer films of FucoPol and chitosan have shown excellent barrier properties to O<sub>2</sub> and CO<sub>2</sub>. The bilayer films revealed to be significantly less permeable to O<sub>2</sub> than single FucoPol and chitosan films. Such properties, together with their production from renewable resources, biodegradability and nontoxicity, make these bilayer films good candidates to be used in food and biomedical applications requiring low oxygen content.

### REFERENCES

- Torres C. *et al.*, J. Biotech., 156:261-267, 2011.
- Ferreira A. *et al.*, Int. J. Biol. Macr., 71:111-116, 2014.
- Luo, Y. *et al.*, Int. J. Biol. Macr., 64: 353-367, 2014.
- Ferreira A. *et al.*, Carb. Polym. 147:8-15, 2016.
- Ullsten N. *et al.*, Polym.Test., 22: 291-295, 2003.
- Cerisuelo J. *et al.*, J. Membr. Sci., 423: 247-256, 2012.

### ACKNOWLEDGMENTS

This work was supported by Fundação para a Ciência e Tecnologia (FCT), Portugal, through projects UID/Multi/04378/2013, UID/QUI/50006/2013, PEst-OE/AGR/UI0245/2014 and Ana Rita Ferreira by PhD fellowship SFRH/BD/79101/2011.



## Influence of Friction on Hydrolytic Degradation Polymeric Biomaterials

Wojciech Karalus, Jan Ryszard Dąbrowski

Department of Materials and Productions Engineering,  
Faculty of Mechanical Engineering, Białystok University of Technology, Poland

[w.karalus@doktoranci.pb.edu.pl](mailto:w.karalus@doktoranci.pb.edu.pl)

### INTRODUCTION

Polymer degradation is an irreversible process leading to significant changes in their structure and properties. It can be caused by physical factors (photodegradation), chemical (oxidation, hydrolysis) or biological (biodegradation). Often these factors occur simultaneously. There is little data on the effect of mechanical stresses generated in a polymeric material on degradation processes. The frictional processes, especially in the kinematic joints of the structure, can also have a significant effect on the degradation of polymers. This applies in particular to medical devices, whose durability and reliability to a large extent determine the quality of treatment or rehabilitation of patients.

### EXPERIMENTAL METHODS

The research was based on polyurethane materials synthesized on the basis of: 4,4'-dicyclohexylene oxide diisocyanate (HMDI), polycaprolactanediol (PCL), and ethylene glycol (sample A) or glycerol (sample B) was used as the chain extender. The tests were carried out on a biotribometer that was provided by the Białystok University of Technology. The friction pair was made of cylindrical samples with a diameter of 6 mm and a disc made of inert corundum ceramics. The samples were subjected to friction tests for 2 hours a day for 56 days. Confocal microscope was used for surface observations of tested samples.

### RESULTS AND DISCUSSION

After the 14th day of friction tests, the friction coefficient of samples A and B started destabilize, as shown in the graph above. The coefficient of friction for sample A increased by oscillating around 0.35-0.42, while for sample B the friction coefficient decreased by oscillating between 0.31 and 0.36 in relation to the results carried out within the first 7 days (Fig. 1). Probable cause of changes in the coefficient of friction change in the internal structure of the tested polymers, which is particularly visible after the 14th day of friction tests. This may be evidence of the accelerated hydrolytic degradation process of the polymer materials under study.

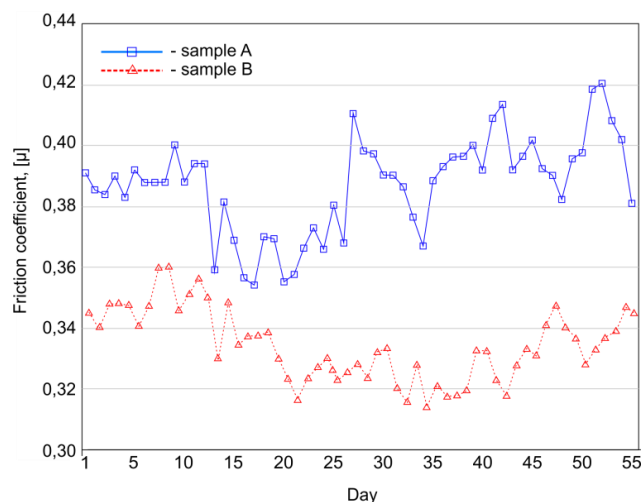


Fig. 1. Coefficient of friction of the tested materials

### CONCLUSION

The obtained test results indicate a significant friction diversity of the materials tested. The B sample with the glycerol-based chain extension was characterized by lower resistance of movement. The nature of the friction coefficient is indicative of changes occurring within the macromolecular compound, which is also confirmed by microscopic studies.

### ACKNOWLEDGMENTS

Special thanks to prof. J. Ryszkowska from Warsaw University of Technology for polymers used in tests. Research has been supported by the Białystok University of Technology within the grant MB/WM/7/2016.

## Production of Hydroxyapatite–Poly(vinyl alcohol) Based Scaffold for Drug Delivery from Orange Spiny Oyster Seashell (*Spondylus Barbatus*)

Serap Ayaz Seyhan<sup>1</sup>, Dilek Bilgic Alkaya<sup>1</sup>, Sumeyye Cesur<sup>2,3</sup>, Faik Nuzhet Oktar<sup>4</sup>, Oguzhan Gunduz<sup>2,3</sup>

<sup>1</sup>Department of Analytical Chemistry, Faculty of Pharmacy, Marmara University, 34668 Istanbul, Turkey

<sup>2</sup>Department of Metallurgy and Materials Engineering, Faculty of Technology, Marmara University, Turkey

<sup>3</sup>Advanced Nanomaterials Research Laboratory, Faculty of Technology, Marmara University, Turkey

<sup>4</sup> Department of Bioengineering, Faculty of Engineering, Marmara University, Turkey

[sayaz@marmara.edu.tr](mailto:sayaz@marmara.edu.tr)

### INTRODUCTION

Hydroxyapatite (HA), tricalcium phosphate (TCP), octacalcium phosphate, amorphous calcium phosphate, dicalcium phosphate have attracted great attention towards biomedical applications because of their similarity to the bone mineral, good bioactivity, biocompatibility and osteoconductivity. However, there is very limited information about converting Orange Spiny Oyster Seashell (*Spondylus Barbatus*) (it was collected in Istanbul) (Fig. 1) to HA. Poly (vinyl alcohol) (PVA), is a water soluble and semi-crystalline polymer. PVA has good chemical and thermal stability, is nontoxic and biocompatible with a wide spectrum of applications. There are several studies in order to control drug delivery, decrease the toxicity of drugs and also for novel biomedical applications. It is necessary to be able to control the release of the drug within the body by using drug delivery systems. The objective of the present paper is to synthesize pure and biocompatible a PVA composite reinforced by hydroxyapatite (HA) obtained from Orange Spiny Oyster Seashell (*Spondylus Barbatus*) and is to determine the feasibility of loading model drug into HA-PVA composite.



Fig. 1. Orange Spiny Oyster Seashell



Fig. 2. Synthesis by Ultrasonic Stirrer Method

### EXPERIMENTAL METHODS

Orange Spiny Oyster Seashell (*Spondylus Barbatus*) was washed, dried, crushed and ball milled until a powder of 100 µm particles size was obtained. Raw powder was stirred with an ultrasonic stirrer at 80°C for 15 min in ultrasonic equipment (Fig. 2). Equivalent amount of H<sub>3</sub>PO<sub>4</sub> was added drop by drop into the solution. The reaction lasted for 8h. Then, to evaporate the liquid part, the mixtures were put into an incubator at 100°C for 24 h and the resultant dried sediments were collected. In the preparation of HA particles in the presence of polymer (PVA), the raw powder was slowly added to polymer (%1 PVA) solution and was stirred with an ultrasonic stirrer at 80°C for 15 min in ultrasonic equipment. Equivalent amount of H<sub>3</sub>PO<sub>4</sub> was added drop by drop into the solution. HA-PVA added to mg/mL model drug solution. Afterward the suspensions were brought to equilibrium under gentle stirring for 24.

### RESULTS AND DISCUSSION

HA powder was synthesized from Orange Spiny Oyster Seashell (*Spondylus Barbatus*) by chemical precipitation method. XRD analysis indicated phase purity and crystallinity of HA powder. TG/DTA result showed that seashell is mainly composed of calcium carbonate (CaCO<sub>3</sub>). Model drug loaded HA-PVA composite underwent different in-vitro tests including, FTIR, SEM and drug release. The in-vitro drug release was investigated using buffer phosphate (pH=7.4) solution.

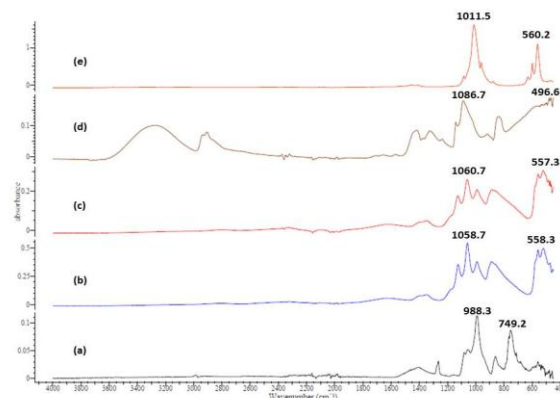


Fig. 3. FTIR spectrums of (a) orange spiny oyster seashell raw, (b) ultrasonic (HA), (c) HA+PVA, (d) PVA, (e) commercial HA.

FTIR spectra (as shown in Fig. 3) shows the characteristic peaks of HA and HA+PVA. As observed in Figure 4. b, c, peaks of orange oyster seashell verify that orange oyster seashell shows similar properties with HA.

### CONCLUSION

The goal of this research is to synthesize pure and biocompatible a PVA composite reinforced by hydroxyapatite (HA) obtained from *Spondylus Barbatus* and is to determine the feasibility of loading model drug into HA-PVA composite. The obtained powders are characterized using XRD, DTA/TGA, FTIR, SEM and drug release.

### REFERENCES

1. D. Agaogullari et al., Acta Physica Polonica A. 121: 23-26, 2012.
2. A. Singh., Bull. Mater. Sci. 35(6): 1031–1038, 2012.
3. R. Narayan et al. Biomaterials Science: Processing, Properties, and Applications V, Published by John Wiley & Sons, Canada, 188-203, 2015.
4. A.M.C. Santos et al. Materials Letters. 176: 122–126, 2016.

## Investigation of Chitosan / Tricalcium Phosphate (TCP) Composite Powders from Scotch Bonnets (*Semicassis granulata*) as a Drug Controlled Release Matrices

Dilek Bilgic Alkaya<sup>1</sup>, Serap Ayaz Seyhan<sup>1</sup>, Sumeyye Cesur<sup>2,3</sup>, Oguzhan Gunduz<sup>2,3</sup>, Faik Nuzhet Oktar<sup>2,4</sup>

<sup>1</sup>Department of Analytical Chemistry, Faculty of Pharmacy, Marmara University, 34668 Istanbul, Turkey

<sup>2</sup>Department of Metallurgy and Materials Engineering, Faculty of Technology, Marmara University, Turkey

<sup>3</sup>Advanced Nanomaterials Research Laboratory, Faculty of Technology, Marmara University, Turkey

<sup>4</sup>Department of Bioengineering, Faculty of Engineering, Marmara University, Turkey

[dbilgic@marmara.edu.tr](mailto:dbilgic@marmara.edu.tr)

### INTRODUCTION

Hydroxyapatite (HA) and tricalcium phosphate (TCP), which is calcium phosphate based bioceramics are favorable towards its application as protein drug carrier as it is highly compatible with protein or peptide drugs. The shell is rich in calcium carbonate. Thus, snails' shells can be used as a source for bioceramic production Scotch bonnets (*Semicassis granulata*) (Fig. 1), belongs to the helmet family, is a medium sized to large species of sea snail. Chitosan is a promising biopolymer for drug delivery systems. Because of its beneficial properties, chitosan is widely used in biomedical and pharmaceutical fields. The present study was being done to prepare chitosan coated composite loaded with amoxicillin. The profile of amoxicillin release from chitosan composite system was studied under various conditions similar to those of some corporeal fluids.



Fig. 1. Scotch bonnets (*Semicassis granulata*)

### EXPERIMENTAL METHODS

Local snails' shells (Scotch bonnets) were collected in Istanbul. They were washed, dried, crushed and ball milled until a powder of 100  $\mu\text{m}$  particles size was obtained. A second part of the raw powder and chitosan was stirred with an ultrasonic stirrer at 80°C for 15 min and in ultrasonic equipment. It was observed that the chitosan added in polymerization medium during the composite preparation. Equivalent amount of  $\text{H}_3\text{PO}_4$  was added drop by drop into the solution. The reaction lasted for 8h. Then, to evaporate the liquid part, the mixtures were put into an incubator at 100°C for 24 h and the resultant dried sediments were collected. The obtained TCP material was characterized with scanning electron microscopy and X-ray diffraction methods. It was found that the bioceramic material consisted of TCP and various related phases. Amoxicillin was loaded into TCP composite by diffusion filling process and coated with 1% aqueous chitosan solutions to develop TCP - amoxicillin respectively. Amoxicillin loading capacity and release kinetics of amoxicillin loaded chitosan coated composite in PBS (pH 7.4) were evaluated.

### RESULTS AND DISCUSSION

TCP powder was synthesized from snail shell (*Scotch Bonnet*) by chemical precipitation method. XRD analysis indicated phase purity and crystallinity of TCP powder. TG/DTA result showed that snail shell is mainly composed of calcium carbonate ( $\text{CaCO}_3$ ).

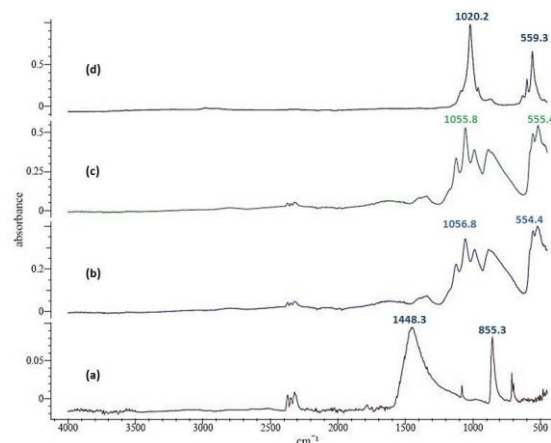


Fig. 2. FTIR spectrums of (a) scotch bonnets raw, (b) hotplate, (c) ultrasonic stirrer and (d) TCP.

FTIR spectra (as shown in Figure 4.d) shows the characteristic peaks of TCP. As shown in Figure 2. b,c, peaks of scotch bonnets verify that scotch bonnet shows similar properties with TCP.

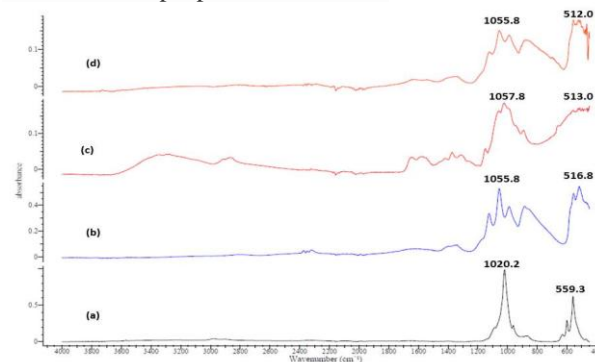


Fig. 3. FTIR spectrums of (a) TCP, (b) ultrasonic stirrer, (c) chitosan, (d) TCP+chitosan

### CONCLUSION

Calcium phosphate based composite powders are favorable towards its application as protein drug carrier as it is highly compatible with protein or peptide drugs. In the present study, it has been demonstrated that composite also highly compatible with amoxicillin and pH dependent release of amoxicillin was demonstrated in PBS

### REFERENCES

1. Susmita Bose and et al Acta Biomaterialia A, 8; 401–1421,2012.
2. D. Kel Key Engineering Materials. 493-494 : 287-292,2012.
3. Anjuvan S., Bull of Mat Sci., 35:1031-1038, 2012.
4. M.Öner.Ceramics Inter:37: 2117-2125,2011.

## Luminescence Phenomena of Carbon Dots – Molecular Insight

Wiktor Kasprzyk, Tomasz Świergosz, Szczepan Bednarz, Karolina Walas, Dariusz Bogdał

Faculty of Chemical Engineering and Technology, Cracow University of Technology, Poland  
[wkas@chemia.pk.edu.pl](mailto:wkas@chemia.pk.edu.pl)

### INTRODUCTION

Recently, much attention has been devoted to the synthesis of fluorescent carbon and/or polymer dots (CD) basing on citric acid (CA). These materials have great potential and wide spectrum of possible applications (Biology, Medicine, Solar Energy Production, Analytical Chemistry and Environmental Protection). Furthermore, they exhibit low cytotoxicity, high photostability and extremely high fluorescence quantum yields up to ~90%. However, the origin of their intriguing fluorescence properties still remains a topic of fierce debate among researchers<sup>1, 2, 3, 4</sup>.

### EXPERIMENTAL METHODS

We described two protocols for the synthesis and purification of carbon dots derived from citric acid and urea. Then we separated pure fluorescent small molecular compounds from CDs using preparative HPLC. Afterwards 1D and 2D NMR and HR-ESI-MS analyses were conducted for structure elucidation.

### RESULTS AND DISCUSSION

Here, we present results of our investigations on the chemical structure of the moieties responsible for high quantum yield, the blue and green luminescence of CDs derived from low-temperature microwave assisted pyrolysis of citric acid in the presence of urea. In the course of this research, we have used chromatographic methods for separation of green fluorescence fraction from CDs and elucidated its chemical structure through detailed NMR analyses. We explained the difference in optical properties of materials prepared under hydrothermal (sealed vessel) and solvent free, microwave-assisted (open vessel) conditions by elucidation of chemical structures of fluorescent compounds formed. Consequently, the understanding of the mechanism of CDs derived from citric acid and urea became feasible.

### CONCLUSION

We showed the importance of the presence of molecular fluorophores on luminescence properties of CDs. Consequently, the understanding of the mechanism of CDs derived from citric acid and urea became feasible.

### REFERENCES

References must be numbered. Keep the same style.

1. Bhattacharyya, S. et al. *Nat. Commun.* 2017, 13, 1.
2. Zhu, S. et al *B. Nano Today* 2016, 11, 128.
3. Kasprzyk, W. et al *Chem. Commun. (Camb)*. 2013, 49, 6445.
4. Kasprzyk, W. et al *RSC Adv.* 2015, 5, 34795.

### ACKNOWLEDGMENTS

The authors gratefully acknowledge Professor Sławomir Wybraniec and Dr Joanna Ortyl for sharing their equipment and knowledge concerning mass spectrometry and fluorescence spectroscopy.



## The Influence of CNT Modification on Osteo-differentiation

Eliška Mázl Chánová<sup>1,3</sup>, Kristýna Venclíková<sup>1</sup>, Petr Knotek<sup>2</sup>, Dana Kubies<sup>1</sup>, Olga Janoušková<sup>1</sup>, Jana Kredatusová<sup>1</sup>, Ying Yang<sup>3</sup>

<sup>1</sup>Institute of Macromolecular Chemistry AS CR, Czech Republic

<sup>2</sup>Department of General and Inorganic Chemistry, University of Pardubice, Czech Republic

<sup>3</sup>Institute for Science&Technology in Medicine, Keele University, Great Britain

[chanova@imc.cas.cz](mailto:chanova@imc.cas.cz)

### INTRODUCTION

A major challenge in bone bioengineering is to create a scaffold material able to sustain the growth and proliferation of bone cells and allow high pressure load conditioning into functional bones. An ideal scaffold material should provide mechanical support, microenvironment for proliferation and differentiation of bone cells. Cells in their natural in vivo environment interacts with their surroundings in the nanometer scale and it has been suggested that the nanostructure of biomaterials is critical to start differentiation.<sup>1</sup>

Carbon nanotubes (CNT) are very promising scaffold material. Due to their unique properties, such as high strength, stiffness, electrical and/or thermal conductivity and high aspect ratio, CNTs are of great interests for their applications in the nano-composites, particularly with polymers.<sup>2</sup> Nevertheless, the wide and long term use of CNTs in biomedical applications is hampered as pristine CNTs were proved to be toxic and may be hazardous to human health. Combining oxidation and biomimetic functioning of CNT could enable CNT a smart biomaterial in regenerative medicine and other related applications.

### EXPERIMENTAL METHODS

CNT-COOH and CNT-NH<sub>2</sub> were modified with bifunctional poly(ethylene oxide) (PEO) of various shape (linear, star) and molecular weight (3 kDa and 10 kDa) using carbodiimide chemistry. The resulting CNT-PEO were further grafted with RGDS-containing oligopeptides via click chemistry strategies (Huisgen cycloaddition, Michael addition). Starting and modified CNTs were characterized by thermogravimetric analysis.

The effect of CNT modification on cell viability and differentiation was tested upon standard tissue culture plate (TCP), in suspension and/or as a part of the polymer coatings in cell culture with MG63 cell line and primary MSC cells in basal and conditional media. Selected samples were loaded to evaluate the effect of mechanical stimulation.

The images of live cell morphology were taken in regular time intervals. Cell viability was determined by AlamarBlue Assay following manufacturer's protocol. The cell differentiation was evaluated by osteopontin detection by Western-blotting analysis using SDS-PAGE analysis optimized for testing the samples in presence of CNT. The total protein content was assessed by BCA Assay. Selected samples were stained with Alizarin red.

### RESULTS AND DISCUSSION

The change of thermal properties of grafted CNT determined by TGA proved the successful modification.

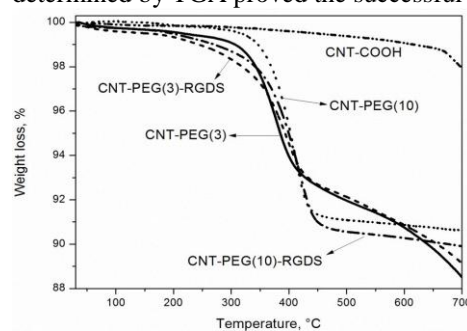


Fig. 1. TGA analysis allowed determining the content of organic component grafted to CNT.

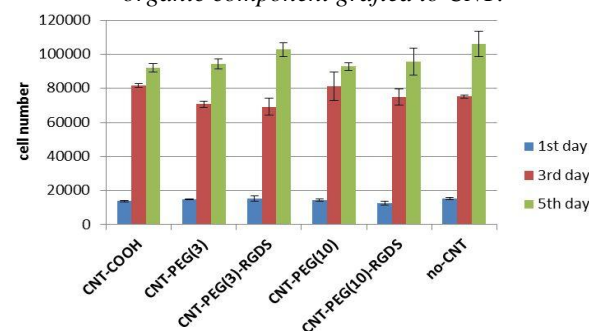


Fig. 2. Evaluation of initial proliferation of MG63 on TCP with CNTs added into the basal culture media as cell numbers after 1, 3, 5 days of growth using cell viability assay.

### CONCLUSION

The set of modified CNTs were prepared. The TGA analysis proved that the CNTs grafting with functionalized PEG enabled the immobilization of RGDS-containing oligopeptides on the CNTs' surface. Their performance in cell culture has been studied under different condition. The effect of CNT modification on cell viability and differentiation were dependent to the grafted active groups on CNT.

### REFERENCES

- References must be numbered. Keep the same style.
- Li X. *et al.*, *Biomaterials* 29:3306-3316, 2008
  - Spitalskya Z. *et al.* *Prog Polym Sci* 35:357-401, 2010

### ACKNOWLEDGMENTS

This work was supported by MEYS of CR within the International Mobility of Researches – MSCA-IF (CZ.02.2.69/0.0/0.0/17\_050/0008473) under the OP Research, Development and Education, and within the National Sustainability Program II (proj. BIOCEV-FAR LQ1604), and the project “BIOCEV” (CZ.1.05/1.1.00/02.0109).

## Fluorescent Molecular Sensors for Rapidly and Nondestructive Measurement of Polymer Materials

Wiktor Kasprzyk<sup>1</sup>, Joanna Ortyl<sup>1,2</sup>, Anna Chachaj-Brekiesz<sup>3</sup>, Monika Topa<sup>1</sup>, Maciej Pilch<sup>1</sup>, Emilia Hola<sup>1</sup>, Paweł Fiedor<sup>1</sup>

<sup>1</sup>Cracow University of Technology, Faculty of Chemical Engineering and Technology, Laboratory of Photochemistry and Optical Spectroscopy, Warszawska 24, 31-155 Cracow, Poland

<sup>2</sup>Photo HiTech Ltd., Park Life Science, Bobrzynskiego 14, 30-348 Cracow, Poland

<sup>3</sup>Jagiellonian University, Faculty of Chemistry, Ingardena 3, 30-060 Cracow, Poland

### INTRODUCTION

Molecular chemical sensors, especially optical luminescent sensors, technologies are rapidly growing topic in science and product design, embracing development in chemistry, biochemistry and life science research. It is expected that in the XXI century opticochemical sensors science and technology will address two major problems that present a great challenge. One is related to topic with applications of sensors in different field of science such as material science for example polymer industry.

During the past few years monitoring of polymerization processes using fluorescent probes has been the most popular and powerful tools that can be used in order to understand the physical and chemical processes that occur at the molecular level<sup>1</sup>. This is possible because their fluorescence is sensitive to the polarity and/or microviscosity of the molecular environment in which the probe molecules are located. One of the most important applications of fluorescent probes in polymer chemistry is monitoring of a photopolymerization process. Theoretically, every process that causes change of the system polarity or microviscosity should be able to be monitored by using fluorescent probes. However, depending on the type of the process and the monitoring parameters, appropriate structure and characteristics of the probe are required. Therefore, there are no completely versatile probes.

Most of known fluorescent probes suitable for monitoring of free radical polymerization, usually do not perform well in cationic polymerization systems, because typical fluorescent probes used for free radical systems contain basic amino groups in their structure, necessary to boost their fluorescence efficiency. Usually these probes are not suitable for cationic polymerization, because they interfere with the polymerization process. To date, only a few fluorescent probes suitable for cationic polymerization systems have been reported<sup>2,3</sup>. Thus, there is a need for new fluorescent probes, which will be able to monitor the cationic polymerization processes without undesired side-effects. In this communication, we report the performance of new fluorescent molecular probes based on 1,6-diphenylquinolin-2-one derivatives as a fluorescent probe for monitoring progress of cationic photopolymerization.

### EXPERIMENTAL METHODS

Triethylene glycol divinyl ether (TEGDVE, Aldrich) and diphenyliodonium hexafluorophosphate (Alfa Aesar) were applied as a model monomer and a cationic photoinitiator, respectively. The photocurable compositions were prepared by dissolution of the photoinitiator and each probe (1,6-diphenylquinolin-2-

one derivatives) in TEGDVE monomer, so as to obtain the concentrations  $5.0 \cdot 10^{-3}$  mol/dm<sup>3</sup> of the probe and 1 wt % of the photoinitiator.

### RESULTS AND DISCUSSION

1,6-diphenylquinolin-2-one derivatives probes perform well in monitoring of cationic photopolymerization of a divinyl ether, while Coumarin 1 probe, which was used as a reference probe, usually used for free radical polymerization systems, failed. A regular kinetic profile is obtained with the new probes, using fluorescence intensity of the probe (I) normalized to the intensity (I<sub>0</sub>) before polymerization, as the polymerization progress indicator.

### CONCLUSION

In this communication new fluorescent probes based on 1,6-diphenylquinolin-2-one derivatives were characterized and their principal applications are presented. It was found those derivatives are well adaptable for the monitoring of cationic and free radical photopolymerization processes with good sensitivity.

### REFERENCES

1. Kamińska I., Ortyl J., Popielarz R., *Polymer Testing*, 42, 99–107, 2014.
2. Ortyl J., Wilamowski J., Milart P., Galek M., Popielarz R., *Polymer Testing*, 48, 151-159, 2015.
3. Ortyl J., Milart P., Popielarz R., *Polymer Testing*, 32, 708 -715, 2013.

### ACKNOWLEDGMENTS

This work was supported by the Foundation for Polish Science (Warsaw, Poland) within the project POWROTY (Contract No. POWROTY/2016-1/4).

## Biocompatibility of the Polymer Middle Ear Prosthesis

Magdalena Ziabka

AGH University of Science and Technology, Faculty of Materials Science and Ceramics,  
Department of Ceramics and Refractories, al. Mickiewicza 30, 30-059 Krakow, Poland  
[ziabka@agh.edu.pl](mailto:ziabka@agh.edu.pl)

### INTRODUCTION

A medical device is defined as implantable if it is either partly or totally introduced, surgically or medically, into the human body and is intended to remain there after the procedure [1-2]. Implants used in ossicular replacement prostheses must demonstrate appropriate biological properties, such as: biocompatibility, stability, no cytotoxicity. Due to the risk of infection (otitis media and chronic otitis media), it is desirable to use an antibacterial agent for illness prevention during the ossicular reconstruction [3]. The reconstruction of the ossicular chain is very often performed by using artificial prostheses made out of titanium, ceramics or bone. In this research polymer middle ear prostheses – the otoimplants modified with silver nanoparticles AgNPs were investigated *in vivo*.

### EXPERIMENTAL METHODS

The otoimplants were manufactured by means of extrusion and injection moulding method, using the Multiplas machine (Multiplas Enginyery Co., LTD, Taiwan) fitted with a special steel moulding form. The two types of the implants were injected: pure ABS (poly)acrylonitrile butadiene styrene and ABS with addition of silver nanoparticles (AgNPs).

The procedure of implantation was performed in the Animal Facility of the Faculty of Pharmacy CM UJ Krakow (the consent no 251/2015 issued by the Ist Local Ethical Committee on Animal Testing in Krakow). The experiment was performed according to the PN ISO 10993-6 guidelines [4]. The research model was the white male adult Wistar rat (*Rattus Norvegicus*). The animals were kept in standard conditions at the stable temperature of about 20°C and 12:12h light cycle.

The middle ear prostheses made of pure ABS and ABS with addition of nanosilver were sterilised at a low temperature gas plasma (the Sterrad 120 apparatus) using hydrogen peroxide vapour in the double-cycle (2 x 45 minutes) and implanted into the rats' glutemus muscles. The animals were divided into two groups for 30, 90-day cycles, 5 rats in every series.

After a set period of time (30, 90 days) rats were decapitated, then the tissue samples were extracted and prepared (frozen in liquid nitrogen, cut into 9µm thick slices with a cryostat microtome for histological and microstructural assessment. To identify the reaction for foreign body and healing process reaction by the May-Grunwald Giemsa (MGG) method was performed.

### RESULTS AND DISCUSSION

After 30 days of implantation the local inflammation was observed around the prosthesis in the tissue samples. In some cases there was an acute inflammatory infiltration. It is worth noting that both kinds of

implants (ABS and ABS/AgNPs) led to similar immunological reactions. Observed inflammation resulted from the tissue damage and was the natural response to a foreign body. After a three month there was the regenerating muscle tissue present in the implantation site. The first visible differences were noted between the two types of implants.

The granulation tissue area was visibly smaller for the otoimplants modified with AgNPs and getting replaced by the regenerating muscle tissue. This may lead to the conclusion that the presence of silver nanoparticles not only didn't exert toxic effect but facilitated the healing process. Similar results recently published by Gravante et al. [5] and Rigo et al. [6] were observed for silver nanoparticle (AgNPs)-based dressing. They found that Acticoat™ Flex 3 was the dressing with the shortest healing times for deep partial thickness burns. This data confirms that the healing process is not impeded during the treatment with AgNPs.

### CONCLUSION

The otoimplants may eliminate bacteria during inflammation in the middle ear. On the bases of *in vivo* research it was proved that ABS modified with silver nanoparticles prostheses are biocompatible for surrounding tissue. Also the AgNPs incorporated into polymer medical devices ensure long-lasting antibacterial effect without any inflammation and toxic reaction for sounding tissue.

### REFERENCES

1. ISO 13485:2003. Medical devices -- Quality management systems -- Requirements for regulatory purposes.
2. Council Directive 90/385/EEC of 20 June 1990 on the approximation of the laws of the Member States relating to active implantable medical devices.
3. Ziabka M., et al. *Molecules* 2017, 22(10), 1681.
4. PN-EN ISO 10993-6: 2016, Biological evaluation of medical devices. Tests for local effects after implantation.
5. Gravante G., et al. *Ann. R. Coll. Surg. Engl.* 2010, 92, 118–123.
6. Rigo Ch., et al. *Int J Mol Sci.* 2013, 14(3), 4817–4840.

### ACKNOWLEDGMENTS

This work was financially supported by the National Centre for Research and Development grant no: LIDER/ 154/L-6/14/NCBR/2015.

## Adjunctive Hemostatic Application of Highly Adhesive Drug Loadable Powder for Partial Hepatectomy Bleeding in a Swine Model

Eunhye Lee<sup>1</sup>, Sukyung Ahn<sup>1</sup>, Yonghai Nam<sup>1</sup>, Keunsu Kim<sup>1</sup>, Don Haeng Lee<sup>1,2</sup>

<sup>1</sup>Utah-Inha DDS and Advanced Therapeutics Research Center, Incheon, Republic of Korea

<sup>2</sup>Division of Gastroenterology & Hepatology, Department of Internal Medicine, Inha University Hospital, Incheon Republic of Korea

[eunhye.lee@unidds.com](mailto:eunhye.lee@unidds.com)

### INTRODUCTION

Topical agents can be effective as adjuncts to aid in hemostasis when bleeding is not controllable with general methods. Such adjunctive hemostatic treatments include topical gelatins, collagens, thrombin and fibrin sealants, synthetic glues, and glutaraldehyde-based glues. UI-SAH is a highly adhesive drug-loadable powder that has been developed for adjunctive hemostatic use. The hemostatic effects are achieved by forming a hydrogel and showing high adhesiveness and biodegradation on bleeding site. And besides, amine containing therapeutic molecules such as vancomycin, mitomycin, and gemcitabine can be easily loaded into UI-SAH without chemical modification.

The aims of this study were to confirm 1) the effectiveness of the application of UI-SAH powder in hepatectomy bleeding swine model, 2) the prevention of organ adhesion after gelation at the bleeding site and 3) the feasibility of the drug loading capacity.

### EXPERIMENTAL METHODS

Adjunctive hemostatic application of UI-SAH was evaluated by hepatectomy bleeding in a swine model. After inducing bleeding, we topically applied UI-SAH on the bleeding site. The hemostatic effect and organ-adhesive were observed using blood loss, hemostatic time, hematological analysis, and organ-adhesion (score). The therapeutic effect of drug-loaded UI-SAH was evaluated in tumor bearing mice model.

### RESULTS AND DISCUSSION

Severe bleeding was effectively controlled after applying the UI-SAH and re-bleeding was not observed until 72 h after treatment in a swine. In addition, Hydrogel that were converted from powder immediately after contacting water were act as anti-adhesion barrier. In a tumor bearing mice model, the tumor volume of anti-cancer drug-loaded UI-SAH group was significantly decreased approximately 50% compared with those of positive control group on day 35 after tumor inoculation.



### CONCLUSION

This study confirmed that the adjunctive hemostatic application of UI-SAH is effective for the in partial hepatectomy bleeding model due to high adhesiveness and the suppression of organ adhesion. Furthermore, tumor suppression can be accelerated by loading of the anti-cancer drug in the UI-SAH. The present study suggests that UI-SAH is promising candidate for adjunctive surgical hemostasis and local anti-cancer therapy.

### ACKNOWLEDGMENTS

This research was financially supported by the Ministry of Trade, Industry and Energy(MOTIE) and Defense Acquisition Program Administration(DAPA) through Civil Military Technology program.



## New Crosslinking Diluents for Dental Materials

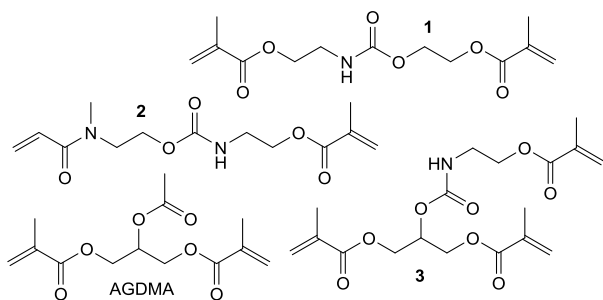
Norbert Moszner, Jörg Angermann, Urs Karl Fischer

Research & Development/Ivoclar Vivadent AG, FL-9494 Schaan, Liechtenstein

[norbert.moszner@ivoclarvivadent.com](mailto:norbert.moszner@ivoclarvivadent.com)

### INTRODUCTION

Tooth-shaded dental restorations are becoming more and more popular. Currently used dental restorative materials are visible-light curing hybrid materials consisting of a resin matrix, which is a mixture of various free radical cross-linking dimethacrylates such as Bis-GMA (2,2-bis[4-(2-hydroxy-3-methacryloyloxypropyl)phenyl]propane) and TEGDMA (triethylene glycol dimethacrylate) as diluent<sup>1</sup>. TEGDMA shows a relative high cytotoxicity and water solubility, and may cause dose-dependent mutagenic effects in mammalian cell cultures. In this context, we synthesized the following crosslinking monomers, which may substitute diluent TEGDMA in dental resins or composites:



### EXPERIMENTAL METHODS

The syntheses of the urethane group containing monomers 1-3 were carried out by addition of 2-isocyanatoethyl methacrylate (IEMA, to the corresponding polymerizable hydroxyalkyl monomers in the presence of bismuth(III) neodecanoate. For the synthesis of glycerol trimethacrylate GTMA, glycerol dimethacrylate (GDMA) was reacted with methacryloyl chloride in the presence of triethylamine/4-(dimethylamino)pyridine (TEA/DMAP). AGDMA was synthesized by acetylation of GDMA with acetic anhydride in ethyl acetate as solvent. Bis-[(2-methacryloyloxyethoxycarbonyl)-amino]-2,2,4-trimethylhexane (UDMA), and bis-(4-methoxybenzoyl)diethylgermanium (Ivocerin<sup>®</sup>, Ivoclar-Vivadent AG, Liechtenstein) were used without purification. The photopolymerization of these monomers and composites was carried by irradiating the samples with a visible light source (400-500 nm, Spectramat, Ivoclar Vivadent AG). Photopolymerizations were also carried out on a Perkin Elmer differential scanning calorimeter (DSC), Pyris Diamond. 0.5 mol% of Ivocerin<sup>®</sup> as photoinitiator was added to each monomer mixture.

### RESULTS AND DISCUSSION

The monomers 1 (130 mPa·s), 2 (1840 mPa·s), and 3 (1020 mPa·s) are liquids showing a higher viscosity compared to TEGDMA (10 mPa·s). AGDMA was obtained as colorless liquid with a viscosity of only 46 mPa·s. The XTT<sub>50</sub>-values determined for the urethane group containing monomers 1, 2, and 3 were > 625, 1086, and 196 µg/mL, respectively. For GTMA or AGDMA determined XTT<sub>50</sub>-values were 121 or 434 µg/mL. These XTT<sub>50</sub>-values confirm a significantly lower cytotoxicity of the synthesized monomers compared to TEGDMA (XTT<sub>50</sub> = 30 µg/mL). The DSC experiments with the pure diluent monomers were carried out using Ivocerin<sup>®</sup> (0.5 mol%) as photoinitiator. The photo-DSC results confirm a significantly increased photopolymerization reactivity of the synthesized urethane unit containing crosslinkers 1 and 2, compared to TEGDMA. The double-bond conversion (DBC) in the homopolymerization of the synthesized monomers were between 43% (GTMA) and 65% (1 or 2) and thereby significant lower compared to TEGDMA (76%). The photopolymerization of multifunctional methacrylates results in polymer networks in which the chain mobility and therefore the accessibility of residual double-bonds are more or less reduced by the formed rigid polymer network structure. Thus, the higher the monomer functionality the lower is the DBC. Therefore, the trimethacrylate monomers 3 (49%) and GTMA (43%) showed the lowest DBC.

For the evaluation of the synthesized diluent monomers in dental composites, resin mixtures with Bis-GMA (7.40 wt.%) and UDMA (8.94 wt.%) with a filler load of 80.00 wt.% were prepared. The flexural strength and flexural elastic modulus of composite were measured. The results obtained for the water stored samples confirm also acceptable mechanical properties of composites with the less cytotoxic diluent monomers 2 and 3, and GTMA.

### CONCLUSION

A number of crosslinking diluents for the free-radical photopolymerization were synthesized and evaluated as alternative for the currently used diluent TEGDMA in a dental composite. It could be shown that the urethane dimethacrylate 1, the urethane hybrid monomer 3, and AGDMA are less cytotoxic and enable the preparation of composites with promising properties.

### REFERENCES

1. Moszner N, Hirt T, J. Polym. Sci. Part A: Polym. Chem. 50: 4369-4402, 2011

## Polymers with Non-Carcinogenic Precursors for Green Electronic Devices

Cristian Ravariu<sup>1</sup>, Dan Edurad Mihaiescu<sup>2</sup>, Bogdan Purcareanu<sup>2</sup>

<sup>1</sup>Department of Electronic Devices Circuits and Architectures, Politehnica University of Bucharest, Romania

<sup>2</sup>Department of Organic Chemistry "Costin Nenitescu", Politehnica University of Bucharest, Romania

[cristian.ravariu@upb.ro](mailto:cristian.ravariu@upb.ro)

### INTRODUCTION

In the last 10 years, the Organic Thin Film Transistors (OTFT) fulminant developed, finding their applications in flexible substrate or mobile phones. The main advantage comes from a room temperature technology, outside of an expensive clean room. The aim of this work is an additional step - moving the organic semiconductor technologies toward green eco-technologies. Traditional organic semiconductors based on polynuclear aromatic hydrocarbons (pentacene<sup>1</sup>, terrylene, other polymers) are susceptible to high toxicity/carcinogenic precursors<sup>2</sup>. This paper strongly envisages OTFT with green polymers grafted on nano-core-shell (NCS) nano-composites, appealing to green chemistry synthesis routes.

### EXPERIMENTAL METHODS

The nano-core-shell materials are structured by a primary core-shell np's ferrite nano-particle ( $\text{Fe}_3\text{O}_4$ ). Synthesis of the II-nd shell is performed by coprecipitation method and specific organic compounds like PABA - para-aminobenzoic acid. PABA is a compound that naturally occurs, respects the molecular conjugation as the main condition to ensure the electronic charge conduction<sup>3</sup> (e.g. alternating single and double bonds between covalently bound carbon atoms) and efficiently binds to the metallic ions of the core. The final material  $\text{Fe}_3\text{O}_4/\text{PABA}$  is achieved by coprecipitation of the ions  $\text{FeII}$  and  $\text{FeIII}$  in  $\text{NaOH}$  solution, under molar ratio of  $\text{Fe}_3\text{O}_4:\text{PABA} = 1:7$ .

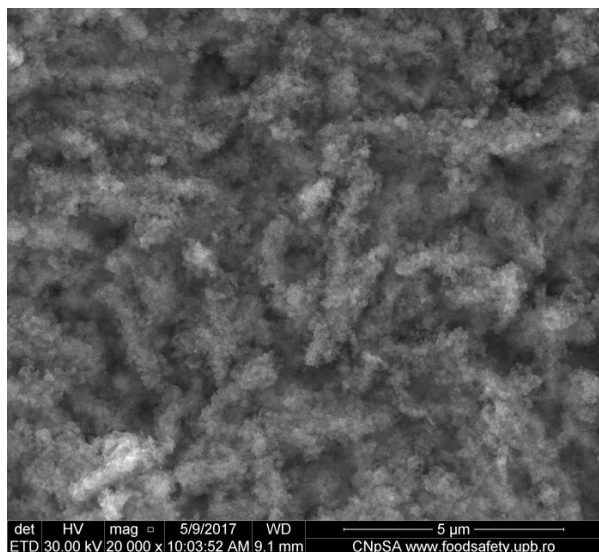


Fig. 1. SEM image of the  $\text{Fe}_3\text{O}_4/\text{PABA}$  system.

### RESULTS AND DISCUSSION

The synthesized  $\text{Fe}_3\text{O}_4/\text{PABA}$  nanoparticles have a hydrodynamic diameter of 71nm, extracted by DLS - Dynamic Light Scattering. The PABA shell presence was identified by FT-IR, finding the characteristics

band of the free group  $-\text{NH}_2$  at  $3160.5 \text{ cm}^{-1}$ . The surface morphology analysis reveals an eterogen structure, with granular clusters of uniform shape and size, separated by aleatory spaces, characterized by SEM, Fig. 1.

A preliminar study of OTFT transistor is simulated in Fig. 2, at  $V_S=0\text{V}$ ,  $V_D=-10\text{V}$ ,  $V_G=-10\text{V}$ .

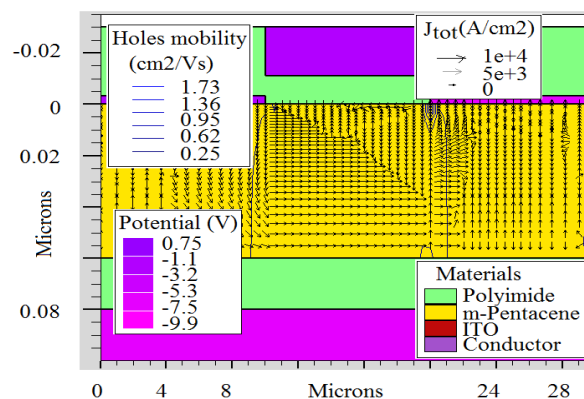


Fig. 2. Potential on electrodes and current vectors in the semiconductor polymer, as modified Pentacene, *p*-type.

The color legend proves the device biasing, besides to the used materials. The negative gate voltage produces a current vectors crowdings to the polymer surface, suggesting an accumulation regim onset. OTFT tests on  $\text{Fe}_3\text{O}_4:\text{PABA}$  materials are in press.

### CONCLUSION

Green electronic technologies for organic transistors, based on non-toxic green polymers attached to NCS nanocomposites were identified. The synthesized  $\text{Fe}_3\text{O}_4/\text{PABA}$  nanoparticles are promising candidate for this purpose. An initial device simulation proved the current flow thru a polymer with molecular conjugation.

### REFERENCES

1. Yang D. *et al*, Pentacene-based photodetector in visible region with vertical field-effect transistor configuration, IEEE Photonics Tech. Lett., 27(3):233-236, 2015
2. Luch A. *et al*, Carcinogenic Polycyclic Aromatic Hydrocarbons, Book Comprehensive Toxicology, 2010.
3. Klauk H, Chem. Soc. Rev., 38: 2643–2666, 2010

### ACKNOWLEDGMENTS

This work was supported by grants of the Romanian National Authority for Scientific Research and Innovation, CNCS/CCCDI UEFISCDI, project number PN-III-P4-ID-PCE-2016-0480 as project 4/2017 (TFTNANOEL) and by the Research Proj. PN-III-P2-2.1-PTE-2016-0160, 49-PTE 2016 (PROZECHIMED).

## Smart Chitosan-based Hydrogels for Targeted Drug Delivery Application

Nga Vo<sup>1</sup>, Lei Huang<sup>2</sup>, Henrique De Paula Lemos<sup>2</sup>, Andrew Mellor<sup>2</sup>, Katarina Novakovic<sup>1</sup>

<sup>1</sup>School of Engineering, Newcastle University, United Kingdom

<sup>2</sup>Institute of Cellular Medicine, Medical School, Newcastle University, United Kingdom  
[n.vo2@newcastle.ac.uk](mailto:n.vo2@newcastle.ac.uk)

### INTRODUCTION

Hydrogels are three-dimensional networks that absorb water while maintaining their distinctive structures. Smart hydrogels contain functional groups that respond to environmental factors such as pH and temperature, variables relevant in physiologic tissues. As these materials are suitable for carrying cargo, including medication, drug release may be directed to a tissue with distinctive pH values, making smart hydrogels promising carriers for delivery in a more controlled way.

In this work, smart pH-responsive hydrogels composed of genipin crosslinked with chitosan and poly ethylene glycol (PEG) were investigated for prospective pH-responsive drug delivery applications. Chitosan contains primary amino groups that are protonated at acidic pH conditions, enhancing gel pore size, swelling and water retention. Genipin was chosen as a crosslinker due to its reaction with molecules comprising amine groups and remarkably low toxicity, which is 5000-10000 times less cytotoxic than glutaraldehyde, the most commonly used crosslinker<sup>1</sup>. PEG was contained within the polymer structure to form a semi-interpenetrating network favoured over fully interpenetrating networks for rapid response rates, tunable pore sizes and minimization of drug burst release effect<sup>2</sup>.

### EXPERIMENTAL METHODS

Several methods were used to investigate the physico-chemical properties of the resulting hydrogels. Fourier Transform Infrared spectroscopy was employed to confirm functional groups in the gel structure and chemical crosslinking between chitosan and genipin. The gels were characterized morphologically using scanning electron microscopy. Gravimetric swelling experiments were used to evaluate the effects of gel compositions and gelation conditions on the crosslinked network. Mechanical properties of the hydrogels were investigated using uniaxial compression test with gels that were immersed in different environments. Differential scanning calorimetry was used to investigate the thermal properties. The cytotoxic effects of these hydrogels with different amounts of crosslinker on mouse fibroblast cells were evaluated by a luminescent assay and the cell morphology was observed by a microscope.

### RESULTS AND DISCUSSION

Electron micrographs indicated that the hydrogels offer a superporous network with a well-defined, interconnected three-dimensional porous structure ranging in pore size from 25 to 200  $\mu\text{m}$  (Fig. 1).

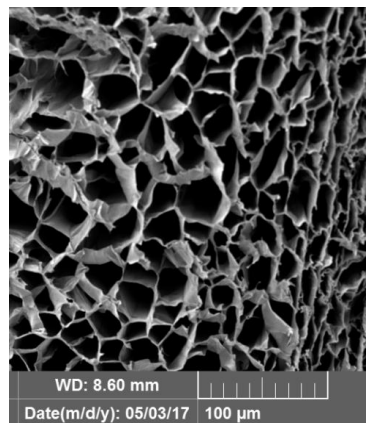


Fig. 1. The electron micrograph of hydrogel sample

In agreement with previously reported studies employing chitosan-based hydrogels, swelling behaviour is directly linked with protonation of amine groups in chitosan chains. Furthermore, amount of each constituent in a hydrogel sample has critical role. While chitosan and genipin directly influence crosslinking density, addition of PEG results in improved elastic properties. For the range of compositions studies, these semi-interpenetrating networks exhibit a compression modulus in the range of 20–50 Pa. The increased modulus compared to hydrogels without PEG is related to the gel stiffness, as the inclusion of PEG fills up more spaces within the network, retarding water penetration into the network. The *in vitro* toxicity test showed that increasing crosslinking density significantly improves the cell attachment and cell viability on hydrogel surface.

### CONCLUSION

This research promotes development of a biocompatible chitosan-PEG-genipin hydrogels as a promising platform in improved controlled payload delivery and in general in tissue engineering. Future work will include investigation of the *in vitro* inflammatory responses of the resulting hydrogels and the release of loaded biomaterials.

### REFERENCES

1. J. Lai, *Int. J. Mol. Sci.* 13:10970-10985, 2012
2. Vega S.L. et al., *European Cells and Materials.* 33:59-75, 2017

### ACKNOWLEDGMENTS

This work was supported by funding from School of Engineering, the Research Excellence Academy scheme, Newcastle University and UK Engineering and Physical Sciences Research Council (EPSRC) grant number EP/N033655/1.



## In Vitro Testing of a Polylactic Polymer Synthesized from Whey

Alexandra Dreancă<sup>1</sup>, Radu Popescu<sup>1</sup>, Marioara Moldovan<sup>2</sup>, Laura Silaghi Dumitrescu<sup>2</sup>, Anca Jurj<sup>3</sup>,  
Ioana Berindan-Neagoe<sup>3</sup>, Ioan Marcus<sup>1</sup>

<sup>1</sup>Faculty of Veterinary Medicine, University of Agricultural Sciences and Veterinary Medicine, Romania

<sup>2</sup>Institute for Research in Chemistry Raluca Rîpan, Babeş-Bolyai University, Romania

<sup>3</sup>Institute of Molecular Biology, Faculty of Medicine, "Iuliu Hațieganu" University of Medicine and Pharmacy, Romania  
[alexandradreanca@gmail.com](mailto:alexandradreanca@gmail.com)

### INTRODUCTION

The polylactic acid (PLA) is an aliphatic polymer achieved from natural and renewable sources<sup>1</sup>. The polylactic polymer and its copolymers represent an important class of biomaterials. Their biocompatibility and biodegradability provide a broad spectrum of applications in different areas of biomedicine, including the regenerative medicine<sup>2</sup>. The main purpose of this research was to test *in vitro* the biocompatibility of a polylactic polymer synthesized from the whey Zonar.

### EXPERIMENTAL METHODS

For experimental synthesis of PLA was used the whey "Zonar", designed & produced by SMEs SC. Embryon Capital Investment, Satu-Mare, Romania) and molasses (provided by Tereos Romania, Ludus). Subsequently, the lactic acid's polymerization was achieved by condensation. The PLA synthesized was characterized through Scanning Electron Microscopy (SEM-Inspect S, FEI Company), with an acceleration voltage of 15 kV and a differential scanning calorimetry (DSC) analysis, using a Mettler Toledo DSC 823e/700°C, in order to reach the melting point of the biomaterial. Testing the cytotoxicity of PLA was performed according to ISO 10993-12<sup>3</sup>. From the PLA extract were achieved seven solutions of different concentrations, respectively 50mg, 25mg, 12,5 mg, 6,25mg, 3,12mg, 1,56mg și 0,78mg per ml, which were tested on a cell culture of osteoblasts at 24 hours. Subsequently, the test was repeated using six solutions of different concentrations, respectively 30mg/ml, 20mg/ml, 10 mg/ml, 5 mg/ml, 2.5 mg/ml and 1.25 mg/ml) which were tested on a fibroblast culture at 48 hours using MTT cell viability & proliferation assay.

### RESULTS AND DISCUSSION

Following the SEM analysis of PLA, there was noticed a homogeneous microstructure of the polymer, without a separation phase. Also, there was obtained a melting point of 174°C (Fig. 2). The cytotoxicity test has revealed a slight decrease in cell viability after 24 hours at the concentrations of 50mg/ml, 25mg/ml and 12,5 mg/ml ( $p \leq 0.01$ ). After 48 hours, the PLA extract has showed a good compatibility with an IC 50 of 64.82 mg/ml (see Fig. 1). The results have proved that the cytotoxicity level of PLA can be determined by the period of time in which the polymers extract acts on the cell culture. In addition, the cellular viability can be affected by the method used to obtain PLA, and by the compounds used in the lactic acid extraction process<sup>4</sup>.

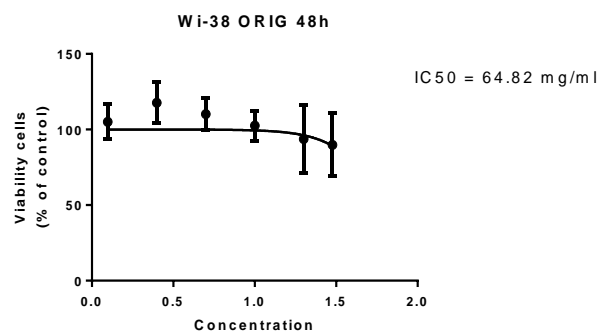


Fig. 1. Assessment of the IC 50 on viability of fibroblasts cells after treatment with PLA extract at 48 hours.

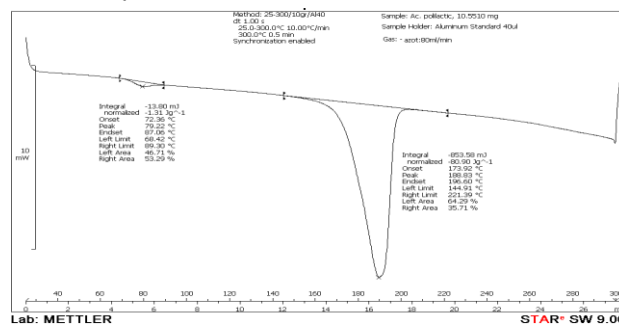


Fig. 2. Analysis of PLA properties through DSC method

### CONCLUSION

Extracting lactic acid from whey and converting it into PLA represents an innovative & promising technology, providing biomaterials for many biomedical fields. The poly-L lactic polymer synthesis from the whey Zonar is a reliable & eco-friendly process, able to provide a low molecular polymer fulfilling 3 essential features, such as nontoxicity, renewability and high biocompatibility.

### REFERENCES

- Shady F. *et al.*, Advanced Drug Delivery Reviews. 2-26, 2016;
- Hamad K *et al.*, Xpress Polymer Letters. 9(5): 435-455, 2015
- Weijia I *et al.*, Biomedical Reports. 3:617-620, 2015
- Vergnol G *et al.*, Journal of Biomedical Materials Research Part B Applied Biomaterials. 00B:000-000. 2015

### ACKNOWLEDGMENTS

This work was supported by a grant of the Romanian National Authority for Scientific Research and Innovation, CNCS/CCCDI-UEFISCDI, project number PN-III-P2-2.1-BG-2016-0335, within PNCDI III"



## Microneedle Arrays Coated with pH-sensitive Charge Reversal Copolymers Improve Dendritic Cell-homing DNA Vaccine Delivery and Immune Responses

Thavasyappan Thambi, Huu Thuy Trang Duong, and Doo Sung Lee

School of Chemical Engineering, Theranostic Macromolecules Research Center, Sungkyunkwan University, Suwon 440-746, Republic of Korea

[thambi1983@gmail.com](mailto:thambi1983@gmail.com)

### INTRODUCTION

Successful delivery of a DNA vaccine to antigen-presenting cells (APCs) and their subsequent stimulation of CD4<sup>+</sup> and CD8<sup>+</sup> T cell immunity remains an inefficient process. In general, the delivery of prophylactic vaccines is mainly mired by low transfection efficacy, poor immunogenicity, and safety issues from the materials employed. Currently, several strategies have been exploited to improve immunogenicity, but an effective strategy for safe and pain-free delivery of DNA vaccines is complicated. Herein, we report the rapid delivery of polyplex-based DNA vaccines using microneedle (MN) arrays coated with a polyelectrolyte multilayer assembly of pH-sensitive charge reversal copolymer and heparin.<sup>1</sup>

### EXPERIMENTAL METHODS

The charge reversal pH-sensitive copolymer was synthesized according to the previously reported procedure. The chemical structure of the copolymer and its working principle was shown in Fig. 1. Biocompatibility of the copolymers was examined by exposing them to the 293T and RAW 264.7 cells. To construct a cationic base layer, MN arrays were coated with polydopamine by dipping the arrays in a dopamine solution. Release of pDNA from MN arrays were investigated by placing MN arrays in PBS (pH 7.4) and citric acid, NaOH buffer (pH 4.03) that were kept on an orbital shaker at 37°C. The cellular uptake of polyplexes was confirmed with RAW 264.7 macrophage cells. The pDNA release was further examined using *in vivo* imaging. Finally, *in vivo* expression of A $\beta$  peptide expression was examined by retrieving the back skin of mice and analysed using ELISA.

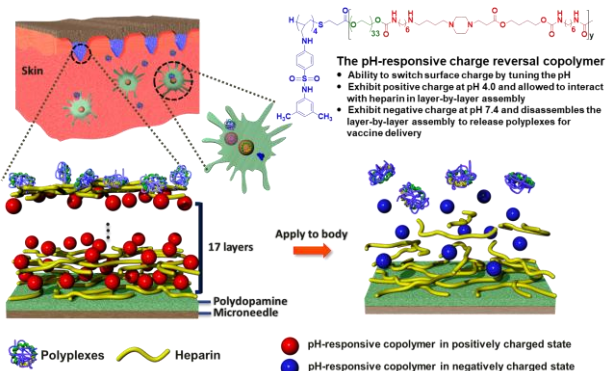


Fig. 1. Schematic illustration of polyplex-coated MNs for cutaneous delivery of DNA vaccines.

### RESULTS AND DISCUSSION

For the synthesis of a charge reversal pH-sensitive copolymer (Scheme 2), carboxylic acid-terminated OSM was first synthesized by the thiol-ene reaction between MPA and SMA in the presence of AIBN as a catalyst and conjugated to the polyurethane copolymer. The copolymer did not show noticeable cell cytotoxicity to the 293T and RAW 264.7 cells. Fig. 2 shows the release and distribution of polyplexes after different route of administration. The vaccination efficacy of the polyplex releasing MNs was examined using an A $\beta$  DNA vaccine (pTarget-Ig-A $\beta$ -Fc). A $\beta$  expression was significantly higher in the mice model treated with MNs compared to SC administration. This is attributed to the length of MNs (330  $\mu$ m) that can reach dermis layer with more APCs than SC injection. In addition, A $\beta$  expression was visualized by immunohistofluorescence via staining with Alexa Fluor 488 secondary antibodies. The MNs coated with DNA vaccines on the top painlessly penetrated the stratum corneum and delivered the DNA vaccines efficiently to the epidermis and dermis for immunization. *In vivo* immunization results demonstrated that targeted delivery of a DNA vaccine encoding A $\beta$  fusion protein to APCs induced robust antigen-specific immune response.

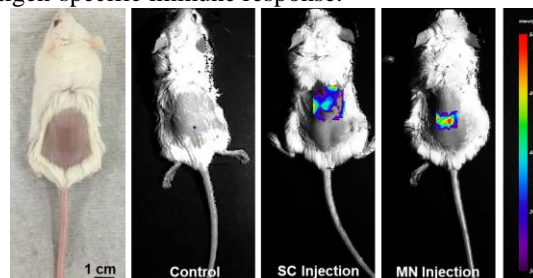


Fig. 2. *In vivo* biodistribution of polyplexes released after injection.

### CONCLUSION

We successfully synthesized a novel charge reversal pH-responsive copolymer as the release-layer for DNA vaccine delivery using microneedles. OSM-*b*-PEG-*b*-PAEU exhibited a rapid pH-responsive change in surface properties, which led to rapid release of polyplexes from MNs into the skin. These results demonstrated the potential utility of this approach for vaccination of Alzheimer's disease.

### REFERENCES

1. Duong HTT. *et al.*, J Control Release. 269:225-234, 2018

### ACKNOWLEDGMENTS

This research was supported by the National Research Foundation of Korea (NRF) funded by The Ministry of Science, ICT & Future Planning (NRF-2017R1D1A1B03028061).

## The Effect of Chemical Composition on Crosslinking Kinetics of Methylcellulose/Agarose Hydrogel

Beata Niemczyk, Paweł Sajkiewicz, Arkadiusz Gradys

Laboratory of Polymers and Biomaterials, Institute of Fundamental Technological Research,  
Polish Academy of Sciences,  
Pawińskiego 5b St., 02-106 Warsaw, Poland  
[bniemczyk21@gmail.com](mailto:bniemczyk21@gmail.com)

### INTRODUCTION

Currently, injectable thermosensitive in-situ gelling hydrogels are investigated as polymeric scaffolds directed toward tissue engineering applications. Their attractiveness is connected with minimally invasive effect of injection to body, solidification within injured tissue providing complete filling of the lesion and effective delivery of therapeutics [1].

Methylcellulose (MC) and rather unique methylcellulose/agarose (MC/AGAR) systems were investigated. The aim of this study was to investigate the kinetics of cross-linking, and mechanical properties of MC and MC/AGAR systems in order to find optimal conditions for tissue engineering applications.

### EXPERIMENTAL METHODS

Methylcellulose METHOCEL A15LV (Sigma Aldrich) was obtained in various concentrations (3; 5; 7 % (w/v)) in demineralized water [2]. The MC aqueous solution was mixed in 1:1 w/w ratio with agarose SEAPREP (Lonza) aqueous solution (1,5%(w/v)) [3, 4].

The cross-linking kinetics of MC and MC/AGAR aqueous solutions were carried out by dynamic mechanical analysis (DMA), using Anton Paar Physica MCR301 rheometer. The oscillatory analysis was performed utilizing small-amplitude sinusoidal deformation. In the temperature range 33-39°C, under isothermal conditions, time dependence of the storage modulus,  $G'$ , the viscous modulus,  $G''$ , and complex viscosity were determined. Observing, that there is no intersection of  $G'$  and  $G''$  curves, the kinetics of cross-linking was deduced from the time derivative of the  $G'$ , providing, as parameters of cross-linking, the time position and the height of the maximum of the time derivative of  $G'$ . Approximation and extrapolation beyond the registered time range with asymmetric double sigmoidal function as well as integration, allowed estimation of the final modulus and complex viscosity of hydrogels, which is crucial from the practical perspective.

Additionally, thermal effects of cross-linking were studied by differential scanning calorimetry (DSC). Measurements were carried out using Pyris 1 DSC (Perkin Elmer). To avoid water evaporation, hermetic pans were used.

### RESULTS AND DISCUSSION

DMA studies revealed that addition of agarose, generally, improves mechanical properties of methylcellulose, what agrees with the data reported in [3].

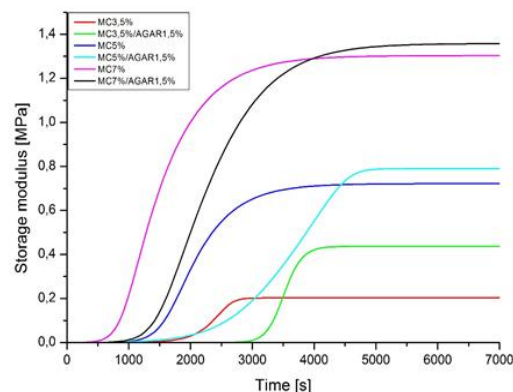


Fig. 1. Storage modulus vs. time for various concentrations of MC and MC/AGAR aqueous solutions at 37°C.

However, as oppositely to [3], it also considerably increases the time of cross-linking, what may be explained as due to the presence of long agarose molecules, which act as steric barriers on the way of methylcellulose crosslinking. As reported in [3], addition of agarose accelerates dehydration of methylcellulose, thereby improves hydrophobic interactions between MC chains. As shown in the Fig 1, the higher the concentration of MC and MC/AGAR, both  $G'$  increases and cross-linking accelerates.

### CONCLUSION

Addition of agarose considerably extends the cross-linking time and improves mechanical properties of methylcellulose hydrogel, making this approach attractive for soft tissue engineering applications as injectable hydrogels.

### REFERENCES

1. Lis A. *et al.*, Polim. Med. 43:302-312, 2013.
2. [http://msdssearch.dow.com/PublishedLiteratur/eDOWCOM/dh\\_08e5/0901b803808e5f58.pdf?filepath=dowwolff/pdfs/noreg/198-02289.pdf&fromPage=GetDoc](http://msdssearch.dow.com/PublishedLiteratur/eDOWCOM/dh_08e5/0901b803808e5f58.pdf?filepath=dowwolff/pdfs/noreg/198-02289.pdf&fromPage=GetDoc)
3. Martin B C *et al.* J. Neural Eng. 5:221, 2008.
4. Rivet C J *et al.* Biomatter; 5:e1005527, 2015.

### ACKNOWLEDGMENTS

Special acknowledgements go to dr. A.Krztoń-Maziopa (Warsaw University of Technology) for access to DMA.

## Synthesis of Biopolymers by Bacterial Strain *Azotobacter Agile 12*

Andrej Dudun<sup>1</sup>, Elizaveta Akoulina<sup>1,2</sup>, Anton Bonartsev<sup>2</sup>, Vera Voinova<sup>2</sup>, Tatiana Makhina<sup>1</sup>, Garina Bonartseva<sup>1</sup>

<sup>1</sup>Research Center of Biotechnology RAS, Russia

<sup>2</sup>Faculty of Biology, M.V.Lomonosov Moscow State University, Russia

[dudunandrey@mail.ru](mailto:dudunandrey@mail.ru)

### INTRODUCTION

Alginates (ALG) and polyhydroxybutyrate (PHB) are two main polymers that can be produced by bacteria of the genus *Azotobacter sp.* These two polymers possess biotechnological importance; ALG, an extracellular polysaccharide, and PHB, an intracellular polyester of the polyhydroxyalkanoates (PHAs) family.<sup>1</sup> Main advantage of bacterial synthesis of polymers is that we can control their properties. Such as molecular weight (MW) for both of them, ratio of guluronic and mannuronic acids and level of acetyl groups in mannuronic acids in ALG.

### EXPERIMENTAL METHODS

**The object of study.** In this work was used strain *Azotobacter agile 12* isolated from soddy-podzolic soils of the Moscow region. Bacterial culture was cultivated in liquid Burk's medium at low concentrations of phosphates and with high aeration.<sup>2</sup>

**Isolation of ALG in culture media.** The alginates were isolated by precipitation with 3X volume of ethanol from the culture medium. Capsular ALG was isolated from the bacterial capsules by processing biomass with a solution of 1M NaCl and 10mM EDTA and further precipitation from supernatant with 3X volume of ethanol and then lyophilised.

**Isolation of PHB from bacterial biomass.** The isolation of PHB from bacterial biomass was carried out by extraction with chloroform for 12 hours at 37°C. Next, the PHB solution was separated from the cell residues by filtration, the next step was the isolation of PHB from the chloroform solution by isopropyl alcohol precipitation. The stage of dissolution in chloroform and precipitation of PHB with isopropyl alcohol was repeated at least 3 times. The PHB was dried at 60°C.

**Determination of ALG and of PHB viscosity.** The molecular weight (MW) of the biopolymers were determined by viscosimetry. The specific viscosity was calculated according to the formula

$$\eta_{sp} = (t - t_0)/t_0,$$

where  $t_0$  is the flow time of the solvent and  $t$  is the flow time of the polymer solution. The molecular weight was calculated according to

the Mark-Houwink equation<sup>3</sup>  $[\eta] = K(M)^a$  with the following coefficients for ALG:

$$K = 7.3 \times 10^{-5}; a = 0.92;$$

$$[\eta] = 7.3 \times 10^{-5} \times (M)^{0.92};$$

And for PHB:

$$K = 7.7 \times 10^{-5}; a = 0.82;$$

$$[\eta] = 7.7 \times 10^{-5} \times (M)^{0.82};$$

where  $M$  is the molecular weight and  $[\eta]$  is viscosity.

### RESULTS AND DISCUSSION

In our early studies we showed that in usual growth conditions (standard Burk's medium) with low aeration yield of PHB is relatively high (80%) and its MW is about 1000-1500 kDa.<sup>4</sup> However in the current studies during cultivation with high aeration yield of PHB was significantly lower (20%), but MW remained the same. Also we obtained large yield of ALG (exo- and capsular) with high MW (Table 1). In the presence of ions  $Ca^{2+}$  the gelling properties of the capsular ALG are better than that of exo-ALG, due to the fact that MW capsular ALG is much higher in comparison with exo-ALG. Such decrease of PHB yield and high MW of ALG can be explained by the special cultivation conditions of the strain, which were grown with an increased level of aeration.

Table 1. Production of ALG and PHB by strain *Azotobacter agile 12*

	g/l	g/g (dry biomass)	Yield capsular ALG (%)	MW (kD)
ALG	2.62	1.37	73	430 (capsular ALG) 112 (exo-ALG)
PHB	0.38	0.20	-	1472

### CONCLUSION

Influence of different growth conditions on synthesis of polymers by the bacterial strain *Azotobacter agile 12* was shown. This strain under high aeration demonstrated the predominance of synthesis ALG over PHB. Such difference in gelling properties of exo- and capsular ALG can be useful for different fields of biotechnology. Further work will provide studying of various fermentation parameters influence on production and composition of ALG and PHB and new fermentation strategies development which can increase ALG and PHB production by bacteria of the genus *Azotobacter sp.*

### REFERENCES

- Galindo E., Peña C., Núñez C., Segura D., Espin D., 2007 Molecular and bioengineering strategies to improve alginate and polyhydroxyalkanoate production by *Azotobacter vinelandii*. *Microbial Cell Factories*, 6 1 16.
- Bonartseva G. A. *et al.* *Appl Biochem and Microbiol*, 53(1):52–59, 2017.
- Usov, A.I., *Usp Khim*, 68(11):1051–1061, 1999.
- Bonartsev A.P. *et al.* *Prep. Biochem. Biotechnol.*, 47(2): 173-184, 2017.

### ACKNOWLEDGMENTS

This work was supported by Russian Science Foundation, project # 17-74-20104.

## Hydrogels Cross-Linked by Trehalose Diacetals with Tunable Degradation Rate in Acidic Solutions as Carriers for pH-triggered Protein Release

Małgorzata Burek<sup>1</sup>, Sylwia Waśkiewicz<sup>2</sup>, Klaudia Kubic<sup>1</sup>, Izabela Nabiałczyk<sup>1</sup>, Ilona Wandzik<sup>1</sup>

<sup>1</sup>Department of Organic Chemistry, Bioorganic Chemistry and Biotechnology,

<sup>2</sup>Department of Physical Chemistry and Technology of Polymers,

Faculty of Chemistry, Silesian University of Technology, Gliwice, Poland

[malgorzata.burek@polsl.pl](mailto:malgorzata.burek@polsl.pl)

### INTRODUCTION

Polymers that undergo physical or chemical changes in acidic solutions are widely studied as drug carriers designed for both localised or prolonged release.<sup>1,2</sup> Besides the obvious body parts such as: skin, gastrointestinal track or vagina, the local acidic environment is characteristic feature of tumour tissues as well as inflammation or ischemia sites. A large pH shift from 7.2–7.4 in the blood or extracellular spaces to 4.0–6.5 in the various intracellular compartments takes also place during cellular uptake. Common strategy of ensuring triggered drug release under such conditions is to provide acid-degradability to polymer through the incorporation of acid-cleavable groups within its structure. Among them, acetals, that are stable at neutral and basic pH, but are susceptible to acid-catalysed hydrolysis, are one of the most frequently utilised. Herein, we present study on hydrogels that are cross-linked by trehalose diacetals. Compared to popular acetal-based cross-linkers which release low molecular weight aldehyde or ketone during hydrolysis, the proposed cross-linkers degrade to trehalose – disaccharide, which is Generally Regarded As Safe by FDA, while aldehyde fragments stay linked with polymer chains (Fig. 1).

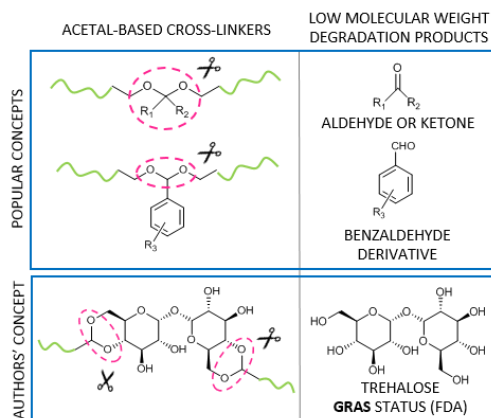


Fig. 1. Chemical structure of acid-cleavable fragment in acetal-based cross-linkers and corresponding low molecular weight degradation products.

### EXPERIMENTAL METHODS

Trehalose diacetals were obtained in acid-catalysed transacetalization reaction between trehalose and various derivatives of benzaldehyde dimethyl acetal.<sup>3</sup> Hydrogels were prepared by redox initiated free radical polymerization as bulk materials. Model protein (bovine serum albumin) was entrapped within hydrogels during their synthesis. NMR spectroscopy was used to confirm the structure of cross-linkers, degradation products as well as to compare hydrolysis rate of variously

substituted cross-linkers in acidic solution. The content of trehalose incorporated within the hydrogels was examined enzymatically by using Trehalose Assay Kit. The internal microstructure of hydrogels was studied by Scanning Electron Microscopy after freezing in liquid nitrogen, freeze-drying and gold covering. Release of model protein in PBS (pH 5.0 or 7.4) at 37°C was determined by using Bradford method. MTS assay was used to evaluate cytotoxicity of degradation products.

### RESULTS AND DISCUSSION

A series of 4,6:4',6'-benzylidene diacetals of trehalose bearing acryloyl functionality was synthesized and further utilised as cross-linking agents in hydrogel synthesis. They were designed taking into account substituent effect in aromatic acetals on the hydrolysis rate, with the aim to obtain materials with various degradation characteristic in acidic solution. Indeed, the trend in the order of degradation rates of the hydrogels followed the trend determined for corresponding acetals. Degradation rate was also influenced by network properties, and increased with increasing cross-linking degree, hydrophobicity of the monomer used as well as matrix density resulting from the monomer concentration during polymerization. Along with the progress in degradation significant changes in the internal microstructure were recorded by SEM. Analysis of degradation solutions by NMR spectroscopy confirmed the formation of polymer with aromatic moieties and free trehalose. Release study of model protein has shown clear correlation to degradation characteristic.

### CONCLUSION

The presented results show that release of physically entrapped protein from hydrogel materials cross-linked by 4,6:4',6'-benzylidene diacetals of trehalose could be easily tuned by substituent effect and network properties. Trehalose cleaved in course of degradation, apart from being nontoxic have also additional advantage in context of protein carriers, as it is a well-known molecular chaperone.

### REFERENCES

1. Binauld S. *et al.*, Chem. Commun. 49:2082-2102, 2013
2. Mura S. *et al.*, Nat. Mater 12:991-1003, 2013
3. Patent application P.423711

### ACKNOWLEDGMENTS

This work was financially supported by the National Science Centre, Poland under the project 2014/15/N/ST8/02707.



## Effect of Bacterial Alginate on Growth of Mesenchymal Stem Cells

Elizaveta Akoulina<sup>1,2</sup>, Anton Bonartsev<sup>1,2</sup>, Garina Bonartseva<sup>2</sup>, Vera Voinova<sup>1</sup>

<sup>1</sup>Faculty of Biology, M.V.Lomonosov Moscow State University, Russia

<sup>2</sup>Research Center of Biotechnology RAS, Russia

[akoulinaliza@gmail.com](mailto:akoulinaliza@gmail.com)

### INTRODUCTION

Alginates (ALG) are polysaccharides produced by brown sea weeds and some bacteria (f.e. *Azotobacter sp.*) are very interesting biopolymers for use in biotechnology. Mostly because of ALGs qualities such as biocompatibility, biodegradation and also because its ability to form gel with bivalent ions like  $Ca^{2+}$ . Bacterial ALG is different from algae ALG by having acetylation. Also by bacterial biosynthesis we can control monomers ratio and molecular weight of biopolymer which makes it more useful for different trends in biotechnology such as tissue engineering for example. Most researches use algae ALG.<sup>3</sup> In this work we compared cytotoxicity of algae and bacterial ALG using mesenchymal stem cells (MSC).

### EXPERIMENTAL METHODS

ALG was produced by strain *Azotobacter chroococcum 7B*, isolated from soddy-podzolic soils of the Moscow region. Bacterial cultures were cultivated in solid Ashby's medium or in liquid Burk's medium.<sup>2</sup>

ALG was isolated from culture media by adding threefold volume of ethanol. Also to get capsule ALG biomass was processed with 0.9% NaCl and 50mM EDTA and after that the samples were centrifuged for 30 min at 15 000 g. Supernatant was isolated and supplemented with a threefold volume of pure ethanol. Cytotoxicity of ALG was examined by week cocultivation experiment with mesenchymal stem cells (MSCs). MSCs were isolated from one week old rats using standard method with collagenase.<sup>4</sup>

ALG of different origin and concentration was added to MSCs while they grow on plastic. Determination of cell number was made by standard XTT test.<sup>5</sup>

### RESULTS AND DISCUSSION

The use of different substances in bioengineering requires an answer to the question: is this material cytotoxic or not. The most common way to test cytotoxicity of this material is to add it into the media with growing cells and to see what happens. In this work we observed influence of ALG of different origin on MSCs growth. Figure 1 shows that adding ALG in medium didn't cause decrease of MSCs growth. Cells grew with bacterial ALG in media even better than without it. But, of course, concentration is an important factor, and lower concentration was better for cells.

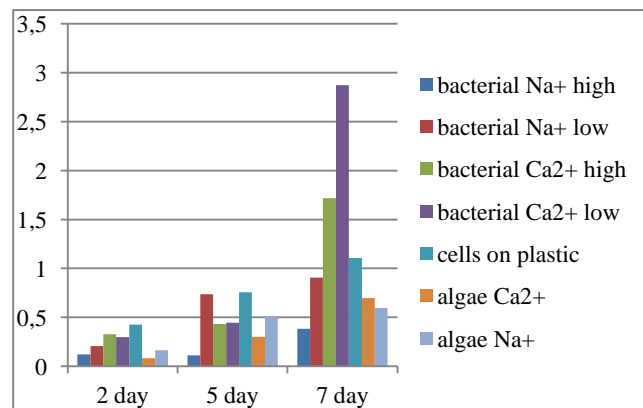


Fig. 1. Cell growth on plastic with bacterial or algae ALG or without.

### CONCLUSION

Thus, ALG of bacteria origin has no cytotoxicity and may even be causing an improvement in cell growth, which gives hope for use of bacterial alginate in biotechnology and biomedicine.

### REFERENCES

1. Bonartsev A.P. *et al.* Prep. Biochem. Biotechnol., 47(2): 173-184, 2017.
2. Bonartseva G. A. *et al.* Appl Biochem and Microbiol, 53(1):52-59, 2017.
3. Bidarra S. J. *et al.* Biomacromolecules 11:1956-1964, 2010.
4. Maniatopoulos C. *et al.* Cell Tissue Res 254:317-330, 1988.
5. Sutherland M.W. *et al.* Free Rnd. RPS, 27(3): 283-289, 1997.

### ACKNOWLEDGMENTS

This work was supported by Russian Science Foundation, project # 17-74-20104. The equipment of User Facilities Centers of M.V.Lomonosov Moscow State University (incl. in framework of Development Program of MSU to 2020) and Research Center of Biotechnology RAS was used in the work.

## Biodegradable non-thermosensitive pseudo-double networks as potential hydrogels to release viable cell sheets for tissue regeneration

Ana Civantos<sup>2,3</sup>, Isabel Casado-Losada<sup>1</sup>, David Acitores<sup>1</sup>, María Eugenia Perez-Ojeda<sup>4,5</sup>, Enrique Martínez-Campos<sup>1,5</sup>, Viviana Ramos<sup>1</sup>, Alberto Gallardo<sup>5</sup>

<sup>1</sup>Tissue Engineering Group, Institute of Biofunctional Studies, Complutense University of Madrid (UCM), Spain  
Associated Unit to the Institute of Polymer Science and Technology (CSIC)

<sup>2</sup>Department of Nuclear, Plasma, and Radiological Engineering, University of Illinois, Urbana-Champaign, USA

<sup>3</sup>Micro and Nanotechnology Laboratory, University of Illinois, Urbana-Champaign, USA

<sup>4</sup>Institute of Organic Chemistry II, Friedrich-Alexander-University of Erlangen-Nürnberg (FAU), Germany

<sup>5</sup>Polymer Functionalization Group, Institute of Polymer Science and Technology, ICTP-CSIC, Madrid, Spain

[ancifle@illinois.edu](mailto:ancifle@illinois.edu)

### INTRODUCTION

Cell sheet detachment platforms avoid the use of aggressive chemical (e.g. trypsin enzyme) and physical (e.g. cell scraping) methods to release cells, therefore, represents a gentler and non-destructive mode of cell harvesting. Keeping intact the ECM structure, this technology allows direct cell sheet transplantation to damage host tissues which has been applied in cornea reconstruction, and periodontal ligament among others<sup>1</sup>. As an interesting alternative to commercially available products such poly-N-isopropylacrylamide (pNIPAm)<sup>2</sup>, is the interpenetrating polymer networks (IPNs) offering easy and biocompatible substrates. In this sense, we have used Vinylpyrrolidone (VP), a non-ionic amphiphilic polymer, which is non-toxic and biocompatible, required properties to use in tissue engineering approaches. These VP pseudo-double networks (Pseudo-DNs) have exhibited good mechanical properties in terms of swelling, compression and elastic modulus, with a strong relationship with degree of crosslinking<sup>1</sup>. This new method allows to design full-adaptable hydrogels in terms of size and thickness<sup>3</sup>. For that reason, in this present work, we have developed a new method to produce VP biodegradable hydrogels with pseudo-double network structure for cell sheet detachment and manipulation.

### EXPERIMENTAL METHODS

Pseudo-DN based on vinylpyrrolidone (VP) and sulfopropyl methacrylate were prepared following a one-step procedure, initiated by UV stimulation. Two different networks were synthesized crosslinkers prepared by Acetal and Michael's addition, VPB and VPA respectively. VPC was synthesized as non-degradable hydrogel (Control). Degradation behavior was evaluated by gravimetric method using different pH buffers till 144h. *In vitro* experiments were performed using C166-GFP (ATCC® CRL-2583™), and mouse macrophagic cell line, RAW 264.7 (ATCC® TIB-71™). Cell viability, proliferation and cell sheet detachment at 5 and 7 day of cell culture were studied through the analysis of cell metabolic activity by Alamar Blue assay (Thermofisher). Images were taken using inverted fluorescence microscope Olympus BX51.

### RESULTS AND DISCUSSION

Biodegradable hydrogels (VPA and VPB) showed 90% of cell viability as non-degradable substrate (VPC) to

C166 GFP cell culture, measured by alamarblue of culture media extracts. Moreover, the hydrogels allowed cell attachment and proliferation for both cell lines, however, VPA presented higher degradation rate and was not stable for cell detachment manipulation (144h). In addition, VPC and VPB, allowed cell proliferation after 144h allowing successful detachment of fully cell sheets. However, VPB showed an increased biocompatibility for RAW 264.7 compared to VPC demonstrating its non-cytotoxic behavior. Cells sheets were easily detached from the substrates by means of a mechanical procedure and subsequently, they were able to attach and proliferate, confirmed by metabolic activity measurement and microphotographs taken. Non-inflammatory response was observed as indicated by the macrophages cell morphology growing on the hydrogels.

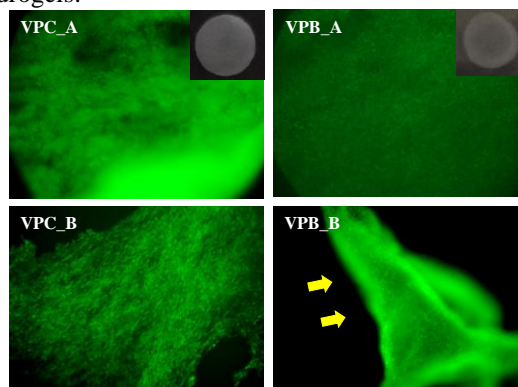


Fig. 1. Detachment experiment of C166-GFP cell sheet (A) before and (after) revealing viable cells. The upper right side, shows the macroscopic differences on the hydrogels (see inserts).

### CONCLUSION

Biodegradable hydrogels based on VP have shown to be suitable for cell sheet manipulation. These degradable substrates can be used to tissue regeneration applications.

### REFERENCES

1. Aranaz, I., *et al.* J. Mater. Chem B, 2(24), 3839-3848 (2014).
2. Kumashiro, Y., *et al.* Ann. Biomed Eng, 38(6), 1977-1988. (2010).
3. Civantos, A., *et al.* (2016). Adv. Mater Interf, 463-495, (2016).

### ACKNOWLEDGEMENTS

The authors gratefully acknowledge support from Grants MAT2010-20001 from the Ministry of Science and Innovation, Spain.

## Surface Functionalization of Ti6Al7Nb Alloy with Biopolymers and DLC-based Coatings Using Plasmochemical Activation

Karol Kyziol<sup>1</sup>, Julia Oczkowska<sup>1</sup>, Karol Wolski<sup>2</sup>, Agnieszka Kyziol<sup>2</sup>, Łukasz Kaczmarek<sup>3</sup>

<sup>1</sup>Faculty of Materials Science and Ceramics, AGH University of Science and Technology, Poland

<sup>2</sup>Faculty of Chemistry, Jagiellonian University, Poland

<sup>3</sup>Institute of Materials Science and Engineering, Łódź University of Technology, Poland

[kyziol@agh.edu.pl](mailto:kyziol@agh.edu.pl)

### INTRODUCTION

Titanium and its alloys are considered to be the most attractive metallic materials for biomedical applications. Ti6Al7Nb has long been favored for biomedical applications because of its excellent properties (*e.g.* relatively low Young's modulus and high biocompatibility)<sup>1</sup>. However, in the case of particular applications surface modification, especially treatment in plasma conditions, is a method to improve blood contact, anti-metallosis properties and hardness of implant<sup>2</sup>. Technological parameters, as well as composition of gas mixture, in plasma process usually consisting of *inter alia* oxygen alter surface properties of the material, such as surface topography or cell adhesion<sup>3</sup>.

Over the last decade, attention in medical applications was focused also on biopolymers due to their biocompatibility, non-toxicity, biodegradability, and capability to adsorb bioactive molecules. Chitosan is one of the most useful biopolymer containing high concentration of nitrogen which prevents thrombosis owing to its chelation ability and fact, that this element is a part of most proteins<sup>4</sup>. However, intensive research is being carried out to develop technology for obtaining durable functional coatings on metallic substrates based on biopolymers.

In this study, biopolymer-based or DLC-based coatings were deposited after plasma pre-functionalization of Ti6Al7Nb substrate in order to improve surface properties, such as surface free energy and biocompatibility. Samples made from Ti6Al7Nb were polished and functionalized in PA RF CVD (Plasma Assisted Radio-Frequency Chemical Vapour Deposition) system. In first stage of surface functionalization of Ti alloy with argon, oxygen, nitrogen and ammonia as reagents (mixed in various volume ratios) in gas mixture were performed.

### EXPERIMENTAL METHODS

The experimental series of un-modified and modified Ti6Al7Nb alloy were characterized with application of SEM-EDS and AFM microscopy. In addition the X-ray diffraction (XRD) technique was used to determine crystal structure of samples after pre-functionalization in plasma conditions. The atomic structure of biopolymer (chitosan) and Si-DLC coatings, obtained of most promising series of experimental series, were characterized using ATR IR and Raman spectroscopy. Additionally, surface energy and cytotoxicity tests *in vitro* were conducted.

### RESULTS AND DISCUSSION

The most profitable composition of gas mixture in the plasma functionalization, before coatings deposition was determined. For example, in the case of Ar/O<sub>2</sub>/NH<sub>3</sub> mixture, plasmochemical modification of Ti6Al7Nb alloy leads to increase of oxygen and nitrogen content up to *ca.* 12.0 at. % and 14.0 at. %, respectively. All obtained surface modified series showed significant changes in the topography of the Ti6Al7Nb surface (Fig. 1).

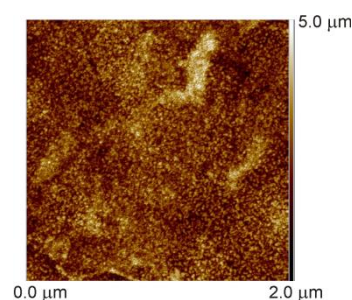


Fig. 1. AFM image (2D) of Ti6Al7Nb surface after surface functionalization with application of Ar/O<sub>2</sub> mixture in plasma conditions

XRD study confirmed the existence of TiO<sub>2</sub> and/or TiN phases on the alloy surface, depending on the chemical composition of plasma during surface functionalization.

### CONCLUSION

In conclusion, it was demonstrated that composition of gas mixture (applied before coatings deposition) has a significant influence on surface topography (also roughness) and content of oxygen atoms in the outer layer. This results in possibility of further post-functionalization with biopolymer application. The obtained coatings on Ti6Al7Nb surface after plasma treatment in Ar/O<sub>2</sub>/NH<sub>3</sub> mixture, in particular chitosan-based ones, are homogeneous, possess good adhesive properties and improved mechanical properties (decreased Young modulus) as well as are characterized by non-cytotoxicity.

### REFERENCES

1. Kulkarni M. *et al.*, In: Nanomedicine, One Central Press, UK, 2014
2. Govindarajan T. *et al.*, Polymers 6, 2309-2331, 2014
3. Mohan L. *et al.*, Appl. Surf. Sci. 268, 288-296, 2013
4. Park S.B. *et al.*, Prog. Polym. Sci. 68, 77-105, 2017

### ACKNOWLEDGMENTS

This work has been financed by Polish National Center for Science, NCN, grant decision DEC-2017/01/X/ST8/00886.



## One-step Sonochemical Fabrication and Embedding of Gentamicin Nanoparticles into Parylene C Implant Coating

Monika Golda-Cepa, Paulina Chytrosz, Aleksandra Chorylek, Andrzej Kotarba

Faculty of Chemistry, Jagiellonian University, Poland

[kotarba@chemia.uj.edu.pl](mailto:kotarba@chemia.uj.edu.pl)

### INTRODUCTION

There is an ongoing demand to enhance reliability and bioacceptability of a huge gamut of new medical devices which in the recent years motivates scientists to face the challenges of modern healthcare. One of the general strategies for implant surface engineering focuses on the application of polymer coatings to fabricate robust, biocompatible and antibacterial interfaces. However, all the biomaterial surfaces can be contaminated during surgery, mostly by bacteria genus *Staphylococcus* and *Pseudomonas*. Patients who underwent a recent surgical procedure and whose immune system is impaired are at high risk of Biomaterials Centered Infection (BCI). There are several strategies to prevent BCI, among them, the direct insertion of antibiotic molecules into the coating on the surface of the medical device is a straightforward promising strategy. Sonochemical irradiation has been proven as an effective technique for the synthesis of nanocrystalline materials, and the precise control of key process parameters (time, power, pulse, amplitude) allows for controlling the size of the nanoparticles and as a consequence targeted elution kinetic.

The aim of the study was to generate the antibiotic nanoparticles under ultrasound irradiation and in-situ embed them into the surface pores of the parylene C.

### EXPERIMENTAL METHODS

Parylene C films were prepared by a CVD (ParaTech Coating Scandinavia AB). The thickness of the parylene C layer was 8  $\mu\text{m}$ . Surface of the polymeric materials were modified with the oxygen plasma (oxygen partial pressure of 0.2 mbar, plasma generator power of 50 W, and exposure time of 8 min).

Gentamicin sulfate nanoparticles (GNPs) were formed and deposited in one-step process on the plasma modified parylene C using an ultrasonic homogenizer (frequency of 20 kHz, amplitude 30%, and time 6 min). Solution of gentamicin sulfate (50 mg/ml) in deionized water was used. The developed system was thoroughly characterized in terms of particle size (NTA, STEM/EDX), surface dispersion (IR-image) and drug release kinetics (UV-Vis).

### RESULTS AND DISCUSSION

The applied sonochemical method resulted in the formation of amorphous gentamicin nanoparticles in majority  $<70$  nm. No evidence for the existence of macroparticles was found in the fabricated samples. The presence of the intact gentamicin molecules and their distribution in the form of the sonochemically obtained NPs were confirmed using IR-image technique. The collected spectra revealed a characteristic band at 1037  $\text{cm}^{-1}$  for gentamicin (group C–N, C–O). The corresponding absorbance maps (20  $\mu\text{m} \times 20 \mu\text{m}$ ) were

collected at this characteristic wavelength. An apparent increase in the absorbance was observed for drug-containing samples when compared to the parent oxygen plasma modified parylene C, indicating the presence and fairly uniform distribution of the GNPs at the micrometric scale. The obtained GNPs/parylene C system was thoroughly evaluated in terms of controlled drug release kinetics. To achieve the desired functionality of the obtained drug-polymer couple, drug elution studies were performed to determine stability and elution kinetics of the gentamicin NPs deposited on the parylene C. For the average sample (2  $\text{cm}^2$ ) drug load was estimated to be  $\sim 4 \mu\text{g}$ . It was found that GNPs/parylene C system provided prolonged drug elution time reaching 7 days. The experimental results were in good agreement with Korsmeyer–Peppas kinetic model ( $k=30.77$ ,  $n=0.308$ ,  $R^2=0.9796$ ), revealing the diffusion-controlled drug release.

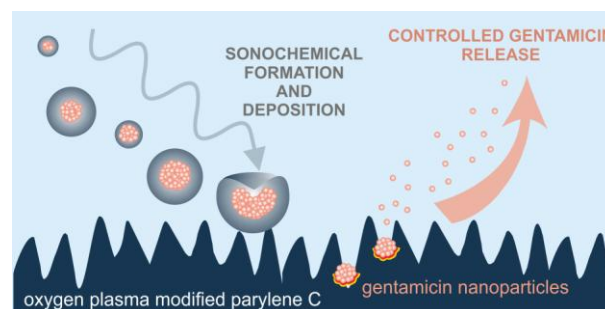


Fig. 1 The overview of the conducted research leading to gentamicin nanoparticles formation, their embedding into parylene C pores and subsequent, controlled release.

### CONCLUSION

A one-step sonochemical method was employed for the first time for gentamicin nanoparticles (GNPs) fabrication and embedding into the surface of parylene C implant coating. It was revealed that the optimization of the applied ultrasound conditions resulted in the formation of GNPs with an average size in the narrow range of 30-70 nm and their docking into the parylene C nanopores, while the molecular structure of the antibiotic was preserved. The obtained surface morphology resulted in controlled elution of the drug up to 7 days, and the kinetics followed the Korsmeyer–Peppas model. The apparent benefits of the proposed sonochemical approach (short preparation time, direct drug accessibility, lack of chemical wastes) are pointed out.

### REFERENCES

1. Golda-Cepa M. *et al.*, Nanomedicine: NBM. Article in press, 2018



## Assessment of Haemo- and Biocompatibility of Different Polyurethane-based Electrospun Vascular Grafts

Vera Chernonosova<sup>1,2</sup>, Alexander Gostev<sup>1</sup>, Andrey Karpenko<sup>1</sup>, Alexander Karaskov<sup>1</sup>, Evgeny Pokushalov<sup>1</sup>, Pavel Laktionov<sup>1,2</sup>

<sup>1</sup>“E. Meshalkin National medical research center” of the Ministry of Health of the Russian Federation, Novosibirsk

<sup>2</sup>Institute of Chemical Biology and Fundamental Medicine, Novosibirsk, Russia

[vera\\_mal@niboch.nsc.ru](mailto:vera_mal@niboch.nsc.ru)

### INTRODUCTION

Clinical efficiency of artificial small diameter vascular grafts (VG) remains poor, owing to blood clotting or neointimal hyperplasia resulting in stenosis<sup>1-2</sup>. Thus, ensuring both the short and long term haemocompatibility requires preventing of clotting after implantation and promoting the formation of the surface layer of endothelial cells. Electrospinning was shown to be a convenient method for VG production, but aforesaid requirements have not been completely satisfied yet. In this study we investigated the interaction of electrospun VGs with blood and endothelial cells. The VGs were produced from solutions of polyurethanes<sup>3</sup> (PU) with biopolymers which were intended to prevent blood clotting and increase cell adhesion.

### EXPERIMENTAL METHODS

Tubular grafts (2 mm diameter, 100 ± 20 µm wall thickness) were produced by electrospinning using the NF-103 setup from following solutions of the components in hexafluoro-2-propanol: 3% PU Tecoflex EG-80A (Lubrizol Inc.) (w/v %); 3% PU with 15% gelatin (GL) (w/w % to PU); 3% PU with 1.5% bivalirudin (BV) (w/w % to PU); 3% PU with 15% GL and 1.5% BV. GL in VGs was fixed by glutaraldehyde (GA) when mentioned.

Donor blood was pumped through the tubular graft using a custom made hydraulic stent for 20 min, 400 ml/min. Concentrations of fibrinogen (FG), D-dimers, APTT, and haemolysis rate were measured using kits from Siemens Healthcare Diagnostics Products GmbH (Germany) against untreated blood. Platelet adhesion was studied by scanning electron microscopy (SEM) on JSM-6460 LV (Jeol).

Human Umbilical Vein Endothelial Cells (HUVEC) were obtained and cultivated on surface of the materials as described elsewhere<sup>4</sup>.

### RESULTS AND DISCUSSION

It was found that fibrinogen and D-dimers levels, but not haemolysis rate, were independent from the chemical composition of VGs (Table 1).

Table 1. Haemostasis parameters in the blood after contact with VGs.

Sample	FG (g/l)	APTT (sec)	D-dimers (µg/ml)	Haemolysis (%)
Control blood	2.23±0.05	30.4±3.9	0.19±0.02	-
PU	2.17±0.02	30.6±3.3	0.17±0.01	2.98±0.74
PU-BV	2.27±0.05	65.73±8.3	0.16±0.01	3.84±1.75
PU-GL	2.27±0.04	31.2±3.7	0.16±0.01	10.46±0.91
GA-treated PU-GL	2.20±0.06	29.8±3.6	0.18±0.01	2.57±0.63
PU-BV-GL	1.97±0.01	120.2±17.4	0.22±0.03	7.27±0.39
GA-treated PU-BV-GL	2.24±0.05	31.2±3.7	0.18±0.01	5.27±1.25

The two-fold increase in the APTT value was observed in blood after contact with PU-BV and PU-GL-BV grafts, GA-treatment of VGs had no effect on APTT value and resulted in the lowest haemolysis level.

SEM demonstrated (Fig. 1) that the addition of BV and GA treatment of VGs decreased the number of platelets on the surface of the grafts. Using AlamarBlue reagent we showed that HUVECs successfully adhere and proliferate on the surface of GA-treated matrices produced from 3% PU with 15% GL and 1.5% BV.

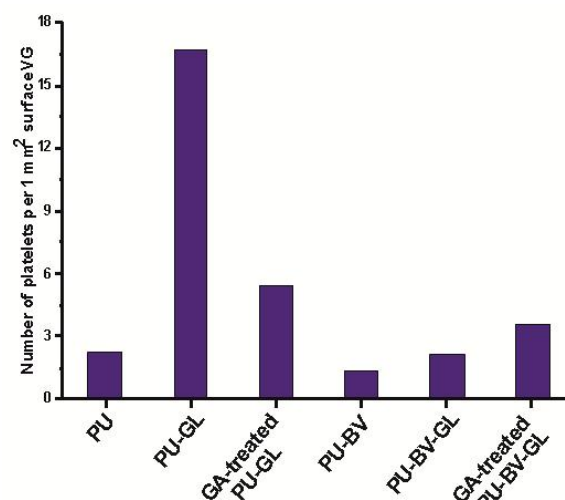


Fig. 1. Platelet adhesion on the surface of the PU-based grafts.

### CONCLUSION

The introduction of BV in VGs had a moderate effect on blood clotting especially after GA treatment. Crosslinking of electrospun VGs from PU with BV also decreased platelet adhesion to the surface of matrices and improved their interaction with endothelial cells. Thus, GA-treated grafts from 3% PU with 15% gelatin and 1.5% bivalirudin demonstrated good haemo- and biocompatibility and are suitable candidates for an *in vivo* study.

### REFERENCES

- Chan-Park M.B. *et al.*, J. Biomed. Mater. Res., Part A. 88A:1104-1121, 2009.
- Kapadia M.R. *et al.*, Circulation.117:1873-1882, 2008.
- Kucinska-Lipka J. *et al.*, Mater. Sci. Eng. C. 46:166-176, 2015.
- Stepanova A.O. *et al.*, Acta Natyrae. 9:79, 2017.

### ACKNOWLEDGMENTS

The study was supported by a grant from the Russian Science Foundation №17-75-30009.

## PLA/Mg Composites Treated with LSP against the Adhesion of Microorganisms

Miguel A. Pacha-Olivenza<sup>1,2</sup>, Amparo M. Gallardo-Moreno<sup>3,2</sup>, José L. González-Carrasco<sup>4,2</sup>, José L. Ocaña-Moreno<sup>5</sup>,  
M. Luisa González-Martín<sup>3,2</sup>

<sup>1</sup>University of Extremadura, Biomedical Sciences, Badajoz, Spain

<sup>2</sup>Networking research Center on Bioengineering, Biomaterials and Nanomedicine (CIBER-BBN), Spain

<sup>3</sup>University of Extremadura, Applied Physics, Badajoz, Spain

<sup>4</sup>National Center for Metals Research (CENIM-CSIC), Madrid, Spain

<sup>5</sup>Polytechnic University of Madrid (UPM) Laser Centre

[mpacoli@unex.es](mailto:mpacoli@unex.es)

### INTRODUCTION

Biodegradable polymeric materials based on polylactic acid (PLA) are currently available for repair applications of bone fractures with low load bearing<sup>1</sup>, gaining popularity due to the avoidance of a removal operation, low immunogenicity, and toxicity. However, their use in clinical practice has been limited to their lack of bioactivity and low mechanical properties<sup>2</sup>. A new strategy to improve the mechanical properties of PLA is the introduction of magnesium (Mg) particles where the polymeric matrix will benefit from the Mg higher strength and modulus, and Mg will benefit from the surrounding protective matrix<sup>3</sup>. Despite these advantages, the composite degrades too fast, and the strength drops sharply just from the initial stages. Gaseous hydrogen and the pH increase associated with the corrosion process might further irritate the injured tissue. A straightforward strategy to tackle hydrogen accumulation is to reduce the corrosion rate by using a promising surface treatment such as Laser Shock Processing (LSP).

A significant problem associated with the use of permanent but biodegradable implants is the appearance of infections<sup>4</sup>. The reason is the fast bacterial colonization of the implant surface by opportunistic microorganisms and the subsequent formation of biofilms<sup>5</sup>.

The purpose of this research is the achievement of information of the characteristics of the early attachment of bacterial strain of *Staphylococcus epidermidis* to polymer-Mg composites treated with LSP.

### EXPERIMENTAL METHODS

PLA was loaded with spherical Mg particles <50 µm in size processed by extrusion and molding by the CENIM-CSIC.

PLA/Mg composite material was subjected to LSP treatment by the UPM Laser Center with different parameters generating 8 different surface finishes.

Bacterial adhesion experiments with the gram-positive strain *Staphylococcus epidermidis* ATCC35983 were carried out with the help of a sterile reusable silicone chamber fixed to the sample surface. Then the bacterial suspension was added to the chamber well and the contact with the alloy surface was allowed for 15, 60, 150 and 90 min. After the adhesion time, the silicone chamber was removed and adhered bacteria were counted using a kit Live/Dead BacLight L-7012.

### RESULTS AND DISCUSSION

The surface of PLA/Mg composite material without LSP treatment generates bactericidal effect on *S. epidermidis* at all times tested. However, when the samples of composite material were treated by LSP, the bactericidal effect appeared after 240 min of contact.

### CONCLUSION

PLA/Mg composites treated with LSP are proposed as a competitive alternative technology to corrosion and stress corrosion cracking which delays the release of Mg from the composite material and, consequently, the bactericidal effect observed in the non-treated samples.

### REFERENCES

1. Maurus P.B. *et al.*, Bioabsorb. Implant Mater Rev Oper Techn Sports Med 12:158, 2004.
2. Bostman O.M. *et al.*, Clin. Orthop. Relat. Res. 371:216,2000.
3. Cifuentes S.C. *et al.*, Mater. Lett. 74:239,2012.
4. Schierholz J.M. *et al.*, J. Hosp. Infect. 49:87,2001.
5. Costerton J.W. Science 284:1318,1999.

### ACKNOWLEDGMENTS

Spanish Junta de Extremadura and FEDER (Grant IB16117&GR15089), and Ministerio de Economía y Competitividad (MAT2015-63974-C4-3-R).

## Physical Surface Changes on a PLA/Mg Composite after Degradation under Physiological Conditions

Daniel Romero-Guzmán<sup>1</sup>, Laura Vazquez-Serrano<sup>1</sup>, Miguel A. Pacha-Olivenza<sup>2,3</sup>, Amparo M. Gallardo-Moreno<sup>1,3</sup>, M. Luisa González-Martín<sup>1,3</sup>

<sup>1</sup>Department of Applied Physics, University of Extremadura, Spain

<sup>2</sup>Department of Biomedical Sciences, University of Extremadura, Spain

<sup>3</sup>Networking Research Center on Bioengineering, Biomaterials and Nanomedicine (CIBER-BBN)  
[mpacoli@unex.es](mailto:mpacoli@unex.es)

### INTRODUCTION

The interaction of any material with the surrounding medium is mediated by physical factors including hydrophobicity, surface tension and surface charge<sup>1</sup>. In the case of biodegradable polymer-based biomaterials both properties can change as time passes due to the polymer degradation. This fact can be more evident when the polymer matrix incorporates soluble metal particles able to dissolve and release ionic species affecting the outer polymer surface and the chemical composition of the surrounding electrolyte.

This work will analyse the hydrophobicity and the electrical potential (zeta potential) of a biodegradable composite PLA/Mg as a function of the degradation time.

### EXPERIMENTAL METHODS

The composite material PLA/Mg was provided by the Centro Nacional de Investigaciones Metalúrgicas (CENIM, CSIC, Madrid), briefly it was a poly-(L,D-lactic) acid (PLA2002D) from NatureWorks with a D-isomer content of 4.25%, molecular weight of 105 kDa and melt flow index (210°C/2.16 kg) of 35.8 g/10 min, and as reinforcement, spherical Mg particles of less than 100 µm in size<sup>2</sup>.

The degradation of the composite was carried out in a physiological buffer PBS (Phosphate Buffered Saline) for different times including 8 h, 24 h and 28 days. These times are relevant for biological analysis including bacterial adhesion experiments and eukaryotic cell proliferation. After the degradation time, samples were dried under nitrogen flow and then stored in a desiccator until their use.

Hydrophobicity and surface tension was obtained through contact angle using the sessile drop technique. Water, formamide and diiodomethane were selected as probe liquids for the measurements. A goniometer G211 (Krüss) was employed in this experimental part.

The zeta potential of the samples was obtained through electrokinetic measurements, in particular, it was employed the information of the streaming current provided by an Electrokinetic Analyser (EKA, Anton Paar) and this transformed into zeta potential by using Helmholtz-Smoluchowski relationships.

The topography of the samples was analysed through back scattering electron dispersion (BSED) and secondary electron (SE) measurement using a Scanning Electron Microscope (SEM) with the objective of observing the degradation of samples.

### RESULTS AND DISCUSSION

The addition of Mg to the polymer matrix diminishes its hydrophobicity, increasing the polar character of the resulting composite. After the composite degradation under physiological conditions, such hydrophobicity also decreases observing the highest changes at short times.

About the zeta potential information, the PLA/Mg samples change their surface charge respect to the polymeric matrix without magnesium particles. In any case, the electrical behaviour depends on the measuring time, which can be related to the release of magnesium ions during the measurement.

### CONCLUSION

The degradation of the PLA/Mg composite modifies the physical properties of its surface. The changes in hydrophobicity and surface tension are more important at initial degradation times. The decrease in the absolute value of the zeta potential in PLA/Mg concerning PLA agrees with the results obtained by Zhao C. et al<sup>3</sup> that showed a better response of cell adhesion on this material.

### REFERENCES

1. Ratner B.D. *et al.*, Biomaterials science: an introduction to materials in medicine, 3rd edn. Academic Press, Amsterdam, 2013
2. Cifuentes S.C. *et al.*, Acta Biomaterialia 32:348-357, 2016
3. Zhao C. *et al.*, Composites Science and Technology 147:8-15, 2017

### ACKNOWLEDGMENTS

Financial support is acknowledged to the Spanish Junta de Extremadura and FEDER grants for the projects IB16117 and GR15089, and to the Ministerio de Economía y Competitividad for the project MAT2015-63974-C4-3-R.

## Characterisation of Partially Polymer Covered Self-expandable Metallic Stents in Esophageal Cancer Treatment: Impact of Long-Term Usage in the Body

Monika Gołda-Cępa<sup>1</sup>, Janusz Włodarczyk<sup>2</sup>, Jarosław Kuźdzał<sup>2</sup>, Paulina Chytrosz<sup>1</sup>, Andrzej Kotarba<sup>1</sup>

<sup>1</sup>Faculty of Chemistry, Jagiellonian University, Poland

<sup>2</sup>Department of Thoracic and Surgical Oncology, Jagiellonian University Medical College John Paul II Hospital, Poland  
[paulina.chytrosz@student.uj.edu.pl](mailto:paulina.chytrosz@student.uj.edu.pl)

### INTRODUCTION

Squamous cell carcinoma of the esophagus is the fourth cause of death in males and seventeenth in females. There is no change or slight decrease in incidence over the last three decades.<sup>1</sup> More than 50% of patients present with unresectable tumour, progressive weight loss and dysphagia, require palliative treatment. Among the many available methods of palliation, stenting is the method of choice. This is because of technical simplicity, wide availability and immediate alleviation of dysphagia. Patients requiring stenting are usually diagnosed with III and IV grade dysphagia and significant weight loss. The stents that are currently used, despite relatively good tolerance, are not free from side-effects and complications. One of the most common problems associated with stenting is granulation tissue overgrowth and stent obstruction. Coverage with a polyurethane or silicone membrane protects from tumour ingrowth, but overgrowth beyond ends of the stent and granulation tissue formation remains an issue.

The aim of the study was to investigate the impact of long-term usage in the body on physicochemical properties of the partially-covered esophageal stents.

### EXPERIMENTAL METHODS

Structural analysis of 16 partially covered self-expandable metallic stents (SEMS) has been subjected after removal due to their dysfunction. SEMS were implanted because of dysphagia due to inoperable esophageal cancer or before chemo-radiotherapy. For the investigations, partially-covered SEMS 7–12 cm long and diameter of 18 mm (Ultraflex Boston Scientific, USA) were used. For the physicochemical investigation as the obtained stents were cut into 1x1 cm coupons. The morphology of the NiTi stent and polyurethane covered surfaces were evaluated by SEM. The properties of polymeric samples were analysed using DSC. The measurements were carried out in a temperature range of 25–600°C with a heating rate of 10°C min<sup>-1</sup> in Ar flow of 50 cm<sup>3</sup> min<sup>-1</sup>.<sup>2</sup> The changes within the surface of polyurethane were followed by contact angle measurements (CA).<sup>3</sup> ATR-FTIR analyses of the polymeric films were performed in order to analyse the structural changes of polyurethane, the spectra were recorded in the range 4000–650 cm<sup>-1</sup>.

### RESULTS AND DISCUSSION

Structural analysis has been subjected of 16 removed prostheses from patients (3 females, 13 males, age 40–80) which were treated in the course of squamous cell carcinoma (14 patients) and adenocarcinoma of the esophagus (2 patients). Among the treated patients, 5 received chemo or chemo-radiotherapy, 5 preoperative

chemo-radiotherapy, 6 did not receive treatment. The microscopic observations revealed surface changes on the metal alloy, mostly cracks, on the used esophageal stents when compared to the reference sample. The changes in surface morphology of polyurethanes covers were observed, mostly as cracks and peeling off 5–10 μm polurethane fragments, as illustrated in Fig. 1. The degradation of the polyurethane films was confirmed with ATR-FTIR, indicating the significant loss of maxima intensity at 2930 cm<sup>-1</sup>, 2860 cm<sup>-1</sup>, 1740 cm<sup>-1</sup>, and 1245 cm<sup>-1</sup> which correspond to the functional –CH<sub>2</sub>, –CO, –CN groups, respectively. The changes in the polymer bulk structure before and after stent implantation were compared in terms of melting temperature ( $T_{melt}$ ). The  $T_{melt}$  for the distal end of the investigated stents were shifted by ~20°C towards higher temperatures which indicates significant changes in the polyurethane covers exposed to the human body environment.

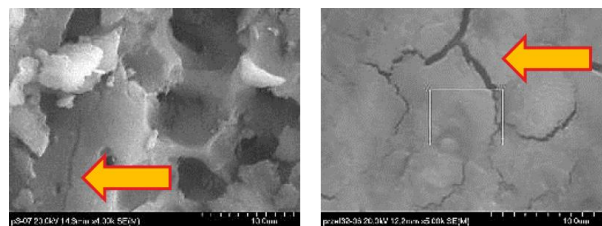


Fig. 1. The cracks (marked by arrows) in polyurethane surface resulting from exposure to the human body environment revealed by SEM images.

### CONCLUSION

The esophageal stents (Nitinol-polyurethane) were examined after prolonged usage in the body. Physicochemical characterization revealed significant changes in the materials bulk and surface morphology as well as surface functional groups (CA, IR). It was concluded, that the degradation strongly depends on the physiological environment (i.e. medical treatment, in-site pH). The main directions for improvement of the stents were pointed out.

### REFERENCES

1. D.M. Parkin *et al.* Cancer J Clin 55:74-108 2005
2. M. Gołda-Cępa *et al.*, RSC Advances 5:48816-48821 2015
3. M. Gołda-Cępa *et al.* Mater Sci Eng C 52:273-281 2015

### ACKNOWLEDGMENTS

The financial support of the project is provided by Collegium Medicum Jagiellonian University grant no. K/ZDF/007542.



## Surface Functionalisation, Nanoroughness and Drug Delivery by Atmospheric Plasma Jet on Scaffolds

A. Patelli<sup>1</sup>, F. Mussano<sup>2</sup>, P. Brun<sup>3</sup>, T. Genova<sup>2</sup>, E. Verga<sup>4</sup>, E. Ambrosi<sup>4</sup>, T. Michieli<sup>1</sup>, G. Mattei<sup>1</sup>, P. Scopece<sup>5</sup>, M. Scatto<sup>5</sup>

<sup>1</sup>Department of Physics and Astronomy, Padova University, via Marzolo 8 35122 Padova, Italy

<sup>2</sup>Department Chirurgical Science, University of Torino, Italy

<sup>3</sup>Department Moleculare Medicine, University of Padova, Italy

<sup>4</sup>Department Molecular Science and Nanosystems, University of Venice, Italy

<sup>5</sup>Nadir S.r.l., c/o Campus Scientifico Università Ca' Foscari Venezia, Via Torino 155b, 30172 Mestre (VE), Italy

[scatto@nadir-tech.it](mailto:scatto@nadir-tech.it)

### INTRODUCTION

Advances in tissue engineering have highlighted how roughness and surface chemistry in the scaffolds can steer cells growth and differentiation. These effects are evident on metallic scaffolds, for example for dental implants which are commercially available as sand blasted, chemically etched and phosphates coated. Alternatively on 3D printed biopolymer scaffolds where roughness is induced by solvent/non-solvent phase separation or by the use of electrospinning fibers, while surface groups are determined by wet or plasma chemistry treatments. The new generation of scaffolds focuses also on smart functions such as the delivery of growth factors or anti-inflammatory drugs and on the possibility to make gradients of the different properties or functions within the same scaffolds.

Here we present an innovative way to control nanoroughness, chemistry and drug delivery just by depositing them locally by spraying smart or inert nanoparticles and fixing them mechanically on the surfaces by an atmospheric plasma coating encapsulation.

### EXPERIMENTAL METHODS

The novel approach has been tested on titanium alloys also with commercial surface treatments (SLA) and on flat molded polycaprolactone (PCL) films. In order to control the roughness at first nanoparticles are sprayed by aerosol on the surfaces. To match the size for focal adhesion the diameter is around 200 nm. Two different type of particles are used: inert silica for roughness control and fluorescent PLA particles to simulate the drug delivery. The particles are fixed on the surfaces by a few hundred nanometers coating obtained by plasma polymerization at atmospheric pressure, employing a jet device provided by Nadir S.r.l.(Italy). The deposited coatings offer ammine or carboxylic functionalization. The surfaces have been characterized by FT-IR, AFM and SEM to evaluate the chemistry and the morphology. The titanium alloys for dental implants have been tested with osteoblasts while PCL with fibroblasts. Cells growth has been evaluated by viability assay, protein absorption, proliferation and focal adhesion, SEM. The release of the fluorophore, simulating a drug release, has been evaluated by the fluorescence released in the growing media.

### RESULTS AND DISCUSSION

The nanoparticles are easily fixed on the surface without substrate and particles damaging or melting. The deposition of the particles allows the control of the roughness on a scale from few microns to the hundreds nanometer range. The roughness increases cells adhesion independently by the chemistry, while the preferred surface chemistry depends on culture media and cells type. Osteoblasts cells adhesion has been increased of 20% relative to commercial large grits and acid etched (SLA) titanium alloys. On the other side compared to smooth PCL substrate fibroblasts adhesion has increased of a factor 10. The release of the fluorophore by the dissolution of the PLA nanoparticles has been verified, confirming that the plasma deposited fixing layer is permeable and that the fluorophore encapsulated is not damaged.

### CONCLUSION

The whole process is in open-air, fast and localized, it is compatible with 3D-printing and allows gradients designs. It offers an easy way to tailor the properties of the scaffolds with long lasting functionalizations. Moreover, it allows to decouple the production problems focusing on surface chemistry, roughness, drug release and mechanical properties singularly.

### ACKNOWLEDGMENTS

This research is co-funded by the H2020 Project – FAST "Functionally Graded Additive Manufacturing Scaffolds by Hybrid Manufacturing" (NMP07, GA n. 685825).

## Improvement of Short Ca-P Whiskers/poly lactide Composites by Surface Modification with Lauric Acid

Monika Biernat, Zbigniew Jaegermann, Paulina Tymowicz-Grzyb, Zdzisław Wiśniewski

Department of Ceramic Technology, Institute of Ceramics and Building Materials, Poland

[m.biernat@icimb.pl](mailto:m.biernat@icimb.pl)

### INTRODUCTION

Poly-L-lactide (PLLA) is a biodegradable polymer widely used in medicine for orthopedic surgery (plates, screws, nails) [1] as well as in tissue engineering scaffolds [2]. Unfortunately, PLLA degrades to acidic monomers which may cause inflammatory and allergic reactions [3] and for some applications mechanical properties of PLLA are too weak. It's also known that PLLA is hydrophobic, what impedes cell seeding, attachment, proliferation and differentiation.

In order to improve mechanical properties and to provide a better environment for cell attachment and proliferation, calcium-phosphates are added into PLLA composites as fillers. Such composites have usually better osteoconductivity than pure PLLA [4]. Hydroxyapatite (HA) whiskers [5], and more resorbable bi- or triphasic calcium-phosphate mixtures [6] are considered as promising reinforcement for polymeric composites.

In this research poly lactide and triphasic calcium-phosphate whiskers were mixed to prepare new biodegradable composites with improved mechanical properties. In order to improve surface chemical compatibility between whiskers and the polymer matrix they were modified with lauric acid.

### EXPERIMENTAL METHODS

Calcium-phosphate (Ca-P) whiskers were synthesized by one-pot single method described in detail before [7]. The obtained whiskers were modified by lauric acid. They were dispersed ultrasonically for 20 min in deionized water. Lauric acid (Sigma-Aldrich) was dissolved in anhydrous ethanol (Avantor), poured into the whiskers suspension and mixed. The solution was stirred for 1h and then the solvent was filtered out. The whiskers were washed with ethanol and dried.

The morphology of the whiskers before and after modification by lauric acid was investigated by SEM and STEM. Functional groups of the samples were identified by FTIR.

In the next step poly lactide - RESOMER® LR 706 S (Evonik) was dissolved in dichloromethane (Avantor) and various amounts of whiskers (modified or unmodified) were added. The suspensions were mixed to homogenize, casted into the molds and then the solvent was evaporated. Composites with 10 wt.%, 20 wt.% or 30 wt.% of Ca-P whiskers were prepared. Then the composites were hot-pressed at 195°C and samples for tensile tests were prepared. The tests were performed on a testing machine with loading speed of 1 mm/min. The fractures of the broken samples were observed by SEM.

### RESULTS AND DISCUSSION

Using the above mentioned procedure the modified Ca-P whiskers were obtained. The presence of some

characteristic bands of lauric acid in the FTIR spectrum of modified whiskers ( $2960\text{ cm}^{-1}$ ,  $2919\text{ cm}^{-1}$ ,  $2850\text{ cm}^{-1}$ ,  $1703\text{ cm}^{-1}$ ) confirmed their surface modification.

Tensile strength tests show that with the increase of whiskers amount, the tensile strength of the composites decreases. However, the composites based on modified whiskers show slightly higher tensile strength than the composites with unmodified whiskers (Table 1). That can be attributed to interfacial bonding improvement.

Table 1. Tensile strength of Ca-P whiskers/poly lactide composites

Sample	Ca-P whiskers/ poly lactide ratio	Tensile strength [MPa] ± standard deviation
Ca-P whiskers/ poly lactide	10/90	40.7 ± 2.9
	20/80	40.5 ± 5.7
	30/70	38.0 ± 6.2
modified Ca-P whiskers/poly lactide	10/90	45.4 ± 2.6
	20/80	41.3 ± 2.4
	30/70	39.6 ± 3.4

SEM observations of fractures of the broken samples show that modified whiskers distribute more homogenously in the polymer matrix and there are no holes after extraction of whiskers from matrix, like in the case of unmodified whiskers.

### CONCLUSION

Ca-P whiskers modified with lauric acid were obtained. Due to the improvement in the distribution and the interfacial bonding, the surface modification by lauric acid increases the mechanical strengths of Ca-P whiskers/poly lactide composites.

### REFERENCES

1. Yu H.X. *et al.*, J. Appl. Polym. Sci. 88:2557-2562, 2003
2. Teo W.E. *et al.*, Acta Biomater. 7:193-202, 2011
3. Sukanumaand J. *et al.*, J. Appl. Biomater. 4:13-27, 1993
4. Emadi R. *et al.*, J. Am. Ceram. Soc. 93:679-2683, 2010
5. Zhou F. *et al.*, Mat. Sci. Eng. C 35:190-194, 2014
6. LeGeros R.Z. *et al.*, J. Mater. Sci. Mater. Med., 14:201-209, 2003
7. Biernat M. *et al.*, Engineering of Biomaterials. 143:17, 2017

### ACKNOWLEDGMENTS

The work was financed from resources assigned to the statutory activity of the Institute of Ceramics and Building Materials in Warsaw.

## PEO-based Films Prepared by Plasma Polymerization from Bulk Precursors

Jana Sedlarikova<sup>1</sup>, Zuzana Kolarova-Raskova<sup>1</sup>, Jaroslav Kousal<sup>2</sup>, Anna Hurajova<sup>1</sup>, Marian Lehocky<sup>1</sup>

<sup>1</sup>Centre of Polymer Systems, Tomas Bata University in Zlin, Czech Republic

<sup>2</sup>Faculty of Mathematics and Physics, Charles University, Czech Republic

[sedlarikova@utb.cz](mailto:sedlarikova@utb.cz)

### INTRODUCTION

Biodegradable polymers play important role in many biomedical applications. Polyethylene oxide (PEO) is known for its antifouling properties and ability to protect the surfaces from microbial attacks<sup>1,2</sup>.

Plasma assisted vacuum thermal deposition uses oligomers released during low pressure thermal decomposition of bulk polymer "precursor" either to form the thin film directly or after plasma re-polymerization. In this way, various properties of the film can be controlled<sup>3</sup>. This method was applied to obtain films based on PEO precursors.

### EXPERIMENTAL METHOD

#### Plasma deposition

PEO of molecular weights from 1500 to 600000 g/mol were used. The deposition setup was described e.g. in Choukourov et al.<sup>4</sup> An RF-powered (13.56 MHz) electrode covered with a glass target was below a heated (up to 330°C) crucible containing a source polymer (precursor). The substrates were placed above the crucible.

#### Characterization of precursors and plasma polymers

PEO polymers after plasma deposition were analyzed by gel permeation chromatography (GPC) using an HT-GPC 220 system (Agilent). Measurement of surface properties was done on Surface Energy Evaluation System by Advex Instruments. Fourier transform infrared spectroscopy in attenuated total reflectance (Nicolet iS10) mode was used. Zeta potential was determined by SurPASS Instrument (Anton Paar). All measurements were performed at laboratory temperature.

### RESULTS AND DISCUSSION

The polydispersity was very high in all samples, Mw distribution curve was more broadened in case of plasma polymer but lower amount of oligomers were present, in comparison to polymer deposited without plasma discharge. As expected, the plasma polymer had higher Mw than their precursor.

The infrared spectra of the films were remarkably similar to the spectra of the precursors, showing good preservation of the precursor polymers' chemical structure.

Zeta potential measurement revealed a decreasing trend in both set of samples. Fig. 1 shows that films prepared with 5W plasma power exhibited higher zeta potential values. The lower values (from -20 to -60 mV) were observed in the samples prepared without power, which corresponds to higher stability. Plasma discharge is responsible for creating many hydrophilic groups (COO, CO-), that can cause low stability of the surface. Results represent average values from 4 measurements; standard deviation was always up to 10%.

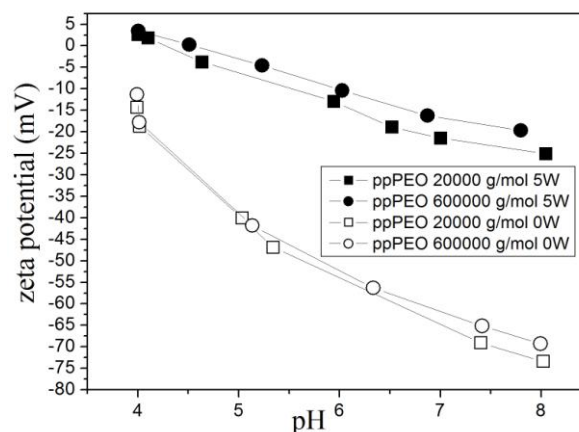


Fig. 1. Zeta potential of PEO thin films prepared without plasma and at plasma power of 5W.

With respect of measured contact angles all tested samples proved to be quite hydrophilic regardless the preparation procedure with or without power.

Concerning the surface energy, the samples treated with plasma deposition at 5 W exhibited slightly higher values with the exception of the polymer with highest tested Mw.

### CONCLUSION

PEO-based films were successfully prepared by plasma assisted vacuum thermal deposition and characterized using contact angle measurement, zeta potential, FTIR-ATR and GPC.

The properties of the films were showed to be tunable by the deposition conditions.

### REFERENCES

- Morent R. et al., Plasma Process Polym. 8:171-190, 2011.
- Santos M. et al., Biosurf Biotribol. 1: 146-160, 2015.
- Choukourov A. et al., Plasma Process Polym. 9: 48-58, 2011.
- Choukourov A. et al., J Phys Chem B. 113: 2984-2989, 2009.

### ACKNOWLEDGMENTS

The work was supported by the grant 17-10813S of the Czech Science Foundation (Grant Agency of the Czech Republic).

## Chitosan and its Derivatives as Biocompatible Coatings and Scaffold Materials

Adriana Gilarska<sup>1,2</sup>, Sylwia Fiejdasz<sup>1</sup>, Czesław Kapusta<sup>1</sup>, Maria Nowakowska<sup>2</sup>, Szczepan Zapotoczny<sup>2</sup>

<sup>1</sup>Faculty of Physics and Applied Computer Science, AGH University of Science and Technology, Mickiewicza 30, 30-059 Kraków, Poland

<sup>2</sup>Faculty of Chemistry, Jagiellonian University, Gronostajowa 2, 30-387 Kraków, Poland  
[adriana.gilarska@vp.pl](mailto:adriana.gilarska@vp.pl)

### INTRODUCTION

Chitosan, a linear polysaccharide obtained by deacetylation of chitin, attracts a lot of attention in recent years. It can be characterized as biocompatible and biodegradable. Furthermore, it exhibits antibacterial and antifouling properties. As biomaterial it has a range of applications in biomedicine: drug delivery, gene therapy, wound healing, tissue engineering<sup>1</sup>. Moreover, its ionic derivatives are soluble in water, which pave the way to many other bio – applications.

Nanoparticle research is a fast developing area of nanotechnology. Among various types of nanoparticles, the ones with magnetic functionality are of special interest. Owing to their remarkable magnetic properties, superparamagnetic iron oxide nanoparticles (SPIONs) and, in particular, magnetite (Fe<sub>3</sub>O<sub>4</sub>) and maghemite (γ-Fe<sub>2</sub>O<sub>3</sub>) can be applied *e.g.* in imaging (MRI)<sup>2</sup> and magnetic hyperthermia<sup>3</sup>. In order to increase their biocompatibility and prevent aggregation, coating materials are often used. Here, we present our results concerning preparation and characterization of iron oxide magnetic nanoparticles coated with ionic derivatives of chitosan and their potential application as building blocks of hybrid magnetic scaffolds.

### EXPERIMENTAL METHODS

Chitosan was modified according to procedures described in literature in order to obtain ionic derivatives<sup>4</sup>. Iron oxide nanoparticles were prepared using co-precipitation method. The synthesis was carried out in aqueous solution using iron salts (FeCl<sub>3</sub>, FeCl<sub>2</sub>), where nanoparticles were formed upon addition of ammonia. During the whole process the reacting solution was sonicated and kept in oxygen-free environment (argon bubbling) in the thermostated bath (20°C). Additionally, nanoparticles were surface-coated with cationic derivative of chitosan (CCh) at the stage of their synthesis. In order to obtain negatively charged nanoparticles, SPIONs were subsequently coated with polyanion using layer by layer (LbL) method. The final products were purified using magnetic filtration. In the next step, hybrid magnetic materials were fabricated by immobilization of polymer-coated SPIONs in hydrogel matrix. Properties of materials prepared were investigated using several methods, *e.g.* DLS, TEM/STEM, XRD, Moessbauer spectroscopy, VSM.

### RESULTS AND DISCUSSION

The obtained nanoparticles were characterized using various complementary techniques regarding their physicochemical, magnetic and biological behaviour. Hydrodynamic diameter of nanoparticles was obtained using Dynamic Light Scattering method and found to be about 100nm. The coating effectiveness and colloidal stability in water was evaluated basing on zeta potential measurements (DLS). The size of magnetic cores was equal to 10nm as revealed by TEM/STEM imaging. The structure of cores was studied using X-ray diffraction and Mossbauer spectroscopy. The results indicate that nanoparticles are of crystalline, nanosized structure. SPION materials revealed to be oxidized magnetite, *i.e.* maghemite. Vibrating Sample Magnetometry measurements confirmed superparamagnetic character of nanoparticles. Biological evaluation regarding the coating used was performed. Preliminary studies concerning hybrid magnetic hydrogels characterization were conducted.

### CONCLUSION

In this work chitosan and its derivatives were shown as versatile biopolymer materials, which can be useful as coatings for magnetic nanoparticles as well as hydrogel scaffold components.

### REFERENCES

1. Dash, M., *et al.*, Prog Polym Sci 36: 981-1014, 2011
2. Jin, R. *et al.*, Curr. Opin. Pharmacol. 18: 18-27, 2014
3. Martinez-Boubeta, C. *et al.*, Sci. Rep. 3 2013
4. Bulwan, M., *et al.*, Soft Matter 5: 4726-4732, 2009

### ACKNOWLEDGMENTS

S.F. acknowledges the financial support from National Science Centre, Poland (grant no. 2016/23/D/ST8/00669).

A.G. has been partly supported by the EU Project POWR.03.02.00-00-I004/16.



## Excimer Laser Micromachining-forming without Influencing the Mechanical Behaviour of Biodegradable Polymers

Magdalena Tomanik<sup>1</sup>, Magdalena Kobielarz<sup>1</sup>, Bogusz Stępak<sup>2</sup>, Arkadiusz Antończak<sup>3</sup>,  
Celina Pezowicz<sup>1</sup>, Jarosław Filipiak<sup>1</sup>

<sup>1</sup>Department of Biomedical Engineering, Mechatronics and Theory of Mechanisms, Faculty of Mechanical Engineering,

<sup>2</sup>Faculty of Microsystem Electronics and Photonics

<sup>3</sup>Laser & Fiber Electronics Group, Faculty of Electronics,

Wrocław University of Science and Technology, Poland

[magdalena.tomanik@pwr.edu.pl](mailto:magdalena.tomanik@pwr.edu.pl)

### INTRODUCTION

Laser technologies, in comparison to the conventional techniques, are suitable for processing micro and nanostructures on polymer surface. By micromachining of biodegradable polymers latticelike structures can be made. However, the reaction due to laser-induced heating of the surrounding material can influence its mechanical behaviour and hence the implant<sup>1-5</sup>.

The excimer laser has a great potential as a precise cutting tool dedicated for complicate contours formation on surface of e.g. stents or scaffolds. In order to determine its suitability for implants manufacturing process, the effects of ArF laser irradiation, above ablation threshold, on mechanical properties of the most commonly used polymers were investigated.

### EXPERIMENTAL METHODS

Taking into consideration the field of application for micromachining, the investigation was carried out on commercial medical poly(L-lactide) (PLLA Evonik L210S) and poly (L-lactide-co-glycolide) (PLGA, Evonik LG857s)<sup>5</sup>. Test specimens were prepared from 350 µm thick polymer sheets, made by compression molding of the granules pre-heated up to 200°C. Optimized process allowed to obtain amorphous poly(L-lactide), for crystalline polymer (PLLA<sub>c</sub>) specimens part of amorphous sheets underwent thermal crystallization process for 5 h in 100°C.

In the investigation an excimer ArF laser (ATLEX300I) with wavelength  $\lambda=193$  µm, impulse time of 5-6 ns and maximum energy of 10 mJ was used. The mechanical properties were determined in tensile test, based on the obtained stress-strain curves the tensile strength and Young's modulus were calculated. From each material group 3 types of specimens were research: non irradiated (reference) and irradiated with 4 impulses with energy density slightly ( $F_1=0.24$  J/cm<sup>2</sup>) and significantly ( $F_2=0.955$  J/cm<sup>2</sup>) above ablation threshold. Statistical analysis was performed using ANOVA and post-hoc Tukey's test. A value of  $p<0.05$  was considered statistically significant.

### RESULTS AND DISCUSSION

Analysing obtained results of Young's moduli (Fig. 1) in none of materials a statistical significant differences between non-irradiated and irradiated specimens were noticed. Moreover, laser treatment did not have significant effects on tensile strength of the PLLA and PLGA specimens (Fig.2). The only statistical significant changes were observed between crystalline poly(L-lactide) specimens, where due to the laser irradiation above ablation threshold, the tensile strength increased.

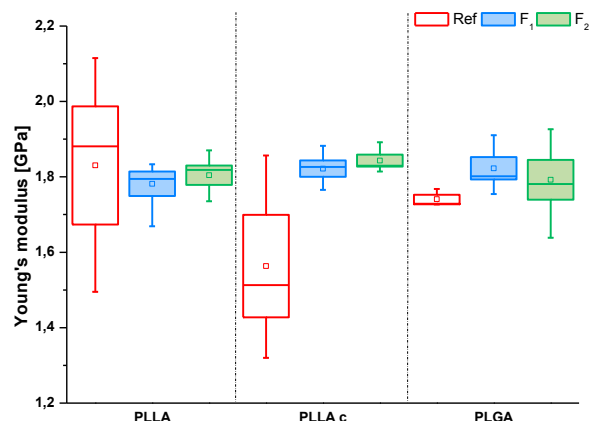


Fig. 1. The Young's modulus [GPa] of the reference and excimer ArF laser irradiated polymers

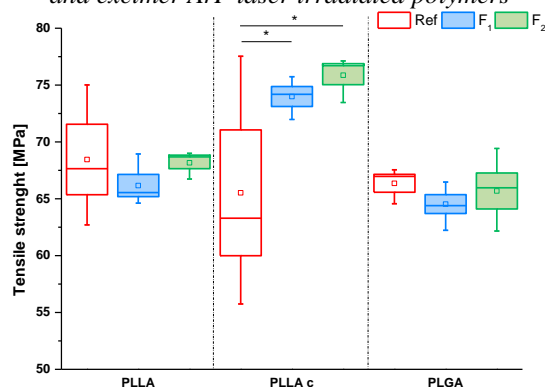


Fig. 2. The tensile strength [MPa] of the reference and excimer ArF laser irradiated polymers;

\*statistical significant difference at  $p<0.05$  level

### CONCLUSION

Conducted experiment allowed to evaluate the presumption that excimer laser can be used as a cutting machine for biopolymers. The thermal effects occurring during the process do not impact the material mechanical properties.

### REFERENCES

1. Kancharla V., *et.al.*, BioMEMS 4(2):105-109, 2002
2. Rytlewski P., Mróz W. *et al.*, J. Mater. Process. Technol. 212(8):1700-04, 2012
3. Slepicka P. *et al.*, Appl. Surf. Sci. 283:438-44, 2013
4. Stępak B. *et.al.*, ACME 14(2):317-326, 2014
5. Tomanik M. *et.al.*, Engineering of Biomaterials / Inżynieria Biomateriałów 19(138):97-97, 2016

### ACKNOWLEDGMENTS

The authors would like to thank the National Science Centre (Grant no: NCN 2013/09/B/ST8/02423) for providing financial support to this project.

## Topographic Evaluation of the Micropatterned Poly(L-lactide) Thin Sheets

Magdalena Tomanik<sup>1</sup>, Katarzyna Łęcka<sup>2</sup>, Arkadiusz Antończak<sup>2</sup>, Celina Pezowicz<sup>1</sup>, Jarosław Filipiak<sup>1</sup>

<sup>1</sup>Department of Biomedical Engineering, Mechatronics and Theory of Mechanisms, Faculty of Mechanical Engineering,

<sup>2</sup>Laser & Fiber Electronics Group, Faculty of Electronics,

Wrocław University of Science and Technology, Poland

[magdalena.tomanik@pwr.edu.pl](mailto:magdalena.tomanik@pwr.edu.pl)

### INTRODUCTION

Laser based technologies are extensively used for polymers surface patterning<sup>3,4</sup>. Different micro- and nano- structures can be obtained thanks to the wide range of beam sizes, therefore can highly improve the biological performance of the material without chemical modification.

Cell behaviour on various types of substrates (materials) is a widely investigated phenomenon<sup>1,2</sup>. Polymer topography such as: height, diameter, and spacing of the patterning, will cause different cell response, which also can be different depending on utilized cell types.

The aim of the study was to evaluate the effect of the CO<sub>2</sub> laser irradiation of poly(L-lactide) thin sheets on the surface wettability and roughness.

### EXPERIMENTAL METHODS

The polymer sheets with an average thickness of 350 μm were extruded from medical poly(L-lactide) (PLLA Evonik L210S) by compression molding of the granules pre-heated up to 200°C. As a result the amorphous poly(L-lactide) sheets with the degree of crystallinity  $X_c \approx 2\%$  were obtained<sup>4</sup>.

Micropatterns on specimens surface resulted from varied laser power used to irradiate the polymer. In the study CO<sub>2</sub> laser with wavelength  $\lambda=10,6 \mu\text{m}$  and maximum average power of 25 W was used and the following powers were applied:  $P_1=24 \text{ J/cm}^2$ ,  $P_2=48 \text{ J/cm}^2$  and  $P_3=71 \text{ J/cm}^2$ .

In order to evaluate the surface properties the roughness ( $R_z$ ), in a direction perpendicular to the beam passage, and wettability measured with H<sub>2</sub>O and PBS solution were determined. Statistical analysis was performed using ANOVA and post-hoc Tukey's test. A value of  $p<0.10$ ,  $p<0.05$  and  $p<0.001$  was considered statistically significant.

### RESULTS AND DISCUSSION

Height profiles of the investigated specimens were obtained along the 1.25 mm line which allowed to calculate the roughness parameter  $R_z$  (Tab. 1). Obtained data has shown that manufacturing technology provides thin polymer sheets of non-rough surface. Through the usage of CO<sub>2</sub> laser surface patterning can be archived and controlled by usage of certain powers.

Tab. 1. The roughness parameter  $R_z$  calculated for surfaces of analysed specimens

	Ref	P <sub>1</sub>	P <sub>2</sub>	P <sub>3</sub>
$R_z$	0.10	0.21	2.87	6.67

Effects of laser irradiation can be also noticed in statistically significant changes of the contact angle in comparison to non- irradiated surface (Fig. 1).

With the increase of the used laser power, as well roughness, the surface becomes more wettable. However Ref and P<sub>1</sub> surfaces provides conditions for almost full PBS drop dissolution ( $\theta=3\div 7.5^\circ$ ) while surfaces P<sub>2</sub> and P<sub>3</sub> are more lyophobic ( $\theta=48\div 53^\circ$ ).

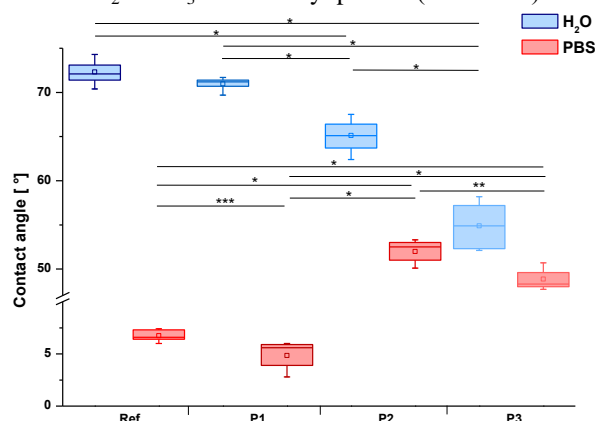


Fig. 1. The wettability of the surface modified with different laser powers; \* $p<0.001$ , \*\* $p<0.05$ , \*\*\* $p<0.10$

### CONCLUSION

Conducted study has shown the increase of surface roughness  $R_z$  with the usage of greater laser power. Moreover, with the progression of the modification the surface becomes more hydrophilic, however the PBS solution divided specimens for well and partially wettable. Obtained results are the part of the project and are in agreement with previously presented data regarding degradation rate of specimens<sup>5</sup>.

### REFERENCES

1. Altomare L. *et.al.*, Acta Biomater. 6: 1948-1957, 2010
2. Ross A.M. *et. al.*, small 8(3):336–355, 2012
3. Stępak B. *et.al.*, ACME 14(2):317-326, 2014
4. Tomanik M. *et.al.*, Engineering of Biomaterials / Inżynieria Biomateriałów 19(138):97-97, 2016
5. Tomanik M. *et.al.*, Engineering of Biomaterials / Inżynieria Biomateriałów 19(138):96-96, 2016

### ACKNOWLEDGMENTS

The authors would like to thank the National Science Centre (Grant no: NCN 2013/09/B/ST8/02423) for providing financial support to this project.

## Extracellular Matrix Substitute with Natural Polysaccharides and Small Peptide

Ewa Stodolak-Zych<sup>1</sup>, Agnieszka Solecka<sup>2</sup>, Julia Golańska<sup>1</sup>, Wiktor Niemiec<sup>3</sup>, Maciej Boguń<sup>4</sup>, Zbigniew Darczyński<sup>4</sup>, Beata Kolesińska<sup>5</sup>

<sup>1</sup>Department of Biomaterials and Composite Materials, Faculty of Materials Science and Ceramics, AGH University of Science and Technology, Krakow, Poland

<sup>2</sup>Department of Biomedical Engineering, Faculty of Electrical Engineering, Automatics, Computer Science and Biomedical Engineering, AGH University of Science and Technology, Krakow, Poland

<sup>3</sup>Department of Silicate Chemistry and Macromolecular Compounds, Faculty of Materials Science and Ceramics, AGH University of Science and Technology, Krakow, Poland

<sup>4</sup>Department of Material and Commodity Sciences and Textile Metrology, Lodz University of Technology, Poland

<sup>5</sup>Institute of Organic Chemistry, Lodz University of Technology, Poland

[stodolak@agh.edu.pl](mailto:stodolak@agh.edu.pl)

### INTRODUCTION

A new approach in the design and manufacture of scaffolds for regenerative medicine or tissue engineering is based on the imitation of the natural extracellular matrix (ECM). Biomimetic scaffolds are obtained by decellularisation methods. This process aims to remove cells (and their potential antigens) that are responsible for triggering an inflammatory response or rejecting the implant. Because of depriving the matrix of cellular components, it is possible to obtain a fibrous and porous structure composed primarily of collagen fibers<sup>1</sup>. Studies have shown that decellularisation process damages important structural elements i.e. elastic fibers. Additionally number of proteoglycans and glycosaminoglycans is significantly reduced after decellularisation.

As an alternative method manufacturing biomimetic scaffolds with natural components we combine material engineering technique (i.e. fibrous scaffolds obtained by wet spinning) with chemical engineering methods (synthesis of small peptides, GAG components). A series of polysaccharides-protein systems based on natural components were manufacturing and characterised in these work. Fibrous polysaccharide substrates were obtained from chitin (CH), butyryl-acetate copolyester chitin (BOC) and their blends (80:20 ratio BOC:CH). Fibrous scaffolds: CH, BOC and BOC:CH were modified with hexapeptide: tryptophan (WWW)<sub>2</sub>, tryptophan-cysteine (WWC)<sub>2</sub> and tyrosine- cysteine (YYC)<sub>2</sub>. The main goal of the treatment was to obtain chemical and microstructural scaffolds mimicking the extracellular matrix.

### EXPERIMENTAL METHODS

The synthesis of the scaffolds was carried out in two stages: dissolving the peptides in the alcohol mixture and then combining them with the polysaccharides matrix (65°C/24h). In the result protein-polysaccharide systems were dried (to 2D form) and/or lyophilized (to 3D form). The structure of biomimetic composition was characterized by analysing the FTIR spectra obtained by the ATR technique (ZnSe/Ge crystal, in range 400-4000cm<sup>-1</sup>, penetration depth 2µm). Polysaccharides-protein substrates have been characterized for their morphology, physical properties (wettability) and structural properties (FTIR/ATR). Their durability in *in vitro* conditions was determined (PBS/37°C/1msc).

Environmental impact on microstructure (fiber diameter before and after hydrolytic degradation, SEM / EDS) and substrate structure (FTIR/ATR) were investigated. The behavior of proteins on the surface of the fibers was determined by model tests using the atomic force microscope (tapping mode AFM, MULTIMODE 8, Bruker).

### RESULTS AND DISCUSSION

Short peptides aggregate observed *in vitro* were result of conformational changes in the peptide chain (Fig. 1). Thus, on the fibers surface in all scaffolds (BOC, CH, BOC:CH) same protein agglomerates were well visible (SEM). Small peptides slightly affecting the fiber diameter or their wettability. Polysaccharides-protein system were stable: pH immersion medium did not change and subtle changes in the FITR-ATR spectrum in the band belongs to amid I and amid II were effect of protein deposition not degradation process. Any change was observed in diameter of fibers.

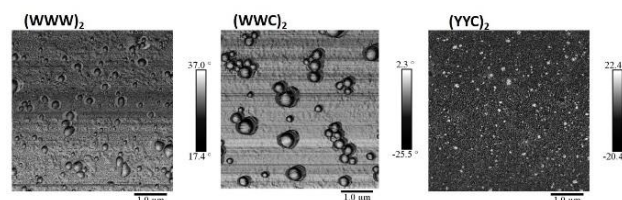


Fig. 1. Peptide aggregates observed in *in vitro* condition. AFM examination

### CONCLUSION

The results showed that the polysaccharides-protein systems are durability in water condition; any important changes in morphology or structure were not observed. Extracellular matrix substitute with natural polysaccharides and small peptide are alternative for scaffold obtaining by decellularization process.

### REFERENCES

- Hinderer S.*et al.*, Adv Drug Deliv Rev. 97:260-9, 2016

### ACKNOWLEDGMENTS

This work has been supported by the National Science Center Poland, under grant no. UMO-2015/19/B/ST8/02594.

## Effective Immobilization of BMPs on Diazo-resin Substrates Composed from Pectin or Chondroitin Sulfate

Magdalena Wyrwal-Sarna<sup>1</sup>, Agata Pomorska<sup>2</sup>, Michal Sarna<sup>3</sup>, Zbigniew Adamczyk<sup>2</sup>, Krzysztof Szczubialka<sup>4</sup>, Andrzej Bernasik<sup>1,5</sup>

<sup>1</sup>Academic Centre for Materials and Nanotechnology, AGH University of Science and Technology, Krakow, Poland

<sup>2</sup>Jerzy Haber Institute of Catalysis and Surface Chemistry, Polish Academy of Sciences, Krakow, Poland

<sup>3</sup>Faculty of Biochemistry Biophysics and Biotechnology, Jagiellonian University, Krakow, Poland

<sup>4</sup>Faculty of Chemistry, Jagiellonian University, Krakow, Poland

<sup>5</sup>Faculty of Physics and Applied Computer Science, AGH University of Science and Technology, Krakow, Poland

[wyrwal@agh.edu.pl](mailto:wyrwal@agh.edu.pl)

### INTRODUCTION

The main aim of this study was the effective immobilization of growth factors: bone morphogenic proteins, BMP-2,4,7 onto versatile polymeric multilayer films (PEM). It was reported that chosen polymeric films enhanced cell viability and proliferation<sup>1</sup>. After adsorption, growth factors are immobilized onto PEM surfaces by electrostatic or covalent photochemical crosslinking. Both approaches were chosen, to compare the best, stable presentation of the BMPs, maintaining the bioactivity of these proteins. Surface immobilization of BMPs will prevent non-specific adsorption of the proteins and uncontrolled release from the surface. Additionally, the dependence of the interaction of proteins each other was examined. Furthermore, thanks to covalent binding BMPs mixtures their osteogenic properties will be enhanced by activation of several signaling pathways<sup>2</sup>. Such a method will reduce the required amount of growth factors for efficient stem cells differentiation.

### EXPERIMENTAL METHODS

Polymeric coatings were composed from diazo-resin (DR) and selected glycosaminoglycans: pectin (Pec) and chondroitin sulfate (Chon). Next, prepared substrates were photocrosslinked before or after protein adsorption. The surface  $\zeta$ -potential was analyzed using SurPass (Anton Paar). UV-Vis spectrometer (Thermo Scientific Evolution 220) was used to confirm an effective photocrosslinking of polymeric layers. Quartz Crystal Microbalance (QCM) (Qsense) was used to analyse the kinetics of structural changes and mass changes of BMPs adsorption on polymeric substrates. Atomic force microscopy (AFM) analysis was conducted using Bruker's BioScope Catalyst AFM. AFM analyzes of substrate topography were performed in distilled water. X-ray photoelectron spectroscopy measurements were performed using a PHI 5000 Versa Probe II (ULVAC-PHI) spectrometer. The type of exposed functional groups were analyzed using angle resolved XPS.

### RESULTS AND DISCUSSION

UV-Vis spectra confirmed an effective photocrosslinking of polymeric layers (Fig. 1). Shifting of the maximum absorption of diazo-resin confirmed the formation of covalent bindings between layers under UV radiation. The effective protein adsorption was confirmed by QCM. This technique gives an insight into the reaction kinetics as well as multilayers structure modification during adsorption. Much more BMPs were

adsorbed on non-crosslinked multilayers. From the dissipate energy it was observed that the substrates became more stiff.

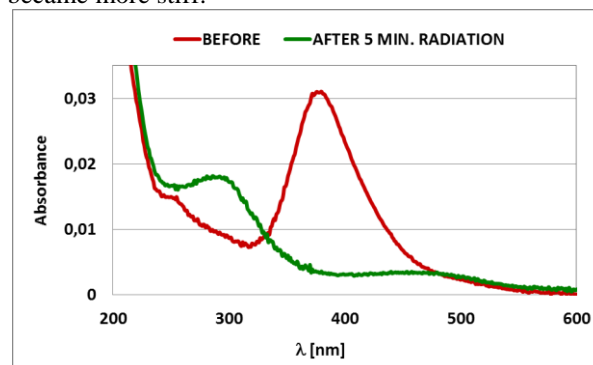


Fig. 1. UV-Vis spectra of deposited (DR/Chon)<sub>6</sub> before and after photocrosslinking.

AFM data showed that the proteins efficiently deposited on the surface of the polymers. This was indicated by differences in the roughness of the polymeric surfaces with and without the proteins. All substrate  $\zeta$ -potential measurements as a function of pH shown that terminal layer: DR, Pec or Chon had negative value at pH 6 (below all proteins pI). XPS measurements confirmed that all deposited polymeric layers penetrate each other. Hydroxyl and ester functional groups are exposed to the surfaces.

### CONCLUSION

The result showed that the polymeric multilayers are effectively photocrosslinked. BMPs adsorb effectively on the polymeric multilayer with DR and Pec or Chon as outer layer. PEM films are versatile substrate for proteins immobilization. Those research will determine the possibility of future usage of such PEM films with BMPs as active coatings of implants or scaffolds enabling the proliferation and differentiation of stem cells.

### REFERENCES

1. Mikulska A. *et al.*, Cell Prolif. 47:516-526, 2014
2. Luu H.H. *et al.*, J. Orthop. Res. 25.:665-677, 2007

### ACKNOWLEDGMENTS

This work was supported by the Polish National Science Centre, project no. 2016/21/D/ST5/01636.



## Raman Microspectroscopic Investigations of Polymer Nanocomposites -Evaluation of Physical and Biophysical Properties

Aleksandra Weselucha-Birczyńska<sup>1</sup>, Anna Kołodziej<sup>1</sup>, Małgorzata Świątek<sup>2</sup>, Łukasz Skalniak<sup>1</sup>, Marta Błazewicz<sup>3</sup>

<sup>1</sup>Faculty of Chemistry, Jagiellonian University, Kraków, Poland

<sup>2</sup>Institute of Macromolecular Chemistry, Academy of Sciences of the Czech Republic, Prague 6, Czech Republic

<sup>3</sup>Faculty of Materials Science and Ceramics, AGH-University of Science and Technology, Kraków, Poland  
[birczyns@chemia.uj.edu.pl](mailto:birczyns@chemia.uj.edu.pl)

### INTRODUCTION

Advanced biomaterial science can significantly improved materials for medical treatment<sup>1</sup>. Carbon nanotubes or carbon nanofibers, are ideal nanostructures for innovative medical applications<sup>2</sup>. However, to use them properly, you need to understand the physical, chemical and biological material properties introduced by the nanoparticle<sup>3</sup>. The Raman microspectroscopy was chosen as a best method of sensing interaction that affects the carbon nanometric systems. Current work is a continuation of our previous studies of nanocomposite polymer membranes<sup>4</sup>.

### EXPERIMENTAL METHODS

The polymer nanocomposites, formed as membranes on the basis of the poly( $\epsilon$ -caprolactone) (PCL), contained identical amounts of carbon nano-additives multi-walled nanotubes (MWCNT), carbon nanofibers (CNF) and respective functionalized nano-structures obtained by oxidative treatment, MWCNT-f, and CNF-f, were studied. The reference membrane was produced from unmodified PCL.

Raman microspectroscopic analysis was carried out to study both faces of the membranes: the top surface that is crystallized during evaporation and the bottom face that adheres to the surface of the vessel onto which the films were cast.

Then, selected samples were subjected to basic biological tests which involved the viability and the morphology of the cells under in vitro conditions.

### RESULTS AND DISCUSSION

Raman spectroscopy was applied as a method for assessment of the degree of crystallinity of thin nanocomposite membranes, of the both sides of the material: on the top and bottom. The homogeneity of both nanomaterials surfaces was also checked the by performing a linear Raman mapping on both surfaces of materials.

In the Raman spectra of all studied nanomaterials the appearance of characteristic polymer matrix bands is expected. One can list here the CH<sub>2</sub> antisymmetric and symmetric stretching at *ca.* 2920 and 2870 cm<sup>-1</sup>, respectively, then 1725 cm<sup>-1</sup> ( $\nu$ C=O) and at 1110 cm<sup>-1</sup> ( $\nu$ COC), skeletal stretching) that are typical of crystalline PCL. These relatively narrow lines reflected the crystalline domains. However, there are also present the broad bands in the spectra that characterizes the amorphous part of the material.

Each of the nanomaterials and each of its faces has its own specificity. Interactions of nanoparticles, of carbon nanotubes and carbon nanofibers, differ.

The attachment and the growth of the U2 cell populations on the polymer and nanocomposite samples were monitored throughout the culture with fluorescence microscopy. Additionally the results of the biological and polymer nanocomposites exhibit significant differences. Cell viability and proliferation revealed a large number of cell, in particular populations on polymeric nanomaterials with carbon nanotubes was significant.

### CONCLUSION

Raman microspectroscopy allow to identify the interaction at the interface of the polymer and the nanoparticles. An increase in the number of cells was observed on the consecutive days of the culture, suggesting unrestricted proliferation of the cells on the tested materials. Raman analysis allowed for the correlation of molecular structure - biological action.

### REFERENCES

References must be numbered. Keep the same style.

1. Zhang L. *et al.*, Nano Today, 4: 66–80, 2009
2. Phong T. *et al.*, Adv. Drug Delivery Rev., 61: 1097–1114, 2009
3. da Rocha E. L. *et al.*, Mater. Sci. Eng. C 34: 270–279, 2014
4. Weselucha-Birczyńska A. *et al.*, Analyst, 140: 2311–2320, 2015

### ACKNOWLEDGMENTS

This project was financed from the National Science Centre (NCN, Poland) on the decision 2013/09/B/ST8/00146 and 2014/13/B/ST8/01195. AK has been partly supported by the EU Project POWR.03.02.00-00-I004/16.

## 2D-Correlation Raman Studies on the Effect of Modifications of Carbon Nanofibers on their Properties and Molecular Structure

Aleksandra Weselucha-Birczyńska<sup>1</sup>, Elżbieta Długoń<sup>2</sup>, Krzysztof Morajka<sup>1</sup>, Marek Michalec<sup>1</sup>, Marta Błazewicz<sup>2</sup>

<sup>1</sup>Faculty of Chemistry, Jagiellonian University, Kraków, Poland

<sup>2</sup>Faculty of Materials Science and Ceramics, AGH-University of Science and Technology, Kraków, Poland  
[birczyns@chemia.uj.edu.pl](mailto:birczyns@chemia.uj.edu.pl)

### INTRODUCTION

Interesting, relatively new fibrous materials are carbon nanofibres (electrospun carbon nanofibers, ESCNFs). They are extremely promising for a medical, industrial and other applications<sup>1-3</sup>. Although the work on these materials has been going on for some time now, from the point of view of medical applications, there is still no coherent theory that explains their effects on living organisms. Raman microspectroscopy and 2D correlation analysis was applied to resolve some details about interactions at the molecular level.

### EXPERIMENTAL METHODS

The membranes formed of carbon nanofibers (ESCNFs) as the unmodified reference sample, then oxidized and also carbonized/graphitized by heating to 1100°C were analyzed.

The Raman microspectroscopy technique has been applied to obtain spectra of studied modified membranes excited with 442 nm, 514.5 nm and 785 nm laser lines. The generalized 2D correlation analysis was performed using Raman spectra as an input data for generating the correlation maps<sup>4</sup>.

Additionally the X-ray diffraction data of these membranes were collected on the Philips diffractometer type X'Pert Pro in the Bragg-Brentano geometry, using CuK $\alpha$  radiation ( $\lambda = 0.154184$  nm).

### RESULTS AND DISCUSSION

The Raman spectra are dominated by the prominent Raman G-band related to the E<sub>2g</sub> active mode appearing near wavenumber of 1580 cm<sup>-1</sup> and the strong and broad D1-band, called the defect band, at ca. 1350 cm<sup>-1</sup>. The degree of crystallinity of analyzed membranes was estimated, as the ratio of the intensity of respective Raman bands. Applying model of two band in the Raman spectra in the range of 1800 – 900 cm<sup>-1</sup>, the D1/G intensity ratio is equal to 1.05±0.06, 1.02±0.02, and 0.27±0.02 for reference membrane, oxidized and heated sample, respectively, for excitation line of 514.5 nm. Modifications introduced during membrane fabrication is also reflected in the size of ordered domains created in the studied membranes. The size of crystalline domains La is equal to 16.13±0.8 nm, 16.45±0.25 nm, and 60.94±5.15 nm for reference membrane, oxidized and heated sample, respectively. One can concluded that oxidation introduces structural modification, changes within fibers alignment. On contrary graphitization leads to significant remodeling of the molecular structure<sup>5</sup>.

Obtained diffractive images indicate an obvious effect of the chemical and thermal treatment on the studied membranes. Oxidation seems to lead to a partial amorphization of material, while graphitization indicates new, different crystalline phase formation.

Two-dimensional Raman correlation allows to obtain additional information about the sample that are not directly visible in collected Raman spectra. By varying the external factor, which is the energy of excitation laser line, the response of the system is modulated. The respective molecular carbon phases give a specific contribution to the observed bandwidth and 2D correlation allows to decode it<sup>6</sup>.

### CONCLUSION

Both methods show the effect of manufacturing and modification techniques on the structure and ordering of the carbon, fibrous membranes. 2D Raman correlation allows to decode particular phases emerging in modified materials, what in consequence increases the spectral resolution.

### REFERENCES

1. Liao S. *et al.*, Biomed. Mater., 1: R45–R53, 2006
2. Cui W. *et al.*, Sci. Technol. Adv. Mater., 11: 014108 (11pp), 2010
3. Pramanik S. *et al.*, Sci. Technol. Adv. Mater. 13: 043002 (13pp), 2012
4. Noda I., Appl. Spectrosc. 47: 1329, 1993
5. Pimenta M. A., *et al.*, Phys. Chem. Chem. Phys., 9: 1276–1291, 2007
6. Weselucha-Birczyńska A. *et al.*, J. Mol. Struct., 1124: 61-70, 2016

### ACKNOWLEDGMENTS

This project was financed from the National Science Centre (NCN, Poland) granted on the decision number 2013/09/B/ST8/00146 and 2014/13/B/ST8/01195.

## Chitosan-based ZnO-doped Bioglass Composite as Carriers of Bioactive Peptides

Lidia Ciolek<sup>1</sup>, Monika Biernat<sup>1</sup>, Zbigniew Jaegermann<sup>1</sup>, Artur Oziębło<sup>1</sup>, Justyna Sawicka<sup>2</sup>, Maria Dzierżyńska<sup>2</sup>, Sylwia Rodziewicz-Motowidło<sup>2</sup>, Milena Deptuła<sup>3</sup>, Michał Piikuła<sup>4</sup>

<sup>1</sup>Department of Ceramic Technology, Institute of Ceramics and Building Materials, Poland

<sup>2</sup>Department of Biomedical Chemistry, Faculty of Chemistry, University of Gdansk, Poland

<sup>3</sup>Department of Embryology, Medical University of Gdansk, Poland

<sup>4</sup>Department of Clinical Immunology and Transplantology, Medical University of Gdansk, Poland

[l.ciolek@icimb.pl](mailto:l.ciolek@icimb.pl)

### INTRODUCTION

Chitosan is widely used in medicine. Its main characteristics include biocompatibility, antimicrobial and hemostatic properties, and biodegradability [1]. Due to the osteoconductive properties it is suitable for hard tissue engineering [2]. Literature reports suggest that chitosan may be used as compound of composites with bioglasses [3]. However biomaterials for regenerative medicine are subjected to continuous improvement in order to amending their integration with body tissues or giving them bactericidal properties. Among antibacterial agents are metals ions (i.e. Zn<sup>2+</sup>) [4], which may be released from bioglasses.

The project aimed at verification if a chitosan based ZnO-doped bioglass composite is proper to be used as a scaffold for bioactive peptides. Potentially such biomaterial could be used in regeneration of bone cavities. A peptide located in polymer scaffold could promote bone regeneration.

### EXPERIMENTAL METHODS

Porous composites based on chitosan solution and ZnO-doped bioglass from CaO-SiO<sub>2</sub>-P<sub>2</sub>O<sub>5</sub> system were fabricated using lyophilization method. Composite microstructure was controlled by the appropriately selected amount of bioglass in relation to the polymer [5]. Selected peptide with a PEPTIDES sequence was incorporated to the obtained composites via their dipping into the peptide solution and lyophilization.

The peptide was synthesized with *Liberty Blue™ Automated Microwave Peptide Synthesizer* on the Rink Amide ProTide resin - Fmoc solid phase peptide synthesis. The purity of the synthesized compound was confirmed by analytical RP-HPLC using a C18 Luna column (4.6 x 250 mm, 5 μm) and a 60 min linear gradient of 5 - 100% acetonitrile in 0.1% aqueous TFA. The counter ion was exchanged to acetate on micro-column with strong cation exchanger solid phase. The level of peptide release from obtained composites was verified.

### RESULTS AND DISCUSSION

The cross-section SEM image of selected composite (fig.1) shows the structure of internally connected open pores of sizes in range of 40 – 300 μm. Specific surface area of the obtained composite was 127,68 ± 0,02 m<sup>2</sup>/g. Before dipping the composite into the peptide solution, it showed bioactivity after incubation in SBF. The formation of apatite layer was indicated by observation of changes in intensity of Si, Ca and P signals.

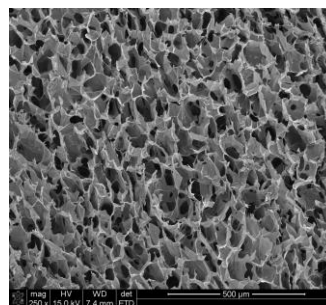


Fig. 1. SEM image of microstructure of chitosan/ZnO doped bioglass composite with peptide

The selected peptide does not show any cytotoxic properties and stimulates proliferation of fibroblast cells, keratinocytes and stem cells.

The results of our tests show very high pace of peptide release from the obtained porous composite (Fig. 2). The peptide did not lose its physical-chemical properties after release.

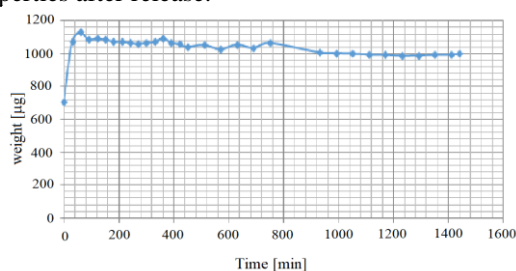


Fig. 2. The level of peptide release from the chitosan/ZnO doped bioglass composite

### CONCLUSION

The results indicates the technological possibility to locate different peptides in chitosan-based ZnO-doped bioglass composite. In future studies we are planning the location of slow-release peptides in the polymer scaffold.

### REFERENCES

1. Di Martino A. *et al.*, *Biomaterials*, 26:5983-5990, 2005
2. Sivashankari PR. *et al.*, *Int. J. Biol. Macromol.*, B. 93: 1382-1389, 2016
3. El-Kady A.M. *et al.*, *Ceram. Int.*, 36:995-1009, 2010
4. Kim T.N. *et al.*, *J. Mat. Sci-Mater. Med.*, 9:129-134, 1998
5. Ciolek L. *et al.*, *Int. J. Appl. Ceram. Technol.*, 14(6):1107-116, 2017

### ACKNOWLEDGMENTS

The work was financed from resources assigned to the statutory activity of the Institute of Ceramics and Building Materials in Warsaw.

Acknowledgment for grant no.

STRATEGMED1/235077/9/NCBR/2014.

## The Development of the Bioactive Particles Combined with Collagen Hydrogels for Tissue Engineering

Justyna Pawlik<sup>1</sup>, Karolina Zazakowny<sup>2</sup>, Katarzyna Cholewa-Kowalska<sup>1</sup>

<sup>1</sup>Department of Glass Technology and Amorphous Coatings, Faculty of Materials Science and Ceramics, AGH University of Science and Technology, Krakow

<sup>2</sup>Department of Inorganic Chemistry, Faculty of Materials Science and Ceramics, AGH University of Science and Technology, Krakow

[pawlikj@agh.edu.pl](mailto:pawlikj@agh.edu.pl)

### INTRODUCTION

Collagen-based biomedical materials with various physical forms, including fibres, films, nanoparticles or hydrogels have been developed for drug carriers, wound dressings, skin replacement and bone substitutes applications<sup>1</sup>. There were several approaches focusing on combining collagen matrix with inorganics particles as calcium phosphate, bioglasses, silica or hydroxyapatite<sup>2-3</sup>. Here we aimed to improve the collagen type I hydrogels by the introduction of bioactive particles, in terms of physico-chemical properties. For this purpose we will introduce the sol-gel bioactive glasses, derived from CaO-SiO<sub>2</sub>-P<sub>2</sub>O<sub>5</sub> system with various CaO:SiO<sub>2</sub> ratio. Those bioactive glasses, are characterized by higher solubility, bioactivity and bone bonding in comparison with melted ones, moreover as reported previously, have been beneficially used as modifiers of synthetic biodegradable polymers and ceramics matrixes<sup>4-8</sup>. In this study we successfully developed the method of introduction of the sol-gel bioglasses into collagen matrix, by the use of genipin as the crosslinking agent, and we evaluate the influence of ceramics particles on the bioactive properties of hydrogels.

### EXPERIMENTAL METHODS

The sol-gel bioactive glasses (SBG) used in this study were fabricated as described in<sup>9</sup>. Collagen type I (rat tail) was purchase from BD Biosciences and Genipin (GNP) (98%) from Bioproducts Co. The hydrogel composites, consist of sol-gel bioactive glasses from CaO-SiO<sub>2</sub>-P<sub>2</sub>O<sub>5</sub> system designed as A2 (high CaO ratio) and S2 (high SiO<sub>2</sub> ratio) and collagen type I (COL I), were obtained with various concentration of SBG with range of 1-5 mg/ml. Hydrogels were fabricated as described in<sup>10</sup>; shortly by mixing Col I with aqueous dispersion of SBG and next with addition of GNP as cross-linking agent. As-prepared composites were incubated at 37°C for 24h, for the gelation process occurred. Hydrogels were characterized under influence of bioglass particles on the microstructure of materials as well as bioactive properties by the SBF test according to<sup>11</sup>. Microstructure of cross-linked composites and after incubation in SBF were evaluated by the SEM/EDS examinations.

### RESULTS AND DISCUSSION

In this study we present method of obtaining collagen and sol-gel bioactive glasses hydrogels, cross-linked by genipin. Our results indicated that it is possible to introduce glass particles into Col I matrix in various concentration with range 1-5mg/ml, that did not impair cross-linking process by genipin presence. The sol-gel

particles size and processing technique of hydrogels were optimized, so the final hydrogels presented homogeneity of particles distribution, with well integrity in collagen matrix. The apatite forming ability of the SBG-Col I composites was assessed by the SBF test, and revealed that after 7 days of incubation, composites modified with A2 glass the surface of materials was covered by the cauliflower-like microspheres, with high intensity of Ca and P as proved by EDS analysis.

### CONCLUSION

We present here a promising research theme for obtaining COL I hydrogels modified by sol-gel bioactive glasses by genipin cross-linking. Our studies show that by proposed technique we are able to obtain hydrogels with wide range of glass particles concentration. Moreover we revealed dependence of the chemical composition of SBGs on the bioactive properties of composites.

As a future investigations we want subsequently widened SBG-COL I hydrogels investigations, by study of chemical interaction between SBG and COL I, and influence of SBG on the hydrolytic degradation and mechanical behaviour of composites.

### REFERENCES

1. Lee C.H., Singla A, Lee Y., *Int. J. Pharm.*, 2001, 221(1).
2. Short AR, Koralla D, Deshmukh A, et al. *J Mat Chem B, Mat. Biol Med.* 2015;3(40):7818-7830.
3. El-Sherbiny IM, Yacoub MH. *Glob Cardio Sci Pract.* 2013, (3):316-342.
4. Laczka M., Cholewa-Kowalska K., Osyczka A.M., *Ceram. Intern.*, 2016, 42(13): 14313-14325.
5. Filipowska J., Pawlik J., et al., *Biomed Mat.*, 2014, 9(6): 065001-15
6. Dziadek M., Pawlik J., et. al., *J Biomed Mat Res. Part B App Biomat.* 2015, 103(8): 1580-1593.
7. Cholewa-Kowalska K., Kokoszka J., *Biomed. Mat.* 2009, 4(5), 1-11, 055007
8. Pawlik J. Widziołek M., et.al., *J Biomed Mat Res A*, 2014, 102(7), 2383-2395.
9. Laczka M., Cholewa-Kowalska K. et.al., *J Mol Struct.*, 1999, 511-512, 223-231.
10. Fiejdasz KS, Szczubiałka J, et.al., *Biomed Mat.*, 2013(8), 035013.
11. Kokubo T, Takadama H, *Biomat.* 2006(27),2907-15.

### ACKNOWLEDGMENTS

The Authors gratefully acknowledge the support of AGH University of Science and Technology (15.11.160.205).



## Synthesis and Characterization of Chitosan-Coated Magnetite Using a Modified Wet Method for Drug Delivery Applications

Yaser E. Greish

Department of Chemistry, United Arab Emirates University, UAE

[y.afifi@uaeu.ac.ae](mailto:y.afifi@uaeu.ac.ae)

### INTRODUCTION

Magnetite ( $\text{Fe}_3\text{O}_4$ ) nanoparticles have been heavily studied for various biomedical applications (1). However, immobilization of drugs onto its surfaces is limited by its surface chemistry and its high affinity towards agglomeration. Therefore, using capping agents during the synthesis of magnetite NPs is a valid approach towards the minimization of NPs agglomeration and to facilitate the immobilization of drugs onto the capping layer (2-3). In this study, the use of chitosan, a known biodegradable natural polymer, during the precipitation of magnetite NPs using a modified wet method is described. The chitosan-coated magnetite NPs are well characterized using various techniques. In addition, the effect of chitosan coating on the magnetic properties of the NPs is carried out.

### EXPERIMENTAL METHODS

Magnetite NPs were prepared using a modified wet method.  $\text{FeCl}_2$  and  $\text{FeCl}_3$  in the proper stoichiometric ratio were slowly added to an alkaline solution. In a parallel experiment, a basic solution containing  $\text{Fe}^{2+}$  and  $\text{Fe}^{3+}$  ions were blended with an acidified chitosan solution, containing up to 3 wt% of chitosan. The pH was maintained above 13, and the precipitated chitosan-coated magnetite NPs were thoroughly washed, dried then characterized using XRD, FTIR, TGA, SEM, and TEM techniques. All samples were also evaluated for their magnetic properties as a function of the initial concentration of chitosan.

### RESULTS AND DISCUSSION

The modified wet method adopted in the current study showed a phase-pure magnetite as the only product, as confirmed by XRD patterns of the prepared NPs. Fig. 1 shows the FTIR spectra of chitosan-coated magnetite NPs. As compared with pure chitosan, all spectra confirm the presence of chitosan onto the surfaces of magnetite NPs. It should be noted that the use of chitosan as a capping agent during the wet synthesis of magnetite NPs stems from the fact that its chemical structure (Fig. 2) indicates the presence of  $-\text{OH}$  and  $-\text{NH}_2$  functional groups that have dual functions.

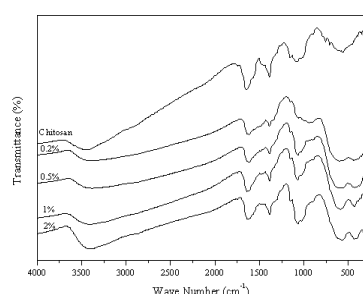


Fig. 1. FTIR spectra of chitosan-coated magnetite NPs

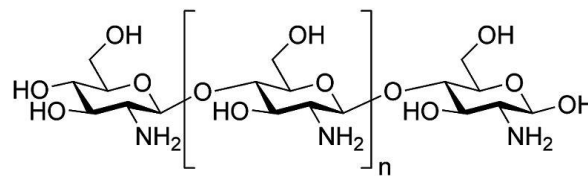


Fig. 2. Chemical Structure of Chitosan

Both groups have affinity towards the surface of magnetite NPs, but due to the chemical structure of chitosan, not all functional groups are used to bind to the magnetite surfaces. Therefore, the presence of unbound groups facilitates the immobilization of the organic drugs onto its surfaces through true chemical reactions. Studying the Thermogravimetric analysis of the chitosan-coated NPs (Fig. 3) confirmed the presence of chitosan coating that increased in thickness with increasing the initial concentration of chitosan. However, results also indicated that above 1 wt% of chitosan resulted in detachment of the adsorbed chitosan extra layers. A typical TEM micrograph of a chitosan-coated NPs is also shown in Fig. 3, where a homogeneous distribution of NPs with an average size of 20 nm could be observed.

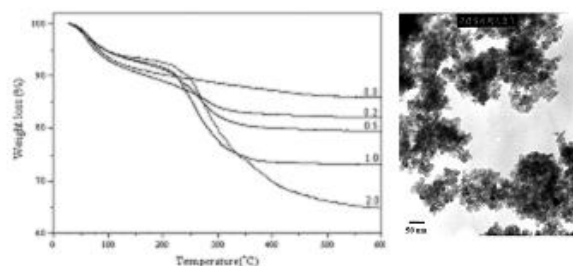


Fig. 3. TGA and a typical TEM of chitosan-coated magnetite NPs

### CONCLUSION

This work demonstrates the optimum coating of magnetite nanoparticles with chitosan to be used for drug delivery applications. The optimally prepared coated NPs have an average particle size of 20 nm.

### REFERENCES

1. Zhao et al. *J Alloys and Compds.* 2009;477:739-43
2. Mahmoudi et al. *Adv Drug Deliv Rev.* 2010.
3. El-kharrag et al. *J. Ceram Sci Technol* 2011;2(4):203-10

### ACKNOWLEDGMENTS

The author acknowledges the funding provided by the UAE University as part of the Zayed Centre of Health Sciences (grant 31R049)

## Stability and Mechanical Properties of Hybrid Hydrogel Materials with Variation of TiO<sub>2</sub> Nanoparticle Concentration with Potential Use as Bones Scaffolds

Karolina Zazakowny<sup>1</sup>, Justyna Pawlik<sup>1</sup>, Joanna Lewandowska-Łańcucka<sup>2</sup>, Joanna Mastalska-Popławska<sup>1</sup>, Kamil Kamiński<sup>2</sup>, Maria Nowakowska<sup>2</sup>, Marta Radecka<sup>1</sup>

<sup>1</sup>Faculty of Materials Science and Ceramics, AGH University of Science and Technology, Kraków, Poland

<sup>2</sup>Faculty of Chemistry, Jagiellonian University, Kraków, Poland

[kzazakow@agh.edu.pl](mailto:kzazakow@agh.edu.pl)

### INTRODUCTION

The hybrid hydrogel materials containing TiO<sub>2</sub> nanoparticles are promising candidates for preparation of bioactive, injectable scaffolds for tissue engineering. Since the scaffolds are placed in the living bodies they must be bioactive and eventually should be either absorbed or degraded after their medical function is completed. Therefore biodegradable biopolymer matrices are frequently used as the scaffolds for bone tissue repair. Among many popular polymeric matrices these obtained from collagen and chitosan are of considerable interest. Collagen, being the component of the bone tissue is a perfect candidate for preparation of the matrix of scaffolds. Whereas chitosan, as a natural polymer is biocompatible and biodegradable and its addition to the matrix should improve its mechanical properties. TiO<sub>2</sub> nanoparticles were recently tested as fillers in polymeric materials aimed to improve properties of bone engineering scaffolds [1]. Since there are many studies showing that hydroxyapatite formation [2] might be strongly accelerated at the surface of TiO<sub>2</sub> particles their incorporation into the polymeric materials can be considered as an effective way to enhance the bioactivity of the resulted inorganic-organic hybrid materials. Polymer gelation takes place at about 37°C, which enables the material to be injected into a specific bone defect site and to form the scaffold at the target site.

### EXPERIMENTAL METHODS

The microstructure of prepared hybrids after mineralization was observed with use of a field emission gun (FEG) scanning electron microscope FEI Europe Company – NOVA NANO SEM 200 equipped with an EDAX energy dispersion spectrometer. The mechanical properties of the tested hydrogels were studied with a Physica MCR-301 (Anton Paar) rheometer equipped with a parallel-plate PP 50 made of stainless steel with a 25 mm diameter. All measurements were performed at 37°C.

### RESULTS AND DISCUSSION

The activity is oriented on optimization of selected TiO<sub>2</sub> nanopowder concentration in the polymeric hybrid materials based on natural polymers (collagen, chitosan) crosslinked with genipin. The introduction of TiO<sub>2</sub> into hydrogel matrices aims to improve mechanical properties and improve the biological activity of materials. The research concerns the development of a material with the highest possible mechanical strength while preserving its biological activity. An anatase TiO<sub>2</sub> nanoparticle with a specific surface area of about 100 m<sup>2</sup>/g was used to prepare sample series.

Based on previous research, it was found that the addition of TiO<sub>2</sub> to the polymer matrix at 1.9 mg/ml resulted in a deterioration in mechanical properties. Within the project studies with materials with lower TiO<sub>2</sub> concentration were performed as well as cytotoxicity on human osteoblastic bone cells (MG-63) with XTT method and defining the rheological properties of the hybrids (G', G'', viscosity) were carried out. As we already showed in previous publication the addition of TiO<sub>2</sub> to polymer hybrids induces the deposition of apatites on the surface of the materials [3]. This effect was not found for polymer matrices that did not contain TiO<sub>2</sub>. There was no significant effect of the polymorphic TiO<sub>2</sub> variation on the properties of the tested systems. Literature reports on other polymer materials with TiO<sub>2</sub> nanoparticles that the addition of oxide, depending on concentration, can affect the mechanical properties by either improving or deteriorating it. This is the reason why it was so important to determine the optimal concentration of TiO<sub>2</sub> that will keep the biological activity without impairing the mechanical properties and may even improve them. The early results suggest that the optimal TiO<sub>2</sub> concentration for collagen hybrids is 0.25 mg/ml and for collagen-chitosan hybrids 0.5 mg/ml. Additionally an effect of the materials degradation in the presence of TiO<sub>2</sub> nanoparticles in the polymer matrix was noticed.

### CONCLUSION

The gained results of the research are the first and fundamental step to solve the scientific problem of obtaining hydrogel hybrid materials with TiO<sub>2</sub> nanoparticles that can be used as bones scaffolds. It was also found that the properties of hybrid materials depend on TiO<sub>2</sub> concentration. The optimal nanoparticle concentration for collagen materials seems to be significantly lower than the one we used in our preliminary research resulting in storage modulus improvement [3].

### REFERENCES

- [1] A.R. Boccaccini, et al., *Mater. Sci. Eng. C* 28 (2008) 1–10.
- [2] T. Kokubo, et al., *Biomater.* 24 (2003) 2161–2175.
- [3] K. Zazakowny, J. Lewandowska-Łańcucka, et al., *Colloids Surf. B.* 2016 (148) 607–614.

### ACKNOWLEDGMENTS

Karolina Zazakowny acknowledges the financial support of Polish National Science Centre, Grant No.18.18.160.0259.

## Plasma-modified Polystyrene Solution Blow Spun Fibrous Scaffolds for 3D Cell Culture

Michał Wojasiński<sup>1</sup>, Marta Błaszczak<sup>1</sup>, Tomasz Ciach<sup>1,2</sup>

<sup>1</sup>Faculty of Chemical and Process Engineering, Division of Biotechnology and Bioprocess Engineering, Warsaw University of Technology, Poland

<sup>2</sup>Central Laboratory of Advanced Materials and Technology CEZAMAT, Warsaw, Poland  
[michal.wojasinski.dokt@pw.edu.pl](mailto:michal.wojasinski.dokt@pw.edu.pl)

### INTRODUCTION

Development and constant improvement of methods for 3D cell culture confirms that 2D approaches are oversimplified. What is more, cell culture on flat surfaces lacks crucial parameters necessary in recreating native 3D tissue structure, thus lacking the physiology of those tissues<sup>1,2</sup>. In our previous research, we described how specific architecture of fibrous materials influences the result of cell culture of cardiac cells, improving cells elongation and arrangement according to the fibers arrangement<sup>3</sup>. Those effects were not observable in classic 2D cell culture on polystyrene. Observations of improved cells interactions with fibrous materials were known since electrospinning allowed production of these materials. However, the commercial production of such fibers was limited by low production rate of electrospinning. Since last decade, the solution blow spinning (SBS) process was introduced to the wider public. Allowing generation of polymer fibers with yield almost, in some cases, 100 times higher than electrospinning solution, blow spinning can become a first-choice technique to produce fibrous materials for 3D cell culture. The only limitation of polymer fibers from solution blow spinning to cell culture are poor wetting properties of those materials. In present research we propose and investigate plasma modification of solution blow spun polystyrene fibers for 3D cell culture of animal cells.

### EXPERIMENTAL METHODS

For production of SBS polymer mats the polystyrene (PS, melt index 14.00 g/10min, Sigma Aldrich) was used. Polymer was dissolved in chloroform in three concentrations 7%w/w, 10%w/w, and 12%w/w to obtain nanofibers, submicron fibers, and microfibers, respectively. Fibers were produced using previously described SBS system<sup>4</sup>. Materials were plasma-modified using Plasma Cleaner (GV10x DS, Asher, ibss Group Inc.) with radio frequency (13.56MHz) plasma in atmosphere 96% of oxygen and 4% of argon. Modification conditions were as follows: pressure 0.42Pa, modification time 30s, and modification power: 30W, 60W, and 90W.

Resulting unmodified materials and plasma-modified fibrous materials were investigated by scanning electron microscopy (SEM) to analyze their morphology, and fiber sizes, gravimetric method to evaluate volumetric porosity, goniometer to analyze water contact angle right after plasma modification and 1, 3 and 6 weeks after modification, FTIR spectroscopy to indicate chemical change in modified materials, and cytotoxicity test (MTT, L929 cell line) to evaluate cytotoxicity of the materials.

### RESULTS AND DISCUSSION

SEM analysis indicated that PS fibers morphology can be affected by plasma modification, especially for the highest modification power – 90W. Fibers tend to melt and fuse together. But, overall mean fiber diameter is not affected by the plasma modification of solution blow spun PS materials. We observed mean fiber diameter: about 300nm - nanofibers, about 550nm - submicron fibers, and about 1200nm - microfibers, regardless of the plasma modification and power of this modification. The same observation was made in terms of the influence of plasma modification on porosity of each class of investigated materials. Mean porosity of nanofibers was about 97%, of submicron fibers – about 96%, and of microfibers – about 94%. Plasma modification of the surface of PS fibrous materials was designed to significantly improve fibrous materials water contact angle. All three classes of materials produced in SBS system exhibited water contact angle about 120-130°. After plasma modification, regardless of modification power the drop was “sucked” into the fibrous material – fully wetted material. Unfortunately, the modification was only temporal. After one week the wettability returns to initial values of water contact angle for every material. Even though, the change in water contact angle is significant, FTIR analysis shows no chemical modification of the polymer within the materials. Results of MTT cytotoxicity tests for all materials are all over 90% of cells viability, which suggest no cytotoxic effect of materials extracts on L929 cells.

### CONCLUSION

Three classes of fibrous plasma-modified polystyrene materials with great, although temporal, wetting properties were produced and proven non-cytotoxic, allowing the application in 3D cell culture and cell research.

### REFERENCES

1. Breslin S. *et al.*, Drug Discov Today. 18:240-249, 2013
2. Haycock J.W. *et al.*, Methods Mol Biol. 695:1-15, 2010
3. Tomecka E. *et al.*, Mater Sci Eng C. 75 :30-316, 2017
4. Wojasiński M. *et al.*, Pol. J. Chem. Technol. 16:43-50, 2014

### ACKNOWLEDGMENTS

Present research was funded by Warsaw University of Technology, Faculty of Chemical and Process Engineering.

## Surface Functionalization of Poly(L-lactide-co-glycolide) with Poly(2-oxazoline)

Anna-Maria Tryba, Katarzyna Reczyńska, Krzysztof Pietryga, Elżbieta Pamuła

AGH University of Science and Technology, Faculty of Materials Science and Ceramics,  
Department of Biomaterials and Composites, Al. Mickiewicza 30, 30-059 Kraków, Poland  
[amtryba@agh.edu.pl](mailto:amtryba@agh.edu.pl)

### INTRODUCTION

Membranes are one of the most important forms of materials used in medicine, e.g. in drug delivery systems, artificial organs, diagnostic devices or as barriers in periodontology. A successful approach widely used in biomaterials science is to design the surface properties of approved materials to specific medical application. A main challenge in this area is the development of processing routes allowing for a simple but efficient surface modification of complex shaped geometries [1]. Our research focuses on biomaterials, and more precisely on implementation of self-assembly principles for surface functionalization of polymeric constructs *via* phase separation between resorbable poly(L-lactide-co-glycolide) (PLGA), water-soluble poly(ethylene glycol) (PEG) [2] and bifunctional poly(2-oxazolines) (POx) [3].

The aim of this study was to functionalize the surface of PLGA membranes with POx in order to change its chemical state and increase hydrophilicity. The latter factors are important in cell adhesion, proliferation and differentiation, thus we hypothesize that applied modification will improve biological performance of PLGA membranes in contact with bone cells.

### EXPERIMENTAL METHODS

The membranes were made from PLGA (85:15, 100 kDa, d = 1.9, CMPW PAN). As a solvent dichloromethane (DCM) and as a pore former PEG (1000 Da), both from Sigma Aldrich, were used. As an amphiphilic POx molecule poly(2-methyl-2-oxazoline-b-2-butyl-2-oxazoline-b-2-methyl-2-oxazoline) and more specifically methyl-P[MeOx37-b-BuOx-23-b-MeOx37-piperidine (P2—P2) (Mn = 8 kDa, d = 1.14, TUD, Dresden) was used. PLGA and PEG were co-dissolved at a concentration of 10% wt/vol in DCM and 1 wt% POx in respect to PLGA was added. The membranes PLGA/Pox were obtained by solvent casting/phase separation and PEG leaching. As references PLGA membranes and PLGA foils without POx were made. Microstructure and topography of the samples were tested with optical microscopy (VHX-900F, Keyence), scanning electron microscopy (SEM, Nova Nano SEM 200) and atomic force microscopy (Exploer, ThermoMicroscopes). Chemical structure was analyzed by FTIR-ATR (Bruker Tensor 27). Wettability and surface free energy was measured on DSA Mk2 (Kruss). Cytocompatibility tests were performed for 1, 3 and 7 days with osteoblast-like MG-63 cells. Live/dead, and viability tests were done.

### RESULTS AND DISCUSSION

PLGA membrane was more smooth at micrometric level ( $R_{rms} = 0.50 \mu\text{m}$ ) as compared to the membrane containing POx ( $R_{rms} = 1.48 \mu\text{m}$ ) (Fig. 1). Wettability results (Fig. 2) suggest that POx was preferentially immobilized on the surface of PLGA, resulting in decreased water contact angle. *In vitro* tests showed that all materials were cytocompatible with MG-63 cells.

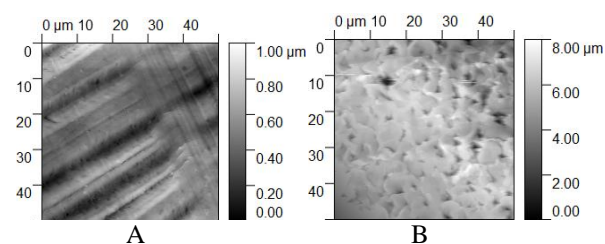


Fig. 1. AFM pictures of control PLGA membrane (A) and PLGA membrane modified with POx (B)

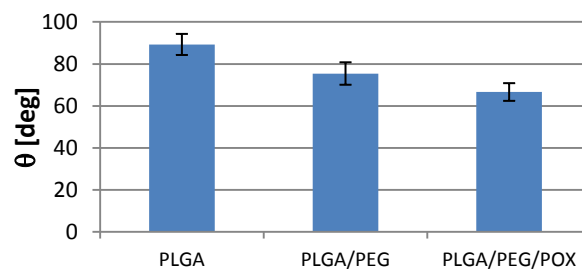


Fig. 2. Water contact angle of PLGA foil, PLGA membrane and PLGA/Pox membrane

### CONCLUSION

It was shown that it is possible to obtain cytocompatible surface-modified PLGA membranes which are more textured at the microscale and have enhanced wettability, thanks to phase separation and preferential adsorption of POx molecules at the interface PLGA-POx-PEG followed by PEG leaching.

### REFERENCES

- [1] Krok, M.; Pamuła, E.; J Appl Polym Sci. 2012,125: E187–E199.
- [2] Pamuła, E.; Błażewicz, S.; Krok, M.; Kościelniak, D.; Dobrzyński, P. Polish Pat. P-391519 (2010).
- [3] Luxenhofer, R.; Schulz, A.; Roques, C.; Lil, S.; Bronich, T.K.; Batrakova, E.V., et al.; Biomaterials. 2010, 31(18): 4972–4979

### ACKNOWLEDGMENTS

This study was supported from Interfaculty Environmental Doctoral Studies (FCB) at the Faculty of Materials Science and Ceramics, AGH University of Science and Technology.



## Self-Assembling Peptides with RGD Motifs as Scaffolds for Tissue Engineering

Graziano Deidda<sup>1,2</sup>, Anthi Ranella<sup>2</sup>, Vamshi Jonnalagadda<sup>3</sup>, Phanourios Tamamis<sup>3</sup>, Estelle Mossou<sup>4,5</sup>, Trevor Forsyth<sup>4,5</sup>, Maria Farsari<sup>2</sup>, Anna Mitraki<sup>1,2</sup>

<sup>1</sup>Department of Materials Science and Technology, University of Crete;

<sup>2</sup>Institute of Electronic Structure and Laser (IESL) & Institute of Molecular Biology and Biotechnology (IMBB), FORTH, Heraklion, Greece;

<sup>3</sup>Artie McFerrin Department of Chemical Engineering, Texas A&M University College Station, TX 77843-3251, U.S.A.;

<sup>4</sup>Institut Laue Langevin, 6 rue Jules Horowitz, 38042 Grenoble Cedex 9, France;

<sup>5</sup>Faculty of Natural Sciences / Institute for Science and Technology in Medicine, Keele University, Staffordshire ST5 5BG, United Kingdom;

[grazianodeidda@gmail.com](mailto:grazianodeidda@gmail.com)

### INTRODUCTION

In the last decade, the development of self-assembled peptides as biocompatible and biodegradable scaffolds for tissue engineering gained increasing interest. [1] We used a combination of theoretical and experimental approaches towards such rational designs. [2] [3] We have been especially focusing on modular designs that consist of a central ultrashort amphiphilic motif derived from the adenovirus fiber shaft. [2] In addition, both the cell attachment tripeptide RGD and a cysteine residue were projected to be incorporated to this central motif in order to allow respectively cell adhesion and metal nanoparticle binding. [4] Subsequently, in place of cysteine residue, photosensitive residues such as tyrosine and tryptophan were contrived to be inserted at the C-terminus as an approach to fabricate fully biocompatible scaffolds via Multi Photon Stereolithography (MPS).

### EXPERIMENTAL METHODS

The techniques utilized to monitor the kinetics of assembly of the peptide-derived networks and their morphology were: X-ray diffraction, TEM, FESEM and AFM. Cell-culture experiments used for viability and cytotoxicity were: MTT assay, LIVE/DEAD test and SEM imaging. An ultraprecise femtosecond (220 fs) laser (Spectra-Physics, 520 nm wavelength in exit) was used to fabricate structures via MPS whilst a UV KrF laser was used for 1-Photon irradiation.

### RESULTS AND DISCUSSION

The designed RGD S-A-peptides proved to be appropriate building blocks with a marked tendency to form higher order assembled networks (Fig. 1). The use of non-linear lithography allowed the fabrication of 3D microstructures on which the cysteine- containing S-A-scaffolds could be efficiently attached to a hybrid zirconia-derived composite in a “scaffold-on-scaffold” strategy for cell attachment (Fig. 2a). In addition, preliminary results indicate that photostructurable S.A. peptides containing Tyr and Trp positively respond to 1P- and 2P- irradiation (Fig. 2b).

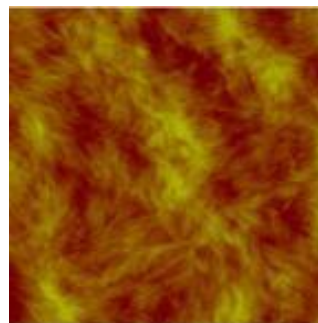


Fig. 1. AFM analysis showed clearly fibril formation of the peptides.

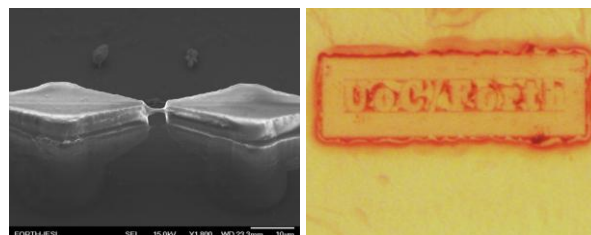


Fig. 2. 3D structures produced by the 2PP technique. a) Zirconia-based «scaffold-on-scaffold» sandwich fabrication following gold metallization and S.A. peptide attachment. b) Photoinitiator-free fabrication for soft-tissue engineering.

### CONCLUSION

These short self-assembling peptides will subsequently be studied for angiogenesis in ischemic in vitro models as they are amenable to offer open-ended possibilities towards multifunctional tissue engineering scaffolds of the future.

### REFERENCES

1. Loo, Y., et al., *Advanced Healthcare Materials*, 2015. 4(16): p. 2557-2586.
2. Tamamis, P., et al., *Journal of Physical Chemistry B*, 2009. 113(47): p. 15639-15647.
3. Deidda, G., et al., *ACS Biomaterials Science & Engineering*, 2016.
4. Terzaki, K., et al., *Biofabrication*, 2013. 5(4).

### ACKNOWLEDGMENTS

This research was supported by “Marie Curie Industry – Initial Training Network (ITN), callFP7-PEOPLE-2012-ITN, [www.angiomatrain.eu](http://www.angiomatrain.eu).

## HypACT Inject Auto Device – an Easy, Fast and Sterile Method to Produce the Best Quality Platelet Rich Fibrin Membrane

Dorottya Kardos<sup>1</sup>, István Hornyák<sup>1</sup>, Melinda Simon<sup>1</sup>, Adél Hinsenkamp<sup>1</sup>, Bence Marshall<sup>1</sup>, Róbert Várdai<sup>2</sup>, Balázs Pinke<sup>3</sup>, László Mészáros<sup>3</sup>, Alfréd Kállay-Menyhárd<sup>4</sup>, Zsombor Lacza<sup>1</sup>

<sup>1</sup>Institute of Clinical Experimental Research, Semmelweis University, Budapest, Hungary

<sup>2</sup>Institute of Materials and Environmental Chemistry, Research Centre for Natural Sciences, Hungarian Academy of Sciences, Budapest, Hungary

<sup>3</sup>Department of Polymer Engineering, Budapest University of Technology and Economics, Budapest, Hungary

<sup>4</sup>Department of Physical Chemistry and Materials Science, Budapest University of Technology and Economics, Hungary

[dorottya.kardos@orthosera.com](mailto:dorottya.kardos@orthosera.com)

### INTRODUCTION

Platelet rich fibrin (PRF) membrane is a second-generation platelet concentrate, produced from autologous blood in a glass tube without any anticoagulant. It is a biocompatible 3D scaffold, containing fibrin clot, platelets, leukocytes and a high concentration of growth factors. It has been tested in numerous clinical situations usually in dental and maxillofacial applications.<sup>1</sup> We produced a sterile, PRF membrane with constant size by HypACT Inject Auto device and we compared the biological and physical properties with PRF membrane made by glass tube.

### EXPERIMENTAL METHODS

We have produced a reproducible, sterile PRF membrane with constant thickness and diameter using the hypACT Inject Auto device. Our aim was to compare the traditional PRF membrane produced in a glasstube (GT-PRF) with the hypACT derived PRF membrane (HI-PRF) based on the following properties: mesenchymal stem cell (MSC) adhesion and proliferation capacity on the membranes, weight loss of the membranes during the culture period, tensile- and strain strength. The examination of the surface and structure characteristics was assessed using electron microscopy and live-dead cell staining using confocal microscopy.

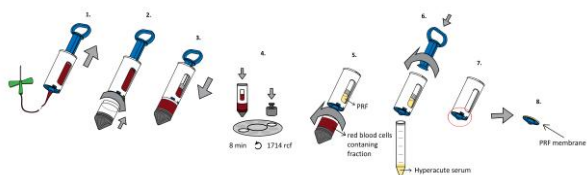


Fig. 1. PRF membrane isolation with hypACT

### RESULTS AND DISCUSSION

There were no significant differences in MSC adhesion, proliferation capacity and in the weight loss of the PRF membranes. There was also no significant difference in the tensile and strain strength values; however the typical stress-strain curves of the two types of membranes were different. The surface and structure of the membranes were similar, but in case of HI-PRF membrane platelets are located in the inside of the membrane, while in case of GT-PRF they are located mostly on the surface.

The biological properties of HI-PRF membrane are at least as good as GT-PRF. Furthermore, we can conclude, based on the stress-strain curve, that HI-PRF is homologous, and more suturable compared to GT-PRF, which could be an advantage in clinical use.

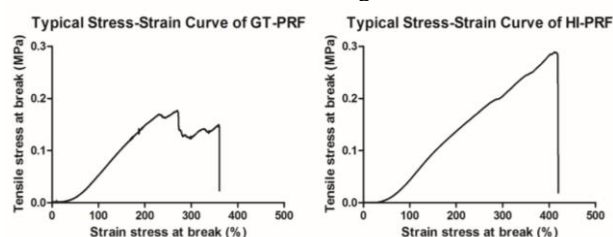
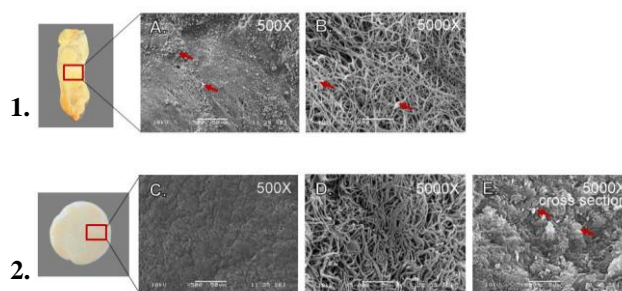


Fig. 2. Typical Stress-Strain Curve of PRF membranes



### 1. Electron microscopy image of PRF membranes

Platelets are located mostly on the surface of GT-PRF, however they are located only inside of HI-PRF.

### CONCLUSION

The hypACT device ensures an easy, fast, and sterile method to isolate PRF membrane from autologous blood. This membrane has the same excellent biological properties as the traditional one.

### REFERENCES

1. Patel GK. *et al.*, J. Periodontol. 1192-1199, 2017

### ACKNOWLEDGEMENTS

I would like to express my thank to Dr. Zsombor Lacza, Dr. István Hornyák and to all of the co-authors, who helped me in the research.

## Wetting Properties and Morphology of Electrospun Fibers from Hydrophobic and Hydrophilic Polymers

Joanna Knapczyk<sup>1</sup>, Marcin Gajek<sup>2</sup>, Urszula Stachewicz<sup>1</sup>

<sup>1</sup>International Centre of Electron Microscopy for Materials Science, Faculty of Metals Engineering and Industrial Computer Science, AGH University of Science and Technology, Poland

<sup>2</sup>Faculty of Materials Science and Ceramics, AGH University of Science and Technology, Poland

[jknapczyk@agh.edu.pl](mailto:jknapczyk@agh.edu.pl)

### INTRODUCTION

The modern development of medicine is possible thanks to the use of new, innovative materials such as biocompatible polymers. Polymers are often used to make new generation dressings, allowing quick wounds healing, where surface properties and wetting are extremely important. This research focused on investigating of the morphology and wettability of electrospun hydrophobic polymer such as polystyrene (PS) and hydrophilic polyamide 6 (PA6).

### EXPERIMENTAL METHODS

Nanofibers were obtained by electrospinning (Apparatus EC-DIG with Climate-control – IME Technologies) from solutions of PS (25%<sub>wt.</sub>) and PA6 (12%<sub>wt.</sub>) dissolved respectively in dimethylformamide and mixture of formic and acetic acids, ratio 1:1.

PS and PA6 nanofiber were analysed by Scanning Electron Microscope (SEM, Merlin Gemini II – ZEISS). To determine the hydrophobicity and hydrophilicity of the obtained nanofibers we measured contact angle with 3 liquids (water, glycerol, formamide). Additionally, surface roughness was verified using confocal microscope (Olympus Lext OLS 4000).

### RESULTS AND DISCUSSION

SEM analyses showed clear differences of electrospun fibers and their diameters, as shown in Fig. 1. The average fiber diameter for PS and PA6 were respectively  $5.48 \pm 0.47 \mu\text{m}$  and  $0.12 \pm 0.02 \mu\text{m}$ .

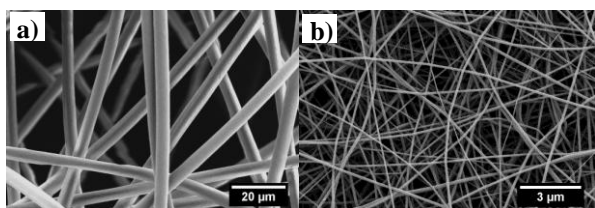


Fig.1. Microstructure in the SEM image of a) PS and b) PA6 electrospun fibers.

Investigating of contact angles confirmed hydrophobicity for PS nanofibers and hydrophilicity for PA6 nanofibers, see Table 1. In Fig. 2, the droplets of water on the electrospun fibers are presented, with a clearly lower contact angle for PA6 than PS fibers.

Table 1. The average values of contact angle with water, glycerol and formamide on electrospun PS and PA6 fibers.

Sample	Liquids	Average Contact Angle [°]	Standard deviation [°]
PS	Water	124.75	4.92
	Glycerol	132.55	1.68
	Formamide	117.81	3.50
PA6	Water	51.58	4.29
	Glycerol	49.44	1.80
	Formamide	27.17	3.34

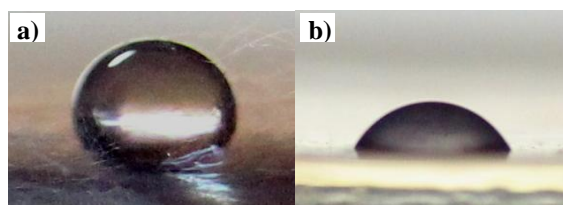


Fig. 2. The droplets of water on electrospun a) PS and b) PA6 fibers.

The confocal microscope showed significant differences in surface roughness of electrospun PS and PA6. The PA6 fibers formed a compact surface with low roughness, while the PS fibers showed much high roughness, as the average diameter is significantly higher in comparison to PA6, see Fig. 1.

### CONCLUSION

The obtained electrospun PS and PA6 fibers significantly differ in their morphology and wettability. The electrospun samples of PS were hydrophobic and PA6 were hydrophilic. Our study showed that roughness of electrospun samples has strongly impact on wetting contact angles. The further studies will explore possibilities of combining hydrophobic and hydrophilic properties of PS and PA6 fibers to create a composite structure.

### REFERENCES

1. Abrigo M. *et. al.*, ACS Appl. Mater. Interfaces, 2015, 7 (14), pp 7644–7652
2. Maitz M.F., Biosurface and Biotribology, 2015, 1 (3), pp 161-176

### ACKNOWLEDGMENTS

The study was conducted within the funding from SONATA BIS 5 project granted by National Science Centre in Poland, No 2015/18/E/ST5/00230.



## Charge Assisted Tailoring of Electrospun PMMA Fibers: Surface Chemistry and Wetting Properties

Daniel Ura<sup>1</sup>, Mateusz Marzec<sup>2</sup>, Andrzej Bernasik<sup>2,3</sup>, Urszula Stachewicz<sup>1</sup>

<sup>1</sup>International Centre of Electron Microscopy for Materials Science, Faculty of Metals Engineering and Industrial Computer Science, AGH University of Science and Technology, Poland

<sup>2</sup>Academic Centre for Materials and Nanotechnology, AGH University of Science and Technology, Poland

<sup>3</sup>Faculty of Physics and Applied Computer Science, AGH University of Science and Technology, Poland  
[urad@agh.edu.pl](mailto:urad@agh.edu.pl)

### INTRODUCTION

Electrospinning is method fabricating polymer fibers for biomedical engineering with ability to tailor polymer surfaces through by using positive and negative polarity of applied voltages. Alternating voltage during electrospinning controls reorientation of functional groups at the surface of polymer fibers<sup>1-3</sup>.

The aim of this study is to determine the effect of voltage polarity on poly(metacrylate methyl) (PMMA) fibers, its surface chemistry and wetting properties of fibrous scaffolds.

### EXPERIMENTAL METHODS

#### Electrospinning

PMMA (12 %wt) dissolved in Dimethylformamide (DMF) was used to produce electrospun fibers, with apparatus EC-DIF integrated with climate system (IME Technologies, The Netherlands). The voltage applied to the nozzle was +/- 10 kV with polymer solution flow rate at 4 ml h<sup>-1</sup>. The humidity in the chamber during electrospinning was H = 35% and temperature T=25°C.

#### Contact Angle Measurements

The electrospun fiber morphology was studied using scanning electron microscope (SEM, Merlin Gemini II, ZEIS) prior contact angle measurement with 3 different liquids: deionized water, glycerol and formamide. Droplets of 3 µl volume were deposited on the fibers surface next the image of the droplet were taken using a camera with macro zoom lens (Canon EOS 700D camera, EF-S 60mm f/2.8 Macro USM zoom lens). The contact angle measurement was performed via ImageJ Software with drop analysis plugin.

#### X-ray photoelectron spectroscopy (XPS)

The surface chemistry of the electrospun PMMA fibers were analyzed with XPS (PHI VersaProbe II) with monochromatic radiation from Al K $\alpha$  (1486.6 eV). The photoelectron take-off angles were set to 90° and the pass energy in the analyzer was set to 23.50 eV to obtain high energy resolution spectra for the C 1s, O 1s regions.

### RESULTS AND DISCUSSION

Electrospun PMMA fibers were successfully produced using positive and negative voltage polarities, as shown in Fig. 1. SEM images of the fibers demonstrated a non-beaded fibrous structure with an average fiber diameter of  $1.44 \pm 0.22 \mu\text{m}$  with positive voltage polarity and  $1.74 \pm 0.32 \mu\text{m}$  with a negative voltage polarity.

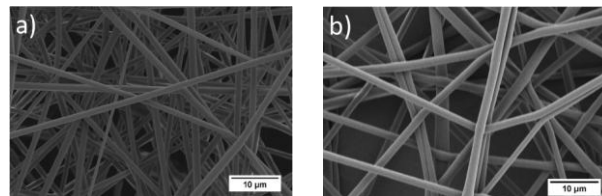


Fig 1. SEM image of electrospun PMMA fiber produced with a) positive and b) negative voltage polarity

Analysis of contact angle on PMMA fibers demonstrated clear differences as fibers produced with negative voltage polarity had higher contact angles for all 3 liquids than for fibers produced with positive voltage polarity, see Table 1.

Table 1. Contact angle results on PMMA fibers produced with positive (+) and negative (-) voltage polarity using water, glycerol, formamide

Voltage polarity	Contact angle [°]		
	Water	Glycerol	Formamide
+	125 ± 3	125 ± 2	39 ± 2
-	132 ± 3	134 ± 2	42 ± 2

The XPS results of PMMA fiber showed variations in oxygen content at the surface of electrospun PMMA fibers with higher O (1s) on electrospun fibers produced with positive voltage polarities.

### CONCLUSION

The electrospinning technique allow to control via applied charges with positive and negative voltage polarities the oxygen content at the PMMA fibers surface. This charge assisted tailoring was confirmed by XPS and observed in contact angle results with 3 liquids with surface tension from 72.2 mN m<sup>-1</sup> to 58.5 mN m<sup>-1</sup>.

### REFERENCES

- Kai, D., Liow, S. S. & Loh, X. J. Biodegradable polymers for electrospinning: Towards biomedical applications. *Mater. Sci. Eng. C* **45**, 659–670 (2015).
- Sharma, J. *et al.* Biocompatible electrospun tactic poly(methyl methacrylate) blend fibers. *Polym. (United Kingdom)* **55**, 3261–3269 (2014).
- Stachewicz, U., Stone, C. A., Willis, C. R. & Barber, A. H. Charge assisted tailoring of chemical functionality at electrospun nanofiber surfaces. *J. Mater. Chem.* **22**, 22935 (2012).

### ACKNOWLEDGMENTS

This research was conducted within the funding from the Sonata Bis 5 project granted by National Science Centre, No 2015/18/E/ST5/00230



## Composite Scaffolds from Poly(3-hydroxybutyrate) and Sodium Alginate for Tissue Engineering

Andrej Dudun<sup>2</sup>, Anton Bonartsev<sup>1,2</sup>, Irina Zharkova<sup>1</sup>, Elizaveta Akoulina<sup>1,2</sup>, Vsevolod Zhuikov<sup>2</sup>, Dariana Chesnokova<sup>1</sup>, Tatiana Makhina<sup>2</sup>, Sergey Yakovlev<sup>1</sup>, Garina Bonartseva<sup>2</sup>, Vera Voinova<sup>1</sup>

<sup>1</sup>Faculty of Biology, M.V.Lomonosov Moscow State University, Russia

<sup>2</sup>Research Center of Biotechnology RAS, Russia

[dudunandrey@mail.ru](mailto:dudunandrey@mail.ru)

### INTRODUCTION

Recent years biodegradable polymers of natural origin, poly(3-hydroxyalkanoates) (PHAs) and alginates (ALGs), have found broad application in medicine and tissue engineering. These polymers are very different in their properties: PHAs are hydrophobic, mechanically strong polyesters, while alginates are hydrophilic, hydrogel-forming, mechanically destructible polysaccharides. However these polymers bring together the fact that PHAs and ALGs can be produced biotechnologically allowing to regulate their properties.<sup>1,2</sup> Particularly, development of composite constructions from these polymers makes it possible to adjust the selected properties, especially mechanics, of the resulting composite PHAs/ALGs constructions for bone and cartilage engineering, where PHAs and ALGs are widely used. Thus, the objective of the work was to create the composite scaffolds from poly(3-hydroxybutyrate) (PHB) and sodium alginate (ALG).

### EXPERIMENTAL METHODS

Both PHB and ALG were produced biotechnologically using a highly effective strain-producer *Azotobacter chroococcum* 7B, which gives the opportunity to acquire high purity polymers with desired properties.<sup>1,2</sup> The produced homopolymer PHB had molecular weight of 155 kDa; the produced ALG had molecular weight of 95 kDa. ratio of mannuronic and guluronic residues 75/25, and acetylation degree 26%.

The scaffolds used in this work were manufactured by two-stage leaching technique. A solution of PHB in trichloromethane with a concentration of 90 mg/ml was filled in glass shape filled with blowing agents: ammonium carbonate and sucrose in a ratio of 1:8. We developed optimal structure for the cultivation of cells, using the sucrose, which was sieved through laboratory sieves U1-ESL (Kraft, Russia) with a mesh size of 315 and 94  $\mu\text{m}$ . Then the obtained PHB scaffolds were filled with 1% ALG solution until full saturation, then they were placed in 5% solution of  $\text{CaCl}_2$  until the complete gelling of alginate in the scaffold and washed.

The microstructure of hybrid scaffolds was investigated by scanning electron microscopy (SEM) using JSM-6380LA (JEOL, Japan) and by wide-field light microscopy (WLM) using stereomicroscope Nikon SMZ1500 (Nikon, Japan). Diameter of micropores was calculated by Image J software using SEM and WLM images, scaffold porosity was also calculated. Ink test was used to determine interconnection of pores in scaffolds. The mechanical properties of obtained constructions were measured by rheometry.

### RESULTS AND DISCUSSION

The produced scaffolds have three-dimensional porous structure with various pore sizes: micropores of  $24 \pm 7 \mu\text{m}$ , macropores of  $370 \pm 65 \mu\text{m}$ . The minimum pore size for cell growth is 75-100  $\mu\text{m}$ , but the optimum range is about 100-135  $\mu\text{m}$ . On average, scaffold porosity amounted to 93%. The hybrid scaffolds were found to have interconnected pore system. Alginate hydrogel completely fill the entire volume of the PHB scaffold, covering tightly all its pores. The filling the scaffold with alginate caused a slight increase in its Young modulus (from 36 to 47 kPa) and a 2-fold decrease in the shear modulus (from 132 to 67).

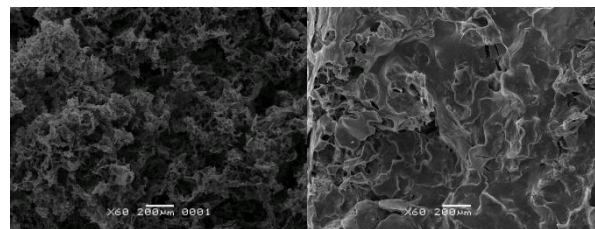


Fig. 1. PHB scaffold without alginate (left) and filled with alginate hydrogel.

### CONCLUSION

Thus, the composite scaffolds from PHB and ALG with desired microstructure and mechanical properties was developed. Further the technique of hybrid PHB/ALG scaffolds production will be used to develop biocomposite scaffolds high loaded highly with mesenchymal stem cells for bone tissue engineering.

### REFERENCES

1. Bonartsev A.P. *et al.* Prep. Biochem. Biotechnol., 47(2): 173-184, 2017.
2. Bonartseva G. A. *et al.* Appl Biochem and Microbiol, 53(1):52–59, 2017.

### ACKNOWLEDGMENTS

This work was supported by Russian Science Foundation, project # 17-74-20104. The equipment of User Facilities Centers of M.V.Lomonosov Moscow State University (incl. in framework of Development Program of MSU to 2020) and Research Center of Biotechnology RAS was used in the work.

**Biophysical Studies on Biocompatible Polymers for Medical Applications - Polyhydroxyoctanoate (PHO)**

Katarzyna Harażna<sup>1</sup>, Tomasz Witko<sup>2</sup>, Daria Solarz<sup>2</sup>, Małgorzata Witko<sup>1</sup>, Marcel Krzan<sup>1</sup>,  
Andrzej Bojarski<sup>3</sup>, Maciej Guzik<sup>1</sup>

<sup>1</sup>Jerzy Haber Institute of Catalysis and Surface Chemistry, Polish Academy of Science, Poland

<sup>2</sup>Faculty of Physics, Astronomy and Applied Computer Science, Jagiellonian University, Poland

<sup>3</sup>Department of Medicinal Chemistry, Institute of Pharmacology, Polish Academy of Science, Poland

[ncharazn@cyfronet.pl](mailto:ncharazn@cyfronet.pl)

**INTRODUCTION**

Sustainability, industrial ecology, eco-efficiency, and green chemistry are guiding the development of the next generation of materials, products, and processes<sup>1</sup>. Biopolymers represent one of the leading sectors for bio-based products and their expected growth is foreseen to be significant within the coming years. Due to their biocompatibility and biodegradability, polymers of natural origin have become not only an alternative to traditional plastics but also have desirable characteristics for their applications in the area of biomedical industry<sup>2</sup>.

**EXPERIMENTAL METHODS**

A detailed examination of a material is a key in finding its suitable applications and also in designing modifications of its structure so that it can be used in a wider scope. Using a microindentation technique the Young's modulus and the hardness of the PHO were determined. By determining the contact angles, we managed to estimate the surface tension of the material. These parameters are crucial in living cells studies, because the characteristic of the substrate, its stiffness and hydrophobicity or hydrophilicity have a direct impact on the behaviour of living cells<sup>3,4</sup>. To verify the biocompatibility, the material was subjected to a cytotoxicity study using dual staining (FDA / PI) on mouse fibroblast cells (MEF 3T3). The shape of the cells and the architecture of their cytoskeleton were analysed, for staining appropriate structures, phalloidin with rhodamine was utilized to visualize actin filaments, and in the case of microtubules, specialized antibodies of the first and second order were used. Observations were carried out using confocal microscopy, thanks to which it was possible to obtain a three dimensional reconstruction of cellular structures.

**RESULTS AND DISCUSSION**

Cytotoxicity tests demonstrated that this material does not damage cells and is fully biocompatible. Confocal observations have shown that the architecture of cells and their cytoskeleton differs from that known from polyacrylamide substrates with similar elasticity or glass supports. This is particularly interesting because the cells exhibit a circular nucleus and heights characteristic for soft substrates and the structure of the cytoskeleton resembles that known from substrates with a higher Young modulus.

**CONCLUSION**

The material is biocompatible, the cells cultivated on its surface show correct morphology and behaviour. Its mechanical properties make it possible to be used in areas where traditional polymers have been used so far.

**REFERENCES**

1. Mohanty A. *et al.*, J. Polym. Environ. 10:19–26, 2002
2. Bugnicourt E. *et al.*, Express Polym. Lett. 8:791–808, 2014
3. Levental I. *et al.*, Soft Matter. 3: 299–306, 2007
4. Wang Y. *et al.*, Proc. Am. Thorac. Soc. 94: 13661–13665, 1997

**ACKNOWLEDGMENTS**

Research funded by The National Centre for Research and Development, grant Lider no. LIDER/27/0090/L-7/15/NCBR/2016 and the project Interdisciplinary PhD Studies "Interdisciplinary for innovative medicine". Katarzyna Harażna acknowledges the support of InterDokMed project no. POWR.03.02.00-00-I013/16.

## Fabrication and Evaluation of Nanofibrous Scaffolds with Polylactide and Hyaluronic Fibers for Skin Substitute

Ewa Stodolak-Zych<sup>1</sup>, Katarzyna Rozmus<sup>1</sup>, Joanna Kubacka<sup>1</sup>, Łukasz Zych<sup>2</sup>, Magdalena Gargas<sup>3</sup>,  
Elżbieta Kołaczowska<sup>3</sup>, Cieniawska Magdalena<sup>4</sup>, Katarzyna Książek<sup>4</sup>, Anna Ścisłowska-Czarencka<sup>4</sup>

<sup>1</sup>Department of Biomaterials and Composite Materials, Faculty of Materials Science and Ceramics,  
AGH University of Science and Technology, Krakow, Poland

<sup>2</sup>Department of Ceramics and Refractories, Faculty of Materials Science and Ceramics,  
AGH University of Science and Technology, Krakow, Poland

<sup>3</sup>Department of Evolutionary Immunology, Institute of Zoology and Biomedical Research, UJ, Krakow, Poland

<sup>4</sup>Academy of Physical Education, Department of Physiotherapy, Section of Anatomy, Krakow, Poland  
[stodolak@agh.edu.pl](mailto:stodolak@agh.edu.pl)

### INTRODUCTION

Skin substitutes are defined as a heterogeneous group of materials that are used to close the wound and take over temporarily or permanently skin functions<sup>1</sup>. They consist natural or synthetic of scaffold (a substitute for the dermis) and fibroblasts, which produce same compounds extracellular matrix (ECM) and ingrown into three-dimensional matrix<sup>2</sup>. Due to their complexity, substitutes can be divided into three classes: first class includes temporary dressings, second class - single-layer skin substitutes, while the third one - complex skin substitutes. Substitutes can be used as protection of damaged tissue, a dressing supporting regeneration before transplantation or as a supplement to the resulting tissue defect. Each of class substitute need porous scaffolds, which can work along or with patient fibroblast.

The aim of this work is to determine the optimal conditions for the electrospinning of nanofibers from polylactide (PLA) and sodium hyaluronate (HA) and to create layered compositions: PLA membrane covered with HA nonwoven fibers (Fig. 1). It was done by modifying parameters such as appropriate amounts of solvents, polymer concentration, mixing temperature and electrospinning process conditions.

Spinning solution were characterized by the surface tension and rheology. Scanning electron microscope (SEM) was used to determine the morphology and diameter of fibers: PLA and HA. The structure of nonwoven fabric PLA/HA was analysed by spectroscopy (FTIR/ATR). Furthermore, biocompatibility evaluation was performed towards fibroblasts (ECM producers), keratinocytes (skin cells) and macrophages (immune cells) in in vitro conditions.

### EXPERIMENTAL METHODS

Commercial polymers: PLA (3251D, NatureWorks), HA (Contipro) were used in the experiment. Mixture of dichloromethane (DCM) and N, N-dimethylformamid (DMF) in 3:1 ratio was used as the solvent in PLA spinning solution. Mixture of ammonia water (WA) and ethanol (EA) in 2:1 ratio was used as the solvent in HA spinning solution. All reagents were from Avator (Poland). In the first part PLA solutions were prepared at various concentrations in a mixture of DCM and DMF with different volume ratios. In the second part, HA solutions of different concentrations of ammonia water with ethyl alcohol (EA). In both parts nanofibers were formed by electrospinning. Evaluation of the nonwoven PLA, HA and PLA/HA morphology was

made by microscopic examination (SEM). The structural characterisation of PLA/HA was used by FTIR-ATR. Other features of membrane were tested during surface free energy test and wettability (DSA 10 Kruss). In biocompatibility studies, cell viability and activity were evaluated<sup>3</sup>.

### RESULTS AND DISCUSSION

The diameter of PLA fibers depends on the concentration of the spinning solution and the temperature of the electrospinning. Stable fibers with comparable diameters (0.65-1.25  $\mu\text{m}$ ) are obtained by increasing the chamber temperature (about 45°C). Their surface is hydrophobic (100°) and the surface energy is maintained at 70 mN/mm. The addition of hyaluronic fibers increases the hydrophilicity of the material and the decrease of surface energy (the polar energy component increases significantly from 35 to 42 mN/mm). HA fibers form a heterogeneous layer on PLA nonwoven, which is confirmed by both physicochemical and structural studies (Fig. 1). All materials were biocompatible but to various degree.

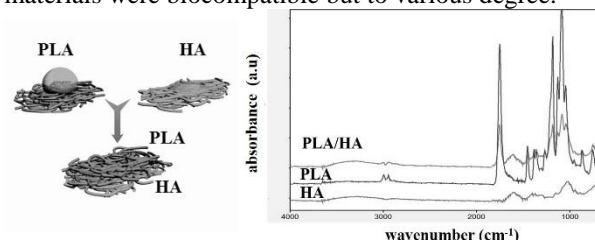


Fig. 1. Idea of skin substitute consisting PLA and HA fibers with the different wettability

### CONCLUSION

The results showed the conditions of formation of submicron PLA fibers and HA fibers. Composition of mixing fibers PLA/HA modified surface properties which improved biocompatibility of cells.

### REFERENCES

1. Ninan N. *et al.*, Polym Rev 55:3-453 2015
2. Ramana Ramya J. *et al.*, Ceram Inter 42:9-1045, 2016
3. Scisłowska-Czarnecka A. *et al.*, J. Appl. Polym. Sci. 127:3256, 2013

### ACKNOWLEDGMENTS

The biological studies were co-funded by the National Science Centre of Poland (grant No. 2014/15/B/NZ6/02519).

## Bacterial Response to PVA/Silver Nanoparticles Wound Dressing

Noemi O. Monteiro<sup>1</sup>, Jean A. N. Silva<sup>2</sup>, Renata N. Oliveira<sup>3</sup>, Rossana M. S. M. Thiré<sup>2</sup>, Olney V. Motta<sup>4</sup>, João C. A. Almeida<sup>1</sup>

<sup>1</sup>Universidade Estadual do Norte Fluminense Darcy Ribeiro – UENF/Center of Bioscience and Biotechnology (CBB), Campos dos Goytacazes - RJ, Brazil

<sup>2</sup>Federal University of Rio de Janeiro – UFRJ, COPPE/Program of Metallurgical and Materials Engineering, Rio de Janeiro - RJ, Brazil

<sup>3</sup>Federal Rural University of Rio de Janeiro – UFRRJ, Post-Graduation Program of Chemical Engineering - PPGEQ / Department of Chemical Engineering, Seropédica – RJ, Brazil

<sup>4</sup>Universidade Estadual do Norte Fluminense Darcy Ribeiro – UENF/Center of Agricultural Science and Technologies (CCTA), Campos dos Goytacazes - RJ, Brazil  
[rossana@metalmat.ufrj.br](mailto:rossana@metalmat.ufrj.br)

### INTRODUCTION

Burns are a serious public health problem due to the high levels of morbidity and mortality<sup>1</sup>. One of the primary problems in the treatment of burns is infection, which can delay healing, increase pain, scarring and in some cases cause death<sup>2</sup>. Hydrogel dressings, such as those based on polyvinyl alcohol (PVA), present most of the characteristics of the ideal dressing. However, they do not possess any intrinsic antimicrobial property. Silver nanoparticles (AgNPs) can be synthesized within PVA hydrogels by gamma radiation giving antimicrobial hydrogels<sup>3</sup>. Understanding the mechanism of action of antimicrobial agents is important for correct prescription of treatment, prevention of resistance and development of improved antimicrobials. The aim of this work was to evaluate the inhibitory effect of PVA/AgNPs films on the growth inhibition and ultrastructural alterations of *Pseudomonas aeruginosa* and methicillin resistant *Staphylococcus aureus*.

### EXPERIMENTAL METHODS

Samples were prepared by the casting technique using aqueous solutions of 10%wt PVA with 0.25%wt AgNO<sub>3</sub><sup>3</sup>. Solutions were poured into Petri dishes and dried in the dark, at room temperature. After drying, the samples were irradiated under ambient conditions with a Co-60  $\gamma$ -source at a dose rate of 0.5, 1.5 or 2.5 kGy.h<sup>-1</sup> for 10 h. PVA/AgNPs films were characterized by X-ray Diffraction (XRD), Scanning Electron Microscopy (SEM) and Atomic Absorption Spectroscopy for Ag content determination. Swelling tests in sterile saline solution were performed gravimetrically for each sample. For microbiological tests, standard strains of *P. aeruginosa* ATCC 15442 and methicillin resistant *S. aureus* (MRSA) ATCC 33591 were used. Antimicrobial activity was assayed by macrodilution and agar diffusion methods. For analysis of the bacteria ultrastructural changes, pieces of PVA/AgNPs films irradiated by 15 kGy were hydrated in Mueller-Hinton broth for 24 h at room temperature. Bacterial inoculum in saline solution was treated with PVA/AgNPs suspension for 8 h. After that, bacteria were processed by Transmission Electron Microscopy.

### RESULTS AND DISCUSSION

Formation of AgNPs was evidenced by the brownish coloration of all samples. Since all samples presented an amount of 1.4%wt Ag atoms despite of radiation dose, there were no significant difference of microstructure, morphology and swelling behaviour of films. The swelling equilibrium degree of the samples (70%) was reached after 30 min of immersion. Samples maintained their structural integrity even after 3 days immersed in saline solution. This is an indication that the PVA/AgNPs films would be able to absorb the exudate from the lesion while maintaining the physical protection against the external environment.

AgNPs presented bacteriostatic effect with significant decrease of the growth of MRSA and *P. aeruginosa*, important bacteria causing multiresistant nosocomial infections. TEM images showed that before treatment with AgNPs MRSA cells presented regular shape, wall and cell division. However, after treatment, electron dense granules in the cytoplasm, formation of vacuoles and cytoplasmic emptying were observed. *P. aeruginosa* cells without treatment had normal regular morphology, cell wall and chromatin, while treated cells showed changes in morphology, membrane and cellular appearance. Moreover, it was possible to observe electron dense granules in the cytoplasm, probably fragmentation of genetic material and marked cytoplasmic emptying.

### CONCLUSION

Results suggested that gamma radiation dose below 25 KGy does not affect significantly the crosslinking degree of PVA molecules, the amount of AgNPs synthesized and the antimicrobial activity of PVA/AgNPs films. AgNPs released from films caused ultrastructural changes in gram-positive and gram-negative bacteria. Accordingly, it can be concluded that PVA/AgNPs films has potential to be used in burn healing treatment, avoiding nosocomial infections.

### REFERENCES

1. World Health Organization (WHO): Fact Sheet, <http://www.who.int/mediacentre/factsheets/fs365/en/>. Accessed on November 28th, 2017.
2. Snell J. A. *et al.*, Critical Care 17:1, 2013.
3. Oliveira R. N. *et al.*, Interface Focus 4:20130049, 2014.

### ACKNOWLEDGMENTS

CNPq and FAPERJ for the financial support.



## Tuning the Mechanical Properties of Alginate-peptide Hydrogels

Guy Ochbaum<sup>1</sup>, Ronit Bitton<sup>1,2</sup>

<sup>1</sup>Department of Chemical Engineering, Ben-Gurion University of the Negev, Beer-Sheva 84105, Israel

<sup>2</sup>Ise Katz Institute for Nanoscale Science and Technology, Ben-Gurion University of the Negev, Beer-Sheva 84105, Israel  
[ochbaumg@post.bgu.ac.il](mailto:ochbaumg@post.bgu.ac.il)

### INTRODUCTION

The challenge in development of surrogate ECMs is to design and prepare synthetic materials capable of influencing cell differentiation, survival and migration through both biochemical interactions and mechanical cues. Current effort in the engineering of synthetic ECM has focused on installing molecular features (peptides) within insoluble scaffolds, either by self-assembly or through covalent modifications of polymer. Apart from inflicting bioactivity, incorporating biomolecules a tissue engineering scaffold may also cause a change in its physical properties, which will indirectly lead to a change in its bioactivity, as hierarchical structural organization and mechanical properties have been shown to affect cellular response to them.

Alginate, a polysaccharide that gels in the presence of divalent ions has been used as an artificial bio-surrounding similar to the natural Extra Cellular Matrix; Covalent bonding peptides to alginates is routinely used tailor alginate's biofunctionality. Here, we investigate the possibility of tuning the mechanical properties of alginate-peptide gels by altering the sequence of the covalently bound peptide.

### EXPERIMENTAL METHODS

We present a systematic investigation of the effect of three RGD-containing peptides, G<sub>6</sub>KRGDY, A<sub>6</sub>KRGDY and V<sub>6</sub>KRGDY, on the physical properties of alginate hydrogels. Characterization of these hydrogels was done by using Small angle X-ray scattering (SAXS) and rheology.

### RESULTS AND DISCUSSION

Alginate/peptide hybrids were prepared by two methods: 1) Covalent binding of the peptide to the alginate backbone (such hybrids were designated 'alginate-peptide'), and 2) direct mixing of peptide and alginate solutions (such hybrids were designated 'alginate + peptide').

Frequency sweep scans of the all the samples (Figure 1) are characteristic of a gel. Comparing storage modulus G' (i.e. gel stiffness) of alginate+peptide gels to that of Alginate-peptide gels shows that for the A<sub>6</sub>KRGDY and V<sub>6</sub>KRGDY peptides, the storage modulus of the alginate-peptide gels was an order of magnitude higher than that of the alginate+peptide gels. In the case of the alginate/G<sub>6</sub>KRGDY gels the G' of alginate-G<sub>6</sub>KRGDY gel was also higher than that of the alginate+G<sub>6</sub>KRGDY gel, yet the differences between the last two is much smaller.

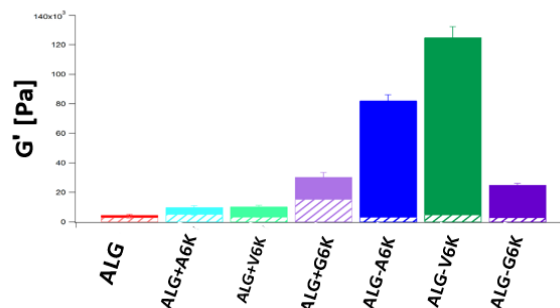


Fig. 1. Trend for the storage modulus at  $\omega = 10$  rad/s during frequency sweep test in water (Solid) and PBS (patterns).

Kratky plots of the SAXS data obtained from alginate peptide gels (Fig 2) show a peak, representing the presence of frozen inhomogeneities in the gel network followed by a straight line characteristic of worm-like chains. The differences between the scattering curves suggest the origin to the differences in the gels' stiffness are the differences between their cross-linked zones.

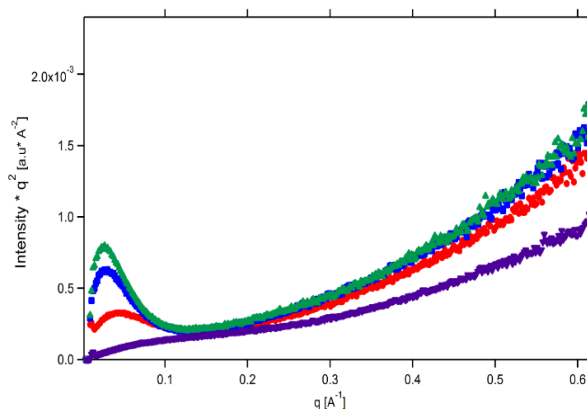


Fig. 2. Kratky plots for alginate gels. Alginate ( $\bullet$ ), alginate-A<sub>6</sub>KRGDY ( $\blacksquare$ ), alginate-V<sub>6</sub>KRGDY ( $\blacktriangle$ ) and alginate-G<sub>6</sub>KRGDY ( $\blacktriangledown$ ) formed by covalent binding.

### CONCLUSION

Our results showed that the ability of peptides to self-assemble in aqueous solutions (i.e. the peptide sequence) is an important factor in tuning the mechanical properties of alginate/peptide gels. Therefore, a detailed structural analysis of the conjugated architecture in solution can be used as a tool to tailor the properties of alginate/peptide hybrid hydrogels.

## Highly Porous 3D Fibrous Scaffolds for Tissue Regeneration

Chae-Hwa Kim, Tae-Hee Kim\*

Technical Textile R&D Group, Korea Institute of Industrial Technology, Ansan, Korea  
[thkim75@kitech.re.kr](mailto:thkim75@kitech.re.kr)

### INTRODUCTION

The tissue engineering strategy involves three critical elements; cells (e.g., stem cells or progenitor cells), signaling molecules (e.g., growth factors), and scaffolds. The scaffold is an artificial extracellular matrix (ECM) and serves as a template for cell growth and tissue regeneration. Ideally, the scaffold should be biocompatible and biodegradable, possess proper mechanical and physical properties, and mimic the in vivo microenvironment to facilitate cell adhesion, proliferation, differentiation, and neo tissue formation<sup>1</sup>. The use of fibres and textiles as components of implantable devices is widespread and covers a broad range of applications in medicine and healthcare. Textiles have been successfully used in close contact with complex biological environments as a part of devices such as heart valve sewing rings, vascular grafts, hernia repair meshes and percutaneous access devices<sup>2</sup>.

In order to be used for scaffolds, the construct should be able to restore biomechanical function and maintain controllable degradation during all stages of manipulation, from cell culture to implantation and thereafter<sup>3</sup>. Recently, several strategies to prepare porous 3D biodegradable scaffolds for tissue engineering have been developed. Interconnected fibre networks have been demonstrated to be particularly interesting as they provide a high porosity, interconnectivity and surface area<sup>4</sup>.

In this study, we have developed totally new concept of fibrous scaffolds by modifying existing textile manufacturing process. To design functional substitutes for damaged tissues and organs, we prepared novel 3D cylinder-type fibrous scaffolds by using “draw texturing” process. The scaffold is designed to have high flexibility and porosity with aligned microfibrillar bulky structure inside the tube having advanced biomimetic structure for cell growth.

### EXPERIMENTAL METHODS

PLA (poly-L-lactic acid) and PLGA [poly (lactide-co-glycolide, Lactide/Glycolide (1:9)) (220den/112fila) filament were prepared by draw texturing process. The PLA yarn was knitted into a tubular structure using a 14 needle circular weft knitting machine, of cylinder diameter 6mm. We could prepare 3D cylinder type scaffolds with microfibrillar bulky fibers inside after PLA, PLGA, and PLA/PLGA draw-textured yarn was inserted into PLA tube and elongated at a ratio of 15% of original length. To provide hydrophilic surface for efficient cell attachment and growth, the scaffolds were treated with oxygen plasma, secondarily coated with collagen and crosslinked by UV. 3D fibrous cylinder type scaffolds were irradiated in the air atmosphere by  $\gamma$ -rays (gamma radiation) to control the degradation rate.

The pore structure and morphology were observed by field scanning electron microscopy, and in-vitro degradation study carried out in phosphate buffered saline (PBS) to explore the interplay of these effects. The potential of scaffolds for tissue engineering was evaluated by investigating the adhesion and proliferation of cells.

### RESULTS AND DISCUSSION

The highly porous 3D fibrous cylinder type scaffolds were successfully prepared. Our scaffolds showed excellent 3-D structure with inter-connected pores.

The degradation study was carried out for 33days. PLGA, PLA/PLGA scaffold showed a sharp drop in pH from day 10 to day 33 and pH decreased as intensity of gamma irradiation increased.

The cell adhesion rate of PLGA scaffolds with collagen coating reached more than 75%, and PLGA material was superior to PLA in cell adhesion and growth. When scaffold was irradiated with 20 kGy of gamma rays, the initial cell adhesion rate was increased compared to the samples not irradiated with gamma rays. The PLGA scaffold showed the highest cell growth. Cell growth generally increases with time, and also influenced by the gamma irradiation intensity increases, the growth rate decreases. PLA/PLGA scaffolds showed the best cell attachment rate, but PLA scaffold was the best growth. Early cell adhesion directly affected cell growth, so scaffolds with high cell adhesion are likely to be advantageous for the better tissue regeneration.

### CONCLUSION

We could prepare highly porous microfibrillar 3D cylinder type scaffolds which had heterogeneous macropore by using draw texturing process. Microfibrillar structure has great potentiality as biomimicking architecture for cell growth and maintaining cell functions. The results suggest that our scaffolds are promising for clinical applications for tissue regeneration in orthopaedics, cardiology, and general surgery, as well as cell culture system for cell therapy.

### REFERENCES

1. X.H.Liu, et al. *Ann. Biomed.Eng.*32:477–486, 2004.
2. King MW, et al. *J. Textile Apparel. Tech, & Management* 1: 1 – 8, 2001.
3. Hollister SJ. *Adv Mater* 21:32–33, 2009.
4. Uzlakoglu K, et al. *Tissue Eng B Rev* 15:17–27, 2009

### ACKNOWLEDGMENTS

This work has been supported by the Korea Institute of Industrial Technology (JA180032)

## Preparation and Characterization of Absorbent Nonwoven Fabrics for Wound Care

YoonJin Kim, Chae-Hwa Kim, Jung Nam Im, Tae-Hee Kim\*

Technical Textile R&D Group, Korea Institute of Industrial Technology, Ansan, Korea

\*[thkim75@kitech.re.kr](mailto:thkim75@kitech.re.kr)

### INTRODUCTION

The wound care product has developed into various types of form, including film, hydrocolloid, foam and nonwoven to meet the causes of injury. When selecting dressings, decisions should be made on the basis of the treatment goal, the timeline for care and how the progress and outcome will be measured. High absorption capacity is the most important characteristics of absorbent nonwoven fabrics<sup>1-2</sup>.

In recent years, various approaches to improve the liquid handling properties have been suggested. The blend fibers were characterized with good moisture absorption<sup>3</sup>.

Hollow viscose rayon (HVR) is a hollow and segmented viscose fiber. The hollow segmented structure gives mechanical stability both in dry and in wet condition. Upon contact with an aqueous liquid, HVR fills completely with the fluid resulting in a significantly higher intrinsic absorbency. HVR can also be cyclically inflated and deflated. The use of HVR can improve high absorption capacity<sup>4</sup>.

In this study, we developed antibacterial absorbent nonwoven fabrics for wound care. Absorbent nonwoven fabrics were prepared by needle-punching and spun lace process in various mixing ratios of HVR and PET. We controlled the water absorption, water retention, and antibacterial property by adjusting the proportion between HVR and PET.

To investigate the potential use of HVR-based nonwoven fabrics as wound dressings, liquid absorption behavior was studied by measuring liquid absorption ratio. Antibacterial activity was quantitatively evaluated against *Staphylococcus aureus* and *Klebsiella pneumoniae*.

### EXPERIMENTAL METHODS

HVR (2 den, 40 mm) and PET(6 den, 42 mm) was purchased from Kelheim fibers and Huvis Co.,Ltd.

Needle-punched composite nonwovens of PET and HVR were prepared by varying HVR percentages in mass per unit area.

Blend ratios of PET and HVR were 10:0, 7:3, 5:5, 3:7, 0:10. Mass per unit area (basis weight) of composite nonwovens ranged from 120 to 130 g/m<sup>2</sup>.

Needle-punched nonwovens were manufactured with needle stroke (800, 1000, 1200 rpm) and antimicrobial effect was given by an eco-friendly antimicrobial agent based on chitosan.

In addition, various nonwoven types as a supporting layer were prepared by needle punching or spunlacing in order to produce a stable absorbent layer.

Free swell absorption test was performed based on modified BS EN 13726-1. The dry specimens were cut into 5 cm × 5 cm and weighed. Then the cut specimens were immersed in 0.9% saline solution for 10 min at room temperature. After the hydration, the specimens

were suspended by using forceps for 30 seconds at one corner in order to allow excess saline solution to drip off. The weights of wet specimens were measured.

The antibacterial properties were evaluated on modified KS K 0693.

### RESULTS AND DISCUSSION

Needle-punched composite nonwovens of PET and HVR were successfully prepared in various mixing ratios and the effects of liquid handling properties were investigated. When investigating the free swell absorption, nonwoven fabrics as an absorbent layer showed excellent free swell absorption with increasing HVR mixing ratios. Both basis weight and content of HVR in composite nonwovens influenced liquid handling properties.

Liquid handling properties reflects the amount of fluid retained by the wound dressings on a gram per gram basis. The liquid absorption and retention per unit area was improved with the increase of basis weight. But as a result of the absorption properties of the composite nonwovens combined with support layer, spunlacing process used for binding two layers exhibited significantly lower absorption than the needle punching process. It means that the composite nonwovens were densely and strongly bonded by spunlacing method, thereby reducing pore size and the space for absorbing liquid.

### CONCLUSION

In this study, we developed the potential use of HVR based absorbent nonwoven fabrics as wound dressing. The experimental results showed that the prepared absorbent nonwoven fabrics would have the optimal comprehensive performance.

When considering liquid handling properties, it is expected that needle-punched PET/HVR absorbent nonwoven fabrics could be a good candidate material for absorbent products such as moist wound dressing and so on.

### REFERENCES

1. Kathryn V. *et al.*, Surgery, 35,9:489-494,2017
2. Deborah S. *et al.*, J. Pharmaceutics and Biopharmaceutics, 127:130-141,2018
3. Kyung Min P. *et al.*, Biomacromolecules. 15,6:1979-1984, 2014
4. Lenzinger B. *et al.*, Walter Roggenstein, 89:72-77,2011.

### ACKNOWLEDGMENTS

This work was supported by Korea Evaluation Institute of Industrial Technology (KEIT) grant funded by the Korea government (MOTIE) (No.10070224).

## L-arginine and Manuka Honey Loaded Nanofibers for Wound Healing Applications

Oana Maria Ionescu<sup>1</sup>, Lenuța Profire<sup>1</sup>, Arn Mignon<sup>2</sup>, Sandra Van Vlierberghe<sup>2</sup>

<sup>1</sup>Department of Pharmaceutical Chemistry, “Grigore T. Popa” University of Medicine and Pharmacy of Iași, Romania

<sup>2</sup>Department of Organic and Macromolecular Chemistry, Ghent University, Belgium

[Ionescu\\_mariuca@yahoo.com](mailto:Ionescu_mariuca@yahoo.com)

### INTRODUCTION

Novel wound dressings based on nanofibers are being widely investigated in the biomedical field due to their high surface area and porosity<sup>1,2</sup>. Chitosan (CS) displays antibacterial effects<sup>3</sup> which could be sustained by honey<sup>4,5</sup>. L-arginine increases the synthesis of collagen and enhances healing<sup>6</sup>. In an acetic acid aqueous solution of chitosan and polyethylene oxide (PEO), the amino groups of the polycation (CS) would be protonized and endow chitosan electrical properties, migrating outward and forming the shell composition under the force of the built-in electric field during conventional electrospinning, with PEO standing as core material with mechanical properties<sup>7,8</sup>. In this study we aim to obtain and characterize L-arginine and Manuka Honey loaded nanofibrous matrices via electrospinning.

### EXPERIMENTAL METHODS

1% wt/v L-arginine monohydrochloride, 10% wt/v Manuka Honey (MH) and both 1% wt/v L-arginine monohydrochloride and 10% wt/v MH were dissolved in PEO 1% wt/v and CS 3% wt/v (1:1 volume ratio) aqueous solution of acetic acid 50% v/v.

### Electrospinning parameters

All solutions were spun using a 21-gauge needle at 18kV, 27.5 cm needle-collector distance and a 1 mL/h flow-rate, relative humidity of 9-22% and a temperature of 18-19°C to obtain randomly oriented fibers.

### Characterization

Before electrospinning, the viscosity of the solutions was measured using a parallel-plate measuring system with rheological measurements depicted in Table 2. The test was performed in triplicate and the data are expressed as means ± SD. Fiber morphology and average diameters as observed by scanning electron microscope and Fibermetric software are shown in Figures 1 and Table 1, with a minimum of 150 fibers checked for calculating the average fiber diameter. The data are expressed as means ± SD. Analysis to confirm the core-shell structure, mechanical, water retention behaviour and in vitro analysis to assay antibacterial activity is ongoing.

### RESULTS AND DISCUSSION

Smooth, uniform, randomly oriented fibers were obtained for all three groups, as depicted in the SEM pictures (Fig. 1).

Table 1. Fiber diameter of the electrospun fibers

Component	Mean Diameter (nm)
PEO/CS/L-Arginine 1% wt/v	227.4±70.51
PEO/CS/MH 10% wt/v	301.4±65.61
PEO/CS/MH 10% wt/v /L-arginine 1% wt/v	275± 101.85

By adding additives to the polymeric solution, both viscosity and fiber diameter increase (Table 1, Fig. 2), which is confirmed by literature data<sup>2,5</sup>.

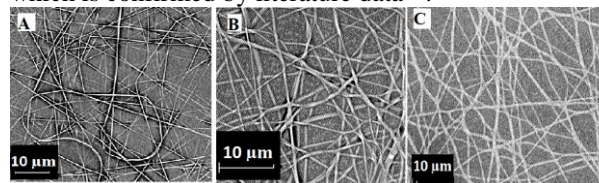


Fig. 1. SEM images of electrospun PEO/CS/L-Arginine 1% wt/v (A), PEO/CS/MH 10% wt/v (B) and PEO/CS/L-Arginine 1% wt/v/MH 10% wt/v (C)

Honey and chitosan have a synergistic effect<sup>9</sup> on the viscosity of MH-chitosan solutions, as can be seen in Table 2. MH also shows thixotropic behaviour because of the presence of high-molecular-weight components (proteins)<sup>10</sup>. As such with the increase of the shear stress, the viscosity decreases.

Table 2. Viscosity corresponding to the characteristic retardation point. After this point an increase in shear rate leads to shear thinning.

Solution	Zero shear viscosity (at 20°C) [Pa.s]
PEO/CS/L-Arginine 1%wt/v	1.14±0.13
PEO/CS/MH 10% wt/v	2.78±1.33
PEO/CS/L-Arginine 1% wt/v/MH 10% wt/v	2.96±1.26

### CONCLUSION

In this work, we successfully developed smooth, continuous L-arginine/MH nanofibers providing a new option for developing wound dressings.

### REFERENCES

- Han G. *et al.*, Adv. Ther. 34:599-610, 2017
- Sarhan W. A. *et al.*, Mater. Sci. Eng. C. 67:276-284, 2016
- Kong M. *et al.* Int. J. Food Microbiol. 144: 51-63, 2010
- Yang X. *et al.*, Mater. Des. 119:76-84, 2017
- White M. B. *et al.*, Wound Repair Regen. 11: 419-423, 2003
- Zhang J-F. *et al.*, Macromolecules, 42:5278-5284, 2009
- Bösiger P *et al.*, Carbohydr. Polym, 181:551-559, 2018
- Sarhan W. A. *et al.*, Carbohydr. Polym, 122:135-143, 2015
- Witczak M. *et al.*, J. Food Eng. 104:532-537, 2011

### ACKNOWLEDGMENTS

The authors thank Ghent University for access to the research infrastructure required for developing and characterizing this type of nanomaterials and Romanian UEFISCDI for the financial support given through the research project PN-II-1.1-MC-2017-2462.



## Collagen Hydrogels Modified by Cyclodextrines Addition

J. Skopinska-Wisniewska, J. Kozłowska, A. Sionkowska

Faculty of Chemistry, Nicolaus Copernicus University in Torun, Poland

[justynak@umk.pl](mailto:justynak@umk.pl)

### INTRODUCTION

Collagen and elastin are the main components of extracellular matrix of connective tissues. For this reason they are extensively studied as materials for tissue engineering [1].  $\beta$ -cyclodextrines are oligosaccharides composed of 7 glucopyranose units. Their hydrophobic interior have a diameter appropriate to the size of molecules like hormones, vitamins and compounds used in cell culture applications [2,3]. In this way, growth factors may be incorporated into protein matrix. The aim of our work was to study the interaction between cyclodextrines and protein matrix.

### EXPERIMENTAL METHODS

The collagen type I was extracted from rat tail tendons and 1% solution in 0.1 M acetic acid was prepared. The 5% and 10% of  $\beta$ -cyclodextrine (CD) and  $\beta$ -cyclodextrine, sulphated sodium (CDS) were added to the samples. The mixtures were incubated 30 min on magnetic stirrer and then dialysed against deionized water.

The mechanical properties were tested using Zwick&Roell machine. The pieces of collagen gels in a shape of cylinder were placed on the bottom disk and pushed by a steel rod with speed 10mm/min.

The swelling degree ( $E_s$ ) was measured by the conventional gravimetric method in 0.05M phosphate buffer saline (PBS) - pH7.4, room temp.  $E_s$  was calculated using the equation  $E_s = (W_s - W_d) / W_d$  ( $W_s$ ,  $W_d$  – the weights of swollen and dry samples, respectively).

### RESULTS AND DISCUSSION

The collagen gels containing  $\beta$ -cyclodextrine are homogenous and transparent. The CD addition causes increasing the stiffness of the gel. The materials modified by CDS are heterogenous and highly cross-linked only in some regions. The 5% addition of CDS decreases of Young's Modulus value, while Coll+10%CDS sample contains part of the gel and sol and can't be tested (Tab. 1).

Tab. 1. Young's Modulus of collagen gel modified by CD and CDS addition.

Sample	E [kPa]	$\sigma$ [kPa]
Coll	8.04±2.93	2.20±0.45
Coll+5%CD	9.66±2.92	1.69±0.26
Coll+10%CD	9.48±2.88	2.11±0.41
Coll+5%CDS	6.61±2.26	1.71±0.33
Coll+10%CDS	-	-

The 5% and 10% addition of CD does not significantly affect the swelling capacity. Whereas, the gels containing CDS exhibit a significantly higher ability to swell (Fig. 1).

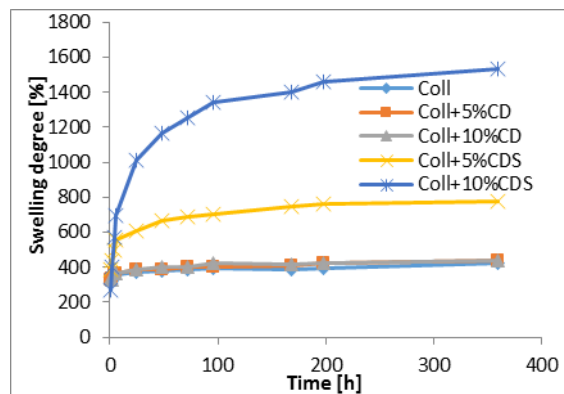


Fig. 1. Swelling ability of collagen gels modified by CD and CDS addition.

### CONCLUSION

The addition of CD to collagen gel improves its stiffness, while CDS reduces Young's Modulus. However, the swelling ability is much higher for gels modified by CDS addition. This is probably caused by heterogeneity in the material structure. The modification collagen gel by CDS addition is more effective, however, a method that allows homogeneous cross-linking should be developed.

### REFERENCES

1. Lee C.H. *et al* Int. J. Pharm. 221:1 – 22, 2001
2. Del Valle E.M., Process Biochem 39:1033-1046, 2004
3. Zhang J. *et al* Adv. Drug Deliv. Rev. 65:1215-1233, 2013

## Interactions of Dermal Papilla Spheroid Array and Acellular Skin Dermis during Hair Follicle Regeneration

Yi-You Huang, Chia-Hsiem Tsai

Institute of Biomedical Engineering, National Taiwan University, Taiwan

[yyhuang@ntu.edu.tw](mailto:yyhuang@ntu.edu.tw)

### INTRODUCTION

Alopecia not only loses function of hair but also cause physiological impacts on the patient. Fabrication of scaffold for regeneration of hair follicle by tissue engineering provides a promising alternative. Successful hair follicle (HF) neogenesis depends on the existence of both capable dermal cells and competent epidermal keratinocytes through epithelial-mesenchymal interaction. Dermal papilla (DP) is a highly specialized mesenchymal cell population and widely applied for hair follicle regeneration engineering. However, DP cells tend to lose their inductivity in vitro. In this study, we developed a strategy for large-scale cultivation of transplantable dermal papilla cellular aggregates by using microfabricated PDMS arrays. We also used three-dimensional (3D) culture system to mimic the real microenvironment and investigate the cell-extracellular matrix (ECM) interactions.

### EXPERIMENTAL METHODS

Due to high biocompatibility and low cell attachment of Poly(dimethylsiloxane) (PDMS), PDMS was used to fabricate the microwells, and provide the hydrophobic surface. High-efficiency of cellular aggregates were formed by relatively hydrophobic culture strategy, i.e. by direct PDMS coating on 96-well plate and PDMS microwell-arrays. Acellular dermal scaffold was fabricated by serial steps of decellularization methods. Two-dimensional (2D) monolayers culture and three-dimensional (3D) culture system were compared by their efficiency and activity.

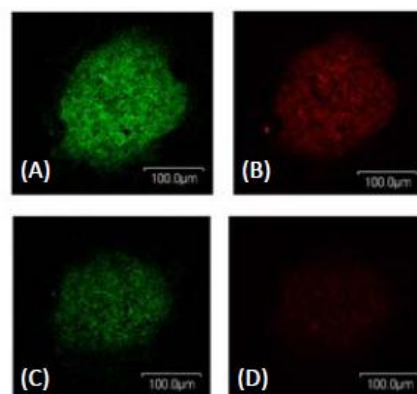
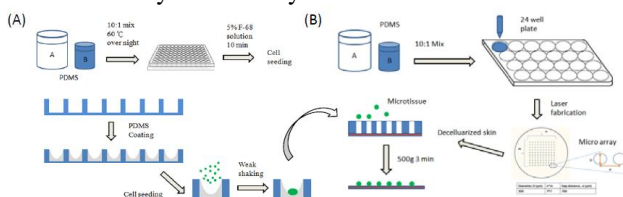


Fig. 1. Immunocytochemistry staining of DP microtissues (A)  $\alpha$ -SMA (B) Versican (C) Vimentin (D) Fibronectin

Discussion should summarize the observations and attempts to place this data into the context of the existing body of literature to express opinions about the significance of the work.

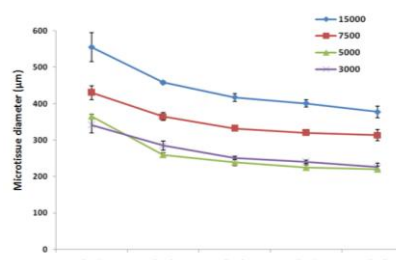
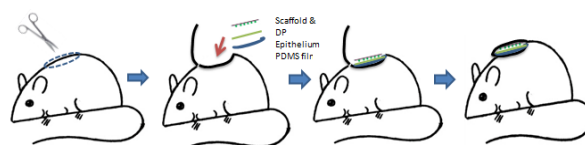


Fig.2



### CONCLUSION

We have successfully developed DP microtissue model by coating PDMS on culture plate, which have uniform size manner and maintain its phenotype in vitro. By using acellular skin dermis as scaffold and combined with PDMS microwell, it provides a concept for in vivo transplantation.

### REFERENCES

1. Hsieh C-H, Wang J-L, Huang Y-Y. Acta Biomaterialia. 7:315-324, 2011.
2. Lin B, Miao Y, Wang J, Fan Z, Du L, Su Y, Liu B, Hu Z, Xing M. ACS applied materials & interfaces. 8:5906-5916, 2016.

### ACKNOWLEDGMENTS

This research was supported by a Grant (MOST 105-2221-E-002-022-MY3) from the MOST, Taiwan.

### RESULTS AND DISCUSSION

Laser-fabricated PDMS micro-array makes microtissues grow in specific arrangement. We found that both rat and human dermal papilla microtissues grow very well in vivo with cell density under 3000 cells/well. Most cells still represented viable within the microtissues for long-term cultivation. The inductivity of DP microtissues were confirmed by the  $\alpha$ -SMA, Versican and Vimentin, the specific markers of DP. These immune-fluorescent staining are highly expressed. In acellular dermal scaffold study, we found that the native cells are almost removed, and the extracellular matrix are kept intact by DNA and GAGs content assays. Decellularized scaffolds possess many good properties compared with artificial scaffolds. Their exceptional cellular affinity and the ability to provide extracellular matrix resembling in vivo environment enable them to provide a proper environment for cellular growth.

## Correlation between viscoelastic properties and curcumin release rate from PVA-Borax/Cellulose nanofiber hydrogels

Gelareh Rezvan, Gholamreza Pircheraghi, Reza Bagheri

Polymeric Materials Research Group (PMRG), Materials Science and Engineering Department,  
Sharif University of Technology, P.O. Box: 11365-9466, Tehran, Iran

[pircheraghi@sharif.ir](mailto:pircheraghi@sharif.ir)

### INTRODUCTION

Nowadays controlled drug release from polymeric vehicles has been accepted as an important approach in pharmacotherapy<sup>1</sup>. Hydrogels are the physically or chemically cross-linked 3D dimensional network of water-soluble polymers which have numerous hydrophilic groups and water content as high as 90 wt%. Along with all proper properties, hydrogels efficiency commonly could be restricted by weak mechanical properties<sup>2</sup>. While, viscoelastic and mechanical properties of hydrogels can be tuned by incorporating nanoparticle reinforcements<sup>3</sup>. Meanwhile, changes in viscoelastic properties of hydrogel would influence its ability for drug loading as well as drug release rate<sup>3</sup>. PVA-Borax (PB) hydrogel is a promising candidate for drug delivery systems. While, due to its weakness in mechanical behaviour, cellulose nanofiber could be added to PB (PB-C) hydrogel as a natural biocompatible reinforcement. In this research, it was tried to find a quantitative correlation between drug release rate and viscoelastic properties of PVA-Borax hydrogel reinforced with cellulose nanofiber.

### EXPERIMENTAL METHODS

In this research, curcumin as a hydrophobic drug encapsulated in Pluronic F127 micelle and loaded into prepared PB-C hydrogels with different content of cellulose nanofiber. Hydrogels were prepared based on solution mixing method described in literature [1]. All the samples consist of 4wt% PVA, 1wt% Borax and 2 or 4wt% cellulose nanofiber.

The curcumin release rate in PBS solution investigated by UV-Vis spectroscopy measurements. While, viscoelastic properties were measured in linear viscoelastic region using a parallel plate oscillatory rheometer.

### RESULTS AND DISCUSSION

Figure 1 reveals that release rate of curcumin is influenced by temperature and hydrogel composition reflected in its rheological properties. In this regard, we have defined the drug release rate coefficient (*DRC*) and viscoelastic properties coefficient (*VPC*) as below equations:

$$DRC = n \times K \quad \text{eq.1}$$

$$VPC = (\omega_c \times \omega_r) / (G'_{\infty}) \quad \text{eq.2}$$

Where *n* is diffusion exponent and *K* is the kinetic constant of curcumin release rate. While,  $\omega_c$ ,  $\omega_r$  and  $G'_{\infty}$  are cross over frequency, resonance frequency and plateau storage modulus.

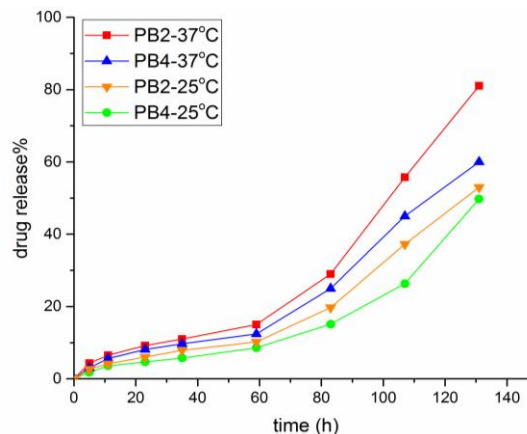


Fig. 1. The release rate of Cur-P from PB-C hydrogels as function of temperature in PBS solution

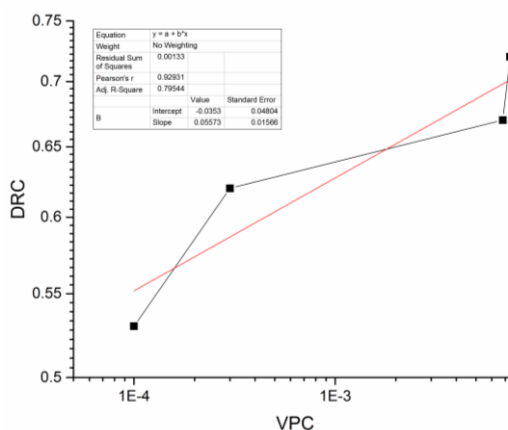


Fig. 2. the power law correlation between drug release rate coefficient (*DRC*) and viscoelastic properties coefficient (*VPC*)

### CONCLUSION

In this work curcumin release rate from PVA-Borax hydrogel reinforced with cellulose nanofiber was investigated. Two parameters, *DRC* and *VPC* were defined which are representative of drug release rate and viscoelastic properties of PB-C hydrogels respectively. The power law correlation between *DRC* and *VPC* of PB-C hydrogel was confirmed.

### REFERENCES

1. Xiao H. *et al.*, *Journal of controlled release*. 73:121-136, 2001.
2. Bhattarai N. *et al.*, *Advanced drug delivery reviews*. 62:83-99, 2010.
3. Hoare T. *et al.*, *Polymer*. 49:1993-2007, 2008.

## Innovative PCL/graphene filament for 3D printing of cartilage scaffolds using fused deposition modeling

Anna Kurowska<sup>1</sup>, Arkadiusz Matuszek<sup>1</sup>, Dawid Holisz<sup>1</sup>, Adam Jabłoński<sup>1</sup>, Magdalena Ziąbka<sup>2</sup>, Ryszard Kwiatkowski<sup>3</sup>, Izabella Rajzer<sup>1</sup>

<sup>1</sup>University of Bielsko-Biala, Department of Mechanical Engineering Fundamentals, Bielsko-Biala, Poland

<sup>2</sup>AGH University of Science and Technology, Faculty of Materials Science and Ceramics, Department of Ceramics and Refractories, Krakow, Poland

<sup>3</sup>University of Bielsko-Biala, Faculty of Materials and Environmental Sciences, Institute of Textile Engineering and Polymer Materials, Bielsko-Biala, Poland  
[irajzer@ath.bielsko.pl](mailto:irajzer@ath.bielsko.pl)

### INTRODUCTION

Fused deposition modeling (FDM) is one of the lowest cost 3D printing methods which is based on layer by layer deposition of extruded polymer through a nozzle using feedstock filaments from a spool<sup>1</sup>. The success of 3D printing is primarily defined by the quality of the filament. Chemical impurities within the filament will affect the printing process. Ideal filament should maintain an absolutely constant diameter across the whole spool. Another important factor is a constant filament roundness across the full length of a spool. Filaments used for biomedical applications are very expensive and usually it is not necessary to use whole spool to produce 3D nasal cartilage implant.

Surgical procedures in the aerodigestive tract are considered potentially contaminated and may be associated with postoperative infectious complications. Recent studies show the high antibacterial efficiency of graphene<sup>2</sup>. Therefore the aim of this work was to develop an innovative filament for FDM in a form of polymer sticks which will contain graphene within its structure in order to obtain antibacterial properties of future nasal cartilage scaffolds.

### EXPERIMENTAL METHODS

Poly( $\epsilon$ -caprolactone) (PCL) (molecular weight: 80 kDA) and graphene nanoplatelets (powder) were purchased from Sigma Aldrich. The filament sticks were fabricated using injection moulding machine (BABYPLAST6/10P). An analysis of the influence of injection moulding parameters on the final sticks properties was done. PCL and PCL/graphene with a diameter of 1.75 mm, were used as filament for the 3D printer. The scaffolds were developed using the Fused Deposition Modelling (FDM) technique. Filament sticks were fused and guided by an extrusion nozzle to form 3D scaffolds. The material left the extruder in a liquid form and solidified upon contact with the fabrication platform. The previously formed layer was the substrate for the next layer. A temperature was maintained just below the solidification point of the material to assure good interlayer adhesion.

The samples were evaluated using a scanning electron microscope (Nova NanoSEM 200, FEI) equipped with EDS analysis. Graphene modified polymeric sticks as well as pure PCL sticks were evaluated by X-ray diffraction method (XRD). Printed samples were observed with a Stereomicroscope (SN) from OPTA-TECH company, equipped with a CMOS 3 camera and OptaViewIS software.

### RESULTS AND DISCUSSION

The microstructure of obtained filament stick is presented in Fig. 1. From the SEM images, it can be observed that graphene nanoplatelets were successfully incorporated into the filament structure. However some graphene agglomerates could also be observed on the surface. After optimization of injection moulding and 3D printing processes parameters, 3D scaffolds were successfully printed and their macroscopic images are presented in Fig. 2.

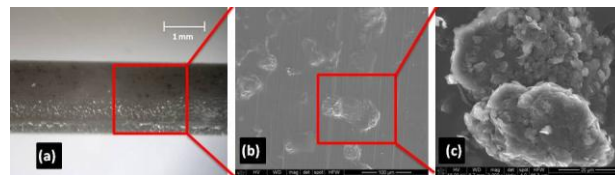


Fig. 1. Microscopic images of PCL/graphene filament.

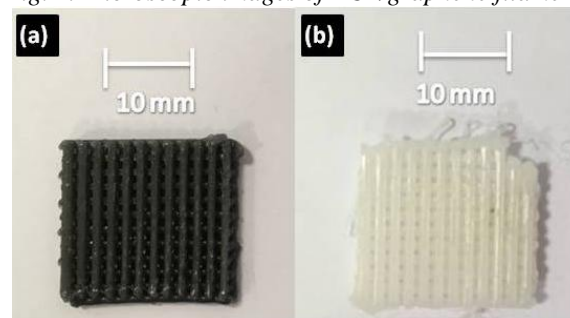


Fig. 2. Images of scaffolds printed with FDM method. (a) PCL/graphene; (b) pure PCL.

### CONCLUSION

Scaffolds were successfully printed using polymeric sticks (modified with graphene) fabricated by injection moulding method. It is expected that after implantation this 3D printed scaffold will provide 3D porous structure which will promote the growth of cartilage and the antibacterial properties of graphene will ensure proper postoperative regeneration of scaffold implantation side.

### REFERENCES

1. Rajzer I. *et al.*, J. Biomech. 2:5-11, 2011
2. Yousefi M. *et al.*, Mater. Sci. Eng. C 74:568-581.

### ACKNOWLEDGMENTS

This work was supported by the National Science Centre, Poland in the frame of project: "Layered scaffolds for nasal cartilages reconstruction fabricated by 3D printing and electrospinning" 2015/18/E/ST5/00189 (Sonata Bis 5).



## Novel Perspectives of Polymer-based Scaffolds for Biomedical Applications

Małgorzata Sekuła<sup>1,\*</sup>, Patrycja Domalik-Pyzik<sup>2,\*</sup>, Sylwia Noga<sup>1,3</sup>, Elżbieta Karnas<sup>1,3</sup>, Karolina Kosowska<sup>2</sup>,  
Martyna Hunger<sup>2</sup>, Natalia Złocista-Szewczyk<sup>2</sup>, Joanna Jagiełło<sup>4</sup>, Ludwika Lipińska<sup>4</sup>,  
Kinga Pielichowska<sup>2</sup>, Jan Chłopek<sup>2</sup>, Ewa Zuba-Surma<sup>3,#</sup>

<sup>1</sup> Malopolska Centre of Biotechnology, Jagiellonian University, Krakow, Poland

<sup>2</sup> Department of Biomaterials and Composites, Faculty of Materials Science and Ceramics,  
AGH University of Science and Technology, Krakow, Poland

<sup>3</sup> Department of Cell Biology, Faculty of Biochemistry, Biophysics and Biotechnology,  
Jagiellonian University, Krakow, Poland

<sup>4</sup> Department of Chemical Technologies, Institute of Electronic Materials Technology, Warsaw, Poland

\* These authors contributed equally to this work

Presenting author: [malgorzata.sekula@uj.edu.pl](mailto:malgorzata.sekula@uj.edu.pl), #corresponding author: [ewa.zuba-surma@uj.edu.pl](mailto:ewa.zuba-surma@uj.edu.pl)

### INTRODUCTION

Mesenchymal stem cells (MSCs) represent a class of adult multipotent stem cells. MSCs possess the ability to differentiate into cells of mesodermal origin, including osteoblasts, chondrocytes and adipocytes. They are also characterized with high proliferative capacity and paracrine activity. Moreover, MSCs are easy to harvest from different sources, demonstrate low immunogenicity and represent no ethical concerns in autologous and allogenic transplantations. All these features make MSCs promising tool for medical research.

Growing evidence indicate, that MSCs in combination with biomaterials constitute novel perspectives for tissue engineering and biomedical applications. Novel strategies enhancing biological properties of cells are still required. Thus, utilization of natural polymers, such as chitosan and alginates are promising platforms dedicated for stem cells propagation and differentiation.

### EXPERIMENTAL METHODS

In current study we examined an influence of chitosan- and sodium alginate-based substrates on MSCs functions. MSCs were isolated from human umbilical cord Wharton's jelly (named as hUC-MSCs) by explant method. Then, cells were cultured in DMEM/F12 medium supplemented with 10% FBS in an incubator chamber at 37°C, 5% CO<sub>2</sub> and 95% humidity. Chitosan- and sodium alginate-based matrices were modified with graphene oxide (GO), reduced graphene oxide (rGO) and hydroxyapatite (HAp) and tested as culture surfaces dedicated for hUC-MSCs propagation and chondrogenic differentiation. The morphology, proliferation activity and metabolic potential of hUC-MSCs were analyzed by microscopic analysis, proliferation test and ATPlite luminescence assay, respectively. Moreover, chondrogenic differentiation of hUC-MSCs was performed to evaluate the impact of scaffolds on their differentiation capacity *in vitro*.

### RESULTS AND DISCUSSION

The analysis demonstrated that hUC-MSCs cultured on chitosan and sodium alginate-based substrates, pristine and modified with GO or rGO, may be used as surfaces for cell propagation. We observed morphological differences of hUC-MSCs cultured on both types of tested scaffolds. Interestingly, analysis of proliferation potential as well as metabolic activity of hUC-MSCs suggested high spontaneous differentiation capacity of hUC-MSCs cultured on polymer-based scaffolds, as compared to cells cultured on control plate (tissue culture polystyrene surface). These observations were also confirmed by gene expression analysis and alcian blue staining.

### CONCLUSION

Our results indicated that chitosan and sodium alginate-based substrates exhibit a potential applicability as novel, safe and biocompatible materials for utilization in biomedical applications. However, further analysis is required to elucidate the impact of polymer-based surfaces on therapeutical properties of hUC-MSCs.

### REFERENCES

1. Kobolak J. *et al.*, Methods. 99:62-68, 2016
2. Nombela-Arrieta C. *et al.*, Nat Rev Mol Cell Biol. 12:126-131, 2011
3. Nagamura-Inoue T. *et al.*, World J Stem Cells. 6:195-202, 2014
4. Chen G.Y. *et al.*, Biomaterials. 33:418-427, 2012
5. Huang H. *et al.*, Biomed Mater. 9:035008, 2014

### ACKNOWLEDGMENTS

This study was funded by Symfonia 3 NCN grant: UMO-2015/16/W/NZ4/00071 and STRATEGMED3 NCBR grant: STRATEGMED3/303570/7/NCBR/2017.



# ISBPPB 2018



Polish  
Society for  
Biomaterials



Faculty of Materials  
Science and Ceramics  
AGH-UST



International Society  
for Biomedical Polymers  
and Polymeric Biomaterials